Zoosystematics and Evolution

94 (1) 2018

PENSOFT

museum für naturkunde

ISSN 1435-1935 Zoosyst. Evol. 94 (1) 2018, 1–209

Zoosystematics and Evolution
A Bulletin of Zoology since 1898

Instructions for authors

Scope

Zoosystematics and Evolution (formerly Mitteilungen aus dem Museum für Naturkunde in Berlin, Zoologische Reihe) edited by the *Museum für Naturkunde, Leibniz Institute for Research on Evolution and Biodiversity at the Humboldt University Berlin* is an international, peer-reviewed, life science journal, devoted to whole-organism biology. It mainly publishes original research and review articles in the field of Metazoan taxonomy, biosystematics, evolution, morphology, development and biogeography at all taxonomic levels. Its scope encompasses primary information from collection-related research, viz. taxonomic descriptions and discoveries, revisions, annotated type catalogues, aspects of the history of science, and contributions on new methods and principles of systematics. Entomological papers will also be accepted for review, but authors should first consider submission to the Deutsche Entomologische Zeitschrift. Articles whose main topic is ecology, functional anatomy, physiology, or ethology are only acceptable when of clear systematic or evolutionary relevance and perspective. Review articles and contributions to a discussion forum are welcome, but authors are asked to contact the editors beforehand.

Authors and submission

- Conflicts of interest: Authors must disclose relevant compet- ing interests, both financial and personal.
- Ownership: Authors must declare that the submitted work is their own and that copyright has not been breached in seeking its publication.
- Originality: Authors must declare that the submitted work has not previously been published, and is not being consid- ered for publication elsewhere.

Language and style

- The language of publication is English. There is no general limitation of the length of manuscripts, but please contact the editor before submitting papers exceeding 30 printed pages (approximately 60 manuscript pages including figures).
- Manuscripts should be written in a clear, straightforward style and must not have been published or submitted elsewhere.
- The text should be 12 pt, double-spaced, one-sided, left justified and with a margin of at least 3 cm.
- Use a standard typeface, e.g. Times New Roman as little formatted as possible (without tabulators, several blank spaces, etc.). Avoid footnotes.
- Divide the text into sections using headlines and subheadlines. Do not number the headlines. Inline headers should be set in italics and followed by a full stop.
- The names of genera and species must be in italics.
- Taxonomic descriptions must comply with the rules of the 4th edition of the ICZN (see http://www.iczn.org/).
- Enter the page number on every page.
- Submit figures with a minimum resolution of 300 dpi.
- The preferred file formats are PSD (Photoshop) and TIFF for colour and grayscale illustrations, and EPS for vector graphics.
- JPG files are only accepted in high resolution.

General manuscript structure

If appropriate, the manuscript should be structured using headlines and sub-headlines, but without numbering, according to the following sections:

- Title page
- Abstract
- Introduction
- Materials and Methods
- Results
- Discussion
- Acknowledgements
- References
- Tables with captions
- Figure captions

The publication process

Peer reviewing

Manuscripts are subject to peer review. All manuscripts submitted will be reviewed by at least two experts. Authors are welcome to make suggestions for competent reviewers.

Proofs

Prior to publication of your manuscript you will receive proofs in PDF format. Please correct and return the proofs within two weeks to the editorial office.
We recommend using the standard proofreading marks or – in the case of a few corrections – using page and line numbers.
Do not change the contents of your article. Corrections extending beyond production errors will be carried out at the expense of the author.
The editorial office reserves the right to publish your article with only the editor‘s corrections, if your corrections do not reach us in time.

Publishing

The print and the online versions of your paper are published simultaneously. It is accessible in open access at Pensoft: http://zse.pensoft.net

COPE Membership

This journal endorses the COPE (Committee on Publication Ethics) guidelines and will pursue cases of suspected research and publication misconduct (e.g. falsification, unethical experimentation, plagiarism, inappropriate image manipulation, redundant publication). For further informa- tion about COPE, please see the website for COPE at http://www.publicationethics.org.uk

Zoosystematics and Evolution

94 (**1**) 2018

PENSOFT

museum für naturkunde

Zoosystematics and Evolution
A Bulletin of Zoology since 1898

Zoosystematics and Evolution

2018. Volume 94. Issue 1

ISSN: 1435-1935 (print), 1860-0743 (online)
Abbreviated keys title: Zoosyst. Evol.

In Focus

The cover picture shows a male of *Melanorivulus linearis* sp. n. Photograph by W.J.E.M. Costa.

See paper of **Costa WJEM** Three new species of the killifish genus *Melanorivulus* from the Rio Paraná Basin, central Brazilian Cerrado (Cyprinodontiformes, Aplocheilidae)

Cover design
Pensoft

Zoosystematics and Evolution
A Bulletin of Zoology since 1898

Content of volume **94** (**1**) 2018

Abstract & Indexing Information

Biological Abstracts® (Thompson ISI)
BIOSIS Previews® (Thompson ISI)
Cambridge Scientific Abstracts (CSA/CIG)
Web of Science® (Thompson ISI)
Zoological Record™ (Thompson ISI)

Zoosyst. Evol. 94 (1) 2018, 1–15 | DOI 10.3897/zse.94.14959

PENSOFT

museum für naturkunde

Revision of *Platydoris angustipes* and description of a new species of *Platydoris* (Gastropoda: Nudibranchia) from southeastern Brazil based on comparative morphology

Patricia O. V. Lima[1], Luiz Ricardo L. Simone[1]

1 *Museu de Zoologia da Universidade de São Paulo, Cx. Postal 42494; 04299-970 São Paulo, SP, Brazil*

http://zoobank.org/57027940-2E36-4170-A90C-B8F17E7C72B6

Corresponding author: *Patricia O. V. Lima* (patylima84@gmail.com)

Received 10 July 2017
Accepted 10 November 2017
Published 2 January 2018

Academic editor:
Matthias Glaubrecht

Key Words

Discodorididae
Platydoris angustipes
Platydoris guarani
new species

Abstract

Platydoris angustipes (Mörch, 1863) is a common nudibranch in the Western Atlantic, ranging from Florida, USA, to Rio de Janeiro, Brazil. In this study, we examined the anatomy of *P. angustipes* along its distribution, including its type material. Our analysis shows consistent differences between the Caribbean and Brazilian populations, mainly in the reproductive system, radular teeth and odontophore musculature. This strongly suggests that the two populations actually belong to distinct species. The Brazilian population is described herein as a new species, *Platydoris guarani* **sp. n.**

Introduction

The nudibranch *Platydoris angustipes* (Mörch, 1863) is presently considered a widespread species in the western Atlantic, ranging from the Caribbean to southern Brazil, and reaching Ascension Island to the east (Rosenberg et al. 2009; Padula et al. 2017). It is very commonly found in Brazilian waters (Marcus and Marcus 1967; García et al. 2002; Valdés et al. 2006; Padula et al. 2012; Alvim and Pimenta 2013; Galvão-Filho et al. 2015; Padula et al. 2017).

In their phylogenetic analysis of the genus *Platydoris*, Dorgan et al. (2002) reviewed the morphological data from the literature noting the distribution of *P. angustipes* in the Caribbean Sea, but not in Brazil. However, Alvim and Pimenta (2013), in a taxonomical revision of Discodorididae, list *P. angustipes* for Brazilian waters.

Since there is doubt whether the Caribbean and Brazilian populations of *Platydoris angustipes* are the same taxa, in the present study we performed a detailed comparative anatomical survey of them. This included the holotype, from Saint Thomas (U.S. Virgin Islands), and specimens collected in Honduras, the Virgin Islands and Brazil (Rio de Janeiro state). We were able to recognize significant morphological differences that led us to the description of the Brazilian population as a new species.

Materials and methods

The studied material come from museum collections, consisting of specimens preserved in 70% ethanol. Dissections were performed under a stereomicroscope by standard techniques, with the specimens immersed in fixative (Simone 2004, 2011). The initial steps of the anatomical investigation were done through a longitudinal cut on the tissue covering the dorsal visceral mass. Digestive, circulatory, excretory, reproductive and central

nervous systems were investigated in detail. The terminology used for odontophore muscles was based on Ponder et al. (2008), Simone (2011) and Lima and Simone (2015). Digital photographs were taken at each dissection step. Illustrations were prepared with the aid of a camera lucida. Scanning electron microscopy (SEM) images of the radula were obtained at MZSP.

Institutions abbreviation: CAS – California Academy of Sciences (San Francisco, USA); ZMUC - Statens Naturhistoriske Museum (Copenhagen, Denmark); MZSP – Museu de Zoologia da Universidade de São Paulo (São Paulo, Brazil); UFBA – Universidade Federal da Bahia (Bahia, Brazil).

The following abbreviations are used herein: **aa**: anterior aorta; **ab**: afferent branchial vein; **an**: anus; **am**: ampulla; **ap**: posterior aorta; **au**: auricle; **at**: aortic trunk; **bc**: bursa copulatrix; **bg**: blood gland; **bs**: buccal sphincter; **ce**: cerebral ganglia; **cp**: pedal commissure; **cu**: caecum; **dd**: duct of digestive gland; **dg**: digestive gland; **ds**: salivary duct; **es**: oesophagus; **ev**: efferent branchial vein; **ey**: eye; **fg**: female gland; **ft**: foot; **gb**: buccal ganglia; **gc**: gill circle; **ge**: gonopore; **gf**: gill filament; **gg**: gastro-oesophageal ganglia; **go**: gonad; **gp**: pedal ganglia; **hd**: hermaphrodite duct; **in**: intestine; **mo**: mouth; **m2 – m10**: odontophore muscles; **mt**: oral tube muscle; **ne**: nephrostome; **oc**: odontophore cartilage; **ot**: oral tube; **ov**: oviduct; **pa**: papilla; **pc**: pericardium; **pe**: penis; **pl**: pleural ganglia; **pr**: prostate; **ra**: radula; **rg**: rhinophoral ganglia; **ri**: rhinophore; **rm**: retractor muscle gill; **rp**: reproductive system; **rs**: radular; sac; **rv**: renal vesicle; **sg**: salivary gland; **st**: stomach; **sn**: nervous system; **sp**: spine; **sr**: seminal receptacle; **to**: oral tentacle; **ud**: uterine duct; **va**: vagina; **vd**: vas deferent; **ve**: ventricle; **vp**: reproductive system vein; **vn**: nervous system vein: **vs**: radular sac vein.

Results

Family Discodorididae Bergh, 1891

Genus *Platydoris* Bergh, 1877

Type species. *Doris argo* Linnaeus, 1767, by subsequent designation (O'Donoghue 1929).

Platydoris angustipes (Mörch, 1863)

Figures 1–6

Doris (*Argus*) *angustipes* Mörch, 1863: 32
Platydoris angustipes var. *alaleta* Bergh, 1877: 505, pl. 58, figs. 13-18.
Platydoris rubra White, 1952: 118, fig. 17, pl. 6, fig. 6.
Platydoris angustipes: Ev. Marcus and Er. Marcus 1967: 93, fig. 112; Er. Marcus and Ev. Marcus 1970: 67, fig. 121; Meyer 1977: 301; Humann 1992: 243; Dorgan et al. 2002: 282, figs. 1B, 2B, 11-13; Valdés et al. 2006: 182; Debelius and Kuiter 2007: 245; Camacho-García et al. 2014: 121; Goodheart et al. 2016: 9, fig.4f.

Type locality. St. Thomas, U. S. Virgin Islands.

Redescription. External morphology (Figure 1A–E): Size ~25 mm length, ~20 mm width. Body dorsoventrally flattened and wide (Fig. 1A, B). Foot not exceeding notum (Fig. 1B). Rhinophores with ~19 transverse lamellae, rhinophoral sheaths with small lobes (Fig. 1C). Gill composed of six tripinnate branchial leaves, arranged in branched fashion with anus in middle of rachis; branchial sheaths also with small lobes (Fig. 1E). Mouth opens in anterior ventral region, between anterior region of notum and foot. Digitiform tentacles present. Anterior border of foot bilabiate, with longitudinal groove (Fig. 1B).

Haemocoel organs (Figure 2A–B): Pericardium and posterior half of visceral mass occupying ~15% of haemocoel volume. Buccal mass located anteriorly, occupying ~10% of haemocoel volume. Nervous system positioned dorsally in relation to buccal mass, covered by blood gland, occupying ~5% of haemocoel volume. Reproductive system on right side of animal, occupying ~25% of haemocoel volume. Stomach on left side of animal, intestine with small curve on its anterior portion; digestive gland system occupying ~45% of haemocoel volume.

Circulatory and excretory systems (Figures 1D, E; 2A–C): Pericardial cavity dorsal, located posteriorly to digestive gland and anteriorly to gill circle (Fig. 2A). Afferent and efferent branches located inside each gill filament, flowing from and to afferent and efferent branchial veins, respectively (Fig. 1D). Gill retractor muscle split, originating from base of gill circle, running longitudinally up to half of foot, inserting into dorsal surface of foot (Fig. 2B). Auricle funnel-like (wider anteriorly), with thin walls. Ventricle slightly taller than wide, with thick muscular walls (Fig. 2C). Aortic trunk branches very close to ventricle; anterior artery irrigates reproductive system, buccal mass, odontophore and nervous system posterior artery irrigates stomach and digestive gland (Fig. 2C). Renal vesicle located on dorsal right side of pericardium, near the base of auricle, connecting to inner surface of pericardium, ~1/6 of ventricle size (Fig. 2A). Renal chamber extending from dorsal to medial sinus, anteriorly connected to renal vesicle, extending posteriorly to center of gill circle (Fig. 1E). Nephrostome readily visible. Blood gland clearly divided in anterior and posterior portions (Fig. 2A).

Digestive system (Figures 1E; 2A–B, D–E; 3A–E; 6A–C): Oral tube composed of outer and inner lips, with thick transversal fold; **mt**, three long pairs of retractor muscles of buccal mass, originating on oral tube and running dorsally and ventrally along it; inserting in the side of the body; about four times as wide and three times as long as m10 (Fig. 2D, E). Odontophore oval, connected to oral tube by pair of ventral protractor muscles (**m10**); thin longitudinal dorsal and ventrolateral protractors of oral sphincter originating in anterior region of odontophore and inserted in posterior region of integument, close to oral tube (Figs 2E; 3C). Oral sphincter surrounding chitinous part of oral tube (Fig. 2D). Odontophore muscles: **m2**, pair of strong buccal mass retractor muscles, four times longer than wide, originating on anterior

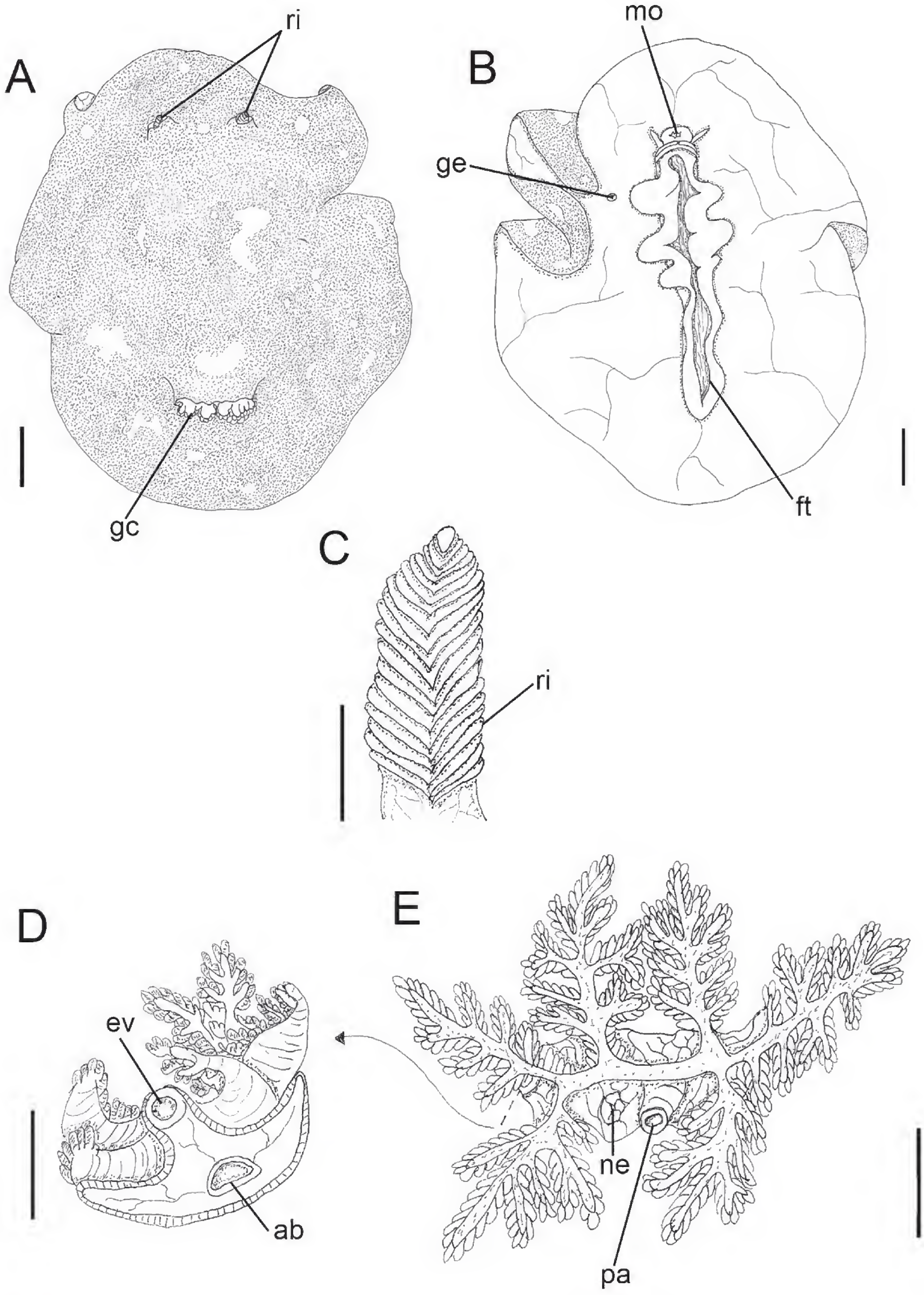

Figure 1. *Platydoris angustipes*, fixed animal **A** dorsal view **B** same, ventral view **C** rhinophore **D** gill filament with transversely sectioned showing afferent and efferent branchial ring **E** gill circle. Scale bars: 5 mm (**A, B**); 1 mm (**C**); 2 mm (**D, E**).

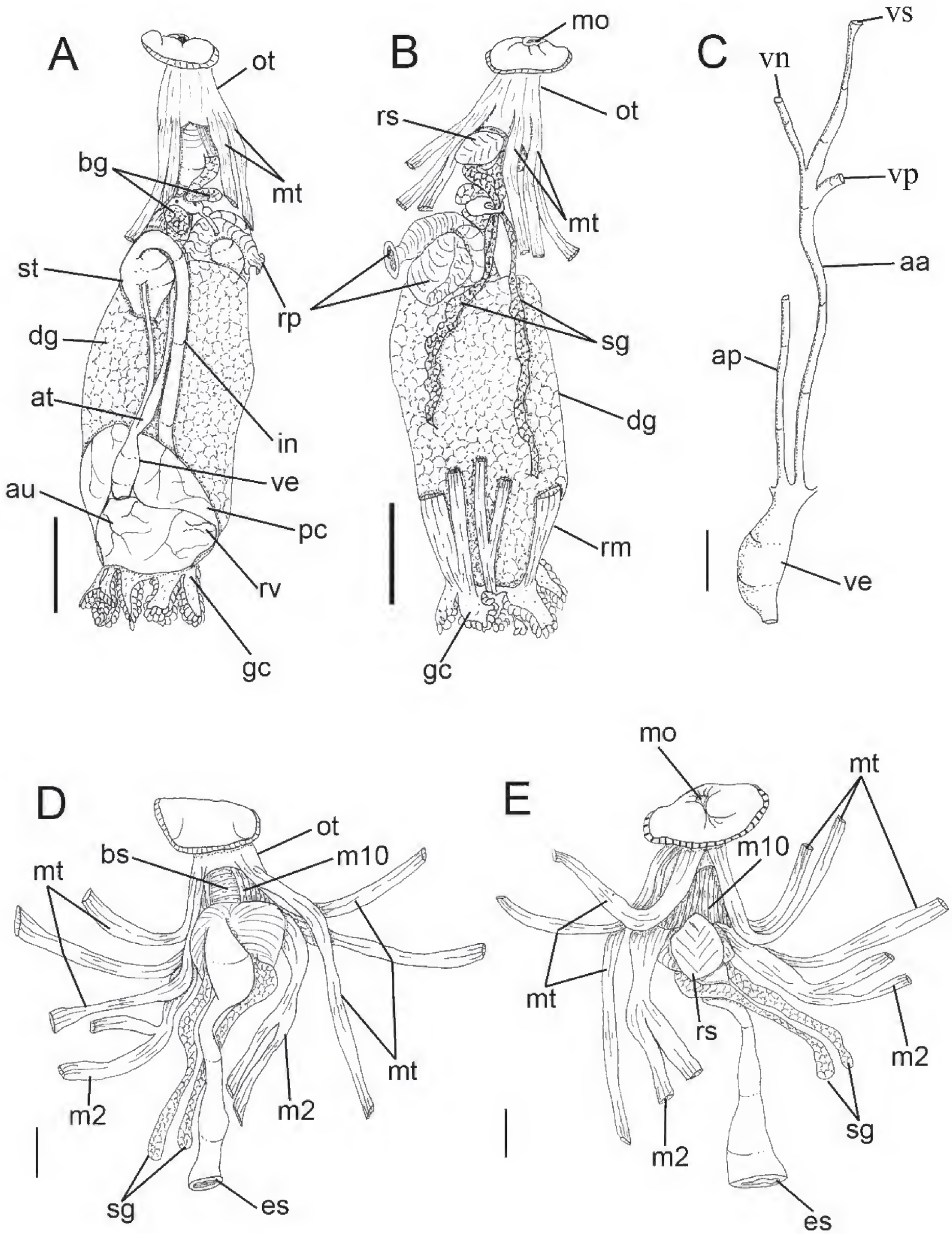

Figure 2. *Platydoris angustipes*. Visceral mass **A** dorsal view **B** same, ventral view **C** circulatory system, dorsal view. Anterior digestive system **D** dorsal view **E** same, ventral view. Scale bars: 5 mm (**A, B**); 2 mm (**C–E**).

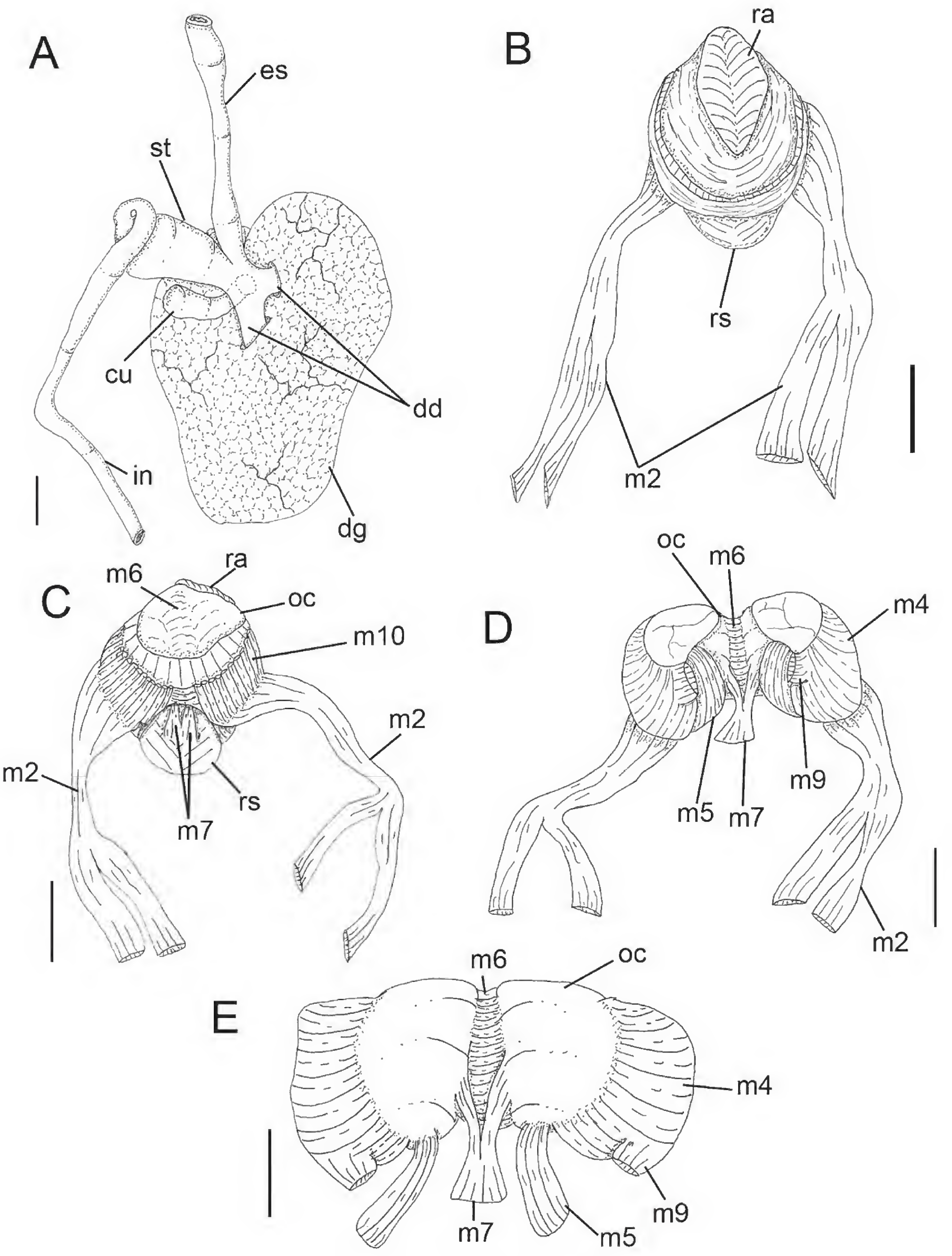

Figure 3. *Platydoris angustipes*. **A** medium digestive system. Odontophore **B** dorsal view with radula **C** same, ventral view **D** same, dorsal view with removed radula **E** same, dorsal view with folded down muscles. Scale bars: 2 mm.

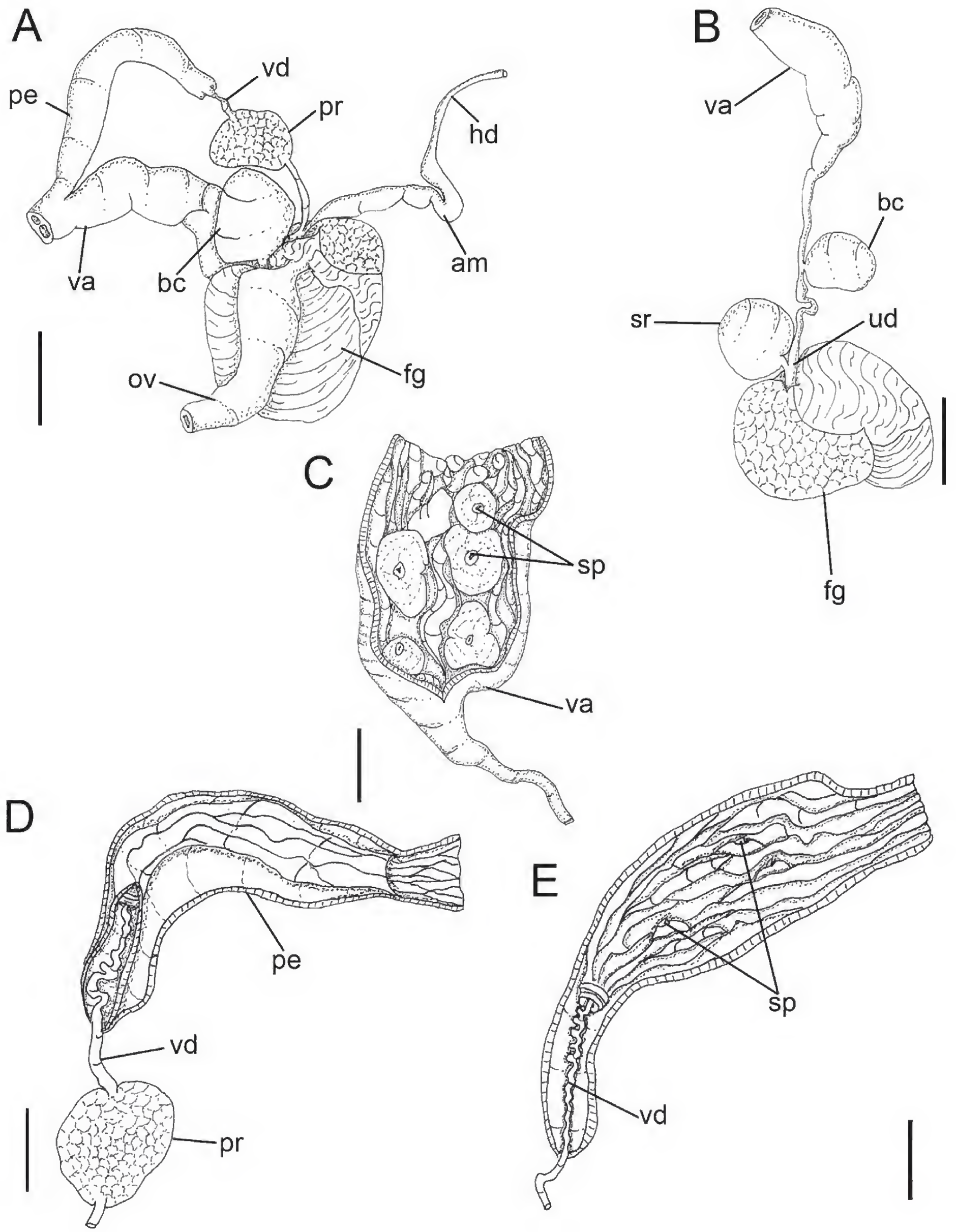

Figure 4. *Platydoris angustipes*. Reproductive system **A** general view **B** detail of connection of uterine duct **C** detail of vagina's spines **D** detail of internal part of insertion of vas deferens **E** detail of penis's spines. Scale bars: 2 mm (**A, B**); 1 mm (**C–E**).

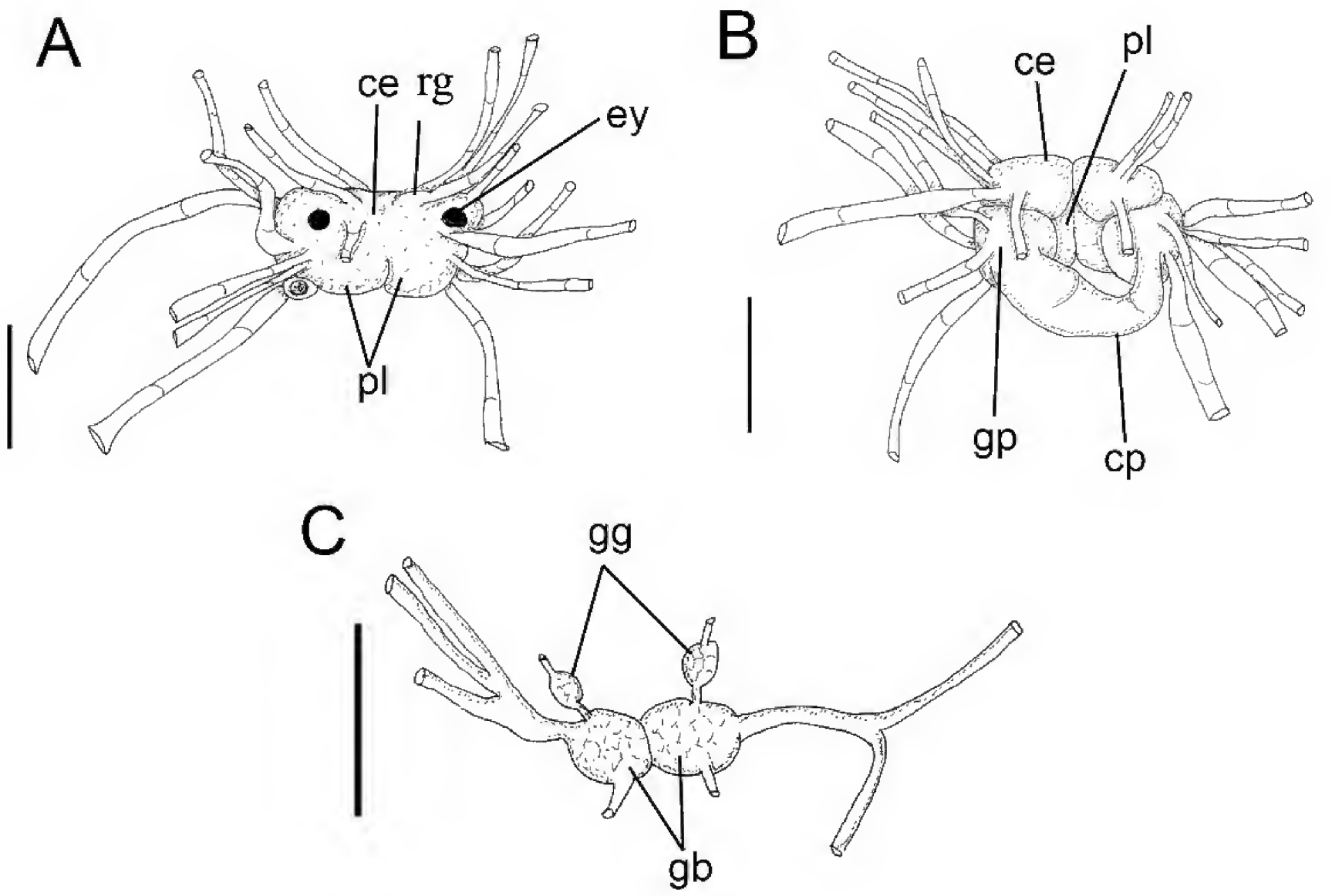

Figure 5. *Platydoris angustipes*. Nervous system **A** dorsal view **B** same, ventral view **C** buccal and gastroesophageal ganglia. Scale bars: 1 mm.

dorsal odontophore, running laterally to m4 and inserted ventrally in dorsal portion of foot, bifurcate on insertion (Fig. 3B–D); **m4**, pair of strong and broad dorsal tensor muscles, as long as wide, covering ~2/3 of cartilage, inserted in ventral portion of subradular membrane (Fig. 3D, E); **m5**, pair of dorsal auxiliary tensor muscles, twice as long as wide, originating on posteriormost region of odontophore cartilage, covering ~1/3 of posterior cavity of odontophore, as long as m4, but with ~1/3 of its width, inserting in ventral side of subradular membrane around radular sac (Fig. 3D, E); **m6**, unpaired horizontal muscle, with transversal fibers connecting to median surface of left and right odontophore cartilages, about same length and half as wide as m4, posterior portion as wide as anterior portion (Fig. 3D, E); **m7**, pair of thin and narrow muscles, originating on inner surface of odontophore cartilages, running together posteriorly, inserting into radular sac (Fig. 3D, E); **m9**, unpaired and horizontal muscle, originating on posterior portion of m4, connecting of the two components of the m4 pair (Fig. 3D, E). Pair of odontophore cartilages elliptical, occupying ~2/5 of odontophore volume (Fig. 3D, E). Subradular membrane thin, strong, translucent. Radular sac ~1/4 as large as odontophore. Radular teeth (Fig. 6A–C): rachidian teeth absent; formula 42 x 62.0.62 (in 25 mm long specimen, CASIZ 76667). Each lateral tooth with broad base, tapering towards apex, hook-shaped, with single terminal cusp; two outermost teeth spatulate. Pair of salivary glands long, tubular; duct inserting in anterior region of esophagus, extending posteriorly to ventral middle region of digestive gland (Fig. 2B). Esophagus simple, originating dorsally to odontophore, inserting directly in anterior region of stomach; internal longitudinal folds with same diameter along entire length (Figs 2D, E; 3A). Stomach oval, occupying ~30% of visceral mass volume, with folds at the center of entire inner surface (Figs 2A; 3A). Common opening for esophagus and stomach located on digestive gland. Intestine with longitudinal folds along its entire length; diameter ~1/2 that of esophagus and more uniform than it (Fig. 3A). Digestive gland dark beige, cone-shaped; largest organ of visceral mass, occupying ~40% of its volume; anterior portion about twice as wide as posterior portion; inner surface of gland sponge-like, bearing two distinct main ducts (Fig. 3A). Anus opening into anal papilla in the center of gill circle, ~1/4 of gill filament length (Fig. 1E).

Genital system (Figure 1B; 2B; 4A–E): Located between buccal mass and digestive gland, mostly dorsally-positioned on right side of animal (Fig. 2B). Genital opening on ventral right side, on anterior third of animal, located between foot and notum (Fig. 1B). Gonad immersed in digestive gland, difficult to distinguish from it. Hermaphrodite duct thin, long. Ampulla located on female gland, elongated and tubular. Prostate rounded, glandular, connected with female gland duct, ~1/3 of ampulla length (Fig. 4A, D). Vas deferens short, ~1/5 of ampulla

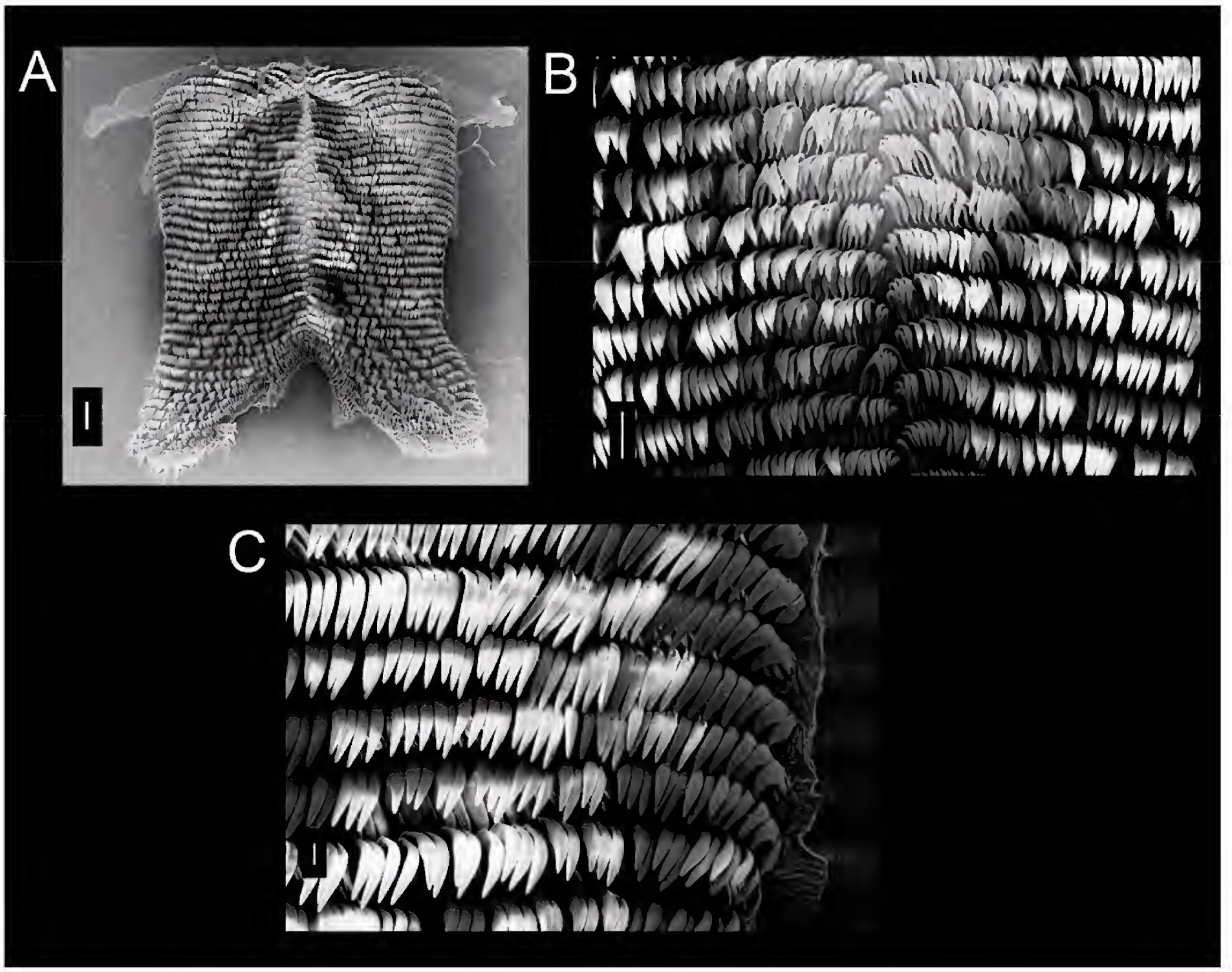

Figure 6. SEM of radula of *Platydoris angustipes*. **A** panoramic view **B** central region with rachidian tooth absent **C** lateral teeth. Scale bars: 300 µm (**A**); 100 µm (**B**); 30 µm (**C**).

(Fig. 4D). Penis' muscle absent. Penis muscular, cylindrical and elongated, about three times longer than prostate; thin folds on internal surface, with cartilage between them and three small tubercles each with a central spine (Fig. 4D, E). Female gland well-developed, rounded, occupying ~1/5% of reproductive system volume; divided into mucus gland (~2/3 of female gland, color beige) and albumen gland (~1/3 of anteriormost region, dilated, irregularly shaped, color dark brown) (Fig. 4B). Oviduct occupying ~1/2 of female gland's volume (Fig. 4A). Uterine duct thin, relatively short, ~1/7 of vagina length; located on the base of seminal receptacle, inserted in female gland near oviduct (Fig. 4B). Seminal receptacle rounded, as large as bursa copulatrix, ~1/3 of vagina length; connected to bursa copulatrix through stalk with ~1/2 of vagina length (Fig. 4B). Bursa copulatrix rounded, ~1/3 of vagina length, connected directly to vagina (Fig. 4B). Vagina cylindrical, elongated, approximately as long as and twice as wide as penis; internal surface with cartilage between folds and five large tubercles each with a central spine; located dorsally in relation to prostate and parallel to penis in genital opening (Fig. 4 A-C).

Nervous system (Figure 5A–C): Located dorsally in relation to odontophore, mostly covered by blood gland. Pair of cerebral and pleural ganglia fused with one another. Pedal ganglia ventrally fused with cerebral and pleural ganglia, but not fused between themselves. Pedal commissure simple, broad and short, surrounding esophagus and salivary glands (Fig. 5B). Buccal ganglia short, located ventrally to odontophore between radular sac and anterior portion of esophagus, connected to cerebral ganglia through long and slender connective tissue, united to gastro-esophageal ganglia by short connective tissue. Gastro-esophageal ganglia circular, ~1/4 of buccal ganglia length (Fig. 5C). Rhinophoral (olfactory) ganglia inconspicuous. Dorsal eyes located on cerebral ganglia (Fig. 5A).

Distribution. United States of America (Florida and Virgin Islands) (Marcus and Marcus 1967; Marcus and Marcus 1970); Cuba (Guanahacabibes Peninsula) (Espinosa et al. 2012); Cayman Islands (Hess et al. 1994); Panama (Bocas del Toro) (Goodheart et al. 2016); Jamaica (Marcus and Marcus 1970); Curaçao (Marcus and Marcus

1970); Trinidad & Tobago (White 1952); Ascension Island (Padula et al. 2017).

Habitat. On reefs, tide pools, from 0 to 73 m depth.

Material examined. CARRIBEAN SEA, West Indies, Lesser Antilles, Martinique, cliffs S of St. Pierre, CASIZ 76667, 1 specimen (William Liltved on "Gloriamaris", 28/ix/1986, 10-85ft – Liltved – West Indies Cruise 1986); HONDURAS, MZSP 75996, 1 specimen (Col. Marcus, P-938); Saint Thomas, ZMUC-GAS 1505, 1 specimen (Riise 152 – Holotype of *Doris angustipes*); Saint Croix, Virgin Island, ZMUC-GAS 2020, 1 specimen (Riise 1860 – Holotype of *Platydoris angustipes alaleta*).

Platydoris guarani sp. n.

http://zoobank.org/632F273F-E1D3-4808-8D68-D21199975575

Figures 7–11

Platydoris angustipes Er. Marcus, 1957: 422, fig. 81-89; Ev. Marcus 1972: 79; García et al. 2002: 53, fig.2K; García et al. 2008: 148; Alvim and Pimenta 2013: 186, figs. 2C; 21–22; Padula et al. 2012: 3 (non Mörch 1863).

Type material. Holotype: BRAZIL, Rio de Janeiro, Ilha Grande, Angra dos Reis, MZSP 86082, 1 specimen (E.P. Gonçalves, L.R. Simone & P. Oristanio, coll., 24/ix/2006, 17m depth, Ponto 3, Pinguino Wreck). **Paratype:** BRAZIL, Rio de Janeiro, Ilha Grande, Angra dos Reis, MZSP 134877, 2 specimens (E.P. Gonçalves, L.R. Simone & P. Oristanio, coll., 24/ix/2006, 17m depth, Ponto 3, Pinguino Wreck).

Type locality. Brazil, Rio de Janeiro state, Angra dos Reis.

Etymology. The specific epithet is a noun in apposition, derived from the native Guarani indigenous people, some tribes of which still reside in Rio de Janeiro.

Diagnosis. Body of orange color, with a white ribbon on its edge and brown spots just above the ribbon (they can be seen both dorsally and ventrally). Radula with outermost teeth not spatulate, with apex hook-shaped; cusp simple and smooth. Presence of m4a and m7b odontophore muscles. Gonad readily visible. Absence of spines on internal surface of penis and vagina.

Description. External morphology (Figure 7A–C): Size ~60 mm length, ~40 mm width. Body color orange with white ribbon on its edge and brown spots just above the ribbon that can be seen both dorsally and ventrally (Fig. 7A–B). Body flattened and wide with small tubercles around dorsum. Rhinophores with ~25 transversal lamellae, very thin; color dark orange; rhinophoral sheaths with very small lobes (Fig. 7C). Gill composed of six white tripinnate branched branchial leaves, arranged in circular fashion surrounding anus; branchial sheaths also with very small tubercles (Fig. 7C). Mouth opens in anterior ventral region, between anterior region of notum and foot. Digitiform tentacles present. Anterior border of foot bilabiate and longitudinally notched.

Haemocoel organs: Of similar proportions as *P. angustipes* (see above).

Circulatory and excretory systems (Figure 8A, B): Same as *P. angustipes*, but with renal vesicle very large, well-developed, of about same length and width as ventricle (Fig. 8B), extending from dorsal to medial sinus, anteriorly connected to renal vesicle, extending posteriorly to center of gill circle and opening in nephrostome (Fig. 8A). Nephrostome pore not readily apparent.

Digestive system (Figures 8C, D; 9A-D; 11A–C): Same pattern as *P. angustipes*, but with the following differences: **m2**, twice as long, not bifurcated on insertion (Fig. 9A, B); **m4a**, pair of thin muscles originating in posterior region of m4 and inserting in the middle of odontophore cartilages, dorsally connected to m7b (Fig. 9D); **m7b**, pair of thin and short muscles originating in posterior region of m6, with joint insertion with posterior part of m7 (Fig. 9C, D). Radular sac ~1/5 as large as odontophore (Fig. 9A, B). Radular teeth (Fig. 11A–C): anterior region broader than in *P. angustipes*; rachidian teeth also absent; formula 35 x 60.0.60 (in 60 mm long specimen, MZSP86082). Each lateral tooth with broad base, tapering towards apex, hook-shaped, with single terminal cusp; outermost teeth narrower than in *P. angustipes*, inner base width ~1/2 lateral teeth width, apex also hook-shaped, cusp simple and smooth (Fig. 11C). Pair of salivary glands long, tubular, bulging in anterior portion and tapering posteriorly; duct inserting in anterior region of esophagus, extending posteriorly to ventral middle region of digestive gland (Fig. 8D). Esophagus simple, originating dorsally to odontophore, inserting directly in anterior region of stomach; longitudinal folds on inner surface with same diameter along esophagus' entire length. Stomach oval, with folds on the center of entire inner surface (Fig. 8C). Common opening for esophagus, stomach and caecum located on digestive gland. Intestine with longitudinal folds along its entire length; diameter similar to that of esophagus; anterior portion S-shaped, about twice longer than in *P. angustipes* (Fig. 8C). Caecum: short elongated sac, located ventrally to stomach, opening in anterior portion of stomach close to esophageal insertion; ~1/12 length and ~1/5 width of stomach (Fig. 8C). Digestive gland dark beige; largest organ of visceral mass; cone-shaped, anterior portion about twice as wide as posterior portion; inner surface of gland sponge-like, bearing distinct main duct. Anus opening into anal papilla on the center of gill circle, similar to *P. angustipes*.

Genital system (Figure 10A–B): Located between buccal mass and digestive gland, longitudinal on right side of animal. Genital opening on right side, on anterior third of animal, located between foot and notum. Gonad circling around all digestive gland, but easy to distinguish, unlike in *P. angustipes*. Hermaphrodite duct thin, long. Ampulla located on female gland, elongated and tubular. Prostate rounded, glandular, of same length as ampulla (Fig. 10A). Vas deferens about same length

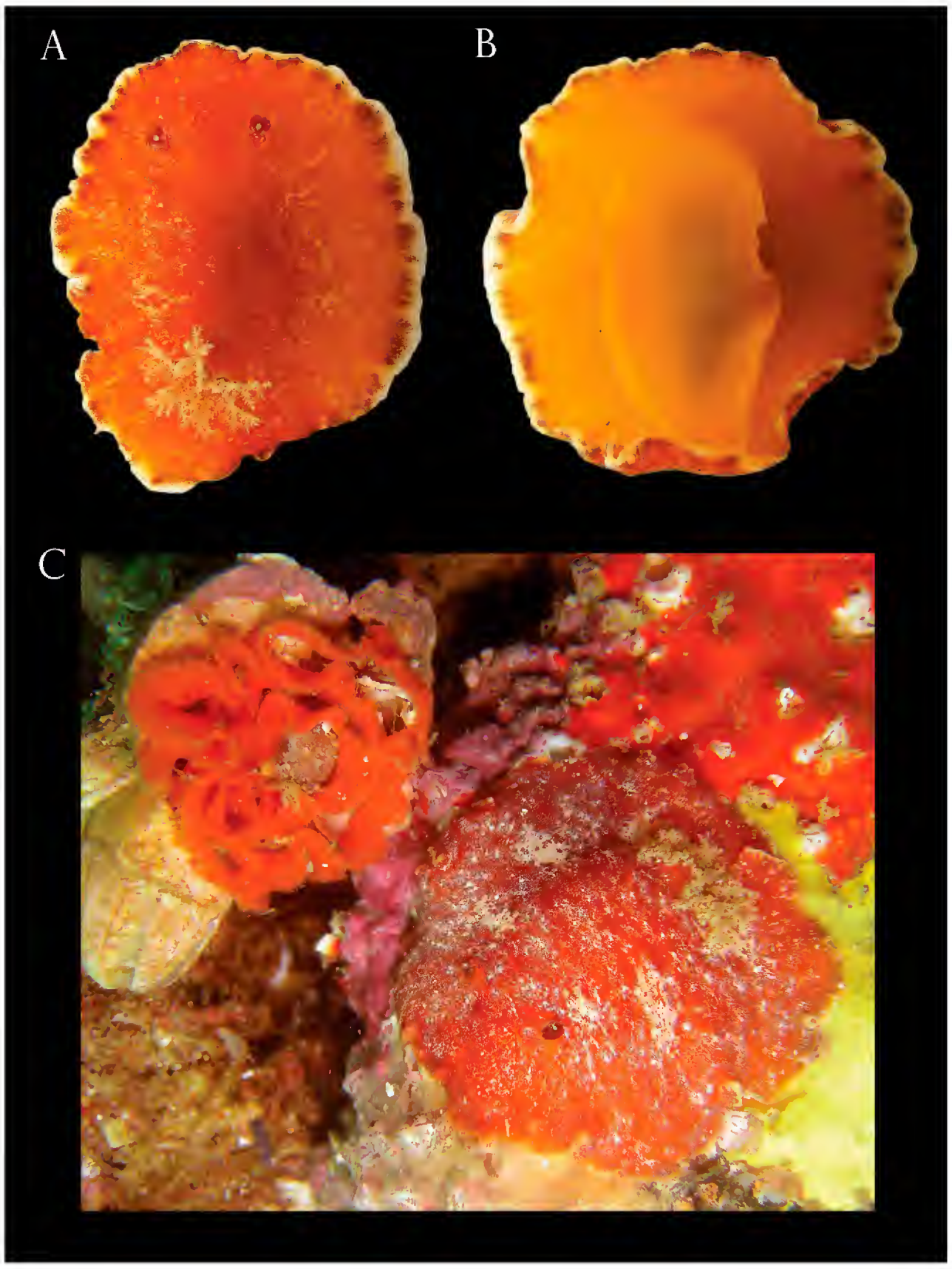

Figure 7. *Platydoris guarani*, living animals. **A.** Dorsal view, specimen from Papagaio, Cabo Frio, Rio de Janeiro (MZSP 97331). **B.** Same, ventral view. **C.** Living animal with spawning, specimen from Enseada da Meia Lua, Cabo Frio, Rio de Janeiro (MZSP 97625). All photograph by V. Padula.

as ampulla Penis muscular, cylindrical and very broad, ~1/2 length and three times wider than ampulla, without spines (Fig. 10A). Female gland well-developed, rounded, occupying ~20% of reproductive system volume; divided into mucus gland (~2/3 of female gland, color beige) and albumen gland (~1/3 of anteriormost region, dilated, irregularly shaped, color dark brown). Oviduct occupying ~1/5 of female gland volume (Fig. 10A). Uterine duct thin, relatively short, length ~1/10 of vagina length, located on the base of seminal receptacle, inserted in female gland near oviduct (Fig. 10B). Seminal receptacle elongate, as long as bursa copulatrix and ~1/3 its width; connected to vagina through stalk with same length and ~1/2 width of vagina (Fig. 10B). Bursa copulatrix rounded, ~1/2 length of vagina, connected to vagina posteriorly to seminal receptacle (Fig. 10B). Vagina cylindrical, very broad, with wide and thick folds, without spines; approximately as long and as wide as penis; positioned dorsally in relation to prostate and parallel to penis in genital opening (Fig. 10B).

Nervous system (Figure): Same as in *P. angustipes*.

Distribution. Brazil (Valdés et al. 2006). Pernambuco: Fernando de Noronha (García et al. 2002); Alagoas: Saco da Pedra (Padula et al. 2012); Bahia: Praia de Itapoã (García et al. 2008); Rio de Janeiro: Cabo Frio: Ilha Comprida; Arraial do Cabo: Prainha (Alvim and Pimenta 2014).

Habitat. Under stones, associated with sponges and ascidians (García et al. 2002), from 0 to 17 m depth.

Material examined. Types. Additional material: BRAZIL, Rio de Janeiro, Enseada da Meia Lua, Cabo Frio, MZSP 97625, 1 specimens (V. Padula, coll., 23/iv/2010); Ilha dos Papagaios, MZSP 97515, 1 specimen (V. Padul, coll., 17/x/2009).

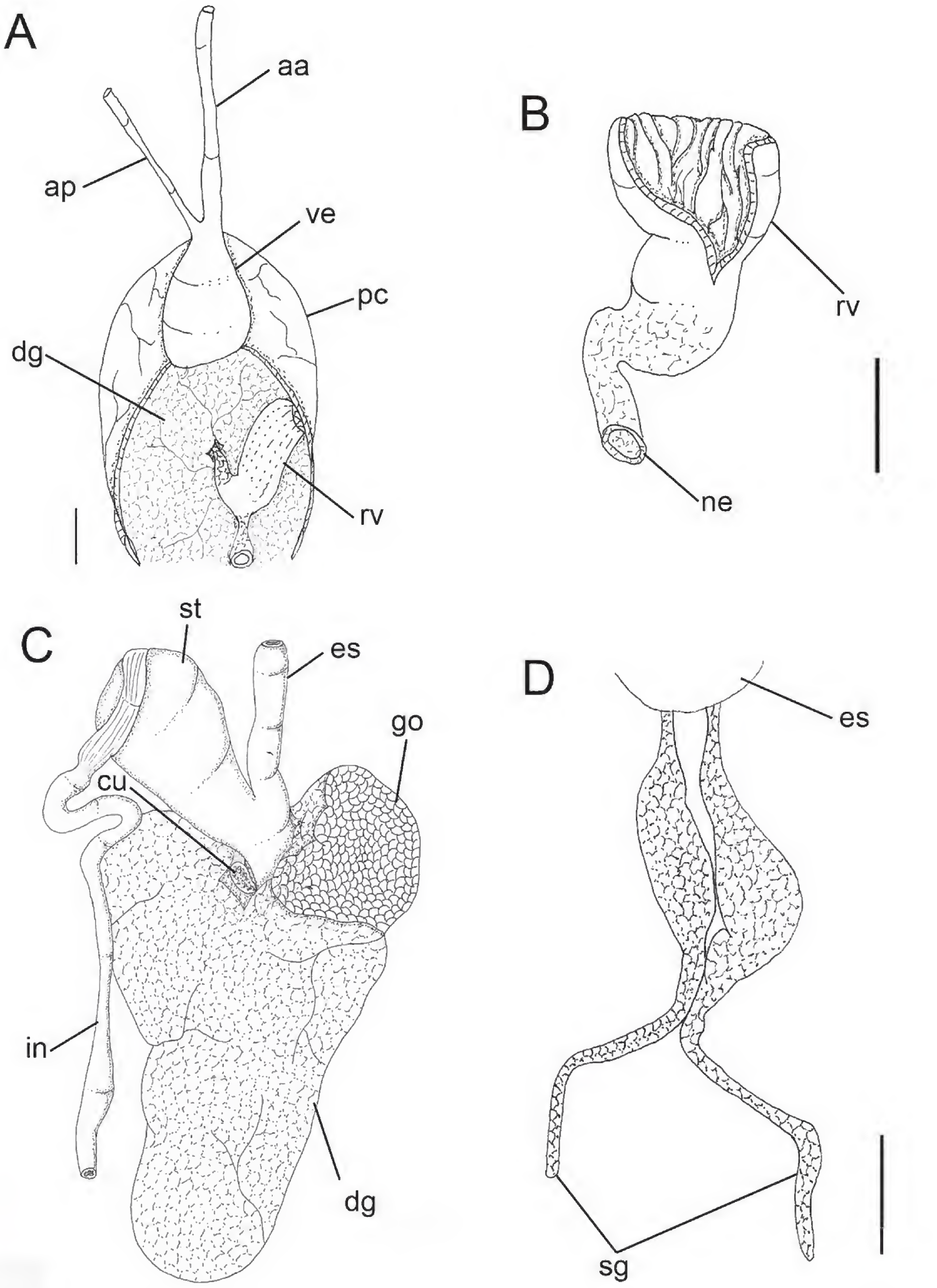

Figure 8. *Platydoris guarani*. **A** circulatory and excretory system, ventral view **B** renal vesicle **C** medium digestive system, dorsal view **D** detail of salivar glands. Scale bars: 2 mm (**A, B, D**); 5 mm (**C**).

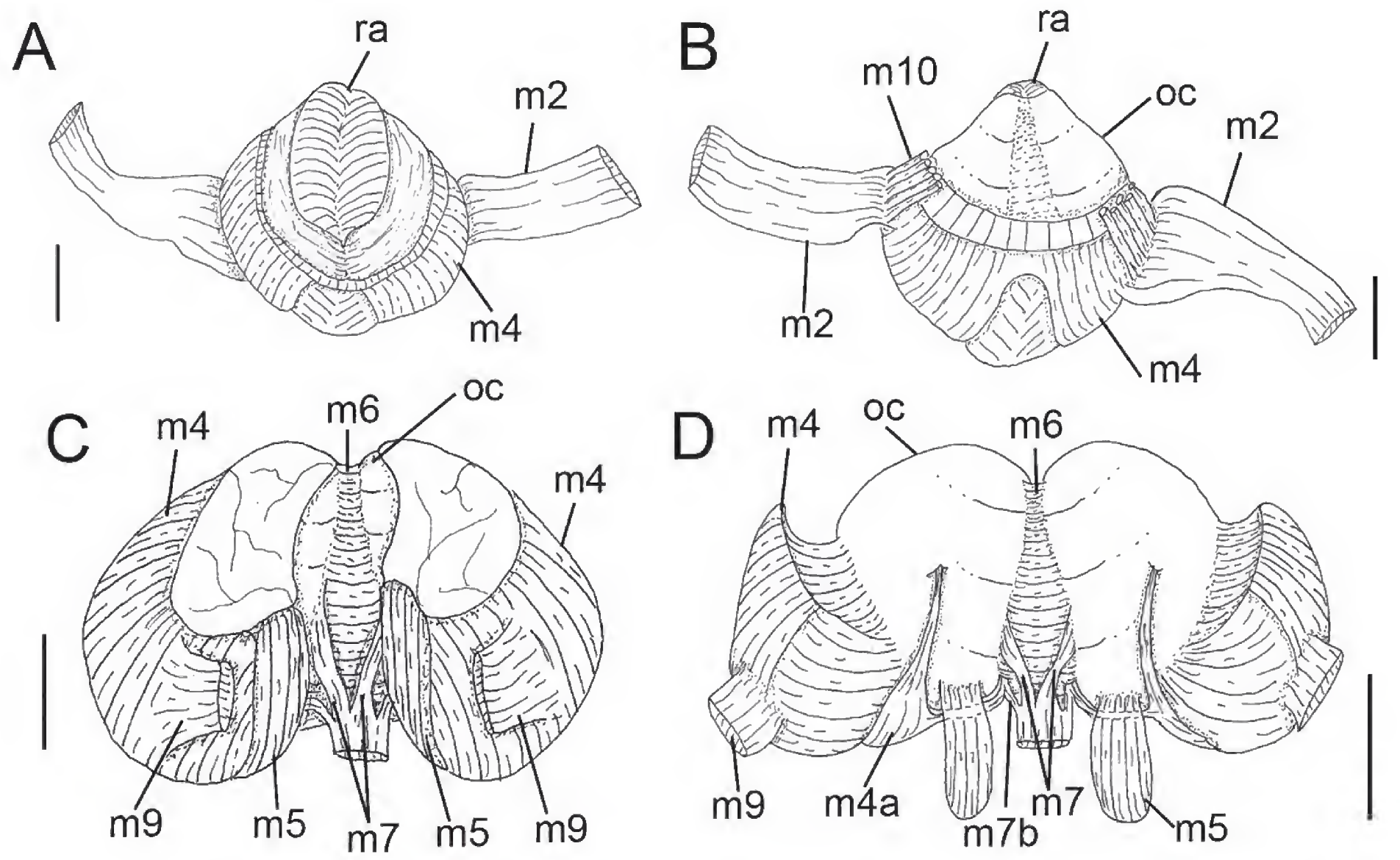

Figure 9. *Platydoris guarani*. Odontophore. **A** dorsal view with radula **B** same, ventral view **C** same, dorsal view with removed radula **D** same, dorsal view, with folded down muscles. Scale bars: 2 mm.

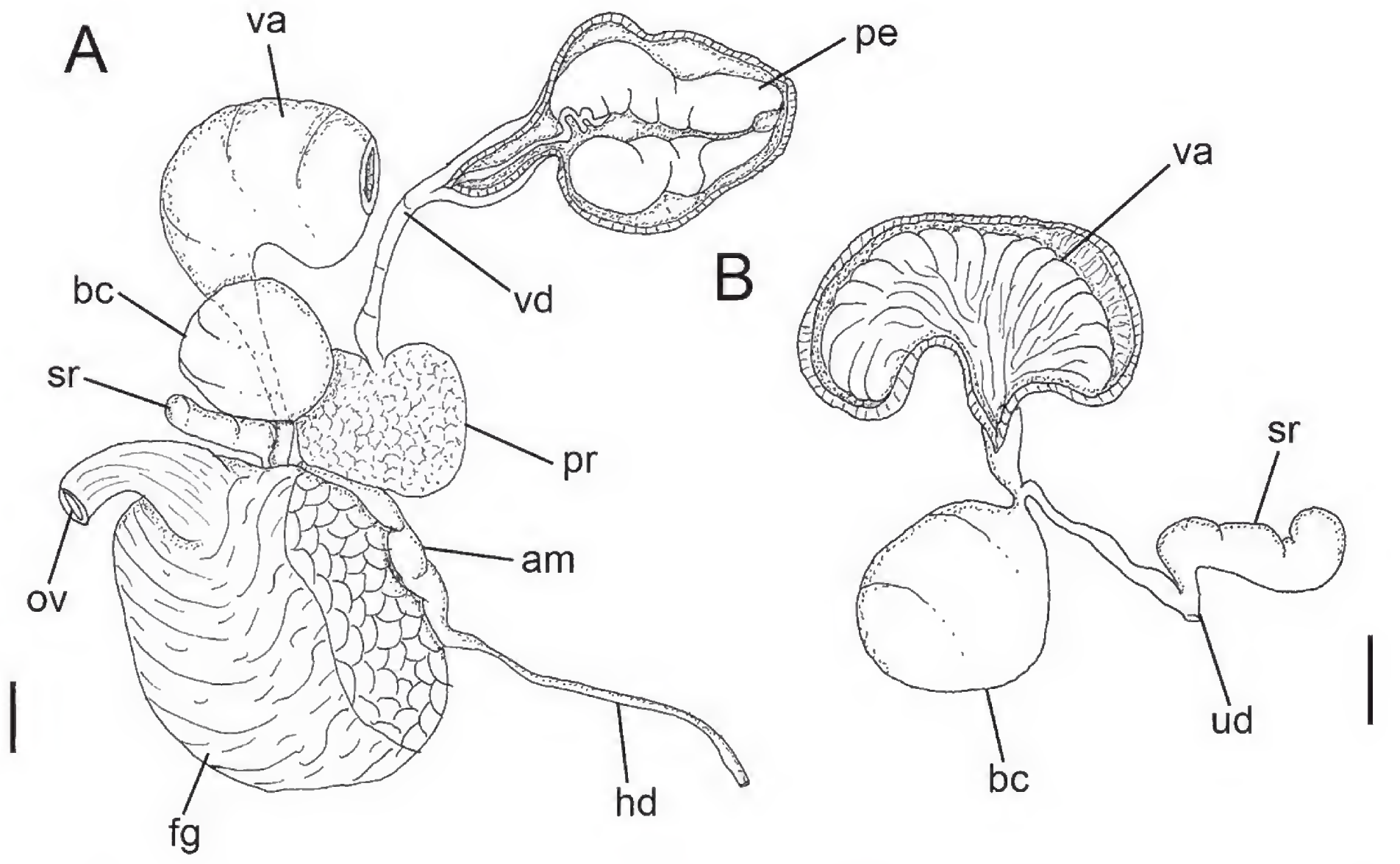

Figure 10. *Platydoris guarani*. Reproductive system **A** general ventral view **B** detail of Bursa copulatrix, seminal receptacle, uterine duct and vagina. Scale bars: 2 mm.

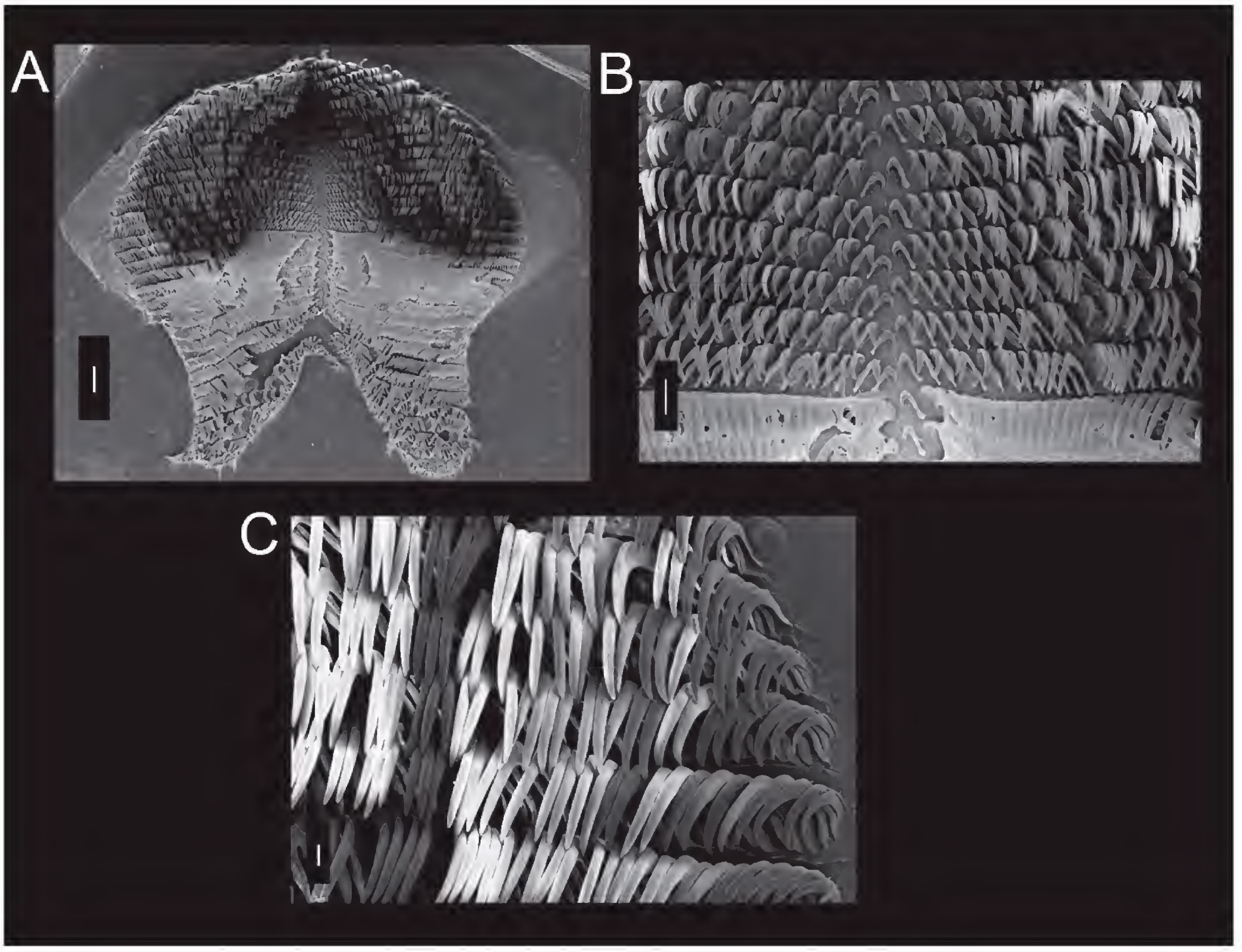

Figure 11. SEM of radula of *Platydoris guarani*. **A** panoramic view **B** central region with rachidian tooth absent **C** lateral teeth. Scale bars: 300 µm (**A**); 100 µm (**B**); 30 µm (**C**).

Discussion

In the previous anatomical and phylogenetic studies including *Platydoris angustipes* (Mörch 1863; Bergh 1877; Marcus and Marcus 1967; Dorgan et al. 2002) and *P. guarani* sp. n. (Marcus 1957; Padula et al. 2012; Alvim and Pimenta 2013), several external diagnostic features have been used to distinguish them, but no suggestions of separating them was ever made. Such features included: the rounded and dorsoventrally flattened body, the foot not exceeding notum, the dorsum covered with small caryophillidia, the digitiform oral tentacles, the bilabiate and longitudinally-notched anterior border of the foot, and the six tripinnate branchial leaves. Moreover, the color pattern of the body of *P. guarani* was deemed distinctive, with a white ribbon on its edge and dark spots on both dorsal and ventral parts of the notum (García et al. 2002; Alvim and Pimenta 2013).

Not all of the differences mentioned above are actually consistent, but the unique set of distinct features found in the present study between the Caribbean and Brazilian specimens, allow the separation in two distinct species. The main diagnostic features are discussed below.

The rhinophore of *P. angustipes* has circa 19 lamellae, while *P. guarani* has circa 25. However, Dorgan et al. (2002) reported 25 lamellae for *P. angustipes* and Alvim and Pimenta (2013) reported 19–25 lamellae for *P. guarani*. As such, this possible diagnostic feature should be studied on a larger sample.

Regarding the circulatory system, the renal vesicle of *P. angustipes* has approximately 1/6 of the ventricle size, while in *P. guarani* this structure is very large, of about the same size as the ventricle. Moreover, the nephrostome in *P. angustipes* is readily visible (Fig. 1E), whereas in *P. guarani* it is not.

Some differences were found in the anterior portion of the digestive system, particularly in the odontophore muscles: mt and m2 are very long in *P. angustipes* (Fig. 2D, E), while those of *P. guarani* are about half the size (Fig. 9A, B); m2 bifurcates on its insertion in *P. angustipes* (Fig. 3C), which is not the case in *P. guarani*. Two muscles occur only in *P. guarani*, namely m7b and m4a (Fig. 9C, D).

In addition, there are visible differences in the midgut. In *P. angustipes* the cecum is circa half the length of the midgut (Fig. 3A), while in *P. guarani* it is much shorter,

about 10% of the midgut (Fig. 8C). The anterior portion of the intestine of *P. guarani* is S-shaped (Fig. 8C), while that of *P. angustipes* is straight (Fig. 3A).

The posterior end of the radula of *P. guarani* (Fig. 11A) is wider than the same region of *P. angustipes* (Fig. 6A). In *P. guarani*, the two outermost lateral teeth are narrower than in *P. angustipes* (about half the width; Fig. 11C) and hook-shaped. The outermost lateral teeth of the radula of *P. angustipes* are wide (Fig. 6C), as observed by Dorgan et al. (2002: fig. 11C), with the two outermost teeth spatulate. The same occurs in *P. guarani* (Marcus and Marcus 1970), but the two outermost spatulate teeth have shorter cusps and several denticles (see fig. 121); this can also be observed in young rows of teeth.

There are also differences in the reproductive system. In *P. angustipes* it is very difficult to distinguish the gonad from the digestive gland, whereas in *P. guarani*, the gonad surrounds the digestive gland, being readily visible (Fig. 8C). In both species, we could not observe the accessory gland (*contra* Marcus 1957; Dorgan et al. 2002; Alvim and Pimenta 2013).

The most significant difference between *P. angustipes* and *P. guarani* is the absence of spines and cuticle in both the vagina and penis of *P. guarani* (Fig. 10A, B). An additional diagnostic feature was given by Dorgan et al. (2002): *P. angustipes* has more spines on the inner surface of the penis (even more than what we observed, only three prominent spines; Fig. 4E).

Furthermore, *Platydoris guarani* is clearly distinguishable from other species of *Platydoris* by the absence of spines and cuticle in both vagina and penis, and absence of the accessory gland. *Platydoris guarani* resembles *P. carolynae* (Dorgan et al. 2002: fig. 29C) in the hook-shape of outermost teeth.

In conclusion, the most characteristic differences between the two populations of *Platydoris*, Brazilian and Caribbean, reside in the digestive system, especially in the odontophore, radula and reproductive system. Based on these findings, *Platydoris angustipes* (Mörch, 1863) is here restricted as a Caribbean species, while the Brazilian population is described as a new species, *Platydoris guarani*. The analysis of additional specimens is still necessary to ascertain which species actually occurs on Ascension Island.

Acknowledgments

We are very grateful to Tom Schiøtte (ZMUC) for loaning the type material of *P. angustipes*; to Lara Guimarães (MZSP) for SEM examination; to Hilton Galvão-Filho (MZSP) for comments on an earlier version of the manuscript; to Vinícius Padula (UFBA) for the photos of live specimens of *P. guarani*. This work was supported by Conselho Nacional de Desenvolvimento Científico e Tecnológico (CNPq, Brazil), proc. 159446/2012-0.

References

Alvim J, Pimenta AD (2013) Taxonomic review of the family Discodoriddae (Mollusca: Gastropoda: Nudibranchia) from Brazil, with description of two new species. Zootaxa 3745(2): 152–198. https://doi.org/10.11646/zootaxa.3745.2.2

Bergh LSR (1877) Malacologische Untersuchungen. In: Reisen im Archipel der Philippinen von Dr. Carl Gottfried Semper. Zweiter Theil. Wissenschaftliche Resultate. Band 2, Theil 2, Heft 12, 495–546 [pls. 58–61]

Camacho-García YE, Pola M, Carmona L, Padula V, Villani G, Cervera JL (2008) Diversity and distribution of the heterobranchs sea slug fauna on the Caribbean of Costa Rica. Cah. Biol. Mar. 55: 109–127.

Debelius H, Kuiter RH (2007) Nudibranchs of the world. ConchBooks, 362 pp.

Dorgan KM, Valdés A, Gosliner TM (2002) Phylogenetic systematic of the genus *Platydoris* (Mollusca, Nudibranchia, Doridoidea) with descriptions of six new species. Zoologica Scripta 31(3): 271–319. https://doi.org/10.1046/j.1463-6409.2002.00105.x

Espinosa J, Ortea EJJ, Sánchez R, Gutiérrez J (2012) Moluscos Marinos Reserva de la Biosfera de la Península de Guanahacabibes. Instituto de Oceanología, La Habana, 325 pp.

Galvão Filho HC, Araújo AK, Silva FV, Azevedo VM, Meirelles CA, Matthews-Cascon H (2015) Sea slugs (Gastropoda: Heterobranchia) from poorly known area in North-east Brazil: filling gaps in Atlantic distributions. Marine Biodiversity Records, 8. https://doi.org/10.1017/S1755267215000494

García FJ, Troncoso JS, Domínguez M (2002) New data on benthic Opisthobranchh Molluscs from the Archipelago of Fernando de Noronha (Brazil), with description of a new species of Aegires Lovén, 1844. Iberus 20(2): 45–56.

García FJ, Álvares MD, Troncoso JS (2008) Opistobranquios de Brasil. Descripcíon y distribucíon de opistobranquios del litoral de Brasil y Del Arquipiélago Fernando de Noronha. Feito, Vigo, S.L., 215 pp.

Goodheart JA, Ellingson RA, Vital XG, Galvão Filho HC, McCarthy JB, Medrano AM, Bhave VJ, García-Méndez K, Jimenéz LM, López G, Hoover CA, Awbrey JD, De Deus JM, Gowacki W, Krug PJ, Valdés A (2016) Identification guide to the heterobranch sea slugs (Mollusca: Gastropoda) from Bocas del Toro, Panama. Marine Biodiversity Records 9(56): 1–31. https://doi.org/10.1186/s41200-016-0048-z

Hess DF, Abbott RT, Hamann J, Meyer K, Millen S, et al. (1994) Marine molluscs of the Cayman Islands. In: Brunt MA, Davies JE (Eds) The Cayman Islands: natural history and biogeography. Kluwer Academic Publishers, The Netherlands, 139–189 https://doi.org/10.1007/978-94-011-0904-8_9

Hummann JC (1992) A warm water Atlantic synonymy, Aphelodoris antillensis equals Chromodoris bistellata (Opisthobranchia: Gastropoda). The Veliger 35: 215–221.

Lima POV, Simone LRL (2015) Anatomical review of *Doris verrucosa* ad Redescription of *Doris januarii* (Gastropoda, Nudibranchia) based on comparative morphology. Journal of the Marine Biological Association of the United Kingdom 2015: 1–18.

Marcus E (1957) On Opisthobranchia from Brazil (2). Journal of the Linnean Society. London, Zoology 43: 390–486.

Marcus Ev (1972) Lista de Opisthobranchia (Mollusca, Gastropoda) coletados pelo Labóratorio de Ciências do Mar, Recife, Brasil. Trabalhos Oceanograficos Universidade Federal de Pernambuco 13: 71–82.

Marcus Ev, Marcus Er (1967) Opisthobranchs from the southwestern Caribbean Sea. Biological Investigations of the Deep Sea, 33. Bulletin of Marine Science 17: 597628.

Marcus Ev, Marcus Er (1970) Opisthobranchs from Curação and faunistically related regions. Studies on the Fauna of Curaçao and other Caribbean Islands 33: 1–129.

Meyer KB (1977) Dorid nudibranchs of the Caribbean coast of the Panama Canal Zone. Bulletin of Marine Science 27(2): 299–307.

Mörch OAL (1863) Contributions à la Faune malacologique des Antilles Danoises. Journal de Conchyliologie 11: 21–43.

Padula V, Bahia J, Correia MD, Sovierzoski HH (2012) New records of opisthobranchs (Mollusca: Gastropoda) from Alagoas, Northeastern Brazil. Marine Biodiversity Records 5: 1–11. https://doi.org/10.1017/S1755267212000346

Padula V, Wirtz P, Schrödl M (2017) Heterobranch sea slug (Mollusca: Gastropoda) from Ascension Island, South Atlantic Ocean. Journal of Marine Biological Association of the United Kingdom: 1–10. https://doi.org/10.1017/S0025315414000575

Ponder WF, Colgan DJ, Healy JM, Nützel A, Simone LRL, Strong EE (2008) Caenogastropoda. In: Ponder WF, Lindberg DL (Eds) Molluscan phylogeny. University of California Press, Los Angeles, 331–383. https://doi.org/10.1525/california/9780520250925.003.0013

Valdés Á, Hamann J, Behrens DW, Dupont A (2006) Caribbean Sea slugs: a field guide to the opisthobranch mollusks from the tropical northwestern Atlantic. Sea Challengers Natural History Books, Silverdale, 289 pp.

Rosenberg G, Moretzsohn F, García EF (2009) Gastropoda (Mollusca) of the Gulf of Mexico. In: Felder DL, Camp DK (Eds) Gulf of Mexico-Origins, Waters, and Biota. Biodiversity. Texas A&M University Press, College Station, Texas, 579–699.

Simone LRL (2011) Phylogeny of the Caenogastropoda (Mollusca), based on comparative morphology. Arquivos de Zoologia 42: 161–323. https://doi.org/10.11606/issn.2176-7793.v42i4p161-323

White KM (1952) On a collection of molluscs from the Dry Tortuga, Florida. Proceedings of the Malacological Society of London 29: 106–120.

Zoosyst. Evol. 94 (1) 2018, 17–27 | DOI 10.3897/zse.94.21321

PENSOFT

museum für naturkunde

Three new species of the killifish genus *Melanorivulus* from the Rio Paraná Basin, central Brazilian Cerrado (Cyprinodontiformes, Aplocheilidae)

Wilson J.E.M. Costa[1]

1 *Laboratory of Systematics and Evolution of Teleost Fishes, Institute of Biology, Federal University of Rio de Janeiro, Caixa Postal 68049, CEP 21941-971, Rio de Janeiro, Brazil*

http://zoobank.org/548D8BB7-0CA6-41ED-ACA6-5BA139A60516

Corresponding author: *Wilson J. E. M. Costa* (wcosta@acd.ufrj.br)

Received 29 September 2017
Accepted 14 November 2017
Published 2 January 2018

Academic editor:
Peter Bartsch

Key Words

Biodiversity hotspot
colour patterns
conservation
systematics
taxonomy

Abstract

Three new species of *Melanorivulus* are described from the upper and middle Rio Paraná Basin, central Brazilian Cerrado. These species are members of the *M. pictus* species group, endemic to central Brazilian plateaus and adjacent areas, and are easily diagnosed by colour pattern characters, but their relationships with other congeners of the group are still uncertain. *Melanorivulus proximus* **sp. n.**, from the middle Rio Aporé drainage, and *M. nigromarginatus* **sp. n.**, from the Rio Corrente drainage, are possibly more closely related to other species endemic to streams draining the slopes of the Caiapó range, whereas *M. linearis* **sp. n.**, from the upper Rio Pardo drainage, middle Rio Paraná Basin, is considered more closely related to *M. egens*, a species also endemic to this part of the Basin. This study corroborates the high diversity of species of *Melanorivulus* in the central Brazilian Cerrado plateaus repeatedly reported in previous studies, indicating once more that different species are often found restricted to short segments of the same river drainage. The intense habitat loss recorded in recent years combined to the high species diversity limited to specific Cerrado freshwater ecosystems, the veredas, indicates that species of *Melanorivulus* endemic to this part of the Brazilian Cerrado are highly threatened with extinction.

Introduction

The Cerrado savannas of central Brazil, with an area of about 2,000,000 km^2, is among the 25 most important biodiversity hotspots of the world (Myers et al. 2000). The present study is directed to a group of small killifishes of the genus *Melanorivulus* Costa, 2006, with species reaching 45 mm of standard length (SL) or less, inhabiting the shallowest parts of the veredas, a typical Cerrado ecosystem comprising streams bordered by the buriti-palm (*Mauritia flexuosa*). About 50 valid species are presently placed in *Melanorivulus*, formerly considered as a subgenus of *Rivulus* Poey, 1860 (Costa 2011). *Melanorivulus* is similar to other South American aplocheiloid killifishes living in similar biotopes, such as *Anablepsoides* Huber, 1992, *Atlantirivulus* Costa, 2008, *Cynodonichthys* Meek, 1904, *Laimosemion* Huber, 1999, *Rivulus* Poey, 1860, which have slender body, short fins and long neural prezygapophyses on caudal vertebrae (Costa 1990). Species of *Melanorivulus* are distinguishable from species of those genera by the presence of black pigmentation concentrated on the whole margin of the caudal fin and on the distal margin of the dorsal and anal fins in females, ventral process of the angulo-articular short or rudimentary, and preopercular canal absent (Costa 2011).

A great diversity of species of *Melanorivulus* has been reported for the Cerrado region drained by the Rio Paraná Basin, the second largest river basin in South America. A total of 14 endemic species have been described for this region (Costa 1989, 2005, 2007a, b, 2008; Nielsen et al. 2016; Volcan and Lanés 2017). These species belong to different and not closely related species groups (Costa et al. 2016): the *M. punctatus* group, containing slender small species, mainly diagnosed by the presence of oblique rows of red dots on the flank in males (e.g., Costa

2005); the *M. pinima* group, easily diagnosed by the reduction of black pigmentation on the head and humeral region in males, presence of longitudinal rows of red dots on the flank, and a longitudinally elongated white to light yellow mark above caudal spot in females (Costa 2007a), and the *M. pictus* group, diagnosed by a deeper body (i.e., body depth reaching about 25 % SL) and oblique red bars on the flank (Costa 2017). Eleven of the 14 endemic species are members of the last group, which are mostly concentrated in the rivers draining the Caiapó range and in the south adjacent areas of the middle Rio Paraná Basin (Costa 2005, 2012).

The *M. pictus* group was first studied by Costa (1989), based on fish collections deposited in the Museu de Zoologia, Universidade de São Paulo, when *M. apiamici* (Costa, 1989), *M. pictus* (Costa, 1989) and *M. vittatus* (Costa, 1989) were described. In September 1994, efforts were directed to firstly sample typical *Melanorivulus* habitats along the Paraná River Basin, but based on the great morphological variability found among populations inhabiting close neighbouring areas, Costa (1995) concluded that all populations of this vast geographical area belong to a single polymorphic species, *M. pictus*. However, after more accurate field studies since 2004, numerous new species have been continuously described for the Paraná and other adjacent river basins (e.g., Costa 2005, 2006, 2012, 2017; Deprá et al. 2017). These studies have indicated that each species is limited to small areas and that different species may inhabit the same river drainage at different altitudes (Costa 2007b, 2017; Volcan et al. 2017). However, some new species collected in recent years are still await formal descriptions. In this paper, three new species of the *M. pictus* group from the Paraná River Basin are described.

Materials and methods

Specimens were captured with small dip nets (40 × 30 cm) and fixed in formalin for a period of 10 days, and then transferred to 70 % ethanol. Collections were made with permits provided by ICMBio (Instituto Chico Mendes de Conservação da Biodiversidade) and field methods have been approved by CEUA-CCS-UFRJ (Ethics Committee for Animal Use of Federal University of Rio de Janeiro; permit number: 01200.001568/2013-87). Material is deposited in Instituto de Biologia, Universidade Federal do Rio de Janeiro, Rio de Janeiro (UFRJ) and Coleção Ictiológica do Centro de Ciências Agrárias e Ambientais, Universidade Federal do Maranhão, Chapadinha (CICCAA). Descriptions of colouration of living fish were based on observations just after collections, in small transparent plastic bottles. Type specimens were photographed live about 24 hours after collection. Measurements and counts follow Costa (1988). Measurements are presented as percentages of standard length (SL), except for those related to head morphology, which are expressed as percentages of head length. Fin-ray counts include all elements. Osteological preparations followed Taylor and Van Dyke (1985); the abbreviation C&S in lists of material indicates those specimens that were cleared and stained for osteological examination. Terminology for osteological structures followed Costa (2006), for frontal squamation Hoedeman (1958), and for cephalic neuromast series Costa (2001). In lists of material, geographical features are written according to Brazilian Portuguese local use (e.g., córrego, ribeirão, rio), allowing more accurate identifications of localities in the field and avoiding common mistakes when tentatively translating them to English.

Results

Melanorivulus proximus sp. n.

http://zoobank.org/79A16259-1DEF-4F9E-8AE1-047802792F3F

Figs 1–2, Table 1

Rivulus pictus (non *Rivulus pictus* Costa, 1989); Costa 1995: 216 (misidentification).

Rivulus scalaris (non *Rivulus scalaris* Costa, 2005); Costa 2005: 79 (misidentification).

Holotype. UFRJ 11681, male, 27.7 mm SL; Brazil: Mato Grosso do Sul state: Cassilândia municipality: stream crossing the road MS-306, Rio Aporé drainage, Rio Paraná Basin, 19°03'54"S, 51°49'56"W, altitude about 515 m asl; W.J.E.M. Costa et al., 20 Sep. 2011.

Paratypes. All from Brazil: Rio Aporé drainage, upper Rio Paraná Basin. Mato Grosso do Sul state: UFRJ 10792, 4 males, 25.6–30.0 mm SL, 1 female, 25.6 mm SL; UFRJ 10793, 1 male, 23.6 mm SL, 1 female, 21.1 mm SL (C&S); collected with holotype. – UFRJ 10788, 6 males, 15.7–27.7 mm SL, 4 females, 24.0–27.4 mm SL; UFRJ 10789, 3 males, 20.9–21.9 mm SL, 2 females, 18.5–20.0 mm SL (C&S); CICCAA 00692, 5 males, 21.9–25.8 mm SL, 5 females, 21.7–25.6 mm SL; Cassilândia municipality: road MS-306, 19°02'15"S, 52°01'57"W, altitude about 540 m asl; W.J.E.M. Costa et al., 20 Sep. 2011.– UFRJ 2207, 8 males, 20.2–27.1 mm SL, 12 females, 17.8–35.4 mm SL.; UFRJ 2280, 1 male, 25.9 mm SL, 2 females, 27.9–28.7 mm SL (C&S); Cassilândia municipality: swamp close to Ribeirão Grande, road MS-306, about 30 km SE from the town of Cassilândia, 19°15'40"S, 51°30'03"W, altitude about 495 m asl; W.J.E.M. Costa et al., 17 Sep. 1994. Goiás state: UFRJ 10821, 1 male, 27.7 mm SL, 1 female, 22.7 mm SL; UFRJ 10822, 4 males, 15.6–18.4 mm SL, 12 females, 16.2–22.1 mm SL; Itajá municipality: Ribeirão Bagageiro, road GO-302, 19°06'17"S, 51°42'15"W, altitude about 455 m asl; W.J.E.M. Costa, B.B. Costa & C.P. Bove, 15 Jan. 2007.

Additional material (non-types). UFRJ 10819, 12; Brazil: Goiás state: Itajá municipality: road GO-302, 19°05'09"S, 51°36'27"W, altitude about 440 m asl; W.J.E.M. Costa et al., 20 Sep. 2011.

Figure 1. *Melanorivulus proximus* sp. n., holotype, UFRJ 11681, male, 27.7 mm SL. Photograph by W.J.E.M. Costa.

Figure 2. *Melanorivulus proximus* sp. n., paratype, UFRJ 10792, female, 26.6 mm SL. Photograph by W.J.E.M. Costa.

Diagnosis. *Melanorivulus proximus* is distinguished from all other congeners of the *M. pictus* group except *M. scalaris* by the presence of irregularly arranged, interconnected oblique red bars on flank, forming Y- and X-shaped marks. *Melanorivulus proximus* is distinguished from *M. scalaris* by: caudal fin base colour pale orangish pink in females (vs. pale yellow); dorsal and anal fin sharply pointed in males (vs. rounded to moderately pointed), dorsal-fin origin at vertical between base of 9th and 10th (vs. between base of 7th and 8th); longitudinal series of scales 29–30 (vs. 31–34); pre-dorsal length longer in males (75.9–78.4 % SL vs. 73.0–75.0 % SL); longer anal-fin base (21.1–24.7 % SL in males and 18.8–21.4 % SL in females vs. 18.1–21.0 % SL in males and 16.2–18.5 % SL in females); and fewer infraorbital neuromasts around orbit (9–10 vs. 11–12).

Description. Morphometric data appear in Table 1. Body relatively deep, subcylindrical anteriorly, slightly deeper than wide, compressed posteriorly. Greatest body depth at vertical just anterior to pelvic-fin base. Dorsal and ventral profiles of trunk slightly convex in lateral view, approximately straight on caudal peduncle. Head moderately wide, sub-triangular in lateral view, dorsal profile nearly straight, ventral profile convex. Snout blunt. Jaws short; teeth numerous, conical, irregularly arranged; outer teeth hypertrophied, inner teeth small and numerous. Vomerine teeth 3–5. Gill-rakers on first branchial arch 2 + 7–8.

Dorsal and anal fins short, sharply pointed in males, rounded to slightly pointed in females. Caudal fin rounded, slightly longer than deep. Pectoral fin rounded, posterior margin reaching vertical at about 90 % of length between pectoral-fin and pelvic-fin bases. Pelvic fin small, longer in males, tip reaching between base of 2nd and 3rd anal-fin rays in males, reaching anus in females; pelvic-fin bases medially in close proximity. Dorsal-fin origin at vertical between base of 9th and 10th anal-fin rays. Dorsal-fin rays 9–11; anal-fin rays 13–15; caudal-fin rays 30–32; pectoral-fin rays 13–14; pelvic-fin rays 7. No contact organs on fins. Second proximal radial of dorsal

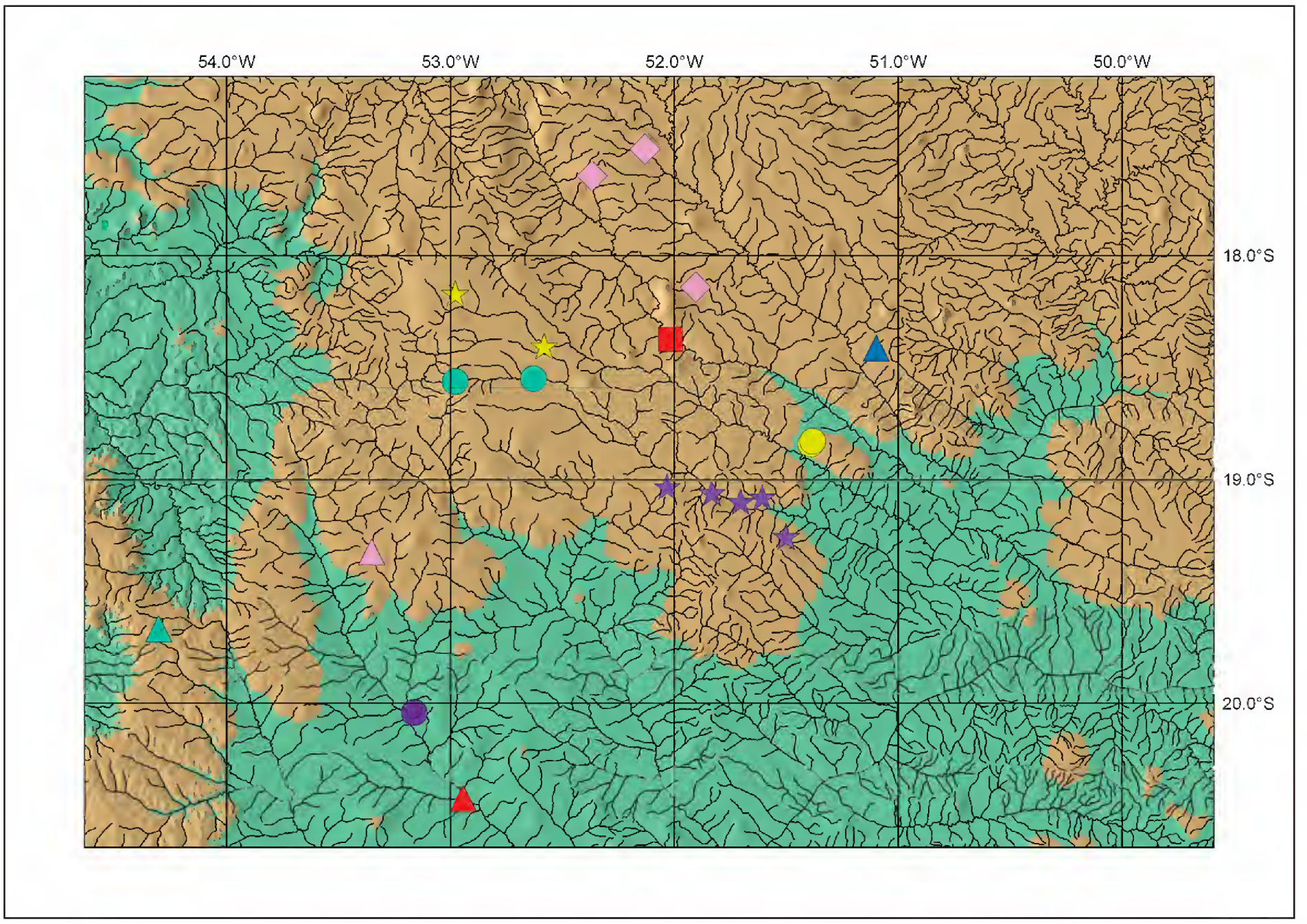

Figure 3. Geographical distribution of killifishes of the *Melanorivulus pictus* species group in the rivers draining the south-eastern slope of the Caiapó range and the adjacent middle Rio Paraná Basin. Blue triangle: *M. vittatus*; light green dot: *M. scalaris*; light green triangle: *M. linearis*; pink lozenges: *M. faucireticulatus*; pink triangle: *M. egens*; purple dot: *M. nigropunctatus*; purple stars: *M. proximus*; red square: *M. rutilicaudus*; red triangle: *M. ofaie*; yellow dots: *M. nigromarginatus*; yellow stars: *M. formosensis*.

fin between neural spines of 18th and 20th vertebrae; first proximal radial of anal fin between pleural ribs of 13th and 14th vertebrae; total vertebrae 30–31.

Scales small, cycloid. Body and head entirely scaled, except anterior ventral surface of head. Body squamation extending over anterior 25 % of caudal-fin base; no scales on dorsal, anal and pectoral-fin bases. Frontal squamation E-patterned; E-scales not overlapping medially; scales arranged in regular circular pattern around A-scale without exposed margins; transverse row of scales anterior to H-scale. Five supraorbital scales. Longitudinal series of scales 29–30; transverse series of scales 8; scale rows around caudal peduncle 16. No contact organs on scales. Cephalic neuromasts: supraorbital 3 + 3, parietal 1, anterior rostral 1, posterior rostral 1, infraorbital 1 + 9–10 + 1, preorbital 2, otic 1, post-otic 2, supratemporal 1, median opercular 1, ventral opercular 1, preopercular 2 + 4, mandibular 3 + 1, lateral mandibular 2–3, paramandibular 1. Lateral line interrupted, alternating sets of 3–4 scales with one neuromast and without neuromasts. Two neuromasts on caudal-fin base.

Colouration in life. ***Males.*** Flank metallic greenish blue to bright blue, with narrow oblique red bars between humeral region and posterior portion of caudal peduncle; bars irregularly arranged, forming chevron-like marks with angle varying in position on flank, often connected to short adjacent bars, forming Y- and X-shaped marks; bars with minute vertical extensions on each scale margin; dorsal portion of flank with oblique rows of red dots; anteroventral portion of flank with rows of red dots, often coalesced to form zigzag red marks. Dorsolateral portion of body, between posterior part of head and anterior part of flank, above humeral region, pale golden. Humeral region with horizontally elongated black spot. Dorsum light brown, venter white. Opercular region greenish golden with dark red reticulation on scale margins; suborbital region yellowish white; lower jaw dark grey. Iris pale yellow, with dark brown bar on anterior and posterior portions. Dorsal fin bluish white, sometimes yellowish on distal portion, with 4–5 transverse, narrow faint red or red stripes. Anal fin pale yellow, base and posterior portion bluish white with row of light red dots or short stripes. Caudal fin pale yellow to bluish white, with 5–6 narrow red or reddish orange stripes. Pectoral fin yellowish hyaline. Pelvic fin orangish pale yellow.

Females. Similar to males, except flank base colour pale greenish golden; dorsal and caudal fin bars dark grey; caudal fin base colour pale orangish pink; and pres-

Table 1. Morphometric data of *Melanorivulus proximus*.

Measurements	Holotype	Paratypes	
	male	males (7)	females (5)
Standard length (mm)	27.7	25.6–30.0	24.0–27.4
Percent of standard length			
Body depth	25.6	22.6–25.0	22.8–23.5
Caudal peduncle depth	15.1	14.1–14.9	13.1–14.2
Pre-dorsal length	78.4	75.9–78.3	76.1–79.7
Pre-pelvic length	57.1	54.7–56.5	55.0–57.9
Length of dorsal-fin base	11.2	10.4–12.8	10.7–12.9
Length of anal-fin base	22.2	21.1–24.7	18.8–21.4
Caudal-fin length	36.9	33.7–39.8	31.6–36.8
Pectoral-fin length	22.8	19.9–22.3	18.9–22.8
Pelvic-fin length	12.4	12.0–13.4	9.1–9.6
Head length	29.3	27.0–29.2	26.9–29.3
Percent of head length			
Head depth	72.0	68.6–72.8	69.3–73.0
Head width	71.1	70.5–73.4	72.7–76.0
Snout length	13.5	13.6–15.2	14.5–16.8
Lower jaw length	18.4	19.9–22.0	19.7–21.8
Eye diameter	33.2	30.3–34.6	30.2–35.7

ence of black spot on dorsal portion of caudal-fin base and dark grey pigmentation concentrated on distal margins of dorsal and anal fins, anterior margin of pelvic fin and entire caudal-fin margin.

Colouration in alcohol. Head and trunk pale brown, fins whitish hyaline; dark marks recorded for live specimens varying from dark brown to black.

Distribution. Middle section of the Rio Aporé drainage, upper Rio Paraná Basin, central Brazil (Fig. 3).

Etymology. From the Latin *proximus* (near, neighbour), referring to its distribution area at the same drainage as *M. scalaris*.

Melanorivulus nigromarginatus sp. n.

http://zoobank.org/FC9E4B2E-47F2-46E4-B779-67CB5B81E667

Figs 4–5, Table 2

Holotype. UFRJ 8434, male, 27.6 mm SL; Brazil: Goiás state: Itarumã municipality: Córrego Lajeado, Rio Corrente drainage, upper Rio Paraná Basin, road GO-178, 18°49'45"S, 51°22'55"W, altitude about 470 m asl; W. J. E. M. Costa et al., 20 Sep. 2011.

Paratypes. Brazil: Estado de Goiás: Município de Itarumã: all from the Corrente River drainage, upper Paraná River Basin. UFRJ 8436, 5 males, 23.4–24.7 mm SL, 8 females, 23.0–27.7 mm SL; CICCAA 00693, 5 males, 19.4–23.5 mm SL, 5 females, 20.4–24.0 mm SL; UFRJ 8435, 1 male, 23.3 mm SL, 5 females, 22.5–25.4 mm SL (C&S); collected with holotype. – UFRJ 8440, 11 males, 25.4–35.6 mm SL, 7 females, 24.7–30.8 mm SL; UFRJ 8442, 4 males, 27.6–32.9 mm SL, 2 females, 26.6–27.9 mm SL (C&S); Córrego Barreiro, road GO-178, 18°50'30"S, 51°23'27"W, altitude 498 m; W.J.E.M. Costa et al., 15 Jan. 2007. – UFRJ 8439, 2 males, 27.0–30.0 mm SL, 1 female, 25.1 mm SL; same locality as UFRJ 8440; W.J.E.M. Costa et al., 20 Sep. 2011.

Diagnosis. *Melanorivulus nigromarginatus* is similar to *M. egens* and *M. linearis*, and distinguished from all other species of the *M. pictus* group by the presence of a black distal marginal stripe on the anal fin in males (vs. absence). *Melanorivulus nigromarginatus* is distinguished from *M. egens* and *M. linearis* by having melanophores strongly concentrated on the post-orbital and humeral regions, forming a stripe (vs. weakly concentrated, not forming distinct marks); presence of red dots on the anteroventral portion of flank (vs. absence); presence of red bars on most portion of caudal fin in males (vs. bars absent in *M. egens* and bars restricted to the dorsal portion of the caudal fin in *M. linearis*); and red chevron-shaped marks irregularly distributed on the flank (vs. regularly). In addition, although not useful to distinguish all specimens, *M. nigromarginatus* often have more scales in the longitudinal series than *M. egens* and *M. linearis* (31–33 vs. 29–31).

Description. Morphometric data appear in Table 2. Body relatively deep, sub-cylindrical anteriorly, deeper than wide, compressed posteriorly. Greatest body depth at vertical just anterior to pelvic-fin base. Dorsal and ventral profiles of trunk slightly convex in lateral view; dorsal and ventral profiles of caudal peduncle nearly straight. Head moderately wide, sub-triangular in lateral view, dorsal profile nearly straight, ventral profile convex. Snout blunt. Jaws short; teeth numerous, conical, irregularly arranged; outer teeth hypertrophied, inner teeth small and numerous. Vomerine teeth 2–5. Gill-rakers on first branchial arch 1 + 8.

Dorsal and anal fins short, tip slightly pointed in males, rounded in females. Caudal fin rounded, slightly longer than deep. Pectoral fin rounded, posterior margin reaching vertical just anterior to pelvic-fin insertion. Pelvic fin small, longer in males, tip reaching between urogenital papilla and base of 2nd anal-fin ray in male, reaching anus in females; pelvic-fin bases medially in close proximity. Dorsal-fin origin at vertical between base of 8th and 9th anal-fin rays. Dorsal-fin rays 10–11; anal-fin rays 13–15; caudal-fin rays 31–34; pectoral-fin rays 13; pelvic-fin rays 6–7. No contact organs on fins. Second proximal radial of dorsal fin between neural spines of 19th and 21st vertebrae; first proximal radial of anal fin between pleural ribs of 13th and 15th vertebrae; total vertebrae 30–32.

Scales small, cycloid. Body and head entirely scaled, except anterior ventral surface of head. Body squamation extending over anterior 25 % of caudal-fin base; no scales on dorsal and anal-fin bases. Frontal squamation E-patterned; E-scales not overlapping medially; scales arranged in regular circular pattern around A-scale without exposed margins. Longitudinal series of scales 30–33;

Figure 4. *Melanorivulus nigromarginatus* sp. n., holotype, UFRJ 8434, male, 27.6 mm SL. Photograph by W.J.E.M. Costa.

Figure 5. *Melanorivulus nigromarginatus* sp. n., paratype, UFRJ 8436, female, 23.8 mm SL. Photograph by W.J.E.M. Costa.

Table 2. Morphometric data of *Melanorivulus nigromarginatus*.

Measurements	Holotype	Paratypes	
	male	males (10)	females (8)
Standard length (mm)	27.6	25.4–35.6	24.7–30.8
Percent of standard length			
Body depth	22.4	23.4–24.7	22.1–24.6
Caudal peduncle depth	14.4	14.2–15.5	13.1–15.0
Pre-dorsal length	74.4	73.7–77.4	76.6–78.5
Pre-pelvic length	55.5	53.9–56.4	56.4–58.8
Length of dorsal-fin base	13.9	12.5–15.7	11.2–13.2
Length of anal-fin base	22.8	21.1–25.0	18.1–21.6
Caudal-fin length	36.6	33.0–38.3	32.7–36.9
Pectoral-fin length	20.6	20.5–23.2	20.4–22.6
Pelvic-fin length	12.3	12.2–15.2	9.4–10.4
Head length	27.0	26.2–27.5	26.8–28.5
Percent of head length			
Head depth	67.8	67.2–73.8	68.6–74.8
Head width	74.4	73.4–77.6	75.6–81.0
Snout length	14.7	13.4–15.5	12.6–15.2
Lower jaw length	20.6	18.1–22.2	16.5–20.8
Eye diameter	32.7	30.6–33.2	29.8–33.0

transverse series of scales 9; scale rows around caudal peduncle 16. No contact organs on scales. Cephalic neuromasts: supraorbital 3 + 3, parietal 1, anterior rostral 1, posterior rostral 1, infraorbital 1 + 10–12 + 1, preorbital 2, otic 1, post-otic 1, supratemporal 1, median opercular 1, ventral opercular 1, pre-opercular 2 + 4, mandibular 3 + 1, lateral mandibular 1–2, paramandibular 1.

Colouration. ***Males***. Flank metallic light green, with narrow oblique red bars between humeral region and posterior portion of caudal peduncle; bars irregularly arranged, forming chevron pattern directed anteriorly, usually fragmented, with angle on flank midline or above it; bars with minute vertical extensions on each scale margin; dorsal portion of flank with oblique rows of red dots; anteroventral portion of flank with rows of red dots. Dorsum light brown, venter white. Side of head light brown on dorsal portion, yellowish white on ventral portion to pale golden on opercle; broad dark grey to black postorbital stripe, continuous to humeral black blotch; lower jaw dark grey. Iris pale yellow, with dark brown bar on anterior and posterior portions. Dorsal fin light yellow, with four to six oblique faint red bars. Anal fin light yellow to orange, basal portion greenish white with five or six orangish red spots, distal margin black. Caudal fin light yellow, with six to eight narrow orangish red bars extending on entire caudal fin, except its ventral-most portion. Pectoral fin hyaline. Pelvic fin light yellow to orange narrow black margin.

Females. Similar to males, except flank base colour pale greenish blue; dorsal and caudal fin bars dark grey;

caudal fin base colour pale orangish pink; absence of black pigmentation on post-orbital and humeral regions; and presence of black spot on dorsal portion of caudal-fin base and dark grey pigmentation concentrated on distal margins of dorsal and anal fins, anterior margin of pelvic fin and entire caudal-fin margin.

Colouration in alcohol. Head and trunk pale brown, fins whitish hyaline; dark marks recorded for live specimens varying from dark brown to black.

Distribution and conservation. Known only from two close small streams in the middle section of the Corrente River drainage, upper Paraná River Basin (Fig. 3).

Etymology. The name *nigromarginatus* (black margin), from the Latin, is a reference to the presence of a black margin on the anal in males.

Melanorivulus linearis sp. n.

http://zoobank.org/9312393A-94FD-4433-9818-88CC6F1666D9
Figs 6–7, Table 3

Holotype. UFRJ 11678, male, 25.1 mm SL; Brazil: Mato Grosso do Sul state: Bandeirantes municipality: Córrego Água Limpa, upper Rio Pardo drainage, Rio Paraná basin, 19°40'01"S, 54°18'13"W, altitude about 620 m asl; W.J.E.M. Costa, B.B. Costa & C.P. Bove, 12 Jan. 2004.

Paratypes. UFRJ 11679, 2 males, 27.9–30.1 mm SL, 7 females, 15.8–23.7 mm SL; UFRJ 11680, 2 males, 20.8–26.0 mm SL, 2 females, 19.5–21.1 mm SL (C&S); CICCAA 00694, 2 males, 19.0–27.2 mm SL, 3 females, 19.6–20.5 mm SL; collected with holotype.

Diagnosis. *Melanorivulus linearis* is similar to *M. egens*, and distinguished from all other species of the *M. pictus* group by the presence of red chevron-shaped marks regularly distributed on the flank (vs. irregularly), absence of distinctive dark marks on humeral region (vs. presence), and absence of red dots on the anteroventral portion of flank (vs. presence). *Melanorivulus linearis* is distinguished from *M. egens* by the presence of red bars restricted to the dorsal portion of the caudal fin in males (vs. absence), presence of black bars on the caudal fin in females (vs. black dots); presence of a pale green spot on humeral region in males (vs. absence); and second proximal radial of the dorsal fin between neural spines of 18th and 19th vertebrae (vs. between neural spines of 19th and 21st vertebrae).

Description. Morphometric data appear in Table 3. Body relatively deep, sub-cylindrical anteriorly, deeper than wide, compressed posteriorly. Greatest body depth at vertical just anterior to pelvic-fin base. Dorsal and ventral profiles of trunk slightly convex in lateral view; dorsal and ventral profiles of caudal peduncle nearly straight. Head moderately wide, sub-triangular in lateral view, dorsal profile nearly straight, ventral profile convex. Snout blunt. Jaws short; teeth numerous, conical, irregularly arranged; outer teeth hypertrophied, inner teeth small and numerous. Vomerine teeth 3–5. Gill-rakers on first branchial arch 1 + 8.

Dorsal and anal fins short, tip slightly pointed in males, rounded in females. Caudal fin rounded, slightly longer than deep. Pectoral fin rounded, posterior margin reaching vertical just anterior to pelvic-fin insertion. Pelvic fin small, longer in males, tip reaching between base of 2nd or 3rd anal-fin ray in males, reaching between anus and urogenital papilla in females; pelvic-fin bases medially in close proximity. Dorsal-fin origin on vertical through base of 8th or 9th anal-fin ray. Dorsal-fin rays 10–11; anal-fin rays 13–15; caudal-fin rays 31–32; pectoral-fin rays 13–14; pelvic-fin rays 7. No contact organs on fins. Second proximal radial of dorsal fin between neural spines of 18th and 19th vertebrae; first proximal radial of anal fin between pleural ribs of 13th and 15th vertebrae; total vertebrae 30–31.

Scales small, cycloid. Body and head entirely scaled, except anterior ventral surface of head. Body squamation extending over anterior 25 % of caudal-fin base; no scales on dorsal and anal-fin bases. Frontal squamation E-patterned; E-scales not overlapping medially; scales arranged in regular circular pattern around A-scale without exposed margins. Longitudinal series of scales 29–31; transverse series of scales 9; scale rows around caudal peduncle 16. No contact organs on scales. Cephalic neuromasts: supraorbital 3 + 3, parietal 1, anterior rostral 1, posterior rostral 1, infraorbital 1 + 9–11 + 1, preorbital 2, otic 1, post-otic 1–2, supratemporal 1, median opercular 1, ventral opercular 1, pre-opercular 2 + 4, mandibular 3 + 1, lateral mandibular 1–2, paramandibular 1.

Colouration. ***Males***. Flank metallic greenish blue, sometimes purplish blue above anal fin, with oblique narrow red bars between humeral region and posterior portion of caudal peduncle; bars regularly arranged, forming chevron pattern directed anteriorly, with angle on flank midline or above it; bars with minute vertical extensions on each scale margin; dorsal portion of flank with few red dots; anteroventral portion of flank without red marks; pale green spot on humeral region. Dorsum light brown, venter white. Side of head light brown on dorsal portion, yellowish white on ventral portion to pale golden on opercle; melanophores dispersed, not forming distinct marks on post-orbital region; lower jaw dark grey. Iris pale yellow, sometimes with dark brown bar on anterior and posterior portions. Dorsal fin light yellow, with four to six oblique red bars through whole fin. Anal fin yellowish orange, basal portion purplish white with six or seven short red bars, distal margin black. Caudal fin light yellow, with six to eight narrow red bars extending between dorsal and middle portions of fin; fin margin dark grey. Pectoral fin hyaline. Pelvic fin light yellow with narrow black margin.

Figure 6. *Melanorivulus linearis* sp. n., holotype, UFRJ 11678, male, 25.1 mm SL. Photograph by W.J.E.M. Costa.

Figure 7. *Melanorivulus linearis* sp. n., paratype, UFRJ 11679, 23.4 mm SL. Photograph by W.J.E.M. Costa.

Table 3. Morphometric data of *Melanorivulus linearis*.

Measurements	Holotype	Paratypes	
	male	males (4)	females (5)
Standard length (mm)	25.1	27.2–30.1	20.7–23.7
Percent of standard length			
Body depth	25.1	23.4–25.1	22.3–23.1
Caudal peduncle depth	15.9	14.4–16.2	12.9–14.1
Pre-dorsal length	75.3	75.4–77.4	77.1–78.7
Pre-pelvic length	57.2	54.6–55.8	54.2–58.0
Length of dorsal-fin base	12.6	12.0–12.8	10.5–12.8
Length of anal-fin base	22.2	19.3–21.6	17.9–19.0
Caudal-fin length	36.8	34.6–36.9	34.2–37.4
Pectoral-fin length	20.8	20.8–21.7	20.8–22.4
Pelvic-fin length	14.8	13.1–15.4	8.6–9.3
Head length	28.2	26.7–29.3	27.8–28.8
Percent of head length			
Head depth	73.1	69.6–72.4	67.7–71.7
Head width	69.7	72.5–74.9	70.5–74.0
Snout length	13.4	12.7–14.8	12.4–14.1
Lower jaw length	15.0	16.2–19.3	16.2–19.5
Eye diameter	32.0	29.7–31.1	32.8–35.3

Females. Similar to males, except flank base colour pale greenish golden; no distinct marks on humeral region; dorsal and caudal fin bars dark grey to black; caudal fin base colour pale white; absence of pale green spot on humeral region; and presence of triangular black spot on dorsal portion of caudal-fin base and dark grey pigmentation concentrated on distal margins of dorsal and anal fins, anterior margin of pelvic fin and entire caudal-fin margin.

Distribution. Known only from the type locality, upper section of the Rio Pardo, middle Rio Paraná Basin, central Brazil (Fig. 3).

Etymology. From the Latin, *linearis* (consisting of lines), an allusion to the red oblique lines regularly arranged on the flank in males.

Discussion

Studies on systematics of *Melanorivulus* have consistently demonstrated the importance of colour pattern characters both to diagnose species and to support monophyletic groups (Costa 2016). According to recent phylogenetic analyses (Costa 2016; Costa et al. 2016), colour pattern characters highly corroborates groups that are supported by other morphological characters, as well as by molecular data. However, the relatively low variability of mor-

Figure 8. *Melanorivulus scalaris*, UFRJ 6494, male, 29.7 mm SL. Photograph by W.J.E.M. Costa.

phometric, meristic and osteological characters among species of the *M. pictus* group makes colour pattern characters essential source to diagnose species and to estimate their relationships, since molecular data are not still available for most species. Consequently, the new taxa herein described exhibit colour patterns characters that in combination easily allow their recognition as new species, but their relationships are still unclear.

Melanorivulus proximus is the second species recorded for the Rio Aporé drainage. *Melanorivulus scalaris* also occurs in the Aporé drainage, but in altitudes between about 740 and 800 m asl, whereas *M. proximus* is here reported for altitudes between about 440 and 540 m asl. The veredas of this drainage were first sampled in 1994, but specimens here recognised as belonging to *M. proximus* were then identified as *M. pictus* (Costa, 1995; see Introduction above for historical context). Costa (2005) described *Rivulus scalaris* Costa, 2005 (= *M. scalaris*) based on material collected in the Ribeirão São Luiz, upper Rio Sucuruí drainage. Specimens collected in the middle section of the Rio Aporé drainage were then tentatively identified as *M. scalaris* and listed as additional material (non-types). Costa (2007) recorded *R. scalaris* to the Rio da Prata floodplains, upper Rio Aporé drainage, in a plateau area where the upper Ribeirão São Luiz and the Rio da Prata are in contact. However, the taxonomic status of the middle Aporé populations was not clarified until now.

The frequent occurrence of irregularly interconnected chevron-shaped red marks on the flank in males of *M. proximus* suggests that it is closely related to *M. scalaris*, in which this colour pattern is always present (Fig. 8). However, the pointed anal fin in males and the strongly pigmented reticulation on the head side in females, suggest that *M. proximus* is more closely related to species endemic to neighbouring drainages that exhibit these derived character states, comprising *M. faucireticulatus* from the Claro and Verde river drainages (Costa 2007b: figs 1–2) and *M. rutilicaudus* from the Rio Verde drainage (Costa 2005: Figs 8–9). In large adult specimens of *M. scalaris* the anal fin tip is not pointed (Fig. 8) and the caudal fin is pale yellow in females (Fig. 9).

Previous studies indicate that the Sucuruí, Aporé, Corrente, Verde and Claro river drainages, which drain the south-eastern slope of the Caiapó range and flow directly to the Rio Paranaíba as part of the upper Rio Paraná Basin, concentrates a great diversity of species of *Melanorivulus* (Costa 2005, 2007a, b, 2008). These species are often members of clades endemic to Caiapó range drainages, including those belonging to the upper Rio Araguaia Basin, on its northern slope (e.g., Costa 2006). However, characters supporting phylogenetic relationships of *M. nigromarginatus*, from the Rio Corrente drainage, with other species of the Caiapó range drainages are ambiguous.

Melanorivulus nigromarginatus is easily distinguished from all other species endemic to the Caiapó range drainages by the presence of a black marginal band on the anal fin in males (Fig. 4), suggesting that it may be more closely related to *M. egens* (Costa 2005: fig. 11) and *M. linearis* (Fig. 6), which also have similar black anal-fin margin, but are endemic to tributaries of the middle section of the Rio Paraná (Fig. 3). Contrastingly, the presence of a distinctive dark humeral spot in *M. nigromarginatus* suggests that it may be more closely related to other species occurring in other Caiapó range drainages (e.g., *M. faucireticulatus*, *M. formosensis*, *M. proximus*, *M. rutilicaudus*, *M. scalaris*, *M. vittatus*). All these species share the presence of a distinct humeral blotch varying from dark red to black (Figs 1–2, 4–5), whereas this derived condition is not present in *M. egens* and *M. linearis* (Figs 6–7). In addition, the presence of orangish pink pigmentation on the caudal fin in females that occur in *M. nigromarginatus* (Fig. 5), *M. proximus* (Fig. 2), *M. faucireticulatus* (Costa 2007b: fig. 2), and *M. rutilicaudus* (Costa 2005: fig. 9), reinforces the hypothesis of close relationships. On the other hand, probably *M. egens* and *M. linearis* from the middle Rio Paraná Basin are closely related species, sharing the presence of red chevron-shaped

Figure 9. *Melanorivulus scalaris*, UFRJ 6494, female, 24.2 mm SL. Photograph by W.J.E.M. Costa.

marks regularly distributed on the flank in males (Fig. 6; Costa 2005: fig. 11).

The present study once more reports the occurrence of different species of *Melanorivulus* inhabiting separate sections of the same river drainage as already described in previous studies (Costa 2007b, 2017; Volcan et al. 2017; Fig. 3). Recently, Costa (2017) compared this distributional pattern to that reported for other vertebrates occurring in the Cerrado, which is explained to be correlated with Miocene topographical reorganization causing geographical isolation of ancestral populations in plateaus and peripheral depressions (Prado et al. 2012; Guarnizo et al. 2016). Although estimates of divergence time among lineages of the *M. pictus* group are not still available, this paleogeographical scenario could explain the present distribution of distinct species of *Melanorivulus* at different altitudinal zones of river drainages.

Costa (2012) reported a strong process of habitat loss in the rivers draining the Caiapó range as a result of the quick expansion of agriculture land use in areas previously occupied by natural vegetation. In recent years, the veredas have often been extirpated after diversion of their water sources for plantation irrigation, as well as widespread deforestation, which has reached their margins when water flow persists. Considering the great diversity of endemic species of *Melanorivulus* inhabiting the Veredas of the Caiapó range and the continuous extirpation of Vereda habitats, this study supports the endangered status of species inhabiting this region.

Acknowledgements

I am especially grateful to Bruno Costa and Claudia Bove for help during several collecting trips in central Brazil. The paper benefited from suggestions provided by P. Bartsch and D. Taphorn. This study was supported by CNPq (Conselho Nacional de Desenvolvimento Científico e Tecnológico - Ministério de Ciência e Tecnologia).

References

Costa WJEM (1988) Sistemática e distribuição do complexo de espécies *Cynolebias minimus* (Cyprinodontiformes, Rivulidae), com a descrição de duas espécies novas. Revista Brasileira de Zoologia 5: 557–570. https://doi.org/10.1590/S0101-81751988000400004

Costa WJEM (1989) Descrição de cinco novas espécies de *Rivulus* das bacias dos rios Paraná e São Francisco (Cyprinodontiformes, Rivulidae). Revista Brasileira de Zoologia 6: 523–534. http://dx.doi.org/10.1590/S0101-81751989000300012

Costa WJEM (1990) Classificação e distribuição da família Rivulidae (Cyprinodontiformes, Aplocheiloidei). Revista Brasileira de Biologia 50: 83–89.

Costa WJEM (2001) The neotropical annual fish genus *Cynolebias* (Cyprinodontiformes: Rivulidae): phylogenetic relationships, taxonomic revision and biogeography. Ichthyological Exploration of Freshwaters 12: 333–383.

Costa WJEM (2005) Seven new species of the killifish genus *Rivulus* (Cyprinodontiformes: Rivulidae) from the Paraná, Paraguay and upper Araguaia river basins, central Brazil. Neotropical Ichthyology 3: 69–82. http://dx.doi.org/10.1590/S1679-62252005000100003

Costa WJEM (2006) *Rivulus kayapo* n. sp. (Teleostei: Cyprinodontiformes: Rivulidae): a new killifish from the serra dos Caiapós, upper rio Araguaia basin, Brazil. Zootaxa 1368: 49–56. http://www.mapress.com/zootaxa/2006f/z01368p056f.pdf

Costa WJEM (2007a) *Rivulus illuminatus*, a new killifish from the serra dos Caiapós, upper rio Paraná basin, Brazil (Teleostei: Cyprinodontiformes: Rivulidae). Ichthyological Exploration of Freshwaters 18: 193–198.

Costa WJEM (2007b) A new species of *Rivulus* from the Claro river drainage, upper Paraná river basin, central Brazil, with redescription of *R. pinima* and *R. vittatus* (Cyprinodontiformes: Rivulidae). Ichthyological Exploration of Freshwaters 18: 313–323.

Costa WJEM (2008) *Rivulus formosensis*, a new aplocheiloid killifish from the upper Corrente River drainage, upper Paraná River basin, central Brazil. Ichthyological Exploration of Freshwaters 19: 85–90.

Costa WJEM (2011) Phylogenetic position and taxonomic status of *Anablepsoides*, *Atlantirivulus*, *Cynodonichthys*, *Laimosemion* and *Melanorivulus* (Cyprinodontiformes: Rivulidae). Ichthyological Exploration of Freshwaters 22: 233–249.

Costa WJEM (2012) Two new species of *Melanorivulus* from the Caiapós hill, upper Araguaia river basin, Brazil (Cyprinodontiformes: Rivulidae). Ichthyological Exploration of Freshwaters 23: 211–218.

Costa WJEM (2016) Comparative morphology, phylogenetic relationships, and taxonomic revision of South American killifishes of the *Melanorivulus zygonectes* species group (Cyprinodontiformes: Rivulidae). Ichthyological Exploration of Freshwaters 27: 107–152.

Costa WJEM (2017) Three new species of the killifish genus *Melanorivulus* from the central Brazilian Cerrado savanna (Cyprinodontiformes, Aplocheilidae). ZooKeys 645: 51–70. https://doi.org/10.3897/zookeys.645.10920

Costa WJEM, Amorim PF, Rizzieri RC (2016) Molecular phylogeny and biogeography of the South American savanna killifish genus *Melanorivulus* (Teleostei: Rivulidae). Vertebrate Zoology 66: 267–273.

Deprá GC, Silva HP, Graça WJ (2017) A new pelvic-less species of *Melanorivulus* Costa (Cyprinodontiformes: Cynolebiidae), with a discussion on the pelvic-fin absence in killifishes. Zootaxa 4300: 111–124. https://doi.org/10.11646/zootaxa.4300.1.6

Guarnizo CE, Werneck FP, Giugliano LG, Santos MG, Fenker J, Sousa L, D'Angiolella AB, dos Santos AR, Strüssmann C, Rodrigues MT, Dorado-Rodrigues TF, Gamble T, Colli GR (2016) Cryptic lineages and diversification of an endemic anole lizard (Squamata, Dactyloidae) of the Cerrado hotspot. Molecular Phylogenetics and Evolution 94: 279–289. http://dx.doi.org/10.1016/j.ympev.2015.09.005

Hoedeman JJ (1958) The frontal scalation pattern in some groups of toothcarps (Pisces, Cyprinodontiformes). Bulletin of Aquatic Biology 1: 23–28.

Myers N, Mittermeir RA, Mittermeir CG, da Fonseca GAB, Kent J (2000) Biodiversity hotspots for conservation priorities. Nature 403: 853–858. doi:10.1038/35002501

Nielsen DTB, Neves PABA, Ywamoto EV, Passos MA (2016) *Melanorivulus polychromus,* a new species of killifish from the rio São José dos Dourados drainage, middle rio Paraná basin, southwestern Brazil, with a redescription of *Melanorivulus apiamici* (Cyprinodontiformes: Rivulidae). Aqua International Journal of Ichthyology 22: 79–88.

Prado CPA, Haddad CFB, Zamudio KR (2012) Cryptic lineages and Pleistocene population expansion in a Brazilian Cerrado frog. Molecular Ecology 21: 921–941. doi: 10.1111/j.1365-294X.2011.05409.x

Taylor WR, Van Dyke GC (1985) Revised procedures for staining and clearing small fishes and other vertebrates for bone and cartilage study. Cybium 9: 107–109. http://sfi.mnhn.fr/cybium/numeros/1985/92/01-Taylor%5b92%5d107-119.pdf

Volcan MV, Klotzeli B, Lanés LEK (2017) Two new species of Melanorivulus (Cyprinodontiformes: Cynolebiidae) from Rio Verde drainage, Upper Rio Paraná basin, Brazil. Zootaxa 4236: 82–94. https://doi.org/10.11646/zootaxa.4236.1.4

Zoosyst. Evol. 94 (1) 2018, 29–56 | DOI 10.3897/zse.94.20116

PENSOFT

museum für naturkunde

An illustrated catalogue of Rudolf Sturany's type specimens in the Naturhistorisches Museum Wien, Austria (NHMW): deep-sea Eastern Mediterranean molluscs

Paolo G. Albano[1], Sara-Maria Schnedl[2], Anita Eschner[2]

1 *Department of Palaeontology, University of Vienna, Althanstrasse 14, 1090 Vienna, Austria*

2 *Natural History Museum, Third Zoological Department, Burgring 7, 1010 Vienna, Austria*

http://zoobank.org/2DC2487C-8832-46D2-9181-EC1F748A3E77

Corresponding author: *Paolo G. Albano* (pgalbano@gmail.com)

Received 8 September 2017
Accepted 16 November 2017
Published 3 January 2018

Academic editor:
Matthias Glaubrecht

Key Words

Type specimens
Pola expeditions
deep-sea
Gastropoda
Bivalvia
Eastern Mediterranean Sea
Adriatic Sea
Greece
Croatia
Rudolf Sturany
Monterosato

Abstract

The "Pola" expeditions were the first to explore the deep Eastern Mediterranean Sea in the 1890s. They remained the most intense surveys in that area for a century and constitute today a fundamental baseline to assess change in the basin, whose fauna is still inadequately described. Solid taxonomic foundations for the study of deep-sea organisms are needed and we here contribute by revising the name-bearing types of mollusc species introduced by Rudolf Sturany on the basis of the "Pola" material from the Eastern Mediterranean Sea stored in the Natural History Museum in Vienna. Sturany introduced 15 names (*Marginella occulta* var. *minor* Sturany, 1896 shall not be considered as the introduction of a new name). He described and established two manuscript names by Monterosato: *Jujubinus igneus* and *Pseudomurex ruderatus*. The genus *Isorropodon* was also introduced together with its type species *I. perplexum*. For each name, we list the available type material, provide the original description and a translation into English and illustrate the specimens in colour and with SEM imaging.

Introduction

The second half of the 19th century was an exciting period for marine exploration: most of the seafaring nations of the time sent out expeditions to investigate the sea. The Austro-Hungarian monarchy did likewise, planning a geographically restricted but intense series of expeditions to the Eastern Mediterranean and the Red Sea (Schefbeck 1996). These expeditions were the joint effort of the important research institutions of the time: The Imperial Academy of Sciences (now the Austrian Academy of Sciences), the Imperial and Royal Court Museum of Natural History (now the Natural History Museum Vienna (NHMW)) and the institutes of Zoology and Chemistry of the University of Vienna. These institutions provided the equipment, knowledge and personnel to plan and successfully conduct the expeditions. The Imperial and Royal Navy provided the ship, the crew and the commander-in-chief Admiral M.B. Sterneck, who had a soft spot for marine biology being a collector of shells and algae since an early age. He proved to be a major player in stimulating and enabling the four expeditions that were organised to the Eastern Mediterranean between 1890 and 1893 and the fifth expedition which surveyed the southern Adriatic Sea in 1894.

The Mediterranean deep sea is remarkably unexplored in comparison to its coastal areas even if it hosts several habitats that can represent biodiversity hot spots, a large share of endemic species and an estimated 66% of species still to be discovered (Danovaro et al. 2010). The "Pola" expeditions were not only the first, but also among the most intense surveys of the Eastern Mediterranean until the 1990s, when the Israel Oceanographic and Limnological Research (IOLR) started the deep-water exploration off the Israeli coast (Galil 2004). The "Thor" (1910), "Meteor 5" (1987), "Meteor 25" (1993) and "Poseidon" (cruise 201/2, 1994) contributed in-between with smaller-scale efforts.

The deep-sea Mediterranean ecosystem is also under siege from several anthropogenic stressors. As an example, climate change may affect the thermohaline circulation reducing its oxygenation (Danovaro et al. 2001) and altering the energy transport from surface waters to the seafloor (Smith et al. 2009). Furthermore, commercial fishing is extending into ever deeper waters with little appreciation of its effects on such a delicate ecosystem (Danovaro et al. 2010). In this context, the "Pola" expeditions constitute a fundamental baseline to assess change in the Eastern Mediterranean. Although not always recognized as such, the NHMW and the other institutions that preserve similar historical samples are a strategic asset in global change research (Johnson et al. 2011, Lister et al. 2011, Albano et al. 2014, Dayan and Galil 2017).

Our aim is to contribute to a solid taxonomic foundation for the study of deep-sea organisms. In particular, we revise the name-bearing types of mollusc species introduced by Rudolf Sturany (malacologist at the NHMW between 1889 and 1922 (Stagl 2012)) on the basis of the "Pola" samples from the Eastern Mediterranean Sea, following the recommendation of the International Commission on Zoological Nomenclature to publish lists of types housed in institutions (ICZN 1999, 72F.4). Similar to the previous effort on Red Sea gastropods (Albano et al. 2017), we also provide detailed illustrations of the type specimens and their diagnostic characters.

Materials and methods

The "Pola" material is entirely stored in the NHMW (Stagl et al. 1996). Type series of Sturany's species were segregated. Most species were represented by holotypes or very small series. In the latter case, we identified the syntypes best matching the original description but refrained from any lectotype designation following recommendation 74G of article 74.7 of the International Code of Zoological Nomenclature ("ICZN Code" in the following text) (ICZN 1999). Some names were termed as varieties of other species. Whenever Sturany clearly clarified the intention of introducing a new name, such names are considered to be of subspecific rank following the article 45.6.4 of the ICZN Code. A taxon list in alphabetical order with page and figure numbers in this paper is provided in Table 1. Any citation to the International Code of Zoological Nomenclature (ICZN 1999) should be considered to its online version which includes all recent amendments.

For each species, we provide references to the original description and figure, the original localities, a list of the type material, the original description and its translation into English. All inventory numbers provided refer to the Mollusca collection of NHMW. The systematic arrangement follows Bouchet and Rocroi (2005) and Bouchet et al. (2010) for gastropods and bivalves, respectively. The reassessment of the current taxonomic status of Sturany's names is beyond the scope of this paper and we relied on the published literature to add comments in this regard. The expeditions surveyed several localities in Greece and Croatia (Fig. 1) whose names were stated in Italian; in our translation, we also use the modern Greek and Croatian names (Table 2).

The NHMW hosts a large collection by Monterosato that was a fundamental reference for Sturany to identify his material. This collection was purchased in 1889, just the year when Sturany started to volunteer in the mollusc collection. The acquisition from December 1889 reads: "*Shells of the Mediterranean Sea ca. 2082 sp.– collection of the zoologist Monterosato, purchased for 500 fl. Ö.W.*" [translated]. In 1897, Sturany – now assistant of the collection – wrote the complete inventory: 2113 inventory numbers altogether. Unfortunately, hardly any of the original labels are preserved within this collection nor is the original list, but Sturany had apparently transcribed all names very carefully.

Some names had been written on labels but never formally described by Monterosato. Such manuscript names have either been described by Sturany (e.g., *Jujubinus igneus*) or rendered available by redescription and illustration (e.g., *Pseudomurex ruderatus*).

Photos were mostly shot with a Nikon SMZ25 microscope; large shells were photographed with a Canon 350D camera, a 50 mm lens and extension tubes. SEM images were taken with a JEOL JSM-6610LV, using low vacuum without any coating. Specimen measurements have been added for holotypes. The map in Fig. 1 was drawn with the oceanmap package (Bauer 2017) in the statistical programming environment R, version 3.3.3 (R Core Team 2017).

Systematic list of taxa

Family Trochidae Rafinesque, 1815

Jujubinus igneus Sturany, 1896 ex Monterosato ms.

Fig. 2

Sturany 1896: 28, plate II, figure 45.

Original locality. Station 260, at Pelagruža, Croatia, 42°23'3"N, 16°21'50"E, 128 m.

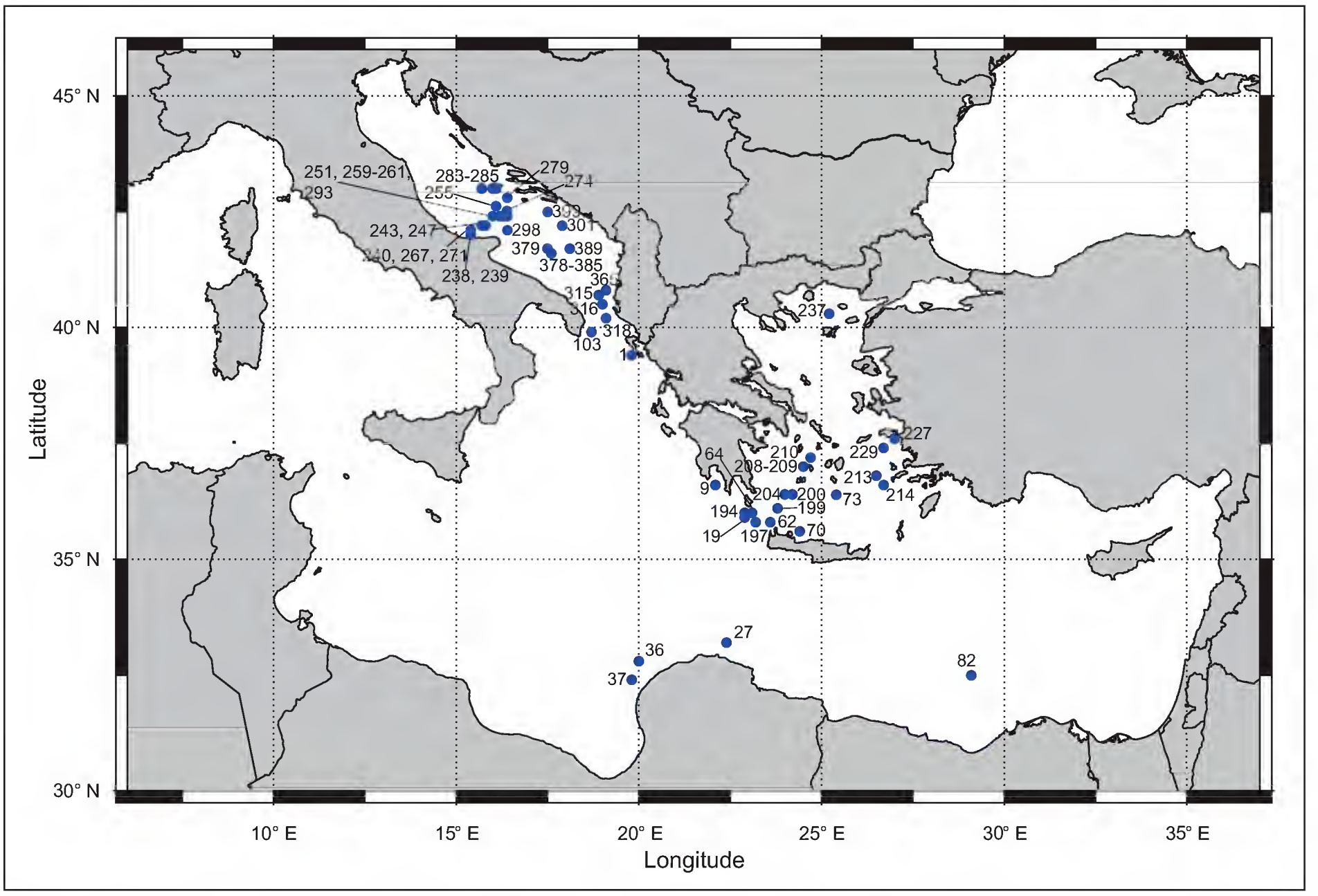

Figure 1. Map of the stations sampled by the "Pola" expeditions to the Eastern Mediterranean (1890-1893) and the Southern Adriatic Sea (1894) which provided molluscan samples and reported in Sturany (1896).

Table 1. List of treated taxa in alphabetic order, with original name, current family placement, and figure in this paper.

Taxon	Current name	Family	Page, Figure
aegeensis, Lyonsia	*Allogramma formosa* (Jeffreys, 1882)	Lyonsiidae	Page 51, figure 14
alexandrina, Taranis	*Taranis moerchii* (Malm, 1861)	Raphitomidae	Page 44, figure 9
amorpha, Lucina	*Myrtea amorpha* (Sturany, 1896)	Lucinidae	Page 47, figure 11
bengasiensis, Fusus	*Fusinus rostratus* (Olivi, 1792)	Fasciolariidae	Page 38, figure 5
berenicensis, Pecchiolia	*Haliris berenicensis* (Sturany, 1896)	Verticordiidae	Page 53, figure 15
cerigottana, Scalaria	*Punctiscala cerigottana* (Sturany, 1896)	Epitoniidae	Page 33, figure 3
corallinoides, Raphitoma nuperrima var.	*Kurziella serga* (Dall, 1881)	Raphitomidae	Page 41, figure 8
igneus, Jujubinus	*Jujubinus exasperatus* (Pennant, 1777)	Trochidae	Page 30, figure 2
implicisculpta, Defrancia	*Pleurotomella eurybrocha* (Dautzenberg & Fischer, 1896)	Raphitomidae	Page 40, figure 7
minor, Marginella occulta var.	–	Marginellidae	Page 38, figure 6
modiolaeformis, Myrina	*Idas modiolaeformis* (Sturany, 1896)	Mytilidae	Page 45, figure 10
perplexum, Isorropodon	*Isorropodon perplexum* (Sturany, 1896)	Vesicomyidae	Page 48, figure 13
pianosana, Fusus craticulatus var.	*Hirtomurex squamosus* (Bivona Ant. in Bivona And., 1838)	Muricidae	Page 36, figure 4
pseudacanthodes, Raphitoma nuperrima var.	*Kurziella serga* (Dall, 1881)	Raphitomidae	Page 41, figure 8
ruderatus, Pseudomurex	*Hirtomurex squamosus* (Bivona Ant. in Bivona And., 1838)	Muricidae	Page 38, figure 4
striatus, Axinus flexuosus var.	*Thyasira striata* Sturany, 1896	Thyasiridae	Page 47, figure 12

Type material. NHMW 72399: 3 syntypes (specimens preserved in ethanol, but apparently without the animal inside).

Additional material. NHMW 27441: 8 shells, Palermo, Italy (Monterosato coll.).

Original description. *Von Station *260 (128 m).*

Die vorliegenden drei Exemplare sind circa 7,5 mm hoch und 5,7 – 6 mm breit. Von den 8 – 9 Umgängen sind die oberen rosenroth, die übrigen zart olivengrün mit rosenrothen und hellgelben Flecken oder Strichen. Die Spiralstreifen bestehen aus Reihen von groben

Table 2. Stations of the "Pola" expeditions to the Eastern Mediterranean Sea listed by Sturany (1896) where molluscs were collected.

Station number	Locality	Coordinates	Depth [m]
1	"Westlich von Corfu" [west of Corfu, Greece]	39°23'N, 19°48'20"E	-615
9	"Vor der Bucht von Kalamata (Griechenland)" [off the Bay of Kalamata, Greece]	36°38'55"N, 22°4'36"E	-1050
19	"Südlich von Cerigo" [south of Kythira, Ionian Sea, Greece]	35°56'N, 22°54'50"E	-1010
27	"An der afrikanischen Küste" [off the African coast, NE of Benghazi]	33°11'18"N, 22°22'56"E	-1765
36	"Nördlich von Benghazi an der afrikanischen Küste" [north of Benghazi, Libya]	32°46'40"N, 19°58'30"E	-680
37	"Nordwestlich von Benghazi an der afrikanischen Küste" [north of Benghazi, Libya]	32°25'14"N, 19°49'57"E	-700
62	"Im Norden der Westküste von Creta" [north of the west coast of Crete, Greece]	35°48'N, 23°34'E	-755
64	"Südwestlich von der Insel Cerigo" [southwest of the island of Kythira, Ionian Sea, Greece]	35°59'N, 22°56'E	-660
70	"Vor der Plaka-B. von Creta (Candia)" [off the Bay of Plaka (north of Vamos) in Crete, Chania, Greece]	35°39'N, 24°23'E	-805
73	"Nördl. Ausgang des Hafens von Santorin (Cycladen)" [northern entrance of the harbour of Santorini (Cyclades), Greece]	36°26'N, 25°24'E	-381
82	"Nördlich von Alexandrien" [north of Alexandria, Egypt]	32°30'N, 29°8'E	-2420
103	"Südlich vom Cap St. Maria di Leuca (Jon. Meer) [south of St. Maria di Leuca Cape, Ionian Sea, Italy]	39°54'N, 18°44'E	-134
194	"Zwischen Cerigo und Cerigotto" [between Kythira and Antikythira, Ionian Sea, Greece]	36°3'N, 23°6'E	-160
197	"Zwischen Cerigo und Candia (Creta)" [between Kythira and Chania (Crete), Greece]	35°45'N, 23°11'E	-608
199	"Südöstlich von Cerigo (Meer von Candia)" [southwest of Kythira, Sea of Crete, Greece]	36°9'N, 23°50'E	-875
200	"Mitten zwischen Cap Malea und Santorin (Meer von Candia)" [between Cape Maleas and Santorini (Sea of Crete), Greece]	36°23'N, 24°11'E	-880
204	"Zwischen Cap Malea und Milo (Meer von Candia)" [between Cape Maleas and Milos, Sea of Crete, Greece]	36°25'N, 24°2'E	-808
208	"Mitten zwischen Milo und Serpho (Cycladen)" [between Milos and Serifos (Cyclades), Greece]	37°0'N, 24°28'E	-414
209	"Ebenda" [as above]	36°59'N, 24°29'E	-444
210	"Östlich von Serpho (Cycladen)" [east of Serifos (Cyclades), Greece]	37°12'N, 24°43'E	-287
213	"Nördlich von Stampaglia (Astropalia), Sporaden" [north of Astypalaia, Dodekanese, Greece]	36°47'N, 26°29'E	-597
214	"Östlich von Stampaglia, Sporaden" [east of Astypalaia, Dodekanese, Greece]	36°37'N, 26°43'E	-533
227	"Ebenda" [as above]	37°37'N, 26°58'E	-92
229	"Nördlich von Samos" [north of Samos, Greece]	37°54'N, 26°43'E	-580
237	"Südwestlich von Samotraki (Äg. M.) [southwest of Samothraki, Aegean Sea, Greece]	40°17'N, 25°13'E	-588
238	"Nördlich von Tremiti" [north of Tremiti Islands, Adriatic Sea, Italy]	42°2'40"N, 15°27'7"E	-98
239	"Ebenda" [as above]	-	-70
240	"Zwischen Tremiti und Pianosa" [between Tremiti Islands and Pianosa Isl., Adriatic Sea, Italy]	42°9'N, 15°22'37"E	-104
243	"In der Linie von Tremiti und Pianosa" [between Tremiti Islands and Pianosa Isl., Adriatic Sea, Italy]	42°11'40"N, 15°40'50"E	-103
247	"Bei Pianosa" [Pianosa Isl., Tremiti Islands, Adriatic Sea, Italy]	42°13'20"N, 15°50'42"E	-111
251	"Vor Pelagosa" [off Pelagruža, Croatia]	42°23'24"N, 16°1'42"E	-129
255	"Bei Pelagosa" [at Pelagruža, Croatia]	42°34'18"N, 16°9'15"E	-176
259	"Bei Pelagosa" [at Pelagruža, Croatia]	42°23'40"N, 16°20'45"E	-174
260	"Bei Pelagosa" [at Pelagruža, Croatia]	42°23'3"N, 16°21'50"E	-128
261	"Bei Pelagosa" [at Pelagruža, Croatia]	42°23'8"N, 16°12'42"E	-101
267	"Bei Lagosta" [at Lastovo, Croatia]	42°9'0"N, 15°22'37"E	-117
271	Not specified	42°2'0"N, 15°27'7"E	-112
274	Not specified	42°31'44"N, 16°27'50"E	-191
279	"Bei Cazza" [at Sušac, Croatia]	42°47'0"N, 16°21'10"E	-132
283	"Zwischen Lissa und Busi" [between Vis and Biševo, Croatia]	42°58'24"N, 16°3'24"E	-102
284	"Zwischen Comisa und Busi" [between Komiža and Biševo, Croatia]	43°2'24"N, 16°0'10"E	-94
285	"Zwischen St. Andrä und Lissa" [between Sveti Andrija and Vis, Croatia]	42°58'20"N, 15°43'10"E	-133
292	Not specified	42°24'44"N, 16°17'42"E	-171
293	"Östlich von Pelagosa" [east of Pelagruža, Croatia]	42°23'0"N, 16°21'59"E	-131
298	"Südöstlich von Pelagosa" [southeast of Pelagruža, Croatia]	42°9'0"N, 16°21'27"E	-485
301	"Südöstlich von Pelagosa" [southeast of Pelagruža, Croatia]	42°11'0"N, 17°51'30"E	-1216
315	"Strasse von Otranto, in der Höhe von Valona" [Strait of Otranto, off Valona, southern Adriatic Sea]	40°40'20"N, 18°51'30"E	-840
316	"Strasse von Otranto" [Strait of Otranto, southern Adriatic Sea]	40°32'45"N, 18°58'0"E	-760
318	"Strasse von Otranto, nach der Ausfahrt von Valona" [Strait of Otranto, at the entrance of Valona, southern Adriatic Sea]	40°13'10"N, 19°3'40"E	-932
365	"Strasse von Otranto" [Strait of Otranto, southern Adriatic Sea]	between 40°46'6"N, 19°3'E and 40°36'N, 18°31'E	-776
378	"Südliche Adria" [southern Adriatic Sea]	41°36'8"N, 17°35'7"E	-950
379	"Südliche Adria" [southern Adriatic Sea]	41°41'N, 17°30'5"E	-1138
385	"Südliche Adria" [southern Adriatic Sea]	41°37'N, 17°38'E	-1196
389	"Südliche Adria" [southern Adriatic Sea]	41°42'N, 18°5'40"E	-1205
399	"Südlich von Meleda" [south of Mljet, Croatia]	42°32'20"N, 17°28'40"E	-218

Körnchen und zwischen ihnen stehen derbe Querstreifen. Die Zahl der Spiralstreifen ist von der vorletzten Windung an bis hinauf zum Embryonalgewinde 5, ein Hervortreten des über der Naht stehenden Streifens als Wulst, wie dies hauptsächlich für die Art Tr. erasperatus *Penn. charakteristisch ist, ist kaum wahrnehmbar. Um den verdeckten Nabel herum verlaufen concentrisch 7 gelb und rosenroth gefleckte Rippen und ausserdem noch nahe dem Kiele der letzten Windung 1–2 schwächere ungefleckte Kreise. Die Querstreifung hier auf der Unterfläche des Gehäuses ist zarter und enger als die auf der Oberseite sichtbare.*

Diese Beschreibung passt im Allgemeinen auch auf die von March. Monterosato mit Jujubinus igneus *bezeichneten Exemplare, die sich in der Sammlung des Hofmuseums befinden, und deshalb habe ich diesen Collectionsnamen auch hier für die Aufschrift gewählt. Es wären für die Monterosato-Exemplare nur noch die lebhaftere rothe Färbung (Zurücktreten der olivgrünen Farbe und Prävaliren von Gelb und Rosenroth) zu erwähnen und das deutlichere Hervortreten des Suturalwulstes, der hier lebhaft roth und gelb gefleckt ist.*

Ich möchte Tr. igneus *Monteros. in coll. als eine Varietät von* Tr. exasperatus *Penn. hinstellen, wobei ich der von Bucquoy, Dautzenberg und Dollfus in dem Werke „Les Mollusques marins du Roussillon,u p. 362–369 ausgesprochenen Auffassung der beiden einander verwandten Arten* exasperatus *Penn. und* striatus *L. folge, muss jedoch auch bemerken, dass diese Art (nämlich* exasperatus*) mit Rücksicht auf die dort namhaft gemachte Synonymie mit* Trochus (Zizyphinus) exiguus *Pulteney (Kobelt, Prodr.p.238; Carns, Prodr. p.259) zusammenfällt.*

Brusina und Stossich führen Tr. exiguus *Pult. als* crenulatus *Brocchi für die Adria an.*

Translation. From station *260 (128 m).

The three specimens at hand are approximately 7.5 mm high and 5.7 – 6 mm wide. The uppermost of the 8 – 9 whorls are pink, the others are pastel olive green with pink and bright yellow marks or lines. The spiral cords consist of tubercled rows and rough horizontal stripes in-between. There are five spiral cords counting from the penultimate whorl up to the protoconch. There is hardly any prominent varix above the suture which is a typical feature in *Tr. exasperatus* Penn. Seven concentrically blended yellow and rose spotted cords frame the covered umbilicus. Moreover, close to the keel of the last whorl there are one to two unspotted cords. Here on the bottom of the shell, the lateral cords are tighter and finer than those visible on the whorls.

Overall, this description matches the specimens described by March. Monterosato as *Jujubinus igneus* in the collection of the Hofmuseum (Imperial Museum of Natural History), therefore I chose this name. Only the livelier red colour (receding of the olive green colour and prevailing of yellow and pinkish) and the here bright red and yellow spotted, prominent sutural varix are important characters.

I would like to describe *Tr. igneus* Monteros. in coll. as a variety of *Tr. exasperatus* Penn., following the notion of "Les Mollusques marins du Roussillon" p.362–369 by Bucquoy, Dautzenberg and Dollfus. However, I have to remark that this species (*exasperatus*) falls within the considerable synonymy of *Trochus* (*Zizyphinus*) *exiguus* Pulteney (Kobelt, Prodr. p. 238; Carus, Prodr. p. 259).

Brusina and Stossich mention *Tr. exiguus* Pult. as *crenulatus* Brocchi for the Adriatic.

Comments. Sturany identified these shells by comparison to specimens in the Monterosato collection (NHMW 27441) which closely match the specimens found in the "Pola" expedition (Fig. 2 A-F). However, Monterosato never formally introduced the name. Therefore, the variety *igneus* has to be considered a new subspecific name introduced by Sturany following the provisions of art. 45.6.4 of the ICZN code. This name is considered a junior synonym of *Jujubinus exasperatus* (Pennant, 1777) (MolluscaBase 2017). The name *Trochus* (*Jujubinus*) *igneus* was used also by Brusina (1896), whose work postdates Sturany's one because he explicitly mentioned the preprint of Sturany's work, and later by Locard (1904).

Family Epitoniidae Berry, 1910

***Scalaria cerigottana* Sturany, 1896**

Fig. 3

Sturany 1896: 9, plate I, figures 3–4.

Type locality. Station 194, Kythira and Antikythira, Ionian Sea, Greece, 36°3'N, 23°6'E, 160 m.

Type material. Holotype: NHMW 13001, height 4.68 mm.

Original description. *Von Station 194 (160 m).*

Das einzige Exemplar dieser neuen Art besitzt nur 5$^{1}/_{2}$ Umgänge, indem der Apex des Gehäuses fehlt.

Auf jedem Umgange stehen 10 mächtige Querrippen. Diese sind aber nicht gleichmässig stark entwickelt, sondern es tritt hier und dort eine besonders dicke und hohe Rippe auffallend hervor, und gleich darauf folgt wieder eine solche unter dem Mittelmasse. Zwischen den einzelnen Rippen und über sie selbst hinweg ziehen zahlreiche (mehr als 20) Spiralstreifen, welche sich, mit dem Mikroskop betrachtet, als feine Furchen repräsentieren. (Fig. 4.) In diesen Furchen reihen sich kleine Grübchen aneinander, welche die Kreuzungspunkte von ursprünglich vorhandenen, bei unserem Exemplare aber nicht mehr sichtbaren Querfurchen mit den noch deutlich vorhandenen Spiralfurchen vorzustellen scheinen. (Man vergleiche diesbezüglich die mikroskopische Skulptur von Scalaria funiculata *Watson.)*

Die Rippen senken sich oben wie unten bogenförmig, also nicht winkelig, wie bei den nächstverwandten Ar-

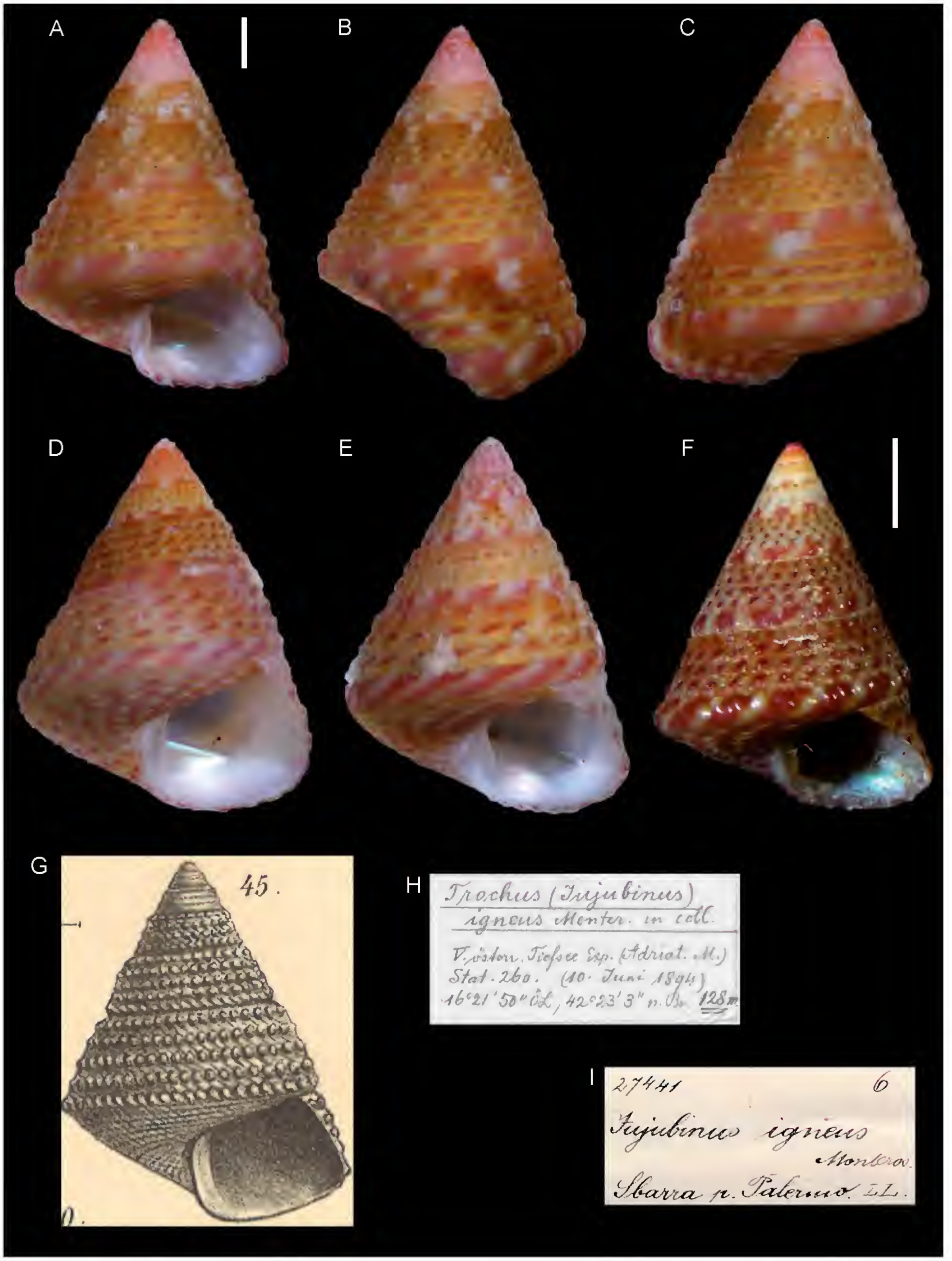

Figure 2. *Jujubinus igneus* Sturany, 1896 ex Monterosato ms. **A-C**. Syntype NHMW 72399a, station 260, Pelagruža, Croatia, 128 m: front (A), side (B) and back (C) views. **D–E**. Syntype NHMW 72399b and c: front views. **F**. NHMW 27441 (Monterosato coll.): front view. **G**. Original figure in Sturany, 1896. **H**. Original label of lot NHMW 72399. **I**. Original label of lot 27441. Scale bar: 1 mm.

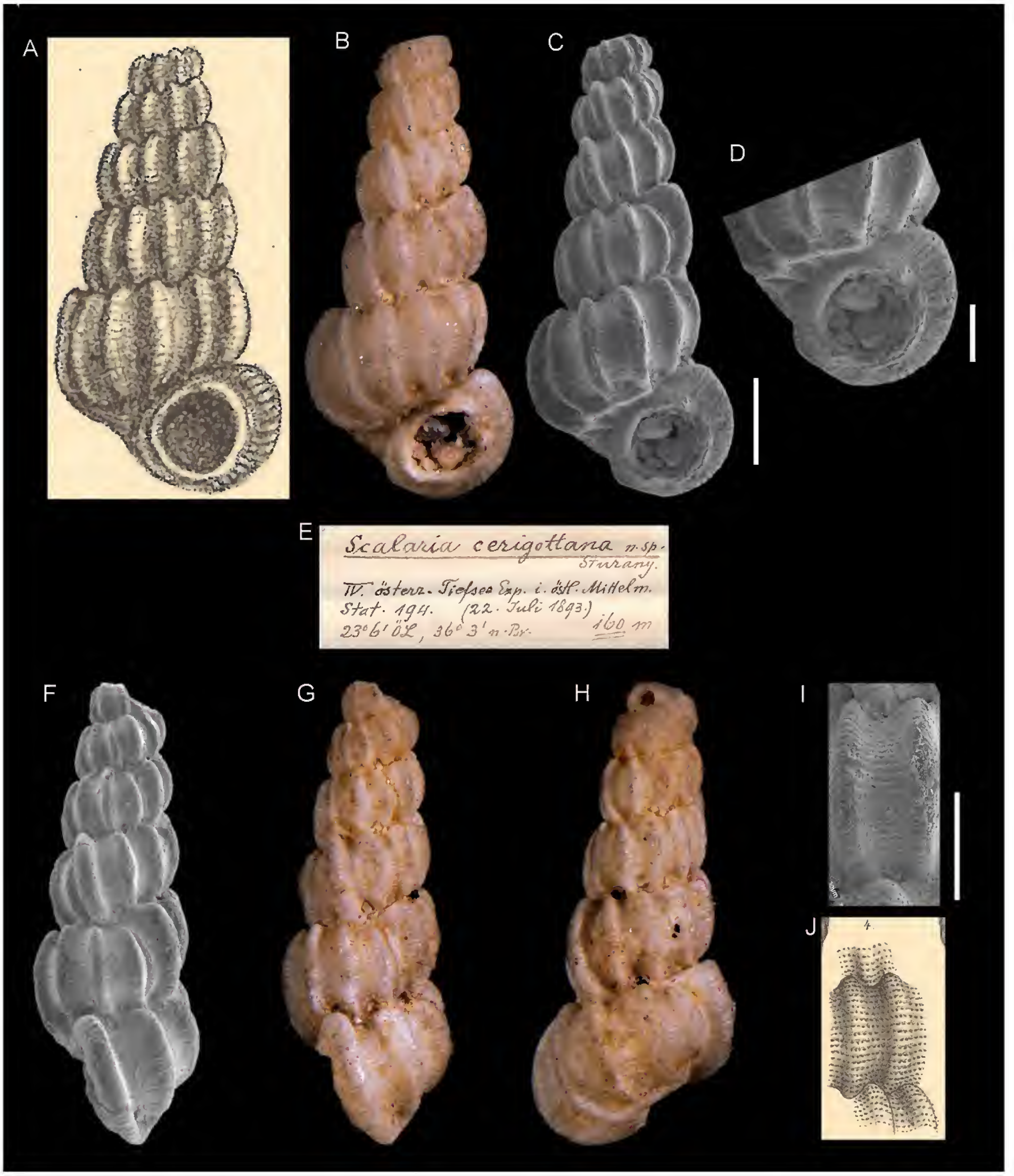

Figure 3. *Scalaria cerigottana* Sturany, 1896, Station 194, between Kythira and Antikythera, Ionian Sea, Greece, 160 m. **A**, **J**. Original figures in Sturany, 1896. **B–D, F–I**. Holotype NHMW 13001: front (**B–C**), side (**F–G**), and back (**H**) views, aperture (**D**), microsculpture (**I**). **E.** Original label. Scale bar: 1 mm (**B–C**, **F–H**); 0.5 mm (**D**, **I**).

ten, in die tiefe Naht; rings um den Nabel aber bilden sie durch wulstige Querverbindungen ihrer unteren Enden einen förmlichen Kiel. Dem kreisrunden Mundrand steht außen eine mächtige Rippe so nahe an, dass er wie verdoppelt aussieht.

Höhe des Gehäuses 5 mm, Breite 2,2 mm; Durchmesser der Mündung 1 mm.

Die Art ist am nächsten verwandt mit Scalaria funiculata *Wats. von Pernambuco (Report on the scient. Res. of the Voyage of H.M.S. Challenger, Zool. Vol. XV,p. 141, pl. IX, fig. 4) und unterscheidet sich von dieser hauptsächlich durch das weniger zugespitzte Gehäuse und die ungleichmäßige Berippung. Ferner stehen ihr nahe* Scalaria longissima *Seg. (Kobelt Prodr. p. 77) und die fossilen*

Formen Turbo torulosus *Brocchi (Conch. foss. subapp. 2. ed., vol. II, p. 163, pl. VII, fig. 4),* Scalaria plicosa *Phil. (Enum. Moll. Sicil. vol. II, p. 146, tab. XXIV, fig. 25),* Nodiscala cavata *de Boury (Bull. Soc. Mal. Ital. XIV, 1889, p. 173, tab. IV, fig. 13).*

Translation. From station 194 (160 m).

The single specimen of this new species shows only 5 ½ whorls, as the apex is missing from the shell. Each whorl has 10 prominent axial ribs which are not developed equally, but some here and there are remarkably thick and high, surrounded by others smaller than average. In between the ribs and covering them are numerous (more than 20) spiral threads, which look like small grooves under the microscope (Fig. 4). Small pits ornament the threads. They seem to be crossing points of the spiral threads with axial lines which are no longer visible in our specimen (in this regard compare the microsculpture of *Scaria funiculata* Watson).

In contrast to closely related species, the ribs sink into the deep suture in a curved manner, not angled. However, they form a keel around the umbilicus through the thick interconnections of their lower ends. A thick varix is present on the lip and makes it seem duplicated.

The shell is 5 mm high, 2.2 mm wide and the diameter of the mouth is 1 mm.

The most closely related species is *Scalaria funiculata* Wats. of Pernambuco (Report on the scient. Res. of the Voyage of H.M.S. Challenger, Zool.Vol.XV, p. 141, pl. IX, fig. 4) and can be distinguished from it by the less pointed shell and the uneven rib pattern. Other closely related species are *Scalaria longissima* Seg. (Kobelt Prodr. p.77) and the fossil forms *Turbo torulosus* Brocchi (Conch. foss. subapp. 2. ed., vol. II, p. 163, pl. VII, fig. 4), *Scalaria plicosa* Phil. (Enum. Moll. Sicil. vol. II, p. 146, tab. XXIV, fig. 25), *Nodiscala cavata* de Boury (Bull. Soc. Mal. Ital. XIV, 1889, p. 173, tab. IV, fig. 13).

Comments. A valid taxon accepted as *Punctiscala cerigottana* (MolluscaBase 2017).

Family Muricidae Rafinesque, 1815

***Fusus craticulatus* var. *pianosana* Sturany, 1896**

Fig. 4G, K

Sturany 1896: 25-26, plate II, figures 40–41.

Original locality. Station 243, between Tremiti Islands and Pianosa Isl., Adriatic Sea, Italy, 42°11'40"N, 15°40'50"E, 103 m.

Type material. not found.

Original description. *Von Station 243 (103 m); 1 Exemplar.*

Das 31 ½ mm hohe und 16 mm breite Gehäuse ist eine Missbildung, indem der Stiel doppelt ausgebildet wurde. Der ursprünglich angesetzte Stiel steht links ab und bildet einen tiefen nabelartigen Trichter, während ihn rechts der neugebildete an Länge überragt. Die Mündung beträgt zusammen mit dem Stiele, der, nebenbei bemerkt, nirgends mit seinen Rändern verwachsen, sondern durchgehend offen rinnenförmig ist, 15 ½ mm in der Länge. Vom Apex ist ein kleines Stück abgebrochen, 7 Windungen sind erhalten.

Die Sculptur der Umgänge erinnert an die der Coralliophilen. Eine Anzahl von mit Schuppen mehr minder reich besetzten Spiralreifen läuft über sie hinweg; an den oberen Umgängen sind 3 bis 5 solcher Reifen vorhanden, und zwar sind sie ziemlich gleich, stark (breit) und noch wenig beschuppt; an den letzten zwei Windungen treffen wir schon bedeutend mehr, und hier wechseln stärkere (breite) und schwächere (schmale) ziemlich regelmäßig ab, d. h. zwischen zwei starke oder Hauptreifen erscheint meistens ein ganz zarter, aber deshalb nicht schuppenloser Reifen eingeschoben. Querwülste sind auf den letzten Wildungen 8–9 vorhanden, oben etwas weniger. Der Aussenrand der Mündung ist entsprechend den dort endigenden Spiralreifen gezackt.

Für die Coralliophila squamulosa *Phil. (Kobelt, Prodr. p. 15; Carus, Prodr. p. 380) ist das Exemplar erstens zu gross, und zweitens hat es nur 9 Querfalten auf dem letzten Umgange, während jene Art 12 bis 13 haben soll. Vielleicht aber sind Herrn March. Monterosato ähnliche Formen vorgelegen, als er sich entschloss, die* Coralliophila squamulosa *als Varietät von* Murex brocchi, *resp.* Fusus craticulatus *zu erklären (Monterosato, Nuova Rivista, p. 39).*

*In der Monterosato-Collection des naturhistorischen Hofmuseums in Wien sind zwei sehr interessante, der hier in Rede stehenden Form nahe kommende Exemplare mit der Determination „*Pseudomurex sp. nov.*? (*ruderatus *Monts ms.)" aufbewahrt. Sie sind blos durch eine viel größere Anzahl von Spiralreifen, welche überdies auch viel gleichmässiger stark sind, zu unterscheiden, sowie durch die relativ minder schlanke Form (Höhe 26 ½, Breite 15 mm.). Ich habe eines dieser Exemplare zum Vergleiche abgebildet (Taf. II, Fig. 42 und 43).*

Von dem echten Fusus craticulatus *Brocchi (=*Hadriana brocchi *Mont.), zu dem ich unser Exemplar vorläufig als Varietät stellen muss, ist dieses aber ebenfalls durch die bedeutend stärker beschuppten Reifen und die geringere Anzahl derselben unterschieden.*

Translation. From station 243 (103 m); 1 specimen.

The shell is 31 ½ mm high and 16 mm wide. A deformation led to doubled development of the siphonal canal. The original siphonal canal is pointed towards the left and forms a deep, umbilicus-resembling funnel, while it is overtopped in length by the secondary siphonal canal to the right.

The mouth opens into the siphonal canal, whose margins never touch each other, is continuously open and 15 ½ mm long. The apex is slightly damaged, seven whorls are preserved.

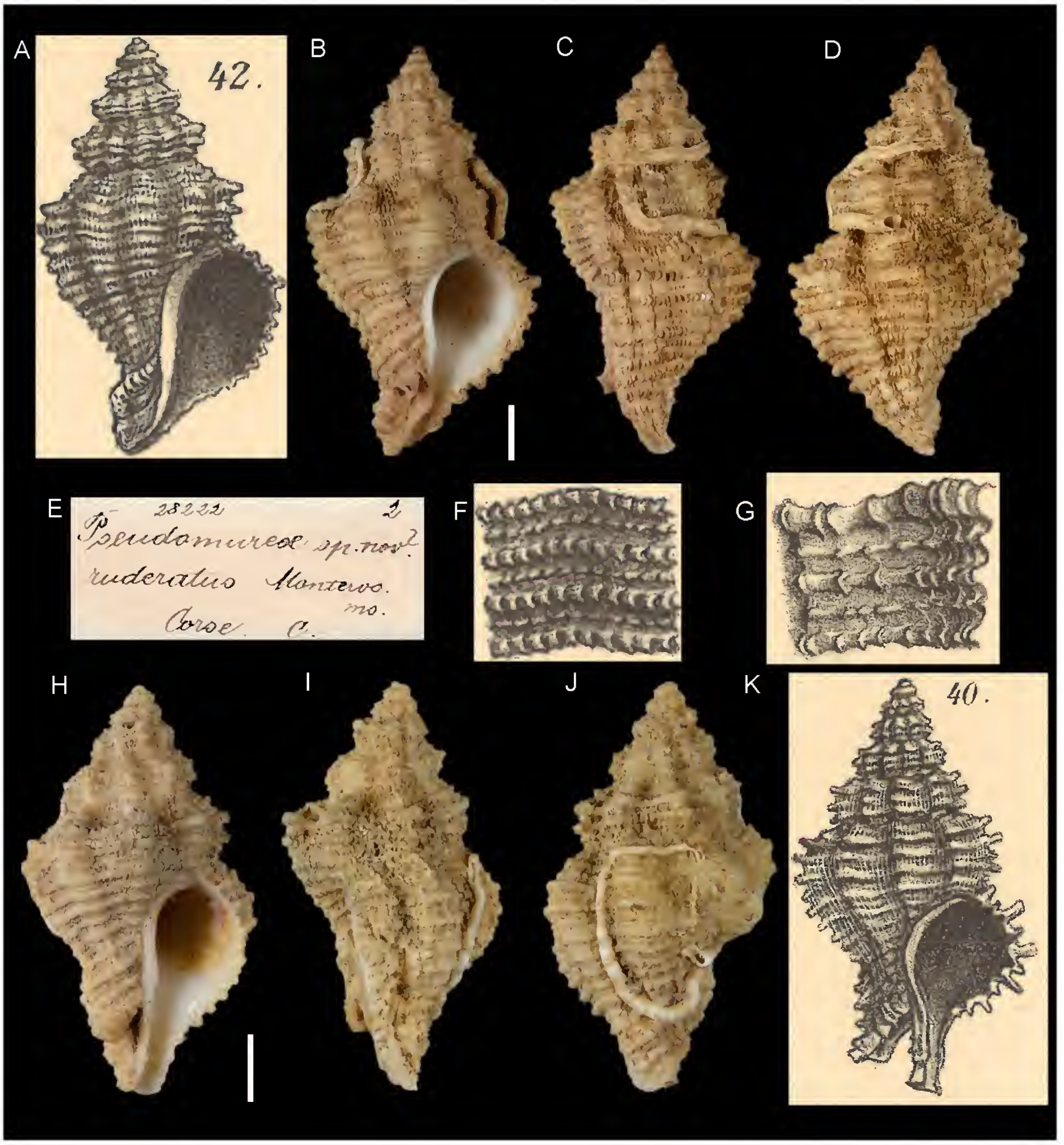

Figure 4. A–F, H–J. *Pseudomurex ruderatus* Sturany, 1896 in Monterosato ms., Corsica, France. Original figures in Sturany, 1896 (**A**, **I**). Specimen NHMW 28222a: front (**B**), side (**C**) and back (**D**) views, original label (**E**). Specimen NHMW 28222b: front (**H**), side (**I**) and back (J) view. **G**, **K**. *Fusus craticulatus* var. *pianosana* Sturany, 1896, Station 243, between Tremiti Islands and Pianosa Isl., Adriatic Sea, Italy, 103 m, original figures in Sturany, 1896. Scale bars: 1 mm.

The sculpture of the whorls resembles those of the coralliophilas; it is accompanied by a number of spiral cords covered unevenly with scales. On the top whorls, there are 3 to 5 such formations which are even and strong (broad) and show only few scales. On the last two whorls, we find considerably more, which alternate quite regularly between stronger (broader) and weaker (narrower) formations. One narrow, scale covered cord is periodically found after two strong spiral stripes. On the last whorls there are varices which are slightly less prominent on the top whorls. The lip is toothed, corresponding to the spiral stripes ending there.

The specimen is too large to be *Coralliophila squamulosa* Phil. (Kobelt, Prodr. p. 15; Carus, Prodr. p. 380) and it has only nine lateral folds on the last whorl, while that species supposedly has 12 to 13. Perhaps though, Mr. March. Monterosato was looking at similar forms when he decided to attribute

Coralliophila squamulosa as a variety of *Murex brocchi,* resp. *Fusus craticulatus* (Monterosato, Nuova Rivista, p. 39).

There are two very interesting specimens stored in the Monterosato collection of the Imperial Museum of Natural History, which resemble the available specimen and are determined as "*Pseudomurex sp. nov*.? (*ruderatus* Monts ms.)". They can be distinguished merely due to a much larger number of spiral stripes, which are also more even in thickness, as well as a relatively less slender shape (height 26 ½ mm, width 15 mm). I have depicted one of these specimens as a comparison (Plate II, Fig. 42 and 43).

However, it is distinguished from the real *Fusus craticulatus* Brocchi *(=Hadriana brocchi* Mont.) by stronger scale coverage on the spiral stripes and a smaller number of those very stripes.

Comments. Sturany introduced the name *pianosana* for a variety of *Fusus craticulatus* Brocchi, 1814 found during the "Pola" expeditions; it has a subspecific rank according to the art. 45.6.4 of the ICZN Code. This name is currently considered a junior synonym of *Hirtomurex squamosus* (Bivona Ant. in Bivona And., 1838) (MolluscaBase 2017).

***Pseudomurex ruderatus* Sturany, 1896 in Monterosato ms.**

Fig. 4A–F, H–J

Sturany 1896: 26, plate II, figures 42–43.

Original locality. Corsica, France (from label accompanying the type material).

Type material. NHMW 28222: 2 syntypes, Corsica, France (Monterosato coll.).

Original description and translation. see *Fusus craticulatus* var. *pianosana*.

Comments. Sturany introduced the name *Pseudomurex ruderatus* on the basis of two shells and a label of the Monterosato collection. He stated the main differences from similar species, illustrated the shells and rendered the name available. This name is currently considered a junior synonym of *Hirtomurex squamosus* (Bivona Ant. in Bivona And., 1838) (MolluscaBase 2017).

Family Fasciolariidae Gray, 1853

***Fusus bengasiensis* Sturany, 1896**
Fig. 5

Sturany 1896: 8, plate I, figures 1–2.

Type locality. Station 36, north of Benghazi, Libya, 32°46'40"N, 19°58'30"E, 680 m.

Type material. Holotype: NHMW 13000, height 45.23 mm.

Original description. *Von Station 36 (680 m); subfossil.*

1 Exemplar von 45 ½ m Länge und 18 ½ mm grösster Breite; die Länge der Mündung beträgt 28 mm, wovon etwa 15 mm auf den oben offenen Stiel kommen, die Breite derselben 9 mm.

Die Spitze des Gehäuses fehlt und nur mehr 6 Windungen sind erhalten. Ein besonders an den untersten Windungen stark hervortretender Kiel verläuft etwas unter der Mitte und bildet überall da, wo er die spärlich vertretenen Querwülste durchkreuzt, von oben nach unten abgeflachte Fortsätze. Die Anzahl derselben richtet sich also nach derjenigen der Querwülste, dies sind 6 auf der letzten Windung und 8–9 auf den übrigen. Ober- und unterhalb des Kieles verlaufen in grösserer Anzahl Spiralreifen, ganz wie bei Fusus rostratus *in der Dicke (Stärke) etwas variabel, aber nicht geschuppt, sondern nur verwischt quergestreift. Die Naht schneidet tief ein. Der Innenrand der Mündung ist über dem Spindelrande in einer zur letzten Windung senkrecht stehenden, wellenförmig geschwungenen Platte losgelöst. Der Stiel ist ein wenig um seine Axe gedreht.*

Auf den ersten Blick möchte man die eben beschriebene Form wohl für eine Varietät von Fusus rostratus *Oliv. halten, doch wäre diese Deutung im Hinblicke auf den unter die Mitte gerückten, exorbitant scharf vortretenden Kiel nicht gerechtfertigt.*

Translation. From station 36 (680 m); subfossil.

One specimen of 45.5 mm length and 18.5 mm greatest width; the mouth is 9 mm wide and 28 mm long, 15 of which belong to the siphonal canal which is open on top. The apex of the shell is missing and only 6 whorls are preserved. A keel which is especially prominent on the lowest whorls runs in the lower half of the whorl and forms two flattened protuberances wherever it crosses the sparse axial ribs. Therefore, the number of these protuberances corresponds to the number of axial ribs, which is 6 at the body whorl and 8–9 at the spire whorls. A greater number of spiral cords run above and below the keel. They vary slightly in thickness, resembling those in *Fusus rostratus*, but without scales and are only poorly transversely ribbed. The suture is deep. The inside of the aperture is loosened above the columellar lip in an undulated callus which is perpendicular to the last whorl. The siphonal canal is bent.

At first appearance, the form described here could be mistaken for a variety of *Fusus rostratus* Oliv., however, this interpretation would not be justified, due to the centred, exorbitantly sharp protruding keel.

Comments. *F. bengasiensis* is considered a junior synonym of *Fusinus rostratus* (Olivi, 1792) (Buzzurro and Russo 2007).

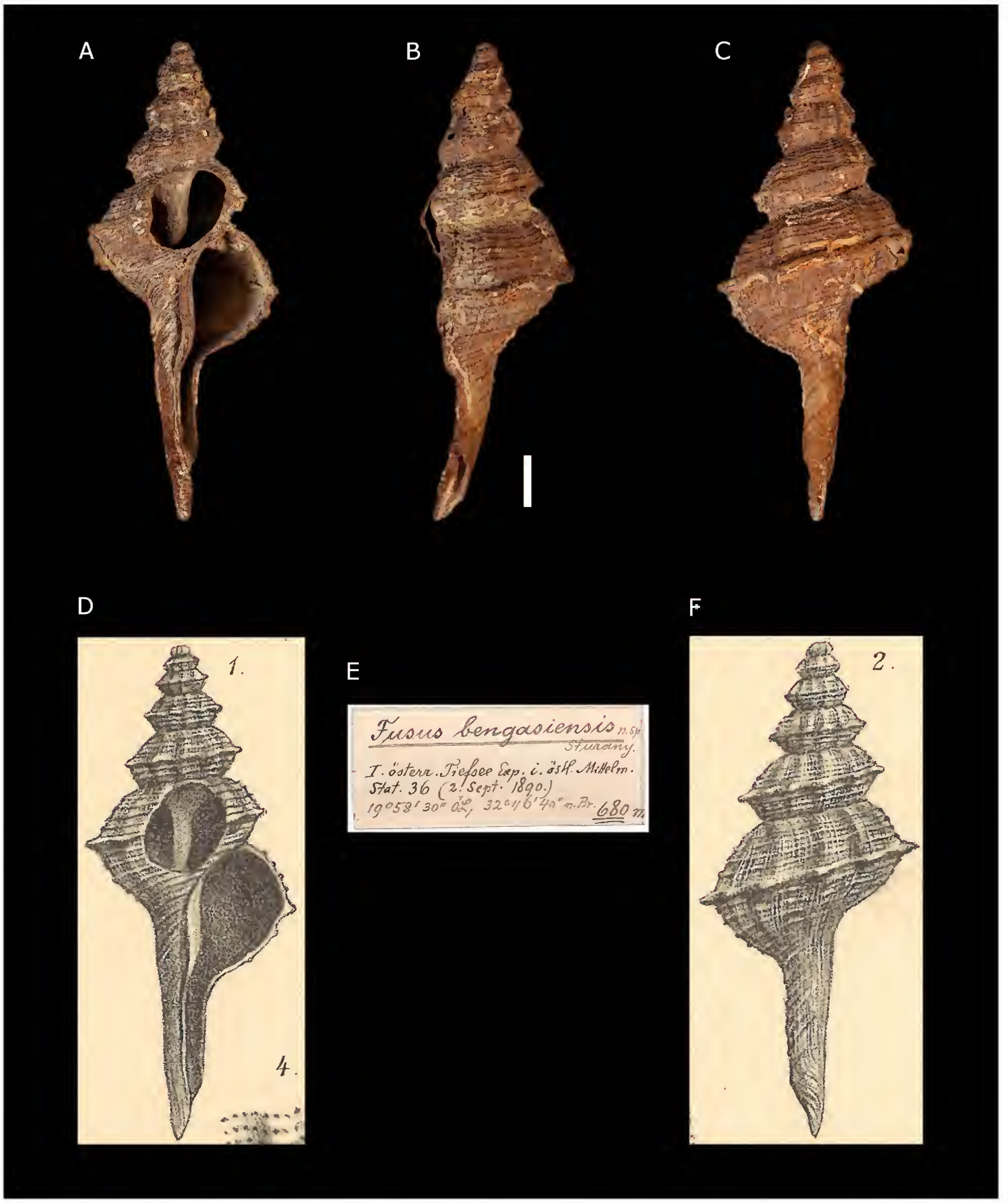

Figure 5. *Fusus bengasiensis* Sturany, 1896, Station 36, north of Benghazi, Libya. **A–C**. Holotype NHMW 13000: front (**A**), side (**B**), and back (**C**) views **E**. Original label. **D**, **F**. Original figures in Sturany, 1896. Scale bar: 5 mm.

Family Marginellidae Fleming, 1828

***Marginella occulta* var. *minor* Sturany, 1896**
Fig. 6

Sturany 1896: 9, not illustrated.

Examined material. NHMW 13012: 2 specimens, station 194. NHMW 99998: 1 specimen, station 36.

Original description. *Von den Stationen 36 (680 m) und 194 (160 m).*

Es liegen von Station 194 zwei Exemplare von 2,3 mm Höhe und 1,7 mm Breite vor, von Station 36 ein größeres mit den Massen 3,1: 2,1 mm. Nur letzteres stimmt mit dem Typus der Art überein, der sich in der Monterosato-Collection des naturhistorischen Hofmuseums befindet, und den dasselbe nur noch in der Grösse übertrifft. (Exemplare von March. Monterosato messen 2,7 mm in der Höhe und 1,7 mm in der Breite.)

Die kleinen Stücke von Station 194 aber dürften zu der bisher nur in coll. bekannt gewordenen M. (Gibberulina) obtusa *Monter. gehören, mit der sie sich in Form und Ausmass ziemlich decken. (Exemplare von Monterosato sind 2,1 – 2,2 mm hoch und 1,6 – 1,7 mm breit.) Doch erscheint es mir nicht empfehlenswerth, eine Species-Trennung vorzunehmen, da die* M. (Gibberulina) obtusa *Monter. schwerlich etwas anderes als eine kleine Varietät der* M. occulta *Monter. ist. (etwa* M. occulta *Monter.* var. minor = M. (Gibberulina) obtusa *Monter. in coll.*).

Translation. From stations 36 (680 m) and 194 (160 m).

There are two specimens (2.3 mm height and 1.7 mm width) available from station 194. A larger specimen (3.1 : 2.1 mm) is available from station 36. Only the latter matches the type specimen in the Monterosato-Collection of the k.k. Naturhistorisches Hofmuseum (Imperial Museum of Natural History) which is merely surpassed in size (specimens of March. Monterosato are 2.7 mm high and 1.7 mm wide).

The small specimens from station 194, however, should belong to *M. (Gibberulina) obtusa* Monter., only known *in coll*., which is rather congruent in form and size (specimens from Monterosato measure 2.1 – 2.2 mm in height and 1.6 – 1.7 mm in width). Still, I do not consider recommendable to separate the species, because *M. (Gibberulina) obtusa* Monter. is hardly anything but a smaller variety of *M. occulta* Monter. (*M. occulta* Monter. var. *minor* = *M. (Gibberulina) obtusa* Monter. in coll.).

Comments. Sturany identified the small specimens from station 194 as *Marginella obtusa* Monterosato, 1878, considered a *nomen nudum* by Gofas (1992). Sturany clearly stated that he considered this species *schwerlich etwas anderes als eine kleine Varietät der* M. occulta [hardly anything but a smaller variety of *M. occulta*] and that *doch erscheint es mir nicht empfehlenswerth, eine Species-Trennung vorzunehmen* [I do not consider recommendable to separate the species]. He used the "var. *minor*" statement only to highlight the small size of these specimens. Such a statement implies that the name is not available (art. 11.5 of the ICZN code).

Family Raphitomidae Bellardi, 1875

Defrancia implicisculpta Sturany, 1896
Fig. 7

Sturany 1896: 12, plate I, figure 10-12.

Type locality. Station 82, north of Alexandria, Egypt, 32°30'N, 29°8'E, 2420 m.

Type material. Holotype: NHMW 13003, height 3.39 mm.

Original description. *von Station 82 (2420 m); 1 Exemplar.*

Das Gehäuse ist spindelförmig, von graubrauner Farbe und besitzt 6 ½, Umgänge, wovon beinahe 4 auf das sogenannte Embryonalgewinde entfallen. Dieses zeigt, allerdings nur stellenweise, ein fein gegittertes Netzwerk (Fig. 12), während auf den 2 ½ unteren Windungen eine hiervon ganz verschiedene Sculptur (Fig. 11) auftritt. Unterhalb der Naht nämlich liegt ein schmaler, concaver Theil mit vielen bogenförmigen Querstrichen, und auf diesen folgt, durch 1 oder 2 Spirallinien gleichsam abgetrennt, der übrige Theil der Umgangsbreite. Dieser ist convex und trägt derbe Querrippen oder Querwülste (10 auf dem vorletzten, 12 auf dem letzten Umgange), durchkreuzt von ziemlich starken Spiralreifen (3 auf dem vorletzten und 6 auf dem letzten Umgange). Die Mündung ist birnförmig, hat oben am Aussenrande einen kleinen Ausschnitt und ist unten in den Stiel ausgezogen, um welchen ebenfalls einige Spiralreifen verlaufen.

Höhe des Gehäuses 3,5, Breite desselben 2,0 mm; Höhe der Mündung samt Stiel 2 mm.

In der Gestalt ist diese neue Art ähnlich der Defrancia cordieri *Payr. (Kobelt Prodr, p. 143) und deren verwandten Formen, für welche Monterosato die Gattung* Cordieria *aufstellt, und auch mit einer noch nicht publizierten Art, mit* Cordiera hispida *Mont. in coll., welche mir aus der Sammlung des Hofmuseums zum Vergleiche vorliegt, zeigt sie vielfach Ähnlichkeit, doch scheint sie schon durch ihre geringen Dimensionen genügend charakterisiert und unterschieden zu sein.*

Translation. From station 82 (2420 m); 1 specimen.

The gray brown shell is fusiform and has 6 ½ whorls, almost 4 of which belonging to the so-called protoconch. This shows, in some parts, a finely reticulated sculpture (Fig. 12), while on the lower 2 ½ whorls there is a completely different sculpture (Fig. 11). Below the suture lies a slender, concave part with many arched axial lines, which is followed by the remaining part of the whorl's width, separated by 1 or 2 spiral lines. This remaining part is convex and is provided with solid axial ribs (10 on the penultimate, 12 on the last whorl), crossed by rather strong spiral stripes (3 on the penultimate, 6 on the last whorl). The aperture is pear-shaped with a small opening on the upper outer edge and is elongated downwards and blended into the siphonal canal, which is also ornamented by some spiral stripes.

The length of the shell is 3.5 mm, the width 2 mm, and the height of the aperture with the siphonal canal 2 mm.

In its form, this new species resembles *Defrancia cordieri* Payr. (Kobelt Prodr, p. 143), as well as its related forms for which Monterosato establishes the genus of *Cordiera*. It also shows multiple similarities to an unpublished species to date, *Cordiera hispida* Mont. in coll., which is available to me as an object of comparison from

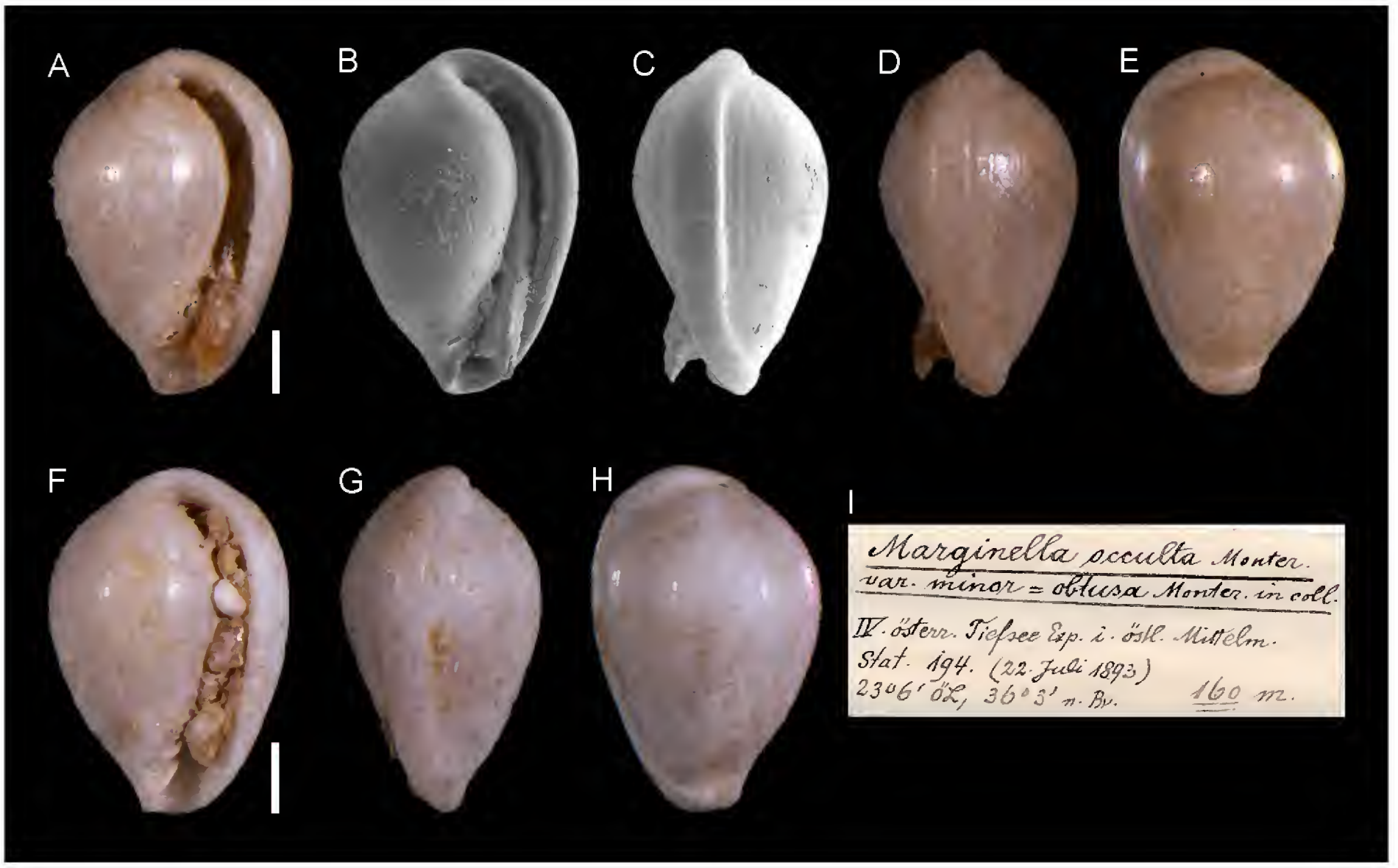

Figure 6. *Marginella occulta* var. *minor* Sturany, 1896, Station 194, between Kythira and Antikythira, Ionian Sea, Greece, 160 m. **A–E**. NHMW 13012: front (**A–B**), side (**C–D**) and back (**E**) views. **F–H**. NHMW 13012: front (**F**), side (**G**) and back (**H**) views. **I**. Original label. Scale bars: 0.5 mm.

the museum collection. However, it seems that the characterization and distinction can be made sufficiently due to its smaller dimensions.

Comments. Currently considered a junior synonym of *Pleurotomella eurybrocha* (Dautzenberg & Fischer, 1896) (Bouchet and Warén 1980).

Raphitoma nuperrima var. corallinoides Sturany, 1896 and var. pseudacanthodes Sturany, 1896
Fig. 8
Sturany 1896: 10-11, plate I, figure 6 (var. pseudacanthodes) and 7 (var. corallinoides).

Type locality. var. *corallinoides*: Station 36, north of Benghazi, Libya, 680 m. var. *pseudacanthodes*: Station 1, west of Corfu, Greece, 615 m; Station 213, north of Astypalaia, Dodekanese, Greece, 597 m.

Type material. var. *corallinoides*: Holotype: NHMW 13013, height 7.27 mm; var. *pseudacanthodes*: NHMW 13014: 1 syntype, station 1; NHMW 13015: 9 syntypes, station 213.

Original description. *Von den Stationen 1, 36, 213 (597–680 m), und zwar von den ersteren je 1 Exemplar, von der letzteren eine grössere Anzahl.*

Auf die Beschreibungen, welche von dieser Art in der Literatur zu finden sind, passen die Exemplare der österreichischen Tiefsee-Expeditionen recht gut, mit den bis jetzt vorhandenen Abbildungen harmonieren sie weniger.

Es soll gezeigt werden, dass nicht alle der vorliegenden Exemplare dem Typus angehören, und deshalb ist es zunächst notwendig, einige Beispiele über Massverhältnisse anzuführen.

[A table with the sizes of the collected specimens follows]

Also nur 1 Exemplar erreicht annähernd die in der Literatur als typisch angegebene Höhe von 12 mm, alle übrigen sind von weit kleineren Dimensionen. Ferner zeigen sie mit Ausnahme von 2 Exemplaren, auf die ich unten als Typen noch zurückkomme, alle eine nicht blos absolut, sondern auch relativ geringe Gehäusebreite als der Typus, der mir in einem leider zerbrochenen ausgewachsenen und einem unfertigen Exemplare aus der Monterosato-Sammlung zum Vergleiche vorliegt. Dieser Typus weist auch eine viel grössere Anzahl von Spiralrippen und Spiralstreifen, welche auf allen Windungen markant hervortreten, auf, während bei unseren Exemplaren die Rippen von der vorletzten Windung bis hinauf zum Embryonalgewinde nur in der Zweizahl vorhanden sind und eine schwache Kante bilden, wie dies bei Pleurotoma (Mangelia) acanthodes *Wats. der Fall ist. Mit dieser von den Bermudas-Inseln und den Azoren stammenden Art haben unsere Exemplare auch die Dimensionen vollständig übereinstimmend, ferner die Skulptur des Embryonalgewindes, und streng genommen besteht eine Verschiedenheit unserer Exemplare von* acanthodes *Wats.*

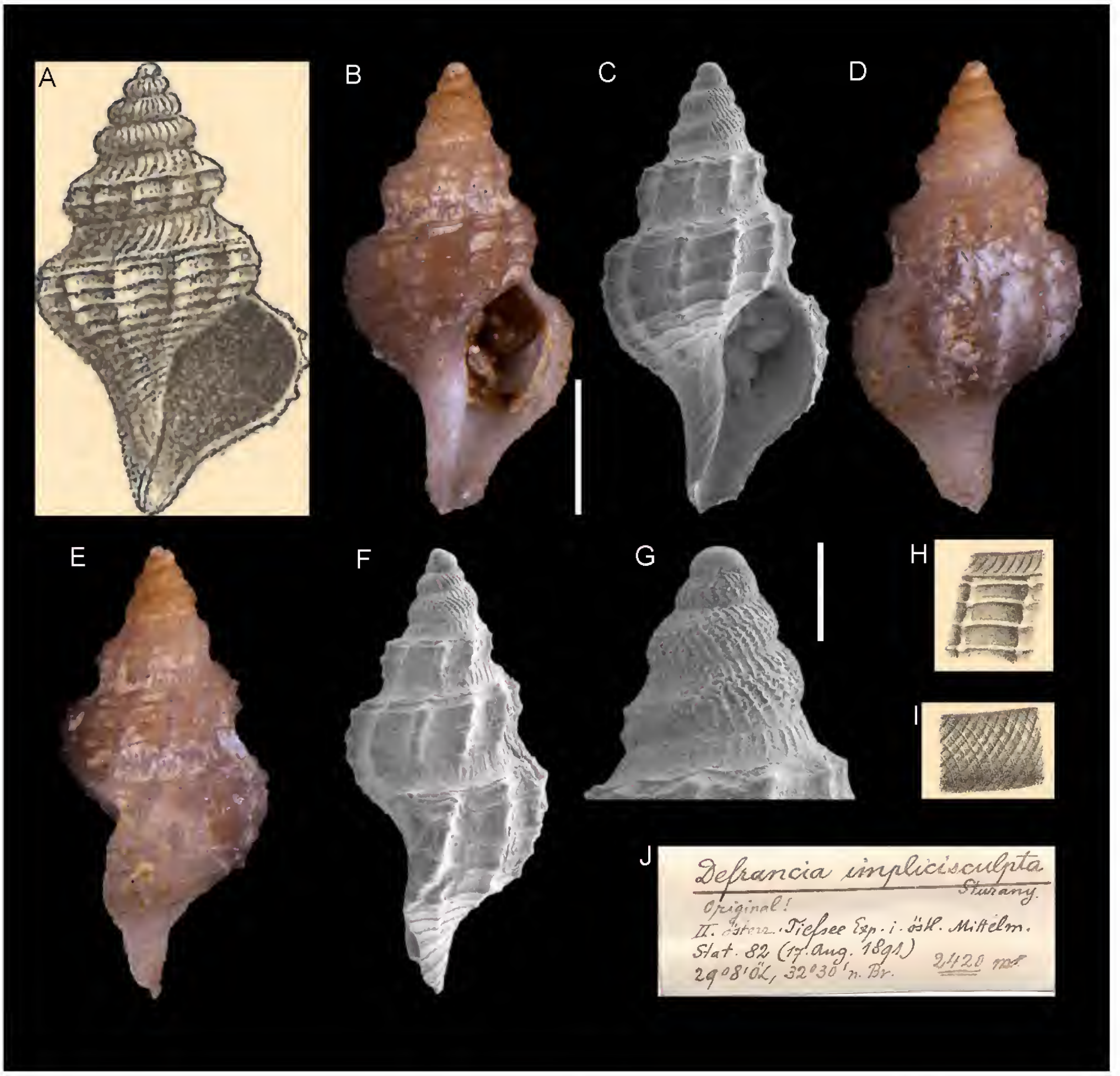

Figure 7. *Defrancia implicisculpta,* Sturany, 1896, station 82, north of Alexandria, Egypt, 2420 m. **A**, **H**, **I**. Original figures in Sturany, 1896. **B–G**. Holotype NHMW 13003: front (**B–C**), back (**D**), side (**E–F**) views and microsculpture (**G**). **J**. Original label. Scale bars: 1 mm (**B–F**), 0.3 mm (**G**).

eigentlich nur in ihrer reichlicheren Körnchensculptur, d. h. zwischen den Spiralrippen der letzten Windung stehen weit mehr Reihen von Punkten oder Körnchen als bei acanthodes, *und ober der ersten Rippe des letzten Umganges, also zwischen ihr und der Naht, 10 bis 12 solcher Reihen. Wegen dieser grossen Ähnlichkeit der Mehrzahl der gesammelten Exemplare mit der Watson'schen Art möchte ich sie von* Raphitoma nuperrima Tib. *als* nov. var. pseudacanthodes *trennen, und dazu das grosse Exemplar von Station 1 (Fig. 6), sowie von Station 213 alle mit Ausnahme jener zwei Exemplare rechnen, welche ich gleich bei der Besprechung der Gehäusebreite ausgenommen habe. Diese muss ich, da sie, wie gesagt, relativ breiter sind, und da sie ferner mehr Spiralrippen besitzen (nämlich circa eben so viel wie die echte* nuperrima *in der Monterosato-Collection des Hofmuseums) als* Raphitoma nuperrima Tib. typ. *isolieren (Fig. 5). Leider sind sie nicht erwachsen.*

Schliesslich ist aber auch das Exemplar von Station 36, welches sich dadurch auszeichnet, dass zwischen den Spiralrippen 1 und 2 auf dem letzten Umgang ein grösserer Zwischenraum ist, als eine besondere Varietät zu bezeichnen, und zwar mit einer zweiten Watson'schen Art, mit Pleurotoma (Mangelia) corallina. *von Westindien zu vergleichen, weshalb ich sie als* nov. var. corallinoides *auffühe (Fig. 7).*

Translation. From stations 1, 36, 213 (597–680 m), one specimen from each of the first two stations and a larger number from the latter station.

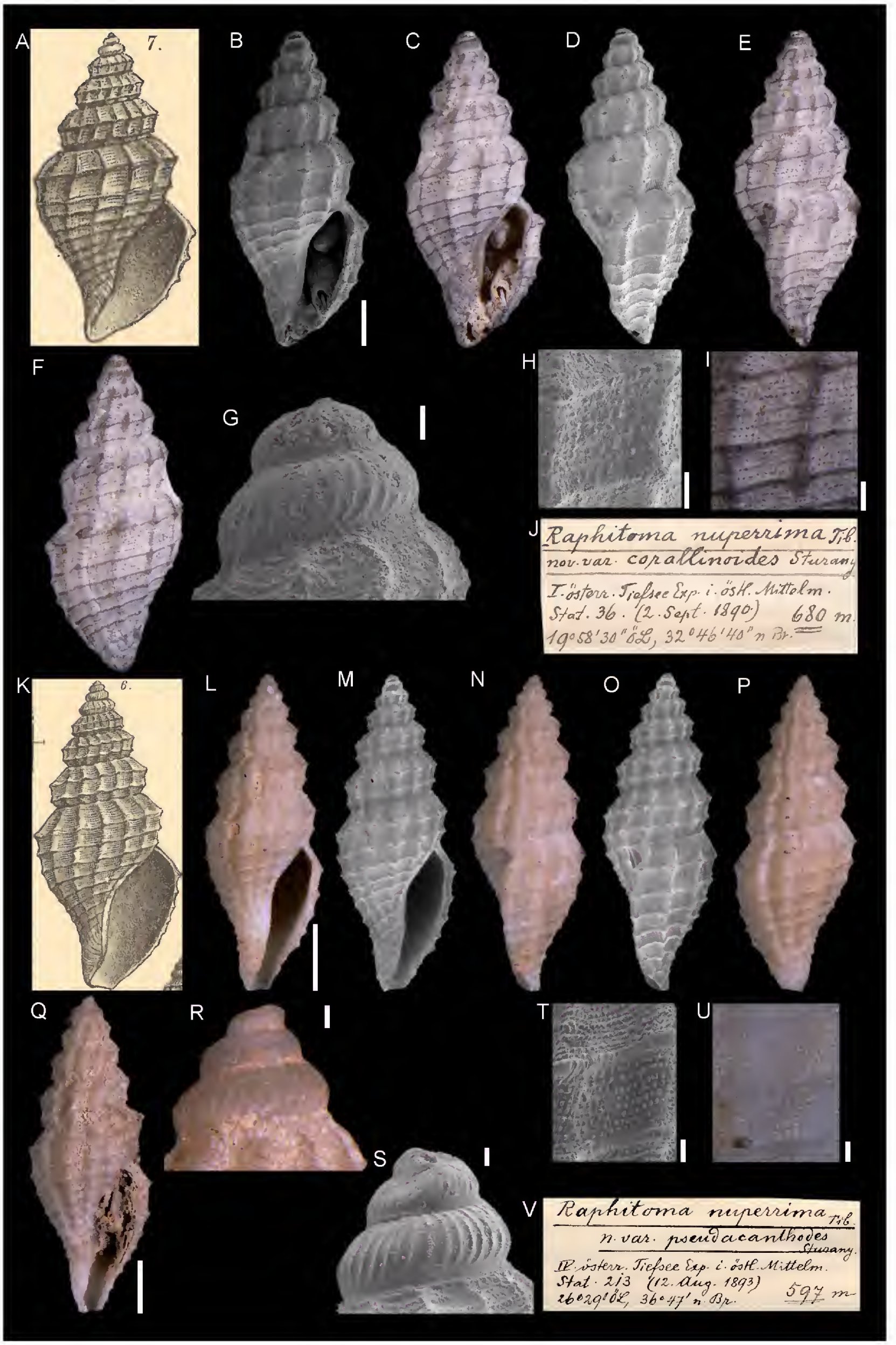

Figure 8. A–J. *Raphitoma nuperrima* var. *corallinoides* Sturany, 1896, holotype NHMW 13013, Station 36, north of Benghazi, Libya, 680 m: original figure in Sturany, 1896 (**A**), front (**B–C**), side (**D–E**) and back (**F**) views, apex (**G**), microsculpture (**H–I**), original label (**J**). **K–P**, **T–V**. *Raphitoma nuperrima* var. *pseudacanthodes* Sturany, 1896, syntype NHMW 13014a, Station 213, north of Astypalaia, Sporades, Greece, 597 m: original figure in Sturany, 1896 (**K**), front (**L–M**), side (**N–O**) and back (**P**) views, microsculpture (**T–U**), original label (**V**). **Q–R**. *Raphitoma nuperrima* var. *pseudacanthodes* Sturany, 1896, syntype NHMW 13014b (same locality as 13014a): front (**Q**), apex (**R–S**). Scale bars: 1 mm (**B–F**, **L–Q**); 0.1 mm (**G**, **R–U**); 0.2 mm (**H–I**).

The specimens of the Austrian deep-sea expedition fit the descriptions currently found in the literature rather well; however, they poorly match the available figures.

It shall be demonstrated that not all of the presented specimens belong to the type, and it is therefore necessary to give some information on the dimensions. Only one specimen reaches the size of 12 mm described in the literature as typical height, all the rest are of far smaller dimensions. Furthermore, with the exception of two specimens, they show a smaller shell not only in absolute terms but also in relation to the type which is available to me as an object of comparison, unfortunately in the form of a broken and juvenile specimen from the Monterosato collection. This type also shows a greater number of prominent spiral ribs and stripes on all whorls, while our specimens show only two ribs from the penultimate whorl upwards to the protoconch, which forms a slight edge, much as it is the case in *Pleurotoma (Mangelia) acanthodes* Wats. Our specimens also correspond completely with this species from the Bermuda Islands and Azores in dimensions, sculpture of the protoconch. Strictly speaking, there is no difference between our specimens and *acanthodes* Wats., except for its richer tubercled sculpture, i.e., between the spiral cords of the last whorl, there are much more rows of granulose structures than there are in *acanthodes*, and above the last rib of the last whorl, namely between it and the suture, there are 10 to 12 such cords. Because of that great similarity of the majority of the collected specimens with Watson's species, I would like to separate it from *Raphitoma nuperrima* Tib. as nov. var. *pseudacanthodes* and include the large specimen from Station 1 (Fig. 6), as well as all those retrieved from station 213 with the exemption of those 2 specimens which I excluded from the review of shell sizes. As mentioned above, I have to isolate them as *Raphitoma nuperrima* Tib. *typ.* (Fig. 5), because they are relatively broader and possess more spiral ribs (approximately as many as the real *nuperrima* in the Monterosato collection of the Imperial Museum). Unfortunately, they are juveniles.

Finally, also the specimen retrieved from station 36 must be designated a remarkable variety. It distinguishes itself by a greater gap between spiral ribs 1 and 2 on the last whorl and must be compared to a second species by Watson, *Pleurotoma (Mangelia) corallina* from the West Indies, which is why I mention it as *nov. var. corallinoides* (Fig. 7).

Comments. Both taxa were considered junior synonyms of *Bela nuperrima* (Tiberi, 1855) (Bouchet and Warén 1980, MolluscaBase 2017) but more likely belong to *Kurziella serga* (Dall, 1881) (S. Gofas, pers. comm. November 2017).

Taranis alexandrina Sturany, 1896

Fig. 9

Sturany 1896: 11-12, plate I, figure 8–9.

Type locality. Station 82, north of Alexandria, Egypt, 32°30'N, 29°8'E, 2420 m.

Type material. Holotype: NHMW 13002, height 3.40 mm.

Original description. *Von Station 82 (2420 m); 1 Schale mit unfertiger Mündung.*

Gehäuse hellbraun, ziemlich dickschalig, aus 5 Umgängen bestehend. Das Embryonalgewinde (1 ½ Windungen) hat eine etwas rauhe Oberfläche, aber keine deutliche Sculptur. Ziemlich unvermittelt beginnt auf der zweiten Umdrehung die von da ab bis zur Mündung scharf ausgeprägte Querrippung. Die Querrippen sind eng aneinandergelagert, durch einen ober der Mitte verlaufenden Spiralkiel gewinkelt und außerdem von einigen Spiralreifen durchkreuzt. Ein solcher, allerdings nur schwach ausgeprägter Spiralreifen zieht gleich unter der Naht dahin; er ist aber nur auf den letzten zwei Umgängen gut kenntlich. Ferner verlaufen auf dem vorletzten Umgange 2 Spiralreifen unter dem Kiele und auf dem letzten Umgang zwischen Kiel und Nabel deren 6 bis 7. Hier entsteht durch die Querrippung und Spiralstreifung ein Maschenwerk aus schiefgestellten Vierecken oder Quadraten, in denen da und dort eine Körnchensculptur angedeutet ist, was sich aber nur bei stärkerer Lupenvergrösserung sehen lässt.

Von den erwähnten Querrippen kommen auf je einen Umgang 22 bis 26 zu stehen.

Die Mündung, leider schadhaft, hat eine birnförmige Gestalt, einen nach links gedrehten, kurzen, ausgussartigen Stiel und einen vermutlich auch im ausgewachsenen Zustande scharfen, äußeren Rand. Der Spindelrand ist breit nach links ausgeschlagen und bedeckt einen ritzförmigen Nabel fast ganz.

Höhe des Gehäuses 3,5, Breite 2, Höhe der Mündung 1,7 mm. Dass das vorliegende Exemplar mit Taranis cirrata Brugn. *(Kobelt Prodr., p. 137) verwandt und in das seinem Ursprunge nach nordatlantische Genus* Taranis *zu stellen ist, davon bin ich nicht vollständig überzeugt; darüber wird sich wohl noch streiten lassen. Es ist kleiner als* Taranis cirrata *und hat um eine Umdrehung weniger; ferner tritt ein Spiralreifen deutlich als Kiel hervor, während die anderen schwächeren zurücktreten. Im Ganzen stimmt wohl die Anzahl der Spirallinien, ob sie nun kielartig oder nur reifenförmig auftreten, bei beiden Formen überein, und auch die Anzahl der Querrippen dürfte dieselbe sein wie bei* Taranis citrrata, *aber wir sehen in den genannten abweichenden Merkmalen und besonders in der Gestaltung der Spindel wichtige Unterschiede.*

Translation. From station 82 (2420 m); 1 specimen with incomplete aperture.

Light brown shell, fairly thick, consisting of 5 whorls. The protoconch (1 ½ whorls) has a somewhat rough surface, but no distinct sculpture. Quite suddenly, sharply pronounced axial ribbing appear at the second whorl and continue until the aperture. The axial ribs are embedded closely together and angled by a central spiral keel and, moreover, crossed by several spiral threads. Such threads, though pronounced only weakly, are already visible right beneath the suture; however, they are only well distinguishable on the

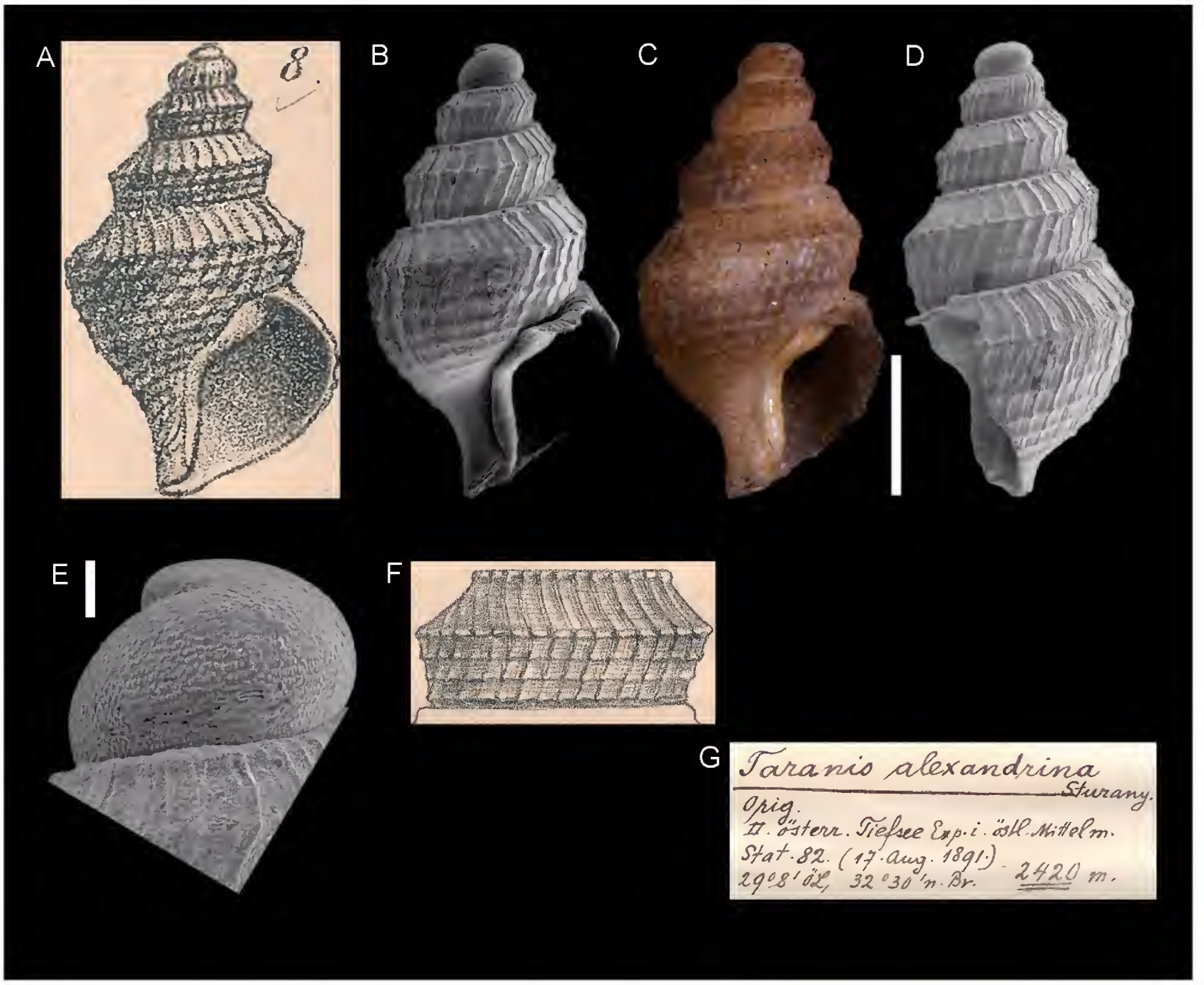

Figure 9. *Taranis alexandrina,* Sturany, 1896, station 82, north of Alexandria, Egypt, 2420 m. **A–F**. Holotype NHMW 13002: original figures in Sturany, 1896 (**A**, **F**), front (**B–C**) and side (**D**) views, apex (**E**). **G**. Original label. Scale bars: 1 mm (**B–D**); 0.1 mm (**E**).

last two whorls. Furthermore, at the body whorl there are 2 spiral stripes beneath the keel and 6 to 7 on the ultimate whorl between keel and umbilicus. As a result of the axial ribbing and spiral stripes, there is a network of slanted rectangles or squares with a hint of a granular sculpture here and there, which is only visible at higher magnification.

Each whorl is equipped with 22 to 26 of the previously mentioned axial ribs.

The unfortunately damaged aperture is pear shaped and has a leftwards rotated, short, nozzle-shaped siphon and a, likely also in the mature state, sharp outer edge. The columella is broadly lashed out towards the left and covers a scar-formed umbilicus almost completely.

Height of the shell 3.5, width 2, aperture height 1.7 mm. I am not entirely convinced that the present specimen is related to *Taranis cirrata* Brugn. (Kobelt Prodr., p. 137) and according to its origin must be placed within the north Atlantic genus *Taranis*. Perhaps this will be further discussed. It is smaller than *Taranis cirrata* and has one whorl less. Furthermore, a spiral stripe is distinctly pronounced as a keel, while the other fainter ones recede. On the whole, probably only the number of spiral lines concur in both forms, whether they appear as a keel or only ring-formed, and also the number of axial ribs seems to be the same as in *Taranis cirrata*, however, we see important differences in the aforementioned traits and especially in the shaping of the columella.

Comments. Considered a junior synonym of *Taranis moerchii* (Malm, 1861) (Bouchet and Warén 1980).

Family Mytilidae Rafinesque, 1815

***Myrina modiolaeformis* Sturany, 1896**
Fig. 10

Sturany, 1896: 20, plate II, figures 34–38.

Original locality. Station 82, north of Alexandria, Egypt, 32°30'N, 29°8'E, 2420 m.

Type material. NHMW 13011: 2 syntypes (1 right and 1 left valve), station 82.

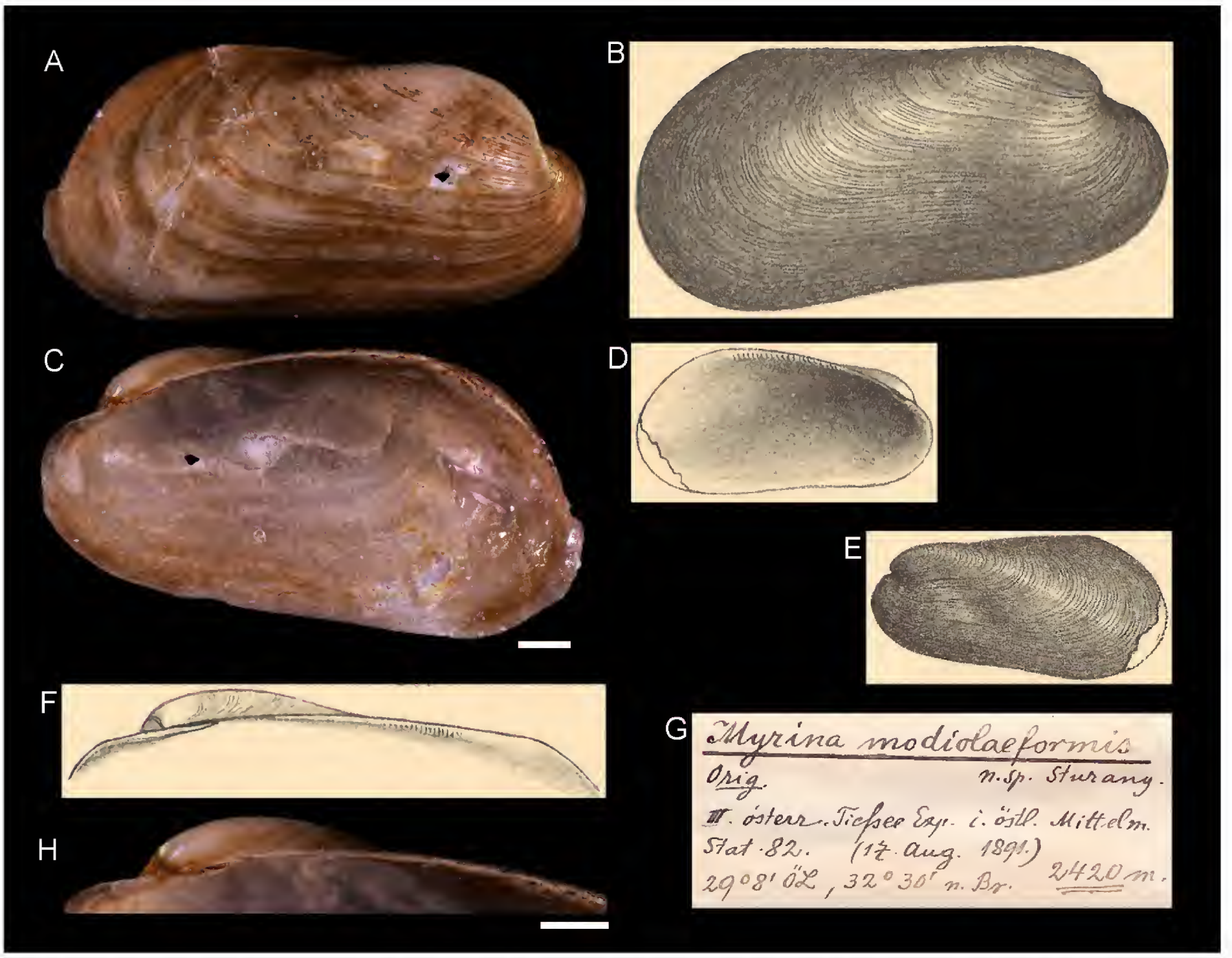

Figure 10. *Myrina modiolaeformis* Sturany, 1896, station 82, north of Alexandria, Egypt, 2420 m. **A**, **C**, **H**. Syntype NHMW 13011a: outer (**A**) and inner (**C**) view, hinge (**H**). **B**, **D–F**. Original figures in Sturany, 1896. **G**. Original label. Scale bars: 1 mm.

Original description. *Von Station 82 (2420 m).*

Es liegt nur eine rechte Schale von 13 mm Länge, 6,7 mm Höhe und 3,2 mm Breite (Dicke) vor, sowie von einem zweiten bedeutend kleineren (ungefähr nur halb so großen) Exemplare die linke Schalenhälfte (Länge 6,8, Höhe 3,5 mm). Die Schalen sind aussen bis auf den Wirbel, der sich weisslich abhebt, nahezu einfarbig hellgelb, innen etwas perlmutterglänzend. Die concentrische Streifung der Aussenseite ist etwas unregelmässig, indem einzelne Streifen stärker hervortreten. Der Wirbel liegt weit nach vorne gerückt, im ersten Fünftel oder Sechstel der Schale. Der hintere Oberrand verläuft bis zu seinem gerundeten Übergang in den Hinterrand ganz gerade. Rückwärts bedeutend höher als vorne gebaut, hat die Schale in ihren Umrissen ungefähr die Gestalt von Modiola (Gregariella) sulcata Risso.

Was mich veranlasste, diese höchst eigenthümlich gestaltete neue Muschel zu dem exotischen Genus Myrina *zu beziehen, ist die Querstrichelung auf der inneren Schlossleiste, wodurch diese wie mit einer grossen Anzahl kleiner, senkrecht gestellter und dicht aneinander gereihter Zähnchen besetzt erscheint. Die grosse rechte Schalenhälfte weist nur hier und dort die verwischten Spuren dieser zahnartigen Striche auf, während sie die linke Schale des zweiten Exemplares unter stärkerer Lupenvergrösserung deutlich erkennen lässt, Hier sind die Querstriche nicht blos auf die hintere Schlossleiste beschränkt, sondern stehen auch direkt unter dem Wirbel auf einem zahnartigen Vorsprung, also ungefähr dort, wo der vordere Oberrand entspringt, ganz ähnlich wie bei der im Challenger-Werk (E. Smith, Lamellibr., pl. XVI, fig. 9) abgebildeten* Myrina coppingeri *Wats. von Nord-Australien.*

Die Zugehörigkeit der hier beschriebenen Muschel zu dem Genus Myrina *ist trotz der angeführten Schlossmerkmale nichts weniger als erwiesen und hierrüber sicher noch nicht das letzte Wort gesprochen.*

Translation. From station 82 (2420 m).

There is only one right valve of 13 mm in length, 6.7 mm in height and 3.2 mm in width (thickness), as well as a left valve of a remarkably smaller (approximately only half the size) specimen (length 6.8, height 3.5 mm). The shells are nearly monochrome yellow, except for the umbo which stands out whitish, and shine lightly of mother-of-pearl on the inside. The concentric stripes on the outside

are slightly irregular, as single stripes stand out more prominent. The umbo is moved far to the front, within the first fifth or sixth of the shell. The rear upper margin is shaped completely straight until its rounded transition into the posterior margin. Being built significantly higher at the posterior than at the anterior, the shell in its outline has roughly the shape of *Modiola (Gregariella) sulcata* Risso. The axial sketchy lining at the hinge margin, which makes it appear as a set with a large number of smaller, vertically and tightly arranged teeth, caused me to place this very peculiarly shaped new bivalve within the exotic genus *Myrina*. The large right valve shows smeared tracks of these teeth-like lines only here and there, while they are clearly visible under higher magnification in the left valve of the second specimen. Here, the axial lines are not limited to the posterior part of the hinge plate, but are also visible directly beneath the umbo on a tooth-like structure, approximately at the position of the beginning of the anterior upper margin, very similar to *Myrina coppingeri* Wats from northern Australia, depicted in the Challenger work (E. Smith, Lamellibr., pl. XVI, fig. 9).

In spite of the mentioned hinge characters, the belonging of the described bivalve to the genus *Myrina* is no less than evident and the last word has certainly not been spoken yet.

Comments. A valid species placed in genus *Idas* (MolluscaBase 2017) recently recorded from cold seep communities in the deep eastern Mediterranean Sea (Olu-Le Roy et al. 2004).

Family Lucinidae J. Fleming, 1828

***Lucina amorpha* Sturany, 1896**
Fig. 11

Sturany, 1896: 16, plate I, figure 22.

Type locality. Station 82, north of Alexandria, Egypt, 32°30'N, 29°8'E, 2420 m.

Type material. Holotype: NHMW 13008 (a right valve), height 9.58 mm, length 10.40 mm.

Original description. *Von Station 82 (2420 m); eine rechte Schalenhälfte.*

Die vorliegende Schale scheint auf den ersten Blick wohl der Lucina spinifera *Mont. (Kobelt Prodr. p. 369; Carus Prodr. p. 152) anzugehören und ein deformiertes Exemplar zu sein unterscheidet sich aber doch wesentlich in folgenden Punkten:*

1. Das Möndchen (lunula) ist hier eine schmale, aber tiefe Grube; daher der Umriss der Schale ein ganz anderer als bei Lucina spinifera. *2. An der Grenze von Unter- und Hinterrand schneidet eine breite winkelige Bucht tief in die Schale und setzt sich bis zur Mitte der Schalenhöhe radial als Konkavität fort (ähnlich wie im Genus* Axinus*). Im Inneren der Schale entspricht dieser Einsenkung von außen eine bauchige Verdickung. 3. Die Anzahl der konzentrischen Streifen (Rippen), welche schwächer sind und näher aneinander gerückt stehen als bei* L. spinifera, *beträgt ca. 66 (gegen ca. 40 bei* L. spinifera*). 4. Der hintere Oberrand zieht vom Wirbel in leichtem konvexen Bogen nach hinten und unten und lässt eine Reihe von schwachen Höckern, die Endigungen der konzentrischen Streifen, erkennen. Doch endigt nicht jeder Streifen, sondern etwa bloß jeder zweite mit einem solchen Höcker.*

Das Schloss stimmt vollständig mit dem von L. spinifera *überein, und auch der Wirbel ist wie dort glatt und nach vorne und innen geneigt. Die Farbe ist nahezu rein weiß, die Wölbung der Schale eine schwache. Die Länge der Schale beträgt 11, die Höhe 9,5 mm.*

Translation. From station 82 (2420 m); one right valve.

At a first glance, the shell at hand seems to be perhaps a deformed specimen belonging to *Lucina spinifera* Mont. (Kobelt Prodr.p. 369; Carus Prodr. p. 152), but is after all clearly distinguished regarding the following points:

1. The lunula, in this case, is a narrow but deep cavity, therefore the outline of the shell is quite a different one than in *Lucina spinifera*. 2. At the boundary between ventral and posterior margin, a broad, cornered cove cuts deep into the shell and continues radially as a concavity (similar to the genus *Axinus*) further to the middle of the shell height. On the inside of the shell, this depression corresponds to a bulbous thickening from the outside. 3. The number of concentric ridges, which are fainter and stand closer together than in *L. spinifera*, amounts to approximately 66 (compared to about 40 in *L. spinifera*). 4. The posterior upper margin runs from the umbo back- and downwards in a slightly convex curve and bears a row of faint humps at the endings of the concentric lines. However, not each one of these lines, but only approximately every second one, ends in such a hump.

The hinge is identical to that of *L. spinifera*, and also the umbo is smooth and tilted forwards and inwards as it is there. The colour is nearly clear white, the curvature of the shell is weak. The length of the shell is 11, the height 9.5 mm.

Comments. Currently accepted as *Myrtea amorpha* (Sturany, 1896) (MolluscaBase 2017) and recently recorded from cold seep communities in the deep eastern Mediterranean Sea (Olu-Le Roy et al. 2004). Its shape is totally unusual for lucinids and is indeed due to an accident during growth.

Family Thyasiridae Dall, 1900

***Axinus flexuosus* var. *striatus* Sturany, 1896**
Fig. 12

Sturany 1896: 17, plate I, figures 23.

Type locality. Station 82, north of Alexandria, Egypt, 32°30'N, 29°8'E, 2420 m.

Type material. Holotype: NHMW 13009 (a right valve), height 7.09 mm, length 7.37 mm.

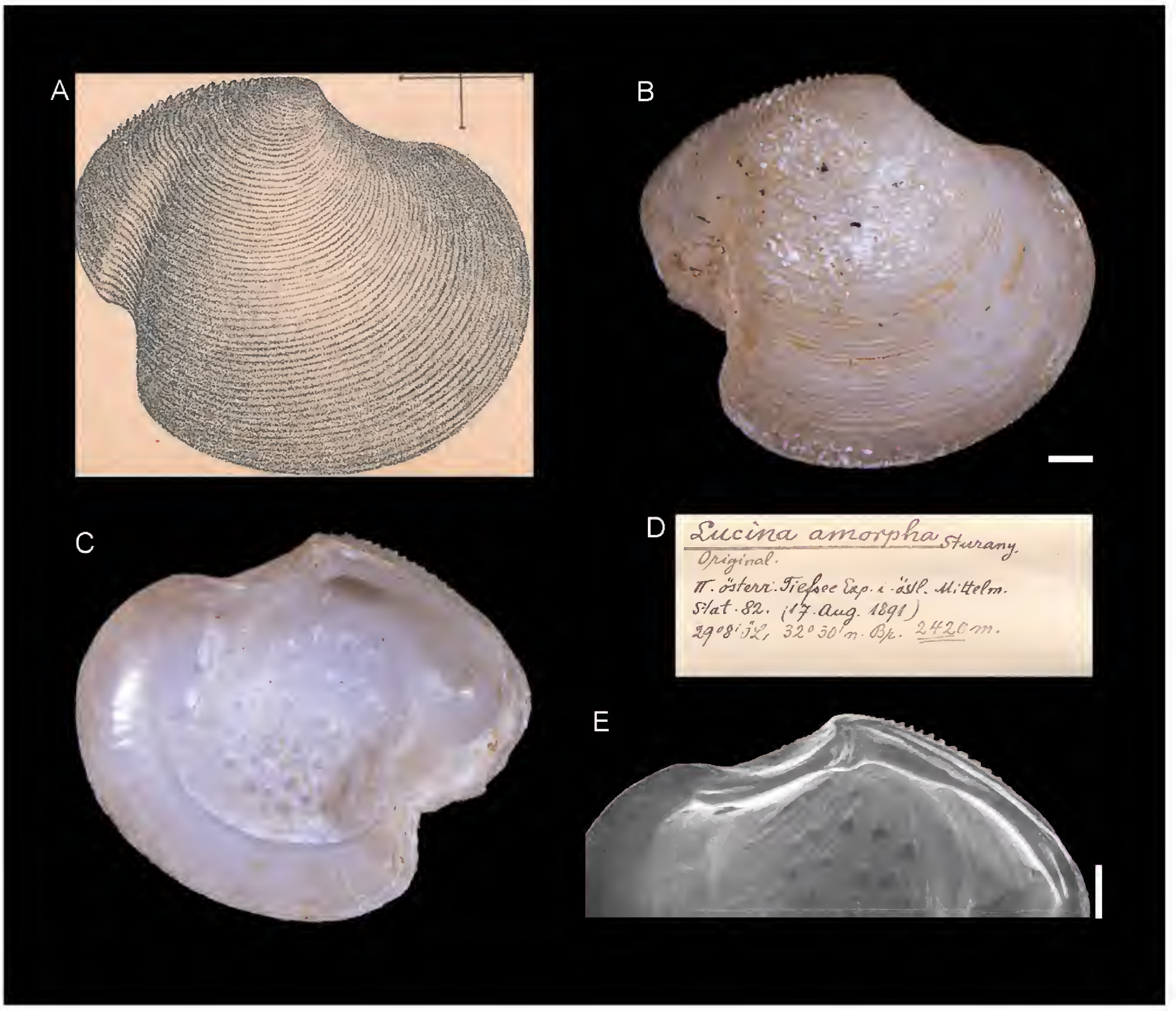

Figure 11. *Lucina amorpha* Sturany, 1896, station 82, north of Alexandria, Egypt, 2420 m. **A**. Original figure in Sturany, 1896. **B**, **C**, **E**. Holotype NHMW 13008: outer (**B**) and inner (**C**) views, hinge (**E**). **D**. Original label. Scale bar: 1 mm.

Original description. *Von Station 82 (2420 m.); eine rechte Schalenhälfte.*

Die stärkere concentrische Streifung der Schale, die noch weiter als im Typus nach vorne gerückte Stellung des Wirbels und der weniger gewölbte Unterrand zwingen zur Abtrennung der Form als eine Varietät von Axinus flexuosus *Mont. und verrathen auch eine gewisse Verwandtschaft mit der bisher nur im Norden gefundenen* Axinus sarsii *Phil. – Die Länge der Schale beträgt 7,5, die Höhe 7 mm.*

Translation. From station 82 (2420 m); one right valve.

The shells stronger concentric stripes, the position of the umbo which is moved further to the front than in the type specimen, and the lesser arched ventral margin require a separation of this form as a variety of *Axinus flexuosus* Mont. and also suggest a certain relation to *Axinus sarsii* Phil., which was only found in the north to this date – the length of the shell is 7.5, the height 7 mm.

Comments. Currently accepted as *Thyasira striata* Sturany, 1896 (MolluscaBase 2017) and recently recorded from cold seep communities in the deep eastern Mediterranean Sea (Olu-Le Roy et al. 2004).

Family Vesicomyidae Dall & Simpson, 1901

***Isorropodon perplexum* Sturany, 1896**

Fig. 13

Sturany 1896: 17, plate I, figures 24–27.

Original locality. Station 82, north of Alexandria, Egypt, 32°30'N, 29°8'E, 2420 m.

Type material. NHMW 13010: 11 syntypes (3 left and 8 right valves), station 82.

Original description. *Von Station 82 (2120 m)*

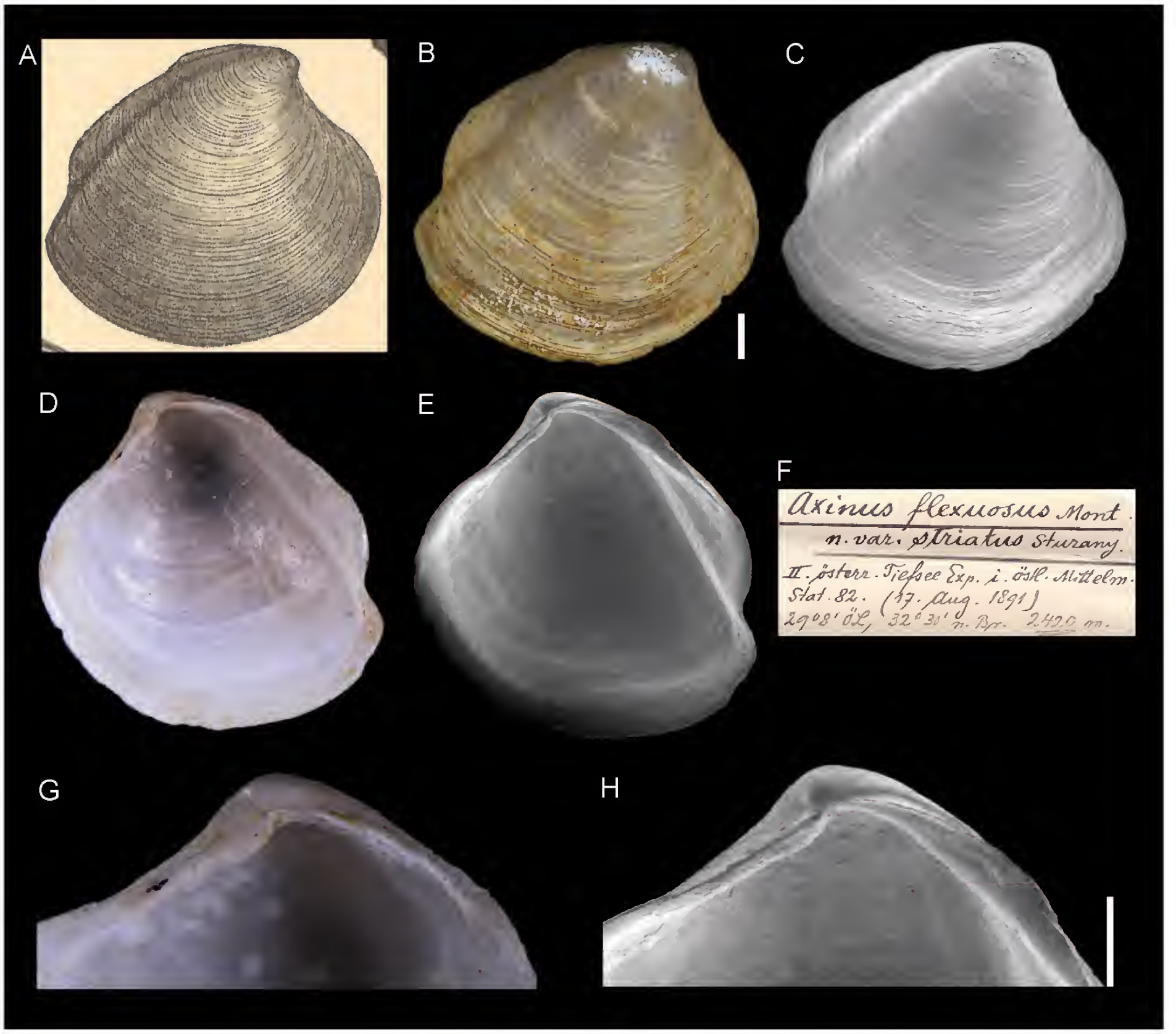

Figure 12. *Axinus flexuosus* var. *striatus* Sturany, 1896, station 82, north of Alexandria, Egypt, 2420 m. **A**. Original figure in Sturany, 1896. **B–E**, **G**, **H**. Holotype NHMW 13009: outer (**B–C**) and inner (**D–E**) views, hinge (**G–H**). **F**. Original label. Scale bar: 1 mm.

Es liegt von dieser rätselhaften, neuen Muschel eine größere Anzahl linker und rechter Schalenhälften vor, die in ihren Massverhältnissen ziemlich verschieden, also durchaus nicht konstant sind und von denen kaum zwei zusammenpassen. Von Farbe sind die Schalen außen weiß, gelb oder braun, innen weißlich mit gelbem Saume am Rande oder einfarbig gelblich bis grau ohne Saum. Vorne und rückwärts sind sie zumeist gleichmässig abgerundet, seltener lässt sich rückwärts die schwache Andeutung eines schnabelförmigen Endes konstatieren, indem der Unterrand an seinem Übergange in den Hinterrand eine leichte Einbuchtung zeigt. Die Außenseite der Schale ist dicht concentrisch gestreift; die Innenseite, glatt und glänzend, weist zwei längliche senkrecht stehende Muskeleindrücke auf und rückwärts eine sehr seichte Mantelbucht. Der Wirbel steht in der vorderen Hälfte der Schale und neigt sich mit seiner Spitze nach vorne und innen; vor demselben ist eine lunula-artige Vertiefung wahrzunehmen.

Das Schloss ist ziemlich kompliziert. In der rechten Schale (Fig. 26) steht direct unter dem Wirbel ein waagrechter, von oben nach unten komprimierter, langgestreckter Zahn, und vor dem Wirbel, nämlich unter dem vorderen Oberrande und von diesem durch eine Rinne getrennt, ein zweiter, ebenfalls waagrechter und abgeflachter Zahn. Die beiden Zähne sind wohl an ihrer Basis miteinander verbunden, lassen aber oben, resp. an der nach dem Innern der Schale gekehrten Partie eine Höhlung zwischen sich. Hinter dem Wirbel verläuft eine Leiste parallel mit dem Oberrande.

In der linken Schale (Fig. 27) fällt dem Auge des Beschauers sofort eine grosse Zahnpartie auf, welche unter dem Wirbel steht und, senkrecht zur Längsebene der Schale betrachtet, zwei mit ihren konvexen Seiten aneinander gelehnte Bogen erkennen lässt, wodurch sie das Aussehen eines Doppelzahnes gewinnt. Diese Zahnpartie kommt beim Schließen der Muschel jedenfalls in die Höh-

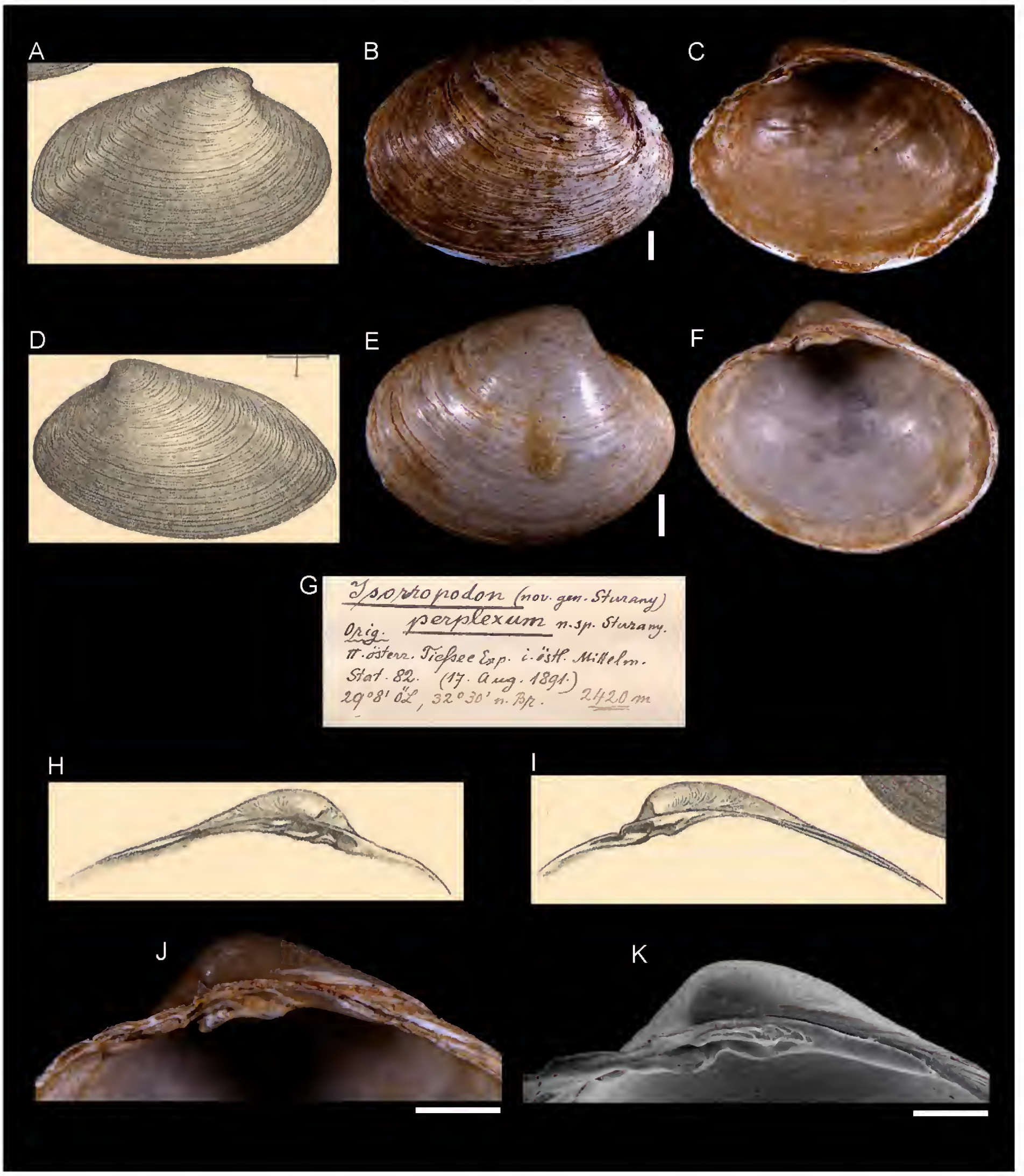

Figure 13. *Isorropodon perplexum* Sturany, 1896, Station 82, north of Alexandria, Egypt, 2420 m. **B–C**, **K**. Syntype NHMW 13010a: outer (**B**) and inner (**C**) views, hinge (K). **E–F**, **J**. Syntype NHMW 13010b: outer (**E**) and inner (**F**) views, hinge (**J**). **G**. Original label. **A**, **D**, **H–I**. Original figures in Sturany, 1896. Scale bar: 1 mm.

lung zu liegen welche sich zwischen den beiden großen Zähnen der rechten Schale ausdehnt, und zwar dürfte sich an jeden derselben einer der 2 oben erwähnten Bögen anlegen. Zwischen dem „Doppelzahne" und dem unter dem Wirbel flächenartig verbreiterten Oberrande liegt analog dem Verhalten in der rechten Schale eine Rinne und über derselben, also direkt am Oberrande ein kleiner abgeplatteter Zahn oder – was aber nur bei einem Exemplar der Fall ist – 2 waagrechte und einander parallel gestellte Zähnchen. Auch in der linken Schale zieht hinter dem Wirbel eine stellenweise fast zahnartig vorspringende Leiste parallel zum hinteren Oberrande dahin.

Das derartig beschaffene Schloss ist ähnlich dem von Cypricardia lithophagella *Lam. (Kobelt Prodr. p. 390), und mit Rücksicht darauf halte ich es für passend, das neue Genus* Isorropodon. *welches mit der obigen, vor-*

läufig allerdings nur nach der einzigen vorliegenden Art entworfenen Beschreibung charakterisiert ist, im Systeme unmittelbar hinter Cypricardia *zu stellen.*

[A table with the sizes of the collected specimens follows]

Translation. From station 82 (2420 m)

There is a large number of right and left valves of this mysterious new bivalve, which are quite diverse in their sizes and of which scarcely any fit together.

The color on the outside of the shell is white, yellow, or brown and whitish on the inside with a yellow margin or monochrome yellowish to gray with no margin. Anterior and posterior sides are in most cases equally rounded. In some rarer cases, there is a faint suggestion of a beak-formed ending, showing a slight dent at the transition of the ventral margin to the posterior margin. The outer surface of the shell is densely concentrically lined; the inside, smooth and shiny, shows two elongated vertical muscle scars and a very superficial/shallow pallial sinus at the posterior. The umbo is located at the anterior half of the shell and its tip tilted to the front and inside. At its front, a lunular-like indentation can be noticed.

The hinge is quite complex. In the right valve (Fig. 26), directly beneath the umbo there is an horizontal elongated tooth, compressed from top to bottom. In front of the umbo, namely beneath the anterior lower margin and separated by it through a groove, there is a second, also horizontal and flattened tooth. The two teeth are connected at their base, but leave a cavity above, respectively at the inwards turned part, between them. Behind the umbo, a bar advances parallel to the upper margin.

In the left valve (Fig. 27), a large set of teeth beneath the umbo strikes the viewer. Perpendicularly to the longitudinal plane of the shell, two curves become visible, leaning together at their convex sides, which makes the teeth seem double-toothed. When the shell closes, this set of teeth is embedded in a caving which is stretched between the two large teeth of the right valve and it seems as the aforementioned curves dock each of them. Between the "double tooth" and the upper margin which is broadened beneath the umbo, there is a groove and above, directly at the upper margin, a small flattened tooth, analogous to the right valve. Only in one specimen we find two horizontal and parallel arranged teeth instead. Also in the left valve there is a bar advancing behind the umbo parallel to the posterior upper margin which is prominent and tooth-like in some parts.

The hinge of this sort is similar to that of *Cypricardia lithophagella* Lam. (Kobelt Prodr. p. 390), and considering this, I find appropriate to introduce the new genus *Isorropodon* which is characterized by the described hinge and stands in the system directly behind *Cypricardia*.

Comments. The genus *Isorropodon* Sturany, 1896 was also introduced and is currently considered a valid genus within the vesicomyid subfamily Pliocardiinae (Krylova and Sahling 2010). *I. perplexum* is considered a valid specis (MolluscaBase 2017) and has been recently recorded from cold seep communities in the deep eastern Mediterranean Sea (Olu-Le Roy et al. 2004). Types noted and species described in detail by von Cosel and Salas (2001).

Family Lyonsiidae P. Fischer, 1887

***Lyonsia aegeensis* Sturany, 1896**
Fig. 14

Sturany 1896: 15, plate I, figures 14–16.

Original localities. Station 199, southwest of Kythira, Sea of Crete, Greece, 36°9'N, 23°50'E, 875 m; Station 213, north of Astypalaia, Dodekanese, Greece, 36°47'N, 26°29'E, 597 m; Station 237, southwest of Samothraki, Aegean Sea, Greece, 40°17'N, 25°13'E, 588 m.

Type material. NHMW 13004: 1 syntype (a complete specimen), station 199; NHMW 13005: 1 syntype (a right valve), station 237; NHMW 13006: 1 syntype (3 fragments), station 213.

Original description. *Von den Stationen *199 (875 m, 1 vollständiges Exemplar), 213 (597 m, Fragment) und 237 (588 m, 1 rechte Schalenhälfte).*

Das vollständige Exemplar von Station 199 ist 17 mm lang, 10 mm hoch und 7,2 mm breit. Es ist sehr nahe mit Lyonsia formosa *Jeffr. verwandt (Kobelt Prodr. p. 321; Carus Prodr. p. 170; E. Smith, Challenger-Report, Lamellibr., p. 72, pl. VI, fig. 3–3b) und würde sich vielleicht, wenn es möglich wäre, eine Reihe von* Lyonsien *vergleichend zu studieren, bloss als eine Varietät von* L. formosa *erweisen. Vorläufig aber muss ich die vorliegende Form isolieren, da sie im Vergleiche zu dem im Challenger-Werke abgebildeten* formosa*-Exemplare in folgenden Punkten abweicht:*

1. Die Größe der Schale ist eine viel bedeutendere, die allgemeine Form eine gestrecktere. 2. Der Wirbel liegt nahezu in der Mitte, während denselben das Challenger-Exemplar (vide d. Ansicht von oben!) mehr gegen das Vorderende gerückt hat. 3. Die vom Wirbel bis ungefähr zur Mitte des Unterrandes ziehende Radialerhöhung ist schwach angedeutet und nur durch eine Reihe blasenförmiger Auftreibungen der Epidermis kenntlich. Der zweite Kiel, welcher vom Wirbel zum hinteren Unterrand der Schale zieht, ist deutlich markiert und beschreibt einen Bogen, dessen Convexität nach vorne zu liegt, während sich beim Challenger-Exemplar dieser Kiel in seinem oberen Theil mit einer schwachen Convexität dem hinteren Oberrande nähert. 4. Hinter dem zweiten Kiele folgen 11 ebenfalls radial ausstrahlende Rippen mit dicht aufsitzenden Dörnchen (gegen 7 beim Challenger-Exemplar!) und in der vorderen Hälfte der Schale kommen zu den für L. formosa *charakteristischen 6 oder 7 stärkeren Querwülsten noch etliche schwächere, enger aneinander stehende wellenförmige Erhebungen, welche hier denjenigen Raum bis zum Wirbel einnehmen, der am Challenger-Exemplar hiervon frei zu sein scheint. 5. Schließlich wäre noch zu erwähnen, dass der*

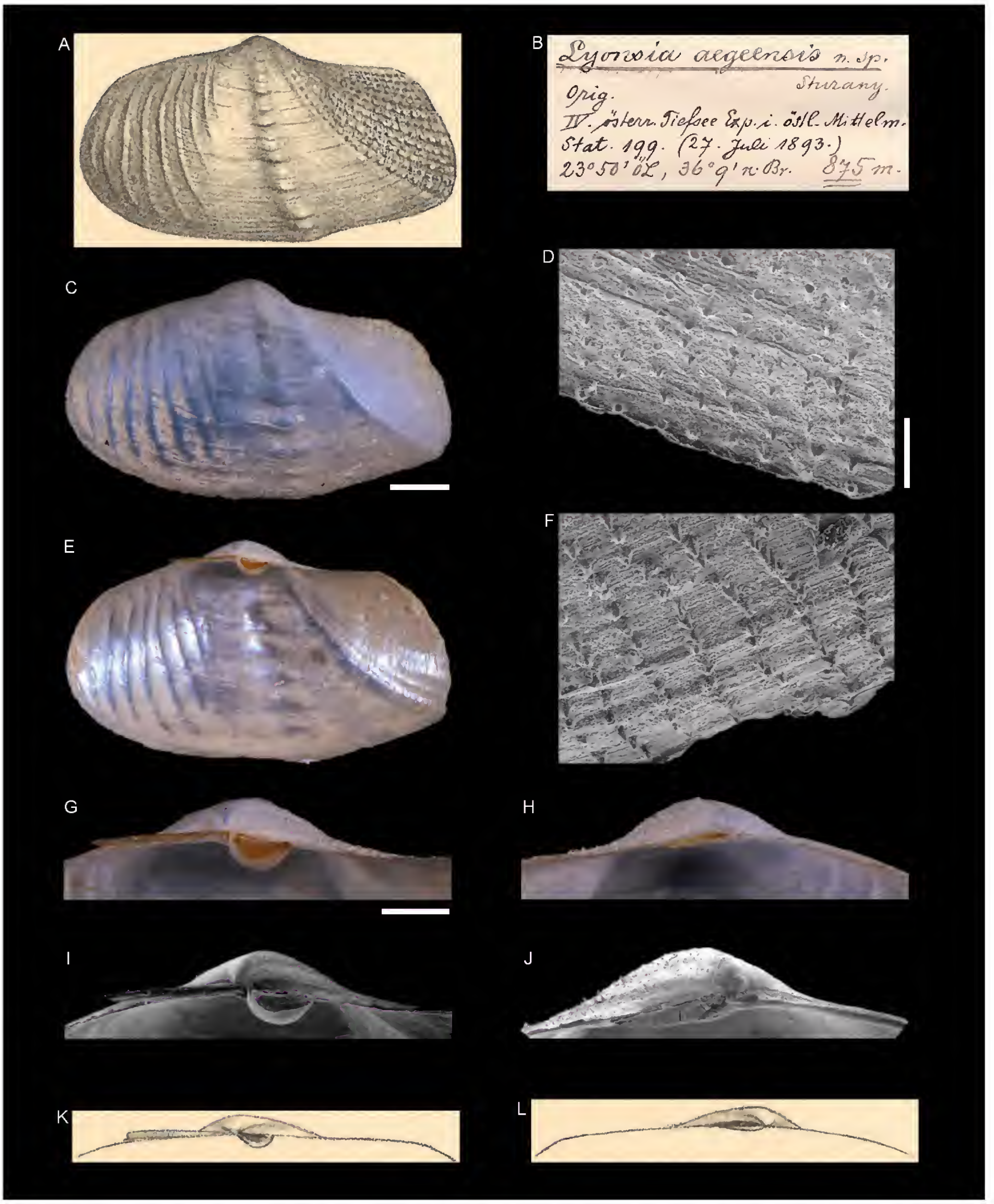

Figure 14. *Lyonsia aegeensis* Sturany, 1896, Station 199, southwest of Kythira, Sea of Crete, Greece, 875 m. **A**, **K**, **L**. Original figures in Sturany, 1896. **B**. Original label. **C–J**. Syntype NHMW 13004: outer view of left valve (**C**), inner view of right valve (**E**), microsculpture (**D**, **F**), hinge right valve (**G**, **I**) and left valve (**H**, **J**). Scale bar: 2 mm (**C, E**), 0.2 mm (**D, F**), 1 mm (**G–J**).

Oberrand mit dem Hinterrande einen deutlichen Winkel bildet, indem er horizontal vom Wirbel ausläuft und mehr plötzlich nach abwärts umbiegt, also nicht, wie dies am Challenger-Exemplar geschieht, langsam und allmählich in den Hinterrand abfällt.

Sehr hübsch ist an dem hier besprochenen Exemplar auch das Ligament mit dem halbkugeligen ossiculum zu sehen. Jede Schale trägt unter dem Wirbel eine horizontal etwas hervortretende, oben ausgehöhlte Platte zur Aufnahme des Ligaments samt dem ossiculum.

Die Schale von Station 237 misst bis bloß 11 1/2 mm in der Länge und 8 1/2 mm in der Höhe.

Translation. From stations 199 (875 m, 1 complete specimen), 213 (597 m, fragment), and 237 (588 m, 1 right valve).

The complete specimen from station 199 is 17 mm long, 10 mm high and 7.2 mm wide. It is very closely related to *Lyonsia formosa* Jeffr. (Kobelt Prodr. p. 321; Carus Prodr. p. 170; E. Smith,

Challenger-Report, Lamellibr., p. 72, pl. VI, fig. 3–3b) and might turn out to be, if it would be possible to comparably study a range of *Lyonsia*, merely a variety of *L. formosa*. For now, however, I have to isolate the present form, as it differs from the *formosa* specimen depicted in the Challenger work in the following points:

1. The size of the shell is much larger; the general form is more elongated. 2. The umbo is situated nearly in the middle, while it is moved further to the anterior in the Challenger specimen (see view from above). 3. The radial ridge which proceeds from the umbo towards about the middle of the lower margin is faintly indicated and only recognizable through a row of blister-formed swellings of the epidermis. The second ridge, which proceeds from the umbo towards the posterior lower margin of the shell, is clearly marked and describes a curve which is convex to the front, while this ridge is orientated towards the posterior upper margin with a weak convexity in its upper part. 4. There are 11 radially expanding ribs with densely packed spines behind the second keel (as compared to 7 in the Challenger specimen!). In addition to the 6 or 7 more prominent varices which are typical for *L. formosa*, there are several wavy elevations in the anterior half of the shell, which are less developed and positioned closer together. Here, these elevations occupy the space towards the umbo which seems to be open in the case of the Challenger specimen. 5. Finally, it can be mentioned that the upper margin forms a distinct angle with the posterior margin, by ending horizontally from the umbo and suddenly bending downwards, not slowly and gradually bending towards the posterior, as it happens in the Challenger specimen.

The ligament with the hemispheric ossiculum is beautifully visible in the here described specimen. Each shell has a horizontally emerging and upright carved plate beneath the umbo to accommodate the ligament including the ossiculum.

The shell from station 237 is merely 11 ½ mm long and 8 ½ mm high.

Comments. Currently considered a junior synonym of *Allogramma formosa* (Jeffreys, 1882) (MolluscaBase 2017).

Family Verticordiidae Stoliczka, 1870

***Pecchiolia berenicensis* Sturany, 1896**
Fig. 15

Sturany 1896: 15, plate I, figure 17–21.

Type locality. Station 37, north of Benghazi, Libya, 32°25'14"N, 19°49'57"E, 700 m.

Type material. NHMW 13007: holotype (a complete specimen), length 6.70 mm, height 6.31 mm.

Original description. *Von Station *37 (700 m.); 1 Exemplar.*

Diese Muschel ist von weisser Farbe, ungleichschalig, ungleichseitig und in ihren Umrissen von der Gestalt eines schief gestellten, ungleichseitigen Viereckes. Die Wirbel liegen in der vorderen Hälfte der Schale. Der schief abwärts geneigte vordere Oberrand ist muldenförmig vertieft (Abgrenzung der lunula) und geht unter einem rechten Winkel direct in den Unterrand über, welcher stumpfwinkelig ist (mit der Spitze in der Mitte) und rückwärts wieder beiläufig unter einem rechten Winkel in den hinteren, convex gekrümmten Oberrand sich fortsetzt. Von einem Vorder- und Hinterrand ist also hier nicht zu reden.

Die rechte Schale übertrifft die linke an Länge und Höhe. Während jene nämlich 7,5 mm in der Länge und 7,1 mm in der Höhe misst, ist diese nur 7,1 mm lang und 6,4 mm breit. Der Rand der überdies auch stärker gewölbten rechten Schale greift, wenn die Muschel geschlossen ist, etwas über den der linken. Die Dicke der ganzen Muschel beträgt 5,5 mm.

Über die Aussenseite der beiden Schalenhälften laufen 23 Radialrippen, welche auch an der perlmutterartig glänzenden Innenseite durchscheinen, und zwischen diesen stehen feine, gewellte, concentrisch angeordnete Querlinien in grosser Anzahl.

Das Schloss ist ziemlich einfach. In der rechten Schale steht ein starker, konischer Hauptzahn unter dem nach vorne und innen gerichteten Wirbel und rückwärts (unter dem hinteren Oberrande) verläuft eine ziemlich lange, in ihrer mittleren Parthie mässig vorspringende Leiste, welche einen Seitenzahn vorstellt; zwischen beide aber, den Haupt- und Seitenzahn, kommt in eine Vertiefung das hornartige innere Ligament zu liegen. In der linken Schale befindet sich unter dem Wirbel eine Vertiefung zur Aufnahme des Hauptzahnes der rechten Schale, und der hintere Seitenzahn ist hier wieder in Form einer Leiste vorhanden, die aber soweit gegen den Wirbel zu gerückt ist, dass das hornige innere Ligament gerade darunter zu liegen kommt. Ist die Muschel geschlossen, so steht der Seitenzahn der linken Schale gerade vor dem der rechten, und unter dem ersteren liegt, wie gesagt, das Ligament.

An der Bildung des Möndchens (lunula), welches breit herzförmig ist und sehr vertieft liegt, betheiligen sich die beiden Schalen nicht in gleichem Masse. Der vordere Oberrand der rechten Schale ist an der betreffenden Stelle convex vorgezogen und passt in eine entsprechende Concavität des gegenüberliegenden Randes; die von der rechten Schale gelieferte Fläche des Möndchens ist also grösser als die linke.

Die vorliegende Art fällt wohl mit keiner der aus dem Genus Verticordia *oder* Pecchiolia *bisher bekannt gewor-*

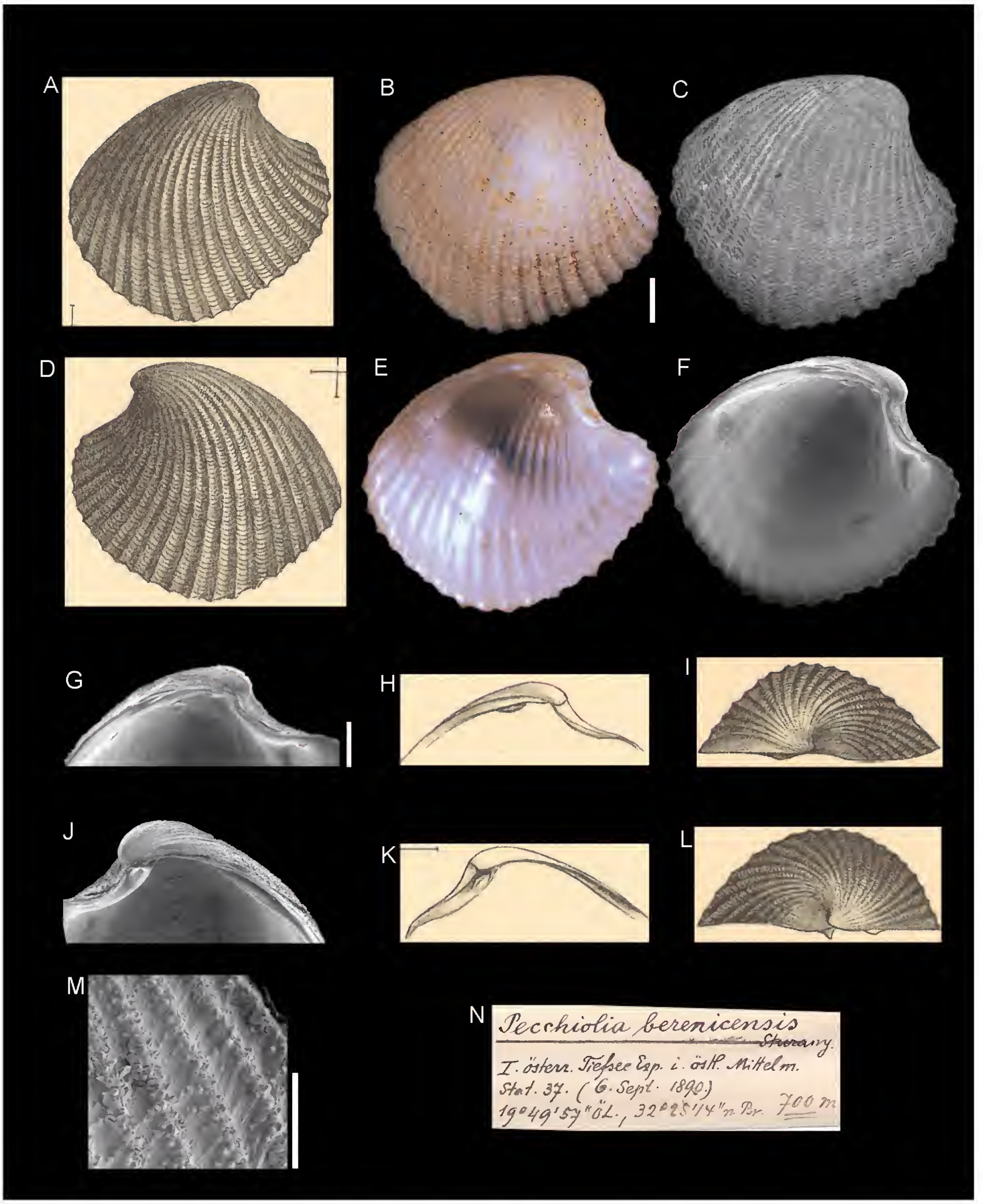

Figure 15. *Pecchiolia berenicensis* Sturany, 1896, Station 37, north of Benghazi, Libya, 700 m. **A**, **D**, **H–I**, **K–L**. Original figures in Sturany, 1896. **B–C**, **E–G**, **J**, **M**. Holotype NHMW 13007: outer view left valve (**B–C**), inner view right valve (**E–F**), hinge detail of right (**G**) and left valve (**J**), sculpture detail (**M**). **N**. Original label. Scale bar: 1 mm (**B–C, E–F, G, J**), 0.5 mm (**M**).

denen zusammen, ist aber mit Pecchiolia insculpta *Jeffr. (P. Z. S. 1881, p. 932, pl. 70, fig. 4.- Kobelt Podr. p. 323; Carus Prodr. p. 165.) aus dem Atlantischen Ocean und dem westlichen Mittelmeere nahe verwandt.*

Translation. From station 37 (700 m); 1 specimen.

This bivalve is white in colour, with a rough surface, unequilateral, and rhomboid in outline. The umbos are located at the anterior half of the shell. The downwards

tilted dorsal margin is depressed (delimiting the lunula) and merges through a right angle directly with the lower margin which has an obtuse angle (with the tip in the middle). Posteriorly, the margin runs again through a right angle towards the posterior, convex bended upper margin. Therefore, there cannot even be any question of an anterior or posterior margin.

The right valve surpasses the left one in length and height. In fact, while that [right] valve measures 7.5 mm in length and 7.1 mm in height, this [left] one is only 7.1 mm long and 6.4 mm wide. The margin of the right valve, furthermore also more strongly arched, slightly surpasses the margin of the left valve when the shells are closed. The thickness of the entire bivalve is 5.5 mm.

There are 23 radial ribs running along the outside of the two valves, which show through the mother-of-pearl shining inside. Between them, there are a large number of delicate, waved concentrically arranged lateral lines.

The hinge is rather ordinary. In the right valve there is a strong, conic cardinal tooth beneath the front- and inwards orientated umbo; proceeding backwards (beneath the posterior upper margin) there is a rather long, in the mid part moderately projected, bar, which lies before a lateral tooth; embedded between the two, the cardinal and lateral tooth, is the horn-like ligament. Situated within the left valve is a deepening beneath the umbo to accommodate the cardinal tooth of the right valve. The posterior lateral tooth is present here again in the form of a bar, which is moved so far against the umbo that the horny inner ligament is placed right beneath it. Whenever the mussel is closed, the lateral tooth of the left valve is placed right in front of that of the right one and beneath the first one lies the ligament, as mentioned before.

The lunula, which is broad and heart-shaped and is positioned very deep, has not the same size in the two valves. The anterior upper margin of the right valve is convex at the relevant position and fits into an equivalent concavity of the opposite margin; the space of the lunula of the right valve is also larger than the part of the left valve.

The species at hand seem not to coincide with any of recognized species of the genera *Verticordia* or *Pecchiolia* to date, however it is closely related to *Pecchiolia insculpta* Jeffr. (P. Z. S. 1881, p. 932, pl. 70, fig. 4.– Kobelt Podr. p. 323; Carus Prodr. p. 165.) from the Atlantic ocean and the western Mediterranean.

Comments. Currently accepted as *Haliris berenicensis* (Sturany, 1896) (MolluscaBase 2017), but its affinity with *Haliris granulata* (Seguenza, 1860) deserves further investigation.

Acknowledgments

We thank Helmut Sattmann, Head of the 3rd Zoological Department of the Natural History Museum in Vienna, who allowed access and work on Sturany's types, and supported the open access publication of this paper. Dan Topa helped during SEM imaging and Nesrine Akkari gave hints on the use of the light microscope. Konstantina Agiadi and Vlasta Ćosović helped determining the modern names of Greek and Croatian localities, respectively. Wolfgang Brunnbauer, librarian of the Zoological Library of the Natural History Museum in Vienna, helped tracing the editions of Sturany's works. PGA is supported by the grant of the Austrian Science Fund (FWF) P 28983-829 'Historical ecology of Lessepsian migration' (PI: P.G. Albano). We thank Serge Gofas, Graham Oliver and Marco Oliverio for their useful comments on the first version of the manuscript.

References

Albano PG, Bongiovanni B, D'Occhio P, Sabelli B (2014) Natural history museums as repositories of endangered diversity: the case of the United States Unionida in the Museo di Zoologia dell'Università di Bologna. Zoosystematics and Evolution 90(2): 105–111. https://doi.org/10.3897/zse.90.8231

Albano PG, Bakker PAJ, Janssen R, Eschner A (2017) An illustrated catalogue of Rudolf Sturany's type specimens in the Naturhistorisches Museum Wien, Austria (NHMW): Red Sea gastropods. Zoosystematics and Evolution 93(1): 45–94. https://doi.org/10.3897/zse.93.10039

Bauer RK (2017) oceanmap: A Plotting Toolbox for 2D Oceanographic Data. R package, version 0.0.9. https://CRAN.R-project.org/package=oceanmap

Bouchet P, Rocroi J-P (Eds) (2005) Classification and nomenclator of gastropod families. Malacologia 47(1–2): 1–397.

Bouchet P, Warén A (1980) Revision of the northeast Atlantic bathyal and abyssal Turridae (Mollusca, Gastropoda). Journal of Molluscan Studies Suppl. 8: 1–119. https://doi.org/10.1093/mollus/46.Supplement_8.1

Bouchet P, Rocroi J-P, Bieler R, Carter JG, Coan EV (2010) Nomenclator of bivalve families with a classification of bivalve families. Malacologia 52(2): 1–184. https://doi.org/10.4002/040.052.0201

Brusina S (1896) Faunistički prilozi sa putovanja yachte "Margite" po Jadranskom moru. Glasnik Hrvatskoga Naravoslovnoga Društva 9: 261–297.

Buzzurro G, Russo P (2007) Mediterranean *Fusinus*. A revision of the Recent Mediterranean species of the genus *Fusinus* Rafinesque, 1815 (Gastropoda: Fasciolariidae). Published by the Authors, 280 pp.

Danovaro R, Dell'Anno A, Fabiano M, Pusceddu A, Tselepides A (2001) Deep-sea ecosystem response to climate changes: The Eastern Mediterranean case study. Trends in Ecology and Evolution 16: 505–510. https://doi.org/10.1016/S0169-5347(01)02215-7

Danovaro R, Company JB, Corinaldesi C, D'Onghia G, Galil B, Gambi MC, Gooday AJ, Lampadariou N, Luna GM, Morigi C, Olu K, Polymenakou P, Ramirez-Llodra E, Sabbatini A, Sardà F, Sibuet M, Tselepides A (2010) Deep-sea biodiversity in the Mediterranean Sea: the known, the unknown, and the unknownable. PloS ONE 5(8): e11832. https://doi.org/10.1371/journal.pone.0011832

Dayan T, Galil B (2017) Natural history collections as dynamic research archives. In: Shavit A, Ellison AM (Eds) Stepping in the same riv-

er twice. Replication in biological research. Yale University Press, 55–63. https://doi.org/10.12987/yale/9780300209549.003.0004

Galil B (2004) The limit of the sea: the bathyal fauna of the Levantine Sea. Scientia Marina 68 (suppl. 3): 63–72. https://doi.org/10.3989/scimar.2004.68s363

Gofas S (1992) Le genre *Granulina* (Marginellidae) en Méditerranée et dans l'Atlantique Oriental. Bollettino Malacologico 28(1–4): 1–26.

ICZN (1999) International code of zoological nomenclature. The International Trust for Zoological Nomenclature, 306 pp.

Johnson KG, Brooks SJ, Fenberg PB, Glover AG, James KE, Lister AM, Michel E, Spencer M, Todd JA, Valsami-Jones E, Young JR, Stewart JR (2011) Climate change and biosphere response: unlocking the collections vault. BioScience 61(2): 147–153. https://doi.org/10.1525/bio.2011.61.2.10

Krylova EM, Sahling H (2010) Vesicomyidae (Bivalvia): current taxonomy and distribution. PloS ONE 5(4): e9957. https://doi.org/10.1371/journal.pone.0009957

Lister AM, Climate Change Research Group (2011) Natural history collections as sources of long-term datasets. Trends in Ecology and Evolution 26(4): 153–154. https://doi.org/10.1016/j.tree.2010.12.009

Locard A (1904) Coquilles des Mers d'Europe. Turbinidæ. Annales de la Société d'Agriculture, Sciences et Industrie de Lyon 8(1): 31–89.

MolluscaBase (2017) Accessed at http://www.molluscabase.org on 2017-07-27

Olu-Le Roy K, Sibuet M, Fiala-Médioni A, Gofas S, Salas C, Mariotti A, Foucher J-P, Woodside J (2004) Cold seep communities in the deep eastern Mediterranean Sea: composition, symbiosis and spatial distribution on mud volcanoes. Deep-Sea Research I 51: 1915–1936. https://doi.org/10.1016/j.dsr.2004.07.004

R Core Team (2017) R: A language and environment for statistical computing. R Foundation for Statistical Computing, Vienna, Austria. URL https://www.R-project.org/.

Schefbeck G (1996) The Austro-Hungarian Deep-sea Expeditions. In: Uiblein F, Ott J, Stachowitsch M (Eds) Deep-sea and extreme shallow-water habitats: affinities and adaptations. Österreichische Akademie der Wissenschaften, Biosystematics and Ecology Series 11: 1–27.

Smith CR, De Leo FC, Bernardino AF, Sweetman AK, Martinez Arbizu P (2008) Abyssal food limitation, ecosystem structure and climate change. Trends in Ecology and Evolution 23: 518–528. https://doi.org/10.1016/j.tree.2008.05.002

Stagl V (2012) Sturany, Rudolf (1867-1935), Zoologe. Österreichisches Biographisches Lexikon 1815-1950 14 (63): 11.

Stagl V, Sattmann H, Dworschak PC (1996) The material of the Pola Red Sea expeditions (1895-1898) in the collections of the Natural History Museum in Vienna. Österreichische Akademie der Wissenschaften, Biosystematics and Ecology Series 11: 29–41.

Sturany R (1896) Berichte der Commission für Tiefsee-Forschungen. XVIII. Zoologische Ergebnisse. VII. Mollusken I (Prosobranchier und Opisthobranchier; Scaphopoden; Lamellibranchier) gesammelt von S.M. Schiff "Pola" 1890–1894. Denkschriften der Kaiserlichen Akademie der Wissenschaften, Mathematisch-Naturwissenschaftliche Classe 63: 1–36.

von Cosel R, Salas C (2001) Vesicomyidae (Mollusca: Bivalvia) of the genera *Vesicomya*, *Waisiuuconcha*, *Isorropodon* and *Callogonia* in the eastern Atlantic and the Mediterranean. Sarsia 86: 333–366. https://doi.org/10.1080/00364827.2001.10425523

Zoosyst. Evol. 94 (1) 2018, 57–71 | DOI 10.3897/zse.94.21651

PENSOFT

museum für naturkunde

A review of the montane lacewing genus *Rapisma* McLachlan (Neuroptera, Ithonidae) from China, with description of two new species

Xingyue Liu[1]

1 *Department of Entomology, China Agricultural University, Beijing 100193, China*

http://zoobank.org/39801E33-A9E4-4DE1-8885-C3A78CF5A0C8

Corresponding author: *Xingyue Liu* (xingyue_liu@yahoo.com)

Received 15 October 2017
Accepted 16 December 2017
Published 5 January 2018

Academic editor:
Michael Ohl

Abstract

The genus *Rapisma* McLachlan, 1866 (Insecta: Neuroptera: Ithonidae) is a rare and poorly known lacewing group endemic to Asia. Here I present a revision of the *Rapisma* species from China, with description of two new species, namely *Rapisma changqingensis* **sp. n.** and *Rapisma chikuni* **sp. n.** The Chinese *Rapisma* now comprises five species that respectively belong to two monophyletic species groups. *Rapisma changqingensis* **sp. n.** represents the northernmost record of the genus, being distributed at the border of eastern Palaearctic and Oriental regions. Moreover, the homology of genital sclerites of *Rapisma* is also updated.

Key Words

Neuropterida
taxonomy
new species
Oriental region

Introduction

The genus *Rapisma* McLachlan, 1866 (commonly called montane lacewings) is one of the extremely rare groups of the holometabolous insect order Neuroptera. The adults of *Rapisma* are a kind of spectacular lacewings, with relatively large body-size and moth-like general appearance. They are characterized by the broad body, the head retracted under stout prothorax, the short antennae, and the broad wings, usually being greenish, yellowish or brownish, with complex venations (see detailed generic characters in the systematic section below). Previously, *Rapisma* was the single representative of the family Rapismatidae (Krüger 1922, Navás 1929), while it is recently assigned to Ithonidae sensu lato, which constitutes three former lacewing families, i.e. Ithonidae sensu stricto, Polystoechotidae and Rapismatidae (Winterton and Makarkin 2010). So far, *Rapisma* is the only extant ithonid genus that occurs in Asia, with distribution area primarily confined to the Oriental region, and it comprises 18 valid described species (Oswald 2017). However, 12 *Rapisma* species are known respectively from a single specimen, suggesting the rareness of this genus.

The most comprehensive study on *Rapisma* refers to Barnard (1981). Subsequently, Barnard and New (1985, 1986) and New (1985) provided considerable additional information on this genus. Nevertheless, *Rapisma* still needs further studies concerning its morphology, phylogeny and biology. First, the homologies of the genital sclerites in *Rapisma*, especially those of gonocoxites complex 9, 10 and 11, should be further interpreted basing on the homology assessment provided by Aspöck and Aspöck (2008). Second, the phylogeny as well as the historical biogeography of *Rapisma* is largely unknown. *Rapisma* was assigned into a monophyletic group together with *Adamsiana* Penny, 1996 from Central America, *Oliarces*

Banks, 1908 from southwestern North America and two fossil genera (*Allorapisma* Makarkin & Archibald, 2009 from the early Eocene of U.S.A. and *Principiala* Makarkin & Menon, 2007 from the Lower Cretaceous of Brazil and England) based on total-evidence data (Winterton and Makarkin 2010), and it was recovered to be the sister group of the latter two fossil genera, suggesting that *Rapisma* might have originated no later than the Early Cretaceous. However, the interspecific relationships among the *Rapisma* species are barely known. Third, considering biology, the knowledge on life history of *Rapisma* is very scarce. It is also interesting to investigate whether the remarkable sexual dimorphism on body and wing coloration (currently found only in a Chinese species *Rapisma xizangense* Yang, 1993) is a common phenomenon in the whole genus.

Rapisma was found from China for the first time in a few years after the aforementioned series of taxonomic works (Yang 1993). Four species were originally described as new species in Yang (1993) from China, namely *Rapisma daianum* Yang, 1993 from Yunnan, *Rapisma yanhuangi* Yang, 1993 from Sichuan, *Rapisma xizangense* Yang, 1993 from Xizang, and *Rapisma zayuanum* Yang, 1993 from Xizang, while one of them (*R. zayuanum*) was synonymized with another sympatrically distributed species (i.e. *R. xizangense*) by Wang et al. (2013) through molecular identification.

In this paper we present a taxonomic revision of *Rapisma* from China, providing descriptions or re-descriptions of all Chinese *Rapisma* species, including two new species. The new species *Rapisma changqingensis* sp. n. from Qinling Mountains extends the northernmost border of the distribution range of *Rapisma* to the transitional zone between eastern Palaearctic and Oriental regions. A revised interpretation on the homologies of genital sclerites of *Rapisma* is also provided.

Material and methods

Specimens for the present study are deposited in the Entomological Museum, China Agricultural University (CAU), Beijing, China; the Institute of Zoology, Chinese Academy of Sciences (IZCAS), Beijing, China; and the Shanghai Entomological Museum, Chinese Academy of Sciences (SEMCAS), Shanghai, China.

Genitalic preparations were made by clearing the apex of the abdomen in a warm, saturated KOH solution for 20–30 min. After rinsing the KOH with acetic acid and water, the apex of the abdomen was transferred to glycerin for further dissection and examination. Habitus photos of adults were taken by using Nikon D800 digital camera with Nikon MICRO NIKKOR 105 mm lens, and the genitalic figures were made by hand drawing under Carl Zeiss Discovery V12 stereo microscope. The terminology of the genitalia generally follows Aspöck and Aspöck (2008).

Results

Genus *Rapisma* McLachlan, 1866

Rapisma McLachlan, 1866: 353. Type species: *Hemerobius viridipennis* Walker, 1853: 276 (original designation).

Generic characters. Medium- to large-sized lacewings (forewing length 19–35 mm). Head (Figs 1–3) partially retracted under prothorax; vertex moderately domed, medially with trace of ecdysial line; clypeus prominent, nearly rectangular. Antennae moniliform, but sometimes subserrate, much shorter than wings (4–11 mm). Compound eyes globular, maximum eye diameter divided by minimum interocular distance (i.e. EI ratio) 0.7–1.1; ocelli absent. Mouthparts mandibulate, mandibles short and broad, margin of labrum excised medially.

Thorax (Fig. 1) stout, covered with fine hairs, prothorax very broad and shield-like. Legs densely setose; tibial spurs absent; length of tarsal segments in approximate ratio 1.0 (basal):0.4:0.35:0.25:0.85 (distal); pretarsal claws broad at base with slight projection on inner side; pretarsus lacking arolium.

Wings (Figs 1–3) broad, with numerous setae on wing margins and veins. Both fore- and hindwing with single nygma between bases of RP+MA and MP, but with trichosors poorly developed, only confined on forewing costal margin.

Forewing broad, greenish, yellowish or brownish. Costal space very broad, particularly at base; costal crossveins usually with marginal forks and with interlink veinlets, most of which are arranged into a longitudinal line on proximal half. Recurrent humeral veinlet present, with several branches. ScA present, short. ScP running free to wing margin, not fused with RA, distally with a few short branches. Subcostal space with many crossveins (number ranging 18–31). RP+MA diverging very near base of R; RP with 3–9 pectinate branches. MA diverging near base of RP and forking repeatedly, with initial branching point either near base of MA or rather distad midpoint of MA. MP diverging into MP1 and MP2 near base; MP1 only forked near wing margin; MP2 profusely and usually dichotomously branched. Cu diverging into CuA and CuP slightly proximad initial branching point of MP. CuA forked only distally; CuP at least initially forked around midpoint; a series of interlink veins present among cua-cup crossveins and longitudinally arranged into a pseudo longitudinal vein. A1 with a few distal branches; A2 and A3 proximally fused, each forked near its base. Simple jugal vein present. Crossvenation exceptionally rich, distal-most crossveins among branches of RP+MA arranged into a gradate series.

Hindwing slightly shorter and narrower than forewing. Frenulum present, short. Venation generally similar to that of forewing, except for the followings. Costal space much narrower than that of forewing, with interlink veinlets among costal crossveins absent. RP with 2–7 pectinate branches. No interlink veinlets among cua-cup crossveins.

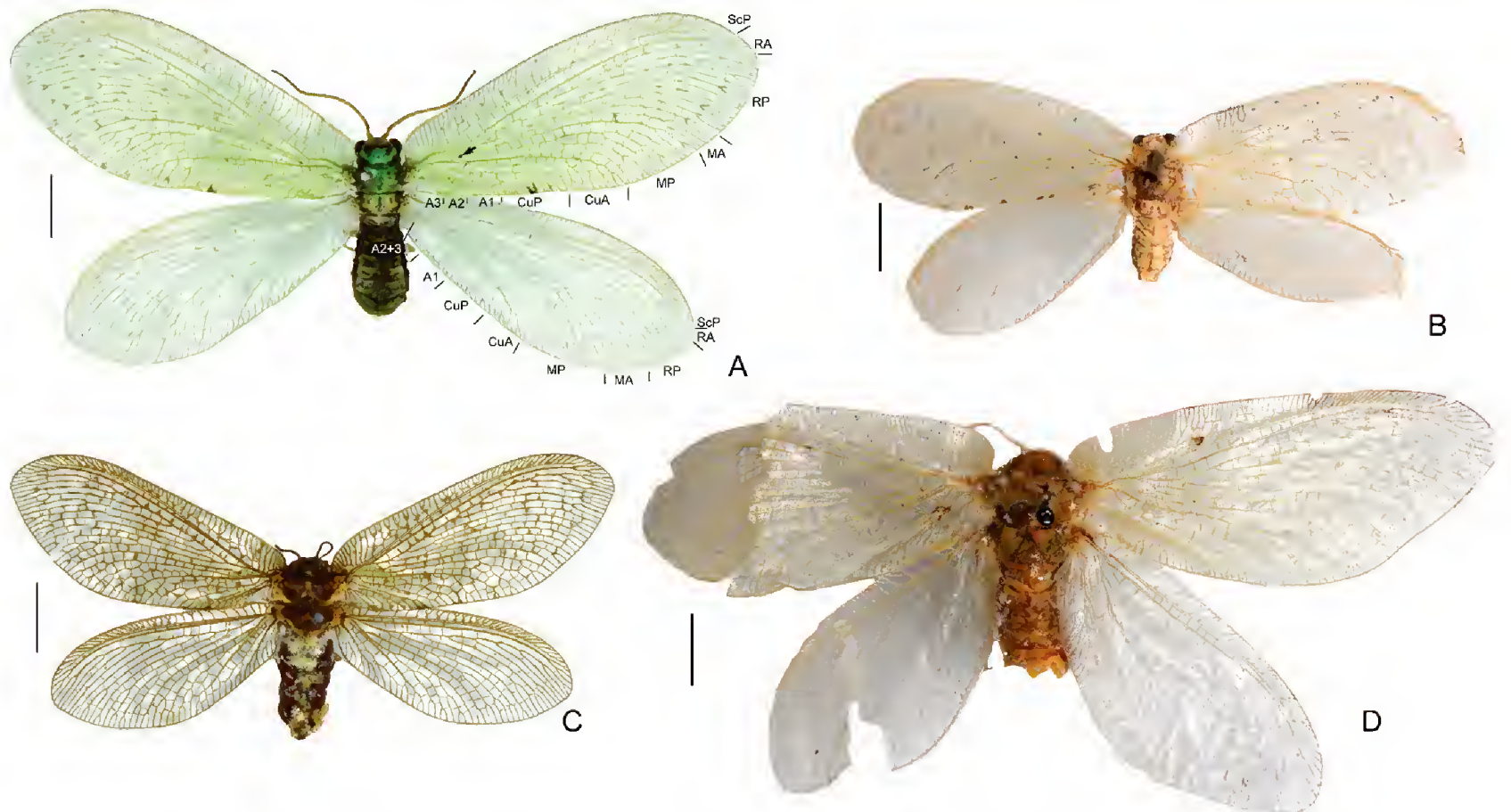

Figure 1. Habitus photos of *Rapisma* spp., (**A**) *Rapisma chikuni* sp. n., holotype male; (**B**) *Rapisma daianum* Yang, holotype male; (**C**) *Rapisma xizangense* Yang, male; (**D**) same species, female (holotype of *Rapisma zayuanum* Yang). Arrow indicates nygma. Scale bar: 5.0 mm.

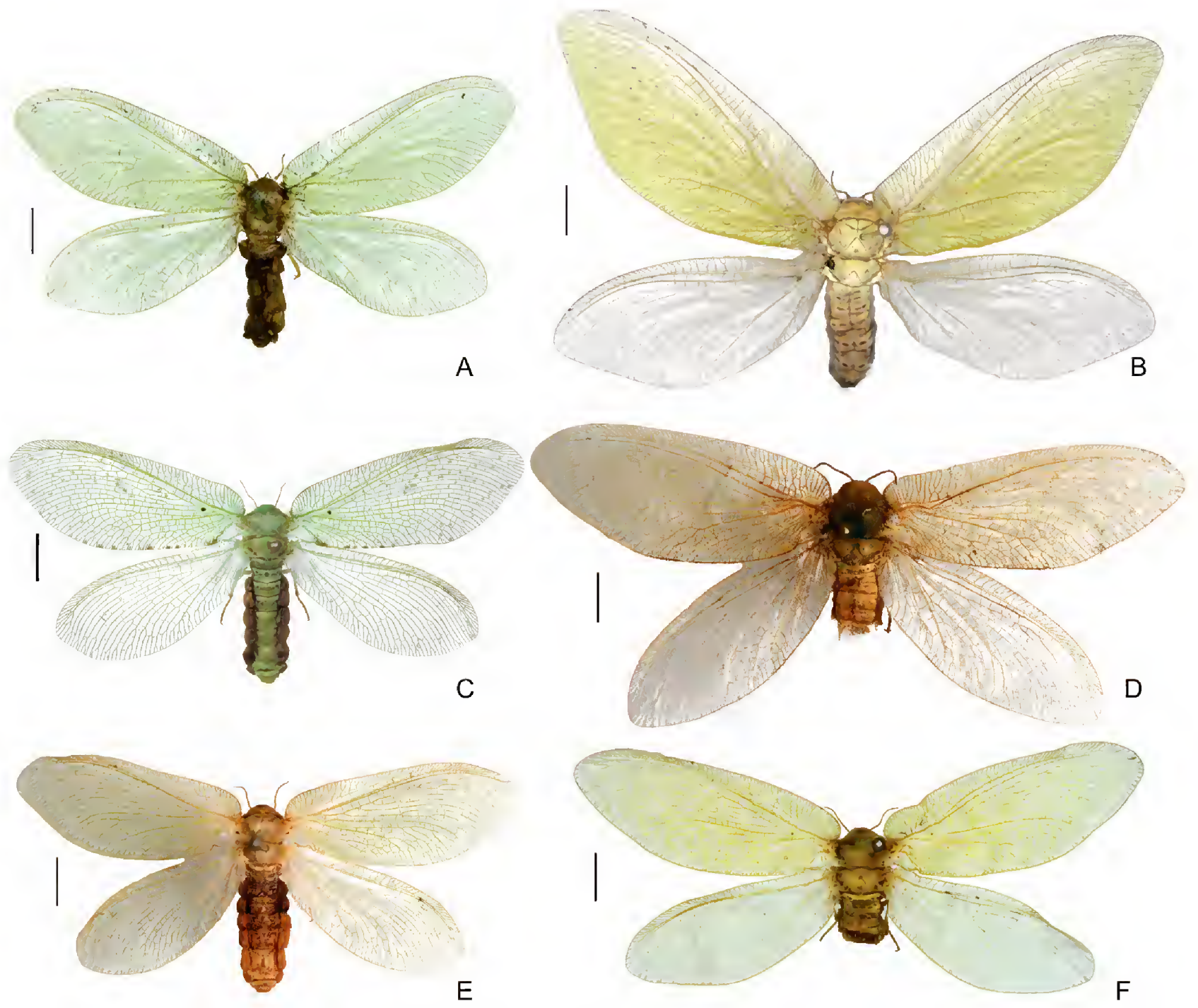

Figure 2. Habitus photos of *Rapisma* spp., (**A**) *Rapisma changqingensis* sp. n., holotype male; (**B**) same species, paratype female; (**C**) *Rapisma yanhuangi* Yang, male; (**D**) same species, holotype female; (**E**) same species, male, lacking forewing dark markings; (**F**) same species, female. Scale bar: 5.0 mm.

Abdomen corpulent. Genital segments much smaller than pregenital segment. Male genitalia (Figs 4–6): Tergum 9 much wider than long; sternum 9 slightly shorter than tergum 9; ectoprocts unpaired in dorsal view; callus cerci present; gonocoxites 9, gonostyli 11 and gonocoxites 11 associated into a complex structure; gonocoxites 9 paired, each of them with a broad lobe (glabrous or covered with many short spines) and a narrow lateral arm, which is articulating laterally on ends of fused gonocoxites 11 (= gonarcus); fused gonocoxites 11 present as a variously shaped arc; gonostyli 11 (= mediuncus lobes) present near posteromedian portion of fused gonocoxites 11, fused, but often showing paired trace, more or less setose; hypandrium internum usually present, but often small and difficult to been found. Female genitalia (Fig. 6): Sternum 7 large; segment 8 much shorter than and slightly retracted in sternum 7, tergum 8 enclosing spiracle; gonocoxites + gonapophyses 8 (= subgenital plate) fused, but usually divided by a transverse suture, posteriorly produced and notched at tip; tergum 9 much shorter than tergum 8, slightly narrowed ventrolaterally; gonocoxites 9 (= ovipositor) rather short and small, valvate, distally with tiny gonostyli 9; a pair of small setose lobes (gonapophyses 9) present posteriad gonocoxites 8 and usually beneath gonocoxites 9; ectoprocts unpaired in dorsal view, laterally with callus cerci; bursa copulatrix medially with a straight channel, anteriorly connected with spermatheca, which constitutes two tubes terminated with a large and a small ovoid sac.

Distribution. China, India, Indonesia, Malaysia, Myanmar, Nepal, Thailand.

Key to *Rapisma* species from China

1 Antennae extremely short, less than 1/5× forewing, moniliform; male gonocoxites 9 glabrous, not bilobed posteroventrally (Figs 6D, 8E, 9E) 2
– Antennae relatively long, ~1/3× forewing length, subserrate; male gonocoxites 9 bilobed and covered with many short spines posteroventrally (Figs 4E, 5) 4
2 Body and forewings brownish in male but greenish in female; male fused gonocoxites 11 in dorsal view distinctly produced posterolaterally (Fig. 6C); Xizang ..... *R. xizangense* Yang
– Body and forewings greenish in both male and female; male fused gonocoxites 11 in dorsal view not produced posterolaterally (Figs 8E, 9E) 3
3 Male head medially without dark marking (Fig. 3E); male fused gonocoxites 11 anteriorly broadly concaved and with a semicircular median notch (Fig. 8C); male gonostyli 11 not prominent posterolaterally (Fig. 8D); female gonocoxites+gonapophyses 8 subtrapezoid, with indistinct transverse suture (Fig. 8H); Shaanxi ..... *R. changqingensis* sp. n.
– Male head medially with dark markings (Fig. 3G); male fused gonocoxites 11 with broadly subtrapezoid anterior incision, but without accessory median notch (Fig. 9C); male gonostyli 11 prominent posterolaterally (Fig. 9D); female gonocoxites+gonapophysis 8 nearly pentagonal, with distinct, arched, transverse suture (Fig. 9H); Sichuan ..... *R. yanhuangi* Yang
4 Male head medially without dark marking (Fig. 3B); male gonocoxites 9 with posteromedian lobes curved anteriad (Fig. 5); southern Yunnan ..... *R. daianum* Yang
– Male head medially with dark markings (Fig. 3A); male gonocoxites 9 with posteromedian lobes not curved anteriad (Fig. 4D); western Yunnan ..... *R. chikuni* sp. n.

Rapisma chikuni sp. n.

http://zoobank.org/D2125C87-5631-44C0-847C-41803F5D2DD5

Figs 1, 3, 4, 10

Diagnosis. Body and forewings generally greenish. Forewing with sparse small grayish brown spots. Male head medially with dark markings on vertex and frons. Antenna subserrate, ~1/3× forewing length. Male gonocoxites 9 paired, covered with many short spines; each with a robust lobe, which laterally bears a digitiform projection and dorsally bears a flat accessory lobe, and with a short, arcuately curved lateral arm; fused gonocoxites 11 generally arched, in dorsal view nearly semicircular, anteromedially strongly concaved, leaving a pair of broadly shell-shaped lobes, which bear a pair of acutely tapering accessory lobes on their laterodistal ends; gonostyli 11 fused, subtrapezoidal, bearing short setae, ventrally with a pair of obtuse processes and with a feebly sclerotized median bar.

Description. Male. Body length 14.5 mm; forewing length 26.6 mm, hindwing length 23.0 mm.

Head nearly semiglobular, slightly retracted under prothorax, visible in dorsal view. Head yellowish; a transverse blackish brown band present on anterior portion of vertex; frons also with a transverse blackish brown band. Compound eyes blackish brown; EI ratio 0.84. Antenna subserrate, 8.5 mm long, with 62 flagellomeres; yellowish, but proximal two flagellomeres and those on distal 1/4 of flagellum slightly darker. Mandibles with tips black.

Pro- and mesothorax greenish, but metathorax yellowish; pronotum anteriorly with a pair of subtriangular blackish brown markings, and posterolaterally with a pair

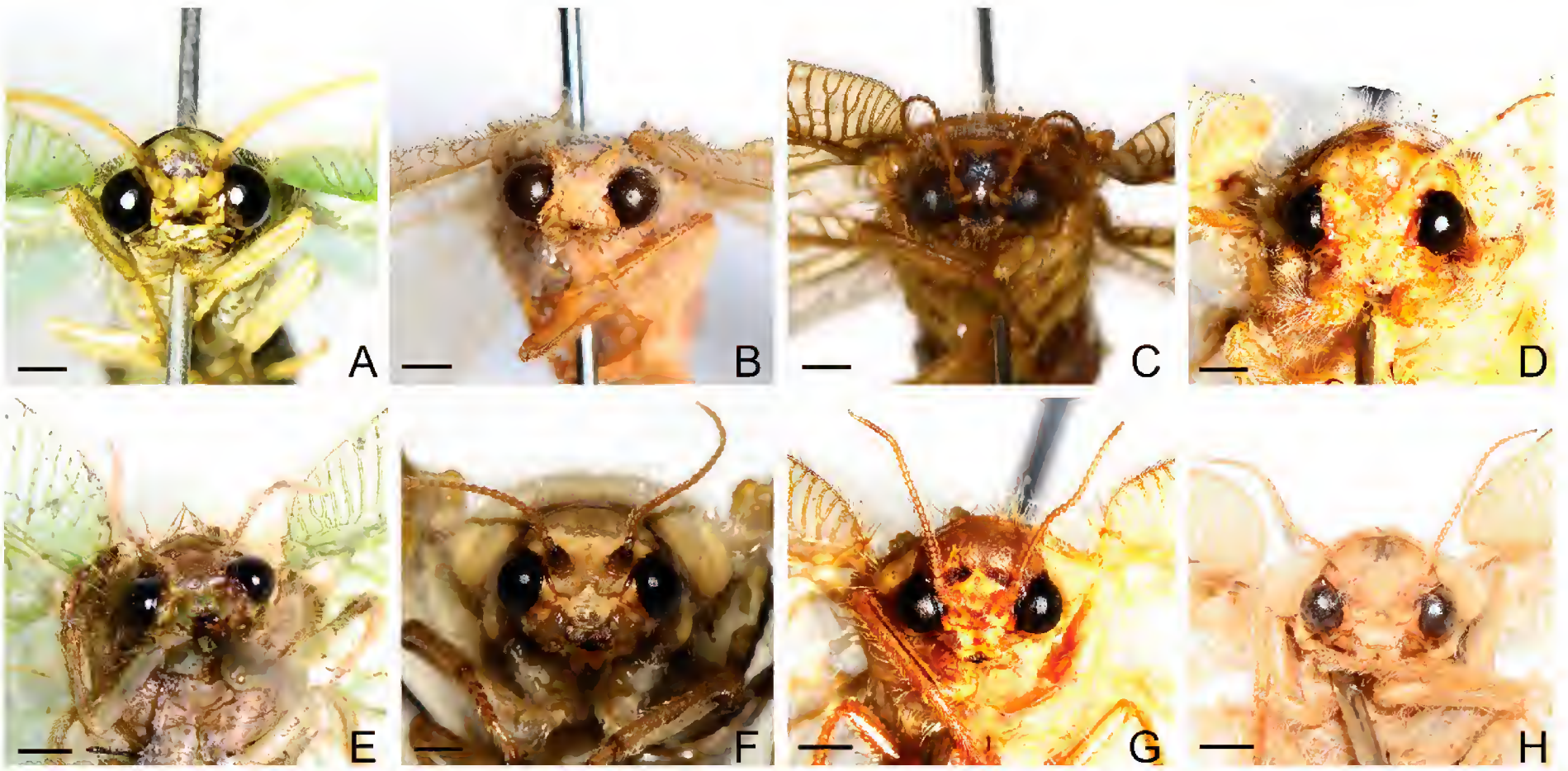

Figure 3. Head of *Rapisma* spp. in frontal view, (**A**) *Rapisma chikuni* sp. n., holotype male; (**B**) *Rapisma daianum* Yang, holotype male; (**C**) *Rapisma xizangense* Yang, male; (**D**) same species, female (holotype of *Rapisma zayuanum* Yang); (**E**) *Rapisma changqingensis* sp. n., holotype male; (**F**) same species, paratype female; (**G**) *Rapisma yanhuangi* Yang, male; (**H**) same species, female. Scale bar: 1.0 mm.

of ovoid blackish brown markings; meso- and metanotum each laterally with a pair of large and a pair of punctiform blackish brown markings. Legs yellowish; pretarsal claws reddish brown, proximally slightly produced.

Forewing greenish, with sparse small grayish brown spots. Trichosors present only along costal margin. A proximal nygma present between RP+MA and MP, blackish, covered with a blackish spot. RP with 7 pectinate branches. Hindwing much paler than forewing, immaculate. A proximal nygma present between RP+MA and MP, yellowish. RP with 4 pectinate branches.

Abdomen brown, with terga and genitalia greenish yellow. Tergum 9 subtrapezoidal, moderately setose. Sternum 9 nearly as long as but narrower than tergum 9, subtrapezoidal, posteriorly slightly concaved. Ectoprocts slightly shorter and much narrower than tergum 9; callus cerci present, slightly prominent. Gonocoxites 9 paired, covered with many short spines; each with a robust lobe, which laterally bears a digitiform projection and dorsally bears a flat accessory lobe, and with a short, arcuately curved lateral arm. Fused gonocoxites 11 generally arched, in dorsal view nearly semicircular, anteromedially strongly concaved, leaving a pair of broadly shell-like lobes, which bear a pair of acutely tapering accessory lobes on their laterodistal ends. Gonostyli 11 fused, subtrapezoidal, bearing short setae, ventrally with a pair of obtuse processes and with a feebly sclerotized median bar. Hypandrium internum relatively large, arrow-shaped, with slenderly foliate lateral lobes.

Female. Unknown.

Material examined. Holotype male, China, Yunnan, Yingjiang, Nabang, Rongshuwang [24°40.48'N, 97°35.33'E], 850 m, 30.VI.2017, Yutang Wang (CAU).

Etymology. The new species is dedicated to Prof. Chikun Yang who made outstanding contributions to the taxonomy of *Rapisma* from China.

Distribution. China (Yunnan).

Remarks. The new species probably belongs to a monophyletic group including *Rapisma corundum* Barnard, 1981 from eastern Myanmar, *Rapisma tamilanum* Barnard, 1981 from southern India, and *R. daianum* from southern Yunnan, China, because these species share some apomorphic characters, e.g. the subserrate male antennae and the posteriorly bilobed male gonocoxites 9. The new species can be distinguished from the related species by the head medially with dark markings, the male gonocoxites 9 with median lobes not curved anteriad, and the male fused gonocoxites 11 broadly shell-like laterally.

Rapisma daianum Yang, 1993

Figs 1, 3, 5, 10

Rapisma daianum Yang, 1993: 147. Type locality: China (Yunnan: Menghai).

Diagnosis. Body and forewings yellowish, possibly greenish in fresh specimens. Forewing with sparse small

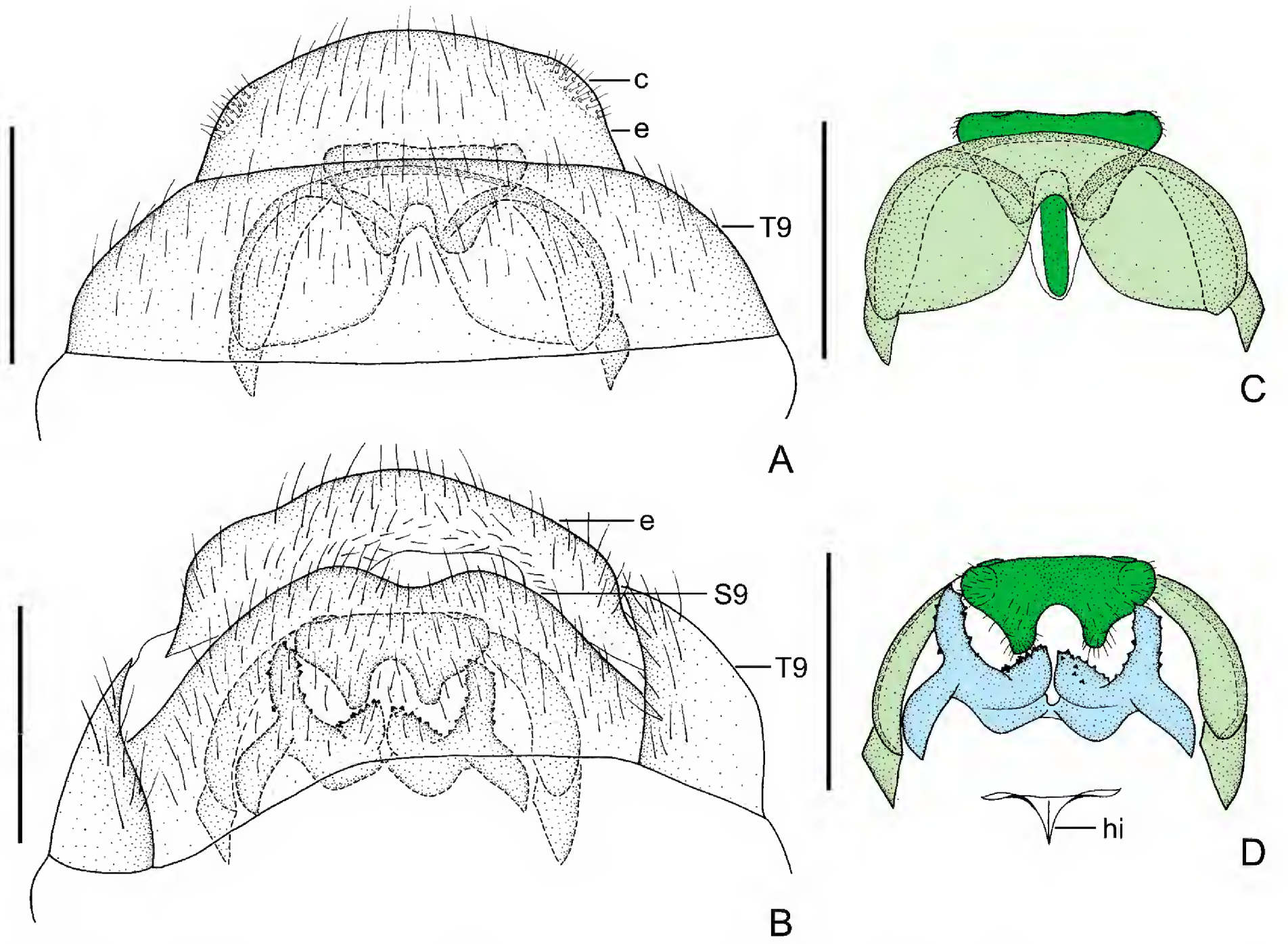

Figure 4. *Rapisma chikuni* sp. n., (**A**) male genitalia, dorsal view; (**B**) male genitalia, ventral view; (**C**) male gonocoxites and gonostyli 11, dorsal view; (**D**) complex of internal male genital sclerites, ventral view. **c** – callus cercus; **e** – ectoproct; **hi** – hypandrium internum; **T** – tergum; **S** – sternum. Gonocoxites 9, gonocoxites 11 and gonostyli 11 are respectively highlighted in pale blue, pale green and green in panels C and D. Scale bar: 1.0 mm.

grayish brown spots. Male head medially without dark marking. Antenna subserrate. Male gonocoxites 9 paired, covered with many short spines; each with a digitiform lobe, which is curved at tip, laterally bears a thick conical projection, and dorsally bears a flat accessory lobe, and with a short, arcuately curved lateral arm; fused gonocoxites 11 generally arched, anteriorly shallowly incised, but anterior margin largely truncate; gonostyli 11 fused, subquadrate, bearing short setae, posteriorly with V-shaped incision, leaving a pair of subtriangular lobes.

Description. Male. Body length 18.0 mm; forewing length 22.0 mm, hindwing length 20.0 mm.

Head nearly semiglobular, slightly retracted under prothorax, visible in dorsal view. Head yellowish, immaculate in general, only with a narrow blackish brown stripe along anterior half of inner margin of compound eye. Compound eyes blackish brown; EI ratio 1.00. Antennae partly damaged, subserrate, yellowish brown to brown, with at least more than 50 antenomeres. Mandibles with tips black.

Thorax yellowish; meso- and metanotum each laterally with a pair of grayish brown markings. Legs yellowish; pretarsal claws reddish brown, proximally slightly produced.

Forewing yellowish, with sparse small grayish brown spots. Trichosors absent. A proximal nygma present between RP+MA and MP, blackish. RP with 6 pectinate branches. Hindwing much paler than forewing, immaculate. A proximal nygma present between RP+MA and MP, yellowish. RP with 3 pectinate branches.

Abdomen yellowish except for pleural portions brown. Gonocoxites 9 paired, covered with many short spines; each with a digitiform lobe, which is curved at tip, laterally bears a thick conical projection, and dorsally bears a flat accessory lobe, and with a short, arcuately curved lateral arm. Gonostyli 11 fused, subquadrate, bearing short setae, posteriorly with V-shaped incision, leaving a pair of subtriangular lobes. Fused gonocoxites 11 generally arched, anteriorly shallowly incised, but anterior margin largely truncate. Hypandrium internum relatively large, arrow-shaped, with slenderly foliate lateral lobes.

Female. Unknown.

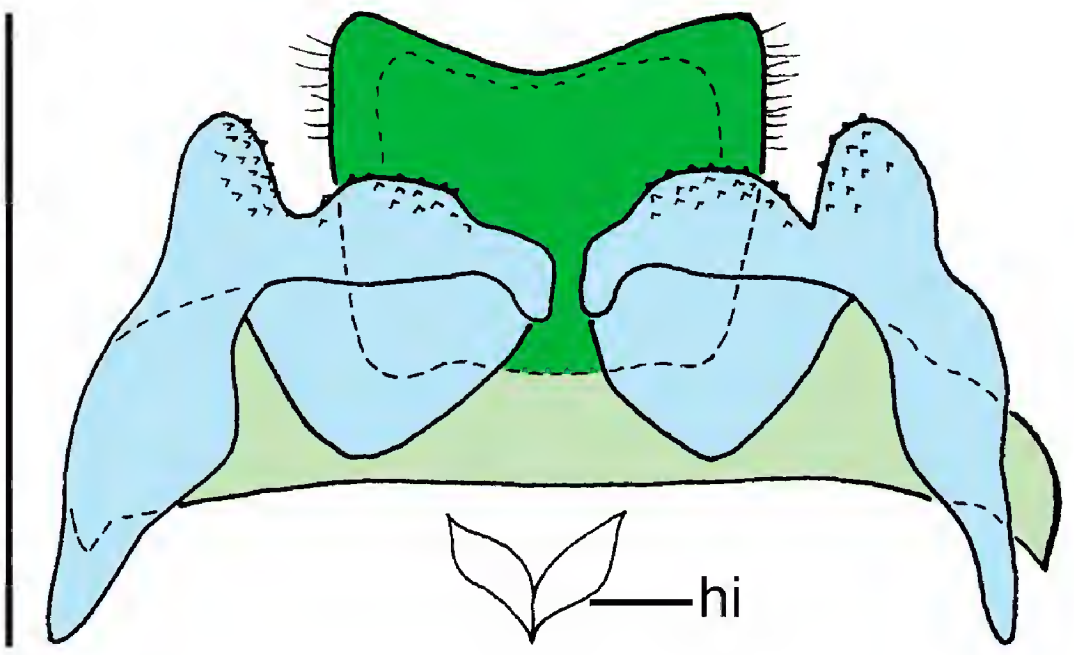

Figure 5. Complex of internal male genital sclerites of *Rapisma daianum* Yang, ventral view. Gonocoxites 9, gonocoxites 11 and gonostyli 11 are respectively highlighted in pale blue, pale green and green. Modified from Yang (1993). Scale bar: 1.0 mm.

Material examined. Holotype male, China, Yunnan, Xishuangbanna, Menghai [ca. 21°57.19'N, 100°27.31'E], 1200–1600 m, 21.VII.1958, Shuyong Wang (IZCAS).

Distribution. China (Yunnan).

Remarks. This species appears to be closely related to *R. corundum* in having similar male gonocoxites 9, while it can be distinguished from the latter species by the forewing with grayish brown spots and the male gonostyli 11 posteriorly with V-shaped incision. In *R. corundum* the forewings are immaculate and the male gonostyli 11 is not incised posteriorly.

Rapisma xizangense Yang, 1993

Figs 2–4, 6, 10

Rapisma xizangense Yang, 1993: 148. Type locality: China (Xizang: Jigong).
Rapisma zayuanum Yang, 1993: 149. Type locality: China (Xizang: Jigong).

Diagnosis. Body and wing coloration greatly differed between males and females, generally brownish in males but greenish in females. Male head medially with dark markings on vertex, frons and clypeus, while female head immaculate. Antenna extremely short, less than 1/5× forewing length. Male gonocoxites 9 paired, glabrous; each with an ovoid lobe, which dorsally bears a subtriangular accessory lobe, and with a slender, arcuately curved lateral arm; fused gonocoxites 11 generally arched, anteriorly shallowly concaved, posteromedially truncate, posterolaterally distinctly produced in dorsal view; gonostyli 11 having subtriangular dorsal lobe with a few short setae, and flat ventral lobe distally with a pair of tufts of long setae.

Description. Male. Body length 13.0–14.0 mm; forewing length 19.0–20.0 mm, hindwing length 16.6–17.0 mm.

Head nearly semiglobular, largely retracted under prothorax, barely visible in dorsal view. Head yellowish brown; a narrow blackish stripe present around compound eye; vertex with a large brown marking, which is sometimes expanded, making vertex almost entirely brown; frons and clypeus medially with a brown marking that is much narrower than vertexal marking. Compound eyes dark brown; EI ratio 0.80. Antennae nearly moniliform, short, 4.4–4.5 mm long, with 27–28 flagellomeres; pale yellowish brown. Mandibles with tips black.

Thorax pale brown, meso- and metathorax slightly paler than prothorax, without any distinct markings. Legs yellowish; pretarsal claws reddish brown, proximally slightly produced.

Forewing brownish, with many small brown spots on crossveins. Trichosors absent. A proximal nygma present between RP+MA and MP, blackish. RP with 8–9 pectinate branches. Hindwing much paler than forewing, immaculate. A proximal nygma present between RP+MA and MP, blackish. RP with 6–8 pectinate branches.

Abdomen brown. Tergum 9 subtrapezoidal, with sparse short setae, posterior margin slightly concaved. Sternum 9 nearly as long as tergum 9, about 1.5 times as wide as long, subtrapezoidal. Ectoprocts nearly as long as tergum 9, ventrally divided into a pair of ovoid lobes; callus cerci present, slightly prominent. Gonocoxites 9 paired, glabrous; each with an ovoid lobe, which dorsally bears a subtriangular accessory lobe, and with a slender, arcuately curved lateral arm. Fused gonocoxites 11 generally arched, anteriorly shallowly concaved, posteromedially truncate, posterolaterally distinctly produced in dorsal view. Gonostyli 11 with a pair of dorsal lobes and a single ventral lobe; dorsal lobe subtriangular, with a few short setae; ventral lobe flat, distally with a pair of tufts of long setae.

Female. Body length 19.1–22.0 mm; forewing length 30.0–31.3 mm, hindwing length 26.0–26.2 mm.

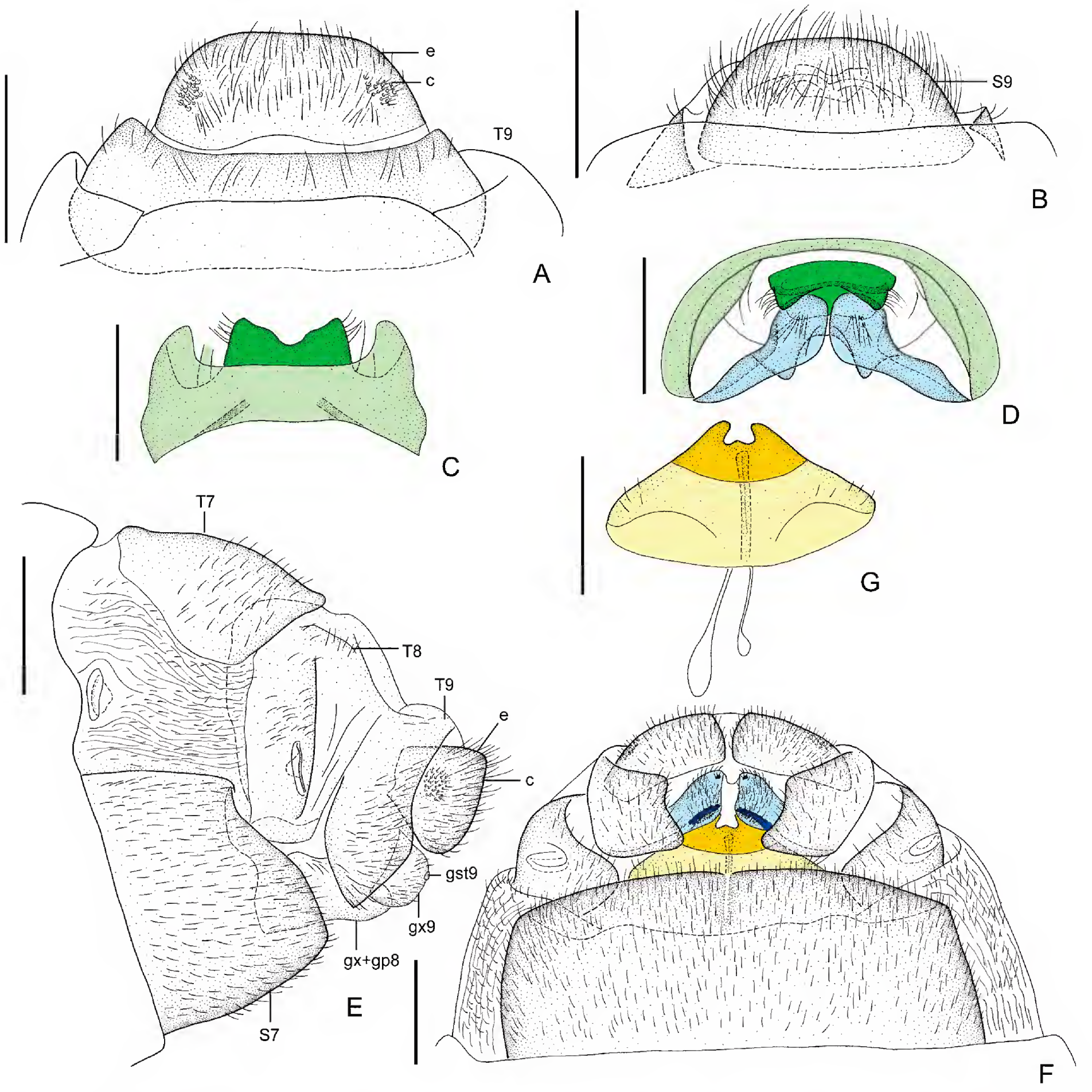

Figure 6. *Rapisma xizangense* Yang, (**A**) male genitalia, dorsal view; (**B**) male genitalia, ventral view; (**C**) male gonocoxites and gonostyli 11, dorsal view; (**D**) complex of internal male genital sclerites, ventral view; (**E**) female genitalia, lateral view; (**F**) female genitalia, ventral view; (**G**) female gonocoxites+gonapophyses 8, ventral view. **c** – callus cercus; **e** – ectoproct; **gx** – gonocoxite; **gp** – gonapophysis; **gst** – gonostylus; **T** – tergum; **S** – sternum. Gonocoxites 9, gonocoxites 11 and gonostyli 11 are respectively highlighted in pale blue, pale green and green in panels C and D. Gonocoxites 9, gonostyli 9 and gonapophyses 9 are respectively highlighted in pale blue, blue, and dark blue in panel F, while gonocoxites 8 and gonapophyses 8 are respectively highlighted in pale yellow and yellow in panels F and G. Scale bar: 1.0 mm (A, B, E, F, G), 0.5 mm (C, D).

Body and forewings in general greenish. Head without dark marking. Forewing sometimes with very indistinct trace of dark spots on a few crossveins.

Sternum 7 large, posteromedially with a narrow groove. Gonocoxites+gonapophyses 8 fused, broadly subtriangular, but divided by an arched transverse suture, notched distally, with a pair of digitiform projections and a weak median projection. Gonocoxites 9 nearly semicircular in lateral view, distally with tiny gonostyli 9; a pair of small setose ovoid gonapophyses 9 present posteriad gonocoxites 8 and beneath gonocoxites 9. Ectoprocts subtrapezoidal in lateral view, slightly broadened posteriad.

Materials examined. Holotype male, China, Xizang, Chayu, Jigong [28°39.17'N, 97°27.21'E], 2300 m, 2.VII.1978, Guangwu Li (IZCAS). 1 female [holotype of *R. zayuanum*], China, Xizang, Chayu, Jigong [28°39.17'N, 97°27.21'E], 2300 m, VIII.1982, Baohai Wang (IZ-

CAS); 1 male, China, Xizang, Chayu [ca. 28°39.17'N, 97°27.21'E], 3.VII.2011, Ye Liu (CAU); 1 female, China, Xizang, Chayu, Shaqiong [ca. 28°39.17'N, 97°27.21'E], 10.VII.2011, Ye Liu (CAU); 1 male, China, Xizang, Chayu [ca. 28°39.17'N, 97°27.21'E], 19.VII.1997, Chaodong Zhu (IZCAS).

Distribution. China (Xizang).

Remarks. This species appears to be closely related to *Rapisma nepalense* Barnard, 1981 from Nepal and *Rapisma almoranum* Barnard, 1981 from northern India in having similar yellowish brown body and medially punctuate head in males as well as male gonocoxite 9 posteriorly with glabrous, ovoid lobe. However, it can be distinguished from *R. nepalense* by the absence of large median dark spot on forewing and the relative broad lobe of male gonocoxite 9, and it differs from *R. almoranum* by the male gonocoxite 9 with a broad lobe and a subtriangular accessory lobe.

Rapisma xizangense is known for the remarkable sexual dimorphism of body and wing coloration (Wang et al. 2013). It may be interesting to figure out whether its related species also have such feature. Barnard (1981) mentioned that *R. almoranum* might be conspecific to *Rapisma viridipenne* (Walker, 1853) from Nepal and northeastern India by having similar forewing marking patterns. So far, *R. viridipenne* is only known from female specimens and its forewing is greenish yellow (Barnard, 1981). If *R. almoranum* and *R. viridipenne* are confirmed to be same species, the sexual dimorphism of body and wing coloration should be also present in this species.

Rapisma changqingensis sp. n.

http://zoobank.org/E7EFEBE1-7CD7-46EF-B57D-DA6D9920C045
Figs 2–3, 7–8, 10

Diagnosis. Body and forewings generally greenish in both males and females. Head medially without dark marking. Antenna extremely short, less than 1/5× forewing length. Male gonocoxites 9 paired, glabrous; each with a broad subtrapezoidal lobe and a slender, arcuately curved lateral arm; fused gonocoxites 11 generally arched, anteriorly broadly concaved but with a semicircular median notch, posteriorly convex in dorsal view; gonostyli 11 having obtuse dorsal lobe with a few short setae, and flat ventral lobe distally with a pair of tufts of long setae.

Description. Male. Body length 18.0 mm; forewing length 25.0 mm, hindwing length 21.7 mm.

Head nearly semiglobular, largely retracted under prothorax, barely visible in dorsal view. Head slightly yellowish green; a narrow blackish stripe present around compound eye and slightly extending toward vertex. Compound eyes blackish brown; EI ratio 0.68. Antenna nearly moniliform, short, 4.0 mm long, with 24 flagellomeres; yellowish throughout. Mandibles with tips black.

Thorax entirely greenish, meso- and metathorax slightly paler than prothorax, without any distinct markings. Legs yellowish throughout; pretarsal claws reddish brown with base yellowish, proximally slightly produced.

Forewing greenish, immaculate. Trichosors absent. A proximal nygma present between RP+MA and MP, whitish. RP with 8 pectinate branches. Hindwing much paler than forewing. A proximal nygma present between RP+MA and MP, whitish. Costal space with a few interlink veinlets among costal crossveins on proximal half. RP with 7 pectinate branches.

Abdomen yellowish green, with terga and genitalia brown. Tergum 9 subtrapezoidal, with sparse short setae. Sternum 9 slightly shorter than tergum 9, about 2.0 times as wide as long, with slightly arcuate posterior margin. Ectoprocts slightly shorter and much narrower than tergum 9, ventrally divided into a pair of ovoid lobes; callus cerci present, slightly prominent. Gonocoxites 9 paired, glabrous; each with a broad subtrapezoidal lobe and a slender, arcuately curved lateral arm. Fused gonocoxites 11 generally arched, anteriorly broadly concaved but with a semicircular median notch, posteriorly convex in dorsal view. Gonostyli 11 with a pair of dorsal and a single ventral lobe; dorsal lobe obtuse, with a few short setae; ventral lobe flat, distally with a pair of tufts of long setae.

Female. Body length 24.8 mm; forewing length 32.0 mm, hindwing length 28.9 mm.

Body and forewings in general greenish. Head without dark marking. Forewing with a few tiny dark spots.

Sternum 7 large, posteromedially with a narrow groove. Gonocoxites+gonapophyses 8 fused, broadly subtrapezoid, notched distally, with a pair of digitiform projections and a weak median projection. Gonocoxites 9 nearly semicircular in lateral view, distally with tiny gonostyli 9; a pair of small setose ovoid gonapophyses 9 present posteriad gonocoxites 8 and beneath gonocoxites 9. Ectoprocts nearly semicircular in lateral view.

Materials examined. Holotype male, China, Shaanxi, Yangxian, Changqing National Nature Reserve, Yangjiagou, 1281 m, 33.6390°N 107.4965°E, 18.VII.2017, Bozun Huang & Zhifei Liu (CAU). Paratype: 1 female, same collecting site as holotype, 24.VII.2017, Puyuan Liu (CAU).

Etymology. The new species is named based on the Changqing National Nature Reserve where type specimens of this species were collected.

Distribution. China (Shaanxi).

Remarks. The new species appears to be closely related to *R. yanhuangi* from Sichuan by the similar body and wing coloration as well as the general characteristics of male genitalia, but it can be distinguished from the latter species by the male head medially without dark marking, the male gonostyli 11 with a pair of dorsal lobes not prominent posterolaterally, and the shape of male fused

Figure 7. Living habitus of *Rapisma changqingensis* sp. n., (**A**) male adult, lateral view; (**B**) female adult, dorsal view.

gonocoxites 11. In *R. yanhuangi* the male head medially possesses several dark markings, the dorsal lobes of male gonostyli 11 are distinctly prominent posterolaterally, and the male fused gonocoxites 11 is differently shaped compared with *R. changqingensis* sp. n.

The two specimens of this new species were collected by accident in a field survey performed by a summer camp for natural education called "Wings of Nature" in Changqing National Nature Reserve, Shaanxi, China. All collectors of these two specimens are middle school

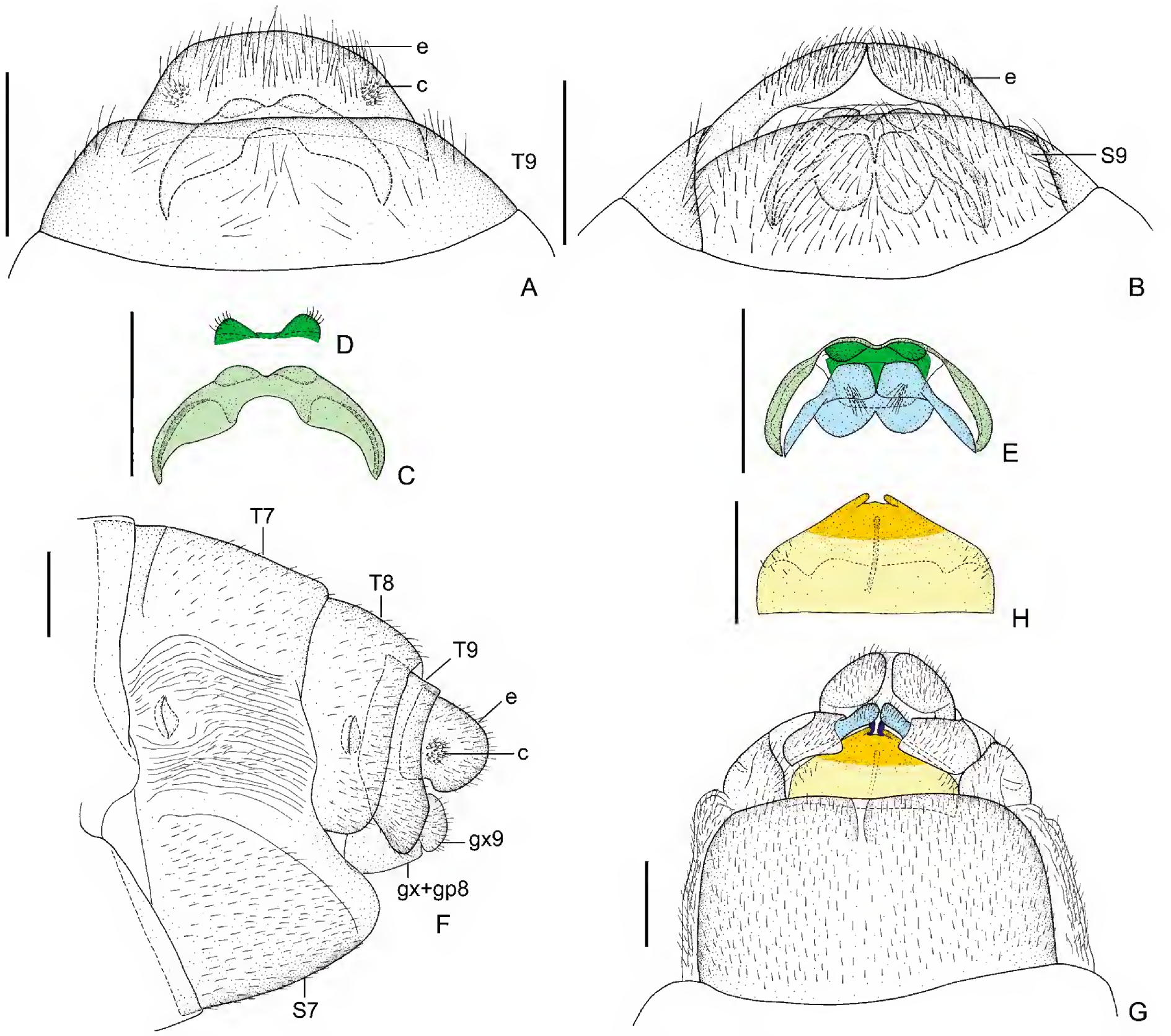

Figure 8. *Rapisma changqingensis* sp. n., (**A**) male genitalia, dorsal view; (**B**) male genitalia, ventral view; (**C**) male gonocoxites 11, dorsal view; (**D**) male gonostyli 11, dorsofrontal view; (**E**) complex of internal male genital sclerites, ventral view; (**F**) female genitalia, lateral view; (**G**) female genitalia, ventral view; (**H**) female gonocoxites+gonapophyses 8, ventral view. **c** – callus cercus; **e** – ectoproct; **gx** – gonocoxite; **gp** – gonapophysis; **T** – tergum; **S** – sternum. Gonocoxites 9, gonocoxites 11 and gonostyli 11 are respectively highlighted in pale blue, pale green and green in panels C–E. Gonocoxites 9 and gonapophyses 9 are respectively highlighted in pale blue and dark blue in panel G (gonostyli 9 present but barely visible in lateral and ventral view), while gonocoxites 8 and gonapophyses 8 are respectively highlighted in pale yellow and yellow in panels G and H. Scale bar: 1.0 mm.

students. The holotype male was found falling in a pond probably from a tree nearby, while the paratype female was found resting on a tree.

The Changqing National Nature Reserve is located at the southern slope of Qinling Mountains, which is commonly considered as a boundary between Palaearctic and Oriental regions in China (Zhang 1999), and it is one of the nature reserves that harbour some endangered wildlife, such as giant pandas, crested ibises, sub-nosed monkeys, etc. The climate of the collecting site of *R. changqingensis* sp. n. is warm temperate, and the vegetation is kind of mixed evergreen broad-leaf and coniferous forest. However, most *Rapisma* species are from subtropical or tropical regions with rainforests. So far, *R. changqingensis* sp. n. represents the northernmost record of *Rapisma*.

Rapisma yanhuangi Yang, 1993

Figs 2–3, 9–10

Rapisma yanhuangi Yang, 1993: 147. Type locality: China (Sichuan: Chongqing).

Diagnosis. Body and forewings generally greenish in both males and females. Head medially with dark mark-

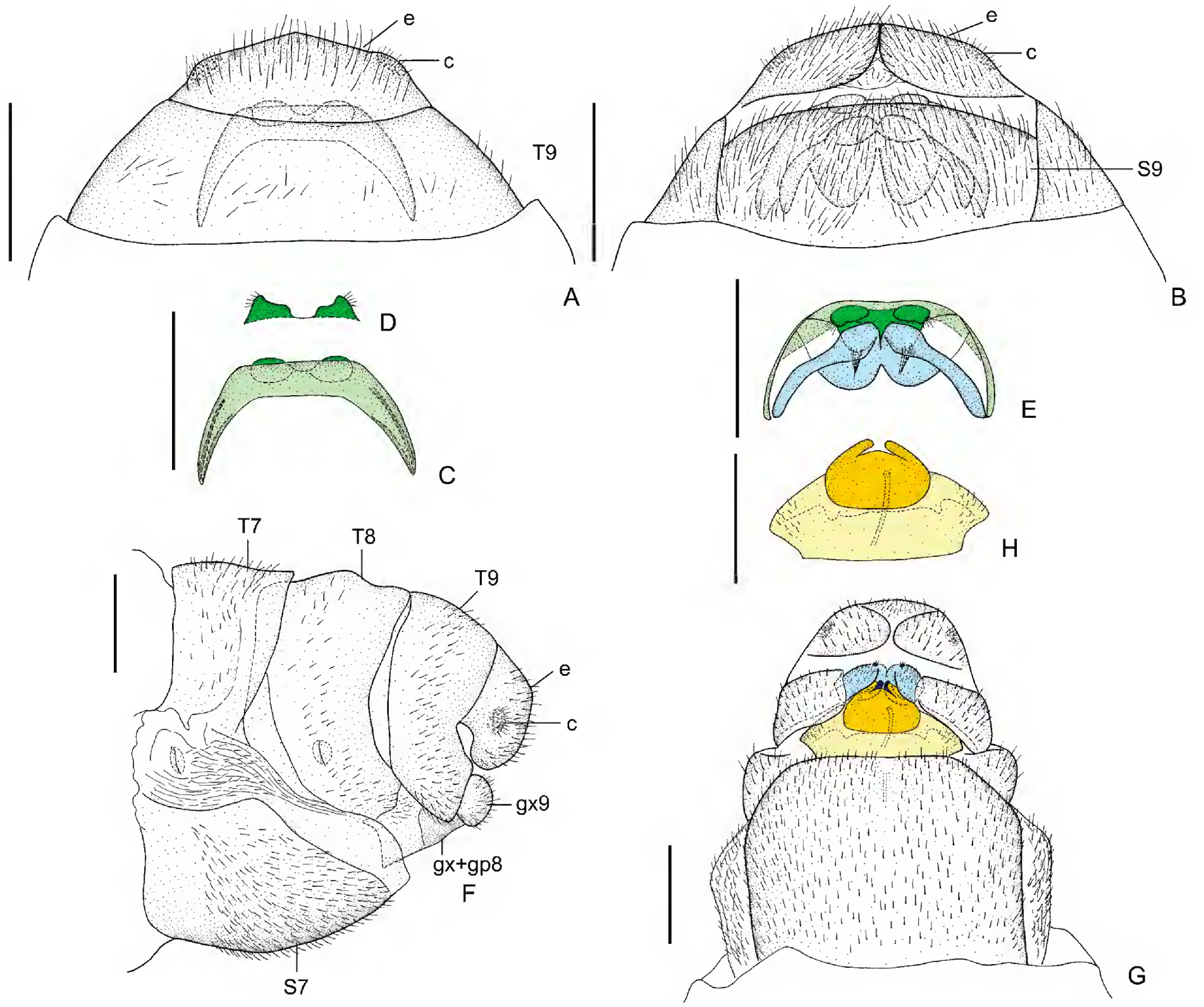

Figure 9. *Rapisma yanhuangi* Yang, (**A**) male genitalia, dorsal view; (**B**) male genitalia, ventral view; (**C**) male gonocoxites 11, dorsal view; (**D**) male gonostyli 11, dorsofrontal view; (**E**) complex of internal male genital sclerites, ventral view; (**F**) female genitalia, lateral view; (**G**) female genitalia, ventral view; (**H**) female gonocoxites+gonapophyses 8, ventral view. **c** – callus cercus; **e** – ectoproct; **gx** – gonocoxite; **gp** – gonapophysis; **gst** – gonostylus; **T** – tergum; **S** – sternum. Gonocoxites 9, gonocoxites 11 and gonostyli 11 are respectively highlighted in pale blue, pale green and green in panels C–E. Gonocoxites 9, gonostyli 9 and gonapophyses 9 are respectively highlighted in pale blue and dark blue in panel G, while gonocoxites 8 and gonapophyses 8 are respectively highlighted in pale yellow and yellow in panels G and H. Scale bar: 1.0 mm.

ings on vertex, frons and clypeus. Antenna extremely short, less than 1/5× forewing length. Male gonocoxites 9 paired, glabrous; each with a broad subtrapezoidal lobe and a slender, arcuately curved lateral arm; fused gonocoxites 11 generally arched, anteriorly with a broad, subtrapezoidal incision, posteriorly truncate, laterally acutely tapering in dorsal view; gonostyli 11 having dorsal lobe posterolaterally distinctly prominent, with a few short setae, and flat ventral lobe distally with a tuft of long setae.

Description. Male. Body length 17.2–20.0 mm; forewing length 20.8–25.8 mm, hindwing length 18.4–22.1 mm.

Head nearly semiglobular, largely retracted under prothorax, barely visible in dorsal view. Head generally pale yellowish green; a narrow blackish stripe present around compound eye; a pair of transverse, ovoid, blackish brown markings present on vertex; several small brownish spots present along midline of frons and clypeus. Compound eyes dark brown; EI ratio 0.78. Antenna nearly moniliform, short, 4.7–4.9 mm long, with 23–26 flagellomeres; pale yellowish brown. Mandibles with tips black.

Thorax entirely greenish, meso- and metathorax slightly paler than prothorax, without any distinct markings. Legs pale yellowish brown, slightly darkened on apices of tibiae and all tarsomeres; pretarsal claws reddish brown, proximally slightly produced.

Forewing greenish, with some small grayish spots on distal half and along posterior margin, but these dark markings sometimes completely reduced. Trichosors absent. A proximal nygma present between RP+MA and

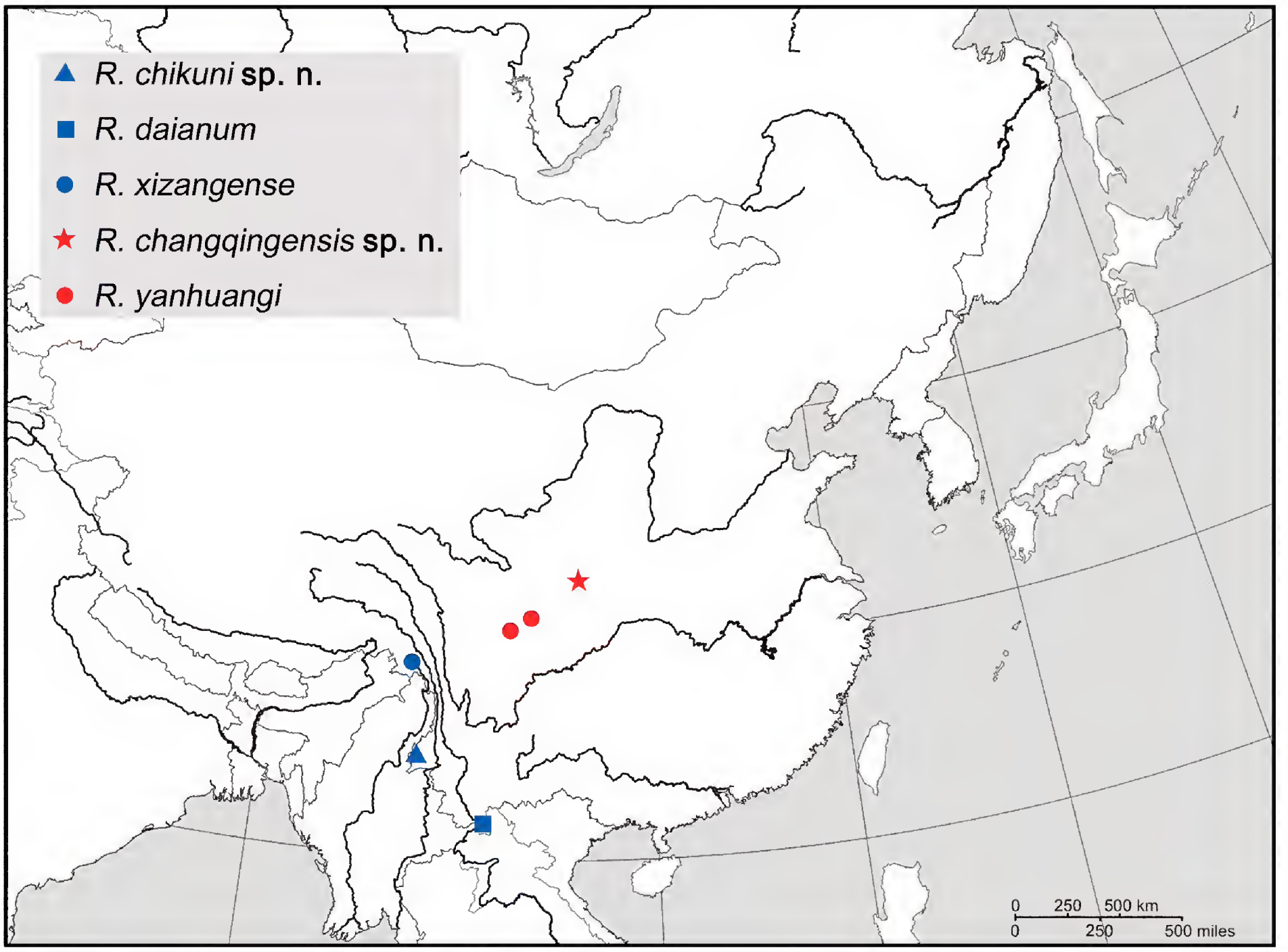

Figure 10. Distribution map of the *Rapisma* species from China.

MP, blackish, sometimes with a distinct black spot. RP with 6–9 pectinate branches. Hindwing much paler than forewing. A proximal nygma present between RP+MA and MP, blackish. RP with 6–7 pectinate branches.

Abdomen yellowish brown, with terga and genitalia greenish. Tergum 9 subtrapezoidal, with sparse short setae. Sternum 9 slightly shorter than tergum 9, about 2.5 times as wide as long, with slightly arcuate posterior margin. Ectoprocts slightly shorter and much narrower than tergum 9, ventrally divided into a pair of ovoid lobes; callus cerci present, slightly prominent. Gonocoxites 9 paired, glabrous; each with a broad subtrapezoidal lobe and a slender, arcuately curved lateral arm. Fused gonocoxites 11 generally arched, anteriorly with a broad, subtrapezoidal incision, posteriorly truncate, laterally acutely tapering in dorsal view. Gonostyli 11 with a pair of dorsal and a pair of ventral lobes; dorsal lobe posterolaterally distinctly prominent, with a few short setae; ventral lobe flat, distally with a tuft of long setae.

Female. Body length 18.0–20.0 mm; forewing length 27.0–27.3 mm, hindwing length 27.0–24.0 mm.

Body and forewings in general greenish. Head slightly darkened on vertex, with or without a dark spot on frons. Forewing without any dark marking.

Sternum 7 large, posteromedially with a narrow groove. Gonocoxites+gonapophyses 8 fused, nearly pentagonal, but divided by an arched transverse suture, notched distally, with a pair of digitiform projections and a weak median projection. Gonocoxites 9 nearly semicircular in lateral view, distally with tiny gonostyli 9; a pair of small setose ovoid gonapophyses 9 present posteriad gonocoxites 8 and beneath gonocoxites 9. Ectoprocts ovoid in lateral view.

Materials examined. Holotype female, China, Sichuan, Chongqing [= Chongzhou, ca. 30°37.29'N, 103°40.13'E], 31.V.1954, Hechang Liu (IZCAS). 4 male 1 female, China, Sichuan, Shimian, Liziping Nature Reserve, Gongyihai Station [29°05.35'N, 102°20.11'E], 2100 m, 22–25. VII.2007, Liu, Zhang, Zhou & Bi (SEMCAS).

Distribution. China (Sichuan).

Remarks. This species was originally described based on a single female specimen (Yang 1993). As the new materials, particularly the female, show almost same characteristics to the holotype female, I identified them to be *R. yanhuangi*. Nevertheless, further confirmation on the present identification should be considered if male specimens from the type locality are found in the future. The new materials of *R. yanhuangi* were collected by light trap. Among the male specimens the greenish forewings possess a few grayish spots or lack any dark spots, while the median dark

spot on frons is present in the holotype female but absent in another female of the new materials. It suggests that identification of *Rapisma* species based solely on head and wing markings must be cautious as these characters are variable among conspecific individuals in some species.

Discussion

Homology of genital sclerites

The genital segments of *Rapisma* are much smaller than the pregenital segments that are rather robust and in dried specimens are sometimes inconspicuous and partly retracted in the preceding pregenital segments. Due to the rareness of *Rapisma* species, very few works deal with the morphology of the genital sclerites of this genus. Barnard (1981) first interpreted the genitalia of *Rapisma* following the homology assessment and terminology proposed by Acker (1960). In this work the male genitalia of *Rapisma* are composed of tergum and sternum 9, tergum 10, paired gonocoxites, gonarcus, mediuncus (including upper mediuncus lobes and lower mediuncus lobes), and hypandrium internum, while the female genitalia constitute terga 8–10, subgenital plate, and paired gonapophyses laterales. It is noteworthy that the female gonostyli of gonapophyses laterales are missing in the illustration of Barnard (1981). However, Yang (1993) illustrated the small gonostyli on the apex of the female ovipositor (= gonapophyses laterales). Aspöck and Aspöck (2008) provided a new homology assessment of the genital sclerites of Neuropterida with revised terminology based on the gonocoxite concept [i.e. the coxopodite concept of Acker (1960) for Neuropterida]. In this work, irrespective of terga and sterna of segments 8–10, the male genital sclerites comprise paired gonocoxites + gonostyli 9 (= gonocoxites), fused gonocoxites and gonostyli 11 (= gonarcus and mediuncus), and hypandrium internum, while the female genital sclerites comprise fused gonocoxites 8 (= subgenital plate) and paired gonocoxites 9 (= gonapophyses laterales). Notably, the sclerites belonging to segment 10 except for ectoprocts are missing in males of *Rapisma*, and the male gonostyli 11 are enlarged, being considered to be a synapomorphy of Ithonidae + Myrmeleontiformia (Aspöck and Aspöck 2008). I basically agree to the homology interpretation for *Rapisma* proposed in Aspöck and Aspöck (2008). Nevertheless, a few amendments are made below.

Concerning the male gonocoxites 9, they are paired, each with a broad lobe and a slender lateral arm, while the broad lobe is modified into two differently shaped parts, i.e. the posteroventral part, being glabrous or covered with many tiny spines, and the anterodorsal part, being flat and broadly ovoid or subtriangular (Figs 4D, 6D). Aspöck and Aspöck (2008) interpreted the former part to be the gonostylus 9 and did not assign the latter part to be a component of segment 9. Compared with the related genera of *Rapisma* (e.g. *Adamsiana*), in which no gonostyli 9 are found in Aspöck and Aspöck (2008), there is no substantial argument to interpret the antero-dorsal lobe to be the gonostylus 9. So, here I interpret that only gonocoxites 9, possibly amalgamated with gonapophysis and gonostyli 9 (but unrecognizable), are present in males of *Rapisma*.

Concerning the female genitalia, it should be first confirmed that the gonostyli 9 are present at the apex of gonocoxites 9 in all female *Rapisma* specimens herein examined (Fig. 6F). Probably, they are present in all *Rapisma* species. Nevertheless, they are very small and could be overlooked as in Barnard (1981) and Aspöck and Aspöck (2008). Furthermore, there is a pair of curious small sclerites present beneath anterior portion of gonocoxites 9 (see Yang 1993: fig. 1; Fig. 6F). They should represent the gonapophyses 9 as similar sclerites are interpreted as gonapophyses 9 in the ithonid genus *Polystoechotes* (see Aspöck and Aspöck 2008: fig. 134). In addition, the fused gonocoxites 8 of *Rapisma* interpreted in Aspöck and Aspöck (2008) is divided anteroposteriorly by a transverse suture (Fig. 6G), and the posterior part is herein considered to be the fused gonapophyses 9, being similar to that in *Polystoechotes* (see Aspöck and Aspöck, 2008: fig. 135).

In general, the genital sclerites of *Rapisma* retain more plesiomorphic features in comparison to other ithonid genera with exceptionally enlarged male ectoprocts, highly specialized female gonocoxites 9, reduced male gonostyli 11, reduced female gonostyli 9, etc. The configuration of male gonocoxites 9 and gonostyli 11 in *Rapisma* is unique among the genera of Ithonidae and may be attributed to the autapomorphies of this genus.

Phylogenetic positions of Chinese *Rapisma*

So far there is no phylogenetic analysis concerning the relationships among *Rapisma* species. Only in Barnard (1981) seven characters were outlined and used to infer the interspecific relationships of this genus, i.e. the presence/absence of dark transverse band on head, the presence/absence of central projection on female gonapophyses 8, the glabrous/spinous male gonocoxites 9, the relatively short/long antennae, the relatively large/small compound eyes, the subserrate/moniliform antennae, and the posteriorly bilobed/undivided male gonocoxites 9 (the former state considered as apomorphic). At present I feel refrain to perform any phylogenetic analysis because there are still a few species with males or females unknown and because the male genitalia of those species from other countries need further examinations given more phylogenetically informative characters could be found. Nevertheless, two groups of species proposed by Barnard (1981) could be justified as they possess some unique apomorphic characters.

First, three species distributed along the southern Himalayas, namely *R. viridipenne*, *R. nepalense*, and *R. almoranum*, form a group based on the glabrous male gonocoxites 9 and the short antennae [*Rapisma burmanum* Navás, 1929 that was originally placed in this group by Barnard (1981) was subsequently removed due to the presence of spinous male gonocoxites 9 (Barnard 1986)]. Thus, three Chinese species, i.e. *R. xizangense*, *R. changqingensis* sp. n., and *R. yanhuangi*, probably belong

to this species group by having the aforementioned apomorphic characters. Within this group, *R. changqingensis* sp. n. and *R. yanhuangi* might form a subgroup because of similar body and wing coloration (both male and female generally greenish) and similarly shaped male gonocoxites 9. The distribution areas of these two closely related species are also near to each other, located at the northeastern edge of Hengduan Mountains and southwestern edge of Qinling Mountains (Fig. 10). Interestingly, these areas are overlapped with the distribution range of giant pandas. The divergence between these two species might be in correlated to geographical isolation formed by certain mountains from these areas. Likewise, given similar range along Himalayas, *R. xizangense* may have close affinity with the other three Himalayan *Rapisma* species, but no definite apomorphy supporting this hypothesis has yet been found.

Second, *R. corundum* from eastern Myanmar and *R. tamilanum* from southern India are considered to form a monophyletic group by the subserrate male antennae and the posteriorly bilobed male gonocoxites 9 (Barnard 1981). Two Chinese species from Yunnan, i.e. *R. chikuni* sp. n. and *R. daianum*, should belong to this species group by having same apomorphic characters.

Most of the other *Rapisma* species are considered to form a group called the *Rapisma malayanum*-complex, which are mainly distributed in western Malaysia but also in Java and Myanmar (Barnard and New 1985, 1986). However, there is no distinct apomorphic character proposed to support the monophyly of this group. From China no species related to this group has yet been found.

Conclusions

This study summarized the present knowledge on the ithonid genus *Rapisma* from China, currently with five species that respectively belong to two monophyletic species group. The morphology of the genitalia of this genus was also further understood. In addition, the distribution region of *Rapisma* is now known to reach the border between Palaearctic and Oriental regions.

Rapisma is the only extant genus of Ithonidae from Asia. The phylogenetic status of this genus in Ithonidae, as well as the phylogenetic relationships among species within the genus, is of high interest and significance for understanding the origin and diversification pattern of the genus. A dated phylogeny of Ithonidae and *Rapisma* as well stand as a key to figure out the above questions, while comprehensive sampling, particularly new materials for molecular works, is required.

Acknowledgements

I want to express my cordial thanks to Mr. Yinong Ni, Mr. Yuchen Zheng, and Dr. Tingting Zhang who led the 2017 field survey of Wings of Nature in Changqing National Nature Reserve, from which the new species *Rapisma changqingensis* sp. n. was found by them and their students. I am also much indebted to Mr. Wenxuan Bi, Mr. Ye Liu, and Mr. Changqing Chen for gifting some *Rapisma* specimens they collected from Yunnan and Xizang, and to Dr. Weibing Zhu and Dr. Haisheng Yin for kindly processing the loan of *Rapisma* specimens deposited in the Shanghai Entomological Museum. My thanks also go to Mr. Yuchen Zheng, Mr. Wenxuan Bi, and Ms. Di Li for taking some pictures and editing illustrations. The present study was funded by the Beijing Natural Science Foundation (No. 5162016), the National Natural Science Foundation of China (No. 31672322) and the Chinese Universities Scientific Fund (No. 2017TC031).

References

Acker TS (1960) The comparative morphology of the male terminalia of Neuroptera (Insecta). Microentomology 24: 25–84.

Aspöck U, Aspöck H (2008) Phylogenetic relevance of the genital sclerites of Neuropterida (Insecta: Holometabola). Systematic Entomology 33: 97–127. https://doi.org/10.1111/j.1365-3113.2007.00396.x

Barnard PC (1981) The Rapismatidae (Neuroptera): montane lacewings of the oriental region. Systematic Entomology 6: 121–136. https://doi.org/10.1111/j.1365-3113.1981.tb00430.x

Barnard PC, New TR (1985) New species in the *Rapisma malayanum*-complex (Neuroptera: Rapismatidae). Neuroptera International 3: 165–173.

Barnard PC, New TR (1986) The male of *Rapisma burmanum* Navás (Neuroptera: Rapismatidae). Neuroptera International 4: 125–127.

Krüger L (1922) Hemerobiidae. Beiträge zu einer Monographie der Neuropteren-Familie der Hemerobiiden. Stettiner Entomologische Zeitung 83: 138–172.

McLachlan R (1866) A new genus of Hemerobidae, and a new genus of Perlidae. Transactions of the Entomological Society of London 15: 353–354. https://doi.org/10.1111/j.1365-2311.1967.tb01441.x

Navás L (1929) Insectos exóticos Neurópteros y afines del Museo Civico de Génova. Annali del Museo Civico di Storia Naturale Giacomo Doria 53: 354–389.

New TR (1985) A new species of Rapismatidae (Neuroptera) from Sabah. Neuroptera International 3: 133–135.

Oswald JD (2017) Neuropterida Species of the World. Version 5.0. http://lacewing.tamu.edu/SpeciesCatalog/Main.

Walker F (1853) Catalogue of the specimens of neuropterous insects in the collection of the British Museum. Part II (Sialides–Nemopterides). Newman, London, 193–476.

Wang YY, Liu XY, Winterton SL, Yan Y, Chang W, Yang D (2013) Comparative mitogenomic analysis reveals sexual dimorphism in a rare montane lacewing (Insecta: Neuroptera: Ithonidae). PLoS ONE 8: e83986. https://doi.org/10.1371/journal.pone.0083986

Winterton SL, Makarkin VN (2010) Phylogeny of moth lacewings and giant lacewings (Neuroptera: Ithonidae, Polystoechotidae) using DNA sequence data, morphology, and fossils. Annals of the Entomological Society of America 103: 511–522. https://doi.org/10.1603/AN10026

Yang CK (1993) The montane lacewings (Neuroptera: Rapismatidae) new to China, with descriptions of four new species. Scientific Treatise on Systematic and Evolutionary Zoology 2: 145–153.

Zhang YZ (1999) Zoogeography of China. Science Press, Beijing, 502 pp.

Zoosyst. Evol. 94 (1) 2018, 73–81 | DOI 10.3897/zse.94.23000

PENSOFT

museum für naturkunde

A new species of *Eisothistos* (Isopoda, Cymothoida) and first molecular data on six species of Anthuroidea from the Peninsular Malaysia

Melvin Chew[1], Azman bin Abdul Rahim[1], Nurul Yuziana binti Mohd Yusof[2]

1 *Marine Ecosystem Research Centre (EKOMAR), Faculty of Science and Technology, Universiti Kebangsaan Malaysia (UKM), Bangi, Selangor, Malaysia*

2 *School of Biosciences and Biotechnology, Faculty of Science and Technology, Universiti Kebangsaan Malaysia (UKM), Bangi, Selangor, Malaysia*

http://zoobank.org/9C28FEF8-BA69-4BCD-A91B-FA910956E2DD

Corresponding author: *Azman bin Abdul Rahim* (abarahim@gmail.com)

Received 13 December 2017
Accepted 15 January 2018
Published 25 January 2018

Academic editor:
Michael Ohl

Abstract

A new species of expanathurid (*Eisothistos tiomanensis* **sp. n.**) is described and illustrated. It was collected from Pulau Tioman, Malaysia and can be distinguished by the unique bipartite shape of its uropodal exopod. *Accalathura borradailei, Apanthura pariensis, A. stocki, Expanathura corallis* and *Mesanthura quadrata* in the Malaysian waters are recorded for the first time. Additionally, six sequences of cytochrome c oxidase subunit I (COI) genes are presented. These are the first molecular evidence of anthuroids from the waters of Malaysia.

Key Words

Isopoda
Anthuroidea
Expanathuridae
Leptanthuridae
Anthuridae
Eisothistos tiomanensis
Accalathura borradailei
Apanthura pariensis
Apanthura stocki
Expanathura corallis
Mesanthura quadrata
Pendanthura tinggiensis
Tinggianthura alba
COI

Introduction

The Anthuroidea Leach, 1814 are a distinctive group of mainly marine isopods (Poore 2009). More than a decade ago, Poore (2001) and Brandt and Poore (2003) revised the taxonomic and evolutionary relationships of what had formerly been treated as a suborder, Anthuridea Monod, 1922. In essence, the former work was a cladistics analysis of family and generic relationships which resulted in the recognition of six families while the latter work replaced Anthuridea with the superfamily Anthuroidea within the Cymothoida Wägele, 1989.

DNA barcoding was first suggested just over two decades ago (Pecnikar and Busan 2014) and it has been utilized for swift reliable biological identifications. It is a taxonomic method that uses a short genetic marker in

an organism's DNA as a unique molecular identifier to a particular species (Hebert et al. 2003a). Hebert et al. (2003b) suggested that the integration of DNA barcoding into traditional taxonomic methods are more efficient in uncovering hidden biodiversity rather than relying on traditional methods alone. On the other hand, due to the increased attention on species barcoding, the issue with questionable and poor quality sequences are becoming more apparent which could possibly harm future systematics studies (Buhay 2009).

Anthuroids have been primarily studied using morphological methods, in particular, dissection of specimens and cladistic analysis. It is only in the recent years that molecular documentations have slowly emerged such as the work of Dreyer and Wägele (2001), Haye et al. (2004), Song and Min (2015a, 2015b) and Wetzer (2001, 2002). Although the Malaysian anthuroids have attracted appreciable taxonomic attention lately (Chew et al. 2014; Chew et al. 2016), no molecular data were provided in their studies. The present study is the first to report molecular properties of anthuroids from this region. In order to ensure that the sequences are reliable genes, molecular gene cloning method was implemented and the sequences were assigned to a Phred quality score of 30.

Methods

Source of specimens and DNA preservation

The specimens in this study were obtained from coral reef areas around Peninsular Malaysia. Coral rubble was collected into a 56 litres bucket with sea water via SCUBA diving and were moderately broken up. About 10 drops of 37 % formaldehyde were added and left to stand for about 30 minutes. Next, the samples were rinsed and washed with seawater passing through a 500 µm sieve. In the field, samples were fixed with about 10 % formalin in seawater. Molecular specimens were obtained in the same manner except that they were laced with about 1 litre of absolute ethanol and left to stand for about 15 minutes. They were placed directly into precooled absolute ethanol (0 ºC) and kept in an icebox which was carried throughout the field sampling to maximize tissue preservation.

Identification and morphological study

At the laboratory, the specimens were sorted and conserved separately in 4 % formalin in water in vials. Specimens were then identified and new species was selected for dissection. Whole bodies and dissected appendages were mounted in glycerol and illustrated under a Leica DMLB light microscope equipped with a camera lucida. Materials are deposited in the Muzium Zoologi, Universiti Kebangsaan Malaysia, Malaysia. The following abbreviations are used: A, antenna; AM, appendix masculina; MD, mandible; MP, maxilliped; MX, maxilla; P, pereopod; PL, pleopod; PLT, pleotelson U, uropod; UN, uropod endopod; UX, uropod exopod; UKMMZ, Universiti Kebangsaan Malaysia Muzium Zoologi.

DNA extraction, PCR amplification, DNA fragment cloning and sequencing

Before extraction, residual ethanol was removed from the tissue by evaporation at room temperature. The samples were left opened covered only with a Kimwipes tissue until they were completely desiccated. DNA was extracted from whole organism using DNeasy Blood and Tissue Kit (Qiagen, USA).

The COI sequences were amplified using the Folmer et al. (1994) universal primers (LCO1490 and HCO2198). The PCR were performed based on the program: initial denaturation period at 95 ºC for 2 minutes and 35 cycles of denaturation at 95 ºC for 30 seconds, annealing at 48 ºC for 45 seconds and extension at 72 ºC for 90 seconds. A final extension was set at 72 ºC for 5 minutes. PCR products were purified using the Qiaquick PCR purification Kit (Qiagen, USA).

Purified PCR products were cloned using *E. coli* Top 10 (Invitrogen) and Thermo Scientific CloneJET PCR Cloning Kit (Thermo Fisher Scientific, USA). Colonies containing the vector along with the cloned PCR fragments were picked with a sterile pipette tip and put in to 20 µl of water. This was mixed and 1 µl was taken as the DNA template for PCR colony screening. Successful clones were purified using the innuPREP Plasmid Rapid Kit (Analytik Jena AG, Germany) and sequences were generated on an automated DNA Sequencer ABI 3100 (Applied Biosystems Inc., USA) using the ABI PRISM Dye Terminator Cycle Sequencing Ready Reaction v3.0 kit (Applied Biosystem Inc., USA).

Bioinformatics screening

Raw COI sequences were assigned to Phred quality score of 30 in order to assess the quality (Ewing and Green 1998). Then, CrossMatch software is used to obtain clean sequences by eliminating the vector sequence (Gotoh 1982). All clones were assembled using the CAP contig assembly program in Bioedit software (Hall 1998).

Results and discussions

Family Anthuridae Leach, 1814

Genus *Apanthura* Stebbing, 1990

Apanthura forceps Negoescu & Brandt, 2001

Apanthura pariensis Negoescu, 1997

Figure 1

Apanthura pariensis Negoescu, 1997: 186-194, figs 6–10.

Materials examined. 43 females, 2 males, UKMMZ-1585, Pangkor Laut, Pulau Pangkor, Perak, Malaysia, 4°11'22.32"N; 100°32'50.22"E (DMS), C. Melvin, 15 April 2014, coral rubble, ~3 m; 9 females, UKMMZ-1586, Pantai Kok, Pulau Langkawi, Kedah, Malaysia, 6°21'56.05"N; 99°40'31.13"E (DMS), C. Melvin, 4 November 2013, intertidal; 8 females, 2 males, UKMMZ-1587, Pantai Kok, Pulau Langkawi, Kedah, Malaysia, 6°21'56.05"N; 99°40'31.13"E (DMS), C. Melvin, 8 March 2015, intertidal.

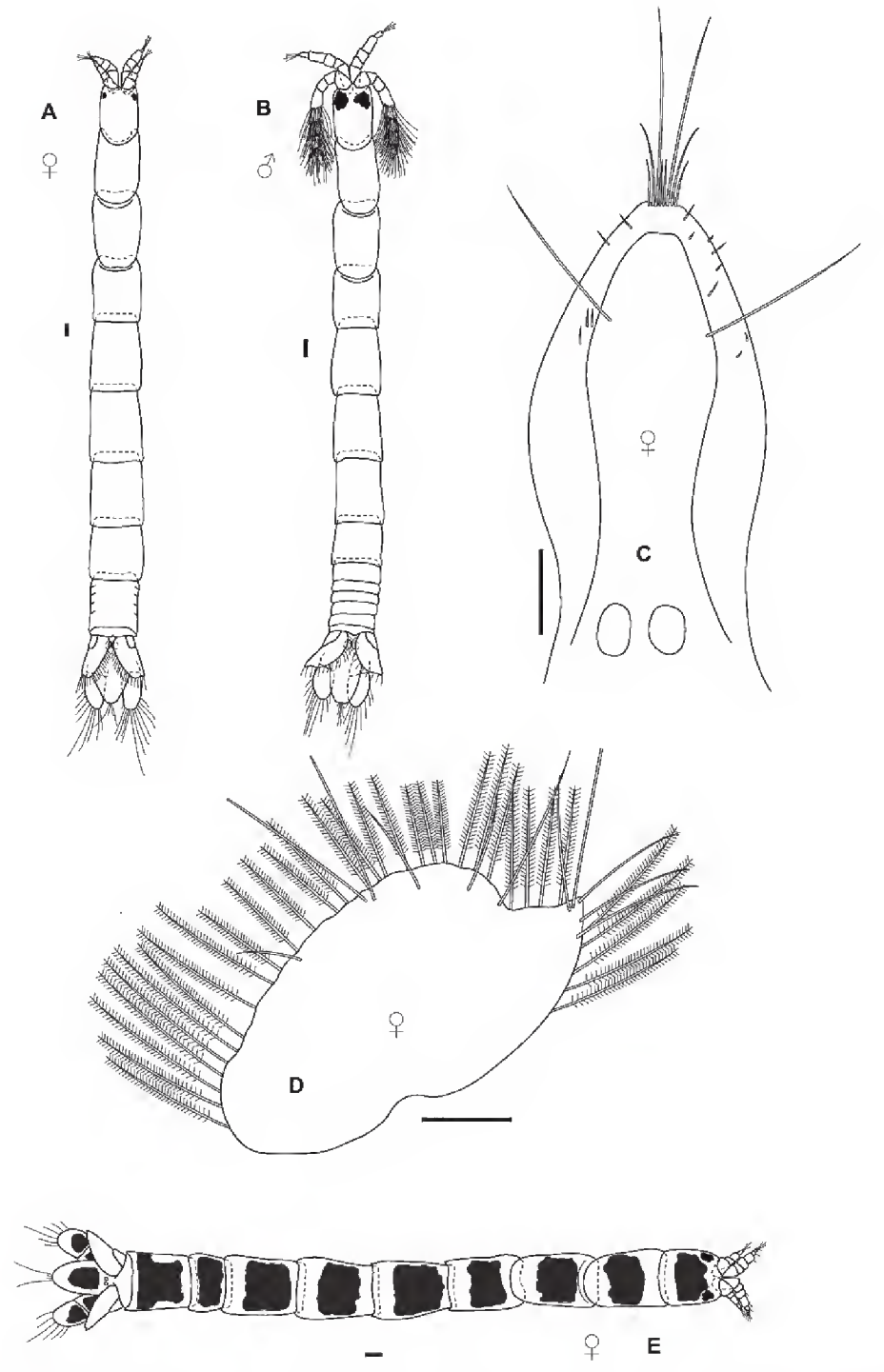

Figure 1. A–D. *Apanthura pariensis*. **A.** female. **B.** male. **C.** pleotelson. **D.** uropodal exopod. **E.** *Mesanthura quadrata*. All scales represent 0.1 mm.

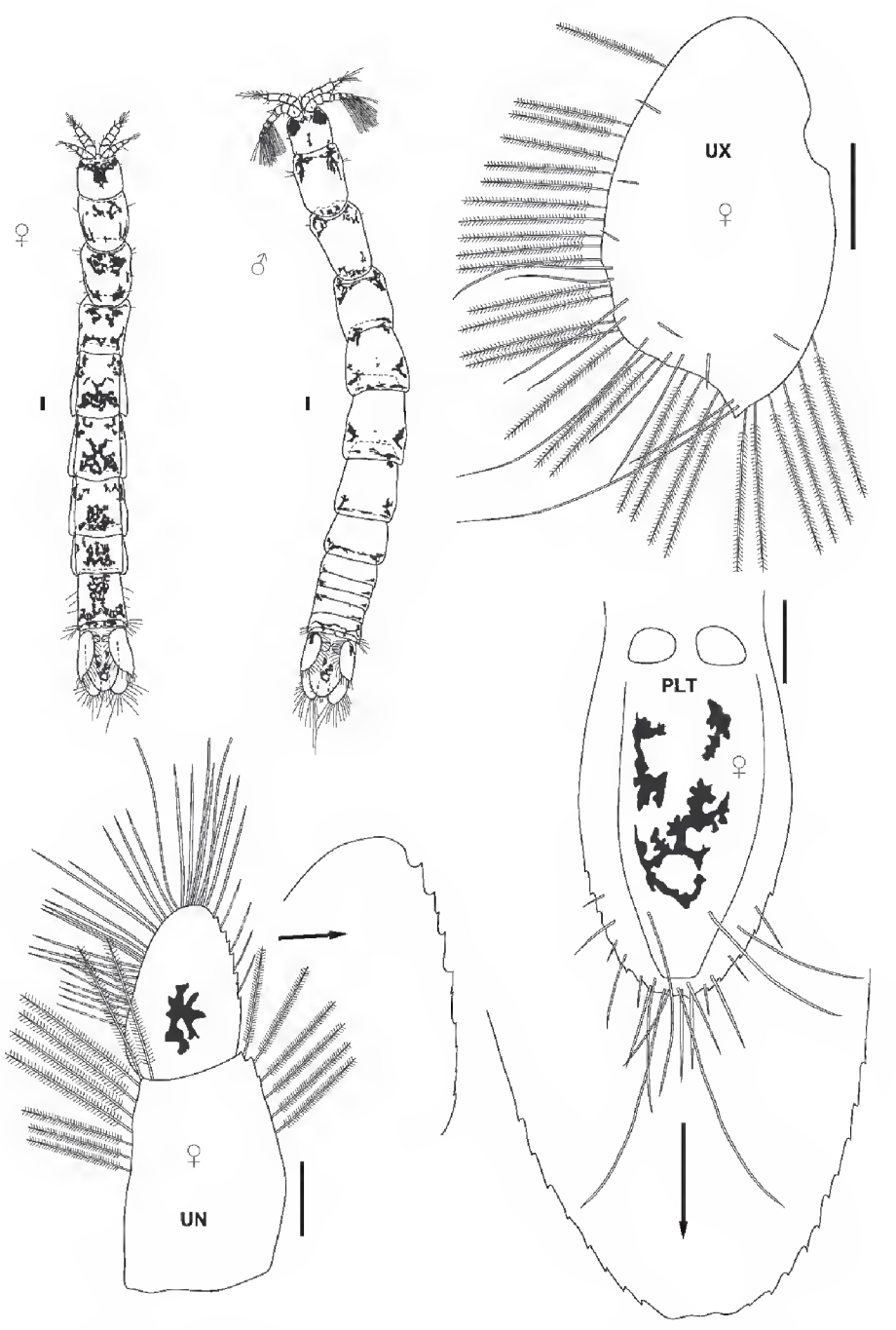

Figure 2. *Apanthura stocki*. All scales represent 0.1 mm.

Distribution. Pari Island, Java Sea, Indonesia (type locality); Pulau Pangkor, Malaysia; Pulau Langkawi, Malaysia.

Molecular data. A 726 base pairs of COI sequence (GenBank: MF680510) was acquired from one individual of *A. pariensis*. No insertion or deletion in the sequence alignment.

Remarks. Negoescu (1997) described in detail the female and manca materials. Fortunately, the male specimen were collected for the first time in the present study. The materials were found particularly from the west coast of Peninsula Malaysia. This is the first record of such species from this country.

Apanthura stocki (Müller, 1991)

Figure 2

Amakusanthura stocki Müller, 1991: 595–600, figs. 30–56.
Apanthura stocki Müller, 1992a: 166.

Materials examined. 1 female, 1 male, UKMMZ-1576, Mentinggi, Pulau Tinggi, Johor, Malaysia, 2°16'21.67"N; 104°7'18.61"E (DMS), C. Melvin, 19 April 2013, coral rubble, ~3 m; 3 females, 1 male, UKMMZ-1577, Kampung Pasir Panjang, Pulau Tinggi, Johor, Malaysia, 2°17'37.96"N; 104°6'1.97"E (DMS) E, C. Melvin, 18 December 2012, coral rubble, ~3 m; 14 females, UKMMZ-1578, Sebirah Kechil, Pulau Tinggi, Johor, Malaysia, 2°18.622'N; 104°05.616'E (DDM), C. Melvin, 18 April 2013, coral rubble, ~3 m; 13 females, 1 male, UKMMZ-1579, Pulau Seri Buat, Pahang, Malaysia, 2°41'13.59"N; 103°55'25.99"E (DMS), C. Melvin, 19 April 2014, coral rubble, ~7 m; 4 females, UKMMZ-1580, Kampung Pasir Panjang, Pulau Tinggi, Johor, Malaysia, 2°17'37.96"N; 104°6'1.97"E (DMS), C. Melvin, 15 June 2015, coral rubble, ~3 m; 27 females, UKMMZ-1581, Batu Bonchek, Pulau Dayang, Johor, Malaysia, 2°28'40.90"N; 104°30'19.12"E (DMS), C. Melvin, 26 July 2016, coral rubble, ~3 m; 6 females, UKMMZ-1582, Teluk Rha, Pulau Aur, Johor, Malaysia, 2°28'17.24"D; 104°30'53.14"E (DMS), C. Melvin, 27 July 2016, coral rubble, ~3 m.

Distribution. Sri Lanka (type locality); Pulau Besar, Malaysia; Pulau Tinggi, Malaysia; Pulau Seri Buat, Malaysia.

Molecular data. A 712 base pairs of COI sequence (GenBank: MF680509) was acquired from one indi-

vidual of *A. stocki*. No insertion or deletion in the sequence alignment.

Remarks. The Malaysian *A. stocki* differs slightly from the original material by its weakly serrated inner margin of uropodal endopod and acute distal margin of uropodal exopod in female.

Genus Mesanthura Barnard, 1914

Mesanthura quadrata Kensley & Schotte, 2000

Mesanthura quadrata Kensley & Schotte, 2000: 2080-2083, figs. 17–18.

Materials examined. 3 immature females, UKMMZ-1595, Pulau Seri Buat, Pahang, Malaysia, 2°41'13.59"N; 103°55'25.99"E (DMS), C. Melvin, 19 April 2014, coral rubble, ~7 m; 1 immature female, UKMMZ-1596, Batu Malang, Pulau Tioman, Pahang, Malaysia, 2°54'15.44"N; 104°6'1.08"E (DMS), C. Melvin, 18 April 2014, coral rubble, ~7 m; 1 female, UKMMZ-1597, Kampung Pasir Panjang, Pulau Tinggi, Johor, Malaysia, 2°17'37.96"N; 104°6'1.97"E (DMS), C. Melvin, 15 June 2015, coral rubble, ~3 m; 1 female, UKMMZ-1598, Sebirah Kechil, Pulau Tinggi, Johor, Malaysia, 2°18.622'N; 104°05.616'E (DDM), C. Melvin, 15 June 2015, coral rubble, ~3 m; 29 juveniles, UKMMZ-1599, Kampung Pasir Panjang, Pulau Tinggi, Johor, Malaysia, 2°17'37.96"N; 104°6'1.97"E (DMS), C. Melvin, 13 October 2012, artificial substrate unit, ~3 m; 1 female, UKMMZ-1560, Sebirah Kechil, Pulau Tinggi, Johor, Malaysia, 2°18.622'N; 104°05.616'E (DDM), C. Melvin, 18 April 2013, coral rubble, ~3 m.

Distribution. Mahé Island, Seychelles (type locality); Pulau Seri Buat, Malaysia; Pulau Tioman, Malaysia; Pulau Tinggi, Malaysia.

Molecular data. n/a.

Remarks. *Mesanthura quadrata* is recorded for the first time from the Southeast Asia region.

Genus *Pendanthura* Menzies & Glynn, 1968

Pendanthura tinggiensis Chew, Rahim & Mohd Yusof, 2016

Pendanthura tinggiensis Chew et al., 2016: 232-238, figs 2–8.

Distribution. Pulau Tinggi, Malaysia.

Molecular data. A 709 base pairs of COI sequence (GenBank: MF680512) was acquired from one individual of *P. tinggiensis*. No insertion or deletion in the sequence alignment.

Remarks. The material used in this study is taken from the study of Chew et al. (2016).

Genus *Tinggianthura* Chew, Abdul Rahim & Haji Ross, 2014

Tinggianthura alba Chew, Abdul Rahim & Haji Ross, 2014

Tinggianthura alba Chew et al., 2014: 1-11, figs 3–9.

Distribution. Pulau Tinggi, Malaysia.

Molecular data. A 658 base pairs of COI sequence (GenBank: MF680513) was acquired from one individual of *T. alba*. No insertion or deletion in the sequence alignment.

Remarks. The material used in this study is taken from the study of Chew et al. (2014).

Family Expanathuridae Poore, 2001
Genus *Eisothistos* Haswell, 1884

Eisothistos tiomanensis sp. n.

*http://zoobank.org/*2C36E902-F854-409D-9FEA-98C41EB299F8
Figure 3–5

Holotype. Adult male, UKMMZ-1559, Labas, Pulau Tioman, Pahang, Malaysia, 2°53'13.71"N; 104°3'54.65"E (DMS), C. Melvin, 18 April 2014, coral rubble, ~15 m.

Description. Holotype, adult male.

Total body length 2.2 mm (tip of rostrum to base of telson), approximately 9.9 times as long as greatest width. Cephalon with minute rostrum; eyes grossly enlarged, containing many ommatidia laterally. Pereonites 1–7 progressively shorter, pereonites 2–3 longest, each 1.3 times as long as pereonite 1, pereonites 4–5 each the same length as pereonite 1, pereonite 6 about 0.7 times length of pereonite 5, pereonite 7 half as long as pereonite 5, pereonites 4–6 anteriorly narrow, subdistally widest, pereonite 7 anteriorly narrow, widest posteriorly. Pleonites 1–5 progressively shorter with pleonites 1–2 of similar length, pleonite 3 about 0.8 times as long as pleonite 2, pleonites 4 about 0.7 times as long as pleonite 3, pleonite 5 shortest half as long as pleonite 4, posterior margin of pleonite 6 with a medial cleft.

Antenna 1 peduncle article 1 subquadrate, articles 2–3 progressively shorter; flagellum of 9 articles with short proximal article bearing numerous aesthetascs, articles 2–9 progressively narrower, articles 2–6 each bearing 2 aesthetascs and 1 seta, articles 7–8 each bearing 1 aesthetasc distally, terminal article with 3 apical setae.

Antenna 2 peduncle articles equal, articles 1–2 each bearing 2 setae, article 3 with 1 seta, article 4 elongate, 2.4 times as long as wide, article 5 longest, twice as long as article 4; flagellum of 6 articles, progressively smaller, articles 1–4 each with 1 distal aesthetasc, article 5 with 2 distal setae, terminal article with 4 apical setae.

Mouthparts reduced.

Pereopod 1 basis 3.3 times as long as greatest width, anterior margin with 1 medial seta, posterior margin with 1 subdistal seta and fine setae; ischium 3.2 times as long

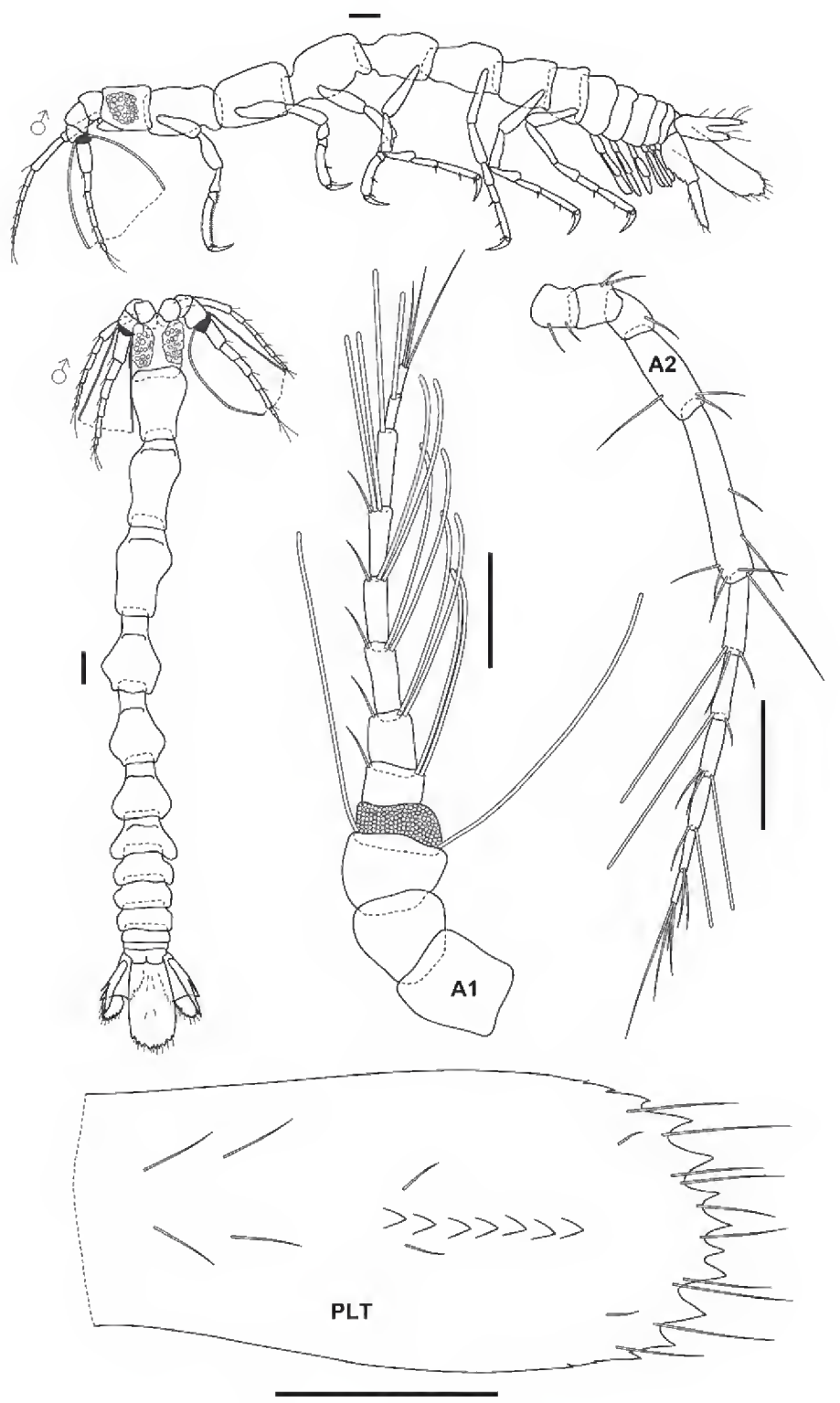

Figure 3. *Eisothistos tiomanensis* sp. n. All scales represent 0.1 mm.

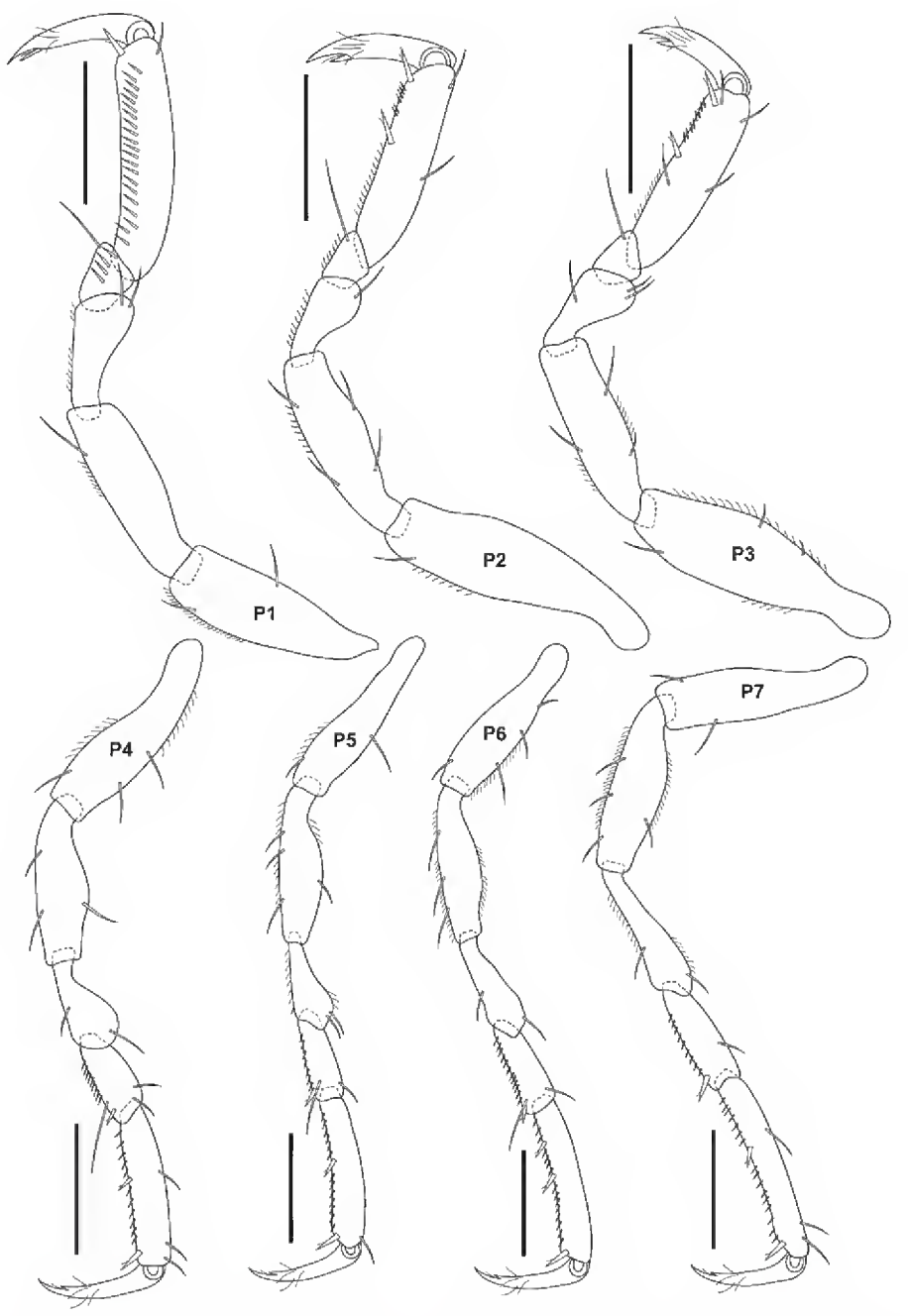

Figure 4. *Eisothistos tiomanensis* sp. n. All scales represent 0.1 mm.

as greatest width, posterior margin subdistally with 1 seta and fine setae; merus anterior margin convex distally, bearing 2 setae, posterior margin with fine setae; carpus anterior margin half the length of posterior margin, posterior margin with 1 seta, with 4 submarginal spinules; propodus 4.4 times as long as greatest width, palm weakly concave with 21 submarginal spinules, anterior margin with 1 distal seta, palmar margin with 1 posterodistal robust seta; unguis half as long as propodus.

Pereopod 2 basis 3.7 times as long as greatest width, posterior margin with 1 subdistal seta and fine setae; ischium 3.1 times as long as greatest width, anterior margin with 2 setae, posterior margin with 2 setae and fine setae; merus anterior margin convex, bearing 1 seta, posterior margin with fine setae; carpus anterior margin half the length of posterior margin, posterior margin with 1 seta and fine setae; propodus 3.9 times as long as greatest width, anterior margin with 2 setae, palmar margin with 1 medial robust seta and 1 posterodistal robust seta, fine setae and subdistal palmar comb; unguis half the length of propodus.

Pereopod 3 basis 3.3 times as long as greatest width, anterior margin with 2 setae and fine setae, posterior margin with 1 seta and fine setae; ischium 3.2 times as long as greatest width, anterior margin with 2 setae and fine setae, posterior margin with 1 seta and fine setae; merus anterior distal margin convex bearing 2 setae, posterior margin with 1 seta, carpus anterior margin one third length of posterior margin, posterior margin with 1 seta; propodus 3.6 times as long as greatest width, anterior margin with 2 setae, palmar margin with fine setae, 2 setae, subdistal palmar comb, 1 medial robust seta and 1 posterodistal robust seta; unguis half as long as propodus.

Pereopod 4 basis 3.9 times as long as greatest width, anterior margin with 2 setae and fine setae, posterior margin with 1 seta and fine setae; ischium 3 times as long as greatest width, anterior margin with 1 seta, posterior margin with 2 setae; merus anterior margin convex, bearing 1 seta, posterior margin with 1 seta, carpus linear twice as long as wide anterior margin with 2 setae, posterior margin with setae comb, 1 seta and 1 robust seta; propodus 4.5 times as long as greatest width, anterior margin with 3 setae, palmar margin bordered with setae comb, 1 medial robust seta and 1 posterodistal robust seta; unguis 0.8 times as long as propodus.

Pereopod 5 basis 4.1 times as long as greatest width, anterior margin with 1 seta, posterior margin with 1 seta and fine setae; ischium 4.1 times as long as greatest width, anterior margin with 1 seta, posterior margin with

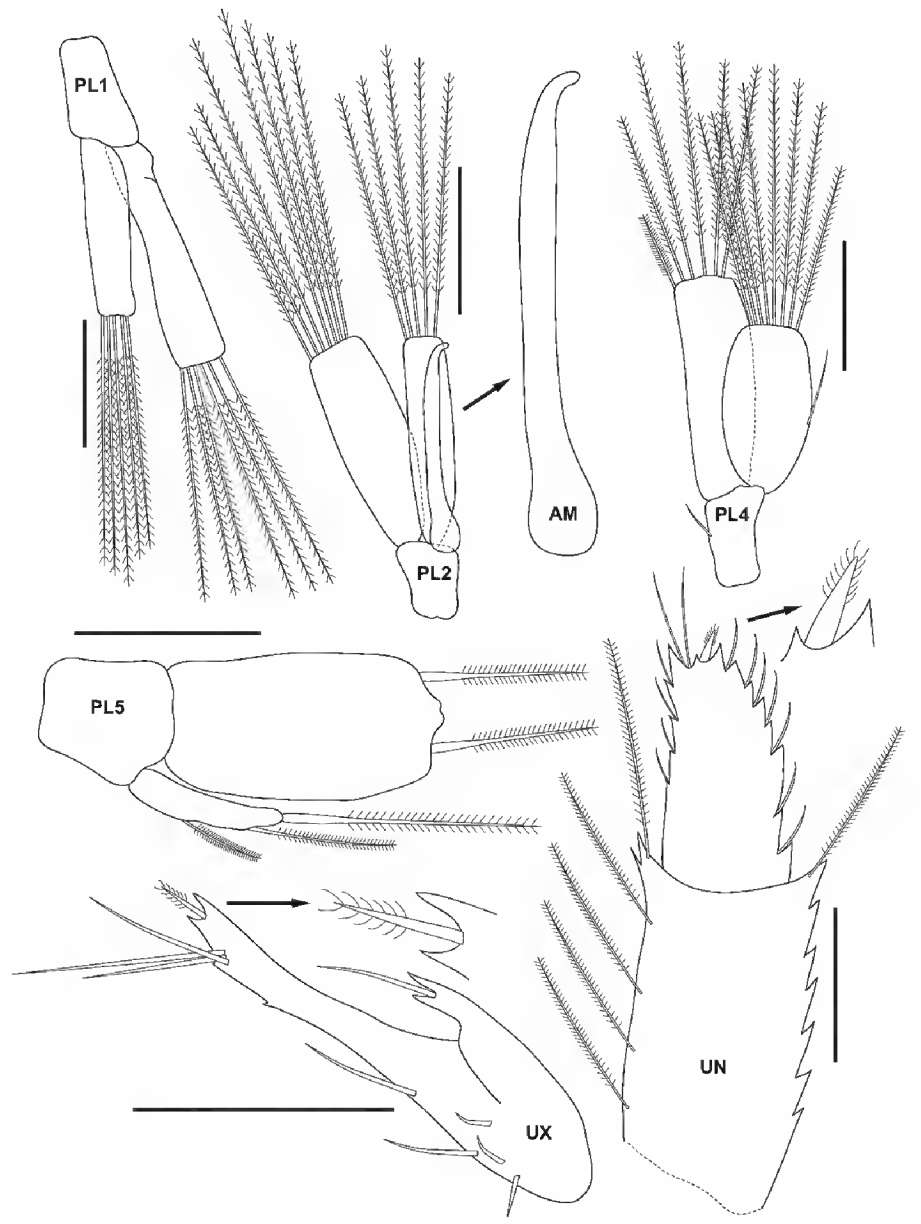

Figure 5. *Eisothistos tiomanensis* sp. n. All scales represent 0.1 mm.

3 setae and fine setae; merus anterior margin subdistally convex, bearing 2 setae, posterior margin with fine setae; carpus linear 2.4 times as long as greatest width, anterior margin with 1 seta, posterior margin with setae comb, 1 distal seta and 1 distal robust seta; propodus 4.6 times as long as greatest width, anterior margin with 1 distal seta, palmar margin bordered with setae comb, 1 medial robust seta and 1 posterodistal robust seta; unguis 0.8 times the length of propodus.

Pereopod 6 basis 4 times as long as greatest width, anterior margin with 3 setae and fine setae, posterior margin with 1 subdistal seta; ischium 3.8 times as long as greatest width, anterior margin with fine setae, posterior margin with 3 setae and fine setae; merus anterior margin convex, bearing 1 seta, posterior margin with 1 seta; carpus linear 2.6 times as long as greatest width, anterior margin with 1 seta, posterior margin bordered with setae comb, distally with 1 seta and 1 robust seta; propodus 5.3 times as long as greatest width, palmar margin bordered with setae comb, proximally with 1 robust seta, medially with 1 robust seta and posterodistally with 1 robust seta; unguis 0.7 times the length of propodus.

Pereopod 7 basis 4.1 times as long as greatest width, anterior margin with 1 seta, posterior margin with 1 seta; ischium 3.2 times as long as greatest width, anterior margin with 1 seta and fine setae, posterior margin with 3 setae and fine setae; merus slender 3.6 times as long as greatest width with anterior margin slightly convex, bearing 1 seta, posterior margin with 1 seta; carpus linear 3.2 times as long as greatest width, anterior margin with 1 seta, posterior margin with setae comb and 1 robust seta; propodus 7.5 times as long as greatest width, anterior margin with 3 setae, palmar margin bordered with setae comb, 1 medial robust seta and 1 posterodistal robust seta; unguis half as long as propodus.

Pleopod 1 with elongated rami, sympod rectangular; exopod slender 4.3 times as long as greatest width, apex truncated bearing 6 plumose setae; endopod shorter than exopod 0.75 times the length of exopod, apex truncated bearing 5 plumose setae.

Pleopod 2 sympod subrectangular; exopod 3 times as long as wide, apex truncated bearing 7 plumose setae; endopod slender 4.8 times as long as greatest width, apex truncated bearing 5 plumose setae; appendix masculina almost as long as endopod, ending in a somewhat hook-like with a rounded end.

Pleopod 3 not available.

Pleopod 4 sympod subrectangular, inner margin with 1 seta; exopod broadened 1.8 times as long as greatest width, apex truncated bearing 8 plumose setae, medial lateral margin with 1 seta; endopod as long as exopod 1.3 times as long as exopod with apical margin truncated bearing 6 plumose setae.

Pleopod 5 shorter than others with sympod subquadrate; exopod much smaller than endopod half as long as endopod bearing 3 plumose setae; endopod broadend 1.8 times as long as greatest width bearing 2 plumose setae, apical margin medially with two small protuberances.

Uropod sympod with serrated inner margin, inner distal margin raised with an acute apex, outer distal margin raised with 2 acute serrations apically; endopod elongate with serrated margin bearing 13 setae, apically with 1 short robust plumose sensory spine; exopod bipartite with 5 setae proximally, medially with a central elongated spike having 3 subdistal setae and apical margin concave bearing 1 short plumose sensory spike, outer margin with a short slender spike bearing 1 seta apically, inner margin obsolete.

Pleotelson 2.2 times as long as greatest width, narrowest anteriorly, widest near posterior end, dorsal surface with 4 pairs of setae and a middorsal row of 7 obscure denticles, subdistal margin with 2 obscure teeth on each side, posterior margin strongly dentate with 10 teeth and 5 pairs of setae.

Etymology. This species is named after the type locality, Pulau Tioman, Malaysia.

Molecular data. n/a.

Remarks. Only one male specimen is available. The male *Eisothistos* in general, differs from the female by its grossly enlarged eyes, antenna 1 with short basal article bearing numerous aesthetascs, reduced mouthparts, pleonites 1–3 elongate and pleopods 1–3 with elongated peduncles and rami (Knight-Jones and Knight-Jones 2002;

Poore 2001; Poore and Lew Ton 2002; Wägele 1979). Though they appear distinctive, their tail-fan shape are more conserved within a species. Hence, it is possible to determine the identity of *Eisothistos* species based on a male specimen. Moreover in this study, the good condition of preserved material and the unique characteristic of its tail-fan, justify a description.

The uropodal exopod form in the *Eisothistos* can be divided into two types. While most possess the tripartite uropodal exopod shape, several others are described with the uncommon bipartite uropodal exopod shape. *Eisothistos tiomanensis* sp. n. belongs to the latter group with *Eisothistos anomala*, *E. corinellae*, *E. macquariensis* and *E. minutus* (Kensley 1980; Poore and Lew Ton 2002; Sivertsen and Holthuis 1980). It differs in having a unique two slender spine-like structure in the uropodal exopod rather than one central slender spike-like structure along with a proximal lobe as in *E. anomala, E. corinellae* and *E. macquariensis*. *Eisothistos minutus* on the other hand, possesses a form similar to the present species. Sivertsen and Holthuis (1980) described it as "a narrow elongate process on the protopod, it ends in two teeth; the protopod seems to have a second similar process laterally, the nature of this process is not clear". Nevertheless, there is no strong robust seta on the apex of the central spike and a seta on the lateral spike. Additionally, there are no teeth present on the dorsal surface of the pleotelson in *E. minutus* while there are 7 obscure denticles present in the new Malaysian species.

Eisothistos sp. n. is readily distinguishable from the other Malaysian species, *E. besar* Müller, 1992 by its bipartite uropodal exopod (tripartite in *E. besar*) and the surface of pleotelson with 7 obsure middorsal teeth (4 distinct middorsal teeth in *E. besar*).

Genus *Expanathura* Wägele, 1981

Expanathura collaris (Kensley, 1979)

Panathura collaris Kensley, 1979a: 823-827, figs 7–9; Kensley and Poore 1982: 635; *Expanathura collaris* Wägele, 1981d: 89, 121–122; Negoescu 1999: 214–220, figs 9–11; Negoescu and Wägele 1984: 118; Negoescu and Brandt 2001: 121–129, figs 14–18; Poore and Lew Ton 2002: 26-32, figs 16–19, 20a.

Materials examined. 54 females, 3 males, UKMMZ-1567, Sebirah Kechil, Pulau Tinggi, Johor, Malaysia, 2°18.622'N, 104°5.616'E (DDM), C. Melvin, 16 May 2013, coral rubble, ~3 m; 12 females, UKMMZ-1568, Mentinggi, Pulau Tinggi, Johor, Malaysia, 2°16'21.67"N; 104°7'18.61"E (DMS), C. Melvin, 19 April 2013, coral rubble, ~3 m; 56 females, 9 males, UKMMZ-1569, Batu Malang, Pulau Tioman, Pahang, Malaysia, 2°54'15.44"N; 104°6'1.08"E (DMS), C. Melvin, 18 April 2014, coral rubble, ~7 m; 35 females, 2 males, UKMMZ-1570, Labas, Pulau Tioman, Pahang, Malaysia, 2°53'13.71"N; 104°3'54.65"E (DMS), C. Melvin, 18 April 2014, coral rubble, ~15 m; 14 females, 4 males, PLAy2-iso4d, Pantai Kok, Pulau Langkawi, Kedah, Malaysia, 6°21'56.05"N; 99°40'31.13"E (DMS), C. Melvin, 8 March 2015, coral rubble, intertidal; 7 females, 1 male, PDYx1-iso4e, Batu Bonchek, Pulau Dayang, Johor, Malaysia, 2°28'40.90"N; 104°30'19.12"E (DMS), C. Melvin, 26 July 2016, coral rubble, ~3m.

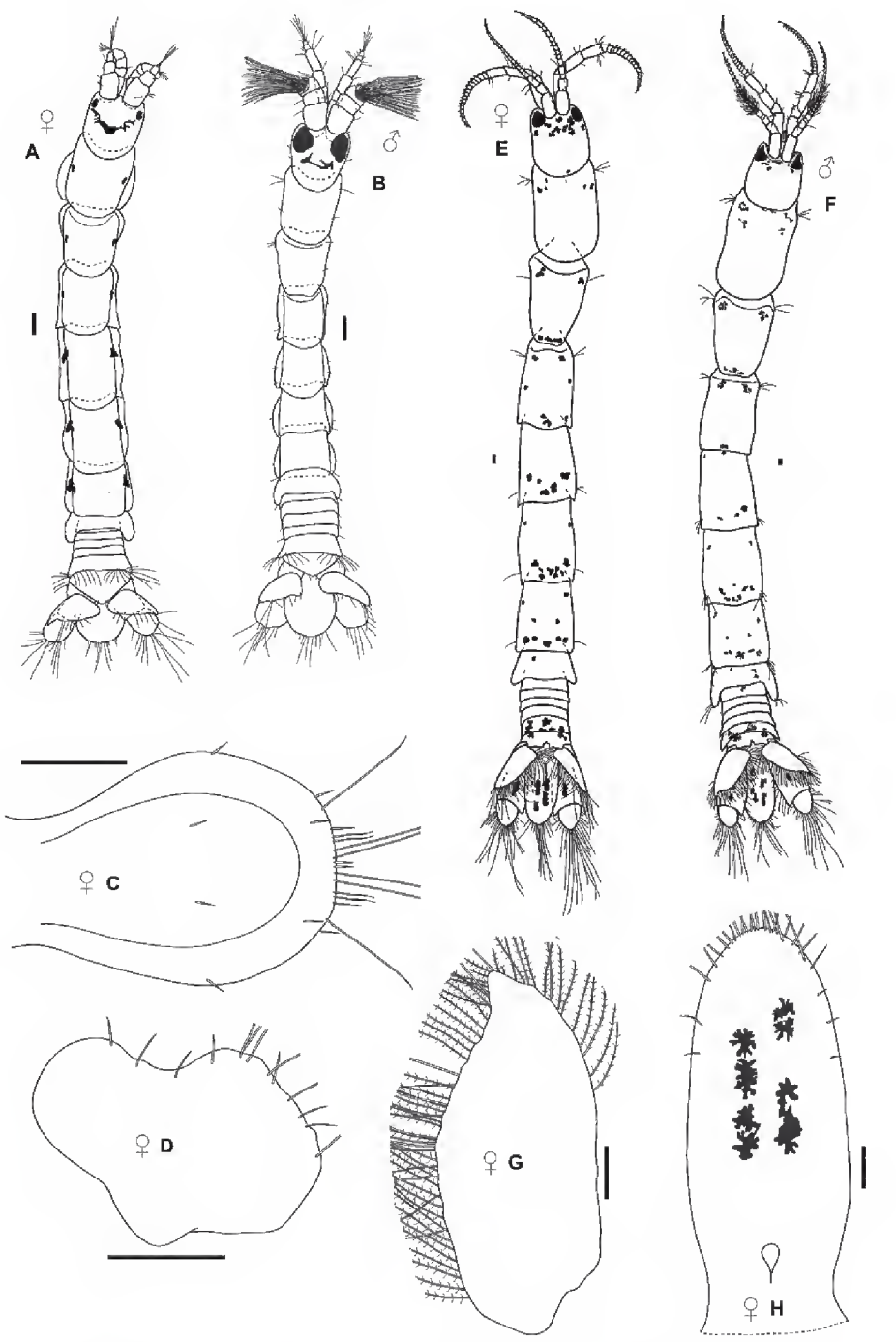

Figure 6. A–D. *Expanathura collaris*. **A.** female. **B.** male. **C.** pleotelson. **D.** uropodal exopod. **E–H.** *Accalathura borradailei*. **E.** female. **F.** male. **G.** uropodal exopod. **H.** pleotelson. All scales represent 0.1 mm.

Distribution. Fiji (type locality); Cook Island; Chesterfield and Melish Reefs, Moorea, Coral Sea; Lord Howe I, Tasman Sea; Papua New Guinea; Northern Territory, Queensland, Australia; Pulau Dayang, Pulau Tinggi, Malaysia; Pulau Tioman, Malaysia; Pulau Langkawi, Malaysia.

Molecular data. A 631 base pairs of COI sequence (GenBank: MF680512) was acquired from one individual of *E. collaris*. No insertion or deletion in the sequence alignment.

Remarks. *Expanathura collaris* is a widespread species dwelling in coral reef rubble especially within the Southeastern Pacific and Australian region (Kensley 1979a; Negoescu 1999; Negoescu and Brandt 2001; Poore and Lew Ton 2002). This is the first record of *E. collaris* from the Southeast Asia region.

Family Leptanthuridae Poore, 2001
Genus *Accalathura* Barnard, 1925

Accalathura borradailei (Stebbing, 1904)

Calathura borradailei Stebbing, 1904: 700, pl. 49A; Chilton 1924: 881
Accalathura borradailei Barnard, 1925: 149; Pillai 1966: 157-158, fig 3.

Materials examined. 35 females, 3 males, UKMMZ-1612, Kampung Pasir Panjang, Pulau Tinggi, Johor, Malaysia, 2°17'37.96"N; 104°6'1.97"E (DMS), C. Melvin, 28 February 2013, coral rubble, intertidal; 34 females, UKMMZ-1613, Kampung Pasir Panjang, Pulau Tinggi, Johor, Malaysia, 2°17'37.96"N; 104°6'1.97"E (DMS), C. Melvin, 18 December 2012, coral rubble, intertidal; 1 female, UKMMZ-1614, Kampung Pasir Panjang, Pulau Tinggi, Johor, Malaysia, 2°17'37.96"N; 104°6'1.97"E (DMS), C. Melvin, 15 June 2015, coral rubble, intertidal; 20 females, UKMMZ-1615, Sebirah Kechil, Pulau Tinggi, Johor, Malaysia, 2°18.622'N; 104°05.616'E (DDM), C. Melvin, 15 June 2015, coral rubble, intertidal; 14 females, 1 male, UKMMZ-1616, Batu Bonchek, Pulau Dayang, Johor, Malaysia, 2°28'40.90"N; 104°30'19.12"E (DMS), C. Melvin, 26 July 2016, coral rubble, ~3 m.

Distribution. Maldives, Fadifolu (type localtiy); Thailand; Chilka Lake, India; Quilon, India; Pulau Tinggi, Malaysia.

Molecular data. A 684 base pairs of COI sequence (GenBank: MF680508) was acquired from one individual of *E. collaris*. No insertion or deletion in the sequence alignment.

Remarks. This is the first record of *Accalathura borradailei* from the waters of Malaysia.

Acknowledgements

The authors would like to thank Universiti Kebangsaan Malaysia, Sultan Iskandar Marine Park–Johor National Parks, and the Department of Marine Park Malaysia. This research was supported by the Universiti Kebangsaan Malaysia under Grant No. LIV-2015-02.

References

Barnard KH (1914) Contributions to the crustacean fauna of South Africa. 3. Additions to the marine Isopoda, with notes on some previously incompletely known species. Annals of the South African Museum 10(11): 325a–358a, 359–440. http://biodiversitylibrary.org/page/1554824

Barnard KH (1925) A Revision of the Family Anthuridae (Crustacea Isopoda), with Remarks on certain Morphological Peculiarities. Journal of Linnean Society London (Zoology) 36: 109–160. https://doi.org/10.1111/j.1096-3642.1925.tb01849.x

Brandt A, Poore GCB (2003) Higher classification of the flabelliferan and related Isopoda based on a reappraisal of relationships. Invertebrate Systematics 17: 893–923. http://dx.doi.org/10.1071/IS02032

Buhay JE (2009) "COI-like" sequences are becoming problematic in molecular systematic and DNA barcoding studies. Journal of Crustacean Biology 29(1): 96–110. https://doi.org/10.1651/08-3020.1

Chew M, Abdul Rahim A, Haji Ross OB (2014) *Tinggianthura alba*: a new genus and species of Anthuridae (Isopoda, Cymothoida, Anthuroidea) from Pulau Tinggi, Johor, Malaysia with an updated key to the genera of Anthuridae. PLoS ONE 9(6): e99072. https://doi.org/10.1371/journal.pone.0099072

Chew M, Rahim ABA, Mohd Yusof NYB (2016) Two new species of *Pendanthura* (Isopoda, Cymothoida, Anthuroidea) from the east coast of Peninsular Malaysia with an identification key to the species of *Pendanthura*. Bulletin Marine Science 92(2): 229–242. https://doi.org/10.5343/bms.2015.1056

Chilton C (1924) Fauna of the Chilka Lake. Tanaidacea and Isopoda. Memoirs of the Indian Museum 5: 875–895.

Dreyer H, Wägele JW (2001) Parasites of crustaceans (Isopoda: Bopyridae) evolved from fish parasites: Molecular and morphological evidence. Zoology 103: 157–158.

Ewing B, Green P (1998) Base-calling of automated sequencer traces using Phred II: Error probabilities. Genome Research 8: 186–194. https://doi.org/10.1101/gr.8.3.186

Folmer OM, Black M, Hoeh R, Lutz R, Vrijenhoek R (1994) DNA primers for amplification of mitrochondrial cytochrome c oxidase subunit I from diverse metazoan invertebrates. Molecular Marine Biology Biotechnology 3: 294–299.

Gotoh O (1982) An improved algorithm for matching biological sequences. Journal of Molecular Biology 162(3): 705–708. https://doi.org/10.1016/0022-2836(82)90398-9

Hall TA (1998) BioEdit: A user-friendly biological sequence alignment editor and analysis program for Windows 95/98/NT. Nucleic Acid Symposium Series 41: 95–98.

Haswell WA (1884) On a new crustacean found inhabiting the tubes of Vermilia (Serpulidae). Proceedings of the Linnean Society of New South Wales 9(3): 676–680. http://biodiversitylibrary.org/page/6602850

Haye PA, Kornfield I, Watling L (2004) Molecular insights into Cumacean family relationships (Crustacea, Cumacea). Molecular Phylogenetics Evolution 30(3): 798–809. https://doi.org/10.1016/j.ympev.2003.08.003

Hebert PDN, Cywinska A, Ball SL, deWaard JR (2003a) Biological identifications through DNA barcodes. Proceedings of the Royal Society B 270: 313–321. https://doi.org/10.1098/rspb.2002.2218

Hebert PDN, Ratnasingham S, deWaard JR (2003b) Barcoding animal life: cytochrome c oxidase subunit 1 divergences among closely related species. Proceedings of Biology Society 270: S96–S99. https://doi.org/10.1098/rsbl.2003.0025

Kensley B (1979) New species of anthurideans from the Cook and Fiji Islands (Crustacea: Isopoda: Anthuridea). Proceedings of the Biological Society Washington 92: 814–836. http://biodiversitylibrary.org/page/35514535

Kensley B (1980) Records of anthurids from Florida, Central America, and South America (Crustacea: Isopoda: Anthuridae). Proceedings of the Biological Society of Washington 93: 725–742. http://biodiversitylibrary.org/page/34599608

Kensley B, Poore GCB (1982) Anthurids from the Houtman Abrolhos Islands, Western Australia (Crustacea: Isopoda: Anthuridae). Proceedings of the Biological Society of Washington 95: 625–636. http://biodiversitylibrary.org/page/34964939

Kensley B, Schotte M (2000) New species and records of anthuridean crustaceans from the Indian Ocean. Journal of Natural History 34: 2057–2121. https://doi.org/10.1080/002229300750022358

Knight-Jones EW, Knight-Jones P (2002) Four new species of *Eisothistos* (Anthuridae: Isopoda) from tubes of *Spirbidae* (Serpuloidea: Polychaeta). Journal of Natural History 36: 1397–1419. https://doi.org/10.1080/00222930110052454

Leach WE (1814) Crustaceology. Edinburgh Encyclopaedia; conducted by David Brewster L.L.D. 7: 383–437, pl. 221. http://biodiversitylibrary.org/page/37187640

Menzies RJ, Glynn PW (1968) The common marine isopod Crustacea of Puerto Rico: A handbook for marine biologists. Studies on the Fauna of Curacao and other Caribbean Islands 27(104): 1–133. http://decapoda.nhm.org/pdfs/4429/4429.pdf

Monod T (1922) Sur un essai de classifi cation rationnelle des isopodes. Bulletin de la Société Zoologique de France 47: 134–140. https://doi.org/10.5962/bhl.part.3467

Müller HG (1991) New species and records of *Amakusanthura*, *Cyathura* and *Haliophasma* from Sri Lanka (Crustacea: Isopoda: Anthuridae). Revue Suisse de Zoologies 98(3): 589–612. https://doi.org/10.5962/bhl.part.79806

Müller HG (1992a) Anthuridae of the genera *Apanthura* and *Cyathura* from Malaysia coral reefs, with description of two new species (Crustacea: Isopoda: Anthuridae). Zoologischer Anzeiger 228: 156–166.

Müller HG (1992b) *Eisothistos besar* n. sp. from a coral reef in the Tioman Archipelago, first member of the genus from southeast Asia (Crustacea: Isopoda). Revue Suisse de Zoologies 99(2): 369–376. https://doi.org/10.5962/bhl.part.79835

Negoescu I (1997) Isopoda Anthuridea results of the Zoological Expedition organized by "Grigore Antipa" Museum in the Indonesia Archipelago (1991). I. Pericarida (Crustacea). Travaux du Museum National d'Histoire Naturelle Grigore Antipa 38: 177–251. https://www.travaux.ro/web/pdf/638-38-177-251%20Negoescu%20%20I.pdf

Negoescu I (1999) Isopoda Anthuridae (Crustacea) from Fiji Islands. Three new species. First record of primary and secondary males in Paranthuridae family. Travaux du Museum d'Histoire Naturelle "Gigore Antipa" 41: 199–280. https://www.travaux.ro/web/pdf/393-41-199-280%20Negoescu%20I.pdf

Negoescu I, Wägele JW (1984) World list of the anthuridean isopods (Crustacea, Isopoda, Anthuridea). Travaux du Museum d'Histoire Naturelle "Gigore Antipa" 25: 99–146. https://www.travaux.ro/web/pdf/25-TMNHNGA-99-146.pdf

Pecnikar ZF, Busan EV (2014) 20 years since the introduction of DNA barcoding: from theory to application. Journal of Applied Genetics 55: 4–52.

Pillai NK (1966) Littoral and parasitic isopods from Kerala: Family Anthuridae.-1. Journal of the Bombay Natural History Society 63(1): 152–161. http://biodiversitylibrary.org/page/47950451

Poore GCB (2001) Families and genera of Isopoda Anthuridea. In: Kensley B, Brusca RC (Eds) Isopod systematics and evolution. Balkema, Rotterdam. Crustacean Issues 13: 63–173.

Poore GCB (2009) *Leipanthura casuarina,* new genus and species of anthurid isopod from Australian coral reefs without a "five-petalled" tail (Isopoda, Cymothoida, Anthuroidea). Zookeys 18: 171–180. http://dx.doi.org/10.3897/zookeys.18.198

Poore GCB, Lew Ton HM (2002) Expanathuridae (Crustacea: Isopoda) from the Australian region. Zootaxa 82: 1–60. https://doi.org/10.11646/zootaxa.82.1.1

Sivertsen E, Holthuis LB (1980) The Marine Isopod Crustacea of the Tristan da Cunha archipelago. Gunneria 35: 1–128. https://www.ntnu.no/c/document_library/get_file?uuid=a84d7dcc-ce88-47f7-9d44-9c2fc3b-7181c&groupId=10476

Song JH, Min GS (2015a) New record of three isopod species (Crustacea: Malacostraca: Isopoda) from South Korea. Korean Journal of Enviromental Biology 33(2): 182–188. https://doi.org/10.11626/KJEB.2015.33.2.182

Song JH, Min GS (2015b) Two new species, *Caenanthura koreana* sp. nov. and *Apanthura koreaensis* sp. nov. (Crustacea: Isopoda: Anthuridae) from South Korea. Zootaxa 3937(2): 362–376. https://doi.org/10.11646/zootaxa.3937.2.7

Stebbing TRR (1900) On Crustacea brought by Dr. Willey from the South Seas. In: Willey A (Ed.) Zoological Results based on material from New Britain, New Guinea, Loyalty Islands and Elsewhere collected during the years 1895, 1896 and 1897 Part V. University Press, Cambridge, 605–690. http://biodiversitylibrary.org/page/21340469

Stebbing TRR (1904) Marine crustaceans. XII. Isopoda, with description of a new genus. In Gardiner JS (Ed.) The Fauna and Geography of the Maldive and Laccadive Archipelagoes Being the Account of the Work Carried on and of the Collections made by an Expedition during the years 1899 and 1900. University Press, Cambridge, 600–721. http://biodiversitylibrary.org/page/10778816

Wägele JW (1979) Morphologische Studien an Eisothistos mit Beschreibung von drei neuen Arten (Crustacea, Isopoda, Anthuridea). Mitteilungen aus dem Zoologischen Museum der Universitaet Kiel 1(2): 1–19.

Wägele JW (1981) Zur Phylogenie der Anthuridea (Crustacea, Isopoda). Mit Beiträgen zur Lebensweise, Morphologie, Anatomie und Taxonomie. Zoologica 132: 1–127.

Wägele JW (1989) Evolution und phylogenetisches System der Isopoda. Stand der Forschung und neue Erkenntnisse. Zoologica (Stuttgart) 140: 1–262.

Wetzer R (2001) Hierachical analysis of mtDNA variation and the use of mtDNA for isopod (Crustacea: Peracarida: Isopoda) systematics. Contributions to Zoology 70: 23–39.

Wetzer R (2002) Mitochondrial genes and isopod phylogeny (Peracarida: Isopoda). Journal of Crustacean Biology 22: 1–14. https://doi.org/10.1163/20021975-99990204

Zoosyst. Evol. 94 (1) 2018, 83–93 | DOI 10.3897/zse.94.22106

PENSOFT

museum für naturkunde

A new species of *Charax* (Ostariophysi, Characiformes, Characidae) from northeastern Brazil

Erick Cristofore Guimarães[1,3], Pâmella Silva De Brito[2,3], Beldo Rywllon Abreu Ferreira[1], Felipe Polivanov Ottoni[1,2,3,4]

1 *Universidade Federal do Maranhão, Departamento de Biologia, Programa de Pós-Graduação em Biodiversidade e Conservação. Av. dos Portugueses 1966, Cidade Universitária do Bacanga, CEP 65080-805, São Luís, MA, Brasil*

2 *Universidade Federal do Maranhão, Departamento de Biologia, Programa de Pós-Graduação em Biodiversidade e Biotecnologia da Amazônia Legal. Av. dos Portugueses 1966, Cidade Universitária do Bacanga, CEP 65080-805, São Luís, MA, Brasil*

3 *Universidade Federal do Maranhão, Laboratório de Sistemática e Ecologia de Organismos Aquáticos, Centro de Ciências Agrárias e Ambientais, Campus Universitário, CCAA, BR-222, KM 04, S/N, Boa Vista, CEP 65500-000, Chapadinha, MA, Brasil*

4 *Universidade Federal do Maranhão, Programa de Pós-Graduação em Oceanografia. Av. dos Portugueses 1966, Cidade Universitária do Bacanga, CEP 65080-805, São Luís, MA, Brasil*

http://zoobank.org/6C9999F9-1EFA-46A1-A3B3-67E4E440945B

Corresponding author: *Erick Cristofore Guimarães* (erick.ictio@yahoo.com.br)

Received 2 December 2017
Accepted 25 January 2018
Published 1 February 2018

Academic editor:
Peter Bartsch

Key Words

Characinae
Characini
freshwater
Maranhão state
Neotropical region
Rio Mearim
Rio Munim
Rio Turiaçu
taxonomy

Abstract

Charax awa sp. n. is herein described from the Rio Mearim, Rio Munim and Rio Turiaçu basins, three coastal river basins of northeastern Brazil located between the Rios Gurupi and Parnaíba basins. These have a complex and still poorly known biogeographic history. This region is ecologically extremely relevant since it comprises three of the main Brazilian biomes, as well as, transition zones between them: Amazônia, Brazilian Cerrado and Caatinga. Therefore, this area has faunal and floristic representatives of these three biomes, which makes it particularly relevant in terms of ecology, biodiversity and conservation. *Charax awa* sp. n. possesses a relatively small orbital diameter (22.1–28.5 % HL), what distinguishes it from most of its congeners, except from *C. notulatus* and *C. caudimaculatus*. It differs from *C. caudimaculatus* by a longer snout, and from *C. notulatus* by the number of scales around the caudal peduncle, as well as by the number of vertebrae. The new species herein described differs from its geographically closely distributed congeners, *C. leticiae*, *C. niger*, and *C. pauciradiatus* mainly by the relative horizontal orbital diameter. It is a "small-eyed" species. In addition, *C. awa* sp. n. can be distinguished from *C. leticiae* by having a maxilla extending to the vertical line posterior to the pupil, near the posterior orbital margin and by having a lower humeral spot distance. It can be distinguished from *C. pauciradiatus* by more scale rows from the pelvic-fin origin to the lateral line and more scale rows from the dorsal-fin origin to the lateral line and it differs from *C. niger* by having more transverse scale rows in space from the humeral spot to the supracleithrum. In addition, it differs from *C. pauciradiatus* and *C. niger* by the absence of bony hooks on anal and pelvic-fins rays of adult males.

Introduction

Characidae is the most species-rich family of Characiformes, comprising about 165 genera and more than 1.150 species, distributed along the river systems between southwestern Texas and Mexico in North America and Patagonia in South America (Nelson et al. 2016; Eschmeyer et al. 2017). *Charax* Scopoli, 1777 is a South American characid genus possessing a midsized (maximum size about 130.0 mm SL) and deep body, being the type genus of the Characidae, comprising 16 valid species (Menezes and Lucena 2014), widely distributed in the Cis-Andean region, occurring in the Amazonas, Paraná, Uruguay, Paraguay, Capim, and Orinoco river basins, as well as in

smaller isolated river basins draining the Guiana Shield, and in the Lagoa dos Patos system, and other coastal lagoons of southern Brazil (Menezes and Lucena 2014).

The distribution of the genus is mainly concentrated in central and northern South America; there is no record for eastern Brazil and none of the valid species was assigned for the coastal river basins of northeastern Brazil by the recent taxonomic revision of the genus (see Menezes and Lucena 2014). However, some records of *Charax* for the coastal river basins of northeastern Brazil were made before the taxonomic revision made by Menezes and Lucena (2014): Martins and Oliveira (2011) recorded *C. gibbosus* for the Rio Mearim basin; Barros et al. (2011) recorded *Charax* sp. for the Rio Itapecuru basin; Martins and Oliveira (2011) recorded *Charax* sp. for the Rio Pericumã basin and Rio Mearim basin.

Charax can be distinguished from all other characid genera by the presence of a deep concavity on the latero-ventral portion of the cleithrum originating a relatively long posterior spiniform projection extending below pectoral-fin base; and an anterior shorter process oriented straight forward or either inclined or bent laterally (Lucena 1987, Mattox and Toledo-Piza 2012: fig 34, Menezes and Lucena 2014). A new species of *Charax* is herein described from the Rio Mearim, Rio Munim and Rio Turiaçu basins, three coastal river basins of northeastern Brazil.

Material and methods

Counts and measurements were taken according to Fink and Weitzman (1974), Menezes and Weitzman (1990) and Menezes and Lucena (2014), on the left side of specimens whenever possible, using a digital caliper with precision of 0.01 mm. Measurements are given as a percentage of standard length (SL), except for subunits of the head, which are given as a percentage of head length (HL). Vertebrae of the Weberian apparatus were not included in the vertebral counts, whereas the fused PU1+U1 of the caudal region was counted as a single element. Counts for supraneurals, vertebrae, rib pairs, branchiostegal rays, gill-rakers, premaxillary, maxillary, and dentary teeth, procurrent caudal-fin rays, and pterygiophores were taken only from cleared and stained paratypes (C&S), prepared according to Taylor and Van Dyke (1985); number of examined specimens are in parentheses. Osteological nomenclature follows Weitzman (1962). Diagnosis was made based on a unique combination of character states, according to Davis and Nixon (1992). Information about congeners was based on both comparative material and literature (e.g Lucena 1987, Mattox and Toledo-Piza 2012, Menezes and Lucena 2014). Institutional abbreviations are: **CICCAA** Coleção Ictiológica do Centro de Ciências Agrárias Ambientais, Universidade Federal do Maranhão, Chapadinha; **CPUFMA** Coleção de Peixes da Universidade Federal do Maranhão, São Luis; **UFRJ** Coleção Ictiológica do Instituto de Biologia, Universidade Federal do Rio de Janeiro, Rio de Janeiro; **MCP** Museu de Ciências e Tecnologia, Pontifícia Universidade Católica do Rio Grande do Sul, Porto Alegre; **USNM** Smithsonian Institution National Museum of Natural History, Washington D.C., U.S.A; **CM** Carnegie Museum of Natural History, Pittsburgh, Pennsylvania, U.S.A; and **MHNM** Museo Nacional de Historia Natural y Antropología, Zoologia, Seccion Ictiología, Ministerio de Educación y Cultura, Montevideo, Uruguay.

Results

Charax awa sp. n.

http://zoobank.org/102A196C-18F0-41B5-913E-C471086EFB69

Fig. 1

Charax gibbosus [*non Charax gibbosus* (Linnaeus, 1758)]: Martins and Oliveira 2011: 196-197.

Charax sp. - Martins and Oliveira 2011:196–197.

Holotype. CICCAA 00752, 101.3 mm SL, Brazil: Maranhão State: Alto Alegre do Pindaré municipality: Igarapé Mineirão, Rio Mearim basin, 3°42'26"S, 45°56'5"W; Guimarães E. C. and Costa C.H.; 03 Dec. 2015.

Paratypes. All from Maranhão State, Brazil: CICCAA 00248, 9, 47.7–90.6 mm SL; CICCAA 00249, 6 (C&S), 42.6–73.8 mm SL; CICCAA 00754, 2, 55.2–68.7 mm SL; collected with holotype. CICCAA 00753, 1 (C&S), 41.4 mm SL, Rio Zutiua (Rio Mearim basin), Santa Inês municipality, 3°43'48"S, 45°35'7"W; Guimarães E. C. and Costa C.H.; 03 Dec 2015.CICCAA 00766, 1 (C&S), 78.5 mm SL, Rio Zutiua (Rio Mearim basin), Santa Inês municipality, 3°43'48"S, 45°35'7"W; Guimarães E. C. and Costa C.H.; 03 Dec 2015. CICCAA 00755, 1, 59.8 mm SL; stream at the Santa Inês municipality (Rio Mearim basin), Santa Inês municipality, 3°40'48"S, 45°19'51"W; Guimarães E. C. and Costa C.H.; 03 Dec 2015.CICCAA 00896, 2, 40.2–48.8 mm SL stream Arapapá (Rio Mearim basin), Alto Alegre municipality; 3°42'30"S, 46°0'19"W; Guimarães E. C. and Brito P. S; 15 Ago 2017.CICCAA 00765, 11, 44.4–68.3 mm SL Lirio stream (Rio Mearim basin), Alto Alegre municipality; 3°38'56"S, 45°46'18"W; Guimarães E. C. and Brito P.S; 15 Ago 2017.CICCAA 00764, 5, 68.4–89.3 mm SL, Olho d'água dos Carneiros (Rio Mearim basin), Santa Inês municipality; 3°43'0"S, 45°28'36"W; Guimarães E. C. and Brito P.S; 11 Ago 2017. CICCAA 00898, 1, 62.2 mm SL, stream at Miranda do Norte municipality (Rio Mearim basin), 3°31'30"S, 44°35'6"W; Guimarães E. C. and Brito P.S.; 13 Ago 2017.

UFRJ 11696, 2, 69.9–70.6 mm SL stream Arapapá (Rio Mearim basin), Alto Alegre municipality; 3°42'30"S, 46°0'19"W; Guimarães E. C. and Brito P.S; 15 Ago 2017. MCP 52700, 4, 45.9–75.1 mm SL Arapapá stream (Rio Mearim basin), Alto Alegre municipality; 3°42'30"S, 46°0'19"W; Guimarães E. C. and Brito P.S; 15 Ago 2017. CPUFMA 98859, 40, 52.2–120.0 mm SL, Rio Turiaçu, (Rio Turiaçu basin), Santa Helena municipality;

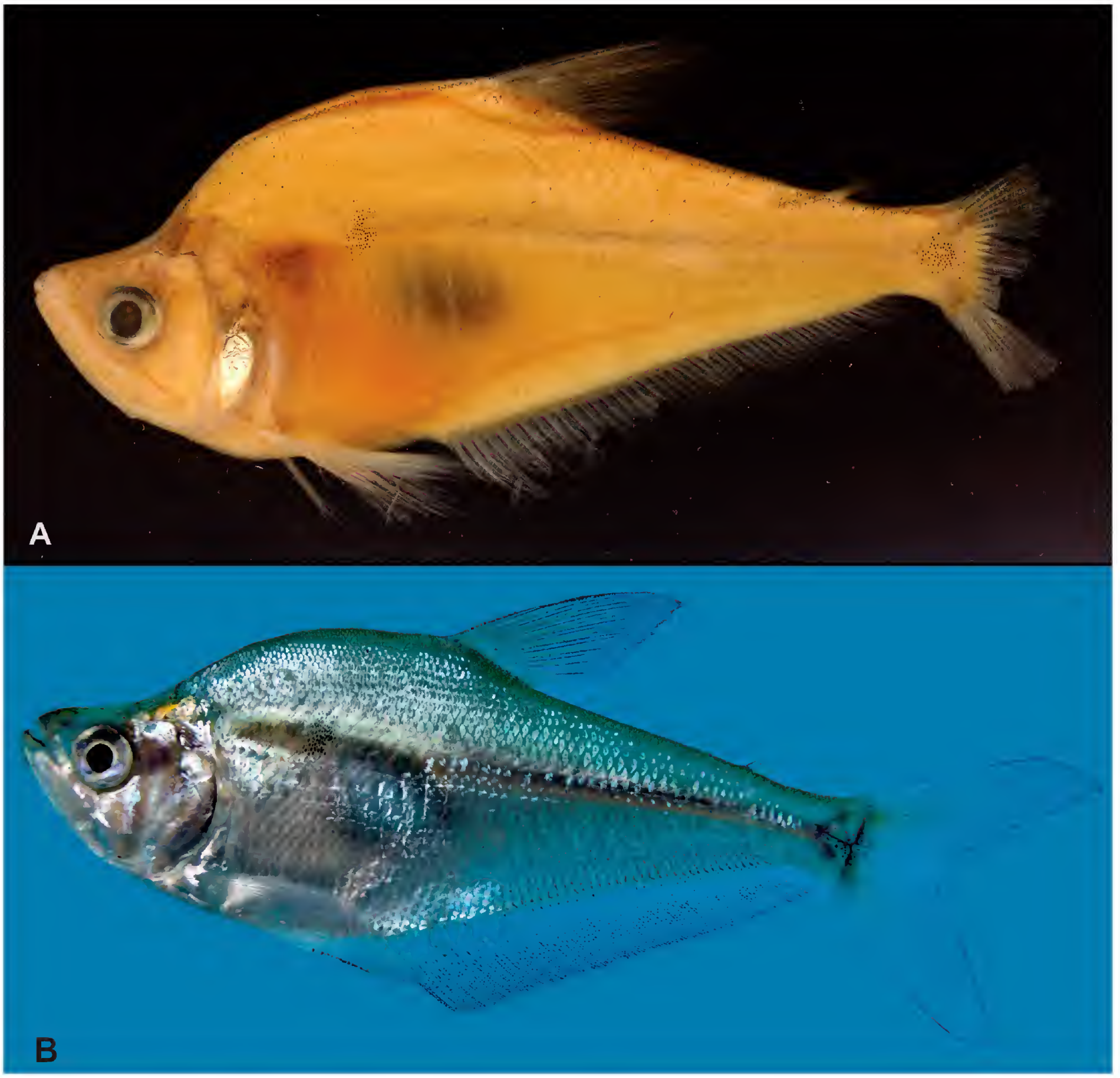

Figure 1. *Charax awa*: (**A**) Holotype, CICCAA 00752, 101.33 mm SL; Brazil, Maranhão, Alto Alegre do Pindaré, Pindaré river drainage, Mearim river basin. (Photographed by Beldo Ferreira). (**B**) Live specimen, paratype, CICCA00898, 62.2 mm SL; Brazil, Maranhão, Miranda do Norte, stream at the Miranda do Norte, Mearim river basin. (Photographed by Erick Guimarães).

2°27’35”S, 45°30’42”W; Piorski et al. 8 Ago 1998. CPUFMA 001747, 18, 76.9–117.3 mm SL, Rio Turiaçu, (Rio Turiaçu basin), Santa Helena municipality; 2°27’35”S, 45°30’42”W; Piorski et al. 17 Abr 2000. CPUFMA 112036, 4, 88.5–88.7 mm SL, Rio Munim, Chapadinha municipality; 3°50’19”S, 43°19’46”W; Nunes et al. 8 Jul 2011. CPUFMA 98136, 3, 85.2–93.7 mm SL, Lago de Viana (Rio Mearim basin), Cajari municipality; 3°22’48”S, 45°2’57”W; Piorski and Pereira, 17 Mar 1998. CPUFMA 98135, 3, 85.6–91.4 mm SL, Lago de Viana (Rio Mearim basin), Cajari municipality; 3°18’54”S, 45°1’40”W; Piorski and Pereira, 17 Mar 1998. CPUFMA 98137, 1, 88.2 mm SL, Lago de Viana (Rio Mearim basin), Viana municipality; 3°15’9”S, 45°4’48”W; Piorski and Pereira, 14 Mar 1998. CPUFMA 97130, 1, 91.3 mm SL, stream Engenho (Rio Mearim basin), Viana municipality; 3°12’26”S, 44°58’5”W; Piorski and Pereira, 6 Dez 1997.

Non type material. All from Maranhão State, Brazil: CPUFMA 98861, 24, 83.5–120.0 mm SL, Rio Turiaçu, (Rio Turiaçu basin), Santa Helena municipality; 2°27’35”S, 45°30’42”W; Piorski et al. 8 Ago 1998. CPUFMA 98862, 23, 79.4–119.1 mm SL, Rio Turiaçu, (Rio Turiaçu basin), Santa Helena municipality; 2°27’35”S, 45°30’42”W; Piorski et al. 14 Ago 1998. CPUFMA 00863, 25, 68.0–113.1 mm SL, Rio Turiaçu, (Rio Turiaçu basin), Santa Helena municipality; 2°27’35”S, 45°30’42”W; Piorski et al. 21 Ago 2000. CPUFMA 00864, 43, 72.3–113.9 mm SL, Rio Turiaçu, (Rio Turiaçu basin), Santa Helena municipality; 2°27’35”S, 45°30’42”W; Piorski

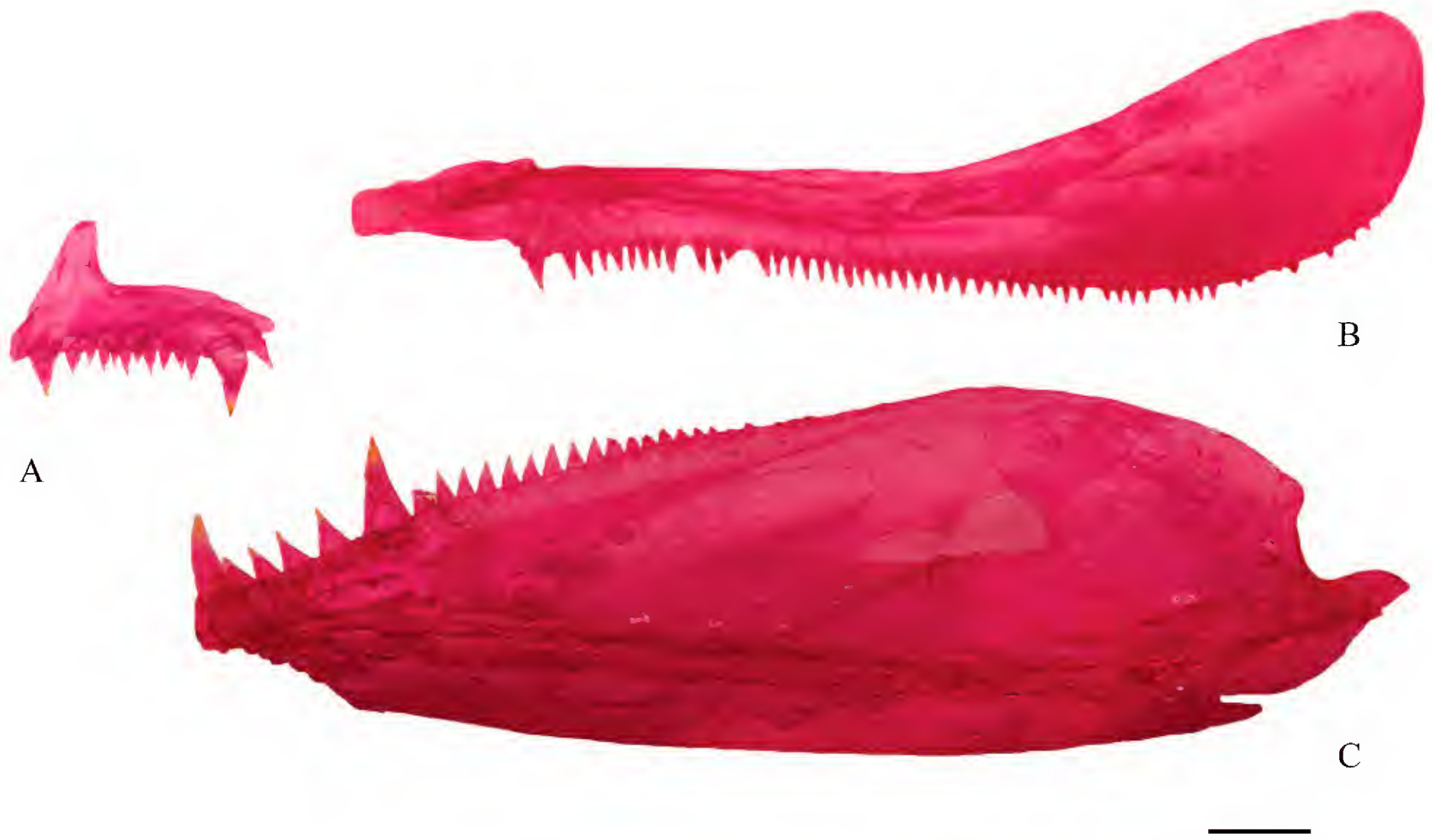

Figure 2. *Charax awa*, CICCAA00249, 73.8 mm SL; Jaws: (**A**) premaxilla, (**B**) maxilla and (**C**) lower jaw. Scale bar 1 mm. (Photographed by Erick Guimarães and Beldo Ferreira).

et al. 16 Out 2000. CPUFMA 00865, 11, 82.3–114.2 mm SL, Rio Turiaçu, (Rio Turiaçu basin), Santa Helena municipality; 2°27'35"S, 45°30'42"W; Piorski et al. 21 Ago 2000. CPUFMA 00866, 31, 82.6–110.3 mm SL, Rio Turiaçu, (Rio Turiaçu basin), Santa Helena municipality; 2°27'35"S, 45°30'42"W; Piorski et al. 15 Out 2000. CPUFMA 00867, 16, 88.7–102.12 mm SL, Rio Turiaçu, (Rio Turiaçu basin), Santa Helena municipality; 2°27'35"S, 45°30'42"W; Piorski et al. 22 Jun 2000.

Diagnosis. *Charax awa* sp. n. can be distinguished from *C. apurensis* Lucena, 1987, *C. condei* (Géry & Knöppel, 1976), *C. delimai* Menezes & Lucena, 2014, *C. gibbosus* (Linnaeus, 1758), *C. hemigrammus* (Eigenmann, 1912), *C. leticiae* Lucena, 1987, *C. macrolepis* (Kner, 1858), *C. metae* Eigenmann, 1922, *C. michaeli* Lucena, 1989, C. *niger* Lucena, 1989, *C. pauciradiatus* (Günther, 1864), *C. stenopterus* (Cope, 1894) *C. tectifer* (Cope, 1870) by the orbital diameter (22.1–28.5% HL vs. 29.6–38.4% HL combined) (Fig. 2). *Charax awa* sp. n. differs from *C. caudimaculatus* Lucena, 1987 by the possession of a longer snout (snout length 23.3–32.8% HL vs. 20.3–22.8% HL); from *C. notulatus* Lucena, 1987 by the number of scales around the caudal peduncle (15–18 vs. 20–22) and by having more vertebrae (35 vs. 32). Furthermore, *Charax awa* sp. n. can be distinguished from *C. condei*, *C. hemigrammus* and *C. stenopterus* by having the lateral line complete (vs. incomplete); from *C. delimai*, *C. metae* and *C. tectifer* by having a toothless ectopterygoid (vs. presence of teeth on ectopterygoid) and having the anal-fin origin always anterior to the vertical through the dorsal-fin origin (vs. anal-fin origin on, or slightly posterior to the vertical through the dorsal-fin origin); from *C. condei*, *C. delimai*, *C. hemigrammus*, *C. metae*, *C. pauciradiatus* and *C. stenopterus* by the number of scale rows from the pelvic-fin origin to the lateral line (11–12 vs. 6–10 combined); from *C. pauciradiatus* by having more scale rows from the dorsal-fin origin to the lateral line (15–18 vs. 13–14). It can be distinguished from *C. niger* by having 8–10 transverse scale rows in space from the humeral spot to the supracleithrum (vs. 5–6); from *C. condei*, *C. delimai*, *C. metae*, *C. rupununi* Eigenmann, 1912 by the number of scale rows around the caudal peduncle (15–18 in *C. awa* sp. n. vs. 12–14 combined in *C. condei* and *C. rupununi*, 19–21 combined in *C. delimai* and *C. metae*). Finally, it differs from *C. leticiae* by having the maxilla extending to a vertical line posterior to pupil, near the posterior orbital margin (vs. maxilla extending slightly beyond vertical through middle of pupil) and from humeral spot distance (35.8–38.0 % SL vs. 39.0–44.0 % SL).

Description. Morphometric data are presented in Tables 1 and 2. Body moderately large (40.2–120.0 mm SL), compressed and moderately deep; greatest body depth slightly in advance of dorsal-fin origin. Dorsal profile of head and body slightly convex on tip of snout, approximately straight from posterior border of posterior nostril to vertical line through posterior border of pupil, concave from that point to about half of distance between pupils and posterior margins of preopercle, strongly convex from that point to dorsal-fin origin, nearly straight along dorsal-fin base and from end of dorsal-fin base to caudal peduncle and slightly concave along caudal peduncle. Ventral pro-

Table 1. Morphometric data of *Charax awa*.

Measurements	Holotype	N	Paratypes	Mean	SD
Standard length (SL)	101.3	107	40.2–120.0	88.4	–
Percentages of standard length					
Depth at dorsal-fin origin	40.0	106	27.7–42.5	37.8	2.8
Snout to dorsal-fin origin	55.0	106	46.5–57.9	52.4	1.5
Snout to pectoral-fin origin	28.4	104	22.8–37.0	28.5	1.8
Snout to pelvic-fin origin	35.5	105	28.6–48.3	37.1	1.8
Snout to anal-fin origin	51.9	103	42.4–65.4	50.3	3.6
Caudal peduncle depth	10.3	102	7.9–14.7	10.1	1.1
Caudal peduncle length	8.0	88	4.9–10.7	7.5	1.3
Pectoral-fin length	21.9	73	14.6–25.9	19.8	2.0
Pelvic-fin length	20.8	67	13.4– 24.7	20.2	2.3
Dorsal-fin base length	12.7	101	8.7–15.2	11.0	1.1
Dorsal-fin height	29.9	64	21.8–49.6	28.7	3.6
Anal-fin base length	53.2	95	42.7–66.2	49.5	3.7
Eye to dorsal-fin origin	44.1	103	36.8–52.9	41.5	2.9
Dorsal-fin origin to caudal-fin base	54.8	101	46.3–69.5	53.9	3.0
Humeral spot distance	37.7	42	32.1–38.0	37.9	3.0
Bony head length	26.7	101	23.9–29.5	26.1	1.0
Percentages of head length					
Horizontal eye diameter	25.4	100	22.1–28.5	25.4	1.6
Snout length	27.2	100	23.2–35.1	26.9	2.4
Least interorbital width	26.2	101	18.9–31.1	25.0	2.2
Upper jaw length	70.6	100	52.1–75.5	62.8	3.9

Table 2. Morphometric data related to the horizontal eye diameter of *Charax awa* presented in separate classes of standard length.

Measurements	N	Paratypes	N	Paratypes
Standard length (SL)	33	40.2–79.2	74	81.6–120.0
Percentages of head length				
Horizontal eye diameter	29	26.1–28.5	71	22.1–25.4

file of head and trunk convex from tip of lower jaw to anal-fin origin, nearly straight along anal-fin base and slightly concave from end of anal-fin base to beginning of procurrent rays. Snout pointed. Lower jaw included in upper jaw when mouth closed. Maxilla extending to a vertical line posterior to pupil, near the posterior orbital margin. Small triangular posteriorly directed projection at intersection between dorsal and posterior margins of hyomandibular (Mattox and Toledo-Piza 2012: figs 24A, 25B).

Dorsal-fin rays ii, 9 (72). Dorsal-fin pterygiophores 10 (8); first dorsal-fin pterygiophore between 4th and 5th vertebrae. Adipose fin present. Unbranched anal-fin rays iv (74) or v (1), branched rays 46 (4), 47 (5), 48 (10), 49 (13), 50 (9), 51 (6), 52 (13), 53 (5), 54 (2) or 56 (1). Anal-fin pterygiophores 46 (2), 47 (2), 48 (1), 49 (2) or 50 (1); first anal-fin pterygiophore between 7th and 8th vertebrae. Pectoral-fin rays i, 13 (3) or 14 (22). Tips of longest pectoral-fin rays reaching slightly beyond middle of pelvic-fin length. Pelvic-fin rays i, 7 (64) or i, 8 (2). Axilar scale on pelvic fin absent. Tips of longest pelvic-fin rays reaching anal-fin rays, between bases of second to seventh branches. Principal caudal-fin ray count 10/9 (59). Dorsal procurrent caudal-fin rays 12 (1), 14 (2), 15(1), 16 (2) or 17 (2). Ventral procurrent caudal-fin rays 7 (3), 8 (2), 9 (1), 1 (10) or 11 (1).

Ventral-most longitudinal series of scales on each side of trunk overlapping one another, delimiting longitudinal gap on region anterior to anus. Scale sheath along anal-fin base. Scales on caudal fin restricted to base of rays. Lateral line complete; perforated scales 53 (1), 54 (3), 55 (8), 56 (10), 57 (4), 58 (2), 59 (4), 60 (7), 61 (4), 62(3) or 63 (1). Horizontal scale rows between dorsal-fin origin and lateral line 15 (27), 16 (20), 17 (5) or 18 (3). Horizontal scale rows between pelvic-fin origin and lateral line 11 (66) or 12 (4). Horizontal scale rows between anal-fin origin and lateral line 12 (2), 13 (37), 14 (16), 15 (7) or 16 (1). Scale rows around caudal peduncle 15 (4), 16 (26), 17 (13) or 18 (3). Scale row along anal-fin base, extending for about two thirds of fin base. Predorsal scales 49 (1), 50 (6), 52 (9), 53 (5), 54(7), 55(3), 56(3), 57 (1), 58 (1), 59 (1), 60 (1), 62 (4), 63 (2), 64 (1), 66 (1), 68 (2). Transverse scale rows between humeral spot and supracleithrum 8 (57), 9 (16) or 10 (1).

Premaxilla and dentary with two canine-like teeth and remaining teeth conical. Maxilla with all teeth conical. Premaxilla with one anterior canine-like tooth followed by set of smaller conical teeth, another canine-like tooth placed on posterior portion of bone, followed by one or two small conical teeth (Fig. 2). Total number of premaxillary teeth 13 (4), 14 (3) or 15 (1). Maxilla with 52 (1), 55 (4), 58 (2) or 60 (1) teeth. Dentary with one canine-like tooth followed by 3–4 conical teeth, another canine-like tooth followed by a posterior row of 16 (3), 18 (4) or 19 (1) conical teeth (Fig. 2).

Ectopterygoid and metapterygoid without teeth. Gill-rakers on lower limb of first gill-arch 13 (2), 14 (3). Branchiostegal rays 3 (1) or 4 (7). Supraneurals 4 (8); first supraneural inserted posterior to neural spine of 4th centrum, and last supraneural inserted anterior to first dorsal-fin pterygiophore. Precaudal vertebrae 12 (8). Caudal vertebrae 23 (8). Total vertebrae 35 (8). Pleural rib pairs 11 (8). Pre- and postzygapophyses minute, approximately triangular in shape, and positioned somewhat parallel to neural zygapophysis of adjacent vertebra (e.g. Mattox and Toledo-Piza 2012: fig. 32A).

Color in alcohol (Fig. 1A). Body pale yellow to light yellow, slightly darker dorsally. Both extreme dorsal and ventral regions of trunk with scattered dark chromatophores. Inconspicuous approximately rounded or slightly elliptical dark brown humeral blotch, extending about three to four scales horizontally and about five vertically. Dorsal part of head, snout, circumorbital region and opercle darker than rest of head. Scattered dark chromatophores on tip of snout and suborbital region. V-shaped lines of chromatophores over myosepta along epaxial and hypaxial muscles, more visible on mid-posterior portion of body. Inconspicuous, approximately triangular shaped dark blotch on caudal-fin base, with posterior dark chromatophores. Inconspicuous clear stripe at anal-fin base. All fins hyaline, or light brown at base, with scattered dark chromatophores more visible on interradial membranes.

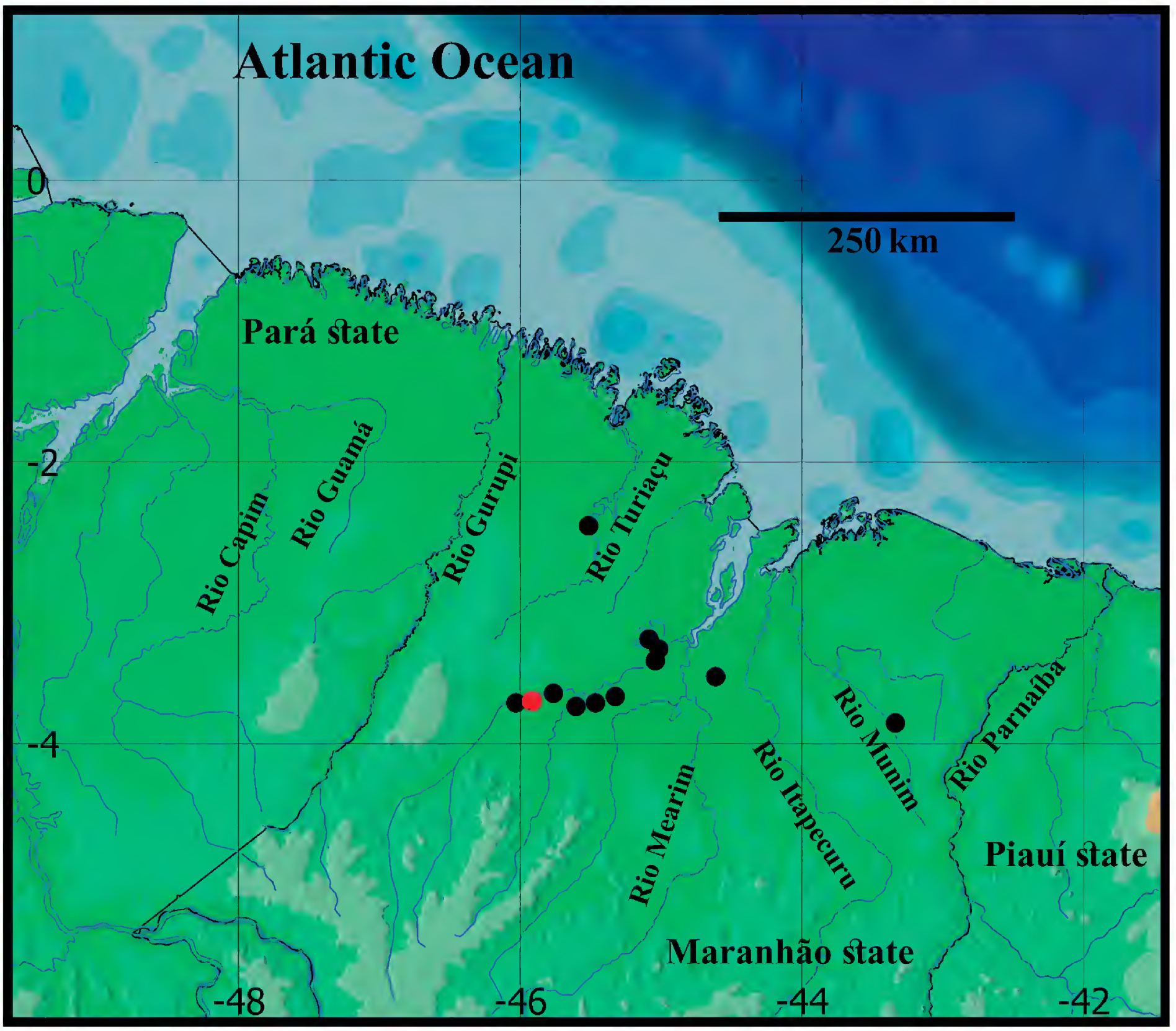

Figure 3. Distribution of *Charax awa* sp. n. Paratypes (black circles) and holotype (red circle).

Anterior portion of first to third unbranched rays of dorsal and first unbranched rays of pectoral and pelvic-fin rays darker than remaining rays.

Color in life (Fig. 1B). Color pattern in life similar to coloration of preserved specimens. Body silver on, anterior portion, and silver to hyaline on posterior portion. Anterior and dorsal portions of trunk darker, and sides of head darker than rest of body. Humeral and caudal-fin base blotches inconspicuous. Dorsal margin of trunk with conspicuous dark brown chromatophores. Purple longitudinal stripe along mid-portion of flank, extending posteriorly to anterior margin of caudal-fin base. Fins hyaline, with scattered dark brown or black chromatophores, more visible on interradial membranes.

Sexual dimorphism. No apparent sexual dimorphism.

Distribution. *Charax awa* is known from the Rio Mearim, Rio Munim and Rio Turiaçu basins, Maranhão state, northeastern Brazil (Fig. 3).

Remarks. The new species herein described differs from its geographically closely distributed congeners, *C. leticiae*, *C. niger*, and *C. pauciradiatus*, with records in the Lower Amazon, Capim, upper Itapecuru and Tocantins river basins (Fig. 4), mainly by the horizontal orbital diameter (see diagnosis section). In addition, *C. awa* sp. n. can be distinguished from *C. leticiae* by having the maxilla extending to a vertical line posterior to pupil, near posterior orbital margin while *C. leticiae* shows the maxilla extending slightly beyond vertical through middle of pupil and by humeral spot distance (32.1–38.0 % SL vs. 39.0–44.0 % SL). It can be distinguished from *C. pauciradiatus* by possessing 11–12 scale rows from the pelvic-fin origin to the lateral line and 15–18 scale rows from the dorsal-fin origin to the lateral line, while *C. pauciradiatus* possess 6–10 and 13–14, respectively, and differs from *C. niger* by having 8–10 transverse scale rows in space from the humeral spot to the supracleithrum, while *C. niger* possess 5–6. Moreover, it differs from *C. pauciradiatus* and *C. niger* by the absence of bony hooks on anal and pelvic-fins rays of adult males. This last character is emphasized in the discussion section.

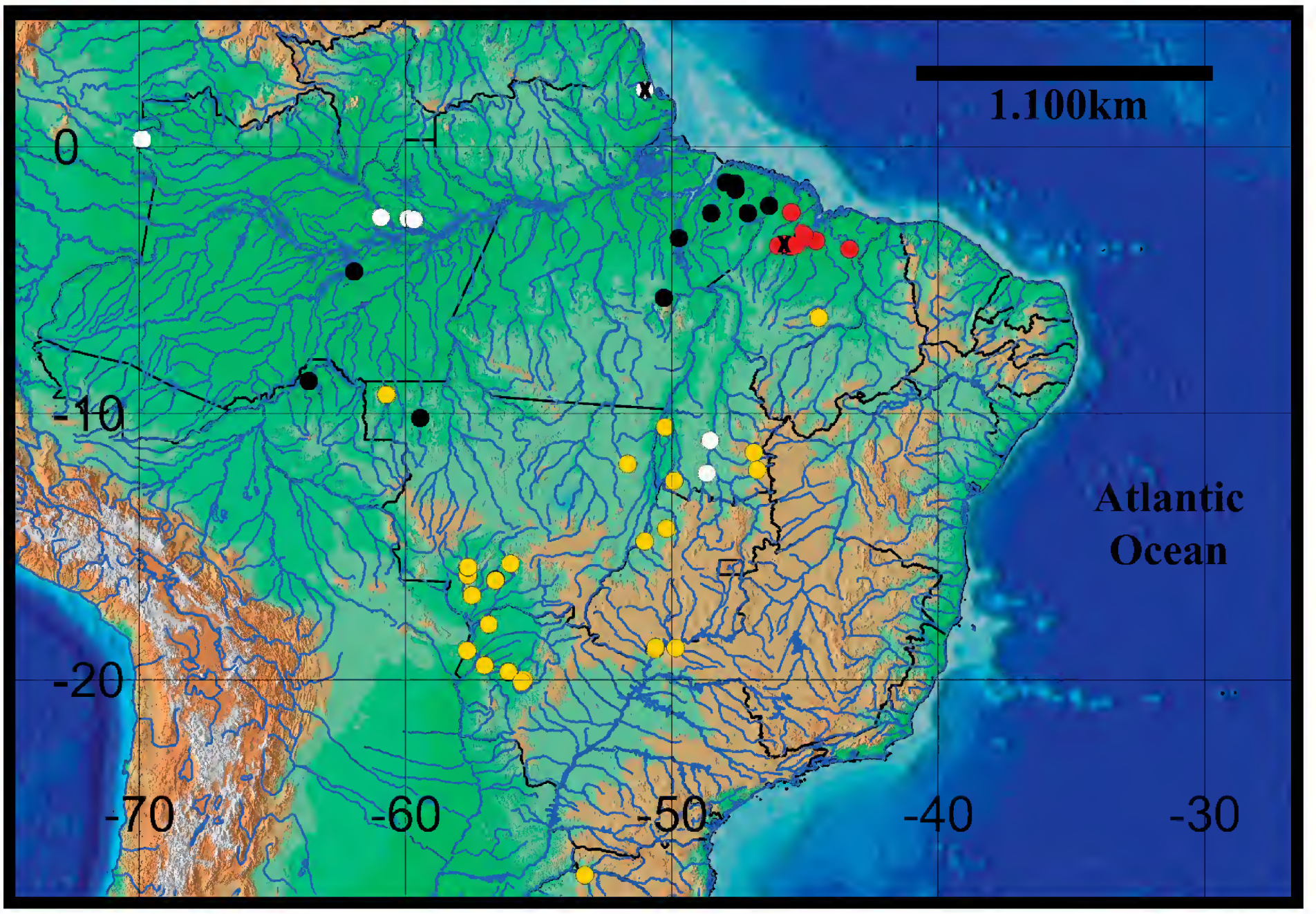

Figure 4. Distribution of *Charax awa* sp. n., *C. leticiae*, *C. pauciradiatus* and *C. niger*. *Charax awa* sp. n. (red circle), *C. leticiae* (yellow circle), *C. pauciradiatus* (black circle) and *C. niger* (white circle). The type localities of the species are marked with an asterisk. Information of this map was based on our examined material and data provided by Lucena 1987, and Menezes and Lucena 2014 . See Suppl. material 1.

In addition, new species herein described differs from *C. gibbosus*, a species incorrectly identified for the same area of *C. awa* sp. n. by the following features:

Charax awa sp. n. possesses a toothless ectopterygoid, absence of bony hooks on anal-fin rays of mature males, 8–10 transverse scales rows between the humeral spot and the suprecleithrum and 49–68 predorsal scales; while *C. gibbosus* has teeth on ectopterygoid, bony hooks on anal-fin rays of mature males, 5–6 transverse scales rows between the humeral spot and the suprecleithrum, and 38–45 predorsal scales.

Etymology. The specific epithet honors the term *Awá*, from Tupi-guarani, meaning "man, people, person", used by the native tribe Guajá, from the Maranhão state, for their self-denomination.

Discussion

Several authors have pointed out that *Charax* constitutes a monophyletic genus within the Characinae (Lucena 1987; Mirande 2010; Mattox and Toledo-Piza 2012; Menezes and Lucena 2014). The sister-group relationship between *Charax* and *Roeboides* was suggested by several authors (Lucena 1998, 2000; Mirande 2009, 2010; Mattox and Toledo-Piza 2012). However, Oliveira et al. (2011) alternatively suggested a different relationship between these two genera, proposing that *Charax* is the sister group of the clade comprising *Roeboides* Günther, 1864 and *Cynopotamus* Valenciennes, 1850. The presence of (1) a well-developed notch on the latero-ventral portion of cleithrum originating a relatively long posterior spiniform projection extending below pectoral-fin base and (2) an anterior shorter process oriented straight forward, or either inclined or bent laterally, was proposed by Lucena (1987) as the synapomorphies of the genus, a hypothesis corroborated by Mattox and Toledo-Piza (2012) and confirmed in the new species herein described (Fig. 5).

Charax awa sp. n. possesses a relatively small eye or orbital diameter when compared to the other congeners, except *C. notulatus* and *C. caudimaculatus* (22.1–28.5 % HL; 26.1–28.5 % HL on specimens below 80 mm SL; and 22.1–25.4 % HL on specimens above 80 mm SL; see Tables 1 and 2). Despite the larger specimens of *C. awa* sp. n. usually have a tendency to have smaller eye diameters when compared to the smaller specimens, the combined range of the eye diameter of these two size categories is even useful for the discrimination of the new species of all the congeners which possess a relatively larger eye diameter (29.6–

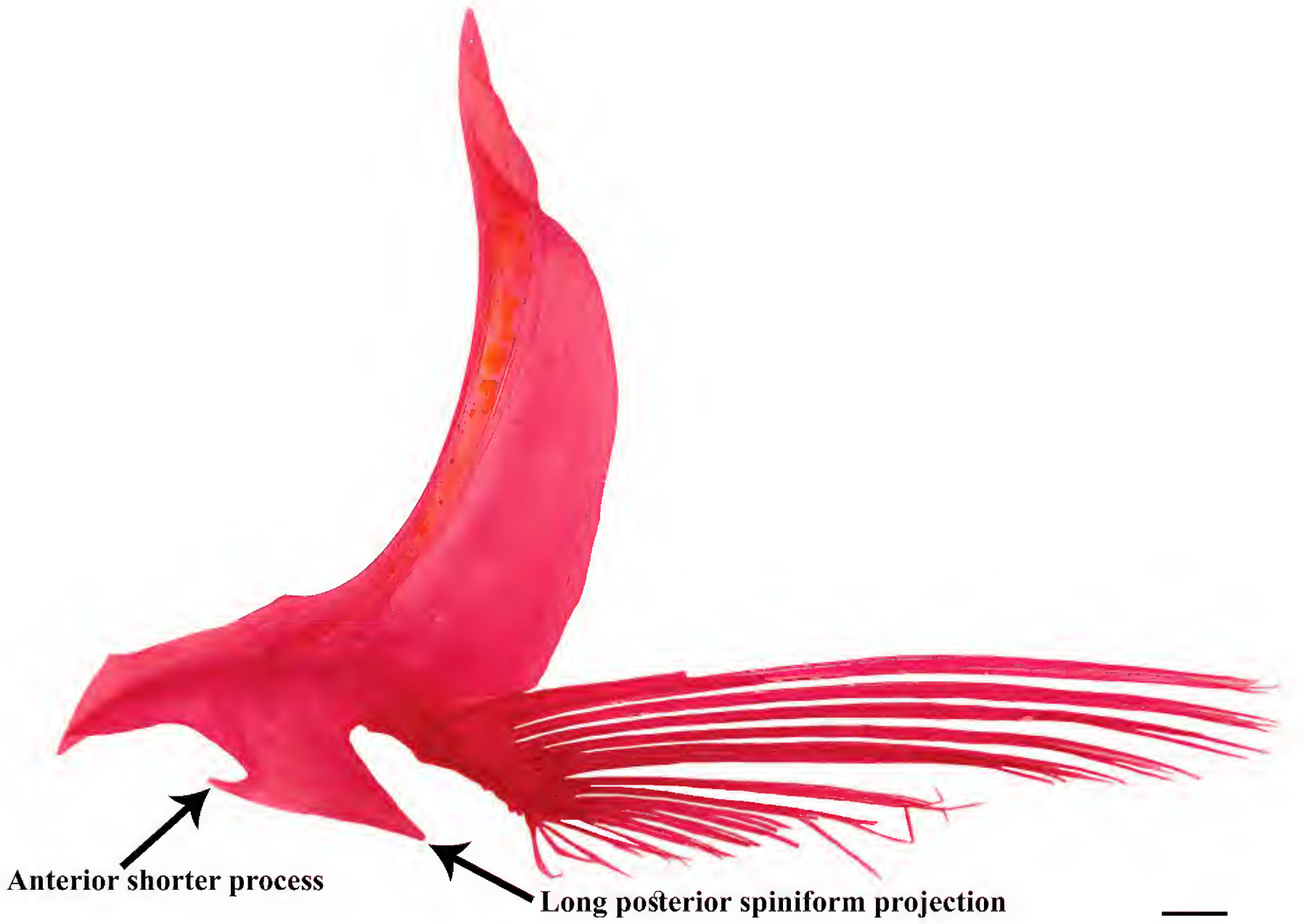

Figure 5. *Charax awa*, CICCAA00248, 73.8 mm SL; Pectoral girdle. Scale bar 1 mm. (Photographed by Erick Guimarães and Beldo Ferreira).

38.4 % HL combined). It is important to emphasize that the eye or orbital diameter is the main diagnostic character of *Charax* according to Menezes and Lucena (2014), which had used this character on their identification key to species of *Charax*, and as the first diagnostic feature in most of the species diagnoses. Other characters widely used by the last taxonomic revision of the genus were the lateral line, different types of scale counts, and the absence or presence or the number of teeth on the ectopterygoid. We confirmed here these characters as useful for species discrimination and taxonomy of the genus.

According to Menezes and Lucena (2014) a sexual dimorphism characterized by the presence of bony hooks on the anal and pelvic-fin rays of adult males is only recorded for *C. pauciradiatus*, *C. michaeli*, *C. gibbosus* and *C. niger* (in the case of the latter two, only in the anal-fin rays). Therefore, they concluded that the absence of these bony hooks is predominant across *Charax*. *Charax awa* sp. n. apparently exhibits this general pattern of the genus, since bony hooks on these fins were not recorded in any of our examined material of the species, including 220 specimens over 84.0 mm SL. Thus, the species apparently does not possess an evident sexual dimorphism.

The river systems of northeastern Brazil, particularly the river basins of its occidental portion, including the region between the Rio Gurupi and Parnaíba basin, remain with their ichthyofauna poorly known and scarcely studied, despite recent efforts to sample and inventory this area (e.g. Soares 2005, Barros et al. 2011, Ribeiro et al. 2014, Ramos et al. 2014, Matavelli et al. 2015, Melo et al. 2017, Piorski et al. 2017). The present study is an example of this state of knowledge. Further refined taxonomic studies will probably unveil more species and new taxa occurring in this area. Despite some freshwater fish species have been described occurring in this region and adjacent areas [e.g. *Corydoras julii* Steindachner, 1906, *Corydoras treitlii* Steindachner, 1906, *Knodus victoriae* (Steindachner, 1907), *Otocinclus hasemani* Steindachner,1915, *Hemiodus parnaguae* Eigenmann & Henn, 1916, *Corydoras vittatus* Nijssen, 1971, *Pterygoplichthys parnaibae* (Weber, 1991), *Auchenipterus menezesi* Ferraris & Vari, 1999, *Roeboides margareteae* Lucena, 2003, *Geophagus parnaibae* Staeck & Schindler, 2006, *Roeboides sazimai* Lucena, 2007, *Platydoras brachylecis* Piorski, Garavello, Arce H. & Sabaj Pérez, 2008, *Cichlasoma zarskei* Ottoni, 2011, *Poecilia sarrafae* Bragança & Costa, 2011, *Hypsolebias coamazonicus* Costa, Amorim & Bragança, 2014, *Anablepsoides vieirai* Nielsen, 2016, *Parotocinclus cabessadecuia* Ramos, Lima & Ramos, 2017 and *Hypostomus sertanejo* Zawadzki, Ramos & Sabaj Pérez, 2017]. Studies on range extension and new records of some freshwater fishes from the area between the mouth of Rio Gurupi and Delta do

Rio Parnaíba (e.g. Barros et al. 2011, Matavelli et al. 2015, Guimarães et al. 2017a, 2017b, Lima et al. 2017), as well as the description of new species (cited above), suggest that the biogeographic history of the river basins of the region is complex and still poorly known. This region is an extremely ecologically relevant area since it comprises three of the main Brazilian biomes, as well as, transition zones between them: Amazônia, Brazilian Cerrado and Caatinga. Therefore, this area has faunal and floristic representatives of these three biomes, which makes it extremely relevant in terms of ecology, biodiversity and conservation (Olson, et al. 2001; Piorski et al. 2008, Fiaschi and Pirani 2009; Miranda et al. 2012).

Comparative material. *Charax caudimaculatus:* USNM 263877, 1, 95 mm SL, Laguna Cococha, Reserva National de Tambopata, Madre de Dios, **Peru.** (Radiograph of a Paratype). USNM 280291, 1, 95.0 mm SL, Laguna Cococha, Reserva National de Tambopata, Madre de Dios, **Peru.** (photograph of holotype).

Charax leticiae: all from **Brazil**: UFRJ: 1576, 4, 66.6–71.1, Goias State, Aruanã municipality. CICCAA 00762, 2, 79.1–80.0 mm SL, Pará State, Parauapebas municipality. CPUFMA121858, 1, 81.0 mm SL, Maranhão state, stream at the Parque Estadual do Mirador (Rio Itapecuru basin), Mirador municipality.

Charax pauciradiatus: all from Maranhão State, **Brazil**. CICCAA00899, 3, 79.1–84.7. Maranhão State, Igarapé Papagaio, Tocantins river basin, São Pedro da Agua Branca Municipality. CPFUMA10860, 6, 88.6–117.46, Igarapé mão-de-onça, Gurupi river basin, Centro Novo Municipality. CPUFMA00868, 9, 103.7–117.94, Gurupi river basin, Centro Novo Municipality. CPUFMA10869, 7, 98.5–113.0, Gurupi river basin, Centro Novo Municipality. CPUFMA11870, 8, 93.9–112.6, Gurupi river basin, Centro Novo Municipality. CPUFMA11871, 3, 89.1–113.2, Gurupi river basin, Centro Novo Municipality.

Charax notulatus: USNM: 360305, 1 (photograph of holotype), 77 mm SL, Guarico State, Cano Falcon, **Venezuela.**

Acknowledgements

We are thankful to Capes (Coordenação de Aperfeiçoamento de Pessoal de Nível Superior) for granting scholarships to ECG and BRF. We also thank Wilson Costa and Nivaldo Piorski for enabling us to study specimens in their care, or for donating specimens; to Vale S.A and Amplo Engenharia e Gestao de Projetos Ltda for the provision of part of the data analyzed in this study. We also thank Clarisse Figueiredo for her English revisions. This paper benefited from suggestions provided by P. Bartsch and three reviewers: two anonymous and W. Costa. This study was supported by FAPEMA (Foundation for Scientific Research and Development of Maranhão - Universal process-00724/17). Material was collected under permits 02001.007241/2004-37 from IBAMA (Brazilian Institute of Environment and Natural).

References

Barros MC, Fraga EC, Birindelli JLO (2011) Fishes from the Itapecuru River basin, State of Maranhão, northeast Brazil. Brazilian Journal of Biology 71(2): 375–380. http://dx.doi.org/10.1590/S1519-69842011000300006

Bragança PHN, Costa WJEM (2011) *Poecilia sarrafae*, a new poeciliid from the Paraíba and Mearim river basins, northeastern Brazil (Cyprinodontiformes: Cyprinodontoidei). Ichthyological Exploration of Freshwaters 21(4): 369–376.

Cope ED (1870) Contribution to the ichthyology of the Marañon. Proceedings of the American Philosophical Society 11: 559–570.

Cope ED (1894) On three new genera of Characinidae. American Naturalist 28(325): 67.

Costa WJEM, Amorim PF, Bragança PHN (2014) Species limits and phylogenetic relationships of red-finned cryptic species of the seasonal killifish genus *Hypsolebias* from the Brazilian semi-arid Caatinga (Teleostei: Cyprinodontiformes: Rivulidae). Journal of Zoological Systematics and Evolutionary 52(1): 52–58. https://doi.org/10.1111/jzs.12041

Davis JI, Nixon KC (1992) Populations, genetic variation, and the delimitation of phylogenetic species. Systematic Biology 41: 421–435. https://doi.org/10.1093/sysbio/41.4.421

Eigenmann CH, Henn AW (1916) Description of three new species of characid fishes. Annals of the Carnegie Museum 10(7): 87–90.

Eigenmann CH (1912) The freshwater fishes of British Guiana, including a study of the ecological grouping of species, and the relation of the fauna of the plateau to that of the lowlands. Memoirs of the Carnegie Museum 5(1): 1–103. https://doi.org/10.5962/bhl.part.14515

Eigenmann CH (1922) The fishes of western South America, Part I. The fresh-water fishes of northwestern South America, including Colombia, Panama, and the Pacific slopes of Ecuador and Peru, together with an appendix upon the fishes of the Rio Meta in Colombia. Memoirs of the Carnegie Museum 9(1): 1–38.

Eschmeyer WN, Fricke R, van der Laan R (Eds) (2017) Catalog of Fishes: Classification. http://www.calacademy.org/scientists/catalog-of-fishes-classification/ [Electronic version accessed 02/12/2017]

Ferraris CJ Jr, Vari RP (1999) The South American catfish genus *Auchenipterus* Valenciennes, 1840 (Ostariophysi: Siluriformes: Auchenipteridae): monophyly and relationships, with a revisionary study. Zoological Journal of the Linnean Society 126(4): 387–450. https://doi.org/10.1111/j.1096-3642.1999.tb00156.x

Fiaschi P, Pirani JR (2009) Review of plant biogeographic studies in Brazil. Journal of Systematics and Evolution, 47(5): 477–496. https://doi.org/10.1111/j.1759-6831.2009.00046.x

Fink WL, Weitzman SH (1974) The so-called Cheirodontin fishes of Central America with descriptions of two new species (Pisces: Characidae). Smithsonian Contribution to Zoology 172: 1–46. https://doi.org/10.5479/si.00810282.172

Géry J, Knöppel HA (1976) Un characin translucide nouveau: *Asiphonichthys condei* n. sp. (Cypriniforme, Characoidei, Characidae). Revue française d'Aquariologie Herpétologie 3(2): 47–54.

Guimarães EC, Ottoni FP, Brito PS, Piorski NM, Nunes JLS (2017a) Range extension of *Gasteropelecus sternicla* (Characiformes) for three coastal river basins of the Eastern Amazon region as well as for the Itacaiunas River drainage of the Tocantins River basin. Cybium 41(1): 72–74. http://sfi-cybium.fr/node/941

Guimarães EC, Ottoni FP, Katz AM (2017b) Range extension of *Piabucus dentatus* (Koelreuter, 1763) for the Pindaré River drainage, Mearim River basin, Brazil (Characiformes: Iguanodectinae). Cybium 41(3): 287–289. http://sfi-cybium.fr/node/2357

Günther A (1864) Catalogue of the fishes in the British Museum. Catalogue of the Physostomi, containing the families Siluridae, Characinidae, Haplochitonidae, Sternoptychidae, Scopelidae, Stomiatidae in the collection of the British Museum 5: 1–455.

Kner R (1858) Zur Familie der Characinen. Sitzungsberichte der Kaiserlichen Akademie der Wissenschaften. Mathematisch-Naturwissenschaftliche Classe 32 (22): 163–168.

Lima RC, Nascimento MHS, Birindelli JLO, Barros MC, Fraga EC (2017) Extension of the distribution of *Megalechis thoracata* (Valenciennes, 1840) (Siluriformes, Callichthyidae) to the basin of the Itapecuru River, northeastern Brazil. Check List 13(4): 327–330. https://doi.org/10.15560/13.4.327

Linnaeus C (1758) Systema Naturae, Ed. X. (Systema naturae per regna tria naturae, secundum classes, ordines, genera, species, cum characteribus, differentiis, synonymis, locis. Tomus I. Editio decima, reformata). Holmiae 1, 824 pp.

Lucena CAS (1987) Revisão e redefinição do gênero neotropical *Charax* Scopoli, 1777 com a descrição de quatro espécies novas (Pisces: Characiformes: Characidae). Comunicações do Museu de Cências da PUCRS, Porto Alegre 40: 5–124.

Lucena CAS (1998) Relações filogenéticas e definição do gênero *Roeboides*, Günther (Ostariophysi; Characiformes; Characidae). Comunicações do Museu de Ciências e Tecnologia da PUCRS, Série Zoologia 11: 19–59.

Lucena CAS (2007) Revisão taxonômica das espécies do gênero *Roeboides* grupo-affinis (Ostariophysi, Characiformes, Characidae). Iheringia Série Zoologia 97(2): 117–136. http://dx.doi.org/10.1590/S0073-47212007000200001

Lucena CAS (1989) Trois nouvelles espèces du genre *Charax* Scopoli, 1777 pour la région Nord du Brésil (Characiformes, Characidae, Characinae). Revue française d'Aquariologie Herpétologie 15(4): 97–104.

Lucena CAS (2000) Revisão taxonômica e filogenia das espécies transandinas do gênero *Roeboides* Günther (Teleostei: Ostariophysi: Characiformes). Comunicações Museu Ciências Tecnologia PUCRS, Série Zoologia 13: 3–63.

Lucena CAS (2003) Revisão taxonômica e relações filogenéticas das espécies de *Roeboides* grupo-microlepis (Ostariophysi, Characiformes, Characidae). Iheringia Série Zoologia 93(3): 283–308. http://dx.doi.org/10.1590/S0073-47212003000300008

Martins MB, Oliveira TG (2011) Amazônia Maranhense: Diversidade e Conservação. Belém: MPEG.

Matavelli R, Campos AM, Vale J, Piorski NM, Pompeu PS (2015) Ichthyofauna sampled with tadpoles in northeastern Maranhão state, Brazil. Check List 11(1): 1550 https://doi.org/10.15560/11.1.1550

Mattox GMT, Toledo-Piza M (2012) Phylogenetic study of the Characinae (Teleostei: Characiformes: Characidae). Zoological Journal of the Linnean Society 165: 809–915. http://dx.doi.org/10.1111/j.1096-3642.2012.00830.x

Melo FAG, Buckup PA, Ramos TPA, Souza AKN, Silva CMA, Costa TC, Ribeiro AT (2017) Fish Fauna of the lower course of the Parnaíba river, northeastern Brazil. Boletim do Museu de Biologia Melo Leitão 38(4): 363–400.

Menezes NA, Lucena CAS (2014) A taxonomic review of the species of *Charax* Scopoli, 1777 (Teleostei: Characidae: Characinae) with description of a new species from the Rio Negro bearing superficial neuromasts on body scales, Amazon basin, Brazil. Neotropical Ichthyology 12(2): 193–228. http://dx.doi.org/10.1590/1982-0224-20130175

Menezes NA, Weitzman SH (1990) Two new species of *Mimagoniates* (Teleostei: Characidae: Glandulocaudinae), their phylogeny and biogeography and a key to the glandulocaudin fishes of Brazil and Paraguay. Proceedings of the Biological Society of Washington 103(2): 380–426.

Miranda JP, Costa JCL, Rocha, CFD (2012) Reptiles from Lençóis Maranhenses National Park, Maranhão, northeastern Brazil. ZooKeys, 246: 51–68. https://doi.org/10.3897/zookeys.246.2593

Mirande JM (2009) Weighted parsimony phylogeny of the family Characidae (Teleostei: Characiformes). Cladistics 25: 574–613. http://dx.doi.org/10.1111/j.1096-0031.2009.00262.x

Mirande JM (2010) Phylogeny of the family Characidae (Teleostei: Characiformes): from characters to taxonomy. Neotropical Ichthyology 8(3): 385–568. http://dx.doi.org/10.1590/S1679-62252010000300001

Nielsen DT (2016) Description of two new species of *Anablepsoides* (Cyprinodontiformes: Cynolebiidae) from Rio Madeira, Amazon drainage, Rondônia state and from Rio Itapecuru basin, Maranhão state, Brazil. aqua, International Journal of Ichthyology 22(4): 165–176.

Nijssen H (1971) Two new species and one new subspecies of the South American catfish genus *Corydoras* (Pisces, Siluriformes, Callichthyidae). Beaufortia 19(250): 89–98.

Nelson JS, Grande TC, Wilson MVH (2016) Fishes of the world. John Wiley and Sons, Hoboken, New Jersey, 651p.

Oliveira C, Avelino GS, Abe KT, Mariguela TC, Benine RC, Ortí G, Vari RP, Castro RMC (2011) Phylogenetic relationships within the speciose family Characidae (Teleostei: Ostariophysi: Characiformes) based on multilocus analysis and extensive ingroup sampling. BMC Evolutionary Biology 11: 275. https://doi.org/10.1186/1471-2148-11-275

Olson DM, Dinerstein E, Wikramanayake ED, Burgess ND, Powell GVN, Underwood EC, Kassem KR (2001) Terrestrial ecoregions of the world: A new map of life on earth a new global map of terrestrial ecoregions provides an innovative tool for conserving biodiversity. BioScience 51: 933–938. https://doi.org/10.1641/0006-3568(2001)051[0933:TEOTWA]2.0.CO;2

Ottoni FP (2011) *Cichlasoma zarskei*, a new cichlid fish from northern Brazil (Teleostei: Labroidei: Cichlidae). Vertebrate Zoology 61(3): 335–342. http://www.senckenberg.de/files/content/forschung/publikationen/vertebratezoology/vz61-3/06_vertebrate_zoology_61-3_ottoni_335.pdf

Piorski NM, Garavello JC, Arce MH, Sabaj Pérez MH (2008) *Platydoras brachylecis*, a new species of thorny catfish (Siluriformes: Doradidae) from northeastern Brazil. Neotropical Ichthyology 6(3): 481–494. http://dx.doi.org/10.1590/S1679-62252008000300021

Piorski NM, Sanches A, Carvalho-Costa LF, Hatanaka T, Carrillo-Avila M, Freitas PD, Galetti PM Jr (2008) Contribution of conservation genetics in assessing neotropical freshwater fish biodiversity. Braz. J. Biol. 68: 1039–1050. http://dx.doi.org/10.1590/S1519-69842008000500011

Piorski NM, Ferreira BRA, Guimaraes EC, Ottoni FP, Nunes JLS, Brito PS (2017) Peixes do Parque Nacional dos Lençois Maranhenses. Vol. 1. Café & Lápis, São Luis, 189 pp.

Ramos TPA, Lima SMQ, Ramos RTC (2017) A new species of armored catfish *Parotocinclus* (Siluriformes: Loricariidae) from the rio

Parnaíba basin, northeastern, Brazil. Neotropical Ichthyology 15(2): e160153. http://dx.doi.org/10.1590/1982-0224-20160153

Ramos TPA, Ramos RTC, Ramos SAQA (2014) Ichthyofauna of the Parnaíba river Basin, Northeastern Brazil. Biota Neotropica 14(1): e20130039. www.biotaneotropica.org.br/v14n1/en/abstract?inventory+bn01014012014

Ribeiro MFR, Piorski NM, Almeida ZS, Nunes JLS (2014) Fish aggregating known as moita, an artisanal fishing technique performed in the Munim river, state of Maranhão, Brazil. Boletim do Instituto de Pesca 40(4): 677–682. http://www.pesca.sp.gov.br/40_4-677-682.pdf

Scopoli JA (1777) Introductio ad historiam naturalem, sistens genera lapidum, plantarum et animalium hactenus detecta, caracteribus essentialibus donata, in tribus divisa, subinde ad leges naturae. Prague, 506 pp.

Soares EC (2005) Peixes do Mearim. Vol. 10. Editora Instituto Geia, São Luis, 143 pp.

Staeck W, Schindler I (2006) *Geophagus parnaibae* sp. n. - a new species of cichlid fish (Teleostei: Perciformes: Cichlidae) from the rio Parnaíba basin, Brazil. Zoologische Abhandlungen, Staatliche Naturhistorische Sammlungen Dresden, Museum für Tierkunde 55: 69–75. http://www.whose-tadpole.net/SNSD/vertebrate-zoology/Zool_Abh/zool_abh_55_2005_69-75.pdf

Steindachner F (1906) Zwei neue *Corydoras*-Arten aus dem Parnahyba und Parahimflusse im Staate Piauhy. Anzeiger der Kaiserlichen Akademie der Wissenschaften, Mathematisch-Naturwissenschaftlichen Classe 43: 478–480.

Steindachner F (1907) Über eine neue *Psilichthys*-Art, *Ps. cameroni* aus dem Flusse Cubataõ im Staate S. Catharina, Brasilien. Anzeiger der Kaiserlichen Akademie der Wissenschaften, Wien, Mathematisch-Naturwissenschaftliche Klasse 44(6): 82–85.

Steindachner F (1915) Ichthyologische Beiträge (XVIII). Anzeiger der Kaiserlichen Akademie der Wissenschaften, Wien, Mathematisch-Naturwissenschaftliche Classe 52(27): 346–349.

Taylor WR, Van Dyke GC (1985) Revised procedures for staining and clearing small fishes and other vertebrates for bone and cartilage study. Cybium 9(2): 107–119. http://sfi-cybium.fr/node/2423

Triques ML (1999) Three new species of *Rhamphichthys* Müller et Troschell [sic], 1846 (Ostariophysi: Gymnotiformes: Rhamphichthyidae). Revue française d'Aquariologie Herpétologie 26(1–2): 1–6.

Weber C (1991) Nouveaux taxa dans *Pterygoplichthys* sensu lato (Pisces, Siluriformes, Loricariidae). Revue Suisse de Zoologie 98(3): 637–643. https://doi.org/10.5962/bhl.part.82074

Weitzman SH (1962) The osteology of *Brycon meeki*, a generalized characid fish, with an osteological definition of the family. Stanford Ichthyology Bulletin 8: 1–77.

Zawadzki CH, Ramos TPA, Sabaj M (2017) *Hypostomus sertanejo* (Siluriformes: Loricariidae), new armoured catfish species from north-eastern Brazil. Journal of Fish Biology 91(1): 317–330. http://dx.doi.org/10.1111/jfb.13349

Supplementary material 1

Distribution of *Charax awa* sp.n., C. leticiae, *C. pauciradiatus*, and *C. niger*

Authors: Erick Cristofore Guimarães, Pâmella Silva De Brito, Beldo Rywllon Abreu Ferreira, Felipe Polivanov Ottoni

Data type: Microsoft Excel Worksheet (.xlsx)

Explanation note: Information of this map was based on our examined material and data provided by Menezes and Lucena (2014).

Link: https://doi.org/10.3897/zse.94.22106.suppl1

Zoosyst. Evol. 94 (1) 2018, 95–108 | DOI 10.3897/zse.94.22501

PENSOFT

museum für naturkunde

Taxonomic and faunistic study of Aulacidae (Hymenoptera, Evanioidea) from Iran, with illustrated key to species

Mostafa Ghafouri Moghaddam[1], Giuseppe Fabrizio Turrisi[2]

1 *Department of Plant Protection, College of Agriculture, University of Zabol, Zabol, P.O. Box: 98615–538, I. R. IRAN*

2 *Via Cristoforo Colombo 8, 95030, Pedara, Catania, Italy*

http://zoobank.org/583BCCD1-F6E1-492A-A0CE-5E1DB5114477

Corresponding author: *Mostafa Ghafouri Moghaddam* (ghafourim@uoz.ac.ir)

Received 24 November 2017
Accepted 24 January 2018
Published 2 February 2018

Academic editor:
Michael Ohl

Abstract

Aulacidae are parasitoids of wood-boring larvae of Hymenoptera and Coleoptera, known in all zoogeographic regions of the World, except Antarctic. Two aulacids, *Pristaulacus compressus* (Spinola, 1808) and the rare *Pristaulacus mourguesi* Maneval, 1935, have been recently collected from Iran, the latter being a new record. Based on available data, the Iranian aulacid fauna includes five species within a single genus, *Pristaulacus* Kieffer 1900. A brief taxonomic treatment, as well as morphometric data and an illustrated key to species, are provided.

Key Words

Pristaulacus
Western Iran
wood-boring
parasitoid
illustrated key

Introduction

The aulacid wasps, Aulacidae Shuckard, 1842 are endoparasitoids of wood-boring larvae Coleoptera (Cerambycidae and Buprestidae) and Hymenoptera (Xiphydriidae). The family Aulacidae is small distinct family in the superfamily Evanioidea. This family includes 262 extant species grouped within only two genera, *Aulacus* Jurine, 1807 with 83 species and *Pristaulacus* Kieffer, 1900 (including the former *Panaulix* Benoit, 1984), with 177 species (Jennings and Austin 2004, Turrisi et al. 2009, Chen et al. 2016, Turrisi and Nobile 2016; Turrisi 2017). According to the online Taxapad (Yu et al. 2012) this family contains four subfamilies and 11 genera, including fossils. Some identified fossils are not completely known and their inclusion within Aulacidae still remains somewhat questionable (Zhang and Rasnitsyn 2004).

Some evidence support strongly a close relationship between Aulacidae and Gasteruptiidae and each group are currently considered as distinct families (Jennings and Austin 2000, Turrisi et al. 2009). However, the current generic classification of the Aulacidae is not sufficiently robust and needs further study. There is strong support for the monophyly of *Pristaulacus* but not for *Aulacus*, which is largely paraphyletic in the cladistics analyses of Turrisi et al. (2009). The faunistic knowledge of Aulacidae is generally unsatisfactory due to their general rarity and difficulty in collecting by conventional methods, e.g., by net; there is a general paucity of available material, even in the large museums (Turrisi 2007).

The Iranian Aulacidae has been recently treated by Ghahari (2012), Lotfalizadeh et al. (2017) and Ghahari and Madl (2017). Nonetheless, continuous sampling in different ecosystems, particularly with Malaise traps, has resulted in new records which we present in this paper, along with an illustrated key to species.

Material and methods

The specimens examined in the present paper have been recently collected using a modified Malaise-trap (Funnel-Townes Style, B. Motamedinia, unpublished: BM-MTF-TS) placed in various localities of Kermanshah province (Western part of Iran), as well as in Eastern provinces (Fig. 1A–B). The traps were a basic Malaise trap supplemented with an additional internal collecting bottle. The insects bump into the black mesh panel and move towards the lighter mesh to escape due to their positive phototropism (van Achterberg 2009); at this point, they encounter the collection bottle and become permanently trapped. However, a considerable number of in-

Figure 1. Malaise traps; locations. **A** Kermanshah province, Dudan, adjacent to the river and valley; **B** Kermanshah province, Harsin, near the foothills; **C** and **D** Additional collecting bottle inside the trap.

sects fail to enter the collecting bottle for various reasons e.g., inappropriate installation of trap or collecting bottle, displacement of the trap by wind, or the particular behavior of the insects (Fig. 1C–D). The collected specimens were killed in 75% ethanol and then glued on triangular cards, according to AXA protocol (van Achterberg 2009). Finally, all of the specimens labeled using new pinning block (Ghafouri Moghaddam et al. 2017).

Specimens were examined under a Nikon® SMZ645 stereomicroscope (Nikon® Inc., Japan). Illustrations of taxonomically important body parts were taken using a Canon® EOS 700D (Canon® Inc., Japan), a simple light source with halogen lamp (manual) and 2× lenses mounted on Hund® Stereomicroscope (Wetzlar Inc., Germany). Multiple images were subsequently processed in Zerene Stacker™ version 1.04 software and post processed in Adobe Photoshop® CS6. The images in the illustrated key were prepared by the second author using voucher specimens already deposited in his private collection. Morphological terminology follows Crosskey (1951), Huber and Sharkey (1993) and Turrisi (2007). Terminology for surface sculpturing follows Harris (1979). A distributional map was generated using SimpleMappr (Shorthouse 2010) and collecting localities are given in Fig. 8. The following abbreviations are used for depositories: **CPTO**: Guido Pagliano collection, Torino, Italy; **DPPZ**: Collection of Department of Plant Protection, University of Zabol, Iran; **DU**: Depository Unknown; **MCSN**: Museo Civico di Storia Naturale "G. Doria", Genova, Italy; **MNHN**: Muséum National d'Histoire Naturelle, Laboratoire d'Entomologie, Paris, France; **NHMW**: Naturhistorisches Museum, Wien, Austria; **ZIN**: Zoological Institute of the Russian Academy of Sciences, St. Petersburg, Russia; **ZMUC**: Zoological Museum, Copenhagen University, Denmark.

Measurements were done with a micro-ruler. Morphometric ratios were measured in tpsDig *ver.* 2.05 (Rohlf 2006), using digitized coordinates of landmarks and capture outlines. It should be noted that we documented measurements to the nearest 0.001 mm with tpsDig, but we conservatively report them to an accuracy of two decimal places. Definitions and abbreviations for the measured characters are shown in Table 1 (see also Figs 2, 3, 5).

Table 1. Abbreviation for morphometric data, measured in the examined material.

Abbreviation	Definition	Explanation
ClL	*Clypeal maximum length*	Full-face view, as in Fig 5A
ClOL	*Clypeus-ocellar line*	Distance between base of clypeus and median ocellus, full-face view (Fig 5A).
ClW	*Clypeal maximum width*	Full-face view, as in Fig 5A
CoL	*Hind coxa maximum length*	In lateral view, as in Fig 3C
CoW	*Hind coxa maximum width*	In lateral view, as in Fig 3C
EL	*Eye maximum length*	Vertical line length of compound eye, full-face view (Fig 2A)
EW	*Eye maximum width*	Horizontal line, width of the compound eye, full-face view (Fig 2A)
FWL	*Fore wing maximum length*	From median margin of first axillary sclerite to distal point of wing blade, as in Fig 3A
FWW	*Fore wing maximum width*	Longest line drawn perpendicular to the length axis, as in Fig 3A
HL	*Head maximum length*	From anterior prominence of head to base of occipital carina, dorsal view (Fig 2B)
HW	*Head maximum width*	Maximum distance between lateral margins of compound eyes dorsal view (Fig 2B)
IOL	*Inter-ocular line*	Shortest distance between inner margin of compound eyes, full-face view (Fig 2A)
MsL	*Mesosoma maximum length*	longest anatomical line that connects the posterior-most point of the propodeal lobe with the anterior-most point of the pronotum, but if one of the reference points is not visible, dorsal view may help, preferentially in lateral view (Fig 2D)
MsW	*Mesosoma maximum width*	In dorsal view, as in Fig 2E
MtL	*Metasoma maximum length*	From base of petiole to base of pygidium, lateral view (Fig. 3B)
OD	*Ocellar diameter*	In dorsal view, as in Fig 2B
OML	*Ocular-mandibular line*	Minimum distance between anterior margin of compound eye and mandibular insertion to head, full-face view (Fig 5A)
OOCL	*Ocular-occipital carina line*	Minimum distance between lateral margin of compound eye and base of occipital carina lateral view (Fig 2C)
OOL	*Oculo-ocellar line*	Shortest distance between margins of compound eye and ocellus, dorsal view (Fig 2B)
OTL	*Oculo-tentorial line*	Minimum distance between anterolateral margin of compound eye and tentorial pit, full-face view (Fig 5A)
PEL	*Petiole maximum length*	From anterior-most margin to posterior margin of petiole, dorsal view (Fig 2F)
PEW	*Petiole maximum width*	Dorsal view, as in Fig 2F
PL	*Propodeum maximum length*	From apex of scutellum to base of petiole, dorsal view (Fig 2E)
POL	*Posterior-ocellar line*	Shortest distance between margin of lateral ocelli, dorsal view (Fig 2B)
PSL	*Pterostigma maximum length*	As in Fig 3A
PSW	*Pterostigma maximum width*	As in Fig 3A
PW	*Propodeum maximum width*	In dorsal view, as in Fig 2E
TL	*Temple maximum length*	Minimum distance between anterior margin of compound eye and base of occipital carina, dorsal view (Fig 2B)

Results

Five species belonging to the genus *Pristaulacus* are recorded from five provinces of Iran (East-Azarbaijan, Guilan, Kermanshah, Shiraz and West Azarbaijan) (Fig. 8). The species recorded for the first time from Iran and from individual provinces are marked with a single (*) or double (**) asterisks, respectively. It should be noted that no depository was mentioned for specimens of both *P. barbeyi* and *P. galitae* from Iran (Ghahari 2012), thus, it has not been possible to examine this material for confirmation. These taxa are marked below with an #.

Illustrated key to Iranian *Pristaulacus* Kieffer

1 Lateroventral margin of pronotum without tooth-like process (**a**) 2

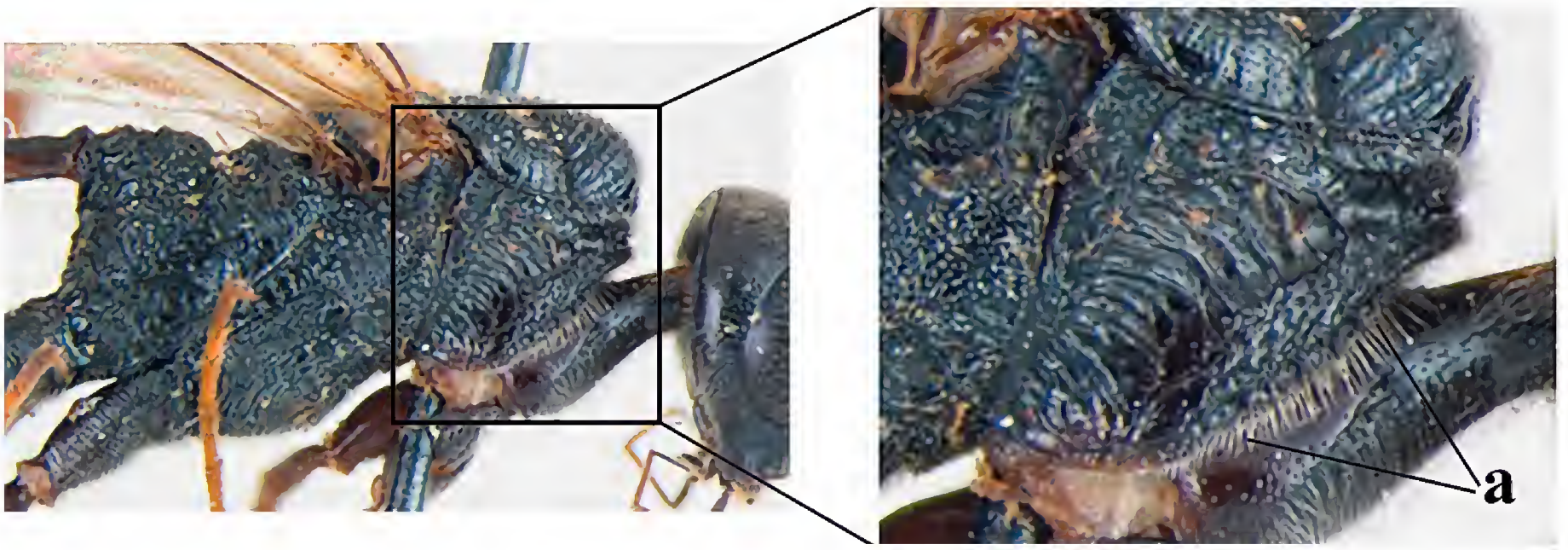

– Lateroventral margin of pronotum with at least one tooth-like process (**aa**) 3

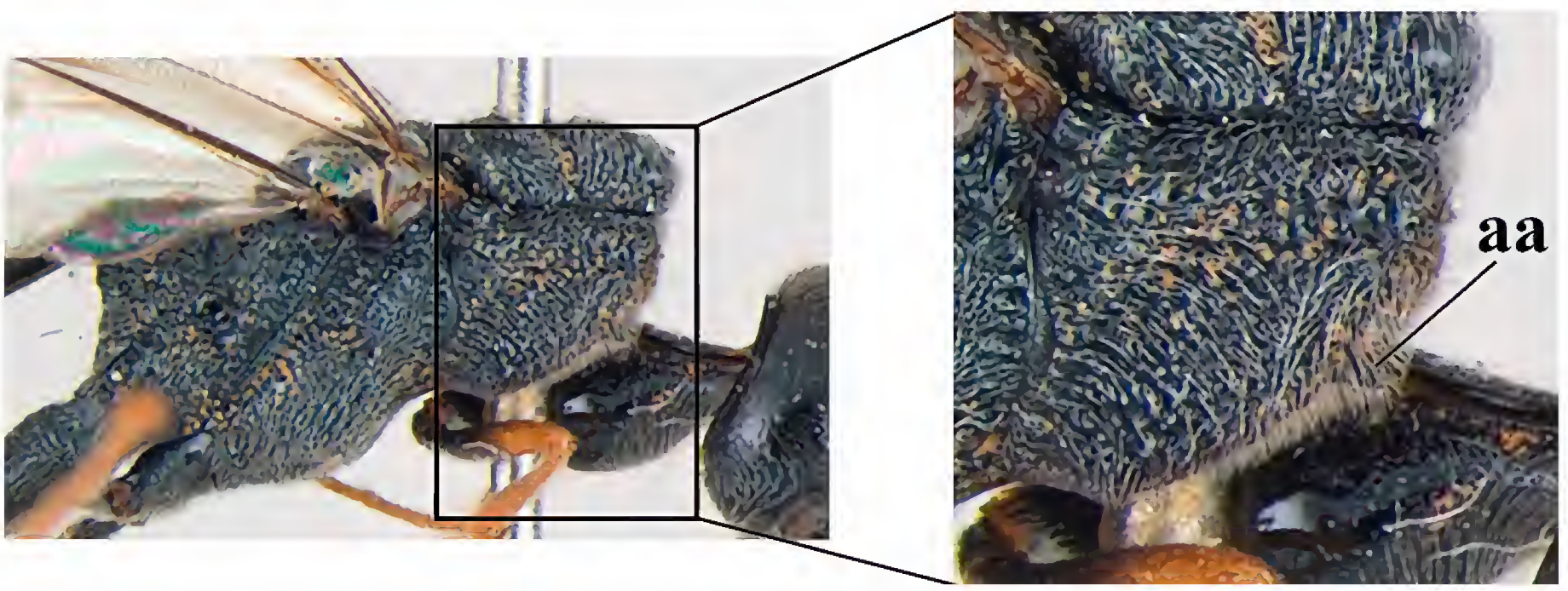

2 Head dull to weakly shiny, extensively transverse striolate (**a**); hind tarsus dark brown; tarsal claw with two tooth-like processes (**b**); petiole stocky and short (**c**).....*P. barbeyi* (Ferrière, 1933)

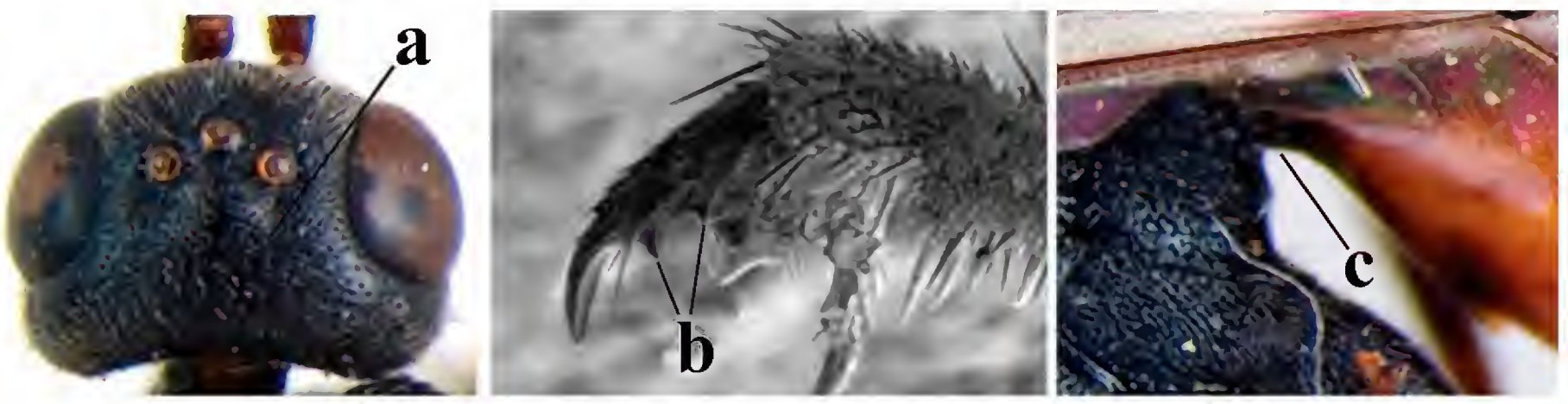

– Head shiny, mostly polished, except frons weakly striolate punctate (**aa**); hind tarsus yellow; tarsal claw with four tooth-like processes (**bb**); petiole slender and elongate (**cc**) ..... *P. gloriator* (Fabricius, 1804)

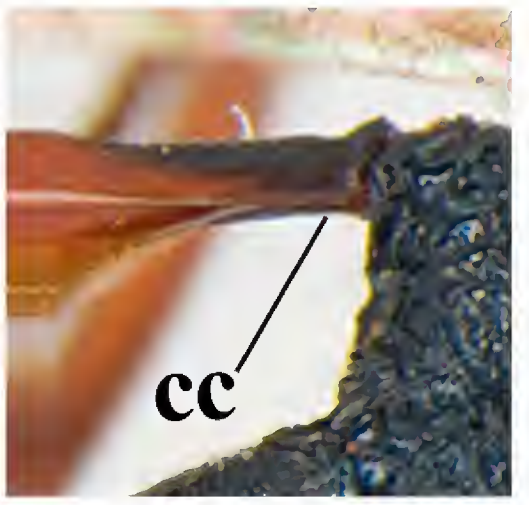

3 Lateroventral margin of pronotum with one tooth-like process (see first couplet) 4

– Lateroventral margin of pronotum with two tooth-like processes (**aa**) ..... *P. compressus* (Spinola, 1808)

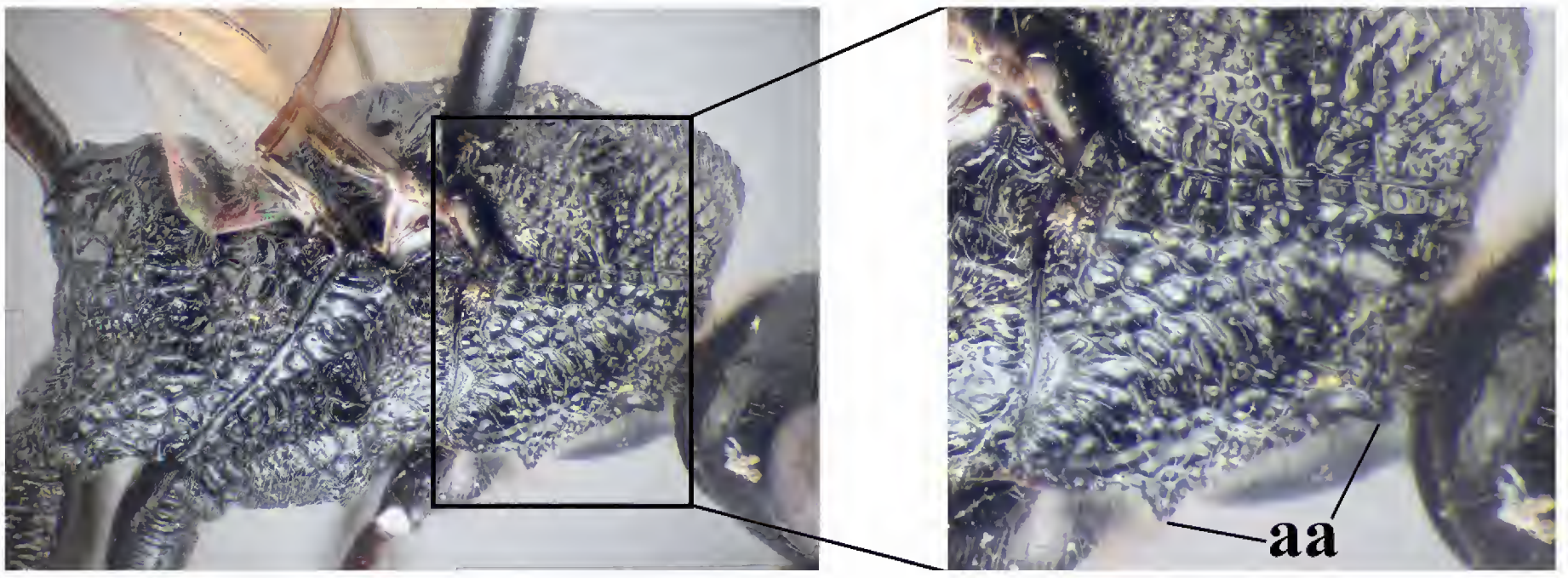

4 Large sized species (body length, excluding ovipositor, 16.5–18.5 mm); occipital carina rim-like, blackish, 0.2× diameter of an ocellus (**a**); hind basitarsus weakly but distinctly curved, 1.5× longer than tarsomeres 2–5 (**b**); ovipositor 1.4× fore wing length ..... *P. mourguesi* Maneval, 1935

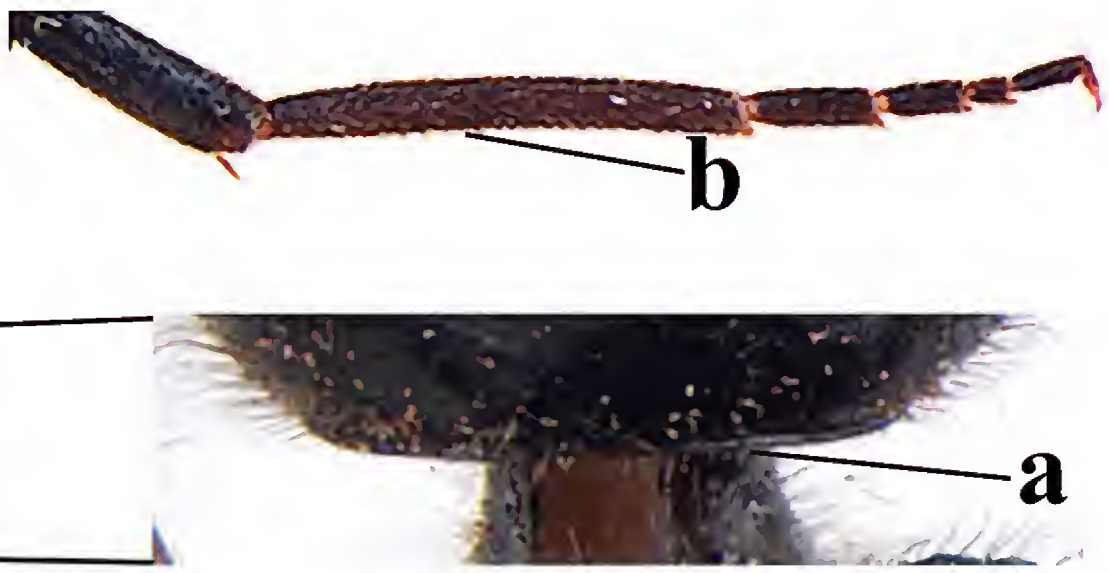

– Medium sized species (body length, excluding ovipositor, 8.0–11.5 mm); occipital carina cerciniform, brownish, 0.5× diameter of an ocellus (**aa**); hind basitarsus straight, 1.1× longer than tarsomeres 2–5 (**bb**); ovipositor 1.2× fore wing length ..... *P. galitae* (Gribodo, 1879)

Family Aulacidae Shuckard, 1842

***Pristaulacus* Kieffer, 1900**

***Pristaulacus barbeyi* (Ferrière, 1933) #**

Odontaulacus barbeyi Ferrière, 1933: 141, Holotype ♀ and paratype ♂. — Algeria, Babor (MNHN).

Distribution. Algeria, Greece, Morocco, Spain, Turkey (Turrisi 2007) and Iran (Ghahari 2012; Turrisi 2013a, b, c).

Distribution in Iran. West Azarbaijan province (Ghahari 2012: DU).

Diagnosis. *P. barbeyi* is a small to medium-sized species, with body length (excluding ovipositor) of 6.7–11.8 mm, fore wing length 5.1–8.1 mm; ovipositor length 1.3× fore wing length (holotype), but variable length among specimens from Turkey. It is readily distinguished by the shape of the head with a very narrow cerciniform occipital carina (width less than 0.2× ocellus diameter), rounded latero-ventral margin of pronotum without tooth-like processes, tarsal claw bearing two tooth-like processes along the inner margin, and a short and stocky petiole.

Hosts. Ghahari (2012) mentioned an unknown Buprestidae as host of this species in Iran, living on *Abies*.

Pristaulacus compressus* (Spinola, 1808) *

Figs 2, 3, 4

Aulacus compressus Spinola, 1808: 48, Holotype ♂. — Italy, Liguria, Habitat in montibus Orerii (MCSN).

Specimens examined. 2♀, DPPZ. Iran, Kermanshah province, Dudan, 35°01′00″N, 46°11′32″E, 1155m, 20.VI.2016, Malaise trap no. 2 mounted in orchard, leg.: M. Zardouei Heidari; 1♀, DPPZ. Iran, Kermanshah province, Harsin, 34°16’18.89”N, 47°36’16.63”E, 1568 m, 05.VII.2016, Malaise trap no. 1 mounted in orchard, leg.: M. Zardouei Heidari.

Distribution. Austria, Bulgaria, Czech Republic, France, Germany, Greece, Hungary, Iran, Iraq, Italy, Lebanon, Morocco, Poland, Romania, Russia (western territories), Slovakia, Spain, Switzerland, Turkey, Ukraine and former Yugoslavia (Madl 1990, Turrisi 2007, 2011, 2013a).

Distribution in Iran. Shiraz (Madl 1990: 114, NHMW), East-Azarbaijan (Lotfalizadeh et al. 2017: DU), and Kermanshah province (**new record**).

Diagnosis. It is a medium sized species with a body length of 8.8–14.2 mm (excluding ovipositor), fore wing length 6.6–9.5 mm. It is readily distinguished by having a wide occipital carina (width equal to ocellus diameter), a pair of tooth-like processes on each latero-ventral margin of pronotum, reddish-orange hind tarsus, and ovipositor length 1.1–1.3× fore wing length.

Morphometric ratios. ClOL/ClL: 1.10; ClL/ClW: 3.33; ClW/OML: 0.69; CoL/CoW: 2.61; EL/EW: 2.42; EL/OML: 2.90; EW/OOCL: 0.40; EW/OTL: 1.21; FWL/FWW: 3.10; HL/ClL: 4.04; HL/TL: 2.07; HW/EW: 9.48; HW/HL: 1.21; IOL/ClOL: 1.36; IOL/EW: 2.91; IOL/HW: 0.30; IOL/OML: 3.48; MsL/MsW: 2.18; MtL/MtW: 2.57; PEL/PEW: 1.90; PL/PW: 0.67; POL/OD: 1.46; POL/OOL: 1.00; SL/SW: 2.89; TL/EL: 1.55.

Hosts. This species was reared from *Chlorophorus adelii* Holzschuh, 1974 (Coleoptera, Cerambycidae) in tree oak, *Quercus* sp. (Madl 1990, Wall 1994). The reared beetle is polyphagous on deciduous trees and is endemic to Iran (Holzschuh 1974).

Remarks. The distribution of this species covers mainly the European area (see Turrisi 2011). It shows some

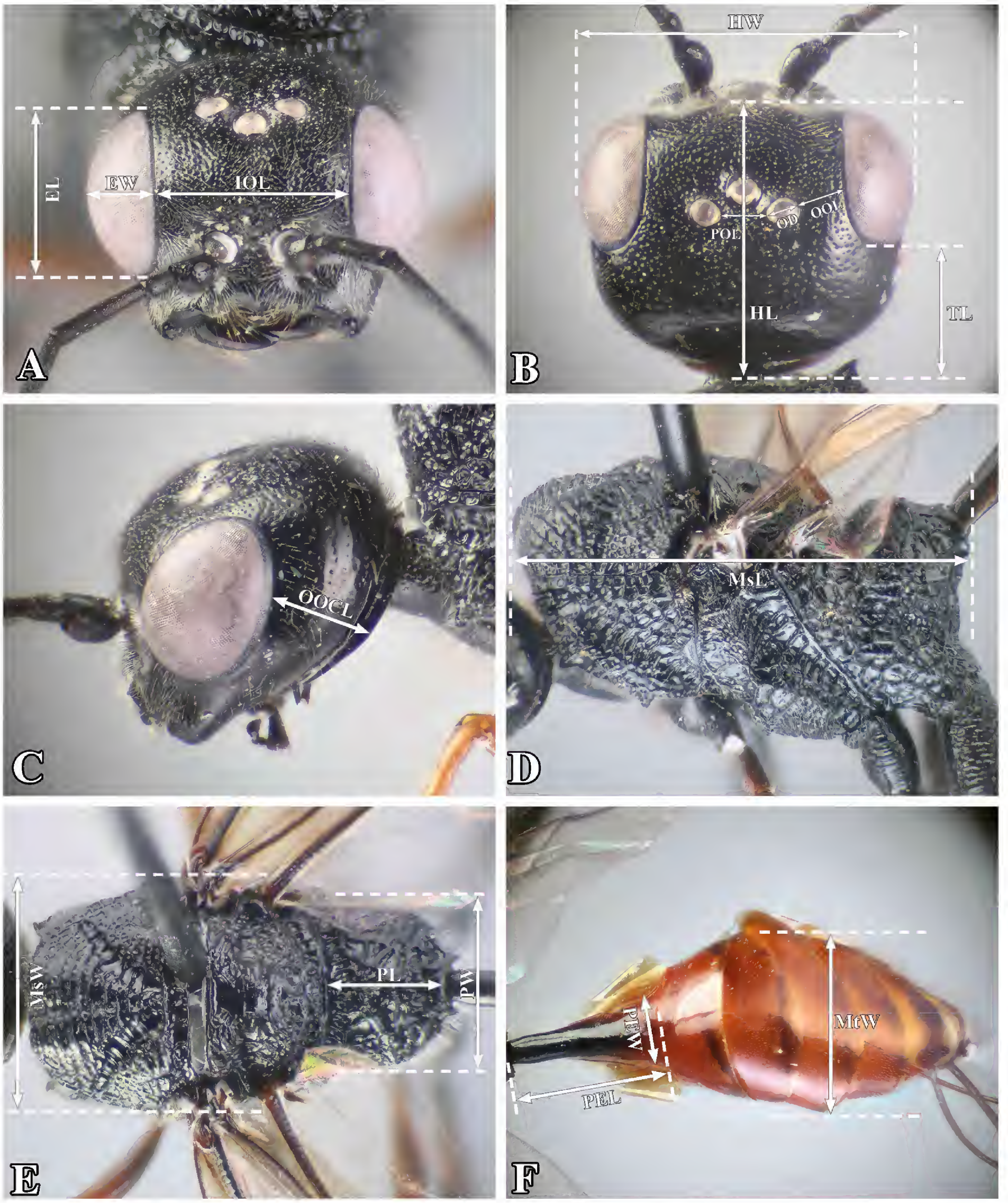

Figure 2. *Pristaulacus compressus* Spinola 1808. female (Iran): **A** face, frontal view; **B** head, dorsal view; **C** head, lateral view; **D** mesosoma, lateral view; **E** mesosoma, dorsal view; **F** petiole and metasoma, dorsal view.

intraspecific variation in colour and sculpture of some parts of the body (Turrisi 2007). The most similar species is *P. lindae* Turrisi, 2000, having hind tarsi blackish brown, metasoma more extensively red orange, different shape of mesosoma, sculpture of prescutum carinulate rugulose, a longer petiole and ovipositor (see Turrisi (2007, 2011 for more details). The head bears a coarser punctuation than European specimens of *P. compressus* and *P. lindae*, but less so than the other two similar species *P. samai* Turrisi, 2011 and *P. rapuzzii* Turrisi, 2011.

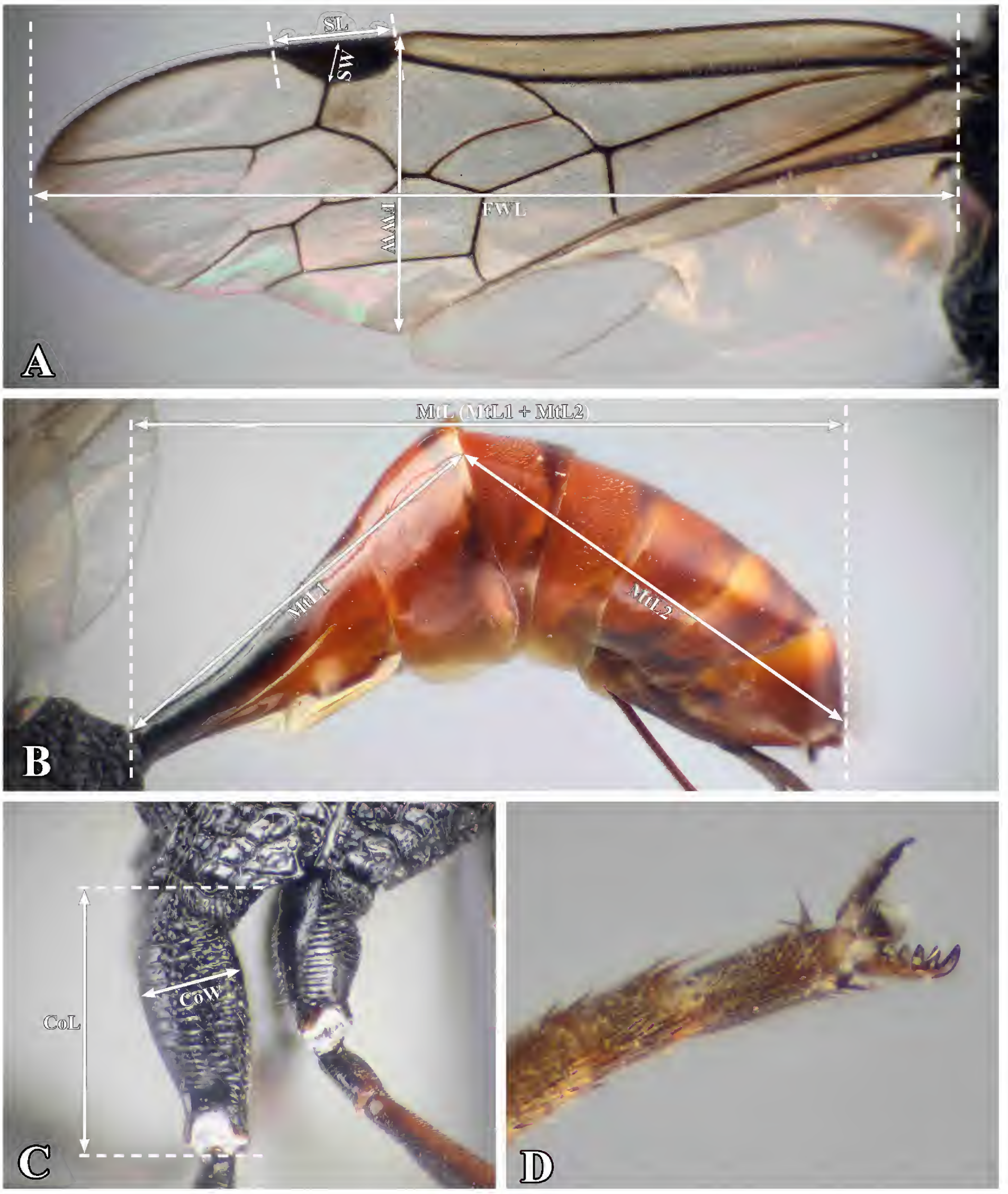

Figure 3. *Pristaulacus compressus* Spinola 1808. female (Iran): **A** fore and hind wing; **B** petiole and metasoma, lateral view; **C** hind coxa, lateral view; **D** hind claw, ventral view.

Pristaulacus galitae (Gribodo, 1879)

Aulacus galitae Gribodo, 1879: 339, Holotype ♀. — Tunisia, Galita Island (CPTO).

Distribution. Algeria, Austria, Bulgaria, Canary Islands (Tenerife), Croatia, Cyprus, Czech Republic, France, Germany, Greece (including Crete and Rhodos), Hungary, Iran, Italy (including Sardinia and Sicily), Morocco, Poland, Romania, Russia (westernmost area), Slovakia, Spain, Tunisia (including Galita Island), Turkey, Ukraine and former Yugoslavia (Turrisi 2007, 2013a, Ghahari 2012, Huflejt and Wiśniowski 2012).

Distribution in Iran. East Azarbaijan province (Ghahari 2012: DU).

Figure 4. *Pristaulacus compressus* Spinola 1808. female (Iran): lateral habitus.

Diagnosis. *P. galitae* is a medium-sized species with a body length of 8.0–11.2 mm (excluding ovipositor), fore wing length 4.5–7.8 mm. It is distinguished by the combination of the following features: shape of the head, with rounded profile of temple, occipital carina moderately wide (0.5× OD), one anterior tooth-like process on each side of latero-ventral margin of pronotum, ovipositor length 1.0–1.2× fore wing length.

Hosts. Ghahari (2012) mentioned specimens reared in Iran from *Trichoferus griseus* # (Fabricius, 1792) (Coleoptera, Cerambycidae) feeding on common fig, *Ficus carica* L. (Moraceae).

Pristaulacus gloriator (Fabricius, 1804)

Bassus gloriator Fabricius, 1804: 99, Holotype ♀. — Germany, Habitat in Germ. Dom. Smidt (ZMUC).

Distribution. Albania, Austria, Czech Republic, Germany, Greece, Hungary, Iran, Italy, Poland, Romania, Russia (European and central areas), Slovakia, Turkey, former Yugoslavia (Turrisi 2007, 2013a, Huflejt and Wiśniowski 2012).

Distribution in Iran. Guilan province (Madl 1990: 114–115, NHMW; Turrisi 2007).

Diagnosis. *P. gloriator* is a medium to moderately large-sized species with a body length of 10.2–15.0 mm (excluding ovipositor), fore wing length 8.2–11.8 mm. It can be easily identified by the shape of the head with a narrow cerciniform occipital carina (width 0.2× OD), a rugulose-carinulate frons, latero-ventral margin of pronotum rounded without tooth-like processes, four tooth-like processes on the inner margin of tarsal claw, and light yellow tarsi.

Hosts. This species was reared from *Paraclytus reitteri* (Ganglbauer, 1881) (Coleoptera, Cerambycidae) feeding on alder, *Alnus* sp. The reared beetle is polyphagous in deciduous trees i.e. *Acer*, *Alnus*, *Carpinus* and *Quercus* (Miroshnikov 2014).

Remarks. This species was previously recorded as *P. holzschuhi* Madl, 1990 from Bandar-e Pahlavi (now called: Bandar-e Anzali - Anzali Port), Assalem, Guilan, Iran (Madl 1990), and is considered as a synonym of *P. gloriator* (Turrisi 2007) (type material examined and deposited in NHMW).

Pristaulacus mourguesi Maneval, 1935 *

Figs 5, 6, 7

Pristaulacus mourguesi Maneval, 1935: 66, Holotype ♀. — France, Pont-Ravatgers (MNHN).

Specimens examined. 2♀, DPPZ. Iran, Kermanshah province, Dudan, 35°01′00″N, 46°11′32″E, 1155m, 20.II.2016, BM-MTF-TS mounted in orchard, leg.: M. Zardouei Heidari; 1♀, DPPZ. same locality label, 05.VI.2016, BM-MTF-TS mounted among Oak forest - *Quercus brantii* Lindley, leg.: M. Zardouei Heidari.

Distribution. Croatia, France, Greece, Hungary (Turrisi 2007, 2013a), Iran (**new record**).

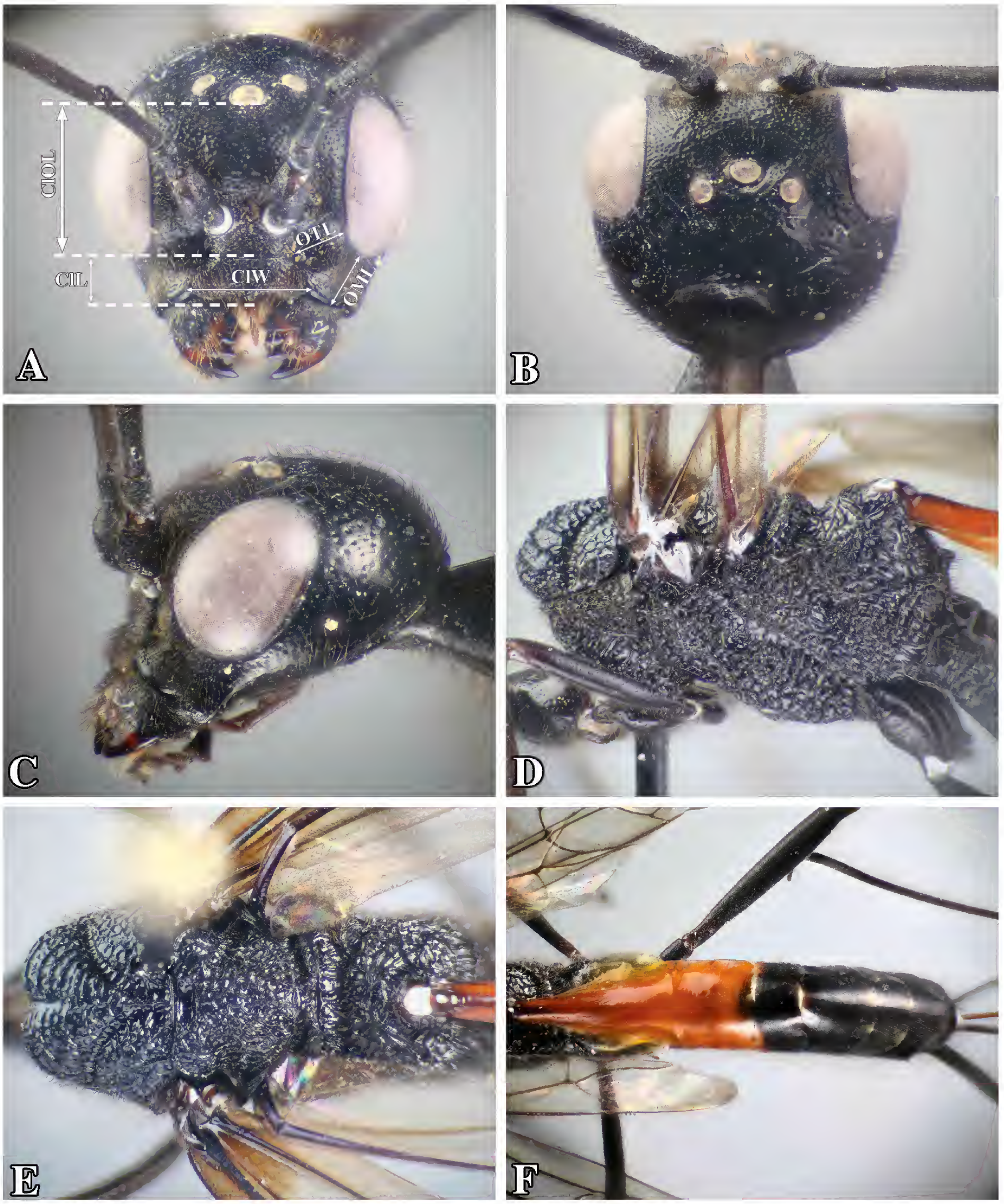

Figure 5. *Pristaulacus mourguesi* Maneval, 1935. female (Iran): **A** face, frontal view; **B** head, dorsal view; **C** head, lateral view; **D** mesosoma, lateral view; **E** mesosoma, dorsal view; **F** petiole and metasoma, dorsal view.

Distribution in Iran. Kermanshah province.

Diagnosis. *P. mourguesi* is one of the largest species among the Palaearctic *Pristaulacus* with a body length varying from 16.5 to 18.5 mm (excluding ovipositor), and fore wing length of 8.8–13.0 mm (♀). It is distinguished by the shape of the head, narrow cerciniform occipital carina (width 0.2× ocellus diameter), hind basitarsus long and slightly curved, 1.5× length of tarsomeres 2-5, and long ovipositor, 1.4–1.6× fore wing length.

Morphometric ratios. CIOL/CIL: 1.21; CIL/CIW: 2.75; CIW/OML: 0.78; CoL/CoW: 2.71; EL/EW: 2.65; EL/OML: 2.72; EW/OOCL: 0.58; EW/OTL: 1.14; FWL/

Figure 6. *Pristaulacus mourguesi* Maneval, 1935. female (Iran): **A** fore and hind wing; **B** petiole and metasoma, lateral view; **C** hind coxa, lateral view; **D** hind claw, ventral view.

FWW: 3.02; HL/ClL: 2.01; HL/TL: 1.97; HW/EW: 5.40; HW/HL: 1.27; IOL/CIOL: 1.27; IOL/EW: 3.26; IOL/HW: 0.60; IOL/OML: 3.35; MsL/MsW: 1.91; MtL/MtW: 6.39; PEL/PEW: 2.39; PL/PW: 0.55; POL/OD: 2.08; POL/OOL: 1.33; SL/SW: 2.62; TL/EL: 0.80.

Hosts. Unknown (Turrisi 2007).

Remarks. This species was previously recorded only from Europe (Turrisi 2007, 2013a). There is a possible record for the Near East without source material (Madl 2012). The closest species is *P. morawitzi* (Semenow, 1892) being medium sized, punctures of head very fine, superficial, and scattered, metasoma pyriform, strongly compressed, nearly entirely reddish orange. See Turrisi (2007) for more details.

Figure 7. *Pristaulacus mourguesi* Maneval, 1935. female (Iran): lateral habitus.

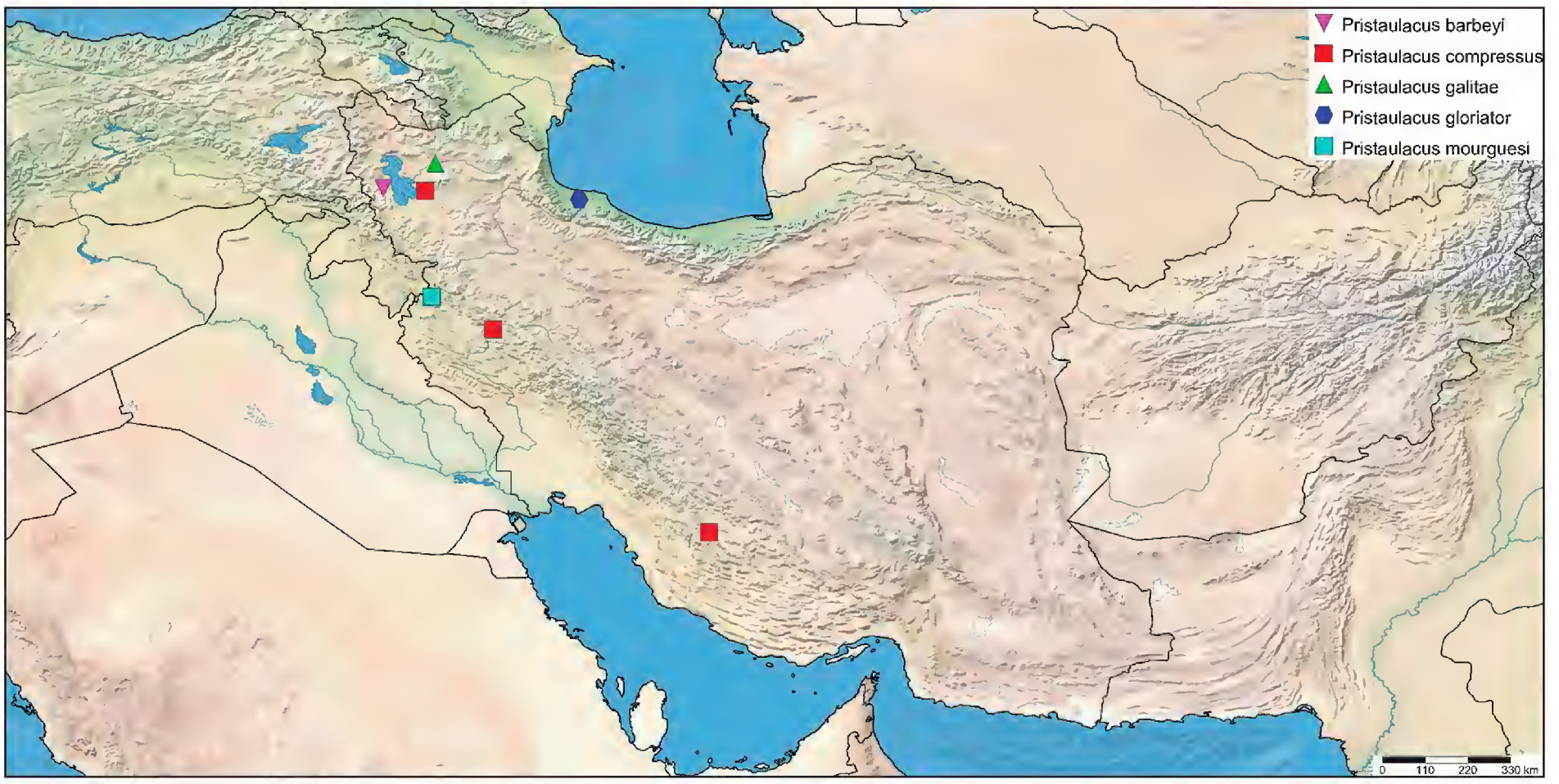

Figure 8. Distribution map of aulacid species in some provinces of Iran.

Discussion

The number of Iranian Aulacidae is raised to five, all within a single genus (*Pristaulacus*). All these species have been collected in Northern and Northwestern (forest habitat) regions, except *P. compressus*, which is recorded from Southern (subdesertic habitat) region.

Jennings et al. (2004) stated that remnant stands of forest are an ideal habitat for their wood-boring hosts. These wasps can be locally abundant in areas undergoing log-

ging or forest fires. The rich fossil record of Aulacidae indicates they were quite abundant in the Mesozoic (Jennings and Austin 2004, Turrisi et al. 2009).

The new specimens have been collected in Zagros forests, which have an area of about 6 million hectares (3.5 percent of Iran), located in the west of Iran with a semi-arid to temperate climate. This wide territory is also referred to as western oak forests (oak-woodland), due to the dominancy of oak species (*Quercus* spp.). The species composition of the woodland vegetation depends on the climatic conditions (Zohary 1973, Kwandrans 2007).

The five species reported in this paper are distributed only in the Western part of the Palearctic region. The results of the present study clearly show the improved efficiency of modern collecting methods for Hymenoptera that are rarely collected with most conventional methods. In addition, the best collecting period seems to be June and this is consistent with those reported in Lotfalizadeh et al. (2017).

Although the research suggests a higher number of species in the Western territories of Iran we predict that the Eastern and Southern parts should also be quite species-rich. Further investigation, especially in poorly collected regions will probably increase the number of known species (Turrisi 2014). The species reported from Iran have ranges included in the Western part of the Palaearctic region. Given the poorly known faunistic situation, it is premature to discuss possible relationships among faunas of Iran and adjacent territories.

Acknowledgements

We are indebted to Ms. Maryam Zardouei Heidari (University of Zabol, Iran) for collecting the specimens and Mr. Amir Nabizadeh Sarabandi (University of Birjand, Iran) for his suggestion and advice on photographing. The authors also express their deep gratitude to Ehsan Rakhshani (University of Zabol, Iran) who offered constructive comments that significantly improved the manuscript. The Museum für Naturkunde Berlin kindly waived the author's fees for this manuscript. The authors thank the anonymous reviewers and the editor for the helpful comments on the manuscript.

References

van Achterberg C (2009) Can Townes type Malaise traps be improved? Some recent developments. Entomologische Berichten 69(4): 129–135.

Benoit PLG (1984) Aulacidae, famille nouvelle pour la faune de l'Afrique tropicale (Hymenoptera). Revue de Zoologie Africaine 98(4): 799–803.

Chen H-Y, Turrisi GF, Xu Z-f (2016) A revision of the Chinese Aulacidae (Hymenoptera, Evanioidea). ZooKeys 587: 77-124. https://doi.org/10.3897/zookeys.587.7207

Crosskey RW (1951) The morphology, taxonomy, and biology of the British Evanioidea (Hymenoptera). Transactions of the Royal Entomological Society London 102(5): 247–301. https://doi.org/10.1111/j.1365-2311.1951.tb00749.x

Fabricius JC (1792) Determinatio generis Ips affiniumque. Actes de la Société d'Histoire Naturelle de Paris 1: 27–35.

Fabricius JC (1804) Systema Piezatorum, Secundum Ordines, Genera, Species, Adiectis Synonymis, Loci, Observationibus, Descriptionibus. Brungsvigae, 440 pp.

Ferrière C (1933) Un nouvel Aulacidae Nord-africain (Hym.). Bulletin de la Société Entomologique de France 38: 140–143.

Ganglbauer L (1881) Bestimmungs-Tabellen der europaischen Coleopteran, IVa. Oedemeridae. Verhandlungen der Kaiserlich-Koniglichen Zoologisch-Botanischen Gesellschaft in Wien 31: 97–116.

Ghafouri Moghaddam M, Rakhshani E, Mokhtari A (2017) An upgrade pinning block: a mechanical practical aid for fast labelling of the insect specimens. Biodiversity Data Journal 5: e20648. https://doi.org/10.3897/BDJ.5.e20648

Ghafouri Moghaddam M, Ghafouri Moghaddam M, Rakhshani E, Mokhtari A (2017) An Upgrade Pinning Block: A Mechanical Practical Aid for Fast Labelling of the Insect Specimens. Biodiversity Data Journal 5: e20648. https://doi.org/10.3897/BDJ.5.e20648

Ghahari H (2012) Two new records of Aulacidae (Hymenoptera: Evanioidea) from Iran. Entomofauna 33: 273–278.

Ghahari H, Madl M (2017) An annotated catalogue of Iranian Aulacidae, Evaniidae and Gasteruptiidae (Hymenoptera: Evanioidea). Zootaxa 4338(2): 341–353. https://doi.org/10.11646/zootaxa.4338.2.8

Gribodo G (1879) Note imenotterologiche. Annali del Museo di Storia Naturale di Genova 14: 325–347.

Harris RA (1979) A glossary of surface sculpturing. Occasional Papers in Entomology 28: 1–31.

Holzschuh C (1974) Neue bockkäfer aus Pakistan, Iran, Anatolien und Mazedonien (Coleoptera: Cerambycidae). Zeitschrift der Arbeitsgemeinschaft Österreichischer Entomologen 25(3/4): 81–100. [In German]

Huber JT, Sharkey MJ (1993) Structure. In: Goulet H, Huber JT (Eds) Hymenoptera of the world: an identification guide to families. Agriculture Canada Research Branch, Monograph No. 1894E, Ottawa, Canada, 13–59.

Huflejt T, Wiśniowski B (2012) Materiały do znajomości krajowej fauny błonkówekz rodziny pokosowatych (Hymenoptera, Aulacidae). Nowy Pam Fizjogr 7(1–2): 25–34.

Jennings JT, Austin AD (2000) Higher-level phylogeny of the Aulacidae and Gasteruptiidae (Hymenoptera: Evanioidea). Hymenoptera: evolution, biodiversity and biological control. CSIRO Publishing, Collingwood, Australia, 154–164.

Jennings JT, Austin AD (2004) Biology and host relationships of aulacid and gasteruptiid wasps (Hymenoptera: Evanioidea): a review. In Rajmohana K, Sudheer K, Girish Kumar P, Santhosh S (Eds) Perspectives on Biosystematics and Biodiversity. (University of Calicut, Kerala, India): 187–215.

Jennings JT, Austin AD, Stevens NB (2004) First record of Aulacidae (Hymenoptera: Evanioidea) from New Caledonia with descriptions of three new species of *Aulacus* Jurine. Austral Entomology 43 (4): 346–352. https://doi.org/10.1111/j.1440-6055.2004.00418.x

Jurine L (1807) Nouvelle méthode de classer les hyménoptères et les diptères. Paschoud. Volume 1: 320 pp.

Kieffer JJ (1900) Note sur le genre *Pristaulacus* Kieff. (Hymén.). Bulletin de la Société entomologique de France 338–339.

Kwandrans J (2007) Diversity and ecology of benthic diatom communities in relation to acidity, acidification and recovery of lakes and rivers. Diatom Monographs 9: 1–169.

Lotfalizadeh H, Masudi-Rad S, Mehrvar A (2017) Review of the superfamily Evanioidea (Hymenoptera) in Iran with four new records. Journal of Insect Biodiversity and Systematics 3(2): 141–151.

Madl M (1990) Über Aulacidae vom Iran (Hymenoptera, Evanioidea). Nachrichtenblatt der Bayerischen Entomologen 39(4): 114–116.

Madl M (2012) Fauna Europaea: Aulacidae. In Mitroiu MD, Madl M, Noyes J (ed) Fauna Europaea: Hymenoptera. by Fauna Europaea version 2.5, http://www.faunaeur.org [accessed 21 July, 2017]

Maneval H (1935) Observations sur des Hyménoptères de la faune Francaise et description d'une espèce nouvelle. Revue Française d'Entomologie 2: 65–76.

Miroshnikov A (2014) In: Konstantinov AS, Ślipiński SA, Solodovnikov Ayu. (Eds) Advances in studies on Asian cerambycids (Coleoptera: Cerambycidae). KMK Scientific Press Ltd., Krasnodar, Moscow, 51–71.

Rohlf FJ (2006) tpsDig. Ver. 2.05. Stony Brook, NY, Department of Ecology and Evolution, State University of New York.

Semenow A (1892) Revisio Hymenopterorum Musei Zoologici Academiae Caesareae Scientiarum Petropolitanae. III. Familia Evaniidae. Bulletin des l'Académie Impériale des Sciences de St.-Pétersbourg, Nouvelle Serie 3, 35: 9–30.

Shorthouse DP (2010) SimpleMappr, an online tool to produce publication-quality point maps. [On Line]. Available from http://www.simplemappr.net [accessed on 19 September 2017]

Shuckard WE (1842) On the Aulacidae etc. The Entomologist, conducted by Edward Newmann, London.

Spinola M (1808) Insectorum Liguriae Species Novae aut Rariores quas in Agro Ligustico Nuper Detexit, Descripsit, et Iconibus Illustravit. Genuae, 262 pp.

Turrisi GF (2000) Gli Aulacidae di Sicilia, con descrizione di *Pristaulacus lindae* n. sp. (Hymenoptera Evanioidea). Bollettino della Società entomologica italiana 132 (3): 259–268.

Turrisi GF (2007) Revision of the Palaearctic species of *Pristaulacus* Kieffer, 1900 (Hymenoptera: Aulacidae). Zoota xa 1433: 1–76.

Turrisi GF (2011) Systematic revision of the sibling species belonging to the *Pristaulacus compressus* group (Hymenoptera: Aulacidae). Insect Systematics & Evolution 42: 1–27. https://doi.org/10.1163/187631211X545132

Turrisi GF (2013a) Review of Aulacidae (Hymenoptera: Evanioidea) from Greece and Cyprus with new records. Entomologia Hellenica 22: 1–9.

Turrisi GF (2013b) *Pristaulacus barbeyi* (Ferrière, 1933), new to Iberian Peninsula (Hymenoptera Aulacidae). Bollettino della Società Entomologica Italiana 145(3): 99–102. https://doi.org/10.4081/BollettinoSEI.2013.99

Turrisi GF (2013c) Addenda - *Pristaulacus barbeyi* (Ferrière, 1933), new to Iberian Peninsula (Hymenoptera Aulacidae). Bollettino della Società Entomologica Italiana 145(3): 99–102. https://doi.org/10.4081/BollettinoSEI.2013.99

Turrisi GF (2014) A new species of *Pristaulacus* Kieffer, 1900 from Laos (Hymenoptera: Aulacidae). Natura Somogyiensis 24: 165–172.

Turrisi GF (2017) The parasitoid wasp family Aulacidae with a revised World checklist (Hymenoptera, Evanioidea). Proceedings of the Entomological Society of Washington 119(sp1): 931–939. https://doi.org/10.4289/0013-8797.119.SpecialIssue.931

Turrisi GF, Jennings JT, Vilhelmsen L (2009) Phylogeny and generic concepts in the parasitoid wasp family Aulacidae (Hymenoptera: Evanioidea). Invertebrate Systematics 23: 27–59. https://doi.org/10.1071/IS08031

Turrisi GF, Nobile V (2016) Description of *Pristaulacus leleji* sp. n. (Hymenoptera: Aulacidae) from Thailand. Evraziatskii Entomologicheskii Zhurnal 15: 152–155.

Wall I (1994) Seltene Hymenopteren aus Mittel-, West-und Sudeuropa (Hymenoptera Apocrita: Stephanoidea, Evanioidea, Trigonalyoidea). Entomofauna 15(14): 137–184.

Yu DSK, van Achterberg C, Horstmann K (2012) Taxapad 2012, Ichneumonoidea 2011. Database on flash-drive. Ottawa, Ontario, Canada. http://www.taxapad.com [accessed 17 september 2017]

Zhang JF, Rasnitsyn AP (2004) Minute members of Baissinae (Insecta: Hymenoptera: Gasteruptiidae) from the Upper Mesozoic of China and limits of the genus *Manlaya* Rasnitsyn, 1980. Cretaceous Research 25(6): 797–805. https://doi.org/10.1016/j.cretres.2004.08.001

Zhang HC, Zheng DR, Zhang Q, Jarzembowski EA, Ding M (2013) Re-description and systematics of Paraulacus sinicus Ping, 1928 (Insecta, Hymenoptera). Palaeoworld 22 (1–2): 32–35. https://doi.org/10.1016/j.palwor.2013.02.001

Zohary M (1973) Geobotanical Foundations of the Middle East, 2 volumes, Fischer, Stuttgart, Amsterdam.

Zoosyst. Evol. 94(1) 2018, 109–135 | DOI 10.3897/zse.94.14698

PENSOFT

museum für naturkunde

Resurrection and re-description of *Plethodontohyla laevis* (Boettger, 1913) and transfer of *Rhombophryne alluaudi* (Mocquard, 1901) to the genus *Plethodontohyla* (Amphibia, Microhylidae, Cophylinae)

Adriana Bellati[1,*], Mark D. Scherz[2,*], Steven Megson[3], Sam Hyde Roberts[4], Franco Andreone[5], Gonçalo M. Rosa[6,7,8], Jean Noël[9], Jasmin E. Randrianirina[10], Mauro Fasola[1], Frank Glaw[2], Angelica Crottini[11]

1 *Dipartimento di Scienze della Terra e dell'Ambiente, Università di Pavia, Via Ferrata 1, I-27100 Pavia, Italy*
2 *Zoologische Staatssammlung München (ZSM-SNSB), Münchhausenstr. 21, 81247 München, Germany*
3 *School of Science and the Environment, Manchester Metropolitan University, Manchester, M1 5GD, UK*
4 *SEED Madagascar, Studio 7, 1A Beethoven Street, London, W10 4LG, UK*
5 *Museo Regionale di Scienze Naturali, Sezione di Zoologia, Via G. Giolitti, 36, I-10123, Torino, Italy*
6 *Department of Biology, University of Nevada, Reno, Reno NV 89557, USA*
7 *Institute of Zoology, Zoological Society of London, Regent's Park, London, NW1 4RY, UK*
8 *Centre for Ecology, Evolution and Environmental Changes (CE3C), Faculdade de Ciências da Universidade de Lisboa, Bloco C2, Campo Grande, 1749-016 Lisboa, Portugal*
9 *Madagascar Fauna and Flora Group, BP 442, Morafeno, Toamasina 501, Madagascar*
10 *Parc Botanique et Zoologique de Tsimbazaza, BP 4096, Antananarivo 101, Madagascar*
11 *CIBIO, Research Centre in Biodiversity and Genetic Resources, InBIO, Universidade do Porto, Campus Agrário de Vairão, Rua Padre Armando Quintas, Nº 7, 4485-661 Vairão, Portugal*

http://zoobank.org/AFA6C1FE-1627-408B-9684-F6240716C62B

Corresponding author: *Angelica Crottini* (tiliquait@yahoo.it)

Received 26 June 2017
Accepted 19 January 2018
Published 2 February 2018

Academic editor:
Johannes Penner

Key Words

Amphibia
Anura
Phrynocara laeve
Plethodontohyla alluaudi
Madagascar
Integrative taxonomy

Abstract

The systematics of the cophyline microhylid frog genera *Plethodontohyla* and *Rhombophryne* have long been intertwined, and their relationships have only recently started to become clear. While *Rhombophryne* has received a lot of recent taxonomic attention, *Plethodontohyla* has been largely neglected. Our study is a showcase of just how complex the taxonomic situation between these two genera is, and the care that must be taken to resolve taxonomic conundrums where old material, multiple genus transitions, and mis-attribution of new material obfuscate the picture. We assessed the identity of the historic names *Dyscophus alluaudi* (currently in the genus *Rhombophryne*), *Phrynocara laeve* and *Plethodontohyla laevis tsianovohensis* (both synonyms of *Rhombophryne alluaudi*) based on an integrative taxonomic approach harnessing genetics, external morphology, osteological data obtained via micro-Computed Tomography (micro-CT) and bioacoustics. We show that (1) the holotype of *Dyscophus alluaudi* is a member of the genus *Plethodontohyla*; (2) the *Rhombophryne* specimens from central Madagascar currently assigned to *Rhombophryne alluaudi* have no affinity with that species, and are instead an undescribed species; and (3) *Phrynocara laeve* and *Dyscophus alluaudi* are not synonymous, but represent closely related species, whereas *Plethodontohyla laevis tsianovohensis* is tentatively confirmed as synonym of *D. alluaudi*. We resurrect and re-describe *Plethodontohyla laevis*, and re-allocate and re-describe *Plethodontohyla alluaudi* on the basis of new and historic material.

* Both authors contributed equally

Introduction

The microhylid subfamily Cophylinae Cope, 1889, endemic to Madagascar, is today recognised as possessing eight genera according to Scherz et al. (2016a): *Plethodontohyla* Boulenger, 1882, *Rhombophryne* Boettger, 1880, *Stumpffia* Boettger, 1881, *Madecassophryne* Guibé, 1974, *Platypelis* Boulenger, 1882, *Anodonthyla* Müller, 1892, *Cophyla* Boettger, 1880 and *Anilany* Scherz, Vences, Rakotoarison, Andreone, Köhler, Glaw & Crottini, 2016. Recent studies (Vieites et al. 2009, Perl et al. 2014) have provided DNA barcoding reference sequences for almost all described and undescribed frog species of Madagascar and have highlighted the presence of a large taxonomic gap in the Cophylinae, which currently comprises over 100 described species (Scherz et al. 2016a, AmphibiaWeb 2018), but which has an estimated further > 40 species yet to be formally described. In spite of the recent efforts in revising the systematics of this subfamily (e.g. D'Cruze et al. 2010, Glaw et al. 2010, Rakotoarison et al. 2012, 2015, 2017, Rosa et al. 2014, Scherz et al. 2016b, Lambert et al. 2017), the genus *Plethodontohyla* has been relatively neglected.

Plethodontohyla in its most updated definition (Wollenberg et al. 2008, Scherz et al. 2016a) comprises moderately small to large terrestrial or scansorial forest frogs (snout-vent length [SVL] 25–100 mm, Glaw and Vences 2007b). Despite sharing a large number of morphological features (e.g. the presence of connected lateral metatarsalia, vomerine teeth, inner [and sometimes outer] metatarsal tubercles, short hindlimbs and males with a single subgular vocal sac; Scherz et al. 2016a), an osteological circumscription to the genus still remains difficult. The ecomorphologies correlate with different skeletal adaptations; for instance, all semi-arboreal taxa (*P. notosticta*, *P. mihanika*) and three predominantly terrestrial species (*P. guentheri*, *P. inguinalis* and *P. fonetana*) possess expanded terminal phalanges (T- or Y-shaped), while all other terrestrial and fossorial taxa possess knob-shaped terminal phalanges. Whereas the clavicle is always absent or highly reduced in terrestrial or fossorial species, it can be present or absent in arboreal species, suggesting repeated loss of these bones (Scherz et al. 2016a, unpublished data), but also the monophyly of these phenetic groups (arboreal and terrestrial/fossorial) has yet to be established. In addition to being a morphologically diverse genus, *Plethodontohyla* has had an exceptionally convoluted taxonomic history.

Plethodontohyla was originally erected by Boulenger (1882) to contain *Callula notosticta* Günther, 1877 (the type species of the genus), *P. inguinalis* Boulenger, 1882 and *P. brevipes* Boulenger, 1882. This circumscription was before its time in recognizing the phenotypic diversity of *Plethodontohyla*, as Boulenger (1882) established the genus containing terrestrial/fossorial (*P. brevipes*) and arboreal and semi-terrestrial (*P. notosticta*, *P. inguinalis*) species. Peters (1883) later erected two genera, *Phrynocara* Peters, 1883 (type species *Ph. tuberatum* Peters, 1883) and *Mantipus* Peters, 1883 (type species *M. hildebrandti* Peters, 1883), each monotypic. Some years later Mocquard (1895) erected another monotypic genus, *Mantiphrys* Mocquard, 1895 (type species *Mantiphrys laevipes* Mocquard, 1895). Over the 20th century, six more species of the genus *Plethodontohyla* were described, plus two in the genus *Phrynocara* and seven in *Mantipus*. Noble and Parker (1926) synonymised *Mantiphrys* with *Mantipus*, and *Phrynocara* with *Plethodontohyla*, and transferred *P. inguinalis* to *Mantipus*. Guibé contributed repeatedly to the species-level taxonomy of these genera (e.g. Guibé 1947, 1974, 1975), but made only one small change at genus-level, which he later reversed (Guibé 1947, 1952, 1978; see below). Blommers-Schlösser and Blanc (1991) later synonymised *Mantipus* with *Plethodontohyla* in their comprehensive monograph on the amphibians of Madagascar (*Mantipus hildebrandti* becoming a junior synonym of *Plethodontohyla inguinalis*). At this point, the genus *Plethodontohyla* contained twelve nominal species, encompassing a wide range of ecomorphologies (terrestrial, fossorial and semi-arboreal) and sizes, from the 22 mm *P. minuta* to the 100 mm *P. inguinalis*.

Andreone et al. (2005) produced the first comprehensive molecular dataset for the subfamily Cophylinae, where it became clear that several members of the genus *Plethodontohyla* were more closely related to *Rhombophryne testudo* Boettger, 1880—which had, until that point, been alone in the monotypic genus *Rhombophryne*—but refrained from making any taxonomic arrangements until more data were available. Frost et al. (2006) also recovered the paraphyly of *Plethodontohyla* first identified by Andreone et al. (2005), and transferred three species to *Rhombophryne* (*R. alluaudi*, *R. coudreaui* and *R. laevipes*). Based on the more comprehensive molecular analysis of the subfamily (Wollenberg et al. 2008) another four species (*R. minuta*, *R. coronata*, *R. guentherpetersi*, *R. serratopalpebrosa*) were transferred to *Rhombophryne* (Glaw and Vences 2007b). Since then, no more species have moved between these two genera except *R. matavy* which was erroneously transferred to *Plethodontohyla* by Peloso et al. (2016), but returned to *Rhombophryne* by Scherz et al. (2016a).

The taxon *Dyscophus alluaudi* Mocquard, 1901 was originally described with the type locality 'Fort Dauphin' (or Tolagnaro; Fig. 1), but was later transferred to *Plethodontohyla* by Noble and Parker (1926). It was then moved to *Mantipus* by Guibé (1947), but was later returned by him to *Plethodontohyla* without comment (Guibé 1978), presumably based on the similarity of its pectoral girdle to that of *Mantipus angeli* Guibé, 1947, which he synonymised with *Plethodontohyla tuberata* (Guibé 1952). Another taxon, *Phrynocara laeve* Boettger, 1913, was described from Sakana, East Madagascar, a locality reported to be a magnificently preserved piece of jungle (Boettger 1913). This taxon was transferred to *Plethodontohyla* by Noble and Parker (1926), initially with an incorrect emendation (*Plethodontohyla laeve*),

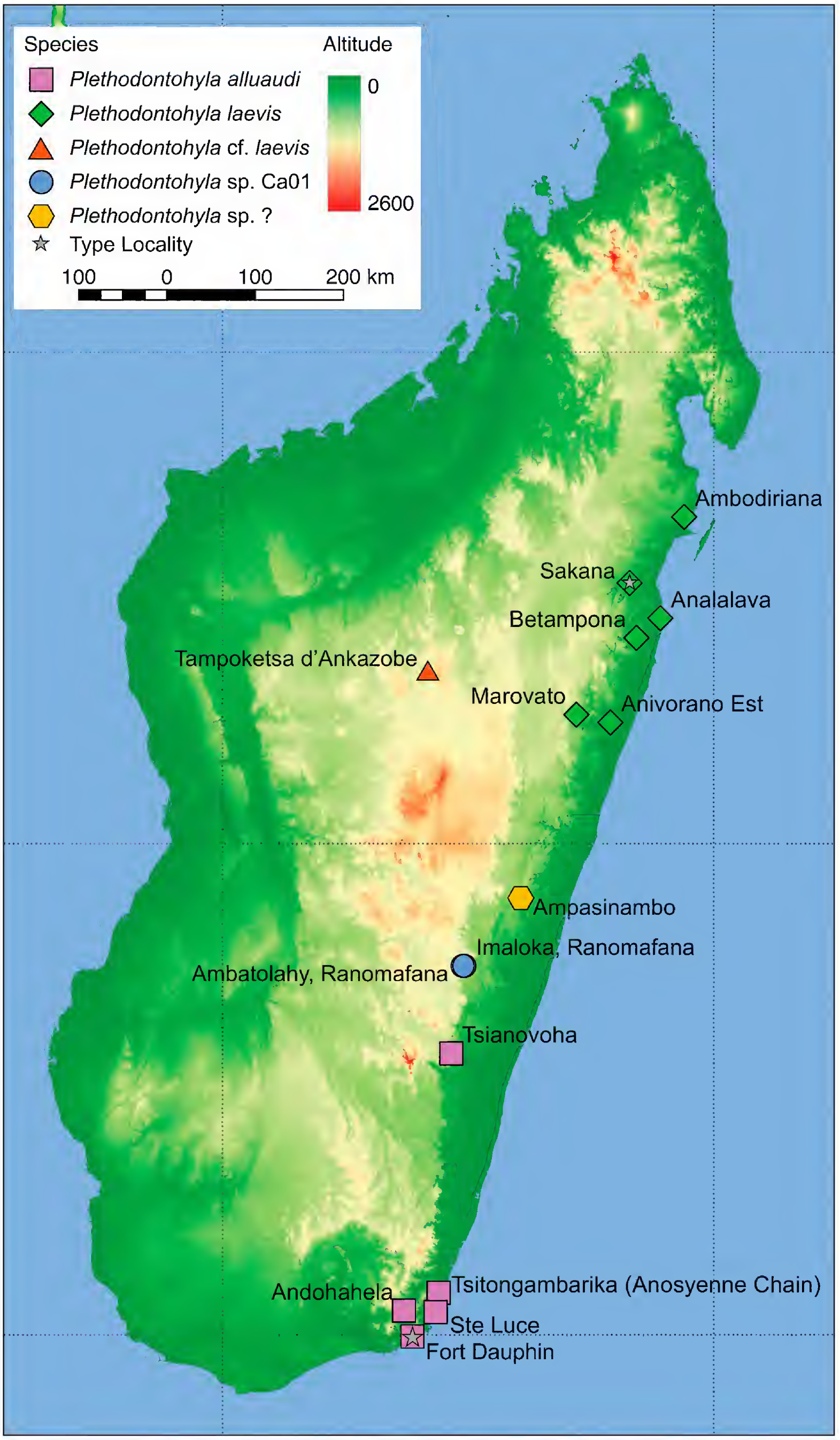

Figure 1. Locality records of *Plethodontohyla laevis*, *P. alluaudi*, and *P.* sp. Ca01, including the uncertain records of two members of this complex (*P.* cf. *laevis* and *P.* sp.) from Blommers-Schlösser (1975).

later corrected to *P. laevis* by Parker (1934). A supposed subspecies of *Plethodontohyla laevis*, *P. l. tsianovohensis* Angel, 1936, was later described from Tsianovoha (approximately 22°07'60.00"S, 047°19'60.00"E; 112 m above sea level [a.s.l.], collected by R. Heim between 1934 and 1935, Fig. 1), a lowland forest in the Vatovavy-Fitovinavy region in eastern Madagascar, but was synonymised with *P. laevis* by Guibé (1978). *Plethodontohyla laevis* was then synonymised with *P. alluaudi* by Blommers-Schlösser and Blanc (1991). Following Blommers-Schlösser (1975), who assigned a specimen collected in Mandraka to *Mantipus alluaudi*, Glaw and Vences (1992), in their first edition of the field guide to the amphibians and reptiles of Madagascar, attributed a specimen of a cophyline frog from Andasibe in central eastern Madagascar also to *P. alluaudi*. Subsequently collected specimens from this region became the genetic reference material for the taxon (Andreone et al. 2005). On the basis of genetic data from these specimens, *P. alluaudi* was transferred to *Rhombophryne* by Frost et al. (2006), where it has since remained.

Recently, individuals of a species of terrestrial cophyline microhylid were found in Betampona Special Reserve (Fig. 1), a small but relatively well-maintained lowland rainforest fragment in eastern Madagascar (Rosa et al. 2012). Genetic analysis revealed these specimens to belong to the genus *Plethodontohyla*, and they were referred to as *P.* sp. Ca3 by Vieites et al. (2009) and Scherz et al. (2016a) (also called *P.* sp. aff. *brevipes* [Ca FJ559294] by Rosa et al. 2012).

In this study, we examined these specimens from Betampona, and found them to have strong affinities with the holotype of *Phrynocara laeve*. This suggested that at least *Phrynocara laeve* was incorrectly attributed to the genus *Rhombophryne*, and prompted questions regarding the genus-level assignment of *Dyscophus alluaudi*. To resolve these questions, we investigated the morphology and osteology of the type material of *Dyscophus alluaudi*, *Phrynocara laeve*, and *Plethodontohyla laevis tsianovohensis* (Fig. 2). We then studied the morphology, osteology and genetics of the *Rhombophryne* species from Andasibe currently assigned to *R. alluaudi*, recently collected material of *P.* sp. Ca3 from Betampona, and of specimens of '*R. alluaudi*' from near Tolagnaro. We base our study on the integration of data from external and internal (osteological) morphology, natural history, congruence between mitochondrial and nuclear DNA differentiation and bioacoustic analyses.

Materials and methods

In anticipation of the main outcomes of our research, we hereafter use *Plethodontohyla laevis* and *P. alluaudi* in reference to these two names, except when discussing the type material, where we refer to the species by their original names (*Phrynocara laeve* and *Dyscophus alluaudi*, respectively).

Voucher specimen collection

New specimens were collected either during the day by searching the leaf litter, or at night using torches and headlamps, sometimes guided by the male advertisement call. Representative voucher specimens were euthanized, and then fixed in 90% ethanol or 10% buffered formalin, rinsed in water and preserved in 70% ethanol. Live colouration was photographed at the time of capture.

Locality information were recorded using a GPS, datum WGS84. Field numbers FAZC, ACZC and ACZCV, FGZC, and PBZT-RJS refer to F. Andreone, A. Crottini, F. Glaw, and J.E. Randrianirina, respectively. Tissue samples (taken before specimen fixation) were obtained from hindlimb muscle or tongue, and preserved separately in 99% ethanol.

Institutional abbreviations used herein are as follows: ZSM = Zoologische Staatssammlung München, Germany; SMF = Naturmuseum Senckenberg in Frankfurt am Main, Germany; UADBA-A = Amphibian collections of the Université d'Antananarivo Département de Biologie Animale, Madagascar (currently Mention Zoologie et Biodiversité Animale, Faculté des Sciences, Université d'Antananarivo, Antananarivo); MRSN = Museo Regionale di Scienze Naturali, Torino, Italy; MNHN = Muséum National d'Histoire Naturelle de Paris, France; ZFMK = Zoologisches Forschungsmuseum Alexander Koenig, Bonn, Germany; ZMA = Zoölogisch Museum Amsterdam (transferred to Naturalis Biodiversity Center in Leiden), Netherlands; BMNH = Natural History Museum, London, United Kingdom.

Morphological measurements

Measurements of preserved specimens were taken by MDS with a calliper to the nearest 0.01 mm, rounded to the nearest 0.1 mm (ratios calculated before rounding to avoid compound rounding errors): SVL (snout-vent length), HW (maximum head width), HL (head length, from the rictus to the snout tip), ED (horizontal eye diameter), END (eye-nostril distance), NSD (nostril-snout tip distance), NND (internarial distance), TD (horizontal tympanum diameter), HAL (hand length, from the radioulnar-carpal articulation to the tip of the longest finger), FORL (forelimb length, given by the sum of HAL, lower arm length [LAL] and upper arm length [UAL]), FOL (foot length, from the tarsal-metatarsal articulations to the tip of the longest toe), TARL (tarsus length), FOTL (foot length including tarsus, given by the sum of FOL and TARL), TIBL (tibia length), HIL (hind-limb length, given by the sum of FOL, TARL, TIBL and thigh length [THIL]), IMCL (maximum length of inner metacarpal tubercle). Examined specimens are listed in Table 1. Note that measurements of *Plethodontohyla brevipes* are from specimens that match the original description of that species in having a uniform brown dorsum and slightly granular dorsal skin. Terminology and description scheme follow Vences et al. (2003), Glaw and Vences (2007a) and Glaw et al. (2007) to allow for better comparison to other *Plethodontohyla* species.

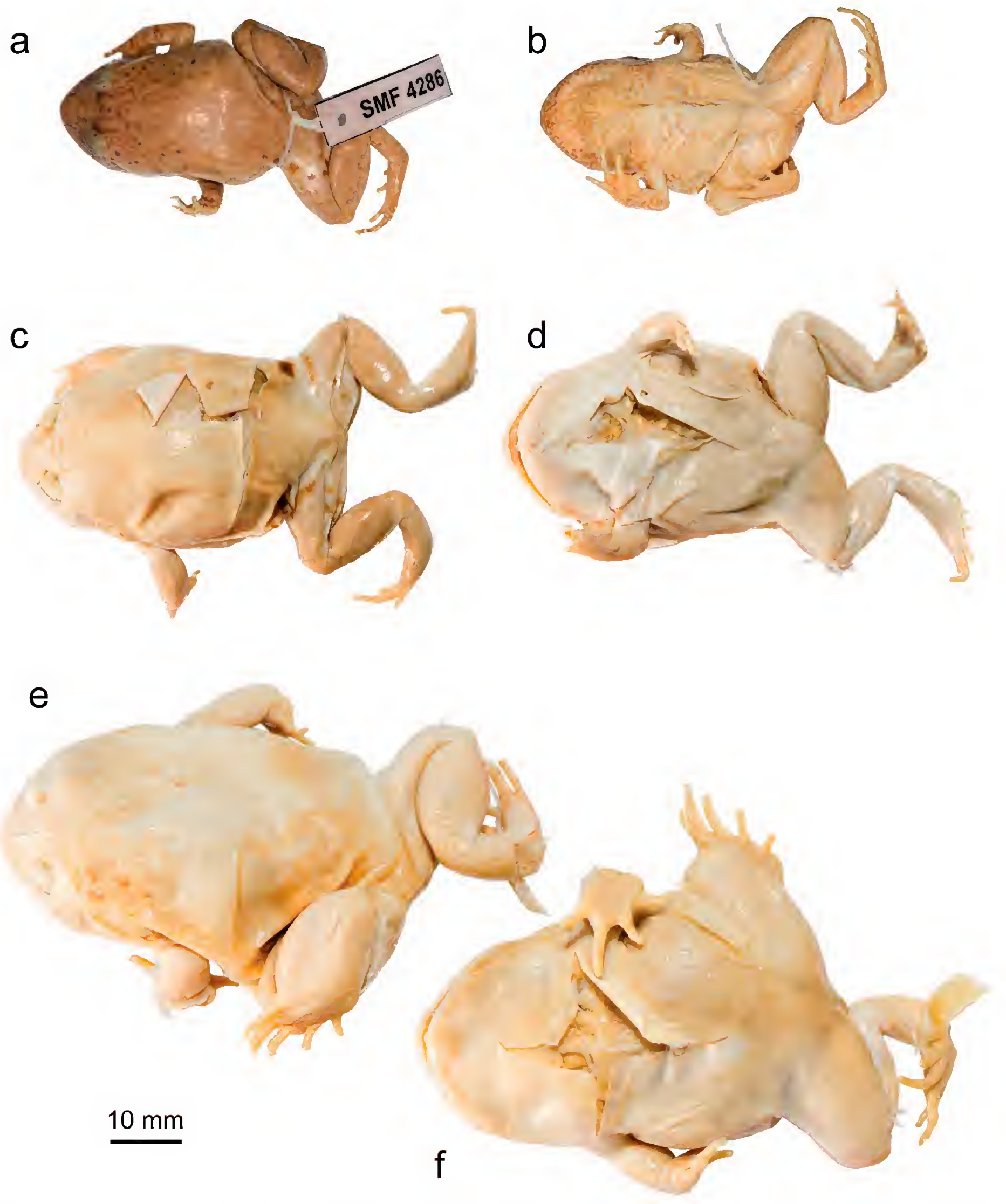

Figure 2. Photographs of the holotypes of (**a–b**) *Phrynocara laeve* (SMF 4286), (**c–d**) *Dyscophus alluaudi* (MNHN 1901.235) and (**e–f**) *Plethodontohyla laevis tsianovohensis* (MNHN 1936.47) in dorsal (**a, c, e**) and ventral (**b, d, f**) view.

Osteological analyses

The holotypes of *Phrynocara laeve* (SMF 4286), *Dyscophus alluaudi* (MNHN 1901.235) and *Plethodontohyla laevis tsianovohensis* (MNHN 1936.47), and one specimen assigned below to *Plethodontohyla laevis* (MRSN A6340) from Betampona, one specimen assigned below to *P. alluaudi* (ZSM 89/2004) from Andohahela and one specimen of the *Rhombophryne* species formerly assigned to *P. alluaudi* by Glaw and Vences (1992) from Andasibe (ZSM 3/2002) were scanned using X-ray micro-Computed Tomography (micro-CT), in a phoenix|x nanotom m cone-beam micro-CT scanner, following protocols used previously

Table 1. Morphological measurements of the holotypes of *Phrynocara laeve*, *Dyscophus alluaudi*, *Plethodontohyla laevis tsianovohensis* and of the recently collected specimens assigned to *P. laevis*, *P. alluaudi*, *P.* sp. Ca01, *P. brevipes* and *Rhombophryne* sp. analysed for this study (all measurements in millimetres except ratios values). For abbreviations, see the measurements section of the Materials and methods. Abbreviations not included in the text: HT, holotype; F, female; M, male; J, juvenile.

Collection Number	Species	Locality	Status	Sex	SVL	HW	HL	HW/HL	ED	ED/HL	END	NSD	NND	TD	TD/ED	HAL	UAL	LAL	HAL/SVL	FORL	FORL/SVL	TIBL	TIBL/SVL	TARL	FOL	FOTL	HIL	HIL/SVL	IMCL
MNHN 1901.235	***Dyscophus alluaudi***	**Fort Dauphin**	**HT**	**F**	**47.4**	**19.8**	**10.7**	**1.85**	**3.7**	**0.35**	**2.7**	**2.1**	**4.5**	**1.9**	**0.53**	**10.8**	**4.5**	**6.9**	**0.23**	**22.2**	**0.47**	**16.0**	**0.34**	**8.9**	**16.2**	**25.1**	**59.2**	**1.25**	**2.7**
MNHN 1936.47	***Plethodontohyla laevis tsianovohensis***	**Forest of Tsianovoha**	**HT**	**F**	**58.0**	**26.8**	**15.7**	**1.71**	**4.2**	**0.27**	**3.3**	**3.0**	**5.5**	**2.5**	**0.58**	**16.0**	**4.5**	**10.2**	**0.28**	**30.8**	**0.53**	**22.6**	**0.39**	**12.6**	**25.0**	**37.6**	**85.4**	**1.47**	**3.3**
UADBA-A 27994	*Plethodontohyla alluaudi*	Andohahela		_	28.8	13.2	7.9	1.67	2.8	0.36	1.9	1.6	2.8	0.9	0.33	7.6	4.1	5.1	0.26	16.8	0.58	11.1	0.39	6.1	12.2	18.4	40.5	1.41	1.5
ZSM 89/2004	*Plethodontohyla alluaudi*	Andohahela		_	29.1	14.5	8.1	1.79	2.6	0.33	2.1	1.4	3.0	1.7	0.66	7.0	3.5	5.2	0.24	15.8	0.54	10.8	0.37	6.1	12.0	18.1	41.2	1.41	1.5
SMF 4286	***Phrynocara laeve***	**Sakana**	**HT**	**F**	**38.1**	**16.5**	**10.5**	**1.56**	**3.8**	**0.36**	**2.5**	**2.1**	**4.2**	**1.5**	**0.40**	**8.8**	**5.1**	**7.3**	**0.23**	**21.2**	**0.56**	**14.8**	**0.39**	**8.6**	**15.9**	**24.5**	**54.5**	**1.43**	**1.9**
ZSM 189/2016	*Plethodontohyla laevis*	Analalava		J	28.1	11.7	8.3	1.41	3.1	0.37	1.8	1.5	2.8	1.2	0.40	6.8	3.5	5.6	0.24	16.0	0.57	11.1	0.40	6.2	12.0	19.4	44.5	1.58	1.4
MRSN A6181	*Plethodontohyla laevis*	Betampona		F	41.5	17.3	10.9	1.59	3.5	0.33	2.6	1.9	4.0	1.2	0.33	9.4	5.6	7.5	0.23	22.5	0.54	15.5	0.37	8.2	11.9	19.3	51.3	1.24	2.1
MRSN A6674	*Plethodontohyla laevis*	Marovato		F	42.2	18.6	10.8	1.72	3.9	0.36	2.9	1.9	3.9	2.0	0.52	10.3	4.6	7.6	0.25	22.5	0.53	16.4	0.39	8.8	15.9	23.3	59.2	1.40	2.0
MRSN A6340	*Plethodontohyla laevis*	Betampona		M	33.0	15.0	8.4	1.79	3.2	0.38	2.5	1.8	3.4	1.4	0.44	7.8	3.3	5.9	0.24	17.1	0.52	13.1	0.40	7.0	13.4	20.8	48.9	1.48	1.7
MRSN A6189	*Plethodontohyla laevis*	Betampona		F	40.9	16.7	10.0	1.68	4.1	0.41	3.0	2.0	3.9	1.4	0.35	8.5	5.6	6.9	0.21	21.0	0.51	15.4	0.38	8.4	14.9	22.3	54.3	1.33	1.7
MRSN A6787	*Plethodontohyla laevis*	Anivorano Est		M	40.3	16.4	10.4	1.58	3.6	0.35	2.2	1.8	3.8	1.6	0.44	8.8	4.2	7.0	0.22	20.0	0.50	14.5	0.36	8.2	14.2	21.6	52.7	1.31	1.8
ZSM 980/2013	*Plethodontohyla laevis*	Betampona		M	36.8	15.8	9.7	1.62	3.7	0.38	2.5	1.8	3.2	1.6	0.44	7.9	4.5	7.0	0.21	19.4	0.53	13.9	0.38	8.1	13.7	21.1	52.1	1.42	2.0
ZSM 855/2006	*P.* sp. Ca01	Ranomafana, Imaloka		F	27.7	12.5	6.9	1.81	2.4	0.35	1.8	1.3	2.6	1.5	0.63	6.4	3.8	4.0	0.23	14.3	0.52	10.8	0.39	5.9	11.6	17.5	40.0	1.44	1.1
ZSM 856/2006	*P.* sp. Ca01	Ranomafana, Imaloka		F	31.9	12.9	7.6	1.70	3.0	0.40	1.8	1.3	2.6	1.6	0.55	6.5	3.6	5.2	0.21	15.3	0.48	11.8	0.37	6.4	12.3	18.7	42.1	1.32	1.4
ZSM 0649/2003	*Plethodontohyla brevipes*	Ranomafana, National Park		_	32.1	12.2	7.9	1.54	2.8	0.35	2.3	1.4	3.0	2.2	0.79	7.2	4.2	5.5	0.22	16.8	0.52	12.2	0.38	6.6	12.6	19.2	44.9	1.40	1.0
ZSM 2605/2007	*Plethodontohyla brevipes*	Ranomafana, Talatakely		_	29.9	12.4	7.2	1.71	2.6	0.36	2.3	1.4	2.7	1.9	0.72	6.8	3.7	5.1	0.23	15.7	0.53	12.2	0.41	6.9	11.8	18.7	42.7	1.43	1.3
ZSM 0851/2006	*Plethodontohyla brevipes*	Ranomafana		M	29.9	11.5	7.5	1.53	2.4	0.33	2.1	1.3	2.6	1.5	0.60	6.9	3.2	5.1	0.23	15.2	0.51	12.4	0.42	6.6	12.2	18.8	43.8	1.46	1.5
ZSM 0853/2006	*Plethodontohyla brevipes*	Ranomafana, Ranomena		_	27.5	11.1	6.9	1.60	2.8	0.41	1.9	1.4	2.7	2.1	0.74	5.7	3.4	4.9	0.21	13.9	0.51	11.3	0.41	6.3	11.4	17.7	40.3	1.47	1.1
ZSM 0854/2006	*Plethodontohyla brevipes*	Ranomafana, Imaloka		_	32.4	13.0	8.0	1.63	2.7	0.34	2.1	1.2	2.7	1.9	0.70	7.0	4.1	4.9	0.22	16.0	0.49	12.2	0.38	6.7	12.1	18.8	43.2	1.34	1.3
ZSM 0852/2006	*Plethodontohyla brevipes*	Ranomafana		M	29.6	11.9	7.1	1.66	2.4	0.34	2.0	1.3	2.6	1.7	0.72	7.1	3.4	5.6	0.24	16.1	0.54	12.5	0.42	6.8	13.4	20.2	45.6	1.54	1.4
ZSM 466/2005	*Rhombophryne* sp.	Andasibe		_	39.9	20.1	11.9	1.70	3.4	0.29	2.6	1.9	4.0	2.6	0.75	9.3	5.1	7.3	0.23	21.7	0.54	16.2	0.41	9.2	17.8	27.0	61.0	1.53	2.0
ZSM 3/2002	*Rhombophryne* sp.	Andasibe		_	36.4	17.0	10.7	1.59	3.0	0.28	2.4		3.5	1.9	0.63	7.0	4.7	5.7	0.19	17.4	0.48	14.8	0.41	8.5	15.7	24.2	55.4	1.52	1.8
ZFMK 52765	*Rhombophryne* sp.	Andasibe		M	42.6	18.9	11.0	1.71	3.4	0.31	2.2		3.9	1.8	0.54	8.8	4.8	7.0	0.21	20.7	0.49	17.1	0.40	9.5	17.2	26.7	62.1	1.46	2.7

Figure 3. Individuals of *Plethodontohyla laevis* in life, illustrating the diversity of colour patterns from different sites of the species known distribution range: (**a**) MRSN A6188 from Betampona in dorsolateral and (inset) ventral view; (**b**) MRSN A6181 from Betampona in dorsolateral view; (**c**) FAZC 13898 from Betampona in dorsolateral view (Photos by Gonçalo M. Rosa); (**d**) MRSN A6787 from Anivorano Est in dorsolateral and (inset) ventral view (Photo by Jasmin E. Randrianirina); (**e**) ZSM 189/2016 from Analalava-Foulpointe in dorsolateral view (Photo by Frank Glaw); (**f**) individual (not collected) from Ambodiriana in dorsolateral view (Photo by Lauric Reynes).

for Madagascan microhylids (e.g. Scherz et al. 2014, 2015a, b, 2016a, b , 2017). The specimens were scanned individually at 140 kV and 80 µA, with a timing of 750 ms, for a total of 20 or 30 minutes (1440 or 2440 images respectively). Reconstruction methods were the same as those used previously (see the aforementioned literature, and especially Scherz et al. 2017). Examination of the internal anatomy of the specimens was conducted in VG STUDIO MAX 2.2 (Volume Graphics GmbH, Heidelberg, Germany). DICOM stacks of the scans and rotational videos are deposited in MorphoSource at the following URL: http://morphosource.org/Detail/ProjectDetail/Show/project_id/396. Portable document file (PDF)-embedded 3D models of select specimens were produced using AMIRA 6.1 (FEI Visualization Sciences Group, Burlington, MA), and are provided as digital Suppl. materials 1–6. Osteological terminology follows Trueb (1968, 1973).

Molecular analyses

Ten samples of *P. laevis* from four different localities (Fig. 3) (seven from Betampona Natural Reserve, one from Marovato, one from Anivorano Est and one from near Analalava-Foulpointe); three samples of *P. alluaudi* (in its new definition but until now referred to as '*P. bipunctata*'; Fig. 4a) from Andohahela (EU341068, Wollenberg et al. 2008), Tsitongambarika (Anosyenne Chain) and Sainte Luce; one sample of *P.* sp. Ca1 Ranomafana (Ambatolahy, EU341067, Wollenberg et al. 2008; Fig. 4b); three samples of *Rhombophryne* sp. (formerly assigned to *R. alluaudi*)

Figure 4. Individuals of (**a**) *Plethodontohyla alluaudi* in dorsolateral and (inset) ventral view (ZSM 89/2004 , until now referred to as *P. bipunctata*; from Andohahela); (**b**) *P.* sp. Ca01 in dorsolateral view (ZCMV 555; from Ambatolahy); (**c**) *P. brevipes* in dorsolateral view (ZSM 649/2003; from Ranomafana); and (**d**) *Rhombophryne* sp. (formerly identified as *R. alluaudi*) in lateral view (ZFMK 52765 from Andasibe) (Photos by Frank Glaw and Miguel Vences).

from Torotorofotsy (ZCMV 968; EU341105, Wollenberg et al. 2008), Andasibe (ZSM 3/2002; AY594112, Andreone et al. 2005) and Tsararano (MRSN A2620; AY594105, Andreone et al. 2005); one sample of all nominal species of the genus *Plethodontohyla* (with the exception of *P. notosticta* for which we included sequences from individuals from two localities, one in the North and one in the South) were used in the molecular analyses (see Table 2 for more details). A homologous sequence of *R. testudo*, the type species of the genus *Rhombophryne*, was also included.

For the newly obtained samples, total genomic DNA was extracted using Proteinase K (10 mg/ml) digestion followed by a standard salt-extraction protocol (Bruford et al. 1992). We amplified one mitochondrial gene fragment (rrnL large ribosomal RNA or 16S rRNA gene) for all newly obtained tissues samples, and one nuclear gene fragment, the pro-opiomelanocortin (POMC) gene, for a subset of samples (see details in Table 2). Standard polymerase chain reactions were performed in a final volume of 25 µl and using 0.75 µl each of 10 pmol primer, 0.4 µl of total dNTP 10 mM (Promega), 0.1 µl of 5 U/ml GoTaq (Promega), 5 µl 5X Green GoTaq Reaction Buffer (Promega) and 4 µl of $MgCl_2$ 25mM (Promega). To sequence a fragment of ca. 550 bp of the 3' terminus of the mitochondrial large ribosomal RNA gene (16S), proven to be suitable for amphibian identification (Vences et al. 2005), we used the primers AC_16S_AR 5'CGCCTGTTTATCAAAAACAT3' and AC_16S_BR 5'CCGGTYTGAACTCAGATCAYGT3' modified from Kocher et al. (1989) and Palumbi et al. (1991), using standard protocols. To sequence the POMC fragment, we used the primers POMC DRVF1 5'ATATGTCATGASCCAYTTYCGCTGGAA3' and POMC DRVR1 5'GGCRTTYTTGAAWAGAGTCATTAGWGG3' (Vieites et al. 2007) as in Vences et al. (2010). Successfully amplified fragments were purified and sequenced at Macrogen Inc., where labelled fragments were analysed on an ABI 3730XL automated DNA sequencer (Applied Biosystems).

Sequences were compared with GenBank sequences, and chromatographs were visually checked and edited, when necessary, using BIOEDIT 7.0.5.3 (Hall 1999). Gaps were included in the hypervariable regions of the 16S to account for indels in the final alignment. All newly determined sequences have been deposited in GenBank (MG273701–MG273723; Table 2). Uncorrected pairwise distances (*p*-distance transformed into percentage using the complete deletion option) amongst individuals of the same species and between ingroup analysed species were computed using MEGA 7.0.21 (Kumar et al. 2016).

Bayesian analyses were conducted in MRBAYES 3.2.2 (Ronquist et al. 2012). The GTR+I+G model was determined by AIC in jModelTest2 (Darriba et al. 2012) as the best-fitting model of substitution. We performed two runs of 10 million generations (started on random trees) and four incrementally heated Markov chains (using default heating values), sampling the Markov chains at intervals of 1,000 generations. Stabilization and convergence of likelihood values were checked by visualizing the log

Table 2. List of samples included for the molecular analyses with their respective localities, voucher and/or field number information, institutional catalogue number (where available) and GenBank accession numbers.

Sample ID	Taxon	Locality	Field number	Institutional catalogue number	Accession nos. 16S	Accession nos. POMC
ACP1109	*Plethodontohyla laevis*	Betampona	–	MRSN A6340	HM364769/ FJ559294	MG273712
ACP1901	*Plethodontohyla laevis*	Betampona	ACZCV 0066	ZSM 980/2013	MG273701	MG273713
ACP1108	*Plethodontohyla laevis*	Betampona	–	MRSN A6189	MG273702	MG273714
ACP1107	*Plethodontohyla laevis*	Betampona	–	MRSN A6181	MG273703	–
ACP2196	*Plethodontohyla laevis*	Betampona	ACZC 6262	–	MG273704	MG273715
ACP2214	*Plethodontohyla laevis*	Betampona	ACZCV 0268	–	MG273705	MG273716
ACP2066	*Plethodontohyla laevis*	Betampona	ACZC 5923	–	MG273706	MG273717
ACP1362	*Plethodontohyla laevis*	Marovato	PBZT-RJS 2020	MRSN A6674	MG273707	MG273718
ACP3171	*Plethodontohyla laevis*	Analalava	FGZC 5239	ZSM 189/2016	MG273708	–
ACP1368	*Plethodontohyla laevis*	Anivorano Est	PBZT-RJS 1830	MRSN A6787	MG273709	MG273719
FGZC161	*Plethodontohyla alluaudi*	Andohahela	FGZC 161	ZSM 89/2004	EU341068	MG273720
ACP1056	*Plethodontohyla alluaudi*	Tsitongambarika (Anosyenne Chain)	FAZC 15423	–	MG273710	MG273721
SE47	*Plethodontohyla alluaudi*	Sainte Luce	–	–	MG273711	–
ZCMV555	*Plethodontohyla* sp. Ca01	Ambatolahy	ZCMV 555	–	EU341067	MG273722
ZCMV968	*Rhombophryne* sp.	Torotorofotsy	ZCMV 968	–	EU341105	MG273723
na	*Rhombophryne* sp.	Tsararano	–	MRSN A2620	AY594105	–
na	*Rhombophryne* sp.	Andasibe	–	ZSM 3/2002	AY594112	–
na	*Plethodontohyla ocellata*	Ambohitsara	ZCMV 88	UADBA uncatalogued	EU341062	–
na	*Plethodontohyla brevipes*	Maharira	ZCMV 270	–	EU341063	–
na	*Plethodontohyla fonetana*	Bemaraha	FGZC 917	ZSM 123/2006	EU341058	–
na	*Plethodontohyla guentheri*	Marojejy	FGZC 2814	ZSM 61/2005	EU341059	–
na	*Plethodontohyla inguinalis*	Vohiparara	–	ZMA 20223	EU341057	–
na	*Plethodontohyla mihanika*	Ranomafana	ZCMV 308	UADBA uncatalogued	EU341056	–
na	*Plethodontohyla notosticta*	Nosy Mangabe	ZCMV 2106	–	EU341061	–
na	*Plethodontohyla notosticta*	Manombo	ZCMV 471	–	EU341060	–
na	*Plethodontohyla bipunctata*	Tolagnaro	RAX 10726	–	KM509181	–
na	*Plethodontohyla tuberata*	Manjakatompo	–	ZSM 375/2000	EU341064	–
na	*Rhombophryne testudo*	Nosy Be, Lokobe	–	ZSM 474/2000	KC180070	–
na	*Scaphiophryne marmorata*	Andasibe	–	ZSM 4/2002	AY834191	–

likelihoods associated with the posterior distribution of trees in the software TRACER 1.5 (Rambaut and Drummond 2007), and occurred after about 3–3.5 million generations. The first four million generations were conservatively discarded, and six million trees were retained post burn-in and summed to generate the majority rule consensus tree (Fig. 5a). The purpose of the presented phylogenetic analyses is: 1) to show that the four analysed populations of *P. laevis* form a monophyletic group; 2) to show the closest phylogenetic relationship of this species to *P. alluaudi* in its new definition and *P.* sp. Ca01 (which might prove to be conspecific with *P. alluaudi*); and 3) to show that the specimens formely assigned to '*Rhombophryne alluaudi*' (from Torotorofotsy, Andasibe, and Tsararano) do not belong to the genus *Plethodontohyla*, rather than provide a phylogenetic hypothesis of the phylogenetic relationships of *Plethodontohyla* species and support for the genus monophyly.

Alternative alleles of the analysed POMC gene fragment were inferred using the PHASE algorithm (Stephens et al. 2001) implemented in the software DNASP 5.10.3 (Librado and Rozas 2009). Haplotype network reconstruction of POMC phased sequences (Fig. 5b) was performed using the software TCS 1.21 (Clement et al. 2000). This software employs the method of Templeton et al. (1992) and calculates the number of mutational steps by which pairwise haplotypes differ, computing the probability of parsimony for pairwise differences until the probability exceeds 0.95 (no manual adjustment of threshold was necessary). The minimum number of mutational steps required to connect the two networks obtained using the parsimony method of Templeton et al. (1992) was identified using the 'fix connection limit' option as implemented in TCS.

Bioacoustic analyses

Vocalizations of *P. laevis* were recorded in the field with a Marantz PMD 660 digital recorder, accessorized with a semi-directional microphone. Calls were successively analysed with the acoustic software ADOBE AUDITION 3.0. Definition of variables and terminology in call descriptions follow Rosa and Andreone (2010), Rosa et

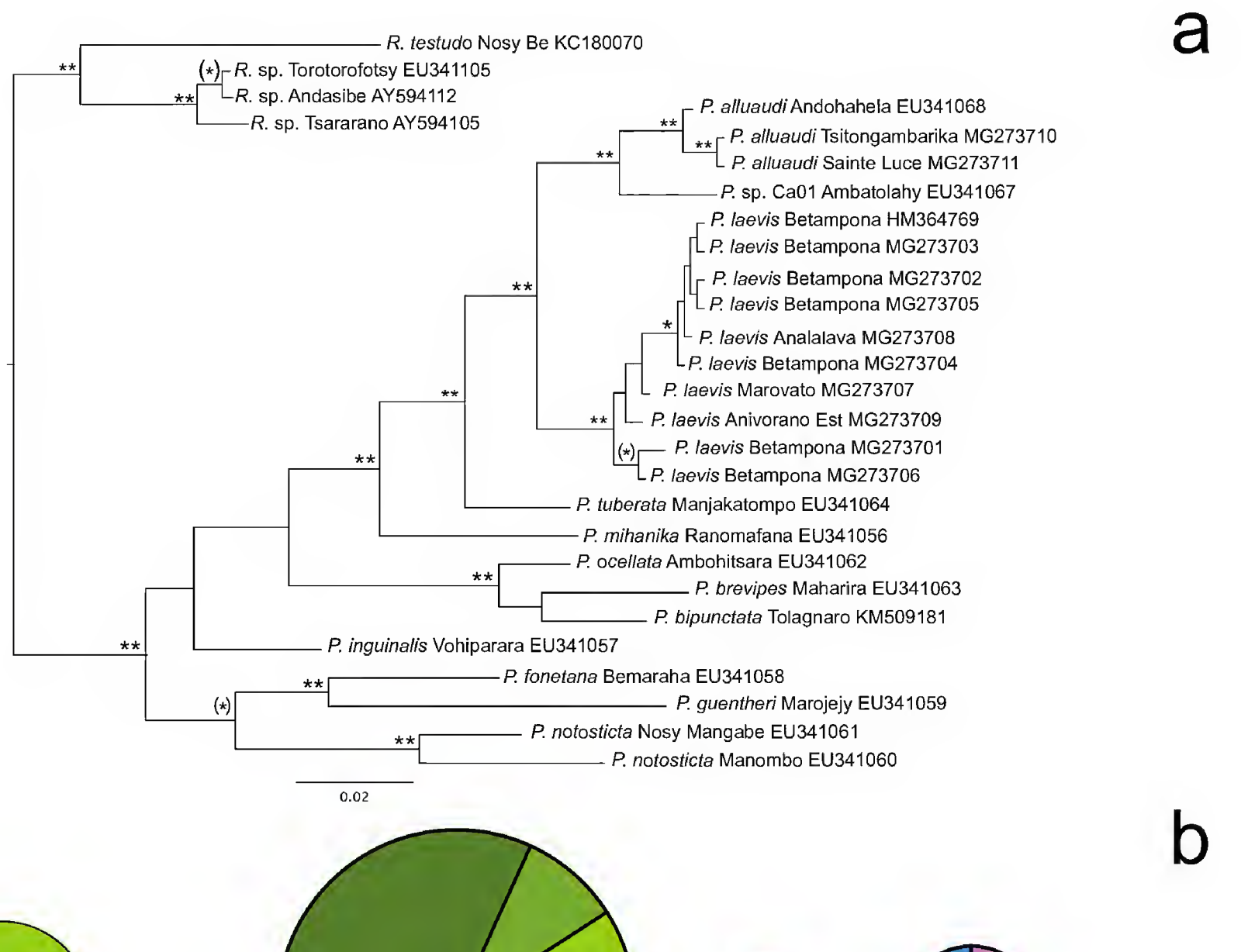

Figure 5. a) Bayesian inference tree based on 529 bp of the mitochondrial 16S. Asterisks denote Bayesian posterior probabilities values: one asterisk enclosed in parentheses, ≥ 90%; one asterisk, ≥ 98%; two asterisks, ≥ 99–100%. **b**) Haplotype network reconstruction for the phased alleles of the nuclear POMC gene fragment in *P. laevis* from Betampona, Marovato and Anivorano Est, *P. alluaudi* from Tsitongambarika and Andohahela, *P.* sp. Ca01 from Ambatolahy and *Rhombophryne* sp. from Torotorofotsy.

al. (2010, 2011) and Köhler et al. (2017), and calls are compared to described *Plethodontohyla* vocalizations available in the literature (see Table 3). Recordings were re-sampled at 44,100 Hz and 16 bit resolution in mono and with the 'Waveform' extension. Frequency information was obtained through Fast Fourier Transformation (FFT, width 1024 points); the audiospectrogram was obtained with a Hanning window function resolution of 256 bands.

Table 3. Comparative measurements from advertisement calls of *Plethodontohyla* species.

Species	Temp. (°C)	Series of notes	Note duration (ms)	Duration of inter-note intervals (s)	Note repetition rate (n/s)	Dominant frequency (Hz)	Visible harmonics	Reference
P. laevis	21	1	391–422 (407±12.7, n=4)	47 (n=1)	0.04	1820–2530	11	this study
P. alluaudi *	24	1	320–560 (478±109, n=4)	unknown	unknown	1400–2100	0	this study
P. inguinalis	21	1	133–191 (148±18, n=10)	0.85–1.15 (1±0.085, n=10)	0.9	800–1300	1	Vallan et al. (2005)
P. mihanika	24.5	1	150–172 (159±6, n=12)	4–7.2 (5.3±1, n=11)	0.18	1900–2200	4	Vences et al. (2003)
P. notosticta	unknown	1	280–340	2	0.43	1000	unknown	Glaw and Vences (1992)
	19	1	365–412 (391±13.3, n=15)	3.9–5.4 (3.7±0.74, n=14)	0.26	930–1330	9	Rosa et al. (2011); this study

* due to the low quality of the available recordings not all the parameters were possible to obtain.

Temporal measurements are provided as range, followed by mean, standard deviation and number of analysed units (n). We measured air temperature (to the nearest 1 °C) with digital devices at close distance to calling frogs (i.e. temperature information refers to air temperature at the time of recording, not body temperature of the calling specimen). The number of recordings did not allow for temperature corrections.

Results and discussion

We here present evidence that (1) *Dyscophus alluaudi* and *Phrynocara laeve* are both members of the genus *Plethodontohyla*; (2) *Plethodontohyla laevis tsianovohensis* is more similar to *D. alluaudi* than *Ph. laevis*; (3) the osteology and morphology of the holotypes of *Dyscophus alluaudi* and *Phrynocara laeve* indicate that they are not conspecific; (4) the species of *Rhombophryne* currently called *R.* '*alluaudi*' from the Andasibe region has no affinity with that species; (5) populations of *P.* sp. Ca3 from Betampona are conspecific with *Phrynocara laeve*; and (6) populations of a species of *Plethodontohyla* from southern Madagascar, until now referred to as '*P. bipunctata*' (ZSM 89/2004) are conspecific with *Dyscophus alluaudi*. Based on these findings, we resurrect and re-describe *Plethodontohyla laevis,* we transfer *Dyscophus alluaudi* to the genus *Plethodontohyla* and re-describe it.

Identity of the holotypes of *Dyscophus alluaudi*, *Phrynocara laeve* and *Plethodontohyla laevis tsianovohensis*

We examined the type material of *Dyscophus alluaudi*, which is currently assigned to the genus *Rhombophryne*, and its junior synonyms *Phrynocara laeve* and *Plethodontohyla laevis tsianovohensis* (depicted in Fig. 2). As we have intimated previously (Scherz et al. 2016a, b), an increasing body of evidence suggests that the name *D. alluaudi* is misapplied. Our investigation resulted in strong evidence for taxonomic placement of the respective names:

(1) The holotype of *Dyscophus alluaudi*, MNHN 1901.235 (Fig. 2c, d), is an adult ovigerous female specimen measuring 47.4 mm in SVL (for all other measurements see Table 1). It has knob-like terminal phalanges, an unossified pubis, tri-radiate prechoanal vomer with the lateral ramus situated at the midpoint, a strongly descending lateral flange of the frontoparietal, a short maxillary facial process, frontoparietals not extending beyond the level of the neopalatine and a well-developed transverse dorsal ridge on the frontoparietal (Fig. 6, see Suppl. material 1). The pectoral girdle has highly reduced clavicles (remaining just as short thin bony elements near the glenoid socket; indicated by arrows in Fig. 6) and a facet near the middle of the anterior edge of the coracoid. The pectoral girdle has been exposed on the specimen, and a thin cartilaginous extension of the procoracoid runs from the anterior glenoid socket to the facet on the leading edge of the coracoid, and then broadens and runs along it to the omosternum (intact only on the left side); the bony remnants of the clavicles are barely discernable through the dissecting microscope, as they are transparent and very thin. A similar condition to that seen in *Dyscophus alluaudi* was described for the type specimen of *Mantipus angeli* by Guibé (1974; confirmed by M.D. Scherz, personal observation), which is a synonym of *Plethodontohyla tuberata* (Peters, 1883). This state was unknown to Scherz et al. (2016a), suggesting the diagnostic value of the 'absence of clavicles' paired with absence of nasal-frontoparietal contact for *Plethodontohyla* recognition must be refined to include also these reduced lateral elements. The configuration is nevertheless clearly different from *Rhombophryne*, including the reduced clavicles of species like *R. mangabensis* (M.D. Scherz et al. unpublished data).

(2) The holotype of *Phrynocara laeve*, SMF 4286 (Fig. 2a, b), is probably also an adult female (with developing eggs), measuring 38.1 mm in SVL (for all other measurements see Table 1). It lacks clavicles, has knob-like terminal phalanges, an unossified pubis, a tri-radiate prechoanal vomer with the lateral ramus displaced anteriorly, lateral flange of frontoparietal not descending strongly, a short maxillary facial process, frontoparietals extending beyond the level of the neopalatine and a well-developed if discontinuous transverse dorsal ridge on the frontoparietal (Fig. 6, Suppl. material 2). It differs strongly from MNHN 1901.235 in its smaller size (SVL 38.1 *vs.* 47.4 mm), much narrower head (HW/HL 1.56 *vs.* 1.85), longer

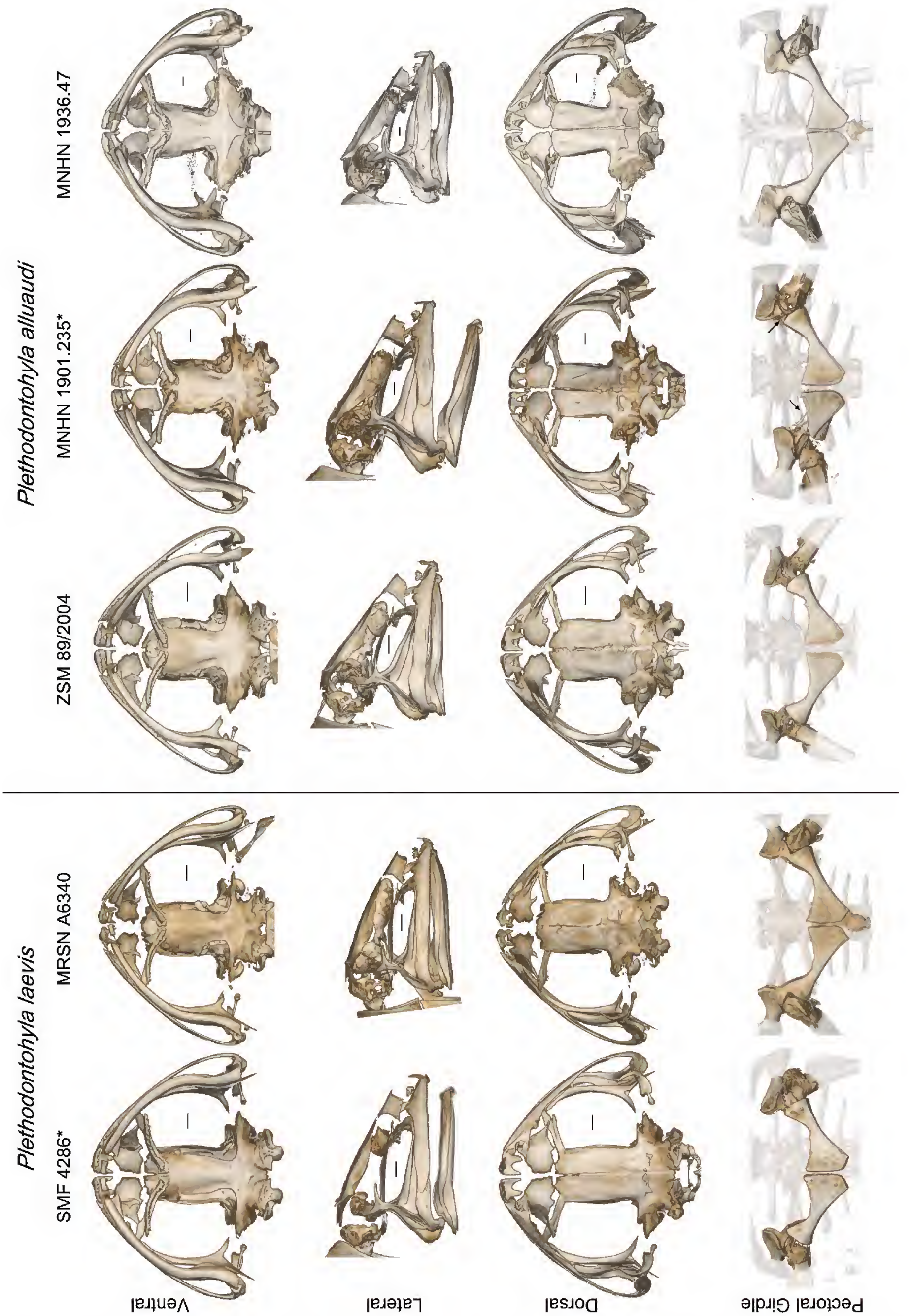

Figure 6. Skull and pectoral girdle morphology of *Plethodontohyla alluaudi* and *P. laevis*. Asterisks indicate the holotypes of each species. Arrows on the pectoral girdle of *P. alluaudi* MNHN 1901.235 indicate the clavicles. Scale bars indicate 1 mm.

relative forelimb length (FORL/SVL 0.56 *vs.* 0.47), longer relative hindlimb length (HIL/SVL 1.43 *vs.* 1.25), the absence of large dark inguinal spots (*vs.* presence), lateral ramus of the prechoanal vomer displaced anteriorly (*vs.* central), frontoparietals exceeding the level of the neopalatine (*vs.* not exceeding the neopalatine) and the weakly descending lateral flange of the frontoparietal (*vs.* strongly). The pectoral girdle is similar to MNHN 1901.235, but has also been damaged, obscuring the state—it nevertheless lacks the ossified clavicles of that specimen. We therefore conclude that it is not a synonym of *D. alluaudi*, but instead a valid species in need of resurrection. Its osteology also suggests that it is a member of the genus *Plethodontohyla*, on the basis of the absence of clavicles and lack of nasal-frontoparietal contact.

(3) The type specimen of *Plethodontohyla laevis tsianovohensis*, MNHN 1936.47 (Fig. 2e, f), is also an adult, ovigerous female measuring 58.0 mm in SVL (for all other measurements see Table 1). It lacks clavicles, but has the same cartilaginous pectoral arrangement as the holotype of *D. alluaudi*, but on the left side it has been damaged so that a second pectoral fenestra is formed medial to the anterior facet of the coracoid, where it ought not to be. In addition, it has knob-like terminal phalanges, an ossified pubis, an almost crescentic prechoanal vomer with a weak lateral ramus, a strongly descending lateral flange of the frontoparietal, a long maxillary facial process, frontoparietals not extending beyond the level of the neopalatine and a well-developed transverse dorsal ridge on the frontoparietal (Fig. 6, Suppl. material 3). Its affiliations are not quite clear; it is larger in size than either *D. alluaudi* or *Ph. laeve* (SVL 58.0 *vs.* 47.4 and 38.1 mm, respectively), its arms are longer than those of *D. alluaudi* but shorter than those of *Ph. laeve* (FORL/SVL 0.53 *vs.* 0.47 and 0.56, respectively), it has longer legs than both (HIL/SVL 1.47 *vs.* 1.25 and 1.43, respectively), its tympanum is broader than both (TD/ED 0.58 *vs.* 0.53 and 0.40, respectively), and its osteology shares some elements with either species and differs from both in others (e.g. the length of the facial process). Overall, the skeleton and external morphology more closely resembles that of MNHN 1901.235, and we therefore tentatively conclude that *P. l. tsianovohensis* should be left in the synonymy of *D. alluaudi*. However, we emphasise that the *D. alluaudi* and *P. l. tsianovohensis* type specimens do not agree in all aspects of their morphology, and their type localities are separated by at least 300 km (Fig. 1), so this taxon may eventually be recognized as a valid, species-level name (possibly it may represent *P.* sp. Ca01, whose osteology has not been studied here, but see below). It must therefore be re-visited in future treatments of the taxonomy of the *P. alluaudi* complex. In any case, it is the most junior of the available names, and its identity can remain unresolved for the time being.

Identity of recently collected specimens

As a next step, we analysed the osteology and morphology of three more recently collected specimens: (1) ZSM 3/2002, a specimen from Andasibe of the species currently referred to as '*Rhombophryne alluaudi*' following Blommers-Schlösser (1975) and Glaw and Vences (1992); (2) MRSN A6340, a specimen of a species of *Plethodontohyla* collected from near the potential type locality of *Phrynocara laeve* that agrees strongly with the original description of that species; and (3) ZSM 89/2004, a specimen of a species of *Plethodontohyla* collected in Andohahela, near to the type locality of *Dyscophus alluaudi*.

(1) ZSM 3/2002 is genetically a member of the genus *Rhombophryne* (Figs 4d, 5a). Osteologically, it resembles other published and unpublished *Rhombophryne* skeletons (Scherz et al. 2014, 2015a, b, 2016a, b, 2017, unpublished data) and it differs unambiguously from the holotype of *Dyscophus alluaudi*: it has fully developed clavicles (*vs.* rudimentary clavicles present in the holotype of *D. alluaudi*), two independent dorsal processes on the frontoparietal (rather than a more or less continuous ridge) and a fused presacral VIII and sacrum (Suppl. material 4). Additionally, it lacks inguinal spots and any trace of the pattern originally described for *Dyscophus alluaudi*. Thus, it is clear that the taxon *Dyscophus alluaudi* is currently misapplied. Based on its molecular phylogenetic identity (Table 2; Fig. 5a), as well as the presence of curved clavicles and knobbed terminal phalanges, this species is a member of the genus *Rhombophryne*. It does not match any other described species of *Rhombophryne*, and will therefore be described in a forthcoming revision of that genus.

(2) MRSN A6340 is a specimen of *Plethodontohyla* collected at Betampona and genetically similar to other specimens collected at Marovato, Anivorano Est and Analalava-Foulpointe (Table 2; Fig. 5). It is an adult male (collected when calling), measuring 33.0 mm in SVL (for all other measurements see Table 1). It lacks clavicles, has knob-like terminal phalanges, a mostly unossified pubis, a tri-radiate vomer with a lateral ramus displaced anteriorly, lateral flange of frontoparietal not descending strongly, a moderately short maxillary facial process, frontoparietals extending beyond the level of the neopalatine and a well-developed transverse dorsal ridge on the frontoparietal (Fig. 6, Suppl. material 5). In all of these respects, it strongly resembles the osteology of the holotype of *Phrynocara laeve*. Its external morphology also resembles that species, though it differs somewhat in ratios (but note the variability of measurements shown in Table 1). It differs clearly from *Dyscophus alluaudi* and *Pl. laevis tsianovohensis* on the same grounds given above from *Ph. laeve*, i.e. the absence of large dark inguinal spots (*vs.* presence in *D. alluaudi*), lateral ramus of prechoanal vomer displaced anteriorly (*vs.* central), frontoparietal exceeding the level of the neopalatine (*vs.* not exceeding the neopalatine) and the weakly descending lateral flange of the frontoparietal (*vs.* strongly). We therefore conclude that this species is assignable to *Plethodontohyla laevis*, distinct from *Plethodontohyla alluaudi*, and we resurrect and re-describe it below based on data from the holotype and our new material.

(3) ZSM 89/2004 is a specimen collected in Andohahela and genetically belonging to the genus *Plethodontohyla* (Table 2; Figs 4a, 5). This specimen is molecularly

similar to other specimens collected at Tsitongambarika and Sainte Luce and moderately similar to the sequence of a specimen collected at Ambatolahy (Fig. 5). ZSM 89/2004 has close genetic affinities to the specimens that we here confer to *P. alluaudi*, representing a closely related clade (see Fig. 5a). Osteologically, it differs from the holotype of *Phrynocara laeve* (and other specimens conferred to that taxon) in the following respects: lateral ramus of prechoanal vomer central (*vs.* displaced anteriorly), and lateral flange of frontoparietal descending strongly (*vs.* not descending strongly). Its coracoids show distinct facets for the attachment of cartilage, more strongly developed than in *P. laevis*. By comparison, it differs from *Dyscophus alluaudi* in the narrower skull, frontoparietals exceeding the level of the neopalatine, absence of clavicle remnants and the proportions of some skull elements (compare the skulls in Fig. 6, Suppl. material 6). However, we hypothesise that these differences between this specimen and the holotype of *Dyscophus alluaudi* are due to the considerable difference in body size (SVL 29.1 *vs.* 47.4 mm) and that the proportions of the skull and its ossification are correlates of age and size. The differences to *Phrynocara laeve* appear more substantial, despite the similarity in size. Both ZSM 89/2004 and UADBA-A 27994 (FGZC 160) possess inguinal spots and agree in external morphology with *Dyscophus alluaudi*. We therefore attribute these populations from southern Madagascar to *Plethodontohyla alluaudi*, and we re-describe this species below.

Remarks on the identity of *P.* sp. Ca01 and *P. brevipes*

Fig. 4b, c

We note that the specimen representing *P.* sp. Ca01 (ZCMV 555) from Ambatolahy in eastern Madagascar (21°14'37.92"S, 047°25'34.38"E) is genetically very similar to the samples attributed to *P. alluaudi* and phylogenetically represents the sister taxon of the specimens here attributed to *P. alluaudi*. A picture of a specimen of *P.* sp. Ca01, ZCMV 555 (or 556, a second not yet sequenced individual) was depicted as *Plethodontohyla brevipes* on page 125 of Glaw and Vences (2007b) and in Fig. 1 of Scherz et al. (2016a). Two additional specimens belonging to this taxon are currently present in the ZSM collection: ZSM 855/2006 and ZSM 856/2006. Elements of the overall appearance of specimens ZCMV 555 (based on the photograph) and ZSM 855/2006 and ZSM 856/2006 disagree with the description of that species, most notably by the presence of a distinct marking over the back of the head (originally described as 'uniform dark brown above'). In contrast, they bear a remarkable resemblance to *P. alluaudi* and *P. laevis*. These specimens may therefore be closely related to the holotype of *P. laevis tsianovohensis*, which is from an area comparatively near to Ambatolahy. Nevertheless, the taxonomic status of *P.* sp. Ca01, and also the relationships of *Plethodontohyla brevipes* based on its holotype (BMNH 1947.2.10.42), clearly need to be revised. This is however beyond the scope of the current study, and must be conducted in the context of a larger revision of the genus. In the diagnoses against *P. brevipes* presented for the following re-descriptions, we included only measurements from specimens that resemble the original description in having uniformly brown dorsal colouration and slightly granular dorsal skin.

Molecular analyses

Among representatives of the genus *Plethodontohyla*, the mean uncorrected *p*-distance (for the 16S fragment) of *P. laevis* varies between 5.5% (comparison with *P.* sp. Ca01 which may be conspecific with *P. alluaudi*) and 11.5% (comparison with *P. guentheri* and with *P. brevipes*). Our data also reveal some genetic differentiation between the four known populations of *P. laevis*, with an intraspecific mean uncorrected *p*-distance of 1.1% (Table 4). For other intraspecific comparisons and comparisons with other *Plethodontohyla* species see Table 4.

The two Bayesian analyses resulted in largely identical trees, with only minor changes in posterior probability values, and showed that *P. laevis* from the four analysed localities forms a robust monophyletic group (posterior probability [PP] 0.99). Our analyses recovered a moderately supported sister relationship (PP 0.94) for *P. laevis* and the clade composed of *P. alluaudi* in its new definition and *P.* sp. Ca01 from Ambatolahy (Fig. 5a). The mean uncorrected *p*-distance of *P.* sp. Ca01 and *P. alluaudi* is 2.9% and these taxa might indeed represent two populations of the same species. Similarly, the three specimens from Torotorofotsy, Andasibe and Tsararano belonging to the genus *Rhombophryne* apparently are the same taxon (mean uncorrected *p*-distance 0.7%; PP 1.0), although a more extensive phylogenetic analysis of *Rhombophryne* will be required to further confirm this result.

The haplotype network reconstruction of the nuclear POMC gene (Fig. 5b) shows no haplotype sharing between *Plethodontohyla laevis* (from Betampona, Marovato and Anivorano Est) and *P. alluaudi*. Wide haplotype sharing is observed between the three analysed populations of *P. laevis* used in this analysis, with at least two haplotypes (haplotype H1 and H2; Fig. 5b) found in all three populations; and haplotype sharing is observed also between *P. alluaudi* from Andohahela and *P.* sp. Ca01 from Ambatolahy (haplotype H7; Fig. 5b).

The analysis of haplotype network reconstruction fails to recover a single statistically significant haplotype network for the analysed dataset that comprises representative samples of *P. laevis* from three localities, *P. alluaudi* from two localities, *P.* sp. Ca01 and the *Rhombophryne* species from Torotorofotsy, and a minimum of 18 substitutions are required to join these two haplotype networks (see Fig. 5b for details).

***Plethodontohyla laevis* (Boettger, 1913), bona species**

Figs 2a, b, 3, 6–8, Suppl. materials 2, 5

Remarks. This species has been referred to as *Plethodontohyla* sp. 3 'Betampona' by Vieites et al. (2009), *Pletho-*

Table 4. Estimates of evolutionary divergence over sequence pairs within- (bold) and between-species for the analysed 16S rRNA mitochondrial gene fragment. The number of base differences per site averaged over all sequence pairs within and between groups are shown. The analysis involved 28 nucleotide sequences. All positions containing gaps and missing data were eliminated. There were a total of 300 positions in the final dataset. Evolutionary analyses were conducted in MEGA7 (Kumar et al. 2016). The presence of n/c (not computed) in the results denotes cases in which it was not possible to estimate evolutionary distances. '*R.* sp.' refers to the undescribed *Rhombophryne* species formerly assigned to *R. alluaudi*.

	P. alluaudi	*P.* sp. Ca01	*P. laevis*	*R.* sp.	*P. ocellata*	*P. brevipes*	*P. fonetana*	*P. guentheri*	*P. inguinalis*	*P. mihanika*	*P. notosticta*	*P. bipunctata*	*P. tuberata*	*R. testudo*
P. alluaudi	**0.7%**													
P. sp. Ca01	2.9%	**n/c**												
P. laevis	5.8%	5.5%	**1.1%**											
R. sp.	12.4%	12.1%	12.6%	**0.7%**										
P. ocellata	9.0%	9.3%	9.9%	9.4%	**n/c**									
P. brevipes	10.4%	10.7%	11.5%	9.4%	5.0%	**n/c**								
P. fonetana	10.4%	10.0%	9.9%	9.0%	9.3%	11.3%	**n/c**							
P. guentheri	11.1%	10.0%	11.5%	10.3%	11.0%	11.7%	7.7%	**n/c**						
P. inguinalis	9.9%	9.3%	9.6%	8.1%	7.0%	8.7%	7.3%	8.3%	**n/c**					
P. mihanika	9.3%	8.3%	7.0%	10.4%	9.7%	11.7%	7.7%	10.7%	9.0%	**n/c**				
P. notosticta	11.6%	10.8%	10.4%	10.6%	10.5%	10.5%	9.8%	10.3%	9.5%	9.7%	**0.6%**			
P. bipunctata	9.4%	9.3%	9.5%	9.8%	2.3%	3.70%	9.7%	10.7%	6.7%	10.0%	9.5%	**n/c**		
P. tuberata	5.6%	5.7%	7.2%	10.8%	8.7%	10.0%	9.7%	10.0%	8.7%	8.3%	10.7%	9.0%	**n/c**	
R. testudo	12.8%	14.0%	14.2%	8.6%	11.3%	11.70%	13.0%	13.0%	9.3%	12.3%	12.3%	10.3%	11.3%	**n/c**

dontohyla sp. aff. *brevipes* [Ca FJ559294] by Rosa et al. (2011, 2012) and *Plethodontohyla* sp. Ca03 Betampona by Scherz et al. (2016a). Blommers-Schlösser (1975) referred to a male specimen from 'near Tampoketsa d'Ankazobe' (approx. 18°19'05.5"S, 047°06'42.8"E , Fig. 1) as *P. laevis*. This locality from the central highlands is indeed closer to the distribution range of *P. laevis* than to *P. alluaudi* (as refined here), but we consider this record uncertain until the specimen (ZMA 6688) has been examined.

Resurrection of *Plethodontohyla laevis*. As we have shown above, several osteological and morphological characters exist to distinguish the holotypes of *Dyscophus alluaudi* and *Phrynocara laeve*. Osteological characters suggest that both taxa are members of the genus *Plethodontohyla*. Specimens recently collected in Betampona Special Reserve closely match the morphology, osteology and appearance of the holotype of *Phrynocara laeve*. A village named Sakana (in the Vavatenina commune, Toamasina Province) was located by using Google Earth roughly 70 km North of Betampona (17°18'00.00"S, 049°01'59.99"E), and we suspect that this may have been the forest to which Boettger was referring in the original description (Boettger 1913). The newly collected material in Betampona, Marovato, Anivorano Est and Analalava-Foulpointe is genetically and morphologically relatively uniform and it is distinct both from *Plethodontohyla alluaudi* (in its new definition), and from all other nominal *Plethodontohyla* species. We therefore resurrect *Plethodontohyla laevis* (Boettger, 1913) from the synonymy of *P. alluaudi* and we provide a re-description of it based on the re-examination of its holotype (including its osteology via micro-CT scanning), and examination of additional, newly collected material.

Holotype. SMF 4286, an adult female collected by A. Voeltzkow in 1905 in Sakana, East Madagascar.

Referred material. Adult male (ethanol-fixed, DNA sequenced and included in Rosa et al. 2012: Accession number HM364769) MRSN A6340 (FAZC 13902), collected by G.M. Rosa and J. Noël on 18 November 2007 at Betampona Nature Reserve, campsite Maintimbato (17°53'35.5"S, 049°13'41.3"E, 283 m a.s.l.), Toamasina Province, eastern Madagascar. MRSN A6189 (FAZC 13643), adult female (ethanol-fixed and DNA sequenced), collected by G.M. Rosa and J. Noël on 21 February 2007 at Betampona Reserve campsite Maintimbato (17°53'36.9"S, 049°13'37.2"E, 295 m a.s.l.); MRSN A6181 (FAZC 13494), adult female (ethanol-fixed and DNA sequenced), collected by G.M. Rosa and J. Noël on 4 February 2007 at Betampona Reserve, Piste Principal (17°55'40.5"S, 049°12'07.4"E, 355 m a.s.l.); ZSM 980/2013 (ACZCV 0066), adult male (ethanol-fixed and DNA sequenced), collected by A. Crottini, D. Salvi, E. Scanarini and J.H. Velo on the morning of 9 November 2013 at Betampona Nature Reserve, campsite Sahaïndrana (17°53'55.50"S, 049°12'02.4"E, 327 m a.s.l.); UADBA uncatalogued (ACZCV 0268), adult unsexed (ethanol-fixed and DNA sequenced), collected by A. Crottini, D. Salvi, E. Scanarini, F. Andreone, S. Faravelli, J. Noël and Georges on the evening of 20 November 2013 at Betampona Nature Reserve, campsite Sahabefoza (17°54'54.82"S, 049°12'32.31"E, 349 m a.s.l.); MRSN A6674 (PBZT-RJS 2020), adult female (ethanol-fixed and DNA sequenced), collected by J.E. Randrianirina on 17 October 2008 at Marovato (18°41'09.60"S, 048°36'19.80"E, 692 m a.s.l.); MRSN A6787 (PBZT-RJS 1830), adult male (ethanol-fixed and DNA sequenced), collected by J.E. Randrianirina on 12

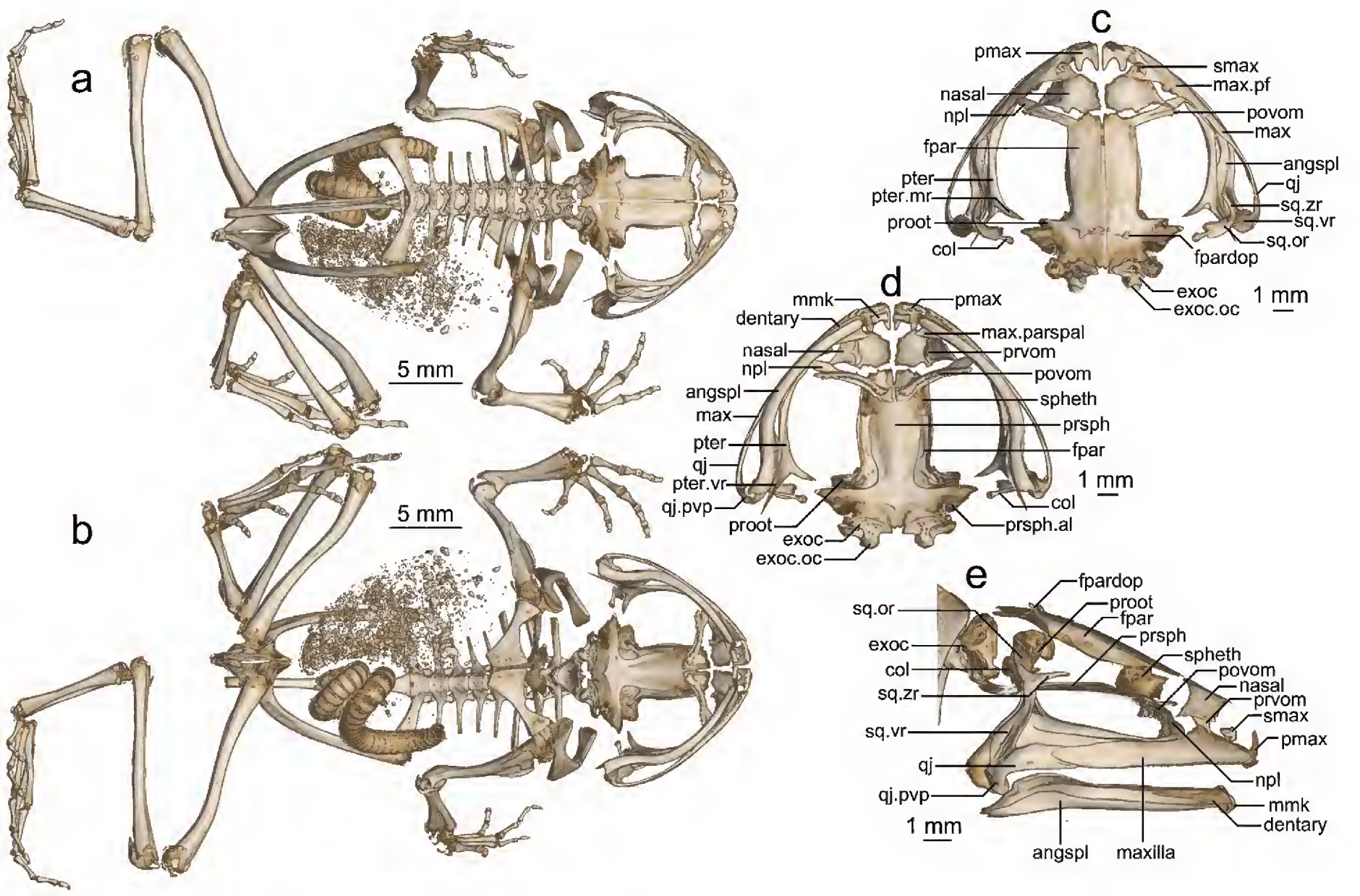

Figure 7. The skeleton of *Plethodontohyla laevis* (SMF 4286) rendered via micro-CT scanning. (**a**–**b**) Full skeleton in (**a**) dorsal and (**b**) ventral view. (**c**–**e**) Skull in (**c**) dorsal, (**d**) ventral and (**e**) lateral view. Abbreviations: angspl, angulosplenial; col, columella; exoc, exoccipital; exoc.oc, occipital condyle of exoccipital; fpar, frontoparietal; fpardop, frontoparietal dorsal process; max, maxilla; max.pf, pars facialis of maxilla; max.parspal, pars palatina of maxilla; mmk, mentomeckelian; npl, neopalatine; pmax, premaxilla; povom, postchoanal vomer; proot, prootic; prsph, parasphenoid; prsph.al, alary process of parasphenoid; prvom, prechoanal vomer; pter, pterygoid; pter.mr, medial ramus of pterygoid; pter.vr, ventral ramus of pterygoid; qj, quadratojugal; qj.pvp, posteroventral process of quadratojugal; smax, septomaxilla; sq.or, otic ramus of squamosal; sq.vr, ventral ramus of squamosal; sq.zr, zygotic ramus of squamosal; spheth, sphenethmoid. For a 3D rotational model, see Suppl. material 2.

October 2008 at Anivorano Est, village d'Ambalatenina, Forêt d'Andrarihitra (18°45'56.94"S, 048°57'07.20"E, 270 m a.s.l.); ZSM 189/2016 (FGZC 5239), juvenile (ethanol-fixed and DNA sequenced), collected by F. Glaw, D. Prötzel and L. Randriamanana, on 1st January 2016 near Analalava-Foulpointe (17°42'25.39"S, 049°27'35.59"E, ca. 30 m a.s.l.).

Diagnosis (see also Tables 1, 5 and Figs 2–3, 6–8). A microhylid belonging to the subfamily Cophylinae, with connected lateral metatarsalia, short hindlimbs, tibiotarsal articulation not exceeding the nostril, inner metatarsal tubercle present, vomerine teeth present, clavicle absent, knob-shaped terminal phalanges, and males with a single subgular vocal sac; therefore attributed to the genus *Plethodontohyla* (see Appendix A of Scherz et al. 2016a). The attribution to the genus *Plethodontohyla* is also supported by molecular phylogenetic evidence from newly collected material (see Fig. 5). The species is characterised by the following suite of characters: (1) moderately large size (male SVL 33.0–40.3 mm; female SVL 36.8–42.2 mm); (2) HW/HL 1.41–1.79; (3) FORL/SVL 0.50–0.57; (4) HIL/SVL 1.24–1.58; (5) TIBL/SVL 0.36–0.40; (6) rounded snout tip; (7) toe tips not enlarged; (8) finger tips not enlarged; (9) knob-shaped terminal phalanges of the fingers and toes; (10) smooth dorsal skin; (11) absence of a distinct dorsolateral colour border; (12) presence of a supratympanic dermal fold; (13) presence of a typically bold and generally white-bordered brown 'X' marking on head; (14) tibiotarsal articulation reaching at least the tympanum and (15) TD/ED 0.33–0.52. Furthermore, the species is separated from all nominal taxa in this genus by an uncorrected pairwise distance of at least 5.5% in the sequenced 16S fragment (comparison with *P. alluaudi* in its new definition and *P.* sp. Ca01).

Plethodontohyla laevis may be distinguished from other members of the genus *Plethodontohyla* as follows: from *P. inguinalis*, *P. notosticta*, *P. guentheri*, *P. mihanika* and *P. fonetana* by non-expanded terminal digits (*vs.* moderately to strongly expanded) and by its knob-shaped terminal phalanges of the fingers and toes (*vs.* T- or Y-shaped) and from all these species except *P. fonetana*

by the absence of a dorsolateral colour border (present in all of these species but only some specimens of *P. inguinalis*). It also differs from *P. notosticta*, *P. guentheri* and *P. mihanika* by having a rounded snout tip (*vs.* generally pointed); from *P. ocellata*, *P. bipunctata*, *P. brevipes*, *P. inguinalis* and *P. tuberata* by smooth skin (*vs.* granular or tubercular); from *P. inguinalis*, *P. notosticta*, *P. guentheri* and *P. mihanika* by the presence of a supratympanic fold running from the posterior border of the eye backward until the forelimb (*vs.* absence); from all species of *Plethodontohyla* except *P. alluaudi* and *P.* sp. Ca01 by the presence of a bold, mostly white-bordered 'X' marking (see Fig. 3 for its variation) on the head (*vs.* absence); from *P. tuberata*, *P. bipunctata*, *P. brevipes* and *P. mihanika* by a tibiotarsal articulation reaching at least the tympanum (*vs.* reaching the insertion of the arms or going beyond the tip of snout in *P. mihanika*); and from *P. ocellata*, *P. bipunctata*, *P. fonetana* and most individuals of *P. brevipes* by lacking two symmetrical and concave thin dorsal folds (*vs.* presence).

Plethodontohyla alluaudi (as newly circumscribed) and *P.* sp. Ca01 are morphologically the most similar species to *P. laevis* (see also Figs 3–4). For distinction from *P. alluaudi*, see the re-description of that species, below. *Plethodontohyla laevis* differs from *P.* sp. Ca01 by larger body size (SVL 33.0–42.2 *vs.* 27.7–31.9 mm) and smaller tympanum (TD/ED 0.33–0.52 *vs.* 0.55–0.63).

Plethodontohyla laevis also resembles *Rhombophryne botabota*, *R. laevipes*, *R. mangabensis* and *R. savaka* in external morphology and in some aspects of its colouration. It may be distinguished from all species by the presence of a bold, mostly white-bordered 'X' marking on the head (*vs.* absence), but additionally it may be distinguished from all four of these species by the absence of clavicles; from *R. laevipes* by its smaller size (SVL 36.8–42.2 mm *vs.* 44.5–56.3 mm), much shorter leg length (HIL/SVL 1.24–1.58 *vs.* 1.75–1.86) and absence of white ocelli in the inguinal region (*vs.* presence); from *R. laevipes* and *R. mangabensis* by its smaller tympanum (TD/ED 0.33–0.52 *vs.* 0.57–0.73); from *R. botabota*, *R. mangabensis* and *R. savaka* by its larger size (SVL 36.8–42.2 mm *vs.* 20.4–32.2 mm); from *R. savaka* by its slightly narrower head (HW/HL 1.41–1.79 *vs.* 1.80), longer relative forelimb length (FORL/SVL 0.50–0.57 *vs.* 0.43), raised supratympanic fold (*vs.* not raised) and absence of a diastema in the vomerine teeth (*vs.* presence); and from *R. botabota* and *R. mangabensis* by generally shorter relative tibia length (TIBL/SVL 0.36–40 *vs.* 0.38–0.45).

Re-description of the holotype (SMF 4286). Specimen in relatively good state of preservation (Fig. 2a, b). Right forelimb fractured (Fig. 7a, b). Ventrally slit down the midline of the whole body. SVL 38.1 mm (for other measurements, see Table 1). Body moderately enlarged and flattened dorsoventrally; head much wider than long and almost as wide as body; snout rounded in dorsal and lateral view; nostrils directed laterally, slightly protuberant, nearer to tip of snout than to eye; canthus rostralis distinct, concave; loreal region concave; tympanum indistinct, rounded, roughly 40% of eye diameter; supratympanic fold from eye to shoulder distinct and straight; tongue ovoid, very broad, posteriorly free and slightly notched; maxillary teeth present; vomerine teeth distinct, forming oblique transverse rows posterior to choanae, laterally approaching the maxillae and medially almost in contralateral contact; choanae ovoid. Arms robust, fingers bearing marked single subarticular tubercles and hands bearing indistinct paired outer metacarpal tubercles; large, slightly protruding inner metacarpal tubercle; fingers without webbing; relative length of fingers 1<2=4<3, fourth finger roughly equal in length to second; finger disks not enlarged; nuptial pads absent. Hindlimbs robust; tibiotarsal articulation reaching the tympanum when hindlimb adpressed along body; tibia length 38.8% of SVL; lateral metatarsalia connected; distinct inner and less distinct outer metatarsal tubercles present; only traces of webbing between toes; relative length of toes 1<2<5<3<4; third toe distinctly longer than fifth. Skin on dorsum and venter smooth; supratympanic fold whitish. Colour of iris indistinguishable.

Colouration. After more than a century in preservative (holotype collected in September 1904) colouration is faded. Dorsum light brown with darker brown-black spots, markings and presence of a bold X-shaped marking bordered with a white line on the head behind the eye. Colouration of the proximal dorsal portion of the hindlimbs mottled with dark brown markings on a cream background colour; the same colouration extends into the inguinal region. Colouration of the distal dorsal portion of the hindlimbs light brown with faint brown crossbands. Sides of head and tympanic region brownish, with darkener flecks. Ventral skin markedly pigmented: throat and chest mottled brown and cream, abdomen and ventral legs cream, becoming increasingly mottled with faint brown distally. The colouration in life of this specimen is not known.

Osteology. In the following, we describe notable and important diagnostic characters of *Plethodontohyla laevis* based on SMF 4286 (Figs 2, 6–7) and the newly collected specimen MRSN A6340 (Fig. 8). PDF-embedded 3D models of these skeletons are provided as Suppl. materials 2 and 5.

Right humerus fractured in SMF 4286. Skeleton of SMF 4286 relatively poorly ossified, such that the carpals, knee and heel joints and pubis are not visible in the micro-CT scans. The skeleton of MRSN A6340 is comparatively well ossified. Vomerine teeth anteriorly convex, long, occupying the whole postchoanal vomer, separated medially by a small gap. Palatine processes of premaxilla subequal in width and length. Prechoanal vomer flat and triradiate, the lateral ramus closer to the anterior end. Premaxilla and maxilla bearing teeth. Nasals large, broad, not in contact with other bones. Sphenethmoid only laterally ossified. Extensive calcification present inside the braincase of MRSN A6340. Posterior ramus of pterygoid

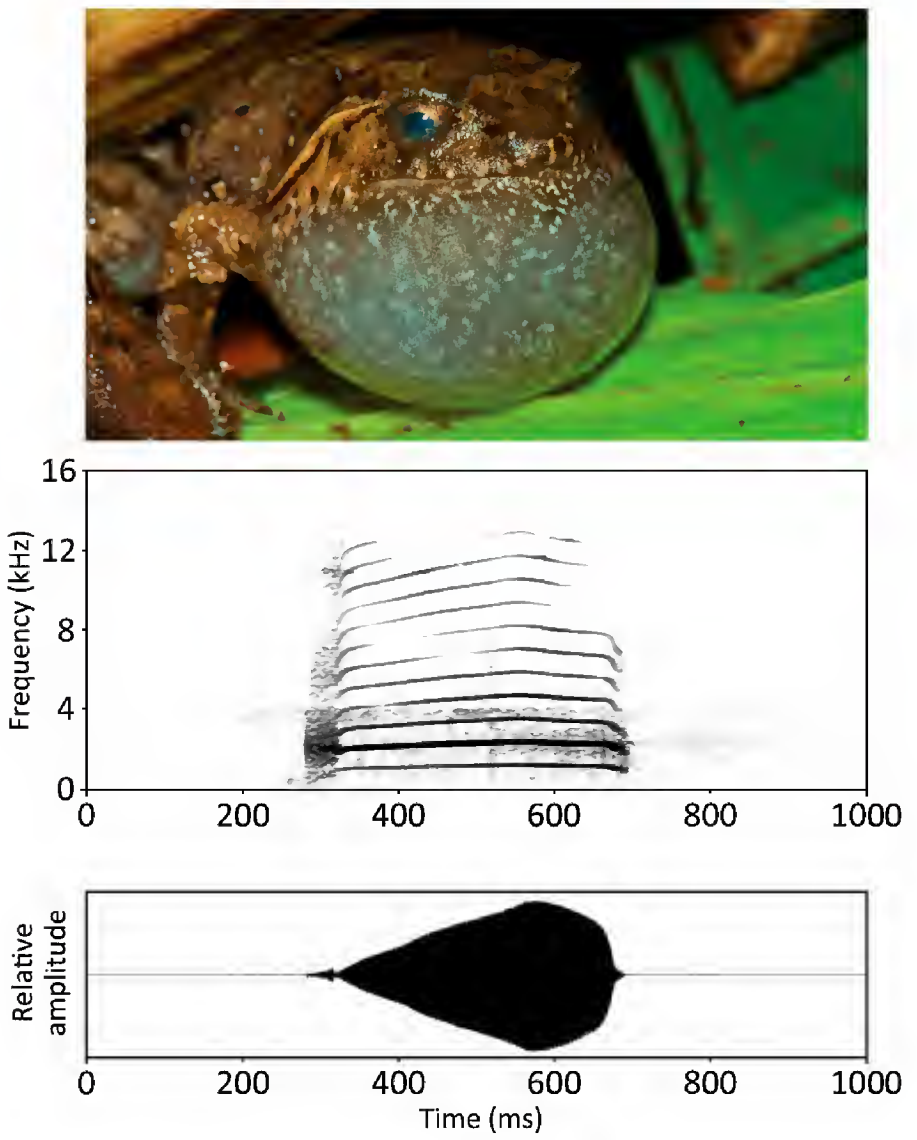

Figure 8. Audiospectrogram and corresponding oscillogram of the advertisement call of *Plethodontohyla laevis* recorded at Betampona Strict Nature Reserve on 18 November 2007 (22:30 h, 21 °C). Calling male MRSN A6340 (top).

extremely long and broad. Transverse ridge across posterior of frontoparietals. Weakly descending lateral flange of frontoparietal. Clavicle absent. Coracoids with weak notches for the attachment of the procoracoid cartilage. Cleithrum broad. Terminal phalanges of fingers knobbed. Finger phalangeal formula 2-2-3-3. Neural spines present on presacrals 2 and 3. Sacrum thin. Iliosacral articulation type IIA/B sensu Emerson (1979). Urostyle bearing a strong, straight dorsal ridge for almost its entire length; articulation bicondylar. Iliac shafts bearing weak dorsal crests; possessing a shallow oblique groove and lacking a dorsal tubercle. Leg bones lacking crests. Toe phalangeal formula 2-2-3-4-3.

Colouration in life based on recently collected material. The colouration in life is remarkably variable. Dorsal colouration is a range of brown tones, while ventral colouration contains elements of grey, black and beige. The most consistent element is a more or less bold, X-shaped marking on the back of the head, with the anterior arms of the X reaching onto the posterior of each eye, and the posterior arms reaching posteriorly to either join the dorsal pattern (typically fading) or remaining clearly distinct in the suprascapular region. This distinctive marking is present in the dorsal colouration also in juveniles (B. Ferrier, personal communication) and is clear in most adults, though it can sometimes be faded and not clearly distinct from the rest of the dorsal colouration. Posterior to this 'X', the dorsum is typically dark brown mottled with black, with generally clearly defined, subsymmetrical light brown markings distributed over the dorsum. In some specimens there are also black spots on the flanks. The lateral head is typically light brown (the colour of the dorsal markings), the supratympanic fold somewhat lighter and the tympanum containing a dark spot. In the inguinal region, black spots and light brown spots merge to form lines, but do not form a clearly defined, single black spot as in e.g. *P. alluaudi*. The dorsal thigh is mottled black with light brown, semi-regular spots, or with moderately defined dark and light crossbands, whereas the dorsal shank is a murky brown with irregular light brown spots or light brown with dark crossbands. The dorsal forelimb is as the shank. The ventral body is beige in base colour, with irregular dark brown mottling over the chin, which can be totally black in males, becoming less regular posteriorly over the abdomen and being free of maculations over the hip. The ventral shank is mostly beige, sometimes with dark spots. A light brown annulus is present before the tip of each finger.

Variation. Morphometric variation is given in Table 1. No remarkable variation in general morphology exists between the holotype and the newly collected material, except that the second finger is shorter than the fourth in newly collected specimens. Colouration variation has been discussed in the above section, and is merely more vivid and distinct in the new material than the holotype. Females lack the single subgular vocal sac that can be highly extensible (Fig. 8). MRSN A6189 and MRSN A6181 are slightly less pigmented than MRSN A6340 and the colouration of the proximal dorsal portion of the hindlimbs (mottled with black markings on a cream background colour) extends forward to lateral midbody and backwards to the tibiotarsal articulation on the ventral side of the hindlimb.

Natural history. Little information is available on this species. The eight new specimens were found active on the ground during the day or during the night, and this species was also found moderately active in dry conditions (after several days of no rainfall). In November 2013 one individual (not collected) was encountered along a drift fence during a rainy night. ZSM 980/2013 was encountered hidden in the leaf litter at the base of a *Ravenala madagascariensis* and ZSM 189/2016 was active in the leaf litter during the day. No information on the reproductive biology of this species is currently known. In 2007, a group of males were heard calling during rainfall. Individuals were calling from within the leaf litter or at the opening of a burrow, into which they can easily disappear upon detection. The holotype has a nearly intact millipede in its stomach (see Fig. 7). This is the only diet record currently available for this species.

Distribution and conservation status. *Plethodontohyla laevis* is known from (1) the type locality Sakana (whence no recent records for the species are known), (2) Betam-

pona Natural Reserve, (3) Marovato, (4) Anivorano Est, (5) Analalava-Foulpointe and (6) the Réserve Privée (RP) d'Ambodiriana (only photographic records are available from this locality) (Figs 1–3). All these sites are distributed at low altitudes in the central- to North-East of Madagascar. Altitudinal distributional range reaches from sea level to ca. 700 m a.s.l.. Due to the severe habitat degradation of the lowland rainforest in the northeast of Madagascar it is likely that the species is locally extinct at its type locality. Surveys in Zahamena Natural Reserve so far failed to report this species, but a more thorough investigation of the area is required to confirm the presence or absence of this species in that area. As noted above, the record of the species from the central highland (Ankazobe) is dubious and must be confirmed by further fieldwork in this area and/or examination of the material cited by Blommers-Schlösser (1975).

The species occurs at least in two protected areas, where it seems to be a relatively abundant although it is a species with secretive habits. Nevertheless, its distribution is highly fragmented, its extent of occurrence is quite limited (minimum convex polygon = 9770.92 km^2) and it is threatened by on-going habitat destruction. These factors (range under 20,000 km^2, severely fragmented distribution and on-going habitat destruction) qualify *P. laevis* as Vulnerable under criterion B1ab(iii) of the IUCN Red List (IUCN 2012).

Acoustic repertoire. Advertisement calls were recorded from a single male (MRSN A6340) at Betampona (Maintimbato: 17°53'35.50"S, 049°13'41.30"E, 283 m a.s.l.) on 18 November 2007, at 22:30 h at an air temperature of 21 °C (Rosa et al. 2011, track #50) (Fig. 8, Table 3). Each call consisted of a single loud note repeated after long, regular intervals, starting as unharmonious sound, but being tonal for most of its duration. They were slightly frequency-modulated in their tonal part and lasted 391–422 ms (407 ± 12.7, n = 4). We recorded one inter-call interval of 47 s. The fundamental frequency of the tonal part was 0.89–1.40 kHz with a dominant frequency band (frequency containing the greatest sound energy) between 1.82–2.53 kHz. Up to 10 harmonics were visible on the spectrogram and no attenuation of any of the harmonics was observed. The call of *Plethodontohyla laevis* is overall quite similar to the other species of this genus, and also members of the genus *Rhombophryne* (e.g. Lambert et al. 2017), but seems to have a lower repetition rate. Although we recorded only one of these long inter-call intervals, the recording was made on a rainy night, with more males calling simultaneously, all with long inter-call intervals.

Plethodontohyla alluaudi (Mocquard, 1901)

Figs 2c, d, 4a, 6, 9, Suppl. materials 1, 3, 6

Remarks. Sequences of this species have been referred to as *Plethodontohyla bipunctata* Andohahela by Wollenberg et al. (2008), Vieites et al. (2009), Perl et al. (2014) and Scherz et al. (2016a). Blommers-Schlösser (1975) referred to a specimen from Ampasinambo (20°31'25.0"S, 048°01'13.7"E) as *P. brevipes*, but later corrected this to *P. alluaudi* (Blommers-Schlösser and Blanc 1991). This locality is between the distributions of *P. alluaudi* (as refined here) and *P. laevis*, and we therefore consider this record uncertain until the specimen (ZMA 6689) has been re-examined.

Identity and redefinition. The original description of *Dyscophus alluaudi* is based on a single specimen of 47.4 mm SVL from the generic locality 'Fort Dauphin'. After the examination and comparison of the type material with recently collected material in south-eastern Madagascar close to the type locality of *Dyscophus alluaudi*, we here reassign this species to the genus *Plethodontohyla*. We therefore re-describe and redefine *Plethodontohyla alluaudi* based on the holotype (including its osteology via micro-CT scanning), on the holotype of *P. laevis tsianovohensis* and the recently collected material from Andohahela, Tsitongambarika and Sainte Luce.

Holotype. MNHN 1901.235, an adult female collected by M. Alluaud in 'Fort Dauphin'.

Referred material. MNHN 1936.0047, holotype of *P. laevis tsianovohensis*, an adult female collected by R. Heim between 1934 and 1935 in Tsianovoha, East Madagascar. ZSM 89/2004 (FGZC 161), an unsexed adult individual (DNA sequenced and included in Wollenberg et al. 2008: Accession number EU341068), collected by F. Glaw, M. Puente, M. Thomas and R. Randrianiaina on 31 January 2004 at Andohahela, (between Isaka-Ivondro and Eminiminy; 24°45'00"S, 046°51'00"E, ca. 230 m a.s.l.), Toliara Province, south-eastern Madagascar; UADBA-A 27994 (FGZC 160), an unsexed adult individual, collected by F. Glaw, M. Puente, M. Thomas and R. Randrianiaina on 31 January 2004 at Andohahela (between Isaka-Ivondro and Eminiminy; 24°45'00"S, 046°51'00"E, ca. 230 m a.s.l.), Toliara Province, south-eastern Madagascar; MRSN uncatalogued (FAZC 15423), unsexed adult individual (ethanol-fixed and DNA sequenced), collected by F. Andreone and G.M. Rosa on 29 February 2012 at Tsitongambarika Forest Reserve (Anosyenne Chain; 24°33'32.10"S, 047°11'24.90"E, 32 m a.s.l.); UADBA-A 62219, an unsexed adult individual, collected by S. Megson on 22 July 2013 at Sainte Luce (24°47'12"S, 047°09'45"E, ca. 19 m a.s.l.), Toliara Province, south-eastern Madagascar; UADBA-A 62224, an unsexed juvenile individual, collected by S. Megson on 17 July 2013 at Sainte Luce (24°46'87"S, 047°10'24"E, ca. 7 m a.s.l.), Toliara Province, south-eastern Madagascar.

Diagnosis (see also Tables 1, 5 and Figs 2, 4, 6, 9). A large microhylid belonging to the subfamily Cophylinae, with connected lateral metatarsalia, short forelimbs (FORL/SVL 0.47–0.58), short hindlimbs,

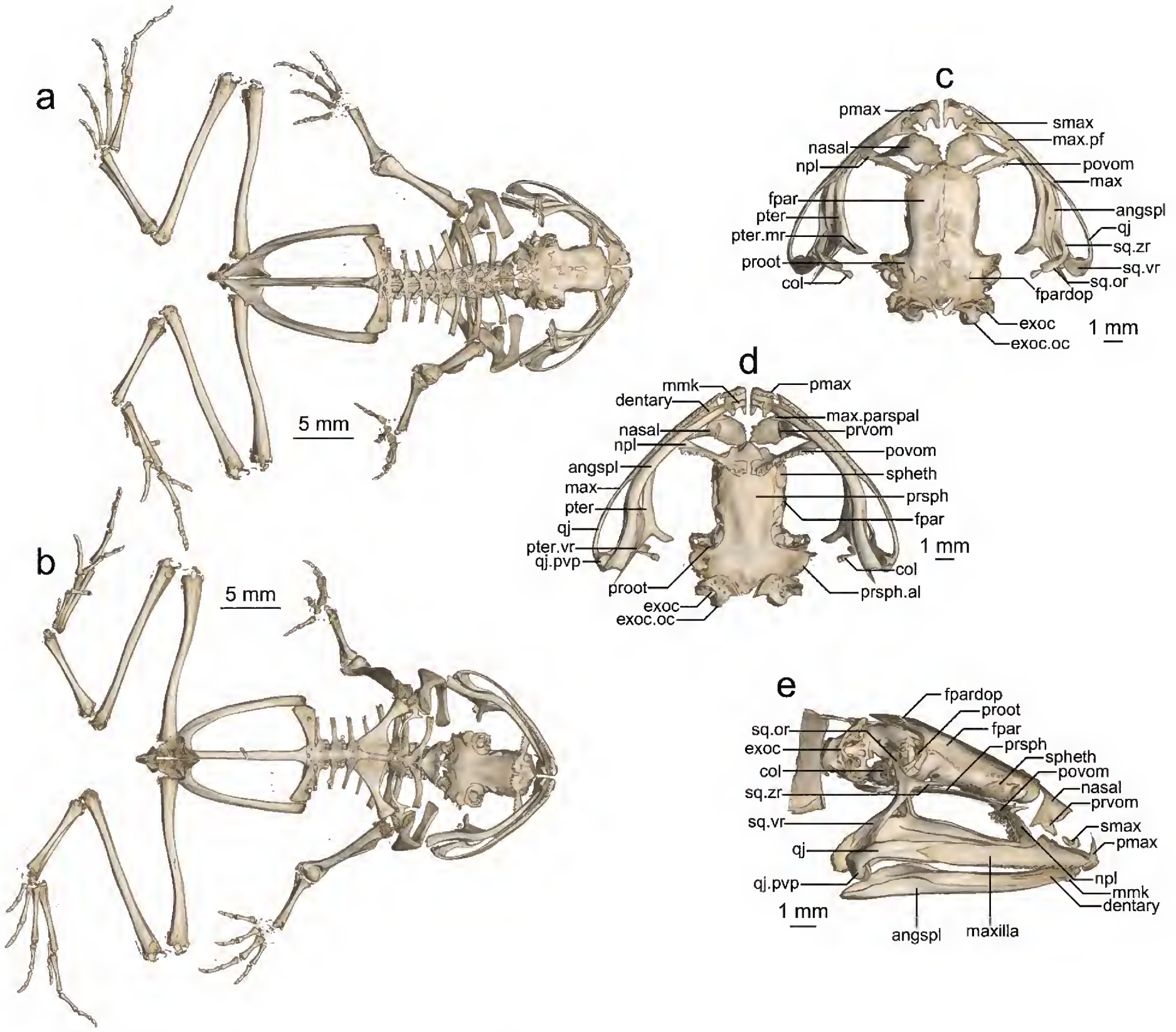

Figure 9. The skeleton of *Plethodontohyla alluaudi* (MNHN 1901.235) rendered via micro-CT scanning. (**a**–**b**) Full skeleton in (**a**) dorsal and (**b**) ventral view. (**c**–**e**) Skull in (**c**) dorsal, (**d**) ventral and (**e**) lateral view. Abbreviations are as in Fig. 7. For a 3D rotational model, see Suppl. material 1.

tibiotarsal articulation reaching the insertion of the arms, inner metatarsal tubercle present, maxillary and vomerine teeth present, clavicle absent or highly reduced, knob-shaped terminal phalanges and males with a single subgular vocal sac; therefore attributed to the genus *Plethodontohyla* (see Appendix A of Scherz et al. 2016a). The attribution to the genus *Plethodontohyla* is also supported by phylogenetic molecular evidence from newly collected material (see Fig. 5). The species is characterised by the following suite of characters: (1) moderately large size (SVL 28.8–58.0 mm); (2) HW/HL 1.67–1.85; (3) FORL/SVL 0.47–0.58; (4) HIL/SVL 1.25–1.47; (5) TIBL/SVL 0.34–0.39; (6) rounded snout tip; (7) toe tips not enlarged; (8) finger tips not enlarged; (9) knob-shaped terminal phalanges of the fingers and toes; (10) smooth dorsal skin; (11) absence of a distinct dorsolateral colour border; (12) presence of a supratympanic fold; (13) presence of a bold white-bordered 'X' marking on head; (14) tibiotarsal articulation reaching the insertion of the arm; (15) TD/ED 0.33–0.66. Furthermore, the species is separated from all nominal taxa in this genus by an uncorrected pairwise distance of at least 5.6% (comparison with *P. tuberata*; genetic distance of 5.8% with *P. laevis*). The genetic distance with *P.* sp. Ca01 is 2.9%.

Plethodontohyla alluaudi may be distinguished from other members of the genus *Plethodontohyla* as follows: from *P. inguinalis*, *P. notosticta*, *P. guentheri*, *P. mihanika* and *P. fonetana* by non-expanded terminal digits (*vs.* moderately to strongly expanded) and by its knob-shaped terminal phalanges of the fingers and toes (vs. T- or Y-shaped) and from all these species except *P. fonetana* by the absence of a dorsolateral colour border (present in all of these species but only some specimens of *P. inguinalis*). It also differs from *P. notosticta*, *P. guentheri* and *P. mihanika* by having a rounded snout

tip (*vs.* generally pointed); from *P. ocellata*, *P. bipunctata*, *P. brevipes*, *P. inguinalis* and *P. tuberata* by smooth skin (*vs.* granular or tubercular); from *P. inguinalis*, *P. notosticta*, *P. guentheri* and *P. mihanika* by the presence of a supratympanic fold running from the posterior border of the eye backward until the forelimb (*vs.* absence); from all species of *Plethodontohyla* except *P. laevis* and *P.* sp. Ca01 by the presence of a bold white-bordered 'X' marking on the head (*vs.* absence); from *P. laevis*, *P.* sp. Ca01, *P. ocellata*, *P. inguinalis*, *P. notosticta*, *P. guentheri*, *P. fonetana* and *P. mihanika* by a tibiotarsal articulation reaching the insertion of the arms (*vs.* see Table 5); and from *P. brevipes* (n = 6) by a generally wider head (HW/HL 1.67–1.85 *vs.* 1.53–1.71, Mann-Whitney U-test, $P = 0.032$), a generally smaller tympanum (TD/ED 0.33–0.66 *vs.* 0.60–0.79, Mann-Whitney U-test, $P = 0.025$), tendency toward larger relative hand size (HAL/SVL 0.23–0.28 *vs.* 0.21–0.24, Mann-Whitney U-test, $P = 0.051$), larger inner metatarsal tubercle (IMTL/FOL 0.13–0.17 *vs.* 0.09–0.13) and presence of a bold 'X' marking on the head (*vs.* absence).

Plethodontohyla laevis and *P.* sp. Ca01 are morphologically the most similar species to *P. alluaudi*. *Plethodontohyla alluaudi* can be distinguished from *P. laevis* by frequent presence of inguinal spots (*vs.* general absence), generally larger tympanum size (TD/ED 0.33–0.66 [0.53–0.66 for three of the four examined specimens] *vs.* 0.33–0.52) and tendency toward larger relative hand size (HAL/SVL 0.23–0.28 *vs.* 0.21–0.25, Mann-Whitney U-test, $P = 0.085$).

Re-description (based on MNHN 1901.235). Specimen in relatively good state of preservation (Figs 2, 6, 9). A cross-shaped incision made over the pectoral girdle, a lateral incision on the left side and a number of incisions on the lower back. A strong transverse fold is present at the posterior head, certainly a fixation artefact. SVL 47.4 mm (for other measurements, see Table 1). Body large and robust; head much wider than long (HW/HL 1.85) and almost as wide as body; snout rounded in dorsal and lateral view; nostrils directed laterally, slightly protuberant, nearer to tip of snout than to eye; canthus rostralis distinct, concave; loreal region concave, oblique; tympanum slightly distinct, rounded, TD/ED 0.53; supratympanic fold from eye to shoulder distinct and curved; tongue ovoid, very broad, posteriorly free and not notched; mandible damaged at the midline so that the two halves are distinguishable externally; maxillary teeth present; vomerine teeth distinct, forming oblique curved rows posterior to choanae, laterally approaching the maxillae and medially almost in contralateral contact; choanae ovoid. Arms robust, fingers bearing marked single subarticular tubercles and hands bearing indistinct outer metacarpal tubercles; large, protruding inner metacarpal tubercle; fingers without webbing; relative length of fingers 1<2<4<3, fourth finger slightly longer than second; finger disks not enlarged; nuptial pads absent. Hindlimbs robust; tibiotarsal articulation reaching the insertion of the arm when hindlimb adpressed along body; TIBL/SVL 0.34; lateral metatarsalia connected; distinct inner and less distinct outer metatarsal tubercles present; only traces of webbing between toes; relative length of toes 1<2<5<3<4; third toe distinctly longer than fifth. Skin on dorsum smooth; supratympanic fold whitish. Colour of iris indistinguishable.

Colouration. After over a century in preservative, the colouration is strongly faded, and several details of the pattern originally illustrated by Mocquard (1901) are only barely distinguishable. The base colouration of the whole specimen is cream-brown. Large dark brown markings in the inguinal region remain, as do oblique dark brown bars on the anterior thigh and faint brown spots on the posterior thigh. A faint trace of the large X-shaped marking on the posterior head is present only as the outlines of this shape. The ventral skin is translucent cream, and muscles are visible through it. No other traces of colouration remain. The colouration in life of this specimen is not known.

Osteology. In the following, we describe notable and important diagnostic characters of *Plethodontohyla alluaudi* based on MNHN 1901.235, MNHN 1936.47 and ZSM 89/2004 (Fig. 6). PDF-embedded 3D models of these skeletons are provided as Suppl. materials 1, 3 and 6.

Ossification is variable, but lowest in ZSM 89/2004 where the knees and carpals are not visible. Vomerine teeth anteriorly convex, with a distinct angle in MNHN 1936.47 not present in the other two specimens, covering the whole postchoanal vomer, separated medially by a small gap. Palatine processes of premaxilla subequal in length, the medial process thinner than the lateral process. Prechoanal vomer flat and triradiate, the lateral ramus around its midpoint, but weak or missing in MNHN 1936.47. Nasals large and broad, not in contact with other bones. Sphenethmoid laterally closed, brain case of ZSM 89/2004 and MNHN1901.235 with some internal mineralisation. Posterior ramus of pterygoid extremely long and broad. Strong transverse ridge across posterior of frontoparietals most raised at its lateral extremities, strongly descending lateral flange of frontoparietal. The right coracoid of MNHN 1901.235 is fractured mid-way along its length. Clavicles are present only in MNHN 1901.235, where they are reduced to thin slivers. The coracoid possesses a strong notch for the attachment of the procoracoid cartilage. Cleithrum broad. Terminal phalanges of fingers knobbed. Finger phalangeal formula 2-2-3-3. Neural spines present on presacrals 2 and 3. Sacrum relatively thin, broadening laterally. Iliosacral articulation type IIA/B sensu Emerson (1979). Urostyle bearing a strong, straight dorsal ridge for almost its entire length; articulation bicondylar. Iliac shafts bearing weak dorsal crests; possessing a shallow oblique groove and lacking a dorsal tubercle. Leg bones lacking crests. Toe phalangeal formula 2-2-3-4-3.

Table 5. Morphological variation in the analysed specimens of *Plethodontohyla* spp. Abbreviations not identified in the text: TT, Toe Tips (1, not enlarged, 2, enlarged); FT, Finger Tips (1, not enlarged, 2, enlarged); TP, Terminal Phalanges (K, knob-shaped, T, T-shaped, Y, Y-shaped); DDL, Dorsolateral Line, a narrow white dorsolateral line delimiting a sharp difference between the dorsal colouration and the uniformly dark flanks, extending from the tip of the snout backward until the inguinal region (+, presence, - absence, (+), not always present); Sk, Skin (1, smooth, 2, granular, 3, with tubercles); RID, Ridge, supratympanic dermal fold (+, presence, - absence); X, bold 'X' marking on the head between the eye bordered by a thin while line (+, presence, - absence); DDF, Dorsal Dermal Folds, two symmetrical and concave thin dorsal folds (+, presence, - absence); TTA, Tibiotarsal Articulation (1, reaching the tympanum, 2, reaching the insertion of the arms, 3, reaching the eye, 4, extending beyond the eye, * at least); ST, Snout tip (1, rounded, 2, pointed).

ID code	Genus	Species	Locality	Sex	Status	TT	FT	TP	DLL	SK	RID	X	DDF	TTA	ST
SMF 4286	*Phrynocara*	*laeve*	**Sakana**	**F**	**HT**	1	1	K	–	1	+	+	–	n/a	1
MRSN A6189	*Plethodontohyla*	*laevis*	Betampona	F	–	1	1	K	–	1	+	+	–	1*	1
MRSN A6181	*Plethodontohyla*	*laevis*	Betampona	F	–	1	1	K	–	1	+	+	–	1*	1
MRSN A6340	*Plethodontohyla*	*laevis*	Betampona	M	–	1	1	K	–	1	+	+	–	1*	1
ZSM 980/2013	*Plethodontohyla*	*laevis*	Betampona	M	–	1	1	K	–	1	+	+	–	1*	1
MRSN A6674	*Plethodontohyla*	*laevis*	Marovato	F	–	1	1	K	–	1	+	+	–	3	1
MRSN A6787	*Plethodontohyla*	*laevis*	Anivorano Est	M	–	1	1	K	–	1	+	+	–	1*	1
MNHN 1901.235	*Dyscophus*	*alluaudi*	**Fort Dauphin**	**F**	**HT**	1	1	K	–	1	+	+	–	2	1
MNHN 1936.47	*Plethodontohyla*	*laevis tsianovohensis*	**Tsianovoha**	**F**	**HT**	1	1	K	–	1	+	+	–	n/a	1
ZSM 89/2004	*Plethodontohyla*	*alluaudi*	Andohahela	–	–	1	1	K	–	1	+	+	–	2*	1
FAZC 15423	*Plethodontohyla*	*alluaudi*	Tsitongambarika (Anosyenne Chain)	–	–	1	1	K	–	1	+	+	–	n/a	1
UADBA-A 27994 (FGZC 160)	*Plethodontohyla*	*alluaudi*	Andohahela	–	–	1	1	K	–	1	+	+	–	n/a	1
ZCMV 555	*Plethodontohyla*	sp. Ca01	Ambatolahy	–	–	1	1	n/a	–	n/a	+	+	–	n/a	1
ZSM 855/2006	*Plethodontohyla*	sp. Ca01	Imaloka	–	–	1	1	K	–	1	+	+	–	1	1
ZSM 856/2006	*Plethodontohyla*	sp. Ca01	Imaloka	–	–	1	1	K	–	1	+	+	–	1	1
MRSN A3221	*Plethodontohyla*	*tuberata*	Manjakatompo	–	–	1	1	K	–	3	+	–	–	2	1
MRSN A2859	*Plethodontohyla*	*ocellata*	Ranomafana	–	–	1	1	K	–	2	+	–	–	1*	1
ACZCV 0101	*Plethodontohyla*	*ocellata*	Betampona	–	–	1	1	K	–	2	+	–	+	1*	1
ZSM 5204/2005	*Plethodontohyla*	*bipunctata*	Andohahela	–	–	1	1	K	–	2	+	–	+	2*	1
ZSM 854/2006	*Plethodontohyla*	*brevipes*	Imaloka	–	–	1	1	K	–	2	+	+	+	2	1
MRSN A2476	*Plethodontohyla*	*inguinalis*	Kalambatritra	–	–	2	2	T	(+)	2	–	–	–	3*	1
MRSN A5653	*Plethodontohyla*	*notosticta*	Sahavontsira	–	–	2	2	T	+	1	–	–	–	3	2
ZSM 61/2005	*Plethodontohyla*	*guentheri*	Marojejy	F	HT	2	2	T	+	1	–	–	–	3	2
ZSM 123/2006	*Plethodontohyla*	*fonetana*	Tsingy de Bemaraha	F	HT	2	2	Y	–	1	+	–	+	1	1
ZSM 1087/2001	*Plethodontohyla*	*mihanika*	Andasibe	M	PT	2	2	T	+	1	–	–	–	4*	2

Colouration in life based on recently collected material. Dorsally a greenish brown colouration, with a distinct dark brown 'X' marking on the posterior head, with the anterior arms of the X over the eyes, and the posterior arms reaching the suprascapular region, bordered with a fine, light brown line. The dorsal colouration is flecked with white, with especially large white spots over the ends of the iliac shafts. A large blackish inguinal spot bordered with a white line is present. The flank colouration is marbled brown with white spots. The supratympanic fold is whitish, and forms a weak colour border between the dorsal colouration and the richer brown lateral head. The arm is anteriorly darker brown, almost blackish. The dorsal thigh is also darker brown, but not blackish. The ventral colouration is translucent and thus peach over the chin and pinkish over the abdomen, invaded on the sides behind the pectoral girdle by brown flecks, but not meeting medially. The ventral thighs are also pinkish, anteriorly and posteriorly with brown flecks. A yellow-cream annulus is present before the tip of each finger.

Variation. Morphometric variation is given in Table 1. The holotype and MNHN 1936.47 are considerably larger than the newly collected material. MNHN 1936.47 apparently lacks inguinal spots, but its colouration is faded to the point where these might have disappeared. UADBA-A 27994 has a considerably smaller tympanum diameter than the other specimens (TD/ED 0.34 *vs.* 0.53–0.66). The holotype has the shortest forelimbs (FORL/SVL 0.47 *vs.* 0.53–0.58) and hindlimbs (HIL/SVL 1.25 *vs.* 1.41–1.47).

Natural history. At Andohahela specimens were found in the leaf litter of rainforest during the day. In Anosyenne Chain (Tsitongambarika) the specimen was found at night under leaf litter not far from the edge of the forest patch. Males from the Sainte Luce population have been heard calling in large choruses from hidden positions after heavy rainfall during the day and night, both inside the forest and in more open areas. During such periods choruses consist of many dozens of individuals. Individuals are extremely hard to detect and cease calling if they notice any distur-

bance, retreating into their burrows and hiding places in the forest floor. Individuals may be seen travelling above ground on rainy nights, particularly in areas in close proximity to small water bodies such as shallow forest streams, the margins of swamps and even in ephemeral mud puddles. At Sainte Luce, one adult specimen was found during the day, in light rainfall, underneath a log in littoral forest; and a juvenile specimen was found during the day in dry weather in severely degraded habitat, inside the shell of a deceased large land snail. The body of this individual became bloated during initial handling. In mature forest, adult individuals have also been observed beneath dead *Pandanus* leaves, under dead fallen trees and dead logs. No feeding or reproductive behaviour has been observed.

Distribution and conservation status. *Plethodontohyla alluaudi* is known from (1) the type locality 'Fort Dauphin' (or Tolagnaro, whence there are no recent records for the species, although this collection site was probably a very generic one), (2) Andohahela National Park, (3) Tsitongambarika Forest Reserve, (4) Sainte Luce and (5) Tsianovoha. Observations in Sainte Luce have been made in two of the largest forest fragments (fragments S7 and S9). All these sites are distributed at low altitudes in the East or south-eastern of Madagascar. Altitudinal distributional range extends from sea level to ca. 230 m a.s.l.. It is not clear where the type locality of this species is, but if it was a forest in the vicinity of Tolagnaro, then it is quite possible that it has been extirpated due to forest destruction there. Surveys in nearby Nahampoana and Mandena forests have so far failed to report this species, but a more thorough investigation of the area is required to confirm the presence or absence of this species in that area.

The species occurs at least in three protected areas, where it seems to be a relatively abundant although it has very secretive habits. Nevertheless, its distribution is highly fragmented, its extent of occurrence is quite limited (minimum convex polygon = 5372.81 km^2) and it is threatened by on-going habitat destruction. As for *P. laevis*, it therefore qualifies as Vulnerable under IUCN Red List criterion B1ab(iii) (IUCN 2012).

Acoustic repertoire. Advertisement calls were recorded from a chorus of males at Sainte Luce (24°46'51.72"S, 047°10'13.14"E; 10 m a.s.l.) on 30 June 2015, around 15:00 h at an air temperature of 24 °C (Table 3). This is a preliminary acoustic description due to the low quality of the available recordings (background noise and overlapping of several calls), which has compromised the obtainment of some parameters (Table 3). The following parameters could be assessed: the call consisted of a single note (soft whistle) repeated after apparently regular intervals. Calls lasted 320–560 ms (478 ± 109, n = 4). The dominant frequency seems to range from 1.4 to 2.1 kHz, however these values should be interpreted with caution since the distance from the calling individuals might complicate the distinction of harmonics. A more accurate bioacoustic analysis will be needed when new data are available.

Taxonomic challenges in cophyline taxonomy

The resurrection of *Plethodontohyla laevis* and transfer of *Dyscophus alluaudi* from *Rhombophryne* to the genus *Plethodontohyla* brings this genus to 11 nominal species (not including the dubious *P. angulifera* Werner, 1903), and *Rhombophryne* down to 18. At present, only two other candidate species are known from *Plethodontohyla* (one from Tsaratanana and *P.* sp. Ca01 from Ambatolahy and Imaloka, which might be conspecific with *P. alluaudi*), but preliminary results suggest that the undescribed diversity in this genus is still widely unexplored and it will probably wind up being as great as it was for *Rhombophryne* (Vieites et al. 2009, Perl et al. 2014), with at least four additional undescribed species still awaiting formal description (A. Crottini et al. unpublished data). With this much-needed clarification of these historical names, we are now finally able to make larger progress on the taxonomy of this genus.

The cophyline microhylids are a case study of the need for an integrative taxonomic approach (Dayrat 2005). Taxonomic action like the synonymisation of *Plethodontohyla laevis* with *P. alluaudi* was made on the basis of external morphological differences and the state of the pectoral girdle, but could not take into account other aspects of skeletal morphology, nor could it account for genetics, as it was done before micro-CT and genetic methods were widely available, and based on single individuals (Blommers-Schlösser and Blanc 1991). Our approach, combining external morphology and osteology without damaging the type specimens of old and recently collected material, and the availability of genetic samples from several populations in Madagascar largely resembling the holotypes of *P. laevis* and *P. alluaudi*, provides a more robust hypothesis on the identities of these species than has been possible in the past.

Cophyline microhylids are still the least understood amphibians of Madagascar and the recent major advances in cophyline taxonomy would not have been possible without the collection of new material. However, more extensive and widespread collection of specimens from across Madagascar is still needed to fully characterize species distribution ranges and clarify their systematics. At least two new genera are still in need of description (Scherz et al. 2016a), basal relationships among the different genera are still poorly resolved, and even at the intra-generic level there are still several unresolved relationships (Scherz et al. 2016a). The intra-genus relationships in *Plethodontohyla* are no exception to this. Although the monophyly of the genus is now relatively well established (Andreone et al. 2005, Wollenberg et al. 2008, Scherz et al. 2016a), one study (Pyron and Wiens 2011) has found them to be polyphyletic, with one poorly supported group (containing *P. inguinalis*, *P. tuberata*, *P. bipunctata*, *P. brevipes* and *P. ocellata*) found to be the sister clade of all cophylines but *Anodonthyla*, and the other group (although with no support) composed of *P. mihanika*, *P. fonetana*, *P. guentheri* and *P. notosticta*, falling sister to the genus *Cophyla*. The former group

would have the name *Mantipus* Peters, 1883 available for it, while the latter would retain the name *Plethodontohyla* Boulenger, 1882. On the other hand, if the species with T- or Y-shaped terminal phalanges would result in a monophyletic group (i.e. if *P. inguinalis* were to move to the group containing *P. notosticta*, *P. fonetana*, *P. guentheri* and *P. mihanika*), the oldest available name for the terrestrial species with knobbed phalanges would be *Phrynocara*. The morphology of the genus combined with the latest available multi-gene phylogeny (Scherz et al. 2016a) suggests however that this group is an eclectic but monophyletic radiation, consisting of several species groups. However, due to the variable external morphology, ecological plasticity, conflicting phylogenetic studies and the availability of many old names and synonyms, an in depth phylogenetic analysis that will assess the species phylogenetic relationships and provide a taxonomic revision of the genus is needed.

Acknowledgments

We are grateful to the Malagasy authorities, in particular the Ministère de l'Environnement et des Forêts, for issuing research and export permits. We extend our thanks to Karen Freeman and Ingrid Porton of Madagascar Fauna and Flora Group. Fieldwork was financially supported by the Saint Louis Zoo's Field Research for Conservation program (FRC# 12-12) of the Wildcare Institute and Gondwana Conservation and Research. We thank Chantal Misandeau and Lauric Reynes for sharing their photographs of the amphibians of Ambodiriana. The Institute for the Conservation of Tropical Environments (ICTE-MICET) provided crucial logistic support. We are grateful to the teams of the Muséum National d'Histoire Naturelle de Paris (France), the Naturmuseum Senckenberg in Frankfurt am Main (Germany) and the Mention Zoologie et Biodiversité Animale, Université d'Antananarivo (Madagascar) for the loan of material pertaining to this paper. We thank the reviewers for their useful comments that significantly improved the manuscript. We are indebted to Miguel Vences for having provided three unpublished POMC sequences used in this work. This work was funded by Portuguese National Funds through FCT - Foundation for Science and Technology under the IF/00209/2014/CP1256/CT0011 Exploratory Research Project. Work of the authors over the past 25 years has been made possible by collaboration accords with the Université d'Antananarivo (Mention Zoologie et Biodiversité Animale) and with the Parc Botanique et Zoologique de Tsimbazaza.

References

AmphibiaWeb (2018) http://amphibiaweb.org/ [accessed on 23 January 2018]

Andreone F, Vences M, Vieites DR, Glaw F, Meyer A (2005) Recurrent ecological adaptations revealed through a molecular analysis of the secretive cophyline frogs of Madagascar. Molecular Phylogenetics and Evolution 34(2): 315–322. http://dx.doi.org/10.1016/j.ympev.2004.10.013

Blommers-Schlösser RMA (1975) Observations on the larval development of some Malagasy frogs, with notes on their ecology and biology (Anura: Dyscophinae, Scaphiophryninae and Cophylinae). Beaufortia 24(309): 7–26.

Blommers-Schlösser RMA, Blanc CP (1991) Amphibiens (première partie). Faune de Madagascar 75: 1–379.

Boettger O (1913) Reptilien und Amphibien von Madagascar, den Inseln und dem Festland Ostafrikas. In Voeltzkow A (Ed.) Reise in Ost-Afrika in den Jahren 1903–1905 mit Mitteln der Hermann und Elise geb. Heckmann-Wentzel-Stiftung. Wissenschaftliche Ergebnisse. Systematischen Arbeiten 3(4): 269–376. Stuttgart, E. Schweizerbart.

Boulenger GA (1882) Catalogue of the Batrachia Salientia & Ecaudata in the Collection of the British Museum. Second edition. Taylor and Francis, London.

Bruford MW, Hanotte O, Brookefield JFY, Burke T (1992) Single-locus and multilocus DNA fingerprint. In: Hoelzel AR (Ed.) Molecular Genetic Analysis of Populations: A Practical Approach. IRL Press, Oxford, 225–270.

Clement M, Posada D, Crandall KA (2000) TCS: a computer program to estimate gene genealogies. Molecular Ecology 9(10): 1657–1659. https://doi.org/10.1046/j.1365-294x.2000.01020.x

Darriba D, Taboada GL, Doallo R, Posada D (2012) jModelTest 2: more models. new heuristics and parallel computing. Nature Methods 9(8): 772–772. https://doi.org/10.1038/nmeth.2109

Dayrat B (2005) Towards integrative taxonomy. Biological Journal of the Linnean Society 85(3): 407–415. https://doi.org/10.1111/j.1095-8312.2005.00503.x

D'Cruze N, Köhler J, Vences M, Glaw F (2010) A new fat fossorial frog (Microhylidae: Cophylinae: *Rhombophryne*) from the rainforest of the Forêt d'Ambre Special Reserve, northern Madagascar. Herpetologica 66(2): 182–191. https://doi.org/10.1655/09-008R1.1

Emerson SB (1979) The ilio-sacral articulation in frogs: form and function. Biological Journal of the Linnean Society 11(2): 153–168. https://doi.org/10.1111/j.1095-8312.1979.tb00032.x

Frost DR, Grant T, Faivovich J, Bain RH, Haas A, Haddad CFB, De Sá RO, Channing A, Wilkinson M, Donnellan SC, Raxworthy CJ, Campbell JA, Blotto BL, Moler P, Drewes RC, Nussbaum RA, Lynch JD, Green DM, Wheeler WC (2006) The amphibian tree of life. Bulletin of the American Museum of Natural History 297: 1–370. https://doi.org/10.1206/0003-0090(2006)297[0001:TATOL]2.0.CO;2

Glaw F, Vences M (1992) A fieldguide to the amphibians and reptiles of Madagascar, 1st edition, Vences & Glaw Verlag, Köln, 335 pp.

Glaw F, Vences M (2007a) *Plethodontohyla guentheri*, a new montane microhylid frog species from northeastern Madagascar. Mitteilungen aus dem Museum für Naturkunde in Berlin, Zoologische Reihe 83(Suppl. 1): 33–39. https://doi.org/10.1002/mmnz.200600023

Glaw F, Vences M (2007b) A field guide to the amphibians and reptiles of Madagascar, 3rd edition. Vences & Glaw Verlag, Köln, 496 pp.

Glaw F, Köhler J, Bora P, Rabibisoa NHC, Ramilijaona O, Vences M (2007) Discovery of the genus *Plethodontohyla* (Anura: Microhylidae) in dry western Madagascar: description of a new species and biogeographic implications. Zootaxa 1577: 61–68. http://www.mapress.com/zootaxa/2007f/z01577p068f.pdf

Glaw F, Köhler J, Vences M (2010) A new fossorial frog, genus *Rhombophryne*, from Nosy Mangabe Special Reserve, Madagascar. Zoosystematics and Evolution 86(2): 235–243. https://doi.org/10.1002/zoos.201000006

Guibé J (1947) Contribution a l'etude du genre *Mantipus*. Mémoires de l'Institut Scientifique de Madagascar 1: 76–80.

Guibé J (1952) Recherches sur les batraciens de Madagascar. Mémoires de l'Institut Scientifique de Madagascar 7: 109–116.

Guibé J (1974) Batraciens nouveaux de Madagascar. Bulletin du Muséum national d'Histoire Naturelle Paris, 3rd series, 171: 1069–1192.

Guibé J (1975) Batraciens nouveaux de Madagascar. Bulletin du Muséum national d'Histoire Naturelle Paris, 3rd series, 323: 1081–1089.

Guibé J (1978) Les batraciens de Madagascar. Bonner zoologische Monographien 11: 1–140.

Hall TA (1999) BioEdit: a user-friendly biological sequence alignment editor and analysis program for Windows 95/98/NT. Nucleic Acids Symposium 41: 95–98. http://jwbrown.mbio.ncsu.edu/JWB/papers/1999Hall1.pdf

IUCN (2012) IUCN Red List Categories and Criteria: Version 3.1. IUCN, Gland, Switzerland and Cambridge, UK.

Kocher TD, Thomas WK, Meyer A, Edwards SV, Pääbo S, Villablanca FX, Wilson AC (1989) Dynamics of mitochondrial DNA evolution in mammals: amplification and sequencing with conserved primers. Proceedings of the National Academy of Sciences of the United States of America 86(16): 6196–6200. https://doi.org/10.1073/pnas.86.16.6196

Köhler J, Jansen M, Rodríguez A, Kok PJR, Toledo LF, Emmrich M, Glaw F, Haddad CFB, Rödel MO, Vences M (2017) The use of bioacoustics in anuran taxonomy: theory, terminology, methods and recommendations for best practice. Zootaxa 4251(1): 1–124. https://doi.org/10.11646/zootaxa.4251.1.1

Kumar S, Stecher G, Tamura K (2016) MEGA7: Molecular Evolutionary Genetics Analysis version 7.0 for bigger datasets. Molecular Biology and Evolution 33: 1870–1874. https://doi.org/10.1093/molbev/msw054

Lambert SM, Hutter CR, Scherz MD (2017) Diamond in the rough: a new species of fossorial diamond frog (*Rhombophryne*) from Ranomafana National Park, southeastern Madagascar. Zoosystematics and Evolution 93(1): 143–155. https://doi.org/10.3897/zse.93.10188

Librado P, Rozas J (2009) DnaSP v5: A software for comprehensive analysis of DNA polymorphism data. Bioinformatics 25(11): 1451–1452. https://doi.org/10.1093/bioinformatics/btp187

Mocquard MF (1895) Sur une collection de reptiles recueillis à Madagascar par M.M. Alluaud et Belly. Bulletin de la Société philomatique de Paris, ser. 8: 112–136.

Mocquard MF (1901) Note préliminaire sur une collection de reptiles et de batraciens recueillis par M. Alluaud dans le sud de Madagascar. Bulletin du Muséum national d'Histoire Naturelle, Paris 7: 251-256.

Noble GK, Parker HW (1926) A synopsis of the brevicipitid toads of Madagascar. American Museum Novitates 232: 1–21. http://hdl.handle.net/2246/4206

Palumbi S, Martin A, Romano S, McMillan WO, Stice L, Grabowski G (1991) The simple fools guide to PCR. Version 2.0. Department of Zoology and Kewalo Marine Laboratory, University of Hawaii, Honolulu, HI.

Parker HW (1934) A Monograph of the Frogs of the Family Microhylidae. Trustees of the British Museum, London.

Peloso PLV, Frost DR, Richards SJ, Rodrigues MT, Donnellan S, Matsui M, Raxworthy CJ, Biju SD, Lemmon EM, Lemmon AR, Wheeler WC (2016) The impact of anchored phylogenomics and taxon sampling on phylogenetic inference in narrow-mouthed frogs (Anura, Microhylidae). Cladistics 32(2): 113–140. https://doi.org/10.1111/cla.12118

Perl RGB, Nagy ZT, Sonet G, Glaw F, Wollenberg KC, Vences M (2014) DNA barcoding Madagascar's amphibian fauna. Amphibia-Reptilia 35(2): 197–206. https://doi.org/10.1163/15685381-00002942

Peters WCH (1883) Über *Mantipus* und *Phrynocara*, zwei neue Batrachiergattungen aus dem Hinterlasse des Reisenden J. M. Hildebrandt von Madagascar. Sitzungsberichte der Akademie der Wissenschaften Königlich Preussischen zu Berlin 1883: 165–168.

Pyron RA, Wiens JJ (2011) A large-scale phylogeny of Amphibia including over 2800 species, and a revised classification of extant frogs, salamanders, and caecilians. Molecular Phylogenetics and Evolution 61(2): 543–583. https://doi.org/10.1016/j.ympev.2011.06.012

Rakotoarison A, Glaw F, Vieites DR, Raminosoa NR, Vences M (2012) Taxonomy and natural history of arboreal microhylid frogs (*Platypelis*) from the Tsaratanana Massif in northern Madagascar, with description of a new species. Zootaxa 3563(1): 1–25. https://doi.org/10.5281/zenodo.215396

Rakotoarison A, Crottini A, Müller J, Rödel MO, Glaw F, Vences M (2015) Revision and phylogeny of narrow-mouthed treefrogs (*Cophyla*) from northern Madagascar: integration of molecular, osteological, and bioacoustic data reveals three new species. Zootaxa 3937(1): 61–89. https://doi.org/10.11646/zootaxa.3937.1.3

Rakotoarison A, Scherz MD, Glaw F, Köhler J, Andreone F, Franzen M, Glos J, Hawlitschek O, Jono T, Mori A, Ndriantsoa SH, Raminosoa Rasoamampionona N, Riemann JC, Rödel MO, Rosa GM, Vieites DR, Crottini A, Vences M (2017) Describing the smaller majority: Integrative taxonomy reveals twenty-six new species of tiny microhylid frogs (genus *Stumpffia*) from Madagascar. Vertebrate Zoology 67(3): 271–398.

Rambaut A, Drummond AJ (2007) Tracer v1.4. http://beast.bio.ed.ac.uk/Tracer [accessed 1 June 2011]

Ronquist F, Teslenko M, van der Mark P, Ayres DL, Darling A, Höhna S, Larget B, Liu L, Suchard MA, Huelsenbeck JP (2012) MrBayes 3.2: efficient Bayesian phylogenetic inference and model choice across a large model space. Systematic Biology 61(3): 539–542. https://doi.org/10.1093/sysbio/sys029

Rosa GM, Andreone F (2010) Bioacoustic data of the recently described *Boophis calcaratus* (Anura: Mantellidae: Boophinae), a cryptic treefrog from Eastern Madagascar. Zootaxa 2426: 61–64. http://www.mapress.com/zootaxa/2010/f/z02426p064f.pdf

Rosa GM, Noël J, Andreone F (2010) The advertisement call of *Mantidactylus aerumnalis* (Anura: Mantellidae), a terrestrial frog from the east coast of Madagascar. Salamandra 46(2): 98–100. http://www.salamandra-journal.com/index.php/home/contents/2010-vol-46/92-rosa-g-m-j-noel-f-andreone/file

Rosa GM, Márquez M, Andreone F (2011) The astonishing calls of the frogs of Betampona. Museo Regionale di Scienze Naturali di Torino, Torino, Italy.

Rosa GM, Andreone F, Crottini A, Hauswaldt JS, Noël J, Rabibisoa NH, Randriambahiniarime MO, Rebelo R, Raxworthy CJ (2012) The amphibians of the relict Betampona low-elevation rainforest, eastern Madagascar: an application of the integrative taxonomy approach to biodiversity assessments. Biodiversity and Conservation 21(6): 1531–1559. https://doi.org/10.1007/s10531-012-0262-x

Rosa GM, Crottini A, Noël J, Rabibisoa N, Raxworthy CJ, Andreone F (2014) A new phytotelmic species of *Platypelis* (Microhylidae: Cophylinae) from the Betampona Reserve, Eastern Madagascar. Salamandra 50(4): 201–214. http://www.salamandra-journal.com/index.php/home/contents/2014-vol-50/378-rosa-g-m-a-crottini-j-noel-n-rabibisoa-c-j-raxworthy-f-andreone/file.

Scherz MD, Ruthensteiner B, Vences M, Glaw F (2014) A new microhylid frog, genus *Rhombophryne*, from northeastern Madagascar, and a re-description of *R. serratopalpebrosa* using micro-computed tomography. Zootaxa 3860(6): 547–560. https://doi.org/10.11646/zootaxa.3860.6.3

Scherz MD, Rakotoarison A, Hawlitschek O, Vences M, Glaw F (2015a) Leaping towards a saltatorial lifestyle? An unusually long-legged new species of *Rhombophryne* (Anura, Microhylidae) from the Sorata massif in northern Madagascar. Zoosystematics and Evolution 91: 105–114. https://doi.org/10.3897/zse.91.4979

Scherz MD, Ruthensteiner B, Vieites DR, Vences M, Glaw F (2015b) Two new microhylid frogs of the genus *Rhombophryne* with superciliary spines from the Tsaratanana Massif in northern Madagascar. Herpetologica 71(4): 310–321. https://doi.org/10.1655/HERPETOLOGICA-D-14-00048

Scherz MD, Vences M, Rakotoarison A, Andreone F, Köhler J, Glaw F, Crottini A (2016a) Reconciling molecular phylogeny, morphological divergence and classification of Madagascan narrow-mouthed frogs (Amphibia: Microhylidae). Molecular Phylogenetics and Evolution 100: 372–381. https://doi.org/10.1016/j.ympev.2016.04.019

Scherz MD, Glaw F, Vences M, Andreone F, Crottini A (2016b) Two new species of terrestrial microhylid frogs (Microhylidae: Cophylinae: *Rhombophryne*) from northeastern Madagascar. Salamandra 52: 91–106. http://www.salamandra-journal.com/index.php/home/contents/2016-vol-52/566-scherz-m-d-f-glaw-m-vences-f-andreone-a-crottini/file

Scherz MD, Hawlitschek O, Andreone F, Rakotoarison A, Vences M, Glaw F (2017) A review of the taxonomy and osteology of the *Rhombophryne serratopalpebrosa* species group (Anura: Microhylidae) from Madagascar, with comments on the value of volume rendering of micro-CT data to taxonomists. Zootaxa 4273: 301–340. https://doi.org/10.11646/zootaxa.4273.3.1

Stephens M, Smith NJ, Donnelly P (2001) A new statistical method for haplotype reconstruction from population data. American Journal of Human Genetics 68: 978–989. https://doi.org/10.1086/319501

Templeton AR, Crandall KA, Sing CF (1992) A cladistic analysis of phenotypic associations with haplotypes inferred from restriction endonuclease mapping and DNA sequence data. III. Cladogram estimation. Genetics 132(2): 619–633. https://www.ncbi.nlm.nih.gov/pubmed/1385266

Trueb L (1968) Cranial osteology of the hylid frog, *Smilisca baudini*. University of Kansas Publications, Museum of Natural History 18: 11–35.

Trueb L (1973) Bones, frogs, and evolution. In: Vial JL (Ed.) Evolutionary biology of the anurans: Contemporary research on major problems. University of Missouri Press, USA, 65–132.

Vallan D, Glaw F, Vences M (2005) The calls of *Pletodontohyla inguinalis* from eastern Madagascar (Amphibia, Microhylidae). Spixiana 28(1): 91–93.

Vences M, Raxworthy CJ, Nussbaum RA, Glaw F (2003) New microhylid frog (*Plethodontohyla*) from Madagascar, with semiarboreal habits and possible parental care. Journal of Herpetology 37(4): 629–636. https://doi.org/10.1670/258-01A

Vences M, Thomas M, Bonett RM, Vieites DR (2005) Deciphering amphibian diversity through DNA barcoding: chances and challenges. Philosophical Transaction of the Royal Society of London Series B 360(1462): 1859–1868. https://doi.org/10.1098/rstb.2005.1717

Vences M, Köhler J, Crottini A, Glaw F (2010) High mitochondrial sequence divergence meets morphological and bioacoustic conservatism: *Boophis quasiboehmei* sp. nov., a new cryptic treefrog species from south-eastern Madagascar. Bonn zoological Bulletin 57(2): 241–255. https://www.yumpu.com/en/document/view/23181939/high-mitochondrial-sequence-divergence-meets-morphological-and-

Vieites DR, Min MS, Wake DB (2007) Rapid diversification and dispersal during periods of global warming by plethodontid salamanders. Proceedings of the National Academy of Sciences of the United States of America 104(50): 19903–19907. https://doi.org/10.1073/pnas.0705056104

Vieites DR, Wollenberg KC, Andreone F, Köhler J, Glaw F, Vences M (2009) Vast underestimation of Madagascar's biodiversity evidenced by an integrative amphibian inventory. Proceedings of the National Academy of Sciences of the United States of America 106(20): 8267–8272. https://doi.org/10.1073/pnas.0810821106

Wollenberg KC, Vieites DR, van der Meijden A, Glaw F, Cannatella DC, Vences M (2008) Patterns of endemism and species richness in Malagasy cophyline frogs support a key role of mountainous areas for speciation. Evolution 62(8): 1890–1907. https://doi.org/10.1111/j.1558-5646.2008.00420.x

Supplementary material 1

PDF-embedded 3D model of the skeleton of *Plethodontohyla alluaudi* holotype (MNHN 1901.235)

Authors: Adriana Bellati, Mark D. Scherz, Steven Megson, Sam Hyde Roberts, Franco Andreone, Gonçalo M. Rosa, Jean Noël, Jasmin E. Randrianirina, Mauro Fasola, Frank Glaw, Angelica Crottini

Data type: Adobe PDF file

Link: https://doi.org/10.3897/zse.94.14698.suppl1

Supplementary material 2

PDF-embedded 3D model of the skeleton of *Plethodontohyla laevis* holotype (SMF 4286)

Authors: Adriana Bellati, Mark D. Scherz, Steven Megson, Sam Hyde Roberts, Franco Andreone, Gonçalo

M. Rosa, Jean Noël, Jasmin E. Randrianirina, Mauro Fasola, Frank Glaw, Angelica Crottini
Data type: Adobe PDF file
Copyright notice: This dataset is made available under the Open Database License (http://opendatacommons.org/licenses/odbl/1.0/). The Open Database License (ODbL) is a license agreement intended to allow users to freely share, modify, and use this Dataset while maintaining this same freedom for others, provided that the original source and author(s) are credited.
Link: https://doi.org/10.3897/zse.94.14698.suppl2

Supplementary material 3

PDF-embedded 3D model of the skeleton of *Plethodontohyla laevis tsianovohensis* holotype (MNHN 1936.47)

Authors: Adriana Bellati, Mark D. Scherz, Steven Megson, Sam Hyde Roberts, Franco Andreone, Gonçalo M. Rosa, Jean Noël, Jasmin E. Randrianirina, Mauro Fasola, Frank Glaw, Angelica Crottini
Data type: Adobe PDF file
Copyright notice: This dataset is made available under the Open Database License (http://opendatacommons.org/licenses/odbl/1.0/). The Open Database License (ODbL) is a license agreement intended to allow users to freely share, modify, and use this Dataset while maintaining this same freedom for others, provided that the original source and author(s) are credited.
Link: https://doi.org/10.3897/zse.94.14698.suppl3

Supplementary material 4

PDF-embedded 3D model of the skeleton of ZSM 3/2002, a specimen of an undescribed *Rhombophryne* species formerly called *Rhombophryne* '*alluaudi*'

Authors: Adriana Bellati, Mark D. Scherz, Steven Megson, Sam Hyde Roberts, Franco Andreone, Gonçalo M. Rosa, Jean Noël, Jasmin E. Randrianirina, Mauro Fasola, Frank Glaw, Angelica Crottini
Data type: Adobe PDF file
Copyright notice: This dataset is made available under the Open Database License (http://opendatacommons.org/licenses/odbl/1.0/). The Open Database License (ODbL) is a license agreement intended to allow users to freely share, modify, and use this Dataset while maintaining this same freedom for others, provided that the original source and author(s) are credited.
Link: https://doi.org/10.3897/zse.94.14698.suppl4

Supplementary material 5

PDF-embedded 3D model of the skeleton of MRSN A6340, a specimen assigned to *Plethodontohyla laevis*

Authors: Adriana Bellati, Mark D. Scherz, Steven Megson, Sam Hyde Roberts, Franco Andreone, Gonçalo M. Rosa, Jean Noël, Jasmin E. Randrianirina, Mauro Fasola, Frank Glaw, Angelica Crottini
Data type: Adobe PDF file
Copyright notice: This dataset is made available under the Open Database License (http://opendatacommons.org/licenses/odbl/1.0/). The Open Database License (ODbL) is a license agreement intended to allow users to freely share, modify, and use this Dataset while maintaining this same freedom for others, provided that the original source and author(s) are credited.
Link: https://doi.org/10.3897/zse.94.14698.suppl5

Supplementary material 6

PDF-embedded 3D model of the skeleton of ZSM 89/2004, a specimen assigned to *Plethodontohyla alluaudi*

Authors: Adriana Bellati, Mark D. Scherz, Steven Megson, Sam Hyde Roberts, Franco Andreone, Gonçalo M. Rosa, Jean Noël, Jasmin E. Randrianirina, Mauro Fasola, Frank Glaw, Angelica Crottini
Data type: Adobe PDF file
Copyright notice: This dataset is made available under the Open Database License (http://opendatacommons.org/licenses/odbl/1.0/). The Open Database License (ODbL) is a license agreement intended to allow users to freely share, modify, and use this Dataset while maintaining this same freedom for others, provided that the original source and author(s) are credited.
Link: https://doi.org/10.3897/zse.94.14698.suppl6

Zoosyst. Evol. 94 (1) 2018, 137–145 | DOI 10.3897/zse.94.22173

PENSOFT

museum für naturkunde

Pantanodontidae (Teleostei, Cyprinodontiformes), the sister group to all other cyprinodontoid killifishes as inferred by molecular data

Pedro H.N. Bragança[1], Pedro F. Amorim[1], Wilson J.E.M. Costa[1]

1 *Laboratory of Systematics and Evolution of Teleost Fishes, Institute of Biology, Federal University of Rio de Janeiro, Caixa Postal 68049, CEP 21941-971, Rio de Janeiro, Brazil*

http://zoobank.org/6F1FBCDE-4F58-48FD-9CE9-645DF8A8E181

Corresponding author: *Pedro H.N. Bragança* (pedrobra88@gmail.com)

Received 9 November 2017
Accepted 24 January 2018
Published 9 February 2018

Academic editor:
Peter Bartsch

Key Words

Phylogeny
Molecular Systematics
Classification
Fluviphylacidae
Poeciliidae
Procatopodidae

Abstract

Pantanodon, containing two African extant species and four European fossil species, for a long time had an uncertain position among the Cyprinodontiformes due to its peculiar morphology. In the last decades, *Pantanodon* has been considered closely related to African lamp-eyes of the Procatopodinae clade, which is contained in the Poeciliidae, a teleost fish family with a broad geographical distribution in Africa and the Americas. However, recent molecular studies have challenged the monophyly of the Poeciliidae, but the position of *Pantanodon* remained uncertain. We analysed one mitochondrial (COI) and five nuclear loci (GLYT1, MYH6, SH3PX3, RAG1, ENC1), a total of 5,083 bp, for 27 cyprinodontiform taxa and 6 outgroups, obtaining a well-supported phylogeny, in which the monophyly of Poeciliidae, as supported by morphological data is refuted. *Pantanodon stuhlmanni*, the type species of the genus, is recovered as the most basal cyprinodontoid lineage and other African taxa formerly placed in Poeciliidae are highly supported as more closely related to European non-poeciliid cyprinodontoid genera than to other taxa. Since the present tree topology is not compatible with the present classification of the Cyprinodontoidei, a new classification using available family group names is provided: Pantanodontidae is used for *Pantanodon*; Procatopodidae, for the African lamp-eye clade; and Fluviphylacidae, for the South American genus *Fluviphylax*. Poeciliidae is restricted to the American livebearers, hence restoring the classification generally used prior to 1981.

Introduction

The teleost order Cyprinodontiformes is a diverse group of small fishes living in freshwater and estuarine environments of all continents, except Oceania and Antarctica. Many of them are popular aquarium fishes, but some species such as guppies and mangrove killifishes are among the most important experimental species used as model organisms for a large spectrum of scientific areas. However, cyprinodontiform classification is still not well established despite continuous efforts to understanding their phylogenetic relationships (e.g. Rosen 1964, Parenti 1981, Costa 1998, Pollux et al. 2014, Pohl et al. 2015).

Prior to Parenti's (1981) phylogenetic analysis, cyprinodontiform classifications were mainly based on sexually dimorphic characters to delimit groups, focusing on the presence and morphology of copulatory organs in males and viviparity (e.g., Garman 1895, Regan 1911). After Hubbs (1924), cyprinodontiforms were often classified in four families of internally fertilizing viviparous taxa: the Anablepidae, Jenynsiidae, Goodeidae, and Poeciliidae, and one diverse oviparous family, the Cyprinodontidae, which was subsequently divided in several subfamilies (e.g. Myers 1931, 1955). Among cyprinodontid subfamilies, Pantanodontinae contained a single genus, *Pantanodon* Myers, 1955, a peculiar group of small spe-

cies with a series of unique osteological features, amongst others, jaw and branchial arch morphology (Whitehead 1962, Rosen 1965). Until 1981, these unique morphological traits found in *Pantanodon* intrigued ichthyologists who did provide complete osteological reviews (Whitehead 1962, Rosen 1965), but still refrained from positioning the genus among other Cyprinodontiformes, and even suggested to place it in a separate family (Rosen 1965). *Pantanodon* presently comprises two African extant species (e.g. Rosen 1965, Seegers 1996) and at least four European fossil species (e.g. Costa 2012a).

In the cyprinodontiform classification provided by Parenti (1981) on the basis of her phylogenetic analysis of morphological characters, oviparous taxa previously placed in a single family, Cyprinodontidae, were distributed among nine different families, belonging to two well supported suborders: the Aplocheiloidei, comprising Aplocheilidae and Rivulidae, and the Cyprinodontoidei, comprising Anablepidae, Cyprinodontidae, Fundulidae, Goodeidae, Poeciliidae, Profundulidae, and Valenciidae. The Poeciliidae then became a more inclusive taxon comprising three subfamilies, the American livebearers being grouped in Poeciliinae, the oviparous African lamp-eyes and *Pantanodon* in Aplocheilichthyinae, and the South American oviparous killifish genus *Fluviphylax* Whitley, 1965 in Fluviphylacinae. Costa (1996) transferred *Fluviphylax* to Aplocheilichthyinae, but Ghedotti (2000) subsequently restricted Aplocheilichthyinae to a single genus and species, *Aplocheilichthys spilauchen* (Duméril, 1861), transferring other oviparous African lamp-eyes, *Pantanodon* and *Fluviphylax* to Procatopodinae.

Recently, some molecular phylogenetic analyses (Pollux et al. 2014, Pohl et al. 2015, Reznick et al. 2017) challenged the monophyly of Poeciliidae sensu Parenti (1981). These studies indicated the African Procatopodinae as the sister group of a clade comprising European non-Poeciliidae cyprinodontoid genera (*Valencia* Myers, 1928 and *Aphanius* Nardo, 1827). In addition, Pollux et al. (2014) and Reznick et al. (2017) based on a broad sample of New World cyprinodontoid taxa supported the South American *Fluviphylax* as the sister group of a Neotropical clade comprising Poeciliinae and Anablepidae, but did not include *Pantanodon* in their analyses. A species of the latter genus, *Pantanodon stuhlmanni* (Ahl, 1924) was tentatively included in a phylogenetic analysis (Pohl et al. 2015), based on two mitochondrial and three nuclear genes. However, the phylogenetic position of *P. stuhlmanni* was not well supported, possibly as a consequence of incomplete data sample. The analysis of the complete concatenated dataset indicated *P. stuhlmanni* as the sister group of a clade comprising all other cyprinodontoids, but this placement was poorly supported. On the other hand, in all single gene trees, *P. stuhlmanni* appeared outside the cypridontiform clade, but again without relevant support. Pohl et al. (2015) then concluded that the phylogenetic position of *Pantanodon* remained largely unresolved.

In order of to test the phylogenetic position of *Pantanodon* and search for a more stable classification, the present study includes a larger gene sample, comprising one mitochondrial and five nuclear genes for representatives of all cyprinodontiform families. A comparative analysis of extant and fossil species of *Pantanodon* provides an updated diagnosis for the genus.

Material and methods

Taxon sampling

Twenty species of Cyprinodontoidei, representing all the main lineages as previously described in morphological (Parenti 1981, Costa 1998, Ghedotti 2000) and molecular studies (Pollux et al. 2014, Pohl et al. 2015), were analysed in this study, in addition to seven species of Aplocheiloidei. Since *Pantanodon* includes only two nominal extant species, *P. stuhlmanni*, the type species, and *P. madagascariensis* (Arnoult, 1963), and the latter has not been collected since the 1960's and is presently considered as extinct (Sparks 2016), only the former species was included in the analysis. Outgroups comprised three representatives of Beloniformes, *Oryzias latipes* (Temminck & Schlege, 1846), *Cheilopogon melanurus* (Valenciennes, 1847), and *Xenentodon cancila* (Hamilton, 1822); two of Atheriniformes, *Labidesthes sicculus* (Cope, 1865) and *Menidia beryllina* (Cope, 1867); and one Cichlidae, *Heterochromis multidens* (Pellegrin, 1900). The latter was used to root the phylogenetic trees, following hypotheses of Ovalentaria relationships, wherein Cichlomorphae is supported as the sister group of Atherinomorphae (Wainwright et al. 2012; Betancur-R et al. 2013). All sequenced specimens used in this study are deposited in the Institute of Biology, Federal University of Rio de Janeiro, Rio de Janeiro (UFRJ) and the Royal Museum for Central Africa, Tervuren (MRAC). In order to avoid large sets of missing data, in three cases when COI sequences were not available for the selected terminal taxa, we used sequences available in GenBank for closely related species: *Aplocheilus panchax* (KU.692279.1) was included as data for *A. lineatus*; *Aphanius anatoliae* (KJ.552353.1), for *A. isfahanensis*; and *Poeciliopsis occidentalis* (HQ.556956.1), for *P. elongata*. A list of species and the respective GenBank accession numbers appear in Supplementary material 1. The material examined for checking morphological diagnostic features of Pantanodontidae is deposited in the following institutions: Institute of Biology, Federal University of Rio de Janeiro, Rio de Janeiro (UFRJ), Royal Museum for Central Africa, Tervuren (MRAC), Museum für Naturkunde, Berlin (MB.f, Palaeontology; ZMB, Ichthyology), Muséum national d'Histoire naturelle, Paris (MNHN.P, Palaeontology; MNHN, Ichthyology) Museum of Zoology, University of Michigan, Ann Arbor (UMMZ), Národní Muzeum, Prague (NMP), and Natural History Museum, London (NHMUK(P), Palaeontology; BMNH, Ichthyology); all material is listed in Supplementary material 2.

Osteological preparations and nomenclature

Osteological studies were made on cleared and stained specimens (c&s) prepared according to Taylor and Van Dyke (1985) and nomenclature for bone structures follows Costa (2006).

DNA sequencing

The genomic DNA was extract from muscle tissue of the right side of the caudal peduncle using DNeasy Blood & Tissue Kit (Qiagen) according to the manufacturer instructions. To amplify the fragments of DNA were used the primers Glyt_F559 and Glyt_R1562, for the Glycosyltransferase gene (GLYT1), myh6_F507 and myh6_R1325, for the cardiac protein encoding gene, Myosin heavy chain 6 (MYH6), SH3PX3_F461, SH3PX3_R1303, SH3PX3_F532 and SH3PX3_R1299, for the SH3 and PX domain-containing 3-like protein (SH3PX3) (Li et al. 2007), RAG1F1, RAG1R2 (Lopez et al. 2004) and H3405 (Hrbek et al. 2007) for the recombination activation gene 1 (RAG1), ENC1_F88, ENC1_F85, ENC1_R975, ENC1_R982 (Li et al. 2007) and the primers ENC1_FPAN (5'-ATGCTGYTWCTGTCTGAYGCCCACCAGTG-3'), ENC1_RPAN (5'-GCYTTBGGRATKATCTCTTTGGC -3') herein developed for the ectodermal neural cortex 1 gene, LCO1490, HCO2198 (Folmer et al. 1994) for the Cytochrome c oxidase subunit I (COI), 16sar-L and 16sbr-H (Palumbi et al. 1991) for the 16S ribosomal RNA gene. The annealing temperatures for the primers ENC1_FPAN and ENC1_RPAN is 59°C. Polymerase chain reactions (PCR) were performed in 30 µl reaction mixtures containing 5 × Green GoTaq Reaction Buffer (Promega), 3.6 mM MgCl2, 1 µM of each primer, 50 ng of total genomic DNA, 0.2 mM of each dNTP and 1U of Taq polymerase. The thermocycling profile was: (1) 1 cycle of 4 minutes at 94 °C; (2) 35 cycles of 1 minute at 92 °C, 1 minute at 49–60 °C (varying according to the primer and the sample) and 1 minute at 72 °C; and (3) 1 cycle of 4 minutes at 72 °C. In all PCR reactions, negative controls without DNA were used to check contaminations. Amplified PCR products were purified using the Wizard SV Gel and PCR Clean-Up System (Promega). Sequencing reactions were made using the BigDye Terminator Cycle Sequencing Mix (Applied Biosystems). Cycle sequencing reactions were performed in 10 µl reaction volumes containing 1 µl BigDye 2.5X, 1.55 µl sequencing buffer 5X (Applied Biosystems), 2 µl of the amplified products (10 –40 ng), and 2 µl primer. The thermocycling profile was: (1) 35 cycles of 10 seconds at 96 °C, 5 seconds at 54 °C and 4 minutes at 60 °C. The sequencing reactions were purified and denatured and the samples were run on an ABI 3130 Genetic Analyzer. Sequences were edited using MEGA 6 (Tamura et al. 2013) and aligned using ClustalW (Chenna et al. 2003). The DNA sequences were translated into amino acids residues to test for the absence of premature stop codons or indels using the program MEGA 6.0.

Gene sampling

For each gene and codon position Measure Substitution Saturation tests were performed according to the model proposed by Xia et al. (2003), considering only fully resolved sites in DAMBE5 (Xia 2013). Preliminary trees were executed for partitions with high saturation level, and the tree topology (symmetrical/asymmetrical) were considered when evaluating the Iss and Iss.c values. The third position of COI and the 16S gene showed substantial saturation as well as the third position of ENC1 nuclear gene and they were then removed from the analysis. The concatenated dataset included the following genes: GLYT, MYH6, RAG1, SH3PX3, the first and the second codon position of ENC1 and the first and second codon position of the mitochondrial gene COI comprising 5,083 bp. A preliminary phylogenetic analysis was performed including the 16S to the concatenated dataset and its inclusion dropped the bootstrap supports and posterior probability values of both shallow and deep nodes. This analysis is presented in Supplementary material 3.

Phylogenetic analysis

The dataset was partitioned according to each gene. The best-fit evolutionary model was calculated for each partition using the Akaike Information Criterion (AIC) determined by the jModelTest 2.1.7 (Darriba et al. 2012). The best model for each partition is presented in Supplementary material 4. To check for major discordance among individual gene trees, maximum likelihood trees were generated for each gene alignment, using MEGA 6 (Tamura et al. 2013). Since separate analyses did not result in conflicting trees, data were concatenated, with the whole dataset containing 5,083 bp. The phylogenetic analyses were conducted through Maximum Likelihood (ML), using the program Garli 2.0 (Zwickl 2006), and Bayesian Inference (BI), using the program MrBayes v3.2.5 (Ronquist et al. 2012). The values of support of the ML analysis were calculated by 1000 bootstrap replications (Felsenstein 1985). BI was conducted using two Markov chain Monte Carlo (MCMC) runs of two chains each for 3 million generations, a sampling frequency of 1000. The quality of the MCMC chains was evaluated in Tracer 1.6, and a 25 % burn-in was removed.

Results

The ML analysis (Fig. 1) generated a tree with most clades receiving high bootstrap values (higher than 95 %), including among them the nodes supporting the Cyprinodontiformes and the Aplocheiloidei. *Pantanodon stuhlmanni* appeared as the sister group of all other cyprinodontoids (91 %), and the clade including all cyprinodontoids except *P. stuhlmanni* was also highly supported (100 %). In the BI analysis (Supplementary material 5), almost the same topology was reached, with the above mentioned clades showing high posterior probability values (above 0.95 %).

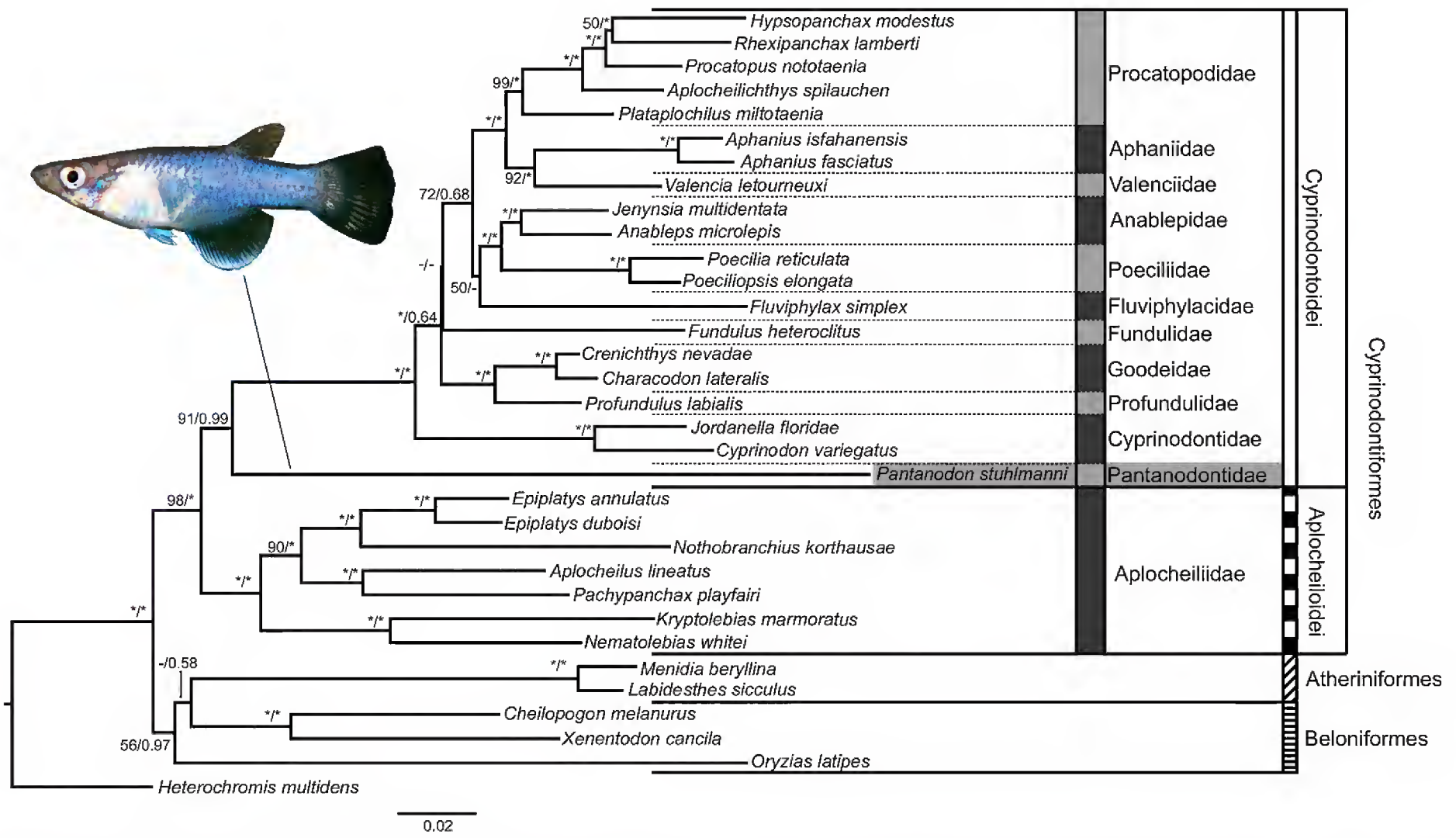

Figure 1. Phylogenetic relationship tree generated by a Maximum Likelihood Analysis of molecular data (5,083 bp, comprising segments of the nuclear genes ENC1, GLYT, MYH6, SH3PX3 and RAG1 and the mitochondrial gene COI). Clade names follows the classification herein proposed. Numbers on each node are bootstrap percentages of the Maximum Likelihood analysis and posterior probabilities of the Bayesian Inference analysis; asterisks indicate maximum values (100 or 1.00 respectively) and a dash refers to values under 50 or 0.50 respectively.

The main difference occurred in the position of *Fluviphylax simplex* Costa, 1996 (sister to a clade comprising only the Anablepidae and the Poeciliidae in ML analysis, vs. sister to a clade comprising the Procatopodidae, represented by *Aplochilichthys spilauchen, Hypsopanchax modestus*, *Plataplochilus miltotaenia*, *Procatopus nototaenia*, *Rhexipanchax lamberti*, Valenciidae, Aphaniidae, Anablepidae, and Poeciliidae in BI analysis), but the relative position of *Pantanodon* was the same in both analyses (Figure 1, Supplementary material 5).

Discussion

Phylogenetic position of *Pantanodon* and African lamp-eyes

The present analysis is consistent with previous morphological and molecular studies in supporting the monophyly of the Cyprinodontiformes, which contains two well established clades, the suborders Aplocheiloidei and Cyprinodontoidei (Parenti 1981, Costa 1998, Pollux et al. 2014, Pohl et al. 2015). However, monophyly of the Poeciliidae as inferred from morphological data (Parenti 1981, Costa 1998, Ghedotti 2000) is refuted. The poecilines are considered to be sister to the Anablepidae, whereas the Procatopodines are closer to the Old world genera *Aphanius* and *Valencia*. Instead of being a taxon belonging to the African lamp-eye clade (= Procatopodinae sensu Ghedotti 2000), *Pantanodon stuhlmanni* is herein supported as the sister group of a clade encompassing all other cyprinodontoids (Fig. 1), thus considered as a member of a separate family, the Pantanodontidae (see Taxonomic implications below). Species of this family exhibit morphological synapomorphies previously used to diagnose the Cyprinodontoidei (Parenti 1981, Costa 1998, 2012b), corroborating its inclusion in this suborder: (1) dentary expanded medially resulting in a robust lower jaw (Fig. 2A), (2) rostral cartilage absent (Fig. 2A), (3) metapterygoid absent (Fig. 2A), (4) dorsal hypohyal absent (Fig. 3C), (5) first basibranchial absent (Fig. 3E), and (6) distal portion of the neural and haemal spines of the preural vertebrae 3 wider than neural and haemal spines of preural vertebrae 4 (Fig. 2D). However, no morphological character was found to support the clade comprising all cyprinodontoids except Pantanodontidae, probably as a result of the high specialised morphology of Pantanodontidae avoiding clear homology assumptions for several structures.

Our analysis highly supports the monophyly of the group ecompassing all African lamp-eyes species, corroborating previous morphological studies (Parenti 1981, Costa 1996), but refuting Ghedotti's (2000) analysis, who considered African lamp-eyes to form a paraphyletic assemblage. According to that study, the species Aplocheilichthys spilauchen is the sister group of a clade including the remaining African lamp-eyes and the American Poeciliinae, represented herein by *Poecilia reticulata* and *Poeciliopsis elongata*. In contrast, the African lamp-eye

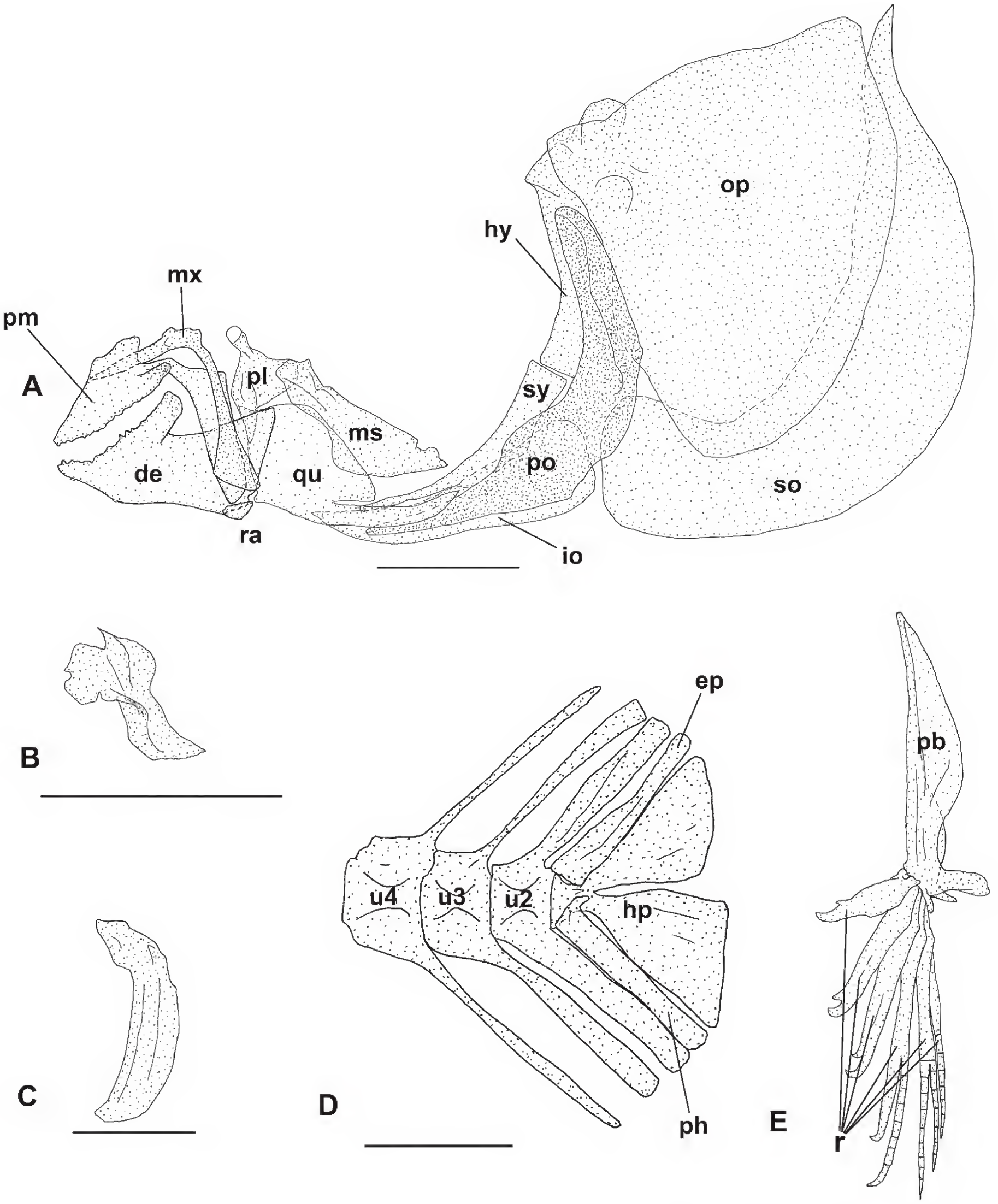

Figure 2. Jaws, jaw suspensorium, opercular apparatus, superficial dermal bones and caudal fin skeleton of *Pantanodon stuhlmanni* and pelvic fin of *P. madagascariensis*: **A**: left jaws, jaw suspensorium and opercular apparatus, lateral view; **B**, left nasal, dorsal view; **C**, left lachrymal, lateral view; **D**, caudal fin skeleton, left lateral view; **E**: pelvic fin bone and rays. Abbreviations: de, dentary; ep, epural; hp, hypural plate; hy, hyomandibula; io, interopercle; ms, mesopterygoid; pb, pelvic bone; ph, parahypural; pl, palatine; pm, premaxila; po, preopercle; qu, quadrate; r, rays; ra, retroarticular; so, subopercle; sy, sympletic; u2–u4, preural centra 2–4. Scale bar = 1mm. Figure 2E was based on illustration present in Rosen (1965), that originally do not have scale bar.

clade is highly supported as the sister group to a clade comprising the European genera *Aphanius* and *Valencia*, whereas the Poeciliinae is considered to be sister to the Anablepidae, both results agreeing with recent molecular phylogenies using different samples, terminal taxa and DNA markers (Pollux et al. 2014, Pohl et al. 2015, Reznkick et al. 2017). The present study also refutes the South American *Fluviphylax* as a member of the African

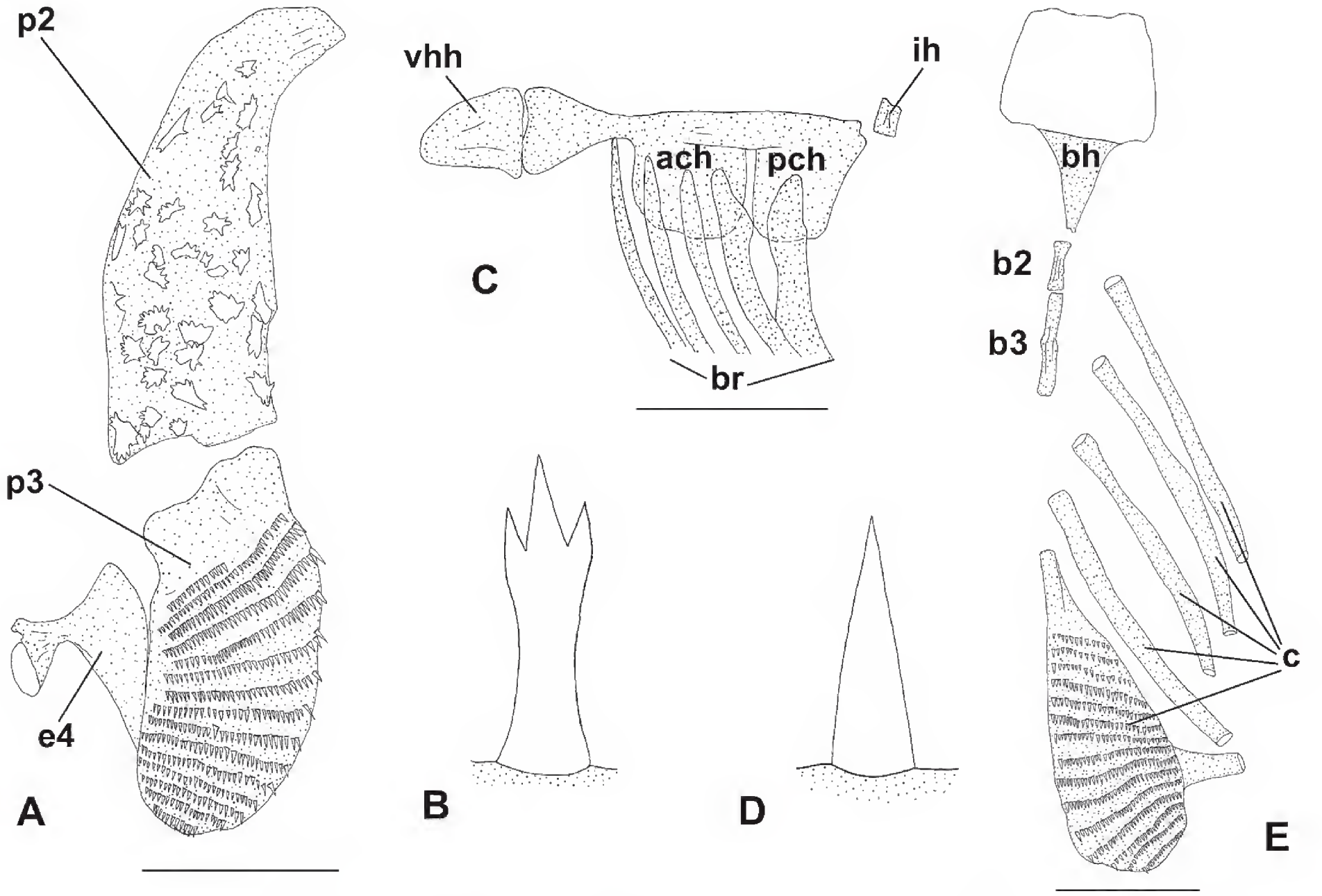

Figure 3. Branchial arches of *Pantanodon stuhlmanni*: **A**, left branchial arches, ventral view of dorsal portion; **B**, third pharyngobranchial tooth, frontal view; **C**, left hyoid bar, lateral view; **D**, fifth ceratobranchial tooth, frontal view; **E**, left and middle branchial arches, dorsal view of ventral portion. Abbreviations: ach, anterior ceratohyal; b1–2, basibranchials 1–2; bh, basihyal; br, branchiostegal rays; c, ceratobranchials; e4,fourth epibranchial; ih, interhyal; p2-3, pharyngobranchials 2 and 3, pch, posterior ceratohyal; vhh, ventral hypohyal. Scale bar = 1mm. Figure 3B and 3D are schematic illustrations of the teeth, thus no scale bar is presented. The cartilaginous hypobranchials are not illustrated in Figure 3E.

lamp-eye clade as supported by morphological studies (Roberts 1970, Parenti 1981, Costa 1996, Ghedotti 2000). Although the position of *F. simplex* is only moderately supported in the analyses, other studies using different molecular data sets indicate that *Fluviphylax* is not closely related to African lamp-eyes (Pollux et al. 2014; Reznick et al. 2017).

Taxonomic implications

The present tree topology indicates relationships not compatible with the current classification of the Cyprinodontoidei. Two families, Cyprinodontidae and Poeciliidae, proposed by Parenti (1981) and subsequent authors using morphological characters, are not monophyletic, highlighting the need for a new classification at the family level. In order to avoid too much impact on the current classification, we herein minimize changes in the classification of the Poeciliidae, using family group names already available. The genus *Pantanodon*, supported as the sister group of all other cyprinodontoids, is placed in its own family, Pantanodontidae Myers 1955, new usage, corresponding to Pantanodontinae of Myers (1955), Whitehead (1962) and Rosen (1965). Procatopodidae Fowler 1916, new usage, is used for the well supported African lamp-eye clade, being equivalent to Aplocheilichthyinae sensu Parenti (1981), and Fluviphylacidae Roberts 1970, new usage, for the South American genus *Fluviphylax*, equivalent to Fluviphylacinae sensu Parenti (1981). Poeciliidae Bonaparte 1831 is restricted to the American livebearers (= Poeciliinae sensu Parenti 1981), restoring Poeciliidae as delimited by authors prior to 1981 (e.g. Hubbs 1924).

The genus *Pantanodon* until recently comprised only two extant species, *P. stuhlmanni*, from brackish water environments of coastal river drainages in Kenya and Tanzania, and *P. madagascariensis* from freshwater environments of forested areas in northern Madagascar drainages (e.g. Whitehead 1962, Arnoult 1963). Costa (2012a) reviewed Tertiary cyprinodontoid fossil taxa from central Europe, transferring three species previously placed in *Prolebias* Sauvage, 1874 to *Pantanodon*: *P. cephalotes* (Agassiz 1839) from the upper Oligocene of d'Aix-en-Provence, southern France; *P. egeranus* (Laube 1901) from the Karpatian, lower Miocene of the Cheb basin,

Czech Republic; *P. malzi* (Reichenbacher and Gaudant 2003) from the upper Oligocene-lower Miocene of Germany. Subsequently, Gaudant (2013) described a new genus, *Paralebias*, for those fossil species. However, since those fossil species exhibit synapomorphies used to diagnose *Pantanodon* (Costa, 2012a) and no unique derived character state was used to diagnose *Paralebias* by Gaudant (2013), the latter genus is here considered as a synonym of the former. More recently, another fossil species was assigned to *Paralebias*, *P. conquensis* Gaudant and Reichenbacher, 2015 from the Miocene of the Tagus Basin, Spain (Gaudant et al. 2015), herein tentatively placed in *Pantanodon* by possessing claw-shaped hooks on the tip of male pelvic fin, an apomorphic diagnostic feature of *Pantanodon*. *Pantanodon*, the only genus of Pantanodontidae here considered as valid, has been diagnosed by several apomorphic conditions: (1) presence of a boomerang-shaped lachrymal (Fig. 2C), (2) extremely reduced nasal (Fig. 2B), (3) dentary and angulo-articular fused in a single structure with coronoid process extending backwards over the quadrate (Fig. 2A), (4) dentary and premaxilla with expanded bone flange (Fig. 2A), (5) tricuspid pharyngeal teeth (Fig. 3B), (6) hypobranchials not ossified (Fig. 3E), (7) epibranchials 1–3 minute or absent (Fig. 3A), (8) second pharyngobranchial tooth plate triangular (Fig. 3A), (9) fifth ceratobranchial and third pharyngobranchial teeth arranged in transverse rows (Fig. 3A, E), (10) fifth ceratobranchial drop-shaped (Fig. 3E), (11) pelvic bone long and narrow (Fig. 2E), and (12) claw-shaped hooks on the tip of outer three or four pelvic-fin rays in males (Parenti 1981, Costa 1998, 2012a). All these characters are herein confirmed in specimens examined (list of specimens examined presented in Supplementary material 2).

Acknowledgments

We are grateful to F. Milvertz and B. Nagy for donating specimens of *P. stuhlmanni* and providing pictures of P. stuhlmanni, to R. Bayer for donating African lamp-eye specimens and to P. Bartsch, G. Clément, B. Ekrt, W. Fink, Z. Gabsi, Z. Johanson, C. Lamour, J. Maclaine, D. Nelson, M. Parrent, P. Pruvost, M. Richter, J. Snoeks, M. Veran, E. Vreven, and F. Witzmann, for hospitality during visits to their institutions. We are also grateful to J.L. Mattos for help during molecular analyses and to reviwers J. Snoeks and L. Machado for improving the manuscript with corrections and suggestions during the review process. Part of this study was conducted by PHNB and WJEMC during a long-term stay at MRAC; special thanks to J. Snoeks for providing us fine conditions to develop researches in his institution. This study was supported by CNPq (Conselho Nacional de Desenvolvimento Científico e Tecnológico – Ministério de Ciência e Tecnologia; grant 141813/2014-8 to PHNB and 200627/2015-5 to WJEMC); FAPERJ (Fundação de Amparo à Pesquisa do Estado do Rio de Janeiro, grant E-26/200.381/2016 to PFA) and CAPES (Coordenação de Aperfeiçoamento de Pessoal de Nível Superior, grant 99999.003613/2015-01 to PHNB).

References

Arnoult J (1963) Un oryziiné (Pisces, Cyprinodontidae) nouveau de l'est de Madagascar. Bulletin du Muséum Nationale de Histoire Naturelle Série 2 (35): 235–237.

Betancur–R R, Broughton RE, Wiley EO, Carpenter K, López JA, Holcroft NI, Arcila D, Sanciangco M, Cureton II JC, Zhang F, Buser T, Campbell MA, Ballesteros JA, Roa–Varon A, Willis S, Borden WC, Rowley T, Reneau PC, Hough DJ, Lu G, Grande T, Arratia G, Ortí G (2013) The tree of life and a new classification of bony fishes. PLOS Currents Tree of Life. Available online at https://doi.org/10.1371/currents.tol.53ba26640df0ccaee75bb165c8c26288.

Chenna R, Sugawara H, Koike T, Lopez R, Gibson TJ, Higgins DG, Thompson JD (2003) Multiple sequence alignment with the Clustal series of programs. Nucleic Acids Research 31: 3497–3500. https://doi.org/10.1093/nar/gkg500

Costa WJEM (1996) Relationships, monophyly and three new species of the neotropical miniature poeciliid genus Fluviphylax (Cyprinodontiformes: Cyprinodontoidei). Ichthyological Exploration of Freshwaters 7: 111–130.

Costa WJEM (1998) Phylogeny and classification of the Cyprinodontiformes (Euteleostei: Atherinomorpha): a reppraisal. In :Malabarba LR, Reis, RE, Vari RP, Lucena ZMS, Lucena CAS (Eds) Phylogeny and classification of Neotropical Fishes. Edipucrs, Porto Alegre, 537–560.

Costa WJEM (2006) Descriptive morphology and phylogenetic relationships among species of the Neotropical annual killifish genera Nematolebias and Simpsonichthys (Cyprinodontiformes: Aplocheiloidei: Rivulidae). Neotropical Ichthyology 4(1): 1–26. https://doi.org/10.1590/S1679-62252006000100001

Costa WJEM (2012a) Oligocene killifishes (Teleostei: Cyprinodontiformes) from southern France: relationships, taxonomic position, and evidence of internal fertilization. Vertebrate Zoology 62: 371–386.

Costa WJEM (2012b) The caudal skeleton of extant and fossil Cyprinodontiform fishes (Teleostei: Atherinomorpha): comparative morphology and delimitation of phylogenetic characters. Vertebrate Zoology 62: 161–180.

Darriba D, Taboada GL, Doallo R, Posada D (2012) jModelTest 2: more models, new heuristics and parallel computing. Nature Methods 9: 772. https://doi.org/10.1038/nmeth.2109

Felsenstein J (1985) Confidence limits on phylogenies: an approach using the bootstrap. Evolution 39: 783–791. https://doi.org/10.1111/j.1558-5646.1985.tb00420.x

Folmer O, Black M, Hoeh W, Lutz R, Vrijenhoek R (1994) DNA primers for amplification of mitochondrial cytochrome C oxidase subunit I from diverse metazoan invertebrates. Molecular Marine Biology and Biotechnology 3: 294–299.

Garman S (1895) The cyprinodonts. Memoirs of the Museum of Comparative Zoology 19: 1–179.

Gaudant J (2013) Occurence of poeciliid fishes (Teleostei, Cyprinodontiformes) in the European Oligo-Miocene: the genus Paralebias nov. gen. Neues Jahrbuch für Geologie und Paläontologie-Abhandlungen 267: 215–222. https://doi.org/10.1127/0077-7749/2013/0305

Gaudant J, Bárron E, Anadón P, Reichenbacher B, Peñalver E (2015) Palaeoenvironmental analysis of the Miocene Arcas del Villar gypsum sequences (Spain), based on palynomorphs and cyprinodontiform fishes. Neues Jahrbuch für Geologie und Paläontologie-Abhandlungen 277: 105–124. https://doi.org/10.1127/njgpa/2015/0503

Ghedotti MJ (2000) Phylogenetic analysis and taxonomy of the poecilioid fishes (Teleostei: Cyprinodontiformes). Zoological Journal of the Linnean Society 130: 1–53. https://doi.org/10.1111/j.1096-3642.2000.tb02194.x

Hrbek T, Seckinger J, Meyer A (2007) A phylogenetic and biogeographic perspective on the evolution of poeciliid fishes. Molecular Phylogenetics and Evolution 43: 986–998. https://doi.org/10.1016/j.ympev.2006.06.009

Hubbs CL (1924) Studies of the fishes of the order Cyprinodontes. Miscellaneous Publications of the Museum of Zoology University of Michigan 13: 1–31.

Li C, Ortí G, Zhang G, Lu G (2007) A practical approach to phylogenomics: The phylogeny of ray-finned fish (Actinopterygii) as a case study. BMC Evolutionary Biology 7: 44. https://doi.org/10.1186/1471-2148-7-44

López JA, Chen WJ, Ortí G (2004) Esociform phylogeny. Copeia 2004: 449–464. https://doi.org/10.1643/CG-03-087R1

Myers GS (1931) The primary groups of oviparous cyprinodont fishes, Order Cyprinodontes (Microcyprini). Stanford University Publications 6: 1–14.

Myers GS (1955) Notes on the classification and names of Cyprinodont fishes. Tropical fish magazine, March, 7.

Palumbi S R, Martin A, Romano S, McMillan WO, Stice L, Grabowski G (1991) The Simple Fool's Guide to PCR, Version 2. University of Hawaii Zoology Department, Honolulu.

Parenti LR (1981) A phylogenetic and biogeographic analysis of cyprinodontiform fishes (Teleostei, Atherinomorpha). Bulletin of the American Museum of Natural History 168: 335–357.

Pohl M, Milvertz FC, Meyer A, Vences M (2015) Multigene phylogeny of cyprinodontiform fishes suggests continental radiations and a rogue position taxon position of *Pantanodon*. Vertebrate Zoology 65: 37–44.

Pollux BJA, Meredith RW, Springer MS, Garland T, Reznick DN (2014) The evolution of the placenta drives a shift in sexual selection in livebearing fish. Nature 513: 233–236. https://doi.org/10.1038/nature13451

Regan CT (1911) The osteology and classification of teleostean fishes of the order Microcyprini. Annals and Magazine of Natural History ser 7 (40): 320–327, pls 1–8. https://doi.org/10.1080/00222931108692944

Reznick DN, Furness AI, Meredith RW, Springer MS (2017) The origin and biogeographic diversification of fishes in the family Poeciliidae. PLoS ONE 12(3): e0172546. https://doi.org/10.1371/journal.pone.0172546

Roberts TR (1970) Description, osteology and relationships of the Amazonian cyprinodont fish Fluviphylax pygmaeus (Myers and Carvalho). Breviora 347: 1–28.

Ronquist F, Teslenko M, Van der Mark P, Ayres DL, Darling A, Höhna S, Larget B, Liu L, Suchard MA, Huelsenbeck JP (2012) MrBayes 3.2: efficient Bayesian phylogenetic inference and model choice across a large model space. Systematic Biology 61: 539–542. https://doi.org/10.1093/sysbio/sys029

Rosen DE (1964) The relationships and taxonomic position of halfbeaks, killifishes, silversides, and their relatives. Bulletin of the American Museum of Natural History 127: 217–168.

Rosen DE (1965) Oryzias madagascariensis Arnoult redescribed and assigned to the East African fish genus *Pantanodon* (Atheriniformes, Cyprinodontoidei. American Museum Novitates 2240: 1–10.

Seegers L (1996) The Fishes of the Lake Rukwa Drainage. Annales du Musée Royal de l'Afrique Centrale, Sciences Zoologiques 287: 1–407.

Tamura K, Stecher G, Peterson D, Filipski A, Kumar S (2013) MEGA6: Molecular Evolutionary Genetics Analysis Version 6.0. Molecular Biology and Evolution 30: 2725–2729. https://doi.org/10.1093/molbev/mst197

Taylor WR, Van Dyke OC (1985) Revised procedures for staining and clearing small fishes and others vertebrates for bone and cartilage study. Cybium 9: 107–109.

Wainwright PC, Smith WL, Price SA, Tang KL, Sparks JS, Ferry LA, Kuhn KL, Eytan RI, Near TJ (2012) The evolution of pharyngognathy: a phylogenetic and functional appraisal of the pharyngeal jaw key innovation in labroid fishes and beyond. Systematic Biology 61: 1001–1027. https://doi.org/10.1093/sysbio/sys060

Whitehead PJP (1962) The *Pantanodon*tinae, edentulous toothcarps from East Africa. Bulletin of the British Museum of Natural History 9: 105–137. https://doi.org/10.5962/bhl.part.16339

Xia X (2013) Dambe5: a comprehensive software package for data analysis in molecular biology and evolution. Molecular Biology and Evolution 30: 1720–1728. https://doi.org/10.1093/molbev/mst064

Xia XH, Xie Z, Salemi M, Chen L, Wang Y (2003) An index of substitution saturation and its application. Molecular Phylogenetics and Evolution 26: 1–7. https://doi.org/10.1016/S1055-7903(02)00326-3

Zwickl DJ (2006) Genetic algorithm approaches for the phylogenetic analysis of large biological sequence datasets under the maximum likelihood criterion. PhD dissertation, Austin, Texas: University of Texas.

Supplementary material 1

List of species, localities and respective Genbank accession numbers

Authors: Pedro Henrique Negreiros de Bragança, Pedro Fasura de Amorim, Wilson José Eduardo Moreira da Costa

Data type: Microsoft Excel Worksheet (.xls) file

Link: https://doi.org/10.3897/zse.94.22173.suppl1

Supplementary material 2

Material examined

Authors: Pedro Henrique Negreiros de Bragança, Pedro Fasura de Amorim, Wilson José Eduardo Moreira da Costa

Data type: Microsoft Word Document (.docx) file

Link: https://doi.org/10.3897/zse.94.22173.suppl2

Supplementary material 3

Maximum Likelihood (A) and Bayesian Inference (B) analysis including the 16S gene.

Authors: Pedro Henrique Negreiros de Bragança, Pedro Fasura de Amorim, Wilson José Eduardo Moreira da Costa

Data type: TIF File (.tif) file

Explanation note: Maximum Likelihood (A) and Bayesian Inference (B) analysis including segments of the nuclear genes ENC1, GLYT, MYH6, SH3PX3, RAG1, the mitochondrial genes 16S and first and second codon position of the COI. In ML, bootstrap values under 50 are not represented, and posterior probability values under 0.5 are not represented in BI.

Link: https://doi.org/10.3897/zse.94.22173.suppl3

Supplementary material 4

Substitution models according to JModeltest 2.1.7

Authors: Pedro Henrique Negreiros de Bragança, Pedro Fasura de Amorim, Wilson José Eduardo Moreira da Costa

Data type: Microsoft Excel Worksheet (.xlsx) file

Link: https://doi.org/10.3897/zse.94.22173.suppl4

Supplementary material 5

Bayesian Inference tree

Authors: Pedro Henrique Negreiros de Bragança, Pedro Fasura de Amorim, Wilson José Eduardo Moreira da Costa

Data type: TIF File (.tif) file

Explanation note: Bayesian inference tree comprising segments of the nuclear genes ENC1, GLYT, MYH6, SH3PX3, RAG1 and first and second codon position of the mitochondrial gene COI (5,083 bp). Numbers on each node are posterior probablity values; values under 50 are not present in the tree.

Link: https://doi.org/10.3897/zse.94.22173.suppl5

Zoosyst. Evol. 94 (1) 2018, 147–161 | DOI 10.3897/zse.94.21754

PENSOFT

museum für naturkunde

Description of a new species of *Homonota* (Reptilia, Squamata, Phyllodactylidae) from the central region of northern Paraguay

Pier Cacciali[1,2,3], Mariana Morando[4], Luciano J. Avila[4], Gunther Köhler[1,2]

1 *Senckenberg Forschungsinstitut und Naturmuseum, Senckenberganlage 25, 60325 Frankfurt a.M., Germany*
2 *Johann Wolfgang Goethe-University, Institute for Ecology, Evolution & Diversity, Biologicum, Building C, Max-von-Laue-Straße 13, 60438 Frankfurt am Main, Germany*
3 *Instituto de Investigación Biológica del Paraguay, Del Escudo 1607, 1425 Asunción, Paraguay*
4 *Grupo de Herpetología Patagónica, IPEEC-CENPAT-CONICET. Puerto Madryn, Chubut, Argentina*

http://zoobank.org/207FF499-30F7-4465-B80E-3C0BD007D4E2

Corresponding author: *Pier Cacciali* (pier_cacciali@yahoo.com)

Received 19 October 2017
Accepted 15 February 2018
Published 28 February 2018

Academic editor:
Johannes Penner

Key Words

Dry Chaco
Gekkota
phylogeny
South America
taxonomy

Abstract

Homonota is a gecko distributed in central and southern South America with 12 species allocated in three groups. In this work, we performed molecular and morphological analyses of samples of *Homonota* from the central region of northern Paraguay, comparing the data with those of related species of the group: *H. horrida* and *H. septentrionalis*. We found strong molecular evidence (based on 16S, Cyt-b, and PRLR gene sequences) to distinguish this lineage as a new species. Morphological statistical analysis showed that females of the three species are different in metric characters (SVL and TL as the most contributing variables), whereas males are less differentiated. No robust differences were found in meristic characters. The most remarkable trait for the diagnosis of the new species is the presence of well-developed keeled tubercles on the sides of the neck, and lack of a white band (crescent-shaped) in the occipital area, which is present in *H. horrida* and *H. septentrionalis*. Nevertheless, in our sample, we found three specimens (one juvenile and two young adults) that exhibit the white occipital band. Thus, this character seems only reliable in adults of the new species. The new species is parapatric to *H. septentrionalis*, both inhabiting the Dry Chaco of Paraguay.

Introduction

Homonota is a gecko, inhabiting mainly xeric and rocky areas in central and southern South America (Cei 1993, Avila et al. 2012), with *Homonota darwinii* reaching the most austral distribution of the genus at 54° latitude south (Morando et al. 2014). Most of the species in the genus are nocturnal, although *H. uruguayensis* can be either diurnal or nocturnal (Carreira et al. 2005). *Homonota horrida* (Burmeister 1861), distributed in Argentina and Paraguay, was the second described species of the genus, after the controversial *H. fasciata* (Duméril and Bibron 1836). This latter species was described from "Martinique", a Caribbean island located out of the distribution of the southern cone Neotropical genus. Both species were considered synonyms by Abdala and Lavilla (1993), which was followed by posterior researchers until recently when Cacciali et al. (2017) found that the type specimen of *H. fasciata* is distinct from the types of *H. horrida*, and recognized them as different taxa. Currently, both species are considered valid, although *H. fasciata* remains a *species inquirenda* because of the lack of information on its distribution and uncertainty in its diagnostic characters (Cacciali et al. 2017). The most recently described species of the genus was *H. septentrionalis* Cacciali, Morando, Medina, Köhler, Motte & Avila, 2017, which is present in the western part of the Dry Chaco (western Paraguay and southern Bolivia). Three groups are currently recognized: *whitii* group composed of *H. whitii* Boulenger, 1885, *H. darwinii* Boulenger, 1885, *H. andicola* Cei, 1978, and *H. williamsii* Avila, Pérez, Minoli & Morando, 2012; *borelli* group with *H. borellii*

(Peracca, 1897), *H. uruguayensis* (Vaz-Ferreira & Sierra de Soriano, 1961), *H. rupicola* Cacciali, Ávila & Bauer, 2007, and *H. taragui* Cájade, Etchepare, Falcione, Barrasso & Álvarez, 2013; and the *horrida* group (indicated as *fasciata* group by Morando et al. 2014) which contains *H. horrida* (Burmeister, 1861), *H. underwoodi* Kluge, 1964, and *H. septentrionalis* Cacciali, Morando, Medina, Köhler, Motte & Avila, 2017. Cacciali et al. (2017) suggested that more revisions are needed to understand the true taxonomic status of *H. fasciata* because currently it is not possible to know to which group it belongs and it is considered *incertae sedis*.

Four species of *Homonota* are recorded in Paraguay: *H. borellii*, *H. rupicola*, *H. horrida*, and *H. septentrionalis*. The most commonly known species was *Homonota horrida* recorded for the "Chaco" (Kluge 1964, Talbot 1978, 1979). Even after the synonymy of *H. horrida* with *H. fasciata* (Abdala and Lavilla 1993) the name *H. horrida* was still used in Paraguayan reports (Aquino et al. 1996, Ziegler et al. 2002). Many specimens of *H. septentrionalis* were referred to as *H. horrida* (those from the westernmost part of the Paraguayan Chaco) according to Cacciali et al. (2017). *Homonota rupicola* is an endemic species found in a rocky hill, east of the Paraguay River; and *H. borellii* was recorded from a few specimens from "Defensores del Chaco" and "Médanos del Chaco" National Parks (Cacciali et al. 2016). Thus, most of the species of *Homonota* from Paraguay are present in the Chaco, which is part of the "Dry Diagonal" formed by Caatinga, Cerrado, and Chaco, characterized by dry seasonal woodlands (Prado and Gibbs 1993). In Paraguay the Chaco is divided in two ecoregions: Humid Chaco and Dry Chaco, and most of the *Homonota* samples are located in the latter (Cacciali et al. 2016).

After the description of *H. septentrionalis*, the same authors continued to study and analyze the taxonomy of Paraguayan samples of *Homonota* from the Chaco, within the framework of a barcoding initiative of the herpetofauna from Paraguay. We performed genetic and morphological analyses among different populations of *Homonota* from the central region of northern Paraguay. Based on genetic and morphological differences, and applying a species delimitation algorithm, we found enough differences to consider these new samples as a different taxonomic unit from those previously recorded for Paraguay. We present here a detailed analysis along with the description of this new species.

Methods

We extracted DNA from three samples of *Homonota* from the central area of northern Paraguay (Occidental Region), which were compared with available sequences of the remaining members of the genus (except *H. fasciata*) to assess its taxonomic relationships in the gene tree. We sequenced fragments of mitochondrial genes rRNA 16S and Cytochrome b (Cytb) and the nuclear gene prolactine receptor (PRLR). Samples used and GenBank accession numbers are specified in Table 1. Samples of 16S were available only for the *horrida* group. To root the tree we included two outgroups (*Garthia gaudichaudii* and *Phyllopezus przewalskii* (Table 1) based on Morando et al. (2014).

Tissue samples were first washed for 15 h with 50 ml Phosphate-buffered saline (PBS) (diluted of 1:9 PBS: H_2O). The DNA extraction was carried out with the DNeasey kit of Qiagen. We used 25 µl of reaction mix for every sample for the PCR (except for PRLR where we used 20 µl). Reagents and concentrations for the PCR mix for the amplification of every gene, are provided in Suppl. material 1: Appendix S1. Primers (produced by Eurofins MWG Operon) used for amplification and sequencing, along with PCR conditions for each gene are detailed in Suppl. material 1: Appendix S2.

We used SeqTrace 0.9.0 (Stucky 2012) for examination of chromatograms and to generate the consensus sequences. We used MAFFT 7 (Katoh and Standley 2013) to automatically align the sequences through its webserver. For alignment of sequences of 16S, we included the Q-INS-i search strategy for corrections with the secondary structure of that gene (Katoh and Toh 2008). We used MSA Viewer (Yachdav et al. 2016) to visualize the alignments and export them to fasta format. We estimated the best substitution model for each gene (separately) with PartitionFinder2 (Lanfear et al. 2016) using the PhyML 3.0 algorithm (Guindon et al. 2010). We used the corrected Akaike Information Criterion (AICc) (Burnham and Anderson 2002) to select the best substitution model, but under the premise that it is not correct to use models that include both +G and +I (Sullivan et al. 1999, Mayrose et al. 2005). Then we chose the subsequent model in the best partition schemes when both were suggested by the AICc.

We performed two phylogenetic analyses, first using a Maximum Likelihood (ML) approach, and then a Bayesian inference (BI) to compare the trees topologies. These analyses were made for each gene individually and for a concatenated dataset of the three genes together. For the ML analysis we used IQ-Tree (Nguyen et al. 2015) through its webserver (Trifinopoulos et al. 2016) using 10,000 non parametric bootstrap replicates plus 10,000 replicates of Shimodaira-Hasegawa approximate likelihood ratio (SH-aLRT) (Anisimova et al. 2011) and 10,000 ultrafast bootstrap (UFBoot) approximation replicates (Minh et al. 2013). We converted the alignment to nexus format in the online server Alter (Glez-Peña et al. 2010) available at http://sing.ei.uvigo.es/ALTER/, to be used in MrBayes v3.2 (Huelsenbeck and Ronquist 2001, Ronquist and Huelsenbeck 2003) for a BI. For this, we ran the analysis in independent duplicates, each with 1,000,000 generations for MCMC with a sampling frequency of 500 generations. We visualized the trees and exported them using FigTree v1.4.3 (available at http://tree.bio.ed.ac.uk/software/figtree/). We considered convergence when the standard deviation of split frequencies was 0.015 or less and when the Potential Scale Reduction Factor approached 1.0 (Gelman and Rubin 1992).

Table 1. Specimens used for genetic analyses and GenBank accession numbers for every gene. Asterisks (*) indicate tissue samples without voucher. Numbers in bold are samples generated for this work.

Species	Voucher	16S	Cytb	PRLR	GenSeq Nomenclature
Homonota andicola	LJAMM-CNP 12493	MD	KJ484188	KJ484274	genseq-3
	LJAMM-CNP 12495	MD	KJ484189	KJ484275	genseq-3
Homonota borellii	LJAMM-CNP 12116	MD	KJ484205	KJ484276	genseq-4
	LJAMM-CNP 12119	MD	KM677796	MD	genseq-4
	LJAMM-CNP 12125	MD	KJ484206	KJ484277	genseq-4
Homonota darwinii	LJAMM-CNP 9266	MD	KJ484191	MD	genseq-3
	LJAMM-CNP 9813	MD	MD	KJ484278	genseq-3
	LJAMM-CNP 11424	MD	KJ484190	MD	genseq-3
Homonota horrida	BYU 47941	MF278828	KJ484192	**MG950402**	genseq-3
	LJAMM-CNP 10493	MD	KM677795	MD	genseq-3
	LJAMM-CNP 10495	MF278829	MD	**MG950403**	genseq-3
	LJAMM-CNP 10576	MF278830	MD	**MG950404**	genseq-3
	LJAMM-CNP 10577	MD	KJ484208	MD	genseq-3
Homonota rupicola	MNHNP-1*	MD	KJ484193	KJ484281	genseq-3
	MNHNP-2*	MD	KJ484194	KJ484282	genseq-3
Homonota septentrionalis	MNHNP 11406	MD	MF278843	MF278849	genseq-2
	MNHNP 11409	MD	MF278844	MF278850	genseq-2
	MNHNP 11873	MF278831	MD	**MG950405**	genseq-3
	MNHNP 12238	MF278832	MD	MD	genseq-1
	SMF 101984	MF278833	MD	**MG950406**	genseq-2
Homonota taragui	LJAMM-CNP 14419	MD	KJ484195	KJ484283	genseq-3
	LJAMM-CNP 14420	MD	KJ484196	KJ484284	genseq-3
Homonota underwoodi	LJAMM-CNP 10923	MD	KJ484197	KJ484286	genseq-4
	LJAMM-CNP 10931	MD	KJ484198	KJ484297	genseq-4
Homonota uruguayensis	UFRGS 2139	MD	MD	KJ484296	genseq-4
	UFRGS 5769	MD	KM677689	MD	genseq-4
	UFRGS 5770	MD	KM677690	MD	genseq-4
	UFRGS 5771	MD	KM677691	MD	genseq-4
Homonota whitii	LJAMM-CNP 14387	MD	KJ484199	MD	genseq-4
	LJAMM-CNP 14388	MD	KJ484200	MD	genseq-4
Homonota williamsii	LJAMM-CNP 4467	MD	KJ484201	KJ484287	genseq-3
	LJAMM-CNP 6517	MD	KJ484202	KJ484288	genseq-2
Homonota sp. n.	SMF 101436	MD	**MG950409**	**MG950407**	genseq-2
	SMF 101438	**MG947388**	**MG950410**	**MG950408**	genseq-2
	SMF 101439	MD	**MG950411**	MD	genseq-2
Outgroups					
Garthia gaudichaudii	E61214	MD	FJ985045	MD	
	IBE_G1(1)	MD	MD	KJ484289	
Phyllopezus przewalskii	LG1093	JN935567	JQ826890	JQ825640	
	LJAMM-CNP 12089	MD	KJ484203	MF278849	

When frequencies did not converge we continued adding 500,000 generations until convergence was achieved.

We assessed the degree of intraspecific divergence within the alignment (removing the outgroups) with the species delimitation test ABGD (Puillandre et al. 2012) through its webserver (http://wwwabi.snv.jussieu.fr/public/abgd/abgdweb.html), using 10 steps of prior minimum and maximum simple genetic distance from 0.001 to 0.1 (default), and 0.5 of relative gap width, since higher (default) values tend to exceedingly split clades (Kekkonen et al. 2015, Yang et al. 2016). For this analysis we used only Cytb which was the mitochondrial gene better represented in our samples, and available for all the species within the genus. The last step using genetic data was the assessment of a species tree based on the clustering proposed by the species delimitation test. To do this we used *BEAST (Drummond et al. 2012) in BEAST 2.4.7 (Ogilvie et al. 2017) under 1,000,000 generations for the mcmc model, visualizing the posterior probability in DensiTree 2.2.6 (Bouckaert et al. 2014).

Additionally, we generated morphological data for 13 specimens (7 males and 6 females) of the new species and

taxa with similar pattern (related taxa of the *horrida* group) looking for potential diagnostic characters. Thus, we used for comparison *H. horrida* (7 males and 5 females) and *H. septentrionalis* (10 males and 12 females), using standard variables (continuous data expressed in mm) already used by Avila et al. (2012) and Cacciali et al. (2017):

SVL snout–vent length, from tip of snout to vent.
TrL trunk length, distance from axilla to groin from posterior edge of forelimb insertion to anterior edge of hind limb insertion.
FL foot length, from the tip of the claw of the 4th straightened toe to the back of the heel.
TL tibial length, measured between the level of the knee and the level of the heel, as shown by Köhler (2014).
AL arm length, from tip of claws of the 3rd finger to elbow.
HL head length, distance between anterior edge of auditory meatus and snout tip.
HW head width, taken at the level of the temporal region, corresponding to the widest part of the head.
HH head height, maximum height of head, at level of parietal area.
END eye–nostril distance, from the anterior edge of the eye to the posterior edge of the nostril.
ESD eye–snout distance, from the anterior edge of the eye to the tip of the snout.
EMD eye–meatus distance, from the posterior edge of the eye to the anterior border of the ear opening.
ID interorbital distance, shortest distance between orbits.
IND internostril distance, shortest distance between nares.
DT number of keeled dorsal tubercles from occipital area to cloaca level.
TVS number of transversal rows of ventral scales, counted longitudinally at midline from the chest (shoulder level) to inguinal level.
LVS number of longitudinal rows of ventral scales, counted transversally at midbody.
SL number of supralabial scales.
IL number of infralabial scales.
4TL number of lamellae under the fourth toe.
3FL number of lamellae under the third finger.

Measurements were taken with digital calipers (precision 0.01), but only the first decimal considered to limit discrepancies. For the morphological analyses only specimens of ~40 mm or larger were included. When paired structures exist, data are presented in left/right orientation, and only the left side was used for statistical analyses. In the color descriptions, the capitalized colors and the color codes (in parentheses) are those of Smithe (1981) for live animals and Köhler (2012) for preserved specimens.

We compared the morphological variation among species through a discriminant function analysis (DFA), testing the normality of the variables with a Shapiro-Wilk (*W*) test (Shapiro et al. 1968, Zar 1999), and for the DFA we only used variables that were normally distributed. We used PAST 3.14 (Hammer et al. 2001) to perform these tests. Meristic (discrete) and metric (continuous) data were analyzed separately. Examined specimens are detailed in Appendix 1. We present a table of localities of the specimens examined in Suppl. material 1: Appendix S3.

Results

The final alignments of 16S, Cytb, and PRLR consisted of 539, 793, and 457 bp, respectively. Alignments and trees are available at TreeBASE (ID: 22305). The best substitution model for 16S was GTR+G, for Cytb TVM+I(1stpos)|TIM+G(2ndpos)|SYM+G(3rdpos), and for PRLRK81(1stpos)|GTR+G(2nd+3rdpos). The complete table with scores is provided in Suppl. material 1: Appendix S4. The topology of the ML (Suppl. material 1: Fig. S1) and BI (Suppl. material 1: Fig. S2) trees using 16S coincide in recognizing three clusters, but the ML tree shows the new species as a sister clade to *H. septentrionalis*, whereas BI shows a trichotomy including *H. horrida*, *H. septentrionalis*, and the new species. Trees of ML and BI based on Cytb have the same topology (Suppl. material 1: Figs S3–S4), with strong support values. In these trees *H. andicola* and *H. whitii* are sister clades, as are *H. darwinii* and *H. williamsii*, and they are sister to the remaining *Homonota* species. The *borellii* group shows *H. uruguayensis* as sister to *H. borellii* + *H. rupicola* + *H. taragui*. Finally, within the *horrida* group, *H. underwoodi* appears as the sister to the remaining *Homonota* with banded coloration pattern. In this part of the tree *H. horrida* is rendered as sister to the clade *H. septentrionalis* plus the new taxon. The topologies of the ML and BI trees using PRLR are also the same (Suppl. material 1: Figs S5–S6). Species in the *whitii* group are clustered together, and the *borellii* group also shows monophyly but with a unresolved polytomy. In the *horrida* group *H. underwoodi* is also suggested as sister to the remaining species, with the new species and *H. septentrionalis* showing the most recent divergence. The trees using the concatenated dataset (with both ML and BI) show similar branch arrangement previously observed in trees of individual genes (Suppl. material 1: Figs S7–S8). Only two samples (UFRGS 2139 of *H. uruguayensis* and LJAMM-CNP 9813 of *H. darwinii*) are not allocated within their respective taxa, probably because some genes are lacking for some species.

The analysis of intraspecific genetic divergence with ABGD results in 12 groups (Suppl. material 1: Appendix S5), which represent nearly all described species (except *H. fasciata*) and the new species, providing evidence for its recognition as a distinct taxon. This is highly congruent with the clusters shown by the gene trees. The species tree shows consensus in the clusters of the three groups of the genus *Homonota*, with slight differences in the branch arrangements. The lower value (density of green lines in Figure 1) shows a trichotomy where the three groups are nested together, and with similar proba-

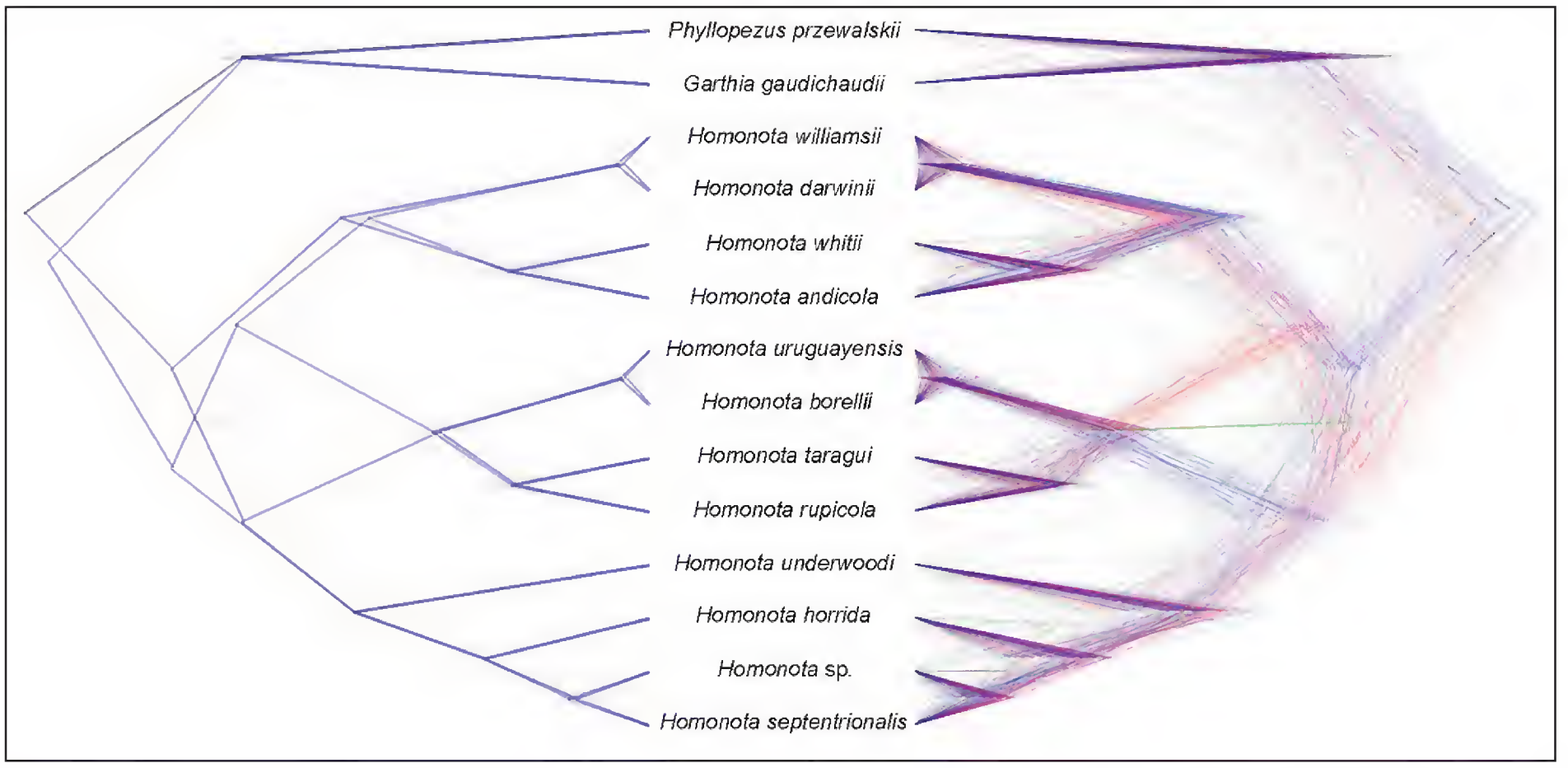

Figure 1. Species tree (left) and density of trees (right) for the species of the genus *Homonota*, based on the genes 16S, Cytb, and PRLR. The intensity in the color of the species tree is proportional to the probability.

Table 2. Normality Shapiro-Wilk (*W*) values for metric (above) and meristic (below) characters showing the *p* value. Values shaded in gray did not reach normality. See Methods section for reference to the acronyms.

	Continuous												
	SVL	TrL	FL	TL	AL	HL	HW	HH	END	ESD	EMD	ID	IND
W	0.978	0.979	0.957	0.987	0.982	0.979	0.976	0.983	0.979	0.967	0.969	0.975	0.952
p	0.503	0.506	0.087	0.849	0.696	0.575	0.401	0.758	0.555	0.199	0.284	0.400	0.050
	Discrete												
	DT	TVS	LVS	SL	IL	4TL	3FL						
W	0.962	0.971	0.965	0.779	0.788	0.913	0.948						
p	0.109	0.291	0.164	$3.05E^{-7}$	$4.65E^{-7}$	0.008	0.023						

bilities a species tree that clusters the *whitii* group as sister to the *borellii* group (density of red lines) and another where the *whitii* group is sister to the *borellii* group + *horrida* group (density of blue lines). Same as observed in the gene trees, *H. underwoodi* is presented as the sister clade to the remaining members of the group, and *H. horrida* sister to the new species of *Homonota* and *H. septentrionalis* with a rather deep divergence between these two taxa.

All continuous morphological variables had normal distributions (Table 2). The DFA for metric data showed that females of the three species are more differentiated than males (Fig. 2). The most contributing variables were SVL and TL for Axis 1, and SVL and TrL for Axis 2 and 3 (Table 3). Given the high eigenvalue of axes 1 and 2 (3.79 and 2.34 respectively, Fig. 2) suggests that the groups are significantly differentiated. For the meristic data, only DT, TVS, and LVS reached normality (Table 2), and DFA with these variables showed a high degree of overlapping without group discrimination and low eigenvalues (Fig. 3), and weak discrimination values (Table 3). Raw metric and meristic data are presented in Suppl. material 1: Tables S1 and S2.

Table 3. Most contributing continuous (Cont.) and discrete (Disc.) variables (highlighted in bold) for Axis 1–3 of the DFA.

	Variables	Axis 1	Axis 2	Axis 3
Cont.	SVL	**0,417**	**1,202**	**–3,447**
	TrL	–0,187	**0,690**	**–1,798**
	FL	0,132	0,401	–0,479
	TL	**0,228**	0,193	–0,417
	AL	0,201	0,213	–0,553
	HL	–0,017	0,357	–0,605
	HW	–0,128	0,218	–0,525
	HH	–0,199	0,187	–0,258
	END	–0,021	0,099	–0,193
	ESD	–0,052	0,111	–0,392
	EMD	0,144	0,134	–0,221
	ID	–0,028	–0,013	–0,302
	IND	0,002	0,127	–0,050
Disc.	DT	**1.424**	–1.232	**–1.338**
	TVS	**2.166**	**1.825**	0.921
	LVS	<0.001	**1.482**	**–1.255**

There is a strong molecular congruence in the recognition of 12 taxa within the genus *Homonota* (three of them with a banded coloration pattern), which added

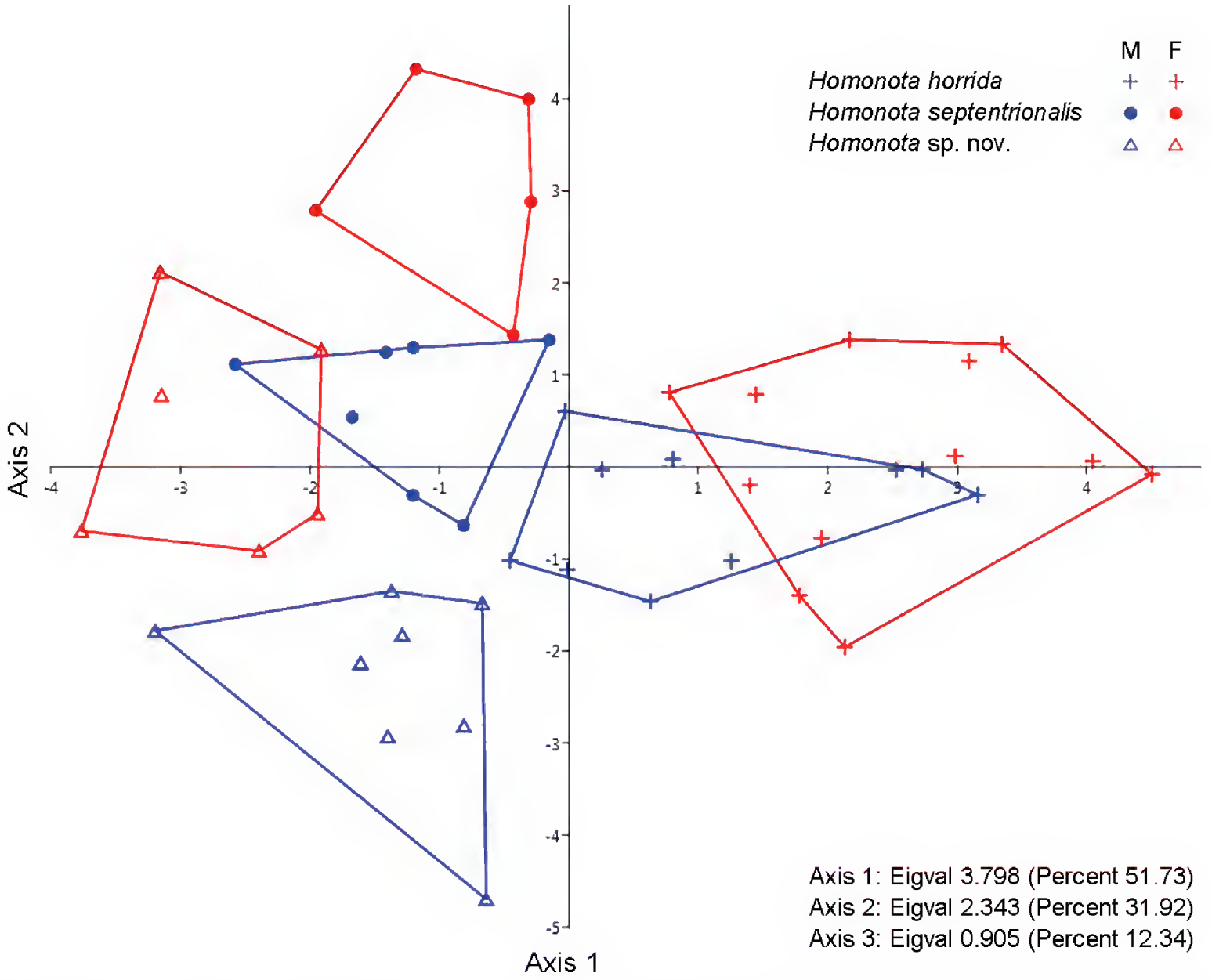

Figure 2. Discriminant Function Analysis scatter plot of individual scores for the three most informative axes for continuous variables of *Homonota horrida*, *H. septentrionalis*, and *Homonota* sp. n. Eigval: Eigenvalues. M: males. F: females.

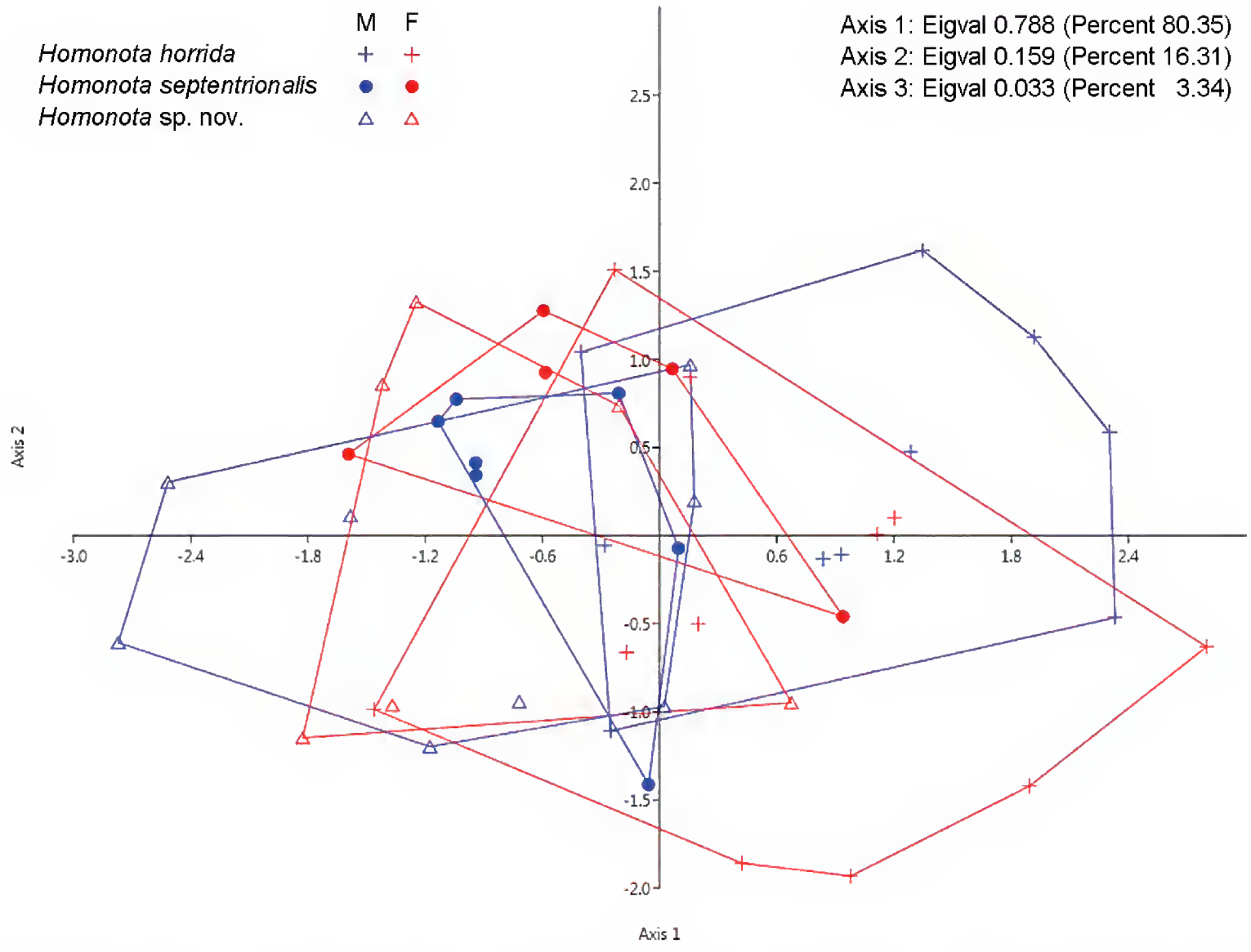

Figure 3. Discriminant Function Analysis scatter plot of individual scores for the three most informative axes for discrete variables of *Homonota horrida*, *H. septentrionalis*, and *Homonota* sp. n. Eigval: Eigenvalues. M: males. F: females.

to the significant differences among the three species with banded pattern based on the DFA, and the additional morphological distinctions discussed below are used to identify the new taxon described here.

Homonota marthae sp. n.

http://zoobank.org/FAB96653-46FF-4291-A23B-0FDB390AC54D

Holotype. SMF 101441 (field number GK-3783) (Fig. 4), adult female, collected on February 17th 2012 by Gunther Köhler in Dry Chaco, near the main house of Estancia Amistad (22.406°S, 60.728°W, elevation ca. 190 masl), Boquerón Department, Paraguay (Fig. 5).

Paratypes. Paraguay: Boquerón Department: Comunidad Ayoreo Jesudi (MNHNP 10744); Comunidad Ayoreo Tunucojai (MNHNP 10534); Estancia Amistad (SMF 101437); Estancia Jabalí (MNHNP 7832); Filadelfia (MNHNP 2795, 2798, 2810, 11790, 11791, 11793, SMF 101436, 101438–40, 101442); 31.5 km S Filadelfia (MNHNP 9726).

Diagnosis. A species of *Homonota* assigned to the *horrida* group given its relationship (based on molecular evidence) with *H. horrida*, and by the color pattern composed of a vertebral and five to seven transversal clear lines appearing as a banded *Homonota* smilar to *H. horrida* and *H. septentrionalis*. *Homonota marthae* has a robust body, and prominently keeled tubercles disposed in four to eight longitudinal rows on the dorsum.

Homonota marthae can be differentiated from all species in the genus, except *H. fasciata*, *H. horrida*, *H. darwinii*, and *H. septentrionalis* by the color pattern of transversal bands on the dorsum (reticulated pattern in the remaining species). *Homonota marthae* is further differ-

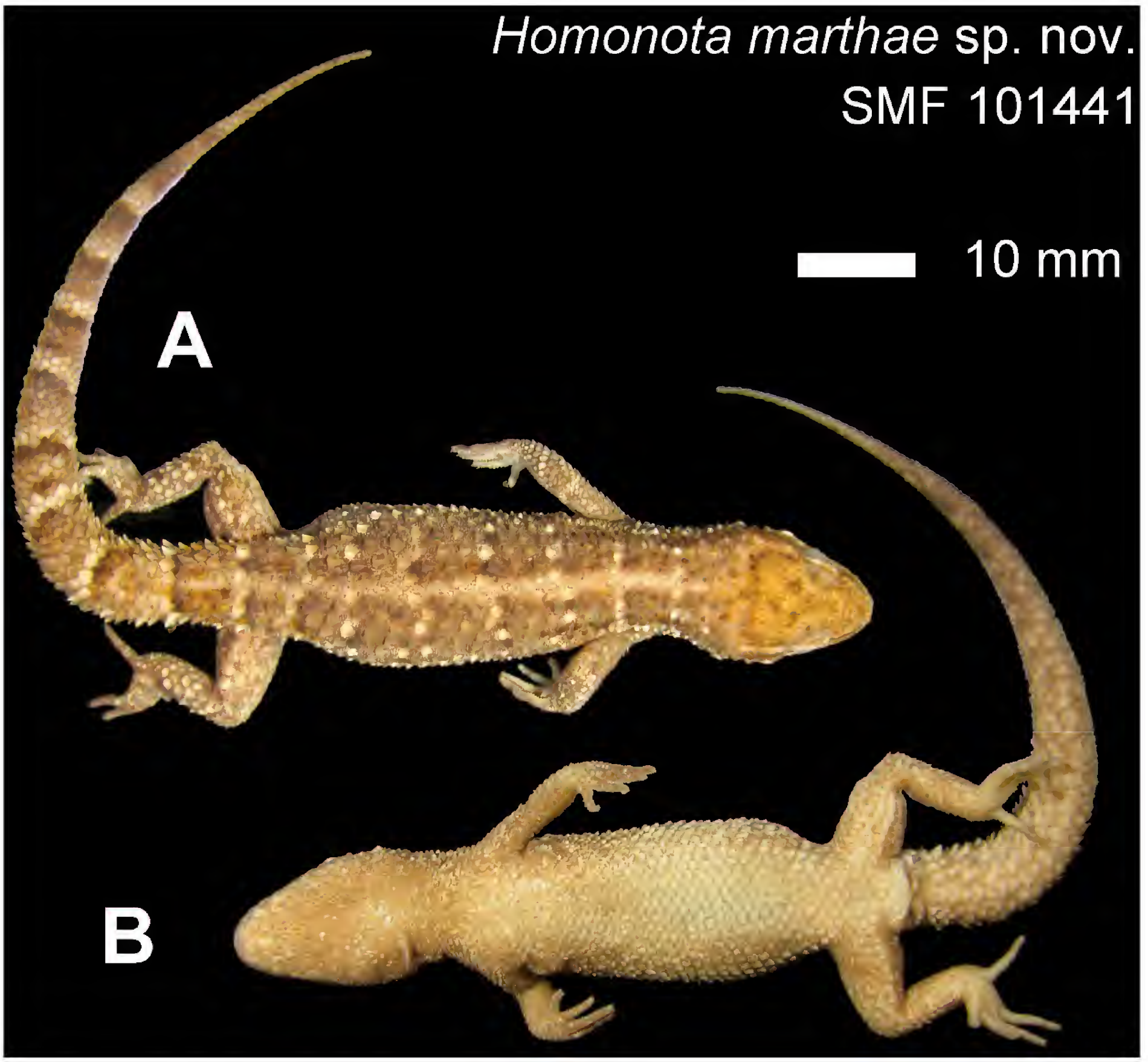

Figure 4. Dorsal (**A**) and ventral (**B**) views of the holotype of *Homonota marthae*.

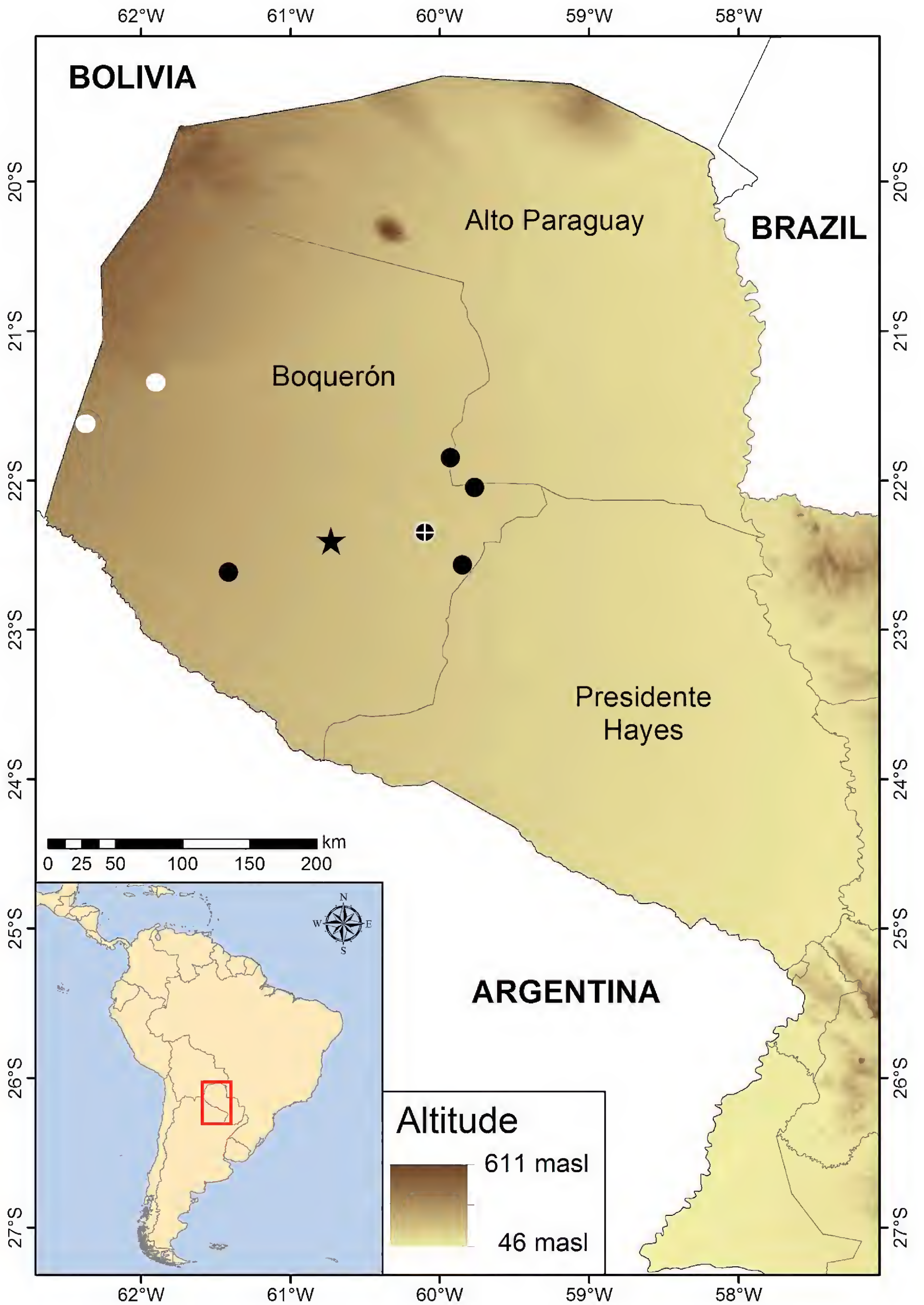

Figure 5. Occidental Region of Paraguay, indicating the political division, showing the known records for *Homonota septentrionalis* (white circles) and the analyzed records of *Homonota marthae* (black circles), and its type locality (star). Circle with a white cross, indicates origin of the genetic samples. High resolution elevation base map (30 seconds resolution) taken from Consortium for Spatial Information (CGIAR-CSI) available on http://www.diva-gis.org/gdata (Jarvis et al. 2008).

entiated from *H. andicola*, *H. whitii*, *H. darwinii*, and *H. underwoodi* by the keeled scales along the whole dorsum (vs. smooth dorsal scales in *H. andicola*, *H. whitii*, and *H. underwoodi*, and keeled scales restricted to the posterior part of the dorsum in *H. darwinii*). It differs from *H. fasciata* by having a serrated edge of the auditory meatus (vs. smooth anterior margin in *H. fasciata*); presence of one or two enlarged tubercles on the upper edge of the auditory meatus (vs. no enlarged tubercles in *H. fasciata*); and a smaller size of the postmental scales (vs. postmentals of the size of the first infralabials in *H. fasciata*). *Homonota marthae* differs from *H. horrida* by the higher position of the ear opening in relation to the level of the mouth (vs. lower positioned in *H. horrida*); from *H. septentrionalis* by more developed keeled tubercles on the sides of the neck (Fig. 6) (vs. less developed tubercles in *H. septentrionalis*). Finally, adults of *H. marthae* differ from these both species by the lack of a white band (usually crescent-shaped) on the occipital area (vs. white occipital crescent-shaped band present in *H. horrida* and *H. septentrionalis*) (Fig. 7). An artificial key for identification of the species of the genus is presented at the end of the work.

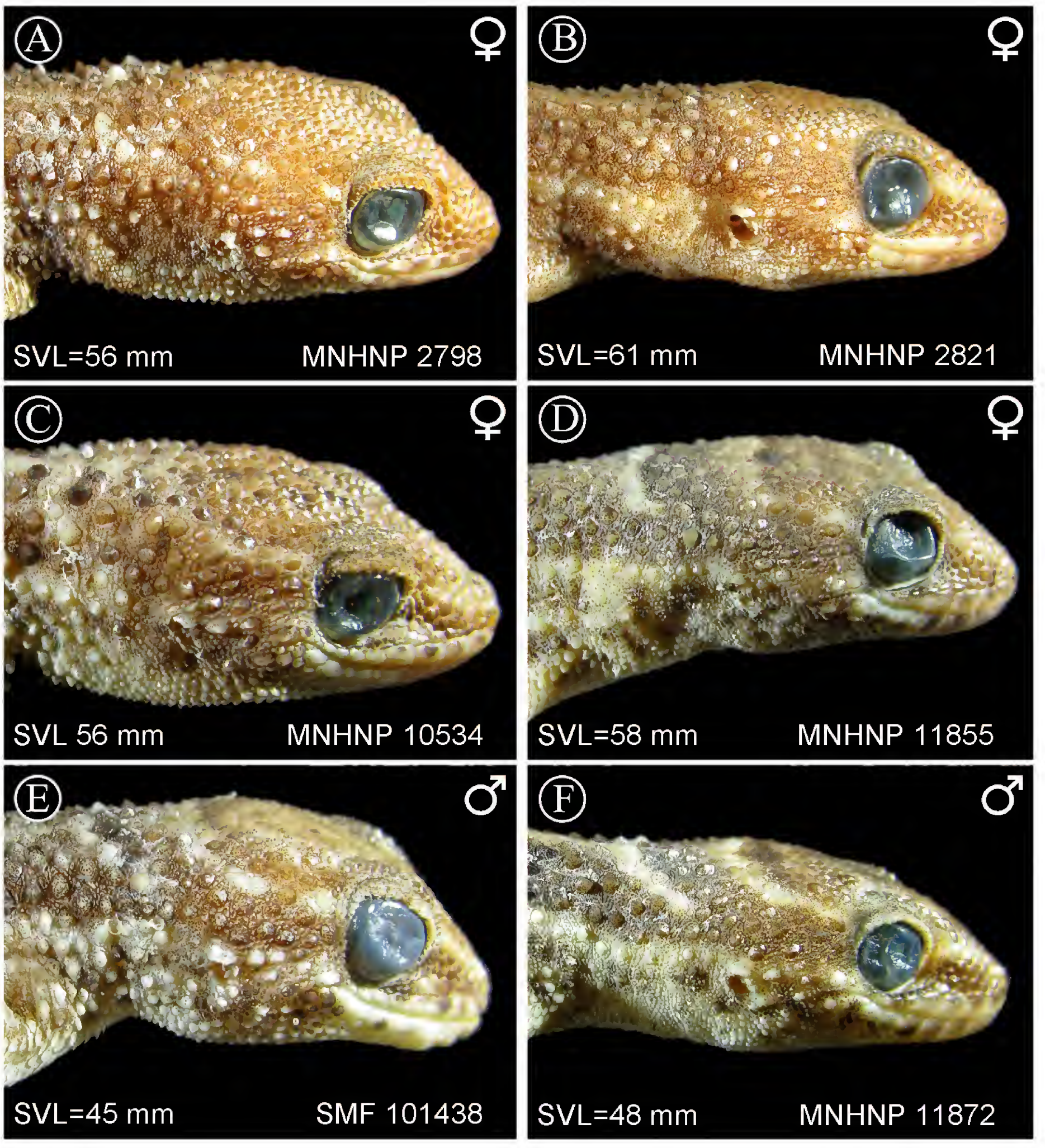

Figure 6. Plate showing the difference in scalation among individuals of similar sizes and same gender, of *Homonota marthae* (**A**, **C**, **E**) and *H. septentrionalis* (**B**, **D**, **F**). Note the more developed keeled tubercles on the sides of the neck in the former species.

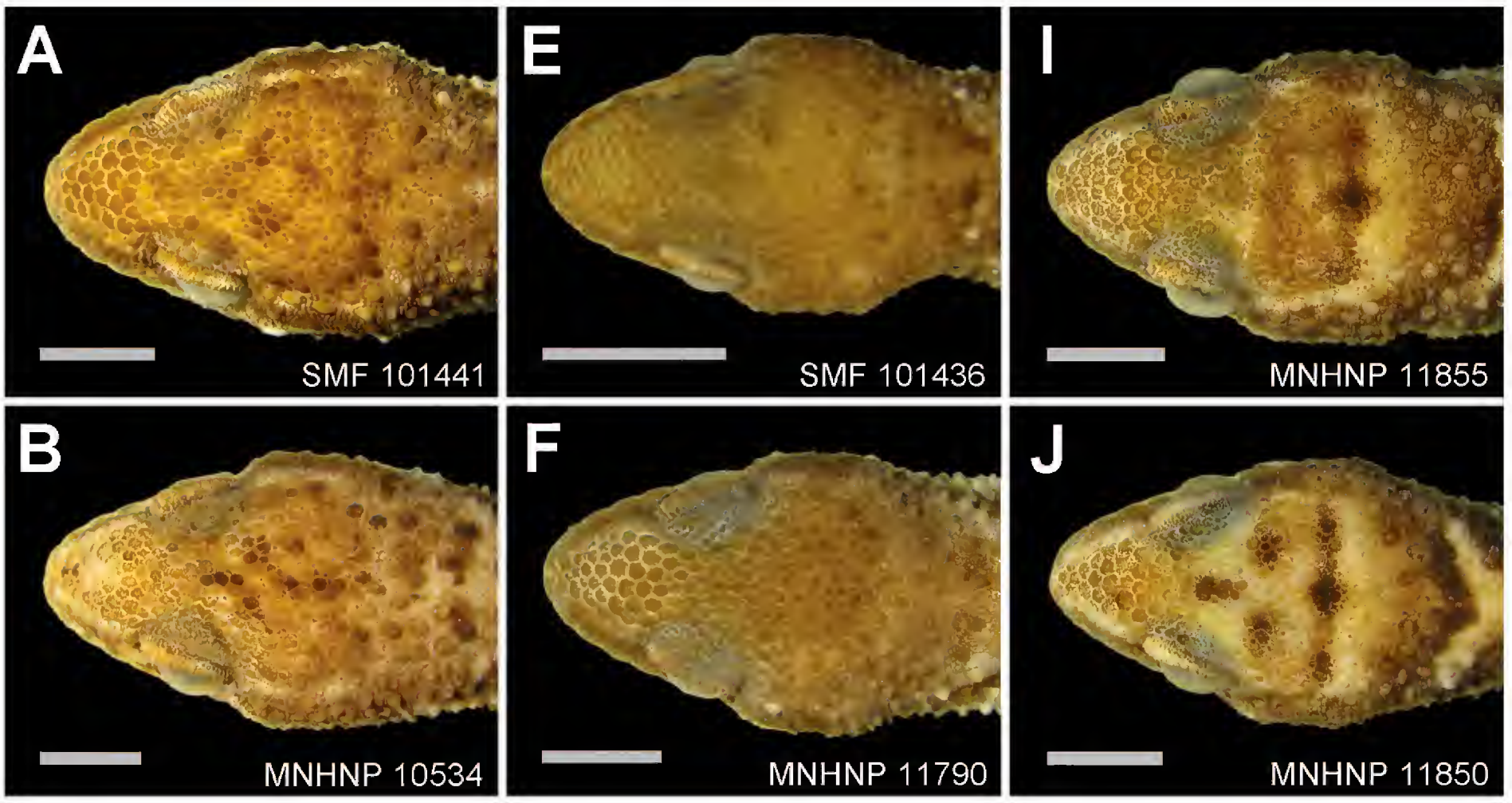

Figure 7. Variation in color patterns of *Homonota marthae* (**A–H**). The lack of the white occipital crescent-shaped line (present in *H. septentrionalis*, **I–L**) is evident in most of the specimens. Scale bars: 5 mm.

Description of the holotype. Adult female, SVL 56 mm (4.1 times the HL), TrL 26 mm, tail length 70 mm, FL 11.0 mm, TL 9.6 mm, AL 13.3 mm, HL 13.6 mm, HW 10.8 mm, HH 8.3 mm, END 4.2 mm, ESD 5.9 mm, EMD 4.7 mm, ID 4.6 mm, IND 2.0 mm; rostral wider (2.7 mm) than high (1.5 mm) with a median groove covering the upper two thirds of the scale; nares surrounded by rostral, supranasal, and postnasal; SL 8/8; one elongated tubercular scale on the mouth commissure; muzzle slightly convex, covered by large homogeneous juxtaposed scales; head covered with big homogeneous juxtaposed scales on the dorsal area, intermixed with small granules; superciliary scales imbricated, associated to spiny-like scales on the posterior half of the orbit; scales on lateral surface of the head heterogeneously covered with strongly conical tubercles intermixed with small granules; auditory meatus oblique and with serrated edge, and one large elongated scale on the upper border; IL 6/6, the last less than half the size of the others; mental bell-shaped; two postmentals less than twice the size of the following posterior scales, contacting the mental, the first IL, and four posterior scales; scales under the head gradually reducing in size posteriorly; dorsal and lateral parts of the neck with granular juxtaposed scales mixed with tubercles;

ventral side of the head covered by imbricate cycloid scales; body dorsally covered with 14–16 rows of strongly keeled scales, separated by one to two small granules in the pleural areas, and three to four granules in the vertebral area; ventral scales cycloid and imbricate arranged in 16 longitudinal rows at midbody; suprascapular, axillary, inguinal regions, and cloacal opening surrounded by small imbricate granules; anterior and dorsal surfaces of limbs covered by large imbricate scales, keeled on the dorsal surface; posterior region of limbs covered by small juxtaposed granules; ventral surface of forelimbs with juxtaposed granules, and ventral surface of hind limbs with large imbricate scales; subdigital lamellae of hands starting from pollex were recorded as follows: 8/8 – 10/12 – 15/13 – 16/16 – 11/11; subdigital lamellae of feet starting from hallux were recorded as follow: 15/13 – 19/17 – 15/16 – 12/12 – 9/9; tail with large imbricated and mucronate scales, 10–12 per caudal whorl.

Coloration of the holotype (in preservative). After five years in preservative, the coloration was recorded as follows: Head Mikado Brown (42) with Warm Sepia (40) speckling on the dorsal surface; Warm Sepia (40) on the sides, with a Light Buff (2) line from nares to orbit, and continuing behind the orbit above the temporal region; supralabials and infralabials Medium Neutral Gray (298) with suffusions of Smoky White (261); and Fawn Color (258) ventrally. Dorsal background color of the body Beige (254) with Vandyke Brown (282) splotches, and poorly defined Chamois (84) transversal lines; Drab (19) laterally, with Dusky Brown (285) and Pale Buff (1) splotches; and Ground Cinnamon (270) ventrally, with Smoky White (261) suffusions. Tail with Grayish Horn Color (268), Sepia (286), and Cream White (52) transversal bands dorsally; Drab (19) laterally; and Smoky White (261) ventrally. Limbs dorsally covered with a reticulation of Drab (19), Chamois (84), and Dusky Brown (285), ventrally grading to Fawn Color (258) in forelimbs, and Ground Cinnamon (270) with suffusions of Smoky White (261) in hind limbs.

Coloration in life. Coloration in life of a young male (SMF 101438) was recorded as follows: Dorsum Mars Brown (223A) with a Tawny Olive (223D) vertebral stripe and transverse lines; dorsum of head Tawny Olive (223D) with a Verona Brown (223B) nuchal band that contains a central Tawny Olive (223D) line; iris Clay Color (123B) with a suffusion of Verona Brown (223B) centrally; dorsal surface of limbs Beige (219D) with Sepia (219) spots; ventral surfaces of head, body and limbs dirty white; dorsal surface of (regenerated) tail light Drab (119C) with scattered Sepia (119) spots; ventral surface of tail Light Drab (119C) with a suffusion of Sepia (119) medially.

Coloration in life of a juvenile female (SMF 101436) was recorded as follows: Dorsal ground color Raw Umber (123) with Raw Umber (223) transverse lines, edged with Pale Horn Color (92) posteriorly. Postocular stripe Ground Cinnamon (239); iris Yellow Ocher (123C) with a suffusion of Dark Drab (119B); dorsal surface of tail Cinnamon Drab (219C) with Sepia (119) bands, borders posteriorly by Chamois (123C); ventral surface of head, body and limbs dirty white, palmar and plantar surfaces Light Drab (119C); anterior portion of ventral tail Beige (219D), with Sepia (119) band on distal portion.

Color variation. One juvenile (SMF 101439, 36 mm SVL) and two young adults (MNHNP 11793, 45 mm SVL; SMF 101438, 45 mm SVL) out of the 17 examined specimens of *Homonota marthae* have a trace of white crescent-shaped band on the occipital area (more visible in the SMF 101439, Fig. 7G), typical of *H. horrida* and *H. septentrionalis*. Nevertheless, many juveniles (such as SMF 101436) show the same coloration as adults (Fig. 7). The specimen MNHNP 7832 has a narrow occipital white band, joined to the postocular lines (Fig. 7C). Some specimens have a darkish coloration (MNHNP 2810, 10744, 11791, 11793) dorsally, and ventrally most of the specimens have a clearer color than the holotype, except for MNHNP 2798, 2810, and 10744. In some specimens (MNHNP 2795, 2798, 2810, 10744) the dorsal color is diffused and the transversal bands are little visible.

Morphological variation. SVL 36–59 mm; TrL 16–27 mm (43.8–48.2% of SVL in females, 40.7–46.7% in males); FL 9–11 mm ($\bar{x}$ 10±0.36) in females, 7–11 mm ($\bar{x}$ 8.7±0.52) in males; TL 8.7–10.1 mm ($\bar{x}$ 9.5±0.2) in females, 8–10.2 mm ($\bar{x}$ 9.1±0.31) in males; AL 9.3–13.7 mm ($\bar{x}$ 12.8±0.28) in females, 11.2–14 mm ($\bar{x}$ 12.4±0.38) in males; HL 9.3–13.8 mm ($\bar{x}$ 13.2±0.19) in females, 11.1–13.5 mm ($\bar{x}$ 12.2±0.31) in males; HW 7.1–11.2 mm (79.4–88% of HL in females, 78.9–85.9% in males); HH 5.5–8.3 mm (52.6–61% of HL in females, 52.6–60.5% in males); END 2.8–5.1 mm (30.8–35.1% of HL in females, 31.4–38.9% in males); ESD 3.9–6.1 mm (40.3–45% of HL in females, 40.5–46.5% in males); EMD 3.1–5 mm (31.3–34.7% of HL in females, 33.8–37% in males); ID 3.8–5.8 mm (33.8–40% of HL in females, 37.1–44.7% in males); IND 1.4–2.1 mm (12.2–16% of HL in females, 11.8–14% in males); SL 5–8; one or two elongated tubercular scales on the mouth commissure; auditory meatus with one large scale on the upper border; IL 5–7; 14–20 longitudinal rows of ventral scales at mid-body; 34–49 transversal rows of ventral scales.

Etymology. This species is named in honor of our indefatigable colleague Martha Motte, who is not only dedicated to safekeeping the herpetological collection of the "Museo Nacional de Historia Natural del Paraguay", but also does a great job in providing selfless support to scientists that are striving to improve the knowledge of the Paraguayan herpetofauna.

Habitat and distribution. *Homonota marthae* is known from the central area of the Paraguayan Dry Chaco in the Department of Boquerón (Fig. 5). The environment is a xeric forest with abundance of thorny vegetation and

almost absence of a herbaceous stratum. Nevertheless, a more detailed analysis of museum collections is advisable for a better knowledge of the distribution of this species.

This species is a dry forest inhabitant, but it is also frequently found in human dwellings. Talbot (1978) recorded the use of logs of Drunken tree (*Chorisia speciosa*: Malvaceae) as shelter by *Homonota* in the Dry Chaco, since the wood of this tree keeps high water levels. Additionally, Cacciali et al. (2007a) demonstrated the use of subterranean caves (usually armadillo burrows) by *Homonota* in several areas of the Paraguayan Chaco.

Discussion

The diversity of species groups within the genus *Homonota* was explored in the last decade, and resulted in the description of *H. williamsii* (Avila et al. 2012) of the *whitii* group, and *H. rupicola* (Cacciali et al. 2007b) and *H. taragui* (Cajade et al. 2013) of the *borellii* group. However, the taxonomy of the *horrida* group (referred to as *fasciata* in Morando et al. 2014) was untouched for many years, and was comprised of two species (*H. horrida* and *H. underwoodi*). Recently, with the description of *H. septentrionalis* by Cacciali et al. (2017), and adding *H. marthae* described herein, the diversity of the *horrida* group currently includes four species. Morando et al. (2014) and Cacciali et al. (2017) presented species trees where the *whitii* group is sister to *horrida* and *borellii* groups. Our deep cluster arrangement is not completely resolved probably due to the use of fewer genes. Nevertheless, there is a strong consensus in the topology of the *horrida* group, where *H. underwoodi* appears as the sister of the remaining taxa (Fig. 1).

No obvious external synapomorphy is known to diagnose the *horrida* group. Three of the four species (*H. horrida*, *H. septentrionalis*, and *H. marthae*) have a pattern characterized by transversal body bands and the presence of a vertebral line. This coloration is different from the remaining species of the genus. The fourth species of the *horrida* group, *H. underwoodi*, has homogeneous body scalation and a completely different pattern, and therefore *H. horrida* and *H. underwoodi* were considered not to be in the same group (Kluge 1964).

The most obvious external difference between *H. marthae* and its presumed closest relative, *H. septentrionalis*, is the lack of a white occipital band in the former taxon, although we found some specimens (mainly juveniles or hatchlings) of *H. marthae* that do have the occipital band. Given that this white occipital band is also present in *H. horrida*, it could be a plesiomorphic character, and therefore the lack of it could be interpreted as the derived state.

Both species seem to inhabit in parapatry the Dry Chaco in Paraguay, and although a major revision of the whole distribution of the group is needed in order to know their actual ranges, *H. septentrionalis* is distributed in the north-westernmost part of the Dry Chaco, whereas *H. marthae* occurs in the central and easternmost areas of the Dry Chaco. Due to the lack of evident geographic barriers between these two species and considering their relatively low morphological variation (especially in males), they remained recognized as a single taxonomic unit until now. Parapatric speciation or breaks to gene flow without evident geographic barriers were observed and discussed by Irwin (2002), and also documented for other geckos in South America's Dry Diagonal, where Werneck et al. (2012) documented a high diversity in sympatric clades of *Phyllopezus* in Caatinga and Cerrado.

The degree of genetic differentiation between these two species is evident, and larger than the degree of morphological differences. Small morphological differentiation or even complete crypsis is common for many organisms, especially when they use the same ecological niche. Specifically for geckos, a recent study showed that it is difficult to find morphological diagnostic characters that match those observed by genetic evidence, as it is the case of the genera *Garthia* and *Homonota*, which are very similar morphologically (Daza et al. 2017). This is in agreement with previous studies that found that molecular genetic tools provided additional evidence for the interpretation of gecko's systematics in the Neotropics (Gamble et al. 2011, Gamble et al. 2012, Morando et al. 2014). The evolutionary processes that led to the molecular differentiation between *H. septentrionalis* and *H. marthae* remain unknown.

Finally, *Homonota marthae* is a common species that resists human perturbation and can be found in rural environments, and although its actual distribution limits are not yet known, and more revisions are needed to target this issue, probably the records of "*Homonota fasciata*" from Defensores del Chaco National Park referred by Cacciali et al. (2016) belong to *H. marthae*, and one of the records of *H. marthae* in Comunidad Ayoreo Tunucojai lays at ~70 km W from Yaguareté Porã Natural Reserve. Thus, we consider that *H. marthae* is not under extinction risk.

Key for identification of the species of the genus *Homonota*

Information to generate the key was based on Cacciali et al. (2007b), Avila et al. (2012), and Cájade et al. (2013). Given that the holotype of *H. fasciata* is completely bleeched, we consider the information on its coloration from the original color description (Duméril and Bibron 1836).

1 Coloration based on irregular or reticulated pattern 2
– Coloration pattern composed of transversal bands 10
2 Dorsal scales homogeneously smooth 3
– Dorsal scales smooth and granular mixed with series of enlarged keeled scales 5

3 Ventral surface of the body immaculate due to lack of chromatophores ..... *H. underwoodi*
– Ventral surface of the body pigmented with chromatophores 4
4 43–49 scales around midbody ..... *H. andicola*
– 55–59 scales around midbody ..... *H. whitii*
5 Series of keeled scales restricted to the posterior half of the dorsum ..... *H. darwinii*
– Series of keeled scales uniformly extended along the whole dorsum 6
6 Dorsal surface of thighs with keeled scales 7
– Dorsal surface of thighs with smooth scales 8
7 Dorsal surface of arms with keeled scales; temporal region with enlarged keeled scales ..... *H. uruguayensis*
– Dorsal surface of arms with smooth cycloid scales; temporal region homogeneously covered by granular scales ..... *H. taragui*
8 146–161 dorsal scales from occipital area to the level of the cloaca; oblique ear opening ..... *H. williamsii*
– 94–139 dorsal scales from occipital area to the level of the cloaca; round ear opening 9
9 45–50 scales around midbody; dorsal surface of the tail with a pattern of thin speckling ..... *H. borellii*
– 54–63 scales around midbody; dorsal surface of the tail with a pattern of black blotches ..... *H. rupicola*
10 Edge of ear opening smooth, without enlarged tubercular scales around; postmentals about five times larger than the scales behind it ..... *H. fasciata*
– Edge of ear opening serrated, with one or two tubercular scales above; postmentals twice larger than the scales behind it 11
11 Tubercles on the dorsal and lateral sides of the neck poorly developed; occipital area with a wide whitish crescent-shaped mark ..... *H. septentrionalis*
– Tubercles on the dorsal and lateral sides of the neck well developed; occipital coloration variable 12
12 Ear opening above the mouth level; occipital area with homogeneous coloration or with a faint reticulation in adults ..... *H. marthae*
– Ear opening at the level of the mouth; occipital area with a wide whitish crescent-shaped mark ..... *H. horrida*

Acknowledgments

Collecting (N° 04/11) and export (N° 02/12) permits were provided by Secretaría del Ambiente. GK thanks Dulcy Vázquez and Thomas and Sabine Vinke for help during fieldwork. We are grateful to Martha Motte (Museo Nacional de Historia Natural del Paraguay - MNHNP) for letting us analyze specimens under her care. For collaboration during collection revisions, we thank Nicolás Martínez (MNHNP) and Cristian F. Pérez (Herpetological collection of the Centro Nacional Patagónico - LJAMM-CNP). We are grateful to the staff (especially Heike Kappes) of the Grunelius-Möllgaard Laboratory (Senckenberg Forschungsinstitut und Naturmuseum Frankfurt - SMF), and to Linda Mogk (SMF) for lab support. PC thanks economic support from the Consejo Nacional de Ciencia y Tecnología (CONACYT, Paraguay) through the Programa Nacional de Incentivo a los Investigadores (PRONII) program. This work is part of an ongoing project of Barcoding of the Paraguayan Herpetofauna, as part of the PhD work of PC, funded by the Deutscher Akademischer Austauschdienst (DAAD, Germany).

References

Abdala V, Lavilla EO (1993) *Homonota fasciata* (Duméril y Bibron, 1836), nombre válido para *Homonota pasteuri* Wermuth, 1965 y *Homonota horrida* (Burmeister, 1861) (Sauria: Gekkonidae). Acta Zoológica Lilloana 42(2): 279–282.

Anisimova M, Gil M, Dufayard JF, Dessimoz C, Gascuel O (2011) Survey of branch support methods demonstrates accuracy, power, and robustness of fast Likelihood-based approximation schemes. Systematic Biology 60(5): 685–699. https://doi.org/10.1093/sysbio/syr041

Avila LJ, Pérez CHF, Minoli I, Morando M (2012) A new species of *Homonota* (Reptilia: Squamata: Gekkota: Phyllodactilidae) from the Ventania mountain range, Southeastern Pampas, Buenos Aires Province, Argentina. Zootaxa 3431: 19–36. http://www.mapress.com/j/zt/article/view/13976

Bouckaert RR, Heled J (2014) DensiTree 2: seeing trees through the forest. bioRxiv, http://dx.doi.org/10.1101/012401

Burmeister H (1861) Reise durch die La Plata Staaten mit besonderer Rücksicht auf die physische Beschaffenheit und den Culturzustand der Argentinischen Republik. Ausgeführt in den Jahren 1857, 1858, 1859 und 1860. H.W. Schmidt, Halle, 515 pp. https://archive.org/details/bub_br_1918_00361310

Cacciali P, Brusquetti F, Bauer F, Sánchez H (2007a) Contribuciones al conocimiento de la biología de *Homonota fasciata* (Sauria: Gekkonidae) en el Chaco paraguayo. Boletín de la Asociación Herpetológica Española 18: 73–77.

Cacciali P, Ávila I, Bauer F (2007b) A new species of *Homonota* (Squamata, Gekkonidae) from Paraguay, with a key to the genus. Phyllomedusa 6(2): 137–146. http://dx.doi.org/10.11606/issn.2316-9079.v6i2p137-146

Cacciali P, Scott NJ, Aquino Ortíz AL, Fitzgerald LA, Smith P (2016) The Reptiles of Paraguay: literature, distribution, and an annotated taxonomic checklist. Special Publications of the Museum of Southwestern Biology 11: 1–373. http://digitalrepository.unm.edu/msb_special_publications/1/

Cacciali P, Morando M, Medina CD, Köhler G, Motte M, Avila LJ (2017) Taxonomic analysis of Paraguayan samples of *Homonota fasciata* Duméril & Bibron (1836) with the revalidation of *Homonota horrida* Burmeister (1861) (Reptilia: Squamata: Phyllodactylidae) and the description of a new species. PeerJ 5: e3523. http://dx.doi.org/10.7717/peerj.3523

Cajade R, Etchepare EG, Falcione C, Barraso DA, Álvarez BB (2013) A new species of *Homonota* (Reptilia: Squamata: Gekkota: Phyllodactylidae) endemic to the hills of Paraje Tres Cerros, Corrientes Province, Argentina. Zootaxa 3709(2): 162–176. http://dx.doi.org/10.11646/zootaxa.3709.2.4.

Carreira S, Meneghel M, Achaval F (2005) Reptiles de Uruguay. Universidad de la República, Montevideo, 639 pp.

Cei JM (1993) Reptiles del noroeste, nordeste y este de la Argentina. Herpetofauna de las selvas subtropicales, Puna y Pampas. Museo Regionale di Scienze Naturali Monografie 14: 1–949.

Corl A, Davis AR, Kuchta SR, Comendant T, Sinervo B (2010) Alternative mating strategies and the evolution of sexual size dimorphism in the side-blotched lizard, *Uta stansburiana*: a population-level comparative analysis. Evolution, 64(1): 79–96. http://dx.doi.org/10.1111/j.1558-5646.2009.00791.x

Daza JD, Gamble T, Abdala V, Bauer AM (2017) Cool geckos: does plesiomorphy explain morphological similarities between geckos from the southern cone? Journal of Herpetology 51(3): 330–342. https://doi.org/10.1670/16-162

Drummond AJ, Suchard MA, Xie D, Rambaut A (2012) Bayesian phylogenetics with BEAUti and the BEAST 1.7. Molecular Biology and Evolution 29: 1969–1973. https://doi.org/10.1093/molbev/mss075

Duméril AMC, Bibron G (1836) Erpetologie générale ou histoire naturelle complete des reptiles. Vol. 3. Libr. Encyclopédique Roret, Paris, 517 pp. https://www.biodiversitylibrary.org/item/99518#page/9/mode/1up

Gamble T, Bauer AM, Colli GR, Greenbaum E, Jackman TR, Vitt LJ, Simons AM (2011) Coming to America: multiple origins of New World geckos. Journal of Evolutionary Biology 24(2): 231–244. http://dx.doi.org/10.1111/j.1420-9101.2010.02184.x

Gamble T, Colli GR, Rodrigues MT, Werneck FP, Simons AW (2012) Phylogeny and cryptic diversity in geckos (*Phyllopezus*; Phyllodactylidae; Gekkota) from South America's open biomes. Molecular Phylogenetics and Evolution 62(3): 943–953. https://doi.org/10.1016/j.ympev.2011.11.033

Gelman A, Rubin DB (1992) Inference from Iterative Simulation Using Multiple Sequences. Statistical Science 7: 457–511. https://doi.org/10.1214/ss/1177011136

Glez-Peña D, Gómez-Blanco D, Reboiro-Jato M, Fdez-Riverola F, Posada D (2010) ALTER: program-oriented conversion of DNA and protein alignments. Nucleic Acid Research 38: W14–W18. https://doi.org/10.1093/nar/gkq321

Guindon S, Dufayard JF, Lefort V, Anisimova M, Hordijk W, Gascuel O (2010) New algorithms and methods to estimate maximum-likelihood phylogenies: assessing the performance of PhyML 3.0. Systematic Biology 59(3): 307–321. https://doi.org/10.1093/sysbio/syq010

Hammer Ø, Happer DAT, Ryan PD (2001) PAST: Paleontological Statistics software package for education and data analysis. Paleontologica Electronica 4: 9. http://palaeo-electronica.org/2001_1/past/issue1_01.htm

Huelsenbeck JP, Ronquist F (2001) Mrbayes: Bayesian inference of phylogeny. Bioinformatics 17(8): 754–755. https://doi.org/10.1093/bioinformatics/17.8.754

Irwin DE (2002) Phylogeographic breaks without geographic barriers to gene flow. Evolution 56: 2383–2394. https://doi.org/10.1111/j.0014-3820.2002.tb00164.x

Jarvis A, Reuter HI, Nelson A, Guevara E (2008) Hole-filled SRTM for the globe Version 4, available from the CGIARCSI SRTM 90m. http://srtm.csi.cgiar.org. [Accessed 02 February 2015]

Katoh K, Standley DM (2013) MAFFT multiple sequence alignment software version 7: improvements in performance and usability. Molecular Biology and Evolution 30(4): 772–780. https://doi.org/10.1093/molbev/mst010

Katoh K, Toh H (2008) Improved accuracy of multiple ncRNA alignment by incorporating structural information into a MAFFT-based framework. BMC Bioinformatics 9: 212. https://doi.org/10.1186/1471-2105-9-212

Kekkonen M, Mutanen M, Kaila L, Nieminen M, Hebert PDN (2015) Delineating species with DNA barcodes: a case of taxon dependent method performance in moths. PLoS ONE 10: e0122481. https://doi.org/10.1371/journal.pone.0122481

Kluge AG (1964) A revision of the South American gekkonid lizard genus *Homonota* Gray. American Museum Novitates 2193: 1–41 .

Köhler G (2012) Color Catalogue for Field Biologists. Herpeton, Offenbach, 49 pp.

Köhler G (2014) Characters of external morphology used in *Anolis* taxonomy—Definition of terms, advice on usage, and illustrated examples. Zootaxa 3774: 201–257. http://dx.doi.org/10.11646/zootaxa.3774.3.1

Lanfear R, Frandsen PB, Wright AM, Senfeld T, Calcott B (2016) PartitionFinder 2: new methods for selecting partitioned models of evolution formolecular and morphological phylogenetic analyses. Molecular Biology and Evolution 34(3): 773–773. https://doi.org/10.1093/molbev/msw260

Mayrose I, Friedman N, Pupko T (2005) A Gamma mixture model better accounts for among site rate heterogeneity. Bioinformatics 21: 151–158. https://doi.org/10.1093/bioinformatics/bti1125

Minh BQ, Thi Nguyen MA, von Haeseler A (2013) Ultrafast approximation for phylogenetic bootstrap. Molecular Biology and Evolution 30(5): 1188–1195. http://dx.doi.org/10.1093/molbev/mst024

Morando M, Medina CD, Ávila LJ, Pérez CHF, Buxton A, Sites JW (2014) Molecular phylogeny of the New World gecko genus *Homonota* (Squamata: Phyllodactylidae). Zoologica Scripta 43(3): 249–260. https://doi.org/10.1111/zsc.12052

Nguyen LT, Schmidt HA, von Haeseler A, Minh BQ (2015) IQ-TREE: A fast and effective stochastic algorithm for estimating Maximum Likelihood phylogenies. Molecular Biology and Evolution 32(1): 268–274. http://dx.doi.org/10.1093/molbev/msu300

Ogilvie HA, Bouckaert RR, Drummond AJ (2017) StarBEAST2 brings faster species tree inference and accurate estimates of substitution rates. Molecular Biology and Evolution 34: 2101–2114. http://dx.doi.org/10.1093/molbev/msx126

Prado DE, Gibbs PE (1993) Patterns of species distributions in the Dry Seasonal Forest of South America. Annals of Missouri Botanical Garden 80(4): 902–927. https://doi.org/10.2307/2399937

Puillandre N, Lambert A, Broullet S, Achaz G (2012) ABGD, Automatic Barcode Gap Discovery for primary species delimitation. Molecular Ecology 21(8): 1864–1877. http://dx.doi.org/10.1111/j.1365-294X.2011.05239.x

Ronquist F, Huelsenbeck JP (2003) MrBayes version 3: Bayesian phylogenetic inference under mixed models. Bioinformatics 19(12): 1572–1574. https://doi.org/10.1093/bioinformatics/btg180

Shapiro SS, Wilk MB, Chen H (1968) A comparative study of various tests of normality. Journal of the American Statistical Association 63(324): 1343–1372. https://doi.org/10.2307/2285889

Smithe FB (1981) Naturalist's Color Guide. Part I. American Museum of Natural History, New York, 23 pp.

Stucky BJ (2012) SeqTrace: A graphical tool for rapidly processing DNA sequencing chromatograms. Journal of Biomolecular Techniques 23(3): 90–93. https://doi.org/10.7171/jbt.12-2303-004

Sullivan J, Swofford DL, Naylor GJP (1999) The effect of taxon sampling on estimating rate heterogeneity parameters of maximum-likelihood models. Molecular Biology and Evolution 16: 1347–1356. https://doi.org/10.1093/oxfordjournals.molbev.a026045

Surget-Groba Y, Thorpe RS (2013) A likelihood framework analysis of an island radiation: phylogeography of the Lesser Antillean gecko *Sphaerodactylus vincenti*, in comparison with the anole *Anolis roquet*. Journal of Biogeography 40(1): 105-116. https://doi.org/10.1111/j.1365-2699.2012.02778.x

Talbot JJ (1978) Ecological notes on the Paraguayan Chaco herpetofauna. Journal of Herpetology 12: 433-435. https://doi.org/10.2307/1563636

Trifinopoulos J, Nguyen LT, von Haeseler A, Minh BQ (2016) W-IQ-TREE: a fast online phylogenetic tool for Maximum Likelihood analysis. Nucleic Acid Research 44: W232–W235. https://doi.org/10.1093/nar/gkw256

Werneck FP, Gamble T, Colli GR, Rodrigues MT, Sites J (2012) Deep diversification and long-term persistence in the South American "Dry Diagonal": integrating continent-wide phylogeography and distribution modeling of geckos. Evolution 66: 3014–34. https://doi.org/10.1111/j.1558-5646.2012.01682.x

Yachdav G, Wilzbach S, Rauscher B, Sheridan R, Sillitoe I, Procter J, Lewis SE, Rost B, Goldberg T (2016) MSAViewer: interactive JavaScript visualization of multiple sequence alignments. Bioinformatics 32(22): 3501–3503. https://doi.org/10.1093/bioinformatics/btw474

Yang Z, Landry JF, Hebert PDN (2016) A DNA Barcode Library for North American Pyraustinae (Lepidoptera: Pyraloidea: Crambidae). PLoS ONE 11: e0161449. https://doi.org/10.1371/journal.pone.0161449

Zar J (1999) Biostatistical Analysis, 4th ed. Prentice-Hall, New Jersey, 929 pp.

Appendix 1

Examined specimens

Homonota horrida

ARGENTINA: La Pampa: Ruta Provincial 1, 23.6 km W from intersection with Ruta Nacional 151 (LJAMM-CNP 10523, 10584); Ruta Provincial 27, 37.7 km S from intersection with Ruta Provincial 14 (LJAMM-CNP 10578–9). Mendoza: 1 km S Punta de Agua (LJAMM-CNP 10493, 10496, 10576–7). Neuquén: 41 km NW Punta Carranza (LJAMM-CNP 8713); 6 km SW Picun Leufu (LJAMM-CNP 13948); Ruta Provinicial 5, 10 km N from Ruta Provincial 7 (LJAMM-CNP 7804); Mina La Casualidad (LJAMM-CNP 14551); Villa El Chocón (LJAMM-CNP 6967–8). Río Negro: Avellaneda (LJAMM-CNP 7670, 7674); Villa Regina (LJAMM-CNP 6520, 6530, 6532–3, 6535).

Homonota septentrionalis

PARAGUAY: Boquerón: Cruce San Miguel (MNHNP 11850, 11855, 11860, 11872); Fortín Mayor Infante Rivarola (MNHNP 12238, SMF 101984); Parque Nacional Teniente Enciso (MNHNP 2821, 9037–8, 9131, 11410, 11421, 11423).

Acronyms

LJAMM-CNP: Colección de herpetología del Centro Nacional Patagónico.

MNHNP: Museo Nacional de Historia Natural del Paraguay.

SMF: Senckenberg Forschungsinstitut und Naturmuseum Frankfurt.

Supplementary material 1

Supplementary information

Authors: Pier Cacciali, Mariana Morando, Luciano J. Avila, Gunther Köhler

Data type: Adobe PDF file

Explanation note: Description of a new species of Homonota (Reptilia, Squamata, Phyllodactylidae) from the central region of northern Paraguay

Link: https://doi.org/10.3897/zse.94.21754.suppl1

Zoosyst. Evol. 94 (1) 2018, 163–193 | DOI 10.3897/zse.94.22120

PENSOFT

museum für naturkunde

Molecular phylogenetic analysis of a taxonomically unstable ranid from Sumatra, Indonesia, reveals a new genus with gastromyzophorous tadpoles and two new species

Umilaela Arifin[1], Utpal Smart[2], Stefan T. Hertwig[3,4], Eric N. Smith[2], Djoko T. Iskandar[5], Alexander Haas[1]

1 *Centrum für Naturkunde - Zoologisches Museum, Universität Hamburg, Edmund-Siemers-Allee 1, 20146 Hamburg, Germany*
2 *Amphibian and Reptile Diversity Research Center Department of Biology University of Texas at Arlington, TX 76019-0498, USA*
3 *Naturhistorisches Museum der Burgergemeinde Bern, Bernastrasse 15 CH-3005 Bern, Switzerland*
4 *Institute of Ecology and Evolution, University of Bern, Baltzerstrasse 6, CH-3012 Bern, Switzerland*
5 *School of Life Sciences and Technology, Institute of Technology Bandung, Jalan Ganeca 10 Tamansari, Bandung 40132, Indonesia*

http://zoobank.org/A0627F44-F87E-46EB-AB98-643CF1F37235

Corresponding author: *Umilaela Arifin* (umilaela@gmail.com)

Received 10 November 2017
Accepted 5 February 2018
Published 9 March 2018

Academic editor:
Matthias Glaubrecht

Key Words

Clinotarsus
Huia
Meristogenys
Morphology
Molecular systematics
Ranidae
Species diversity
Taxonomy

Kata Kunci

Clinotarsus
Huia
Meristogenys
Morfologi
Molekular sistematik
Keanekaragaman spesies
Taksonomi

Abstract

The presence of an adhesive abdominal sucker (gastromyzophory) allows tadpoles of certain species of anurans to live in fast-flowing streams. Gastromyzophorous tadpoles are rare among anurans, known only in certain American bufonids and Asian ranids. To date, *Huia sumatrana*, which inhabits cascading streams, has been the only Sumatran ranid known to possess gastromyzophorous tadpoles. In the absence of thorough sampling and molecular barcoding of adults and larvae, it has remained to be confirmed whether other Sumatran ranid species living in similar habitats, i.e., *Chalcorana crassiovis*, possesses this larval type. Moreover, the taxonomic status of this species has long been uncertain and its taxonomic position within the Ranidae, previously based exclusively on morphological characters, has remained unresolved. To study the diversity and relationships of these frogs and to establish the identity of newly collected gastromyzophorous tadpoles from Sumatra, we compared genetic sequences of *C. crassiovis*-like taxa from a wide range of sites on Sumatra. We conducted bayesian and maximum likelihood phylogenetic analyses on a concatenated dataset of mitochondrial (12S rRNA, 16S rRNA, and $tRNA^{val}$) and nuclear (RAG1 and TYR) gene fragments. Our analyses recovered *C. crassiovis* to be related to *Clinotarsus*, *Huia*, and *Meristogenys*. The DNA barcodes of the gastromyzophorous tadpoles matched adults from the same sites. Herein, we provide a re-description of adult *C. crassiovis* and propose "*C. kampeni*" as a synonym of this species. The molecular evidence, morphological features, and distribution suggest the presence of two related new species. The two new species and *C. crassiovis* together represent a distinct phylogenetic clade possessing unique molecular and morphological synapomorphies, thus warranting a new genus.

Abstrak

Pada beberapa jenis katak tertentu yang hidup di sungai berarus deras, di bagian abdomen berudunya terdapat semacam alat perekat sebagai mekanisme adaptasi pada kondisi habitat tempat tinggalnya. Tipe berudu seperti ini dikenal dengan nama *gastromyzophorous* dan sangat jarang ditemukan, hanya diketahui pada beberapa jenis bufonid di Amerika dan katak ranid di Asia. Hingga saat ini, hanya *Huia sumatrana*, dengan habitat sungai berarus deras, yang diketahui memiliki tipe berudu seperti ini di Sumatra. Tanpa survey menyeluruh dan tanpa *DNA barcoding* untuk katak dewasa dan kecebong, dugaan men-

genai keberadaan katak jenis lain dengan tipe berudu serupa di pulau ini, misalnya *Chalcorana crassiovis*, masih harus dibuktikan. Di sisi lain, status taksonomi jenis ini hingga kini masih belum dapat dipastikan, dan posisi taksonominya dalam famili Ranidae hanya berdasarkan karakter morfologi saja. Oleh karena itu, untuk mengetahui keanekaragaman dan hubungan kekerabatan dari katak-katak jenis tersebut, serta untuk memastikan identitas koleksi berudu *gastromyzophorous* dari Sumatra, kami membandingkan data genetik dari semua taxa yang mirip dengan *C. crassiovis* dari berbagai lokasi di Sumatra. Kami merekonstruksi pohon filogeni dengan menganalisis sekuens DNA dari gabungan fragmen gen mitokondria (12S rRNA, 16S rRNA, dan $tRNA^{val}$) dan gen inti (RAG1 dan TYR) menggunakan metode Bayesian dan Maximum Likelihood. Hasil penelitian kami membuktikan bahwa *C. crassiovis* berkerabat dekat dengan *Clinotarsus, Huia*, dan *Meristogenys*. Sekuens DNA dari berudu gastromyzophorous memiliki kecocokan dengan sekuens DNA katak dewasa dari lokasi yang sama. Dalam paper ini, kami menyajikan deskripsi ulang untuk *C. crassiovis* dan menyarankan agar "*C. kampeni*" menjadi junior synonym dari *C. crassiovis*. Bukti molekuler, karakter morfologi, dan kisaran distribusi menunjukkan bahwa terdapat dua jenis baru yang berkerabat dengan *C. crassiovis*. Ketiganya menunjukkan perbedaan filogenetik yang signifikan, yang dibuktikan dengan adanya synapomorphy pada karakter molekuler dan morfologi yang unik. Oleh sebab itu dibentuk genus baru untuk ketiga jenis ini.

Introduction

A fascinating aspect of Southeast Asian ranid frogs is that some of them possess tadpoles with large abdominal suckers. The presence of this adhesive structure has been referred to as gastromyzophory (Inger 1966). Altig and Johnston (1989) described gastromyzophorous tadpoles as an ecomorphological guild. These tadpoles are adapted to live in fast-flowing streams (McDiarmid and Altig 1999, Altig 2006). Their body profile is streamlined with an extended sloping snout. Their adhesive abdominal sucker allows them to cling to rocks even in the fast-flowing, turbulent water of cascades (Nodzenski and Inger 1990, Gan et al. 2015). The abdominal sucker occupies almost the entire ventral surface of the body immediately posterior to the oral disk; both act together to press the body to the substrate through suction. The sucker has raised thickened lateral and posterior rims that seal against the substrate; the oral disk itself is broadly expanded to almost full body width. On the ventral surface of this sucker, there are spots or bands of brown skin, i.e., keratinized epithelium, probably enhancing friction when the sucker engages with the rock surface (Inger 1985, Gan et al. 2015). The tadpoles are able to loosen the suction momentarily to drag themselves forward by action of their strongly developed jaws; algae and other organic rock overgrowth is scraped off by the jaws and keratodont rows of the oral disk while wandering over the rock surface (Inger 1966, AH pers. observ.). According to our field observations on Bornean *Meristogenys* tadpoles (AH unpubl.), this feeding mode restricts taxa with gastromyzophorous tadpoles to certain habitats and microhabitats: clear rocky streams with considerable water velocity and enough light reaching those rocks to form organic overgrowth for the tadpoles to graze on.

Members of the gastromyzophorous tadpole guild are relatively rare among anurans. They are known only in certain bufonids (e.g., Rao and Yang 1994, Boistel et al. 2005, Matsui et al. 2007, Aguayo et al. 2009, Rueda-Solano et al. 2015) and some Asian ranids: species of *Amolops* Cope, 1865, *Huia* Yang, 1991, *Meristogenys* Yang, 1991, and *Rana sauteri* Boulenger, 1909 (Kuramoto et al. 1984, Yang 1991, Malkmus et al. 2002, Matsui et al. 2006, Ngo et al. 2006, Shimada et al. 2007, Stuart 2008, Gan et al. 2015).

In Asia, *Amolops*, *Huia*, and *Meristogenys* are all genera for which the tadpoles are known to have the gastromyzophorous type (Inger 1966, Yang 1991, Shimada et al. 2015): a total of 69 species are currently listed for these genera (Frost 2017). All adult frogs of this group were mainly recorded along swift rocky hill or mountain streams in forested areas. These frogs usually like to perch themselves on rocks or vegetation in the vicinity of streams. In case of *Meristogenys*, it has been reported that eggs are glued to rock surfaces to keep them from being washed away (Malkmus et al. 2002). In Sumatra, this aforementioned habitat for ranid species with gastromyzophorous tadpoles is very abundant due to the mountainous tolopogy, which stretches longitudinally along the island. To date, *Huia sumatrana* Yang, 1991 has been the only Sumatran ranid positively known to possess gastromyzophorous tadpoles (Yang 1991, Manthey and Denzer 2014). The tadpoles of *H. modigliani* (Doria, Salvidio & Tavano, 1999), a species also recorded from Sumatra, remain unkown. In an extensive field effort, we focused on sampling riverine ranids from fast-flowing or torrential streams. We suspected that there might be species, other than *H. sumatrana*, that inhabit torrential stream habitats in Sumatra and also possess gastromyzophrous larvae. In fact, one of us had found unidentified gastromyzophorous tadpoles in Su-

matra in previous fieldwork (DI unpubl.). It has been known that particularly *Odorrana hosii* (Boulenger, 1891), *Chalcorana crassiovis* (Boulenger, 1920), and/or *C. kampeni* (Boulenger, 1920), are Sumatran ranid species that occur in rocky, fast flowing streams, along with *H. sumatrana*. Potentially, as inferred from the preferred habitat of adults, these taxa could all be candidates for possessing gastromyzophorous tadpoles. The tadpoles of *O. hosii*, however, show that such habitats offer various microhabitats options. The tadpole of *O. hosii* have no abdominal sucker and live in relatively quiet, leaf litter filled side-pools (Inger 1966, Grossmann and Manthey 1997, AH pers. observ.). In case of *C. crassiovis* and/or *C. kampeni,* no information regarding tadpoles is hitherto available and the possibility of a gastromyzophorous tadpoles has remained unverified until now.

Chalcorana crassiovis (Boulenger, 1920) was originally described as *Rana crassiovis* Boulenger, 1920 based on two specimens (BMNH 1947.2.3.99 and BMNH 1947.2.4.1) collected from Kerinci, Sumatra, Indonesia at ~1219 m (4,000 ft.) a.s.l.. In the same publication describing *C. crassiovis*, Boulenger (1920) also re-described *Rana pantherina* van Kampen, 1910 as *R. kampeni*. The short original description of *R. pantherina* by van Kampen (1910) included a figure of one specimen. Boulenger (1920) based his description of *C. kampeni* on a specimen (ZMA unregistered number) collected at Bandar Baru, Batak Mts., Kabupaten (=Regency) Dili Serdang, Provinsi (=Province) Sumatera Utara at ± 900 m a.s.l.. Van Kampen (1923) later recorded another population of *C. kampeni* from Serepai and Sungai Kring in Kerinci. Van Tujil (1995) declared the holotype of *C. kampeni* as lost.

Inger and Iskandar (2005) were the first to report on a large series of *Chalcorana crassiovis* from along the banks of Batang Tarusan, Provinsi Sumatera Barat and provide a re-description of *C. crassiovis* on the basis of these samples. The original description of *C. kampeni* was very similar to that of *C. crassovis* leading Inger and Iskandar (2005) to doubt the validity of *C. kampeni* and to conclude that it may be conspecific with *C. crassiovis*. Inger and Iskandar (2005) considered the larger tympanum of *C. kampeni* only a sexual dimorphism within *C. crassiovis*; judging by its small reported size (36.5 mm, van Kampen 1910), the *C. kampeni* type specimen was probably a male. Despite the conclusion of Inger and Iskandar (2005), the two taxa have not been synonymized and some authors have maintained the name *C. kampeni* and applied it to all known populations previously referred to as *Rana kampeni* (e.g., Frost et al. 2006, Che et al. 2007, Oliver et al. 2015).

To date, no studies have included *Chalcorana crassiovis* (or *C. kampeni*) in a molecular phylogenetic context, and few have included Sumatran congeners (Inger et al. 2009, Pyron and Wiens 2011, Oliver et al. 2015, Chan and Brown 2017). Sound phylogenetic hypotheses based on robust sampling of the *Chalcorana* group remain to be proposed. This is significant given the ensuing debates over the relationships among the Asian Ranidae in recent decades. After its original description by Boulenger (1920) as *Rana crassiovis*, this species has been placed in various genera (i.e., *Hydrophylax* (Frost et al. 2006), *Hylarana* (Che et al. 2007), and *Chalcorana* (Oliver et al. 2015)) on the basis of secondary taxonomic implications from analyses of other, putatively related taxa (Frost 2017). This past history of various placements clearly shows that *C. crassovis* needs to be analyzed in a larger phylogentic context amongst ranids. Phylogenetic analyses of new data have the potential to significantly contribute to the ongoing discussion and ultimately lead to more stable taxonomic amendments.

Considering the confusing and unstable taxonomic history of *Chalcorana crassiovis* and its relatives, it became clear that a thorough resampling and molecular analysis of cascade-dwelling frogs of Sumatra was necessary. Herein, we present our analyses of newly sampled material of *C. crassiovis*. The objectives of this study were: 1) to examine the phylogenetic relationships and taxonomic status of *C. crassiovis* and morphologically similar taxa based on new molecular data; 2) to evaluate the phylogenetic position and taxonomy of material topotypic with *C. kampeni*; 3) to assess material from extensive sampling along the longitudinal axis of Sumatra in an effort to elucidate the diversity and distribution of this group of frogs; 4) to assign samples of collected gastromyzophorous tadpoles to specific species based on molecular evidence.

Materials and methods

Sampling strategy

We conducted rapid biological sampling (Ribeiro-Junior et al. 2008) at sites across Sumatra between 2013–2016. All specimens examined were collected during these sampling activities, and additional specimens were collected during 2008 and 2012 (Fig. 1). Rapid sampling entails visiting many sites but with limited time at each site in order to gather as much data as possible from as many sites as possible. This approach is cost effective and indispensable for sampling potentially cryptic species (Ribeiro-Junior et al. 2008). We collected frogs that were morphologically similar to *Chalcorana crassiovis* at their torrential stream habitats along with any gastromyzophorous tadpoles found in the same streams. The sampling included specimens from the reported type locality of the enigmatic taxon *C. kampeni*. Its type locality, when originally described as *Rana pantherina* van Kampen, 1910 was Bandar Baru, a village in the Kabupaten Deli Serdang, Provinsi Sumatera Utara. We collected stream frogs that are morphologically similar to *C. crassiovis* from the hillside streams of Bandar Baru and consider our materials (Appendix 1) topotypic to the original types of *C. kampeni.* The type locality of *C. crassiovis* is "Korinchi, Sumatra, 4,000 feet" (Boulenger 1920). Today, the modern spelling, "Kerinci" is applied to Mt. Kerinci as well as the Kabupaten Kerinci area; the original description does not provide hints as to where exactly the type specimens were collected from within that area. We visited Mt. Ker-

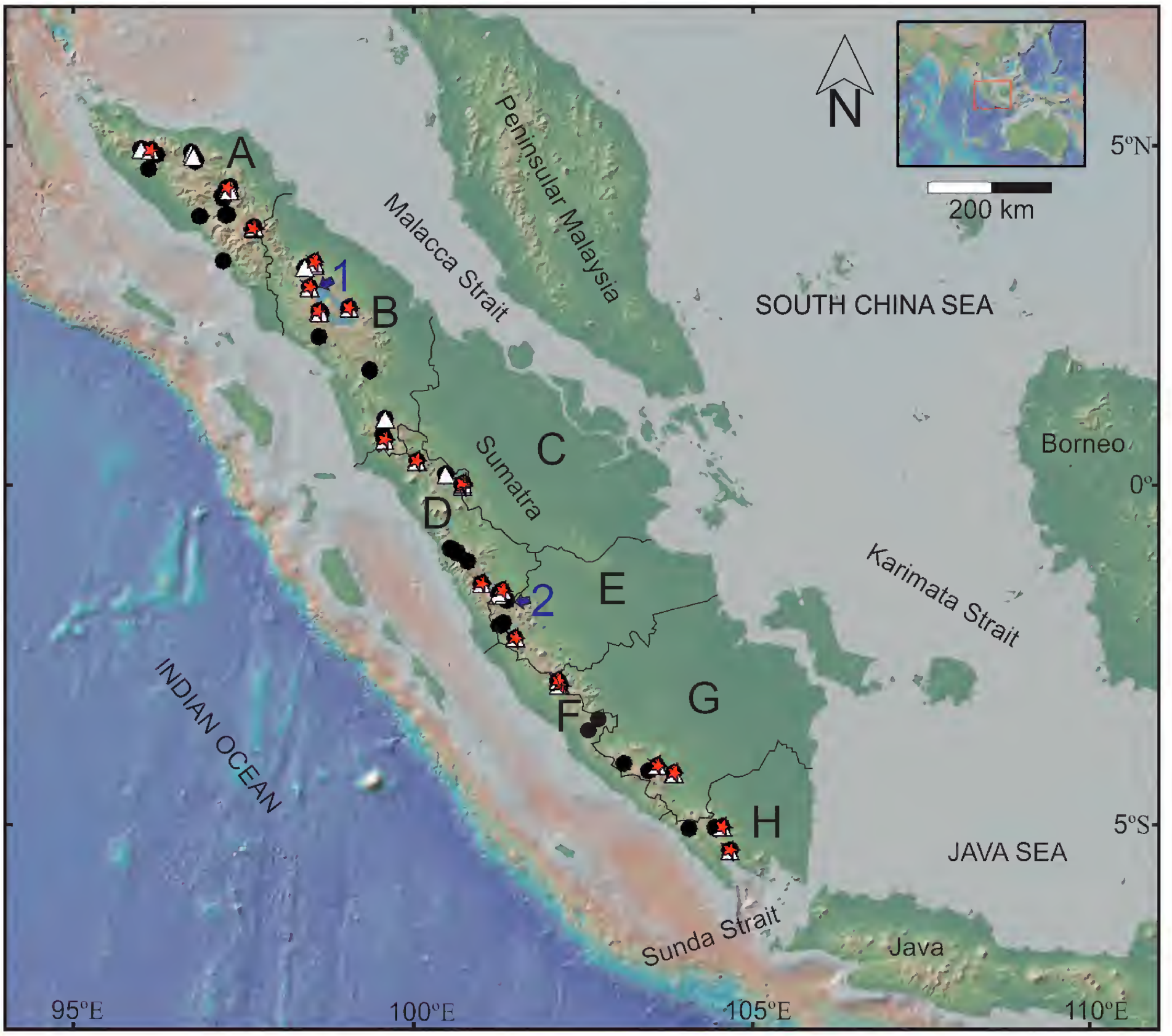

Figure 1. Sampling localities of adult and larva of *Chalcorana crassiovis* specimens for this study. Black circles represent localities of specimens which were examined. White triangles represent localities of specimens which were examined and measured. Red stars represent localities of specimens which were examined, measured, and sequenced. Type locality of *C. kampeni* shown by number 1 (Bandar Baru), number 2 (Kerinci) for *C. crassiovis*. Provinces are shown by alphabet: **A** Aceh, **B** Sumatera Utara, **C** Riau, **D** Sumatera Barat, **E** Jambi, **F** Bengkulu, **G** Sumatera Selatan, **H** Lampung. Borders between provinces are represented by black lines. The map was prepared using GeoMapApp (Ryan et al. 2009).

inci but could not find frogs of the group in question, so our nearest samplings were approximately 10 km north and northeast of Mt. Kerinci and several localities were still within the Kabupaten Kerinci area (Appendix 1).

We followed the general legal guidelines of Germany (Tierschutzgesetz, https://www.gesetze-im-internet.de/tierschg/BJNR012770972.html) for handling and euthanizing the specimens. Each frog was anesthetized slowly and ultimately euthanized in an aqueous solution of chlorobuthanol. Tissue samples of muscle or liver tissue were preserved in either ethanol (96%), RNA later (Sigma Aldrich, USA) or Lysis buffer (0.5 M Tris / 0.25% EDTA / 2.5% SDS, pH 8.2) for DNA analyses. Specimens were fixed in 4% neutral-buffered formalin and then transferred to 70% ethanol for long term storage. All specimens examined in this study are deposited at one of these following museum: The Natural History Museum (**BMNH**), London, United Kingdom; the Museum Zoologicum Bogoriense (**MZB**), Bogor, Indonesia; the Zoologisches Museum Hamburg (**ZMH**), Hamburg, Germany; the Museum of the University of Texas Arlington (**UTA**), Arlington, USA; and the Museum of Vertebrate Zoology (**MVZ**), Berkeley, USA.

In order to uncover the true diversity of *Chalcorana crassiovis,* we acquired DNA sequences from tissue samples of adults (n = 20) from 19 localities across Sumatra. We selected the 20 specimens after a preliminary assessment of the qualitative morphological features of all specimens (n = 329) that were examined. Additionally, we included a subsample of four Sumatran gastromyzophorous tadpoles in the genetic analysis for identification. We

followed the results of previously published studies (Yang 1991, Frost et al. 2006, Oliver et al. 2015) to select potentially related species to compose a diverse and sufficiently comprehensive ingroup in order to test the phylogenetic relationships of our *C. crassiovis* samples. *Staurois* was chosen as the outgroup taxon (Pyron and Wiens 2011). We selected sequence data of *C. chalconota* (Schlegel, 1837), *C. megalonesa* (Inger, Stuart & Iskandar, 2009), *Hydrophylax malabaricus* (Tschudi, 1838), *Hydr. leptoglossa* (Cope, 1868), *Hylarana erythraea* (Schlegel, 1837), *Hyl. macrodactyla* Günther, 1858, *Clinotarsus alticola* (Boulenger, 1882), *Cli. penelope* Grosjean, Bordoloi, Chuaynkern, Chakravarty & Ohler, 2015, and *Staurois guttatus* (Günther, 1858), particularly to serve as generotypic representatives. We applied the name *Cli. penelope* for one sample that was originally loaned under the name *Cli. alticola* (FMNH 268338), because it was identical with available sequences (16S) of *Cli. penelope* (Genbank accession numbers KR827723 [MNHN 2000.4633] and KR827724 [MNHN 930P]; Grosjean et al. 2015).

We added DNA sequences of *Amolops afghanus* (Günther, 1858), *A. indoburmanensis* Dever, Fuiten, Konu & Wilkinson, 2012, *A. marmoratus* (Blyth, 1855), *A. panhai* Matsui & Nabhitabhata, 2006, *Huia sumatrana* Yang, 1991, *H. cavitympanum* (Boulenger, 1893), *H. masonii* (Boulenger, 1884), *H. melasma* Stuart & Chan-ard, 2005, *Meristogenys jerboa* (Günther, 1872) and *M. kinabaluensis* (Inger, 1966) because these taxa have reliably recognizable gastromyzophorous larvae. Finally, we included *Odorrana hosii* (Boulenger, 1891) and *O. livida* (Blyth, 1856) as additional species. *Odorrana hosii* lives syntopically in the same streams with *C. crassiovis*. Sequences of *M. jerboa*, *C. megalonesa, Hyl. macrodactyla, Hydr. malabaricus, Hydr. leptoglossa,* and *O. livida* were obtained from Genbank. The remaining ingroup sequences were generated by this project. The list of voucher specimens (n = 46) comprising the genetic data set is provided in Suppl. material 1.

Laboratory protocols

We extracted DNA from tissue samples (liver, muscle) using Crystal DNA mini Kit (Biolab), PeqGOLD Tissue Kit (Peqlab), or Qiagen DNeasy Blood and Tissue Kit. We then amplified mitochondrial genes (12S rRNA, 16S rRNA, and $tRNA^{val}$) and nuclear genes (recombination-activating gene 1, RAG1, tyrosinase exon 1, TYR) for all frog samples. For tadpoles, we sequenced the 12S rRNA and 16S rRNA (which include $tRNA^{val}$) genes as barcode tool to associate them with adults. Primer information and PCR annealing temperatures applied for this study are provided in Table 1. We cleaned the PCR products using ExoSAP-IT™ and let a contractor (Macrogen, LGC, or Microsynth) sequenced the purified forward and reverse strands. We used GENEIOUS v 8.0 (Kearse et al. 2012, Biomatters Inc., www.geneious.com) to check sequence quality of both strands by comparison to their respective chromatograms, and to assemble and edit if necessary. Furthermore, we aligned sequences for each gene loci using MAFFT v7.017 (Katoh and Standley 2013, module implemented in GENEIOUS v 8.0) with default setting. We eliminated poorly aligned positions and divergent regions of an alignment of each DNA loci using GBLOCK 0.91b (Castresana 2000, Talavera and Castresana 2007) which included in the online software http://www.phylogeny.fr (Dereeper et al. 2008), with setting for a less stringent selection (allows smaller final block and allows gap positions within the final block).

Phylogenetic analyses

We ran PARTITION FINDER v.1.1 (Lanfear et al. 2012) on our concatenated dataset using Bayesian Information Criterion (BIC) to find the best models by testing a variety of models and partitioning strategies for each loci. Four partitions were proposed by the analysis: 12S rRNA, 16S rRNA, and $tRNA^{val}$: GTR+I+ G; RAG1 codon 1, RAG1 codon 2, and TYR codon 1: HKY+I; RAG1 codon 3: HKY+ G; TYR codon 3: K80+G. We then employed Maximum Likelihood (ML) and Bayesian Inference (BI) to infer phylogenetic trees. To explore partitions, we constructed trees using individual loci, concatenated sequences for mitochondrial loci only, concatenated sequences for nuclear loci only, and concatenated sequences for combined mitochondrial and nuclear loci; the later was used for optimal tree reconstruction (Kluge 1989, 2004). ML tree search included 1000 bootstrap replicates in RAXML v. 8 (Stamatakis 2014) and was performed using the CIPRES Science Gateway V 3.3 (Miller et al. 2010, www.phylo.org/sub.sections/portal), with default parameters. We also used the CIPRES Science Gateway to find optimal phylogenetic trees with MR. BAYES v 3.2.6 (Huelsenbeck and Ronquist 2001, Ronquist and Huelsenbeck 2003) in two independent runs, each with four chains, and running for 50 million generations with sampling every 1000 generations. Convergence was assessed by examining all parameters and the effective sample sizes in TRACER v.1.6 (Rambaut et al. 2014) after discarding the first 25% of samples as burn in. We viewed trees that resulted from RAXML and MR. BAYES in FIGTREE v.1.4.3 (http://tree.bio.ed.ac.uk/software/figtree/) and prepared the tree in Fig. 2 using CORELDRAW X6. Nodal support with Bootstrap values (BS) $\geq$ 70 for ML tree (Hillis and Bull 1993) and Posterior Probability value (PP) $\geq$ 0.95 for Bayesian analyses (Huelsenbeck and Ronquist 2001) are herein considered as strong support (Huelsenbeck and Ranala 2004, Mulcahy et al. 2011). We also calculated genetic *p*-distances using MEGA 7.0.25 (Kumar et al. 2016) from 16S ribosomal subunit.

Adult and tadpole morphology

We measured a total of 175 adult *Chalcorana crassiovis* group frogs (males = 133, females = 42). These represent a subsample of all specimens examined (n = 329, Appendix 1). Measurements were taken with digital calipers with 0.01 mm reading accuracy. The subsample of 175 specimens included the sequenced specimens (except for MVZ271526, tissue only). Measurements were taken by UA, following current standards for morphological mea-

Table 1. Gene markers, primer sequences, annealing temperatures and sequence length information.

Markers	Sequence	Annealing temp (°C)	Length (bps)	Citation
12S	12SZ-L: AAAGGTTTGGTCCTAGCCTT 12SK-H: TCCRGTAYRCTTACCDTGTTACGA	52	825	Goebel et al. (1999)
16S+ tRNA^{val}	12sm: GGCAAGTCGTAACATGGTAAG 16sd: CTCCGGTCTGAACTCAGATCACGTAG	51	1406	Pauly et al. (2004), Oliver et al. (2015)
RAG1	Rag1 1F: GCMTTGCTSCCRGGGTATCA Rag1 2R: TCAATGGACGGAAGGGTTTCAATAA	50	801	Oliver et al. (2015)
TYR	Tyr1A: AGGTCCTCTTRAGCAAGGAATG Tyr1G: TGCTGGGCRTCTCTCCARTCCCA	57	579	Oliver et al. (2015)

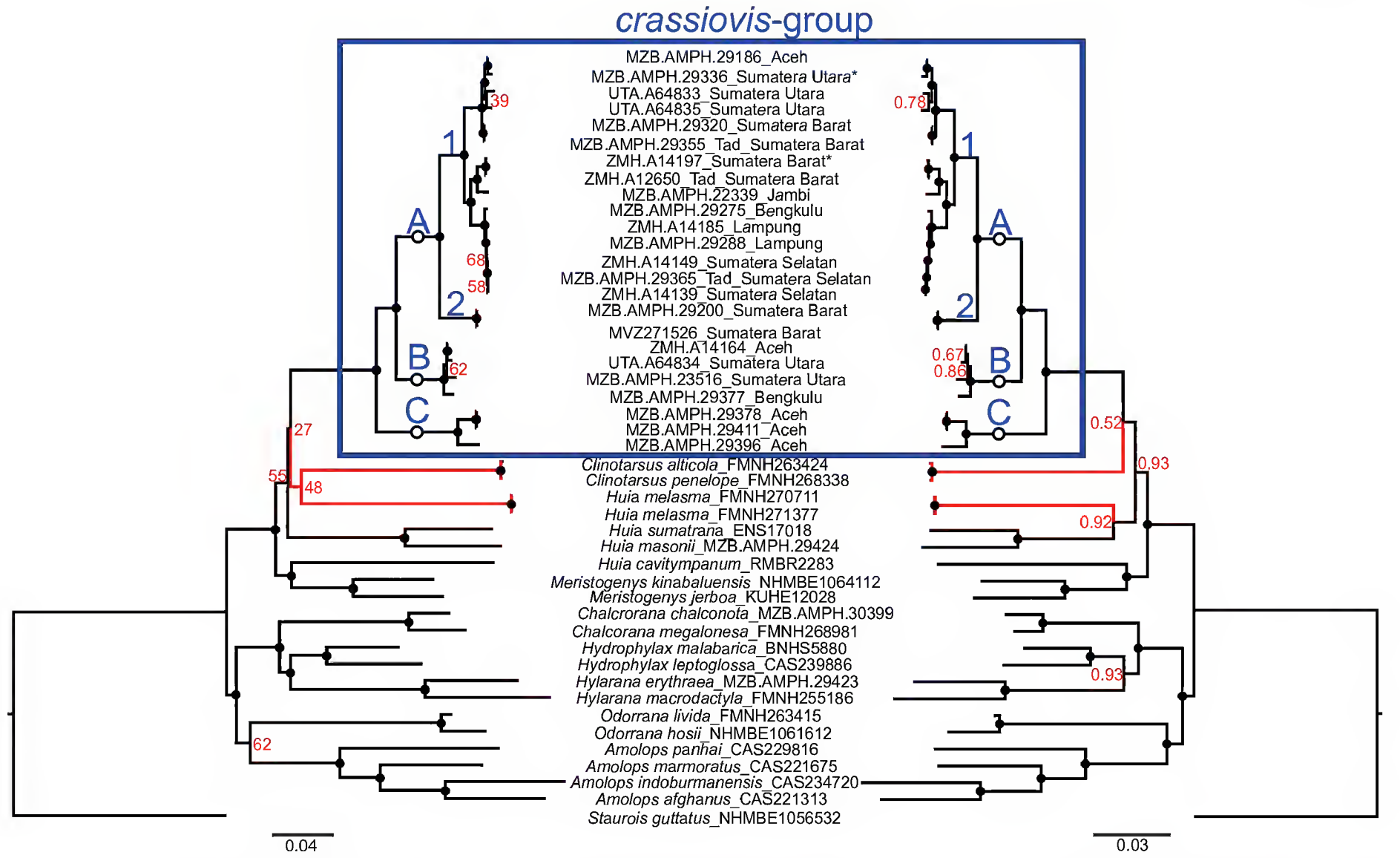

Figure 2. Bayesian (on the right) and Maximum Likelihood (on the left) trees showing the phylogenetic relationship of the *crassiovis*-group. **A, B, C** are distinct lineages within *crassiovis*-group. Black circles represent well supported nodes (PP ≥ 0.95 and BS ≥ 70). Red branches represent relationship between *Clinotarsus* and *Huia melasma*. Tadpole sequences named with specimen number_Tad_locality (province). Adult sequences named with specimen number_locality (province). MZB.AMPH.29336 and ZMH.A14197 were collected from the type locality of *C. kampeni* and *C. crassiovis*, respectively.

surements of frogs (e.g., Matsui et al. 2010, Shimada et al. 2011, Waser et al. 2016, and Watters et al. 2016). All acronyms and definitions of measured distances are explained in Table 2 and illustrated in Suppl. material 2A. We determined sex by the presence of nuptial pads and vocal sacs in males, and their absence and presence of eggs, respectively, in females. We analyzed sexes separately to control for bias resulting from sexual dimorphism.

We collected tadpoles from rocks in fast flowing water using a fishnet and followed the procedures suggested in Haas and Das (2011). We preserved tail tissues of the photographed specimens in either 96% ethanol or RNAlater. We fixed and stored the remaining specimens from the series in neutral-buffered formalin solution (4%). We staged the tadpoles (n = 29) according to the table in Gosner (1960). The range of Grosner stages was 25–42, with the majority of specimens at Stage 25 (n = 12). We assigned the 25 tadpoles that were not sequenced to the respective clade of the genetically examined tadpoles based on their morphological similarity. Standard measurements for tadpoles (Altig 2007, Shimada et al. 2007, Haas and Das 2011, Oberhummer et al. 2014) were taken from digital images with a calibrated digital microscope VHX5000 KEYENCE Corporation, Japan (Table 3 and Suppl. material 2B) by UA. We slightly edited all images in this study using Adobe PHOTOSHOP CS6 (contrast adjustment, background, cleanup, cropping, sharpening). We prepared image plates with CORELDRAW X6.

We followed the morphological terminology of Duellman (2001) and Kok and Kalamandeen (2008). For webbing we used the formula in Guayasamin et al. (2006). We adopted the suggestions for glands cluster definitions from Shimada et al. (2015).

Table 2. Standard measurement for adult specimens used in this study. See Suppl. materials 2A for illustration.

Acronym	Characters	Explanation
SVL	Snout Vent Length	From tip of snout to vent
HL	Head Length	From tip of snout to angle of jaw
HW	Head Width	Maximum width of the head at angle of jaw
SL	Snout Length	From tip of snout to the anterior corner of eye
SN	Snout Narial distance	From tip of snout to center of nares
ED	Eye Diameter	Maximum distance between anterior and posterior corners of eye
EN	Eye Narial distance	From center of naris to anterior circumference of eye
IND	Internarial Distance	Distance between centers of nares
IOD	Interorbital Distance	Minimum distance between upper eyelids
UEW	Upper Eyelid Width	Maximum transverse width of upper eyelid
TYv	vertical Tympanum diameter	Maximum vertical diameter, from the outer edges of tympanic annulus
TYh	horizontal Tympanum diameter	Maximum horizontal diameter, from the outer edges of tympanic annulus
ET	Eye-Tympanum distance	From posterior corner of eye to the anterior edge of tympanum
LAL	Lower Arm Length	From the tip of the elbow to the proximal edge of the palmar tubercle
HAL	Hand Length	From the proximal edge of the palmar tubercle to the tip of Finger III
FE	Femur Length	From center of vent to lateral of knee
TL	Tibia Length	Distance between anterior point of knee and posterior surface of heel with both tibia and tarsus flexed
FL	Foot Length	From proximal end of inner metatarsal tubercle to tip of Toe IV
IMTL	Inner Metatarsal Tubercle Length	Maximum distance between anterior and posterior tip of inner metatarsal tubercle
F1L	Finger I Length	From the proximal edge of subarticular tubercle of Finger I to the tip of Finger I
F2L	Finger II Length	From the proximal edge of subarticular tubercle of Finger II to the tip of Finger II
F3DW	Finger III Disc Width	Maximum width of Finger III disc
T4DW	Toe IV Disc Width	Maximum width of Toe IV disc

Table 3. Standard measurement for tadpole specimens used in this study. See Suppl. materials 2B for illustration.

Acronym	Character	Explanation
BL	Body Length	From snout to the point where the axis of the tail (horizontal septum of myotomes) meets the body wall
BH	Body Height	Maximum body height at trunk
BW	Body Width	Maximum body width
EN	Eye Narial distance	From center of eye to the center of naris
ED	Eye Diameter	Diameter of eye measured horizontally
ES	Eye Snout distance	From tip of snout to the anterior circumference of the eye
IND	Inter Narial Distance	Distance between center of nares
IOD	Inter Orbital Distance	Minimum distance between eyeballs
LFH	Lower Fin Height	Measured at point of maximum tail height
MTH	Maximum Tail Height	Measured from the maximum point of upper fin to the maximum point of lower fin
NL	Narial Length	Maximum aperture of narial opening in dorsal view
ODW	Oral Disc Width	Maximum width of oral disc
SN	Snout Narial distance	From snout to the center of naris
SS	Snout Spiracle distance	From snout to end of spiracle tube
SUL	Sucker Length	From anterior end to posterior end of abdominal sucker
SUW	Sucker Width	Maximum width of abdominal sucker
SSL	Snout and Sucker Length	From the tip of snout and to posterior end of abdominal sucker
TTL	Total Length	From tip of snout to tip of the tail
TAL	Tail Length	Calculated as: Total Lenght (TTL) – Body Length (BL)
TMH	Tail Muscle Height	Maximum tail muscle height at body-tail junction
TMW	Tail Muscle Width	Maximum tail muscle width at body-tail junction
UFH	Upper Fin Height	Measured at point of maximum tail height

Results and discussion

Phylogenetic analyses and morphology

We inferred optimal phylogenetic trees from our concatenated dataset (3611 bps) comprising all gene markers (12S rRNA+16S rRNA+tRNA^{val}+RAG1+TYR), of which 12.16% gaps and undetermined characters state. The best log likelihood of ML tree was -25426.240268.

The tree topologies recovered from ML and BI, respectively, were identical, except for the arrangement of *Clinotarsus* and *Huia melasma* (Fig. 2). Our BI tree (Fig. 2 right) suggested *Clinotarsus* to be sister taxon of the *Chalcorana crassiovis* group and *H. melasma* to be the sister taxon of *H. sumatrana*+*H. masonii*. In the ML tree (Fig. 2 left), however, *Clinotarsus*+*H. melasma* and the *C. crassiovis* group were sister taxa. Based on a dataset of two nuclear markers (RAG1+TYR) and lacking *C. crassiovis*, Stuart (2008) suggested *Clinotarsus*+*H. melasma* to be the sister taxon of a clade comprising other *Huia* species from Sumatra, Java, and Borneo, and *Meristogenys*. In contrast, based on a larger dataset, Pyron and Wiens (2011) identified *Clinotarsus* as sister taxon to *H. sumatrana*+*H. masonii*, whereas *H. melasma* was sister taxon to all other species in a clade comprising *Huia*+*Meristogenys*+*Clinotarsus*. However, all of these scenarios for the arrangement of *Clinotarsus* and *H. melasma* within ranid phylogeny had low nodal support. Consequently, we prefer not to draw any phylogenetic conclusions or recommend taxonomic amendments concerning *Clinotarsus* or *H. melasma*.

With the exception of the incongruence in the position of *Clinotarsus* and *Huia melasma*, both the ML and BI trees confirmed the existence of two major clades each with strong nodal support (Fig. 2): *crassiovis*-group+*Huia*+*Meristogenys*+*Clinotarsus* (PP = 1; BS = 100) and *Amolops*+*Odorrana*+*Hylarana*+*Hydrophylax*+*Chalcorana* (PP = 0.97; BS = 75). This result strongly suggests that *C. crassiovis* is not the closest relative of either *C. chalconota* (generotype) or *C. megalonesa*. DNA barcoding (12S rRNA+16S rRNA+tRNA^{val} genes) successfully matched samples of gastromyzophorous tadpoles to adult in the *crassiovis*-group.

Our results further corroborate previous studies (Stuart 2008, Pyron and Wiens 2011) in that the genus *Huia* is paraphyletic in its current composition. Yet, our phylogenetic trees were different from these previous studies concerning other genera. For example, our trees suggest *Odorrana* to be more closely related to *Amolops* (PP = 0.98, BS = 62, Fig. 2) than to *Chalcorana*+*Hylarana*+*Hydrophylax*. Stuart (2008) and Pyron and Wiens (2011) presented evindence that *Odorrana* was as closely related to some *Rana* or *Lithobathes*, embedded in a more inclusive assemblage (including, among others, *Chalcorana*, *Hylarana*, and *Hydrophylax*, in current generic assignment). To corroborate that was beyond the scope of our analysis and, thus, we did not include samples of *Rana* and *Lithobates*.

Within the clade of the *crassiovis*-group (Fig. 2), unexpected genetic diversity was revealed along the Sumatran transect. Our phylogenetic tree showed three distinct, well supported clades within our samples that previously would have been all be assigned to *Chalcorana crassiovis,* i.e., *Clade* A, Clade B, and Clade C (PP = 1, BS = 100). These three clades showed high genetic divergence among each other (Clade A–B: 6.61–8.53%, Clade A–C: 7.46–9.59%, and Clade B–C: 7.74–8.74%, respectively, Suppl. materials 3). Clade A comprises frogs from northern part of Provinsi Aceh to the southern part of Provinsi Lampung, including samples from the type localities of *C. crassiovis* (ZMH.A14197) and of *C. kampeni* (MZB.AMPH.29336), respectively. We found no evidence, that specimens from the type locality of *C. kampeni* were significantly divergent genetically from the remaining lineages in Clade A (uncorrected *p*-distance = 2.56%). Clade B encompass samples from Aceh, Sumatera Utara, and Bengkulu provinces, whereas Clade C consists of samples from the northern part of Provinsi Aceh. Apart from clearly being genetically distinct, we also found morphological features distinguishing both Clades B and Clade C, respectively, from Clade A. The morphology of our specimens in Clade A, however, fit well the description of *C. crassiovis* (*sensu* Inger and Iskandar 2005 assuming synonymy with *C. kampeni*). In the expanded morphological dataset, both quantitative data (morphometric values and body ratio values) and qualitative data (e.g., skin texture and coloration, iris coloration, pattern of rear of thigh, see Fig. 3) clearly clustered the *C. crassiovis* specimens and their respective geographic division into Clades A–C. Morphological analyses are detailed in the taxonomic section below.

Frogs in Clade A share a similar elevational range (425–1545 m a.s.l.) and a similar habitat type (primary forest or good secondary forest) with Clade C (314–1000 m a.s.l.). Clade A also overlaps in elevational range with Clade B (1190–2033 m a.s.l.). In Aceh, we observed specimens of Clade A and Clade B at the same stream (1190 m a.s.l.), as well as frogs of Clade A and Clade C in another stream (1000 m a.s.l.). These observations suggest independent evolution occurring with the syntopic species. Two genetic samples (MZB.AMPH.29200 and MVZ271526) from Cagar Alam (=Nature Reserve) Rimbo Panti, Kecamatan (=District) Panti, Kabupaten (=Regency) Pasaman, Provinsi (=Province) Sumatera Barat, were separated by 4.05–4.90% uncorrected *p*-distance from their nearest relatives (Suppl. materials 3) and were sister to all other samples in Clade A (Fig. 2). Although this could be indicative of a separately evolving lineage, we could not find unambiguous morphological evidence that could separate these two with certainty from that of the remaining samples in Clade A. Some morphological features in the Rimbo Panti specimens, such as rear of thigh pattern and webbing formula (Fig. 4) overlap with other populations in Clade A. Rimbo Panti specimens (n males = 9, n females = 3) are bigger in size (SVL males = 46.45–48.87 mm, females = 78.00–83.99 mm) com-

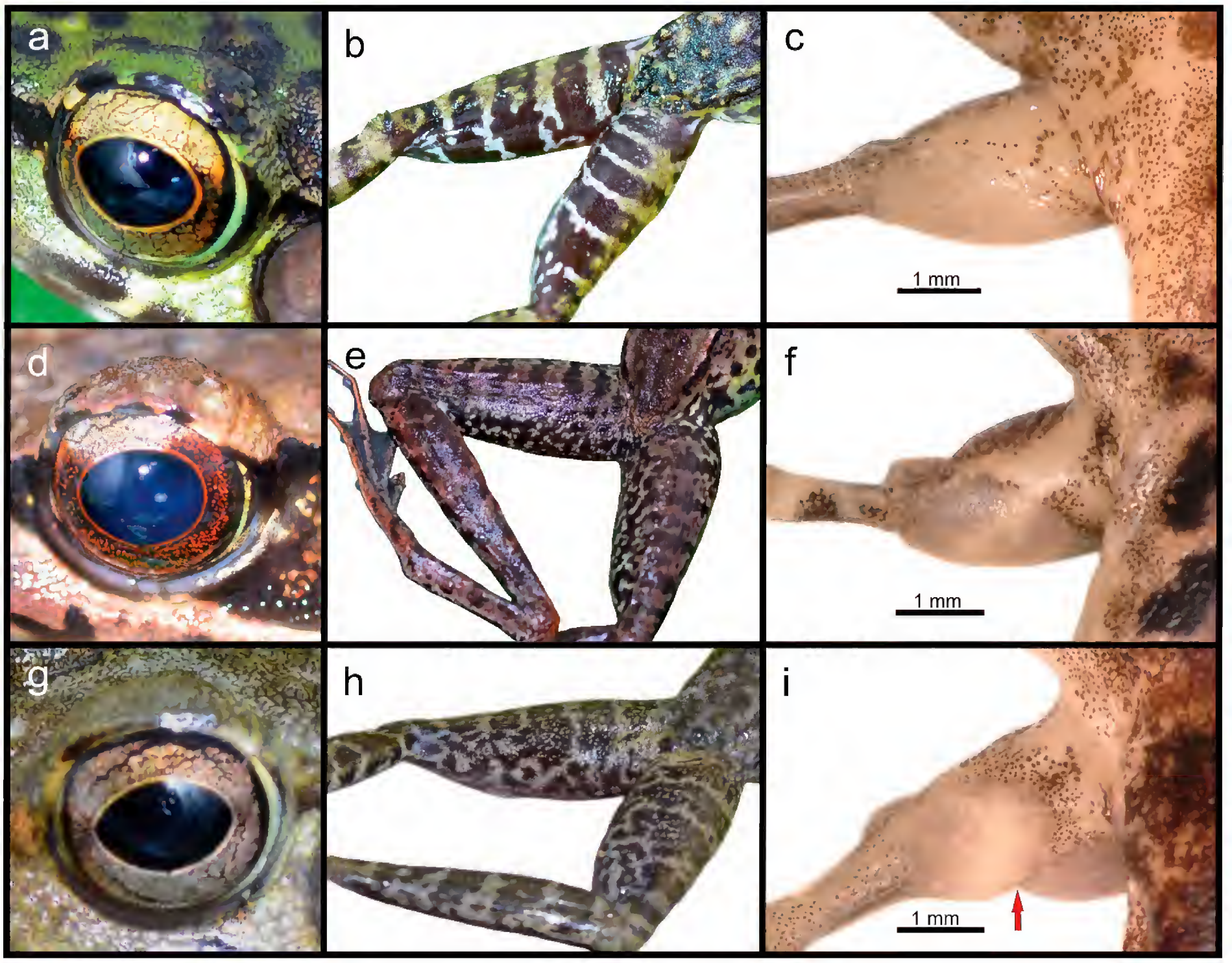

Figure 3. Comparison of three lineages within Clade 1 based on the coloration of iris, the coloration of rear of thigh, and nuptial pad. Clade 1A (**a–c**), Clade 1B (**c–d**) and Clade 1C (**g–i**). Photographs were taken from ZMH.A14197, male, Provinsi Sumatera Barat (**a–c**); ZMH.A14194, female, Provinsi Bengkulu (**d–e**); MZB.AMPH.23524, male, Provinsi Sumatera Utara (**f**); and MZB. AMPH.29396, male, Provinsi Aceh (**g–i**). Photos by U. Arifin.

pared to the remaining samples of this clade (SVL males = 30.30–41.75 mm, females = 40.98–77.73 mm). However, the specimens of Rimbo Panti were collected at 450 m a.s.l. whereas the smallest body size of the remaining specimens of Clade A were from 1355 m a.s.l. at Gunung Kunyit, Kabupaten Kerinci, Provinsi Jambi (SVL males = 30.03–32.81 mm). The rear of thigh of Rimbo Panti specimens is typically mottled, light on dark background (Fig. 4d). The mottling pattern varied among specimens and some specimens are similar in pattern to the specimens from other regions in Clade A. The majority of specimens in Clade A were fully webbed, except for one free phalanx on Toe IV. Six specimens from Rimbo Panti were fully webbed, and six (all males) had webbing only reaching the base of the disc of Toe IV but deeply incised). This webbing pattern is also present in other specimens in Clade A. At present we conservatively consider these differences as interspecific variation, despite the genetic distance.

Three of the four tadpoles sequenced belonged to Clade A and one tadpole belonged to Clade C. Morphological characters such as shape of the jaw sheath and number of keratodont rows showed distinct separation Clades A and C (see below) and were in accordance with the genetically justified assignment.

Taxonomic Amendments: Genus and Species Descriptions

Herein we adopt the Unified Species Concept (de Queiroz 2005) and consider Clades A–C as independently evolving units. Evidence for this assumption is provided by substantial genetic divergence (6.61–9.59%, Suppl. materials 3), robustly supported reciprocal monophyly in phylogenetic analyses, adult and tadpole morphology, geographical distribution, and syntopic occurence. We believe that the establishment of a new genus for the *crassiovis*-group is in place because 1) the group is monophyletic; 2) the group is biogeographically well delimited (endemic to Sumatra); 3) the branch length (Fig. 2) that separates the *crassiovis*-group from any potential relative is substantial and on par with nodes that define other genera in ranids, indicating similar ages of origin. The new genus is comprised of three species, two of which are new to science (Fig. 2).

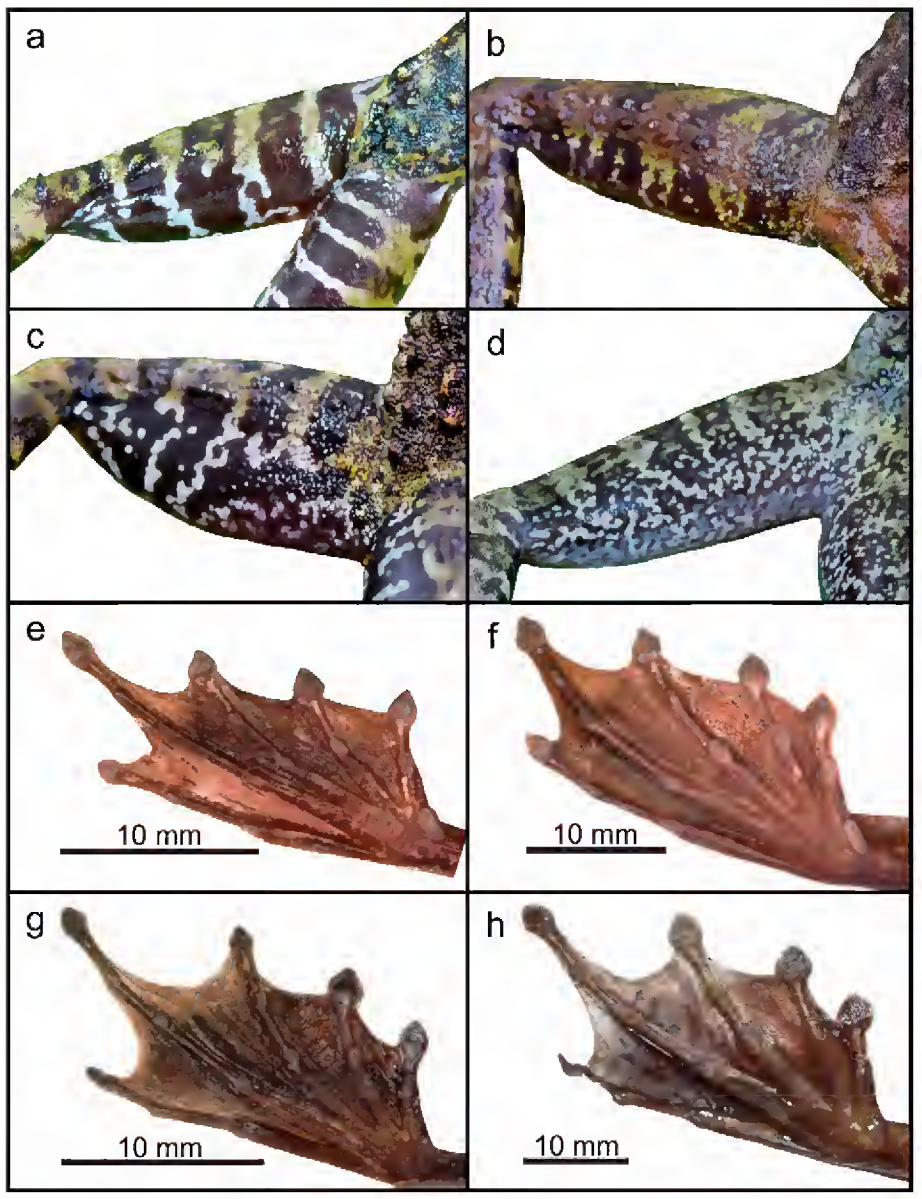

Figure 4. Variation of rear of thigh pattern and webbing on toes of the specimens within Clade 1A. Photographs were taken from ZMH. A14197, male, Provinsi Sumatera Barat (**a, g**); MZB.AMPH.29196, female, Provinsi Aceh (**b**); MZB.AMPH.29320, male, Provinsi Sumatera Barat (**c**); MZB.AMPH.29200, male, Provinsi Sumatera Barat (**d–e**); ZMH.A14170, female, Provinsi Sumatera Barat (**f**); ZMH.A14185, female, Provinsi Lampung (**h**). Photos by U. Arifin

Sumaterana gen. n.

http://zoobank.org/1BC968B1-5D37-4D67-9413-8A4FA811DC83

Fig. 5a–c

Type species. *Rana crassiovis* Boulenger, 1920, Syntypes: two adult females, BMNH1947.2.3.99 and BMNH1947.2.4.1.

Diagnosis. *Sumaterana* gen. n. belongs to a group of ranid torrent frogs, along with *Huia* and *Meristogenys* that possess gastromyzophorous larvae (Inger 1966, Inger and Gritis 1983, Inger 1986, Yang 1991). *Sumaterana* gen. n. species can be diagnosed by a combination of: (1) gastromyzophorous tadpole; (2) larval upper jaw sheaths thick, smooth, broadly arched, with thinner medial section; (3) lower jaw sheaths undivided, smooth, and V-shaped; (4) Labial Tooth Row Formula (LTRF): 8(5–9)/8(1) to 9(5–9)/9(1); (5) infraorbital and postorbital gland clusters present; (6) adult frogs medium sized (SVL males = 27.94–48.87 mm; females = 40.98–83.99 mm); (7) dorsum finely granulated, with or without scattered tubercles; (8) supratympanic fold present (skin fold above the tympanum, starting behind the eye); (9) posttympanic fold absent (vertical skin fold immediately posterior to tympanum); (10) dorsolateral fold absent or present; (11) tibia length 58.08–79.67% SVL; (12) outer metatarsal tubercle absent; (13) inner metatarsal tubercle present; (14) Finger I relatively shorter or subequal to Finger II; (15) width of finger discs larger or subequal to width of toe discs; (16) vocal sacs and nuptial pads present; (17) humeral gland absent.

Comparison. *Sumaterana* gen. n., *Huia*, *Meristogenys*, and *Amolops* can be distinguish from *Chalcorana*, *Clinotarsus*, *Hydrophylax*, *Hylarana*, *Odorrana*, and all other ranids (except, *Rana sauteri*, Kuramoto et al. 1984) by having gastromyzophorous tadpoles. Although *R. sauteri* has gastromyzophorous tadpoles (Kuramoto et al. 1984), Gan et al. (2015) pointed out that *R. sauteri* larvae differs from the gastromyzophorous tadpole of *Huia* and *Meristogenys* in significant features of the sucker (see below). *Amolops* and *R. sauteri* seem only distantly related to *Huia* and *Meristogenys* (Pyron and Wiens 2011; this study), and independent evolution in gastromyzophorous tadpoles must be assumed. We corroborate and expand the conclusion of Manthey and Denzer (2014) that the tadpoles of *Sumaterana* gen. n., *Amolops*, *Huia*, and *Meristogenys* can be distinguished by the shape of their jaw sheaths. The jaw sheath of *Sumaterana* gen. n. is characterized by (followed by *Amolops*; *Huia*; *Meristogenys* features in parantheses): the upper jaw sheath thick, broadly arched, with thinner medial section (thick, broadly arched, without the medial thinning; M-shaped or ∧-shaped; divided; Yang 1991, Manthey and Denzer 2014); lower jaw sheath V-shaped (V-shaped; V-shaped; divided or undivided; Yang 1991, Manthey and Denzer 2014). The number of keratodont rows on the lower lip is eight to nine in *Sumaterana* gen. n. (three to five rows in *Amolops*, except for *A. cremnobatus* with six rows (Inger and Kottelat 1998); six rows or more in *Huia* (Manthey and Denzer 2014); four rows or more in *Meristogenys* (Inger and Stuebing 2009, Manthey and Denzer 2014, Shimada et al. 2015). *Sumaterana* gen. n. has two glandular clusters, infraorbital and postorbital (postorbital and abdominal clusters in *Amolops* (Yang 1991, Inger and Kottelat 1998, Liu et al. 2000, Matsui and Nabhitabhata 2006, Ngo et al. 2006), except for *A. cremnobatus*, postorbital and midlateral clusters (Inger and Kottelat 1998); a combination of infraorbital, postorbital, prespiracular, midlateral, and variably caudal/fin clusters in *Meristogenys* (e.g., Yang 1991, Matsui et al. 2010, Shimada et al. 2011, Shimada et al. 2015); and a combination of caudal/fin, postorbital, midlateral, and infraorbital clusters in *Huia* (Yang 1991; UA pers. observ.).

Adult *Sumaterana* gen. n. can be distinguished from *Huia, Meristogenys,* and *Amolops* by: lacking posttympanic fold (present in *Huia, Meristogenys* and *Amolops*; Yang1991; UA unpubl. data); the disc of Finger III wider or almost equal to that of Toe IV (subequal in *Huia*, less or equal to in *Meristogenys*, wider in *Amolops*; Yang 1991); Finger I length shorter or subequal to that of Finger II (Finger I ≥ Finger II in *Huia*, Finger I > Finger II in *Meristogenys*, Finger I ≤ Finger II in *Amolops*; Yang 1991); lacking an outer metatarsal tubercle (present in *Huia* except for

Figure 5. *Sumaterana* gen. n. species: (**a**) *S. crassiovis* comb. n., ZMH.A14197, male, Provinsi Sumatera Barat; (**b**) *S. dabulescens* sp. n., MZB.AMPH.29396, male, holotype, Provinsi Aceh; (**c**) *S. montana* sp. n., ZMH.A14194, female, paratype, Provinsi Bengkulu. Photos by U. Arifin.

H. cavitympanum, present in *Meristogenys* except for *M. kinabaluensis*; Yang 1991); tibia length relative to SVL 58.08–78.39% (> 70% in *Huia* and in *Meristogenys*; Yang 1991); furthermore, *Sumaterana* gen. n. differs from *Huia* by having a translucent but non-transparent tympanum; tympanum not encased by dark Π-shaped marking (Manthey and Denzer 2014); and dorsolateral folds less distinct or absent. *Sumaterana* gen. n. differs from *Amolops* by having diamond-shaped finger and toe tips (rounded in *Amolops*) and relatively smaller fingers and toe discs.

Etymology. *Sumaterana* is a compound generic epithet created from the Indonesian proper noun Sumatera, the Indonesian name for the island of Sumatra, and *rana*, the feminin Latin word for frog. Sumatera itself is named after the kingdom of Samudra Pasai, which was located along the coast of Aceh, Sumatra from the 13th to the 16th centuries CE. Samudra is a sanskrit word that means gathering of the seas, a place where the Andaman, Java, and South China seas meet the Indian Ocean. *Rana*, was also the very first generic name to be assigned to a member of the *S. crassiovis* group, endemic to the island of Sumatra.

Common name. Sumatran Cascade Frogs (English) and Katak Jeram Sumatra (Bahasa Indonesia).

Phylogenetic definition and content. *Sumaterana* gen. n. is a node-based genus that consists of three known species: *Sumaterana crassiovis* comb. n. (Fig. 2 Clade A, Fig. 5a), *S. montana* sp. n. (Fig. 2 Clade B, Fig. 5c), and *S. dabulescens* sp. n. (Fig. 2 Clade C, Fig. 5b), and their most recent common ancestor. *Chalcorana kampeni* is considered a junior synonym of *S. crassiovis* comb. n. based on Inger and Iskandar (2005) and the new molecular evidence. The monophyletic clade of *Sumaterana* gen. n. is restricted to the island of Sumatra, Indonesia. Our phylogenetic analyses and morphological examination supports these taxonomic recognitions (uncorrected *p*-distances in Suppl. materials 3).

Distribution and habitat. Species of *Sumaterana* gen. n. inhabit riparian habitats in primary or secondary forest in Sumatra, Indonesia. Inhabited streams are typically fast flowing, 5 m wide or less, dominated by big rocks (diameter > 1 m). The known elevational range is from 314–2033 m a.s.l.. Adult frogs of these genus usually perched on rocks or vegetation at the stream. Tadpoles of these frogs can be found in groups attached to the top or sides of rocks in fast moving water.

Sumaterana crassiovis comb. n.

Figs 2 Clade A, 5a, 6a

Rana pantherina Van Kampen, 1910.
Rana crassiovis Boulenger, 1920.
Rana (*Hylorana*) *kampeni* Boulenger, 1920.
Rana (*Hylorana*) *crassiovis* Boulenger, 1920.
Rana (*Hylarana*) *kampeni* Van Kampen, 1923.
Rana (*Hylarana*) *crassiovis* Van Kampen, 1923.
Rana (*Chalcorana*) *kampeni* Dubois, 1992.
Rana (*Chalcorana*) *crassiovis* Dubois, 1992.
Hydrophylax kampeni Frost et al., 2006.
Hydrophylax crassiovis Frost et al., 2006.
Hylarana kampeni Che et al., 2007.
Hylarana crassiovis Che et al., 2007.
Chalcorana kampeni Fei et al., 2010; Oliver et al., 2015.
Chalcorana crassiovis Fei et al., 2010; Oliver et al., 2015.

Syntypes. Two adult females (BMNH1947.2.3.99 and BMNH1947.2.4.1-Fig. 7), Kerinci, Sumatra, Indonesia, 4000 feet (~1219 m a.s.l.), coll. Robinson-Kloss Expedition on the Batrachians. Based on the lack of morphological distinguishing characters (Inger and Iskandar 2005) and low genetic divergence (2.56%, Suppl. materials 3) of topotypic specimens (this study), we consider *C. kampeni* a junior synonym of *S. crassiovis* comb. n..

Referred specimens (283). 262 adults (128 of them: 96 males and 32 females; were measured) and 21 tadpoles collected from Aceh up to Lampung (Appendix 1).

Description. Specimens were assigned to *Sumaterana crassiovis* comb. n. based on comparison of material from Kabupaten Kerinci. *Sumaterana crassiovis* comb. n. is described by the following combination of characters: a medium sized species, SVL in males 30.03–48.87 mm,

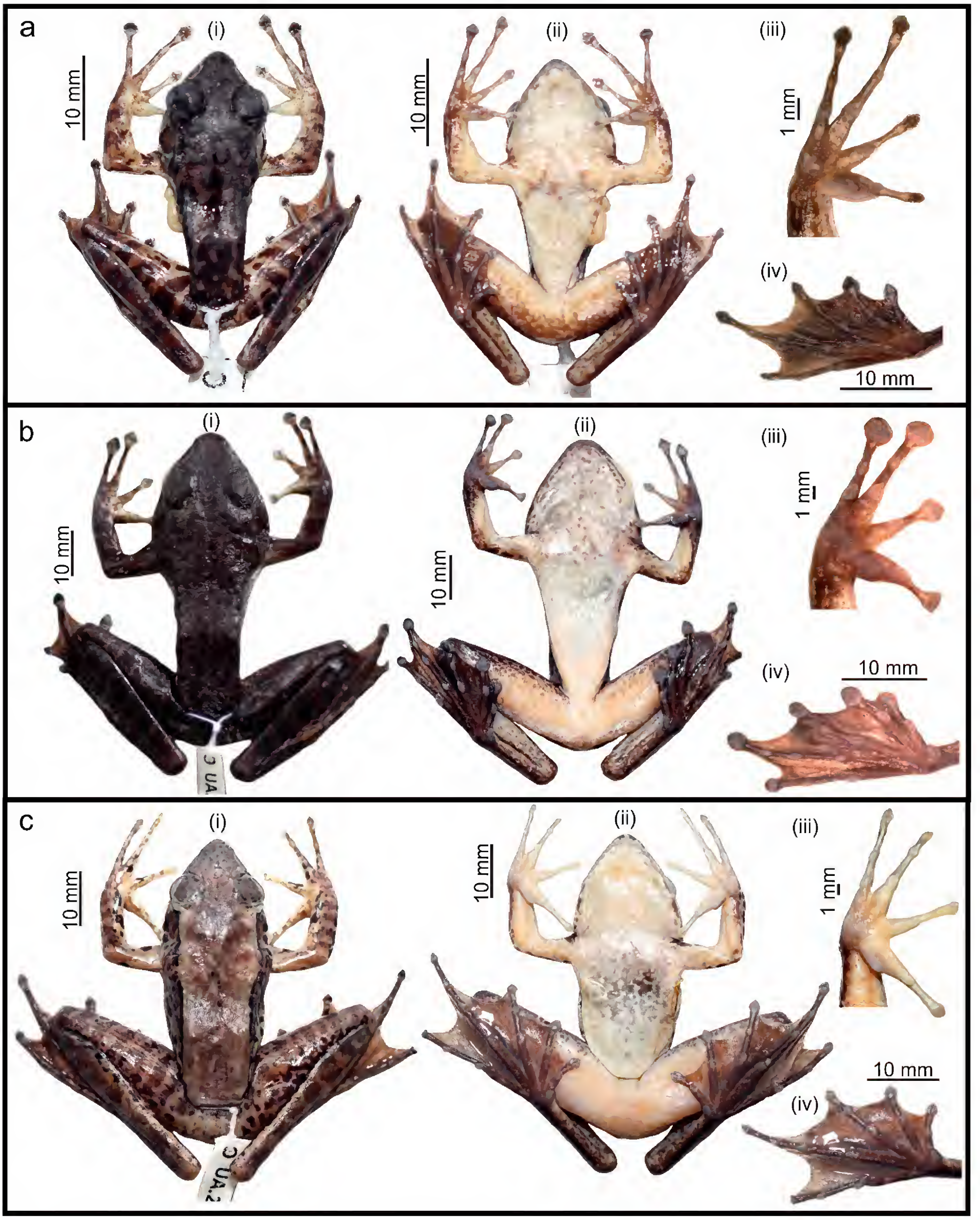

Figure 6. Morphological comparison of (**i**) dorsal, (**ii**) ventral, (**iii**) palmar, and (**iv**) plantar regions of *Sumaterana* gen. n. species. (**a**) *S. crassiovis* comb. n., ZMH.A14197, male, Provinsi Sumatera Barat; (**b**) *S. dabulescens* sp. n., ZMH.A14159, female, paratype, Provinsi Aceh; (**c**) *S. montana* sp. n., ZMH.A14194, female, paratype, Provinsi Bengkulu. Photos by U. Arifin.

females 40.98–83.99 mm; head width subequal to head length; snout rounded, obtusely pointed in dorsal view, slightly protruding in lateral view; nostril closer to snout than to eye; vomerine teeth present, in oblique groups, between choanae; tongue lanceolate; loreal area deeply concave; canthus rostralis sharp, constricted behind nostrils; rictal ridge present; tympanum distinct, translucent (not transparent); interorbital distance 75.96–124.80% width

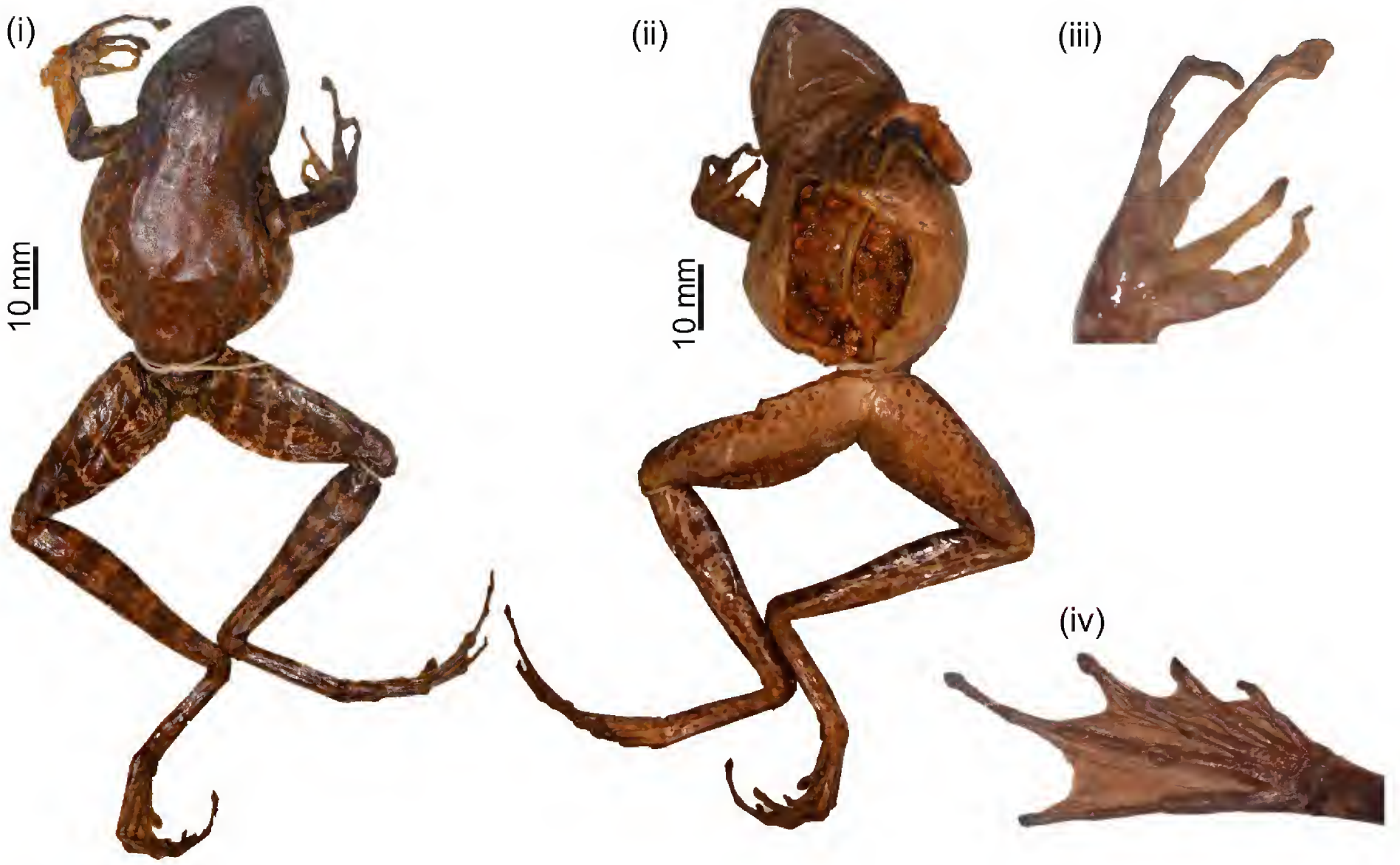

Figure 7. Pictures of dorsal (**i**), ventral (**ii**), palmar (**iii**), and plantar (**iv**) regions of the type species of *Sumaterana crassiovis* comb. n. (BMNH1947.2.4.1, female). Photos by U. Arifin.

of upper eyelid in females, 68.26–120.31% width of upper eyelid in males; pineal spot visible; dorsolateral fold absent; supratympanic fold thick, posttympanic fold absent; dorsum finely granulated with scattered tubercles, variable in size and density; flanks coarsely granulated with few tubercles; venter smooth, granulated posteriorly; rear of thigh usually barred as continuation of thigh dorsal pattern; arm slender, lower arm length 19.03–24.18% SVL in females and 19.58–25.46% SVL in males; hand length 31.54–36.98% SVL in females and 31.77–39.23% SVL in males; fingers long, without webbing; fingertips expanded into discs, diamond-shaped, with circummarginal groove; Finger I < Finger II, Finger III longest; fringes present on the outer phalanges of all fingers; subarticular tubercles distinct; width of Finger III disc > width of Toe IV disc; hindlimbs long, articulation of the heels reaching beyond tip of snout, when limb aligned to body; relative femur length 85.39–94.32% tibia length in females, 85.82–95.02% tibia length in males; length of tibia 60.17–70.52% SVL in females, 58.78–76.44% in males; toes slender and long; tip of toe extended into disc, diamond-shaped, with circummarginal grooves; toe lengths: I < II < III < V < IV, Toe V only slightly longer than Toe III; Toes I, II, III, and V fully webbed, webbing of Toe IV usually one phalanx free ($I(1^{+/-}—1^{+/-})II(1^{+/-}—1^{+/-})III(1^{+/-}—2^{+/-})IV(2^{+/-}—1^{+/-})V$); subarticular tubercles distinct; inner metatarsal tubercle distinct, oval, 92.07–212.77% T4DW in males and 98.80–150.00% in females; outer metatarsal tubercle absent; tarsal fold absent. (Measurements: Tables 4–5).

Coloration. Dorsal skin background green in life, with dark blotches around tubercles, lighter areas on the dorsum forming irregular network pattern; dark line connects the eye and the snout; the upper and lower lips with dark blotches on a light background; iris golden yellow, reddish anteriorly and posteriorly, with a dark netting pattern; tympanum pale brown, encircled by a dark line; flanks lighter than dorsum, lighter ventrad and with dark spots; venter whitish, throat and chest with or without dark marking; distinct cross-bars on dorsal limbs; the rear of thigh with dark vertical bars (usually a continuation from dorsal surface and separated by narrow lighter areas) or mottling (dark marking on lighter background); ventral legs are dusted with brown pigment; webbing color brown. In preservative, dorsal background light brown; flanks becoming gray; iris changed to gray.

Variation. (1) number of tubercles on dorsum and flanks: few to dense; (2) size of tubercles on dorsum: small and round to larger and elongated; (3) dorsolateral fold absent, but row of few small tubercles form incomplete dorsolateral series, dorsal to the posterior of trunk (not in continuation of tympanic fold); (4) dorsal coloration: dark blotches on green background vary from few and isolated, to dense, and forming irregular green background network between the dark blotches; (5) flank color yellowish-green to green (as dorsum), lighter ventrad, with distinct spots; (6) upper and lower lips: whitish to greenish, with dark markings, small distinct bars to wide and connected, lip

Table 4. Morphometric values from all specimens of *Sumaterana* gen. n. examined in this study. Information given for each character as follows: average±st.deviation (first line), min–max (second line).

Character	*S. crassiovis* comb. n.		*S. montana* sp. n.		*S. dabulescens* sp. n.	
	(males, n = 96)	(females, n = 32)	(males, n = 10)	(females, n = 7)	(males, n = 27)	(females, n = 3)
SVL	37.58±4.01 30.03–48.87	67.43±10.42 40.98–83.99	29.98±1.14 27.94–31.56	55.07±2.58 51.61–59.60	37.65±1.45 34.69–40.86	57.30±7.58 48.03–66.60
HL	14.73±1.76 11.92–19.66	26.84±4.04 16.44–32.44	12.01±0.40 11.53–12.83	21.61±0.99 20.42–25.35	14.86±0.53 13.81–15.73	24.13±2.71 20.79–27.43
HW	13.52±1.66 10.96–18.61	24.43±3.72 14.14–29.68	10.88±0.53 9.74–11.79	19.61±1.09 18.04–21.65	14.00±0.59 12.99–15.20	23.03±2.78 19.41–26.18
SL	5.85±0.71 4.52–7.82	10.80±1.66 6.76–13.61	4.99±0.38 4.47–5.53	8.76±0.59 7.83–9.59	5.82±0.22 5.22–6.26	9.55±0.98 8.35–10.74
SN	2.26±0.26 1.78–2.99	3.92±0.64 2.50–5.82	2.15±0.35 1.73–2.77	3.95±0.60 3.11–4.80	2.21±0.14 1.94–2.47	3.39±0.40 2.88–3.85
EN	3.45±0.35 2.62–4.44	6.30±0.95 4.17–8.16	2.70±0.24 2.29–3.14	4.86±0.31 4.58–5.55	3.38±0.13 3.10–3.62	5.33±0.46 4.71–5.80
IND	3.78±0.44 3.03–5.17	6.52±0.94 3.79–7.90	3.50±0.33 3.06–4.01	6.10±0.75 5.04–7.58	3.79±0.19 3.44–4.26	5.95±0.50 5.25–6.40
IOD	3.49±0.34 2.90–4.53	6.13±0.88 4.05–7.99	3.23±0.19 2.96–3.51	5.21±0.40 4.72–5.94	3.41±0.16 3.02–3.76	4.93±0.70 4.03–5.74
UEW	4.07±0.62 2.72–6.05	6.84±1.10 4.18–8.48	2.96±0.18 2.72–3.22	5.21±0.40 4.65–6.00	4.02±0.34 3.41–4.67	5.63±0.56 4.90–6.26
ED	5.62±0.61 4.59–7.70	9.10±1.42 5.68–11.40	4.41±0.35 3.80–4.97	7.23±0.59 6.64–8.29	5.40±0.37 4.76–6.39	7.96±1.06 6.63–9.22
TYv	3.23±0.37 2.39–3.97	3.86±0.59 2.46–4.82	3.08±0.31 2.43–3.40	3.69±0.14 3.50–3.92	3.21±0.23 2.88–3.86	2.99±0.58 2.26–3.67
TYh	3.22±0.36 2.39–4.29	3.84±0.63 2.46–4.82	3.02±0.30 2.44–3.50	3.43±0.14 3.19–3.57	3.12±0.28 2.27–3.70	2.78±0.17 2.58–3.00
ET	1.14±0.29 0.74–2.90	2.74±0.64 1.44–4.01	0.92±0.12 0.70–1.17	2.14±0.17 1.87–2.31	1.20±0.11 1.01–1.50	2.07±0.19 1.90–2.33
LAL	8.26±0.75 6.89–10.06	14.43±2.03 9.00–17.13	7.05±0.31 6.49–7.58	11.63±0.74 10.08–12.45	8.11±0.31 7.74–9.11	12.23±1.23 10.71–13.73
HAL	13.14±1.34 10.77–16.82	23.27±3.34 14.90–30.32	10.85±0.46 10.26–11.72	18.70±0.98 17.41–20.79	12.48±0.42 11.62–13.33	18.25±1.58 16.11–19.87
FE	22.33±2.10 19.29–28.55	40.35±5.89 24.25–50.36	19.75±0.96 18.16–21.14	35.94±1.49 33.97–38.66	22.42±0.81 21.18–24.29	32.44±4.06 27.55–37.50
TL	24.52±2.61 20.74–31.85	44.61±6.31 27.83–55.96	22.17±0.90 20.96–24.20	40.69±1.13 38.29–42.08	23.74±0.72 22.30–25.30	36.01±3.32 31.46–39.28
FL	20.68±2.34 16.26–27.71	38.11±5.57 23.64–49.14	18.82±0.51 18.19–19.53	34.85±1.53 32.30–37.54	19.63±1.31 14.41–22.04	30.27±3.27 25.94–33.85
IMTL	1.75±0.27 1.28–2.62	3.20±0.57 1.72–4.29	1.50±0.13 1.30–1.70	2.70±0.30 2.30–3.27	1.83±0.16 1.51–2.10	2.74±0.26 2.38–2.96
F1L	3.88±0.51 3.02–5.30	7.77±1.34 4.62–10.90	3.46±0.18 3.19–3.84	6.78±0.55 6.07–7.73	3.78±0.18 3.28–4.05	5.62±1.50 3.52–6.96
F2L	4.85±0.59 3.92–6.74	8.89±1.39 5.85–11.79	3.66±0.19 3.30–3.96	6.99±0.53 6.26–8.00	4.55±0.22 4.17–5.19	7.03±0.80 6.01–7.97
F3DW	2.00±0.35 1.29–3.01	3.62±0.62 2.26–5.06	1.16±0.20 0.93–1.54	1.82±0.25 1.40–2.13	2.03±0.16 1.64–2.27	3.00±0.48 2.33–3.46
T4DW	1.36±0.30 0.92–2.26	2.71±0.46 1.72–3.47	1.08±0.21 0.78–1.40	1.82±0.17 1.63–2.20	1.58±0.13 1.30–1.77	2.43±0.32 1.99–2.76

markings absent or very thin in few individuals; (7) ventral dark markings: from none (ventral side whitish) to dark on throat and reaching venter, pale to dark; (8) rear of thigh with dark bars, complete or broken, or occasionally dark mottling on whitish/grayish background (Fig. 4a–d); (9) iris: golden to pale yellow, from faint and thin to dense and dark netting; (10) number of cross bars: 3–4 on lower arm (from elbow to wrist), 4–7 on thigh; (11) Toe IV: from one phalanx free of webbing to webbing reaching intercalary tubercle of Toe IV (Fig. 4e–h). See Fig. 8 for images of *Sumaterana crassiovis* comb. n. from different localities and for morphometric variation Tables 4–5.

Sexual dimorphism. Males significantly smaller than females. Tympanum diameter 45.27–71.68% ED in males, 33.33–48.51% ED in females. Male with distinct undi-

Table 5. Morphometric ratios from all specimens of *Sumaterana* gen. n. examined in this study. Information given for each character as follows: average±st.deviation (first line), min–max (second line).

Character	*S. crassiovis* comb. n.		*S. montana* sp. n.		*S. dabulescens* sp. n.	
	(males, n = 96)	(females, n = 32)	(males, n = 10)	(females, n = 7)	(males, n = 27)	(females, n = 3)
HW/ HL	91.80%±2.75% 86.44%–100.30%	90.97%±2.85% 84.36%–97.32%	90.61%±3.99% 82.85%–95.08%	90.72%±2.30% 87.54%–94.49%	94.21%±2.01% 88.32%–96.87%	95.37%±1.61% 93.36%–97.31%
SL/ ED	104.32%±8.80% 77.76%–125.45%	119.03%±7.66% 106.07%–138.71%	113.90%±13.48% 94.66%–145.53%	121.99%±14.12% 103.02%–144.43%	108.08%±7.18% 94.05%–120.59%	120.50%±3.99% 116.49%–125.94%
EN/ SN	153.27%±12.86% 119.60%–187.64%	162.54%±10.76% 141.08%–187.96%	127.22%±14.95% 107.60%–157.23%	125.25%±16.53% 100.00%–150.80%	153.19%±9.46% 140.27%–177.84%	157.58%±5.31% 150.65%–163.54%
IND/ IOD	108.15%±6.51% 95.83%–143.79%	105.48%±6.82% 91.11%–121.35%	108.01%±5.99% 99.71%–121.88%	116.74%±8.06% 106.78%–128.66%	111.38%±5.47% 102.65%–121.94%	121.74%±7.76% 111.50%–130.27%
IOD/ UEW	86.87%±9.24% 68.26%–120.31%	91.20%±9.72% 75.96%–124.80%	109.33%±3.46% 102.17%–114.14%	98.60%±6.15% 89.33%–105.48%	84.68%±7.10% 72.38%–100.00%	87.24%±3.88% 82.24%–91.69%
TYv/ ED	57.76%±5.57% 46.53%–71.68%	42.59%±3.72% 36.75%–56.83%	74.01%±10.69% 52.31%–89.47%	50.57%±6.19% 43.91%–60.47%	59.63%±4.62% 51.82%–72.94%	37.90%7±.28% 28.18%–45.70%
TYh/ ED	57.45%±5.37% 45.27%–71.68%	42.33%±3.80% 33.33%–56.83%	73.07%±11.60% 52.31%–92.89%	46.46%±4.08% 41.54%–54.67%	58.61%±4.30% 51.82%–69.36%	35.29%±2.68% 32.54%–38.91%
F1L/ F2L	80.08%±4.24% 70.56%–90.80%	86.72%±3.25% 78.97%–93.54%	94.55%±4.18% 87.67%–101.82%	97.05%±2.62% 93.46%–100.89%	83.41%±4.24% 78.03%–94.16%	78.45%±14.09% 58.57%–89.47%
F3DW/ T4DW	148.51%±15.60% 113.73%–197.03%	133.13%±9.69% 112.08%–160.09%	108.13%±8.45% 91.04%–120.00%	93.19%±11.74% 73.68%–108.12%	128.79%±8.42% 105.13%–144.53%	122.94%±4.16% 117.09%–126.38%
FE/ TL	91.16%±2.33% 85.82%–95.02%	90.39%±1.87% 85.39%–94.32%	89.10%±2.63% 85.17%–94.12%	88.33%±2.47% 85.09%–93.45%	94.43%±1.96% 89.40%–97.55%	89.85%±4.00% 86.51%–95.47%
HL/ SVL	39.17%±1.20% 36.22%–42.03%	39.88%±1.24% 37.52%–43.53%	40.09%±1.51% 37.83%–42.88%	38.84%±1.03% 37.16%–40.28%	39.49%±1.13% 37.66%–42.67%	42.22%±0.86% 41.19%–43.29%
HW/ SVL	35.96%±1.46% 33.06%–39.40%	36.27%±1.36% 33.57%–39.68%	36.31%±1.91% 33.66%–39.33%	35.22%±0.59% 34.16%–35.97%	37.20%±1.11% 34.95%–39.01%	40.26%±0.72% 39.31%–41.05%
SL/ SVL	15.56%±0.61% 13.99%–17.05%	16.01%±0.65% 14.70%–17.53%	16.65%±1.23% 14.95%–18.73%	15.74%±0.88% 14.42%–17.04%	15.49%±0.59% 14.46%–16.55%	16.73%±0.52% 16.13%–17.38%
SN/ SVL	6.02%±0.41% 4.81%–7.50%	5.77%±0.24% 5.31%–6.13%	7.18%±1.11% 5.66%–8.86%	7.09%±0.98% 6.01%–8.66%	5.89%±0.38% 5.04%–6.62%	5.93%±0.11% 5.78%–6.02%
EN/ SVL	9.18%±0.47% 8.27%–10.75%	9.37%±0.63% 8.41%–11.02%	9.00%±0.73% 7.44%–10.17%	8.72%±0.25% 8.30%–9.07%	9.00%±0.40% 8.32%–9.64%	9.36%±0.47% 8.71%–9.81%
IND/ SVL	10.06%±0.61% 8.67%–12.62%	9.69%±0.68% 8.05%–10.81%	11.66%±1.01% 10.62%–13.52%	10.91%±0.73% 9.75%–11.96%	10.04%±0.43% 9.23%–11.02%	10.46%±0.60% 9.61%–10.93%
IOD/ SVL	9.31%±0.46% 8.04%–10.75%	9.21%±0.64% 7.26%–10.33%	10.78%±0.51% 10.10%–11.91%	9.36%±0.42% 8.78%–9.96%	9.03%±0.49% 8.17%–10.13%	8.60%±0.16% 8.39%–8.78%
UEW/ SVL	10.81%±0.98% 7.73%–12.90%	10.15%±0.68% 7.73%–11.24%	9.87%±0.59% 8.90%–10.85%	9.50%±0.32% 8.99%–9.90%	10.72%±0.81% 9.18%–12.17%	9.87%±0.34% 9.40%–10.20%
ED/ SVL	14.99%±1.06% 12.82%–19.09%	13.50%±0.84% 11.92%–15.40%	14.72%±1.06% 12.16%–16.10%	13.00%±1.02% 11.80%–14.73%	14.37%±0.85% 12.64%–15.84%	13.88%±0.09% 13.80%–14.00%
TYv/ SVL	8.67%±0.83% 6.80%–10.79%	5.72%±0.45% 4.83%–6.63%	10.80%±1.12% 8.42%–12.96%	6.81%±0.39% 6.42%–7.54%	8.55%±0.52% 7.78%–9.67%	5.26%±0.98% 3.95%–6.31%
TYh/ SVL	8.62%±0.80% 6.42%–10.47%	5.68%±0.42% 4.84%–6.64%	10.73%±1.24% 8.42%–12.36%	6.28%±0.36% 5.68%–6.88%	8.41%±0.55% 7.65%–10.21%	4.90%±0.36% 4.50%–5.37%
ET/ SVL	3.03%±0.79% 2.23%–9.66%	3.98%±0.52% 3.12%–5.08%	3.05%±0.36% 2.38%–3.79%	3.83%±0.19% 3.62%–4.14%	3.18%±0.24% 2.78%–3.79%	3.65%±0.35% 3.32%–4.14%
LAL/ SVL	22.05%±1.22% 19.58%–25.46%	21.41%±1.12% 19.03%–24.18%	23.53%±0.70% 22.48%–24.48%	20.92%±1.52% 19.44%–24.12%	21.61%±0.83% 20.04%–23.05%	21.44%±0.69% 20.62%–22.30%
HAL/ SVL	35.01%±1.51% 31.77%–39.23%	34.47%±1.49% 31.54%–36.98%	36.20%±1.35% 34.17%–38.93%	33.61%±1.47% 30.93%–35.85%	33.26%±1.18% 31.08%–36.00%	32.06%±1.60% 29.83%–33.54%
FE/ SVL	59.54%±2.76% 53.83%–67.33%	59.84%±2.37% 54.62%–63.19%	65.86%±1.38% 63.23%–68.32%	64.63%±2.85% 60.35%–67.80%	59.65%±2.52% 54.95%–64.69%	56.67%±0.49% 56.31%–57.36%
TL/ SVL	65.32%±2.72% 58.78%–75.37%	66.22%±2.71% 60.17%–70.52%	73.97%±2.34% 70.88%–78.39%	73.29%±4.83% 65.28%–79.67%	63.17%±2.51% 58.08%–68.81%	63.20%±2.99% 58.98%–65.50%
FL/ SVL	55.06%±2.44% 49.18%–63.85%	56.46%±2.27% 50.91%–60.23%	62.82%±1.71% 59.52%–65.32%	62.69%±3.42% 57.38%–67.51%	52.25%±3.14% 39.59%–56.93%	53.01%±1.54% 50.83%–54.18%
IMTL/ T4DW	131.80%±22.06% 92.07%–212.77%	117.46%±14.34% 98.80%–150.00%	144.27%±33.28% 97.86%–212.82%	139.17%±19.24% 111.36%–171.78%	115.89%±10.10% 98.75%–138.69%	113.49%±6.59% 104.35%–119.60%

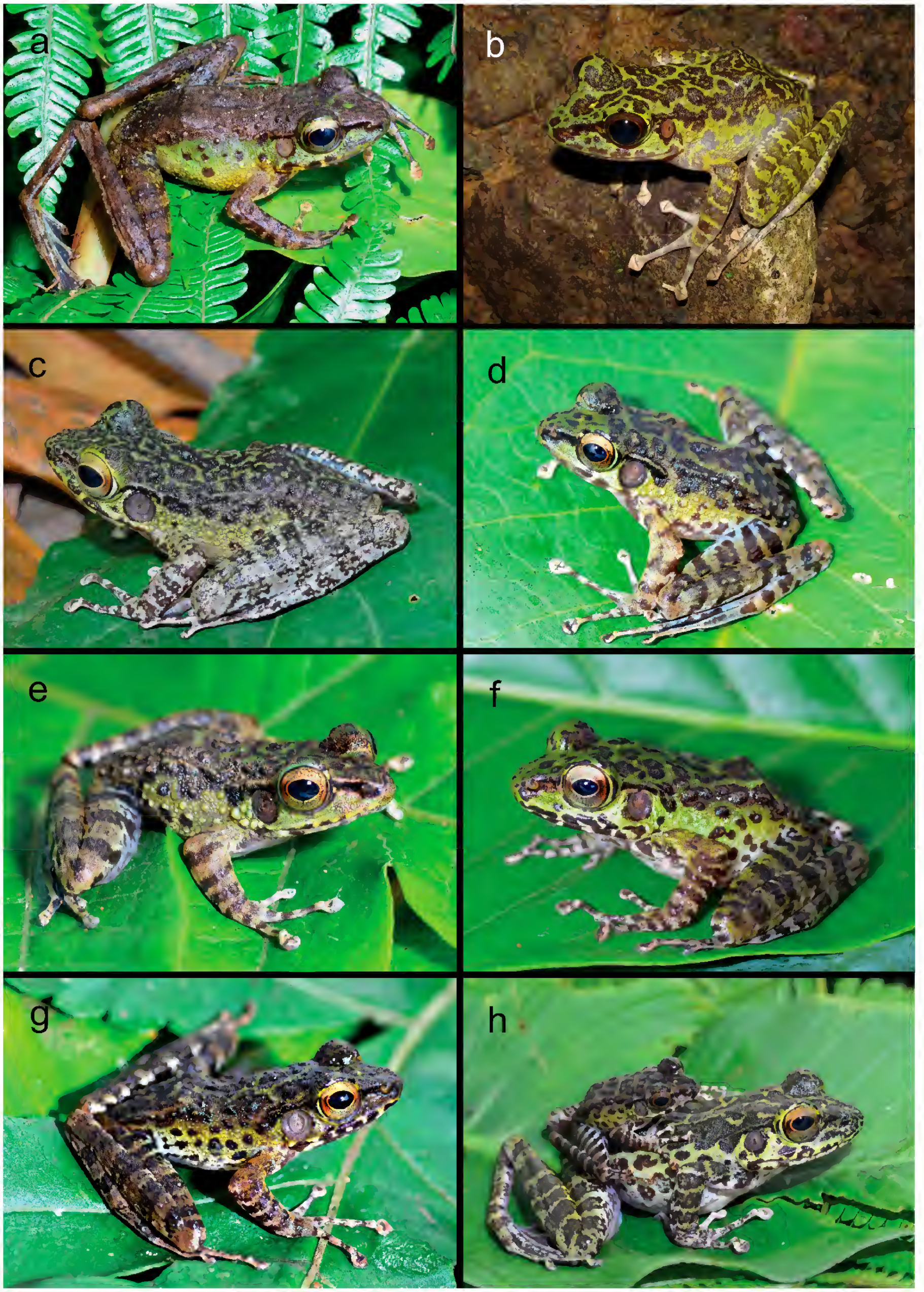

Figure 8. Morphological variation within *Sumaterana crassiovis* comb. n. (**a**) MZB.AMPH.29196, female, Provinsi Aceh, (**b**) Provinsi Sumatera Utara, (**c**) MZB.AMPH.29200, male, Provinsi Sumatera Barat, (**d**) ZMH.A14197, male, Provinsi Sumatera Barat, (**e**) MZB.AMPH.29320, male, Provinsi Sumatera Barat, (**f**) MZB.AMPH.29277, young male, Provinsi Bengkulu, (**g**) ZMH.A14151, male, Provinsi Sumatera Selatan, (**h**) ZMH.A14185 and MZB.AMPH.29296, male and female, Provinsi Lampung. Photos by U. Arifin, except for (b) by A. Irawan.

vided nuptial pads, covering base of the first finger to subarticular tubercle in dorsal and medial surface, paired subgular vocal sacs, humeral glands absent.

Common name. We propose Kerinci Cascade Frogs as the common English name (to replace the old spelling in "*Korinchi Frog*", Iskandar and Mumpuni 2004) and Katak Jeram Kerinci as the Indonesian name.

Distribution and ecological remarks. This species is widespread on the island of Sumatra, ranging from the northern part of Provinsi Aceh to Kabupaten Pasawaran, the southern part of Provinsi Lampung (Fig. 9). Elevational range 425–1545 m a.s.l.. This species is abundant along rocky streams (usually 1–5 m wide) in primary or good secondary forest. The inhabited streams are typically rocky with boulders (usually diameter > 1 m) and with rock formations along the stream, water current velocity 0.2–1.1 m/s (Fig. 10). Males of this species commonly can be observed perching on rocks or vegetation at the stream banks. Females were rarely observed near the streams. It seems that they approach the streams only during breeding activities. Tadpoles were often found in groups, on rocks in the stream, overflown with water in cascading sections.

Tadpoles. Tadpoles were identified (100%) using 12S rRNA+16S rRNA+tRNA^{val} barcoding with adult samples from the type locality. We examined total of 21 tadpoles. Stage 25: MZB.AMPH.29362 (n = 1), ZMH.A12649 (n = 3), MZB.AMPH.29363 (n = 1), MZB.AMPH.29364 (n = 1), Stage 26: MZB.AMPH.29362 (n = 2), MZB.AMPH.29356 (n = 1), ZMH.A12649 (n = 2), MZB.AMPH.29365 (n = 1), Stage 31: MZB.AMPH.29362 (n = 1), Stage 32: MZB.AMPH.29362 (n = 1), Stage 35: MZB.AMPH.29362 (n = 1), ZMH.A12650 (n = 1), Stage 36: MZB.AMPH.29355 (n = 1), ZMH.A12649 (n = 1), Stage 39: MZB.AMPH.29360 (n = 1), Stage 42: MZB.AMPH.29361 (n = 1). One selected tadpole from the lot had 100% match (12S rRNA+16S rRNA+tRNA^{val}) to an adult *Sumaterana crassiovis* comb. n. from the type locality. We refer to ZMH.A12650 (stage 35, Fig. 11a–c) for tadpole description.

Head and trunk approximately oval in dorsal view and dorsoventrally depressed and streamlined, in lateral view; maximum body width 64.40% body length; snout expanded and broadly rounded with emargination laterally setting off snout from body; eyes positioned dorsolaterally, oriented laterally; ED = 2.31 mm; IND/IOD = 48.22%; SN/EN = 44.82%; nostril open without raised rim; positioned anterodorsally and anterolaterally directed; two glands clusters present, infraorbital glands (five on each side) and postorbital glands (one on each side); oral disc ventral, a groove separating upper lip from snout, ODW/BW = 66.33%; oral disc marginal papillae short, arranged in single row; marginal papillae of upper lip present only on sides, on lower lip in uninterrupted row; two short submarginal papillae in lateral area of upper lip; LTRF: 9(6–9)/9(1); upper jaw sheath broad and heavily keratinized, smooth, undivided, thick but with distinct thinner medial section; lower jaw sheath undivided, V-shaped, smooth, and thick; both jaw sheaths finely serrated along their edges; very large abdominal sucker adjoining oral disc posteriorly, SUL/BL = 76.61%, SUW/BW = 89.03%; spiracle sinistral, tube long and posterior half free from body wall, opening directed posteriorly or posterodorsally; anal tube median, free from tail fin, directed posteriorly; strongly muscular tail: TAL/BL = 165.71%, TMH/BH = 71.87%, TMH/MTH = 63.00%; upper fin convex; maximum upper fin height is 30.57% maximum tail height at 49.19% of tail length; tail tip pointed.

In life (Fig. 11a–c), dorsum light brown, orangeish anteriorly and posteriorly to eyes; trunk darker than head; tail muscle light brown with fine-orange stippling; lower flanks region whitish; lateral tail vein very obvious, including dorsal branching along myosepta; upper and lower fins mostly transparent without iridophores; iris black, with dense gold to orange iridescent stippling; abdomen whitish laterally and densely stippled with fine-orange iridophores medially; abdominal sucker mostly transparent with white iridocytes in the center. In preservation, upper side gray with dark stippling; dense-dark stippling laterally; iris black; lens gray; ventral side uniformly transparent with some grey pigments in the anterior region of snout and lateral parts.

Sumaterana montana sp. n.

http://zoobank.org/72D3A049-2C2F-43FC-B38A-483C295BEC08

Figs 2 Clade B, 5c, 6c

Holotype. MZB.AMPH.29377 (female), Gunung Baru, Desa (=village) Seblat Ulu, Taman Nasional (=National Park) Kerinci-Seblat, Kabupaten Lebong, Provinsi Bengkulu, Sumatra, Indonesia (02.88413°S, 102.13073°E), 2033 m a.s.l., 4 May 2014, 20:44, coll. U. Arifin.

Paratypes (10). ZMH.A14194 (female, Fig. 5c and Fig. 6c), approx. 300 m from the holotype locality (02.88525°S, 102.12993°E), 2000 m a.s.l., 3 May 2014, 22:04, coll. U. Arifin and G. Cahyadi. MZB.AMPH.23516 (male) and MZB.AMPH.23517 (female), 02.55397°N, 098.59806°E, 1774 m a.s.l.; MZB.AMPH.23518 (female), UTA.A64829 (female), MZB.AMPH.23519 (male), MZB.AMPH.23520 (male), UTA.A64830 (male), UTA.A64831 (male), UTA.A64832 (male), 2.54691°N, 98.61414°E, 1780 m a.s.l.; vicinity of Tele, Kecamatan Samosir, Kabupaten Toba-Samosir, Provinsi Sumatera Utara, Indonesia, 20 January 2014, coll. E. N. Smith, M. I. Lubis, K. A. O'Connell, and E. Wostl.

Referred specimens (16). See Appendix 1.

Diagnosis. (1) medium sized frog, SVL males (n = 10) 27.94–31.56 mm and females (n = 7) 50.11–63.37 mm; (2) dorsum skin finely granulated, color generally brown with scattered light spots; (3) tympanum distinct and translucent, slightly deep, supratympanic fold present, posttympanic fold absent; (4) dorsolateral fold present, thin, continuation of supratympanic fold to the level of pelvic joint, uninterrupted

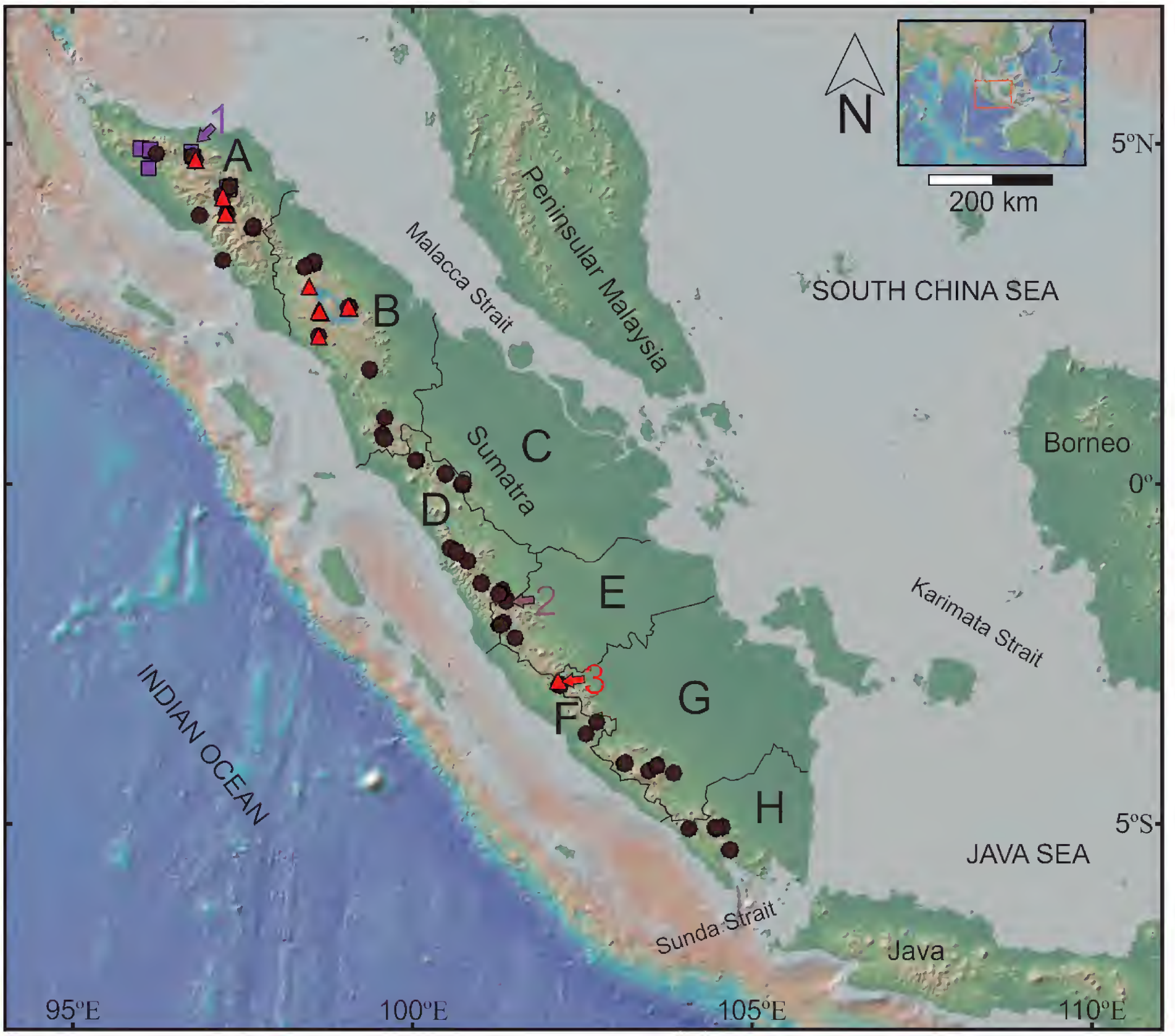

Figure 9. Geographical distribution of *Sumaterana dabulescens* sp. n. (purple squares; type locality purple arrow [**1**]: Jamat, Taman Buru Linge Isaq), *S. crassiovis* comb. n. (brown circles; type locality brown arrow [**2**]: Kerinci), and *S. montana* sp. n. (red triangles; type locality red [**3**]: Gunung Baru, Taman Nasional Kerinci-Seblat). The map was prepared using GeoMapApp (Ryan et al. 2009).

or broken; (5) venter smooth, white or yellowish; (6) tibia length 69.63–79.67% SVL; (7) Finger I 87.67–10.18% Finger II; (8) width of disc of Finger III 73.68–120.00% width of disc of Toe IV; (9) rear of thigh mottled; (10) approx. a quarter of the upper part of iris golden brown and the remaining iris with dense bright red stippling on black background; (11) webbing formula: I(0^{+}—$1^{1/2}$)II(0^{+}—2)III(0^{+}—3^{+})IV(3^{-}—0^{+})V; (12) outer metatarsal tubercle absent, inner metatarsal tubercle present; (13) males with paired vocal sacs, undivided nuptial pad, humeral gland absent.

Comparisons. *Sumaterana montana* sp. n. differs from *S. crassiovis* comb. n. (character in parentheses) in these characters: dorsum color brown with scattered light blotches (green background with dark markings on tubercles, lighter area forming irregular network pattern); iris golden brown in the upper quadrant, below with dense bright red stippling on back background (golden yellow with reddish color in the anterior and posterior sector and dark netting pattern); rear of thigh mottled, light spots on dark background (usually with vertical dark bars on lighter background, as continuation of dorsal thigh); dorsal texture shagreened, generally without tubercles (finely granulated with scattered tubercles); length of Finger I ≈ Finger II (Finger I < Finger II); disc width of Finger III ≈ disc width of Toe IV (disc width of Finger III > disc width of Toe IV); dorsolateral fold present, thin (absent); webbing formula: I(0^{+}—$1^{1/2}$)II(0^{-}—2)III(0^{-}—3^{+})IV(3^{-}—0^{+})V (I($1^{+/-}$—$1^{+/-}$)II($1^{+/-}$—$1^{+/-}$)III($1^{+/-}$—$2^{+/-}$)IV($2^{+/-}$—$1^{+/-}$)V).

Description of holotype. Adult female, gravid; body relatively slender; head width 91.93% head length; snout rounded, slightly pointed in dorsal view, and slightly protruding in lateral view; vomerine teeth present, in oblique groups, between choanae; loreal area deeply concave; canthus rostralis sharp, constricted behind nostrils; rictal ridge

present; eye-nostril distance 133.41% of snout-nostril distance; interorbital distance 99.00% width of upper eyelid; tympanum distinct, translucent, slightly set deep, diameter < 50% ED (TYv/ED = 49.31%, TYh/ED = 44.91%); supratympanic fold present, posttympanic fold absent; pineal spot visible; dorsolateral fold thin, starting in line with supratympanic fold anteriorly to the level of pelvic joint; dorsum and flank skin shagreened; venter skin smooth. Arm slender, lower arm length 19.44% SVL; hand length 32.81% SVL; fingers long, without webbing, tip extended into discs, diamond-like shaped, with circummarginal groove; length of Finger I 96.63% Finger II, Finger III longest; flaps present on the outer phalanges of all fingers; subarticular tubercles distinctive; disc width of Finger III 94.42% disc width of Toe IV. Hindlimbs long, articulation of the heels reach far beyond the tip of snout when limb aligned with body, relative length of femur, foot, and tibia to SVL: 61.01%, 69.63%, and 59.24%, respectively; toe lengths: I < II < III < V < IV, Toe V only slightly longer than Toe III; toe tip extended into diamond-shaped discs; cirmummarginal groove present; webbing formula: I(0^+—$1^{1/2}$)II(0^+—2)III(0^+—3^+)IV(3^-—0^+)V; subarticular tubercle distinct; inner metatarsal tubercle distinct, oval, 152.09% T4DW; outer metatarsal tubercle absent; tarsal fold absent.

Holotype coloration. In life, dorsum and upper head brown with scattered light spots; dark dorsolateral line from eye to groin; flanks brown lighting up ventrad, with yellowish color in the posterior region, and many round dark spots; venter yellowish, dark markings on throat up to half of abdomen; golden brown color in at the upper quarter sector of iris, the remaining parts of iris with dense red stippling on black background; a series of dark spots encircled base of upper eye lid; dark brown line from eye to nostril (along canthus rostralis) towards snout tip, not connected to counterpart at tip of snout; dark brown area between eye and tympanum; tympanum pale brown with darker spot in the center; upper lip background brown, lighter posteriorly, with dark brown spots; lower lip brown with few light spots; arm with four dark cross-bars, from elbow to wrist; dorsal face of thigh and tibia brown, each with 6 dark bars; yellow spots on groin; rear of thigh mottled, whitish and yellow spots on brown background; ventral skin of thigh dusted brown on cream background, denser on both lateral side of posterior region; webbing color brown. Color in preservative similar to life coloration; dorsum brown and markings remain the same; yellowish color on flanks and venter changed into white; iris color became gray.

Holotype measurements (mm). SVL 59.60, HL 23.35, HW 21.65, SL 9.14, SN 4.16, EN 5.55, IND 7.58, IOD 5.94, ED 7.95, UEW 6.00, TYv 3.92, TYh 3.57, ET 2.31, LAL 12.32, HAL 20.79, FE 38.66, TL 41.50, FL 37.54, IMTL 3.27, F1L 7.59, F2L 7.73, F3DW 2.03, T4DW 2.15.

Variation. (1) dorsum color background: light pale brown to dark brown; (2) lighter spots on dorsum, none to dense; variable size; (3) dorsolateral fold: continuous or interrupted, variable thickness; (4) yellowish posterior of flank; pale to brighter; (5) tubercles on flanks: none to many; (6) round dark spots on flanks, few to many; size: small to big; (7) dark marking on throat, chest, and ventrum: none to present and reaching the belly; (8) cross bars on limbs, 3–4 (arm, from elbow to wrist), 5–6 (thigh); variable thickness; (9) mottled pattern on rear of thigh: small, yellow and creamy spots to blotches, on brown background. (Metrics: Tables 4–5).

Sexual dimorphism. Males smaller than females. Tympanum diameter 52.31–92.89% ED in males and 41.54–60.47% ED in females. Adult males with single, undivided nuptial pad covering base of the first finger to subarticular tubercle on dorsal and medial surface. Paired subgular vocal sacs visible, humeral glands absent.

Etymology. The specific epithet is the Latin adjective *montana* in allusion to the distribution of this species at high elevations of the Bukit Barisan mountain range of Sumatra.

Common name. We propose Mountain Cascade Frogs as common English name and Katak Jeram Gunung in Bahasa Indonesia.

Distribution and natural history. Only known from high elevations of northern (Provinsi Aceh and Provinsi Sumatera Utara) and mid (Provinsi Bengkulu) Sumatra (Fig. 9). Known elevation was from 1190–2033 m a.s.l.. The holotype was perching on moss on a root of a dead tree, about 120 cm above a small creek (50 cm wide), ~50 m from Camp 4.5 of Gunung Baru, Desa Ulu Seblat, Taman Nasional Kerinci-Seblat, Kabupaten Lebong, Provinsi Bengkulu (~2000 m a.s.l.). The paratype ZMH.A14194 was observed sitting on the branch, about 300 m away, at the same creek where the holotype was collected, 200 cm above the ground. Accompanying fauna included species of *Rhacophorus* and *Philautus*. Paratypes from the vicinity of Tele, Kecamatan Samosir, Kabupaten Toba-Samosir, Provinsi Sumatera Utara were collected along the stream in the rainforest with patches of coffee plantation. The two specimens of *Sumaterana montana* sp. n. from the stream at Marpunge, Taman Nasional Gunung Leuser, Kabupaten Gayo Lues, Provinsi Aceh were found within low vegetation in the middle of the stream, *S. crassiovis* were abundant syntopically. Specimens from Gunung Sibuatan, Kabupaten Karo, Provinsi Sumatera Utara were found on the stream bank about 1–4 m away from water.

Tadpoles. Unknown.

Sumaterana dabulescens sp. n.

http://zoobank.org/A4E2A0F3-E0DA-43A1-BEEC-0340026C3BCB
Figs 2 Clade C, 5b, 6b

Holotype. MZB.AMPH.29396 (male, Fig. 5b), Desa Jamat, Taman Buru Linge Isaq, Kabupaten Aceh Ten-

Figure 10. (**a–b**) Typical cascading stream habitat of *Sumaterana crassiovis* comb. n. at Taman Nasional Gunung Leuser, Provinsi Aceh. *Sumaterana dabulescens* sp. n. inhabits similar stream habitats. (**c**) Specimen of *S. dabulescens* sp. n. on a rock near a small cascade in its natural habitat at Taman Buru Linge Isaq, Provinsi Aceh. Photos by U. Arifin.

gah, Provinsi Aceh, Sumatra, Indonesia (04.36482°N, 097.24783°E), 440 m a.s.l., 6 March 2014, 20:02, coll. U. Arifin and G. Cahyadi.

Paratypes (24). ZMH.A14159 (female, Fig. 6b) and MZB.AMPH.29398 (female) and five males MZB. AMPH.29400 (male), MZB.AMPH.29402 (male), ZMH. A14161–62 (males), ZMH.A12667 (male), same data as holotype, (20:00–21:31, except ZMH.A12667 at 13:00). UTA.A64917 (male), stream at Enang-Enang Resort, road of Takengon-Bierut, Provinsi Aceh, (04.88649°N, 096.72689°E, 604 m a.s.l.), 7 August 2015, 20:00–21:00, coll. E. N. Smith and F. Akhsani. UTA.A64919 (male), Kabupaten Bener Meriah, Provinsi Aceh, (04.82623°N, 096.74841°E), 924 m a.s.l., 6 August 2015, coll. I. Sidik and F. Akhasani. UTA.A64921 (male), 04.93841°N, 095.98375°E, 314 m a.s.l., UTA.A64922 (male) and UTA.A64923 (male), 04.93852°N, 095.98294°E, 323 m a.s.l., UTA.A64924 (male), 04.93869°N, 095.98250°E, 333 m a.s.l., Kruong Meuriam, Kecamatan Tangse, Kabupaten Pidie, Provinsi Aceh, 6 June 2016, I. Sidik and W. Trilaksono. MZB.AMPH.29381 (male), MZB. AMPH.29383 (male), MZB.AMPH.29385 (male), MZB. AMPH.29387 (male), MZB.AMPH.29389 (male), ZMH. A14154–58 (males), ZMH.A12668 (male), Kecamatan Mane, Kabupaten Pidie, Provinsi Aceh, (4.92091°N, 96.12275°E), 761 m a.s.l., 20 March 2014, coll. U. Arifin and G. Cahyadi.

Referred specimens (22). 13 adults, one juvenile, and 8 tadpoles (Appendix 1).

Diagnosis. (1) medium sized frog, SVL males (n = 27) 34.69–40.86 mm and females (n = 3) 48.03–66.60 mm; (2) dorsum finely granulated with scattered round, distinct tubercles; generally gray with dark gray spots on tubercles; (3) tympanum distinct and translucent (not transparent), supratympanic fold present, posttympanic fold absent; (4) dorsolateral fold absent; (5) venter smooth, granulated posteriorly, white; (6) tibia length 58.08–68.81% SVL; (7) Finger I 58.57–94.16 Finger II; (8) width of disc of Finger III 105.13–144.53% width of disc of Toe IV; (9) rear of thigh mottled; dark blotches on light background; (10) iris silver-gray with dark netting, slightly yellow to orange golden in the upper part; (11) all toes fully webbed to base of discs ($I(1^{+/-}—1^{+/-})II(1^{+/-}—1^{+/-})III(1^{+/-}—1^{+/-})IV(1^{+/-}—1^{+/-})V$); (12) outer metatarsal tubercle absent, inner metatarsal tubercle present; (13) males with paired vocal sacs, divided nuptial pad, humeral gland absent.

Comparison. *Sumaterana dabulescens* sp. n. differs from *S. crassiovis* comb. n. and *S. montana* sp. n. (character in parentheses: *S. crassiovis* comb. n.; *S. montana* sp. n.) by gray dorsum with dark markings on tubercles, lighter area forming irregular network pattern (green background with dark markings on tubercles, lighter area forming irregular network pattern; brown background with lighter sports, Fig. 5); iris color in life silver gray with dark reticulation, slightly yellow to golden in the upper part (golden yellow with reddish color in the anterior and posterior sector and dark netting pattern; golden brown in the upper quadrant of the iris, remaining iris with dense bright red stippling on black background; Fig. 3); rear of thigh mottled, dark blotches on light background (generally barred, dark bars on light background; mottled, light spots on dark background; Fig. 3); dorsal skin texture coarsely granulated with scattered round tubercle, vary in size and density (finely granulated with scattered tubercles, vary in size, shape, and density; shagreened, without tubercles); dorsolateral fold absent (absent; present, thin); length of Finger I < Finger II (Finger I < Finger II; Finger I ≈ Finger II); nuptial pad on male divided (undivided; undivided; Fig. 3); webbing full on all toes (I($1^{+/-}$—$1^{+/-}$)II($1^{+/-}$—$1^{+/-}$)III($1^{+/-}$—$2^{+/-}$)IV($2^{+/-}$—$1^{+/-}$)V; I(1—$1^{1/2}$)II(0—2)III(0—3)IV(3—0)V).

Description of holotype. Male, vocal sacs distinct and paired; nuptial pad distinct, divided, covering dorso-medial face of proximal Finger I to level of subarticular tubercle; humeral gland absent; body relatively slender; head width 90.11% head length; in dorsal view, snout obtusely pointed, in lateral view acutely projecting; canthus rostralis sharp, constricted behind nostrils; loreal area deeply concave; vomerine teeth present, in oblique groups, between choanae; tongue lanceolate; rictal ridge present; eye-nostril distance 177.84% snout-nostril distance; interorbital distance 89.27% width of upper eyelid; tympanum distinct, translucent, diameter > 50% ED (TYv/ED = 64.85; TYh/ED = 69.36%); supratympanic fold distinct, posttympanic fold absent; pineal spot visible; dorsolateral fold absent; dorsum and flanks finely granulated with scattered rounded tubercles on the dorsal region up to the upper part of the flanks; venter skin smooth, finely granulated in the posterior region; hindlimb long, articulation of the heels reach far beyond the tip of snout when limb aligned with body; thigh length 94.90% tibia; tibia 64.02% SVL; fingers slender, without webbing; Finger I 94.16% Finger II, Finger III longest; skin flaps present on the outer phalanges of all fingers; subarticular tubercles on fingers and toes distinct; disc width of Finger III 105.13% disc width of Toe IV; discs of toes and fingers diamond-shaped, both with circummarginal grooves; toe lengths: I < II < III < V < IV, Toe V slightly longer than Toe III; toes fully webbed; inner metatarsal tubercle distinct, oval, 118.59% T4DW; outer metatarsal tubercle absent; tarsal fold absent.

Holotype coloration. In life, dorsum and flanks generally gray; scattered tubercles on the dorsum and the upper part of flanks usually embedded in dark color; lighter area of the dorsum form an irregular network; golden color with dark spot between eye and nostril; upper lip grayish-white with dark spots (right: 4; left: 4); lower lip whitish with dark spots (right: 3; left: 2); iris silver-gray with dark netting, golden orange in the upper part; tympanum gray with light spot in the center; venter, chest, and throat fully whitish; forearm with four distinct dark cross-bars; hind limbs with thick dark cross-bars dorsally (thigh: 5; tibia: 5); rear of thigh with dark mottling on light gray background; legs light brownish ventrally; webbing brown. Dorsal coloration turned from gray with dark spots into uniformly dark brown in preserved specimens; flanks remained gray, lighter ventrad; iris color changed to uniform gray; no color change in the dark markings or pattern.

Holotype measurements (mm). SVL 36.13, HL 14.87, HW 13.40, SL 5.67, SN 1.94, EN 3.45, IND 3.88, IOD 3.66, ED 5.32, UEW 4.10, TYv 3.45, TYh 3.69, ETD 1.19, LAL 7.76, HAL 12.80, FE 21.95, TL 23.13, FL 19.19, IMTL 1.85, F1L 4.03, F2L 4.28, F3DW 1.64, T4DW 1.56.

Variation. (1) dorsum generally with round tubercles, lighter spots vary from few to dense; (2) number of dark-round tubercles on dorsum and flanks: few to many tubercles; (3) size of dark wound tubercles on dorsum and flanks: small to big tubercle; (4) life coloration of dorsum background: lighter grey or slightly grayish-green to dark gray; (5) iris upper sector: light yellow to orange; (6) dark netting of iris: loose to dense; (7) throat, chest, and venter with or without marking, ranging from none to marking reaching venter; (6) marking on upper and lower lip: variable in size; (9) number of cross bars on limbs: 2–4 (arm between wrist and elbow), 4–7 (thigh); (10) thickness of cross bars on limbs: variable; (11) composition of dark color on lighter background of mottling pattern on rear of thigh: dense to less dense dark pattern on lighter background. Metrics in Tables 4–5.

Sexual dimorphism. Males smaller than females. Tympanum diameter 38.54–72.94% ED in males and 28.18–45.70% ED in females. Adult males with divided nuptial pads and vocal sacs, covering dorso-medial face of proximal Finger I to level of subarticular tubercle, humeral gland absent.

Etymology. The species epithet *dabulescens* is an artificial construct of "*dabul*", "gray" in Gayo language, combined with the Latin ending "-*escense*", here in the sense of "tending to be", in allusion to the gray appearance of this species. The Gayo are a local tribe in the Aceh region of Sumatra and after which the Gayo highlands have been named.

Common name. We propose Gayo Cascade Frogs as the English common name and Katak Jeram Gayo as name in Bahasa Indonesia.

Distribution and natural history. Provinsi Aceh, particularly localities in the northern and middle part of Aceh:

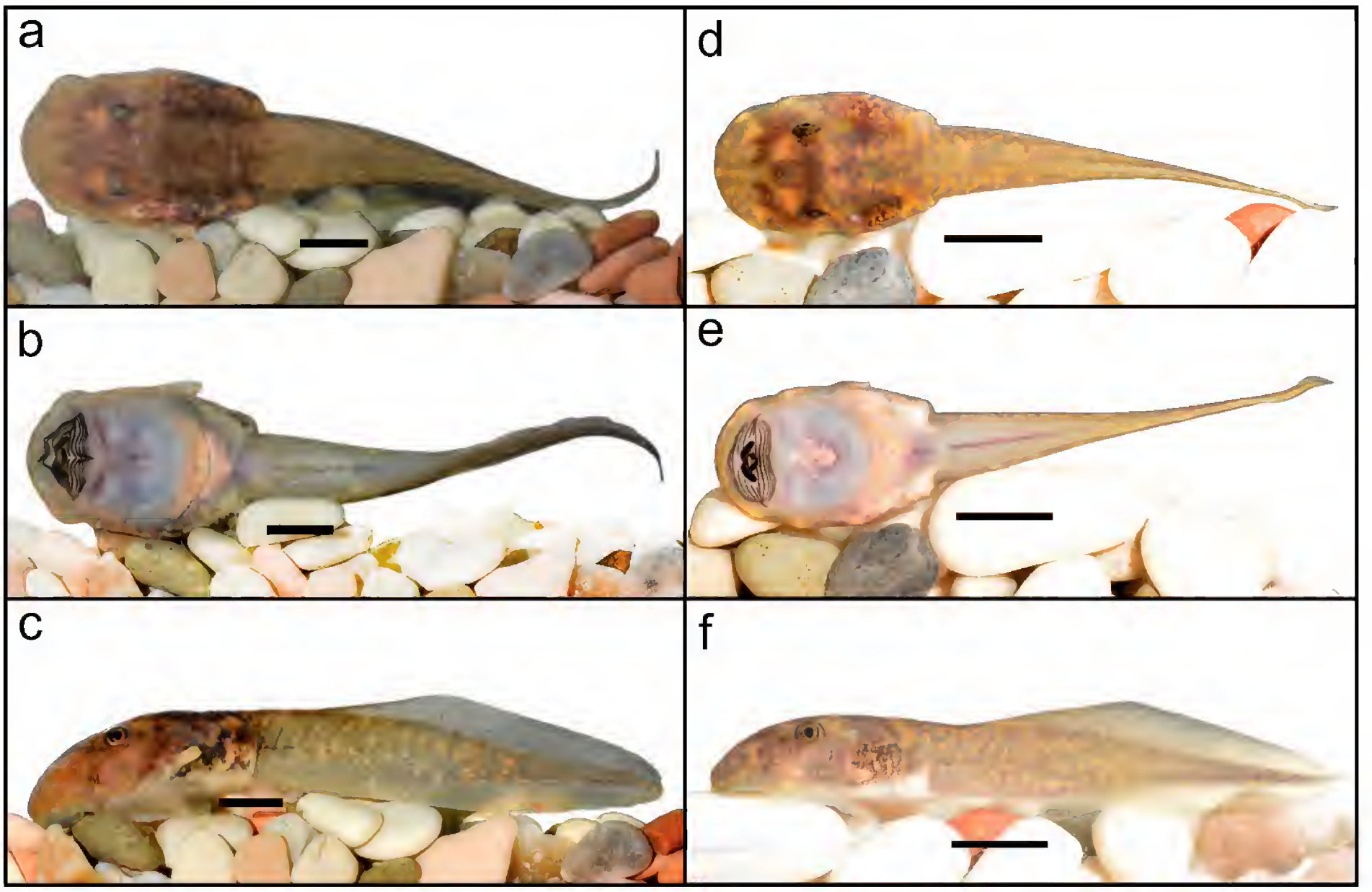

Figure 11. Tadpoles of *Sumaterana crassiovis* comb. n., ZMH.A12650, Provinsi Sumatera Barat (**a–c**) and *S. dabulescens* sp. n., MZB.AMPH.29411, Provinsi Aceh (**d–f**) showing dorsal, ventral, and lateral view. Scale 5 mm. Photos by U. Arifin.

Kecamatan Mane, Kabupaten Pidie; Krung Meuriam, Kecamatan Tangse, Kabupaten Pidie; Kabupaten Bener Meriah; Road Takengon-Bierut, Enang-Enang Resort, Kabupaten Aceh Tengah, and Taman Buru Linge–Isaq, Kecamatan Takengon, Kabupaten Aceh Tengah (Fig. 9). Known elevation for this species was 314–1000 m a.s.l.. The holotype was caught 100 cm above water level on a rock wall at the stream slope. The paratypes were perching on vegetation above the stream (15–200 cm above water) or on rocks in the stream or at the stream bank. The other specimens were collected from rocks or vegetation either in stream or approx. 30–100 cm away from the water (e.g., Fig. 10c). Tadpoles were collected between 23:00–24:00 from rocks (diameter ~1 m) in a fast flowing stream (4 m wide), local protected forest, Kecamatan Mane, Kabupaten Pidie.

Tadpoles. We examined eight tadpoles of *Sumaterana dabulescens* sp. n.. Stage 25: UA20140336 (n = 5), ZMH.A12655 (n = 1), Stage 28: MZB.AMPH.29411 (n = 1), Stage 37: MZB.AMPH.29413 (n = 1). Tadpole assignment to species was justified by 100% genetic match (12S rRNA+16S rRNA+ $tRNA^{val}$) of the selected tadpole to an adult from the same locality (Fig. 2). For the following description we refer to MZB.AMPH.29413 (Stage 37) because this specimen has the most advanced developmental stage in the series: in dorsal view, body slightly rectangular, snout broadly rounded, body rounded at both posterior corners; in lateral view, dorsoventrally depressed, streamlined; maximum body width 65.51% body length; eyes dorsolateral, oriented laterally; ED = 1.61 mm; IND/IOD = 48.01%; SN/ES = 45.23%; nostrils directed anterolaterally; nostril opens without raised rim; infraorbital gland cluster (left: 6 glands; right: 3) and postorbital gland cluster (two in each side) present; oral disc ventral, a groove separating upper lip from snout, oral disc width 68.00% body width; edge of oral sucker protruding snout contour in dorsal view; oral disc marginal papillae short, arranged in a single row; on upper lip marginal papillae present only on lateral parts, on lower lip in uninterrupted row; two short submarginal papillae in lateral area of upper lip; LTRF: 8(5–8)/8(1); upper jaw sheaths broad, heavily keratinized, smooth, undivided, thick but medial part conspicuously thinner than lateral parts; lower jaw sheaths undivided, smooth, V-shaped, thick; both jaw sheaths finely serrated along their edges; very large abdominal sucker in posterior continuation of oral disc, SUL/BL = 70.47%, SUW/BW = 82.94%; spiracle sinistral, tube long, posterior half free from body wall; spiracle directed posterodorsally; anal tube median, free from tail fin, directed posteriorly; strong muscular tail: TMH/BH = 76.19%, TMH/MTH = 66.74%; upper fin convex; maximum upper fin height is approx. 34.99% MTH at approx. 49.00% TAL; tail tip pointed.

In life, dorsal coloration of body and tail densely mottled with brown and golden blotches on a grayish background with dense fine dark stippling; lower flanks with a conspicuous wedge-shaped white area; tail muscle dark with dense-dark stippling overlain by yellowish-golden

to orange mottling; lateral tail vein visible in first third of tail, including dorsal branching along myosepta; upper and lower fin mostly transparent, stippled with melanophores, especially towards the fin margin; yellowish-golden stippling also present in the upper and lower fin; iris background color black, with dense golden to orange iridophore stippling; abdomen whitish laterally and densely stippled with golden iridophores medially; golden iridophores stippling also present in the anterior region of the snout and oral disc; abdominal sucker mostly transparent except for the central spot with golden iridocytes and scattered pigment along the rim. In preservative: color of dorsal region became gray with dense darker dots and dark brown mottling; darker region were obvious on the upper flanks and between eyes and naris; iris all black; lens grayish-white; ventrally uniformly transparent with dark pigments in the anterior region of snout, oral disc, and lateral.

Body proportions between Stage 25, Stage 28, and Stage 37 were variable, e.g., BW/BH in Stage 25 (165.01%) > in Stage 28 (160.72%) > in Stage 37 (144.97%); SUW/BW in Stage 25 (89.58%) > in Stage 28 (86.66%) > in Stage 37 (82.94%); TAL/BL in Stage 25 (153.74%) < Stage 37 (174.06%) < in Stage 28(183.00%); TMH/BH in Stage 25 (61.38%) < in Stage 37 (76.19%) < in Stage 28 (84.71%); TMH/MTH in Stage 25 (60.53%) < in Stage 37 (66.74%) < in Stage 28 (71.00%). Variation: Body shape in the Stage 25 and Stage 28 were oval; the posterior region gradually arched towards the end of the body (e.g. Stage 28; Fig. 11d–f). Color patterns were also variable among the specimens. For example, in life, MZB.AMPH.29411 (Stage 28, Fig. 11d–f) had less mottling on upper side of body and tail than MZB.AMPH.29413 (Stage 37), more extensive golden color in the iris, smaller orange blotches in the tail region, very few golden spots in both upper or lower fin region, golden iridopores and pigments were less in the ventral region. In preservative, MZB.AMPH.29411 is lighter than MZB.AMPH.29413.

Species keys of *Sumaterana* sp. n. in the context of Southeast Asian Ranidae

1 Highly stream-adapted, gastromyzophorous tadpoles abdominal sucker present 2
– Abdominal sucker absent ..... *Abavorana*, *Amnirana*, *Chalcorana*, *Clinotarsus*, *Hylarana*, *Odorrana*, *Pulchrana*, *Staurois*
2 Expanded, rounded finger and toe tips ..... *Amolops*
– Expanded finger and toe tips, pointed and diamond shaped 3
3 Posttympanic and dorsolateral folds well developed, thick dark ∏-shaped over tympanum ..... *Huia*
– Posttympanic and dorsolateral folds well developed, no thick dark ∏-shaped over tympanum, endemic to Borneo ..... *Meristogenys*
– Posttympanic fold absent, dorsolateral folds present or absent, no thick dark ∏-shaped over the tympanum, endemic to Sumatra ..... 4, *Sumaterana*
4 Poorly developed dorsolateral folds, F1 subequal to F2 in length, F3DW subequal to T4DW, dorsum shagreened, brown, sometimes slightly tuberculate ..... *S. montana*
– Dorsolateral folds absent, F1 shorter than F2, F3DW wider than T4DW, dorsum green or greyish with darker markings, finely granulated and tuberculate 5
5 Undivided nuptial pad in males, green dorsal background in life, rear of thighs with dark bars ..... *S. crassiovis*
– Divided nuptial pad in males, gray dorsal background in life, rear of thighs with dark mottling or blotches ..... *S. dabulescens*

Conclusive summary

The taxonomic status of the taxon previously known as *Chalcorana crassiovis* has been problematic for a long time. The case was confounded by the description of a morphologically similar species (*C. kampeni*), the loss of the *C. kampeni* type specimen, insufficient sampling, and a lack of evidence beyond morphology (*viz.*, molecular data). After the original description by Boulenger (1920), only Inger and Iskandar (2015) collected substantial numbers of specimens from that taxonomic group. The exclusively morphological evidence in their validated the existence and provided a re-description of *C. crassiovis*, while questioning the existence of *C. kampeni*. Some authors still continue treating *C. crassiovis* and *C. kampeni* as distinct species, by implication of other evidence. Our study is the first to conduct molecular analyses for these doubtful taxa in a phylogenetic context. Our phylogenetic hypotheses strongly support *C. crassiovis* as a distinct lineage, and a diverse, monophyletic group (Fig. 2) that is not closely related to other species previously assigned to the genus *Chalcorana*. Our comprehensive sampling along the Sumatran transect yielded specimens with astonishing genetic diversity and morphological differences among the clades comprising the *crassiovis*-group (Fig. 2). We recommend all taxa in Clades A–C to be moved to the proposed new genus *Sumaterana* gen. n.. The new genus currently comprises three known species: *S. crassiovis* comb. n., *S. montana* sp. n. and *S. dabulescens* sp. n.. We consider them to represent valid species (*viz.*, independently evolving lineages) as indicated by genetic, morphological, and ecological differences in comparison to other related species (see above). Furthermore, our molecular data reveal the presence of gastromyzophorus larvae in the species belonging to *Sumaterana* gen. n..

Samples from the type localities of *Sumaterana crassiovis* comb. n. and "*Chalcorana kampeni*" were nested in Clade A in the phylogenetic analysis (Fig. 2) with small amounts of genetic divergence (uncorrected *p*-distance 2.56%, Suppl. materials 3). Furthermore, Inger and Iskandar's (2005) morphological description of *C. crassiovis* and Boulenger's (1920) original description matched our Clade A samples well, except for small differences. For example, according to Inger and Iskandar (2005) the tubercles on the dorsum were large and rounded, but in our samples some tubercles were also elongated and variable in size. Inger and Iskandar (2005) noted Finger I equal or slightly longer than Finger II, but in our samples Finger I was consistently shorter than Finger II. This may partially be attributed to different methods of finger length comparison. Inger and Iskandar (2005) reported skin flaps on the outer phalanges of the second and third fingers. We observed flaps present on the outer phalanges of all fingers, although not all of them are movable. This character is difficult to express unambiguously in verbal form (i.e., some may consider them fringes rather than flaps) and graded character states can occur on different fingers. Thus, we do not believe our observations contradict Inger and Iskandar (2005). Based on low genetic divergence within Clade A, morphological homogeneity among samples corroborating the original description of the type (Boulenger 1920) and the re-description by Inger and Iskandar (2005), and the inclusion of topotypic specimens of both previously named taxa, we recommend "*C. kampeni*" be considered a junior synonym of *S. crassiovis* comb. n..

In this study we included four known species of *Huia* (*H. cavitympanum*-type species, Borneo; *H. sumatrana*, Sumatra; *H. masonii*, Java; and *H. melasma*, the mainland Asia). Nevertheless, we were unable to solve the phylogenetic problem of *Huia*, which has previously been considered paraphyletic (Stuart 2008, Pyron and Wiens 2011). Our study perpetuates this conundrum as the type species of *Huia* (*H. cavitympanum*) was shown to be the sister taxon to Bornean *Meristogenys* in our analyses, rather than monophyletic with the other *Huia* species in our dataset. One possibility would have been to subsume all members of the assemblage (*Sumaterana* gen. n., *Meristogenys*, *Huia*, and *Clinotarsus*) under one name (*Clinotarsus*, the oldest available name). We did not choose this option in order to ensure taxonomic stability and because valuable biological information associated with the current monophyletic groups would be dissolved in one genus, such as island endemism (*Sumaterana* gen. n./*Meristogenys*), differences in adult and tadpole morphology and tadpole peculiarities (species of today's *Clinotarsus* with non-gastromyzophorous tadpoles). Because of the low support in parts of his tree, Stuart (2008) refrained from taxonomic amendments concerning *Huia*, and so do we. Much more effort needs to be invested to solve the perplexing phylogenetic uncertainties concerning *Huia*.

Another interesting subject arises from the optimized phylogenies in our analyses (Fig. 2) with respect to the evolution of larval gastromyzophory in Southeast Asian ranids. Previously all Asian ranid taxa with gastromyzophorous tadpoles were grouped under the genus *Amolops* (Inger 1966). Yang (1991) split the group into *Amolops*, *Huia*, and *Meristogenys* based on adult and tadpole morphological characters. Molecular systematic studies, however, suggested that the assemblage of *Amolops*, *Huia*, and *Meristogenys* was para- or polyphyletic (Frost et al. 2006, Stuart 2008, Pyron and Wiens 2011). Our phylogenetic analyses indicate that gastromyzophorous tadpoles have likely evolved independently, once in the most recent common ancestor of the group *Huia*+*Sumaterana* gen. n.+*Meristogenys* and again in the ancestor of *Amolops*. Tadpoles from both clades are perplexingly similar morphologically (Noble 1929, Gan et al. 2015), yet molecular evidence implies separate origins. Interestingly, although *Clinotarsus* does not possess gastromyzophorous tadpoles, this genus is nested within *Huia*+*Sumaterana* gen. n.+*Meristogenys* (Stuart 2008, Pyron and Wiens 2011, this study). Therefore, it could be hypothesized that larval gastromyzophory might have been lost secondarily in *Clinotarsus*. Further studies are needed to test and understand the evolution of this larval type in these frogs.

A third case of ranids with gastromyzophorous tadpoles has been reported in *Rana sauteri* (Boulenger, 1909). Its tadpoles are clearly more morphologically (Kuramoto et al. 1984) and biogeographically (Taiwan) distant to *Amolops*, *Huia*, and *Meristogenys*. Gan et al. (2015) summarized that in *R. sauteri* the edge of the abdominal sucker was not as sharply defined as in *Amolops*, *Huia*, and *Meristogenys* (sucker is completely free and rim raised), particularly at the posterior. Moreover, the sucker seems to work differently in *R. sauteri*: the musculus diaphragmatopraecordialis is absent in *R. sauteri*, but well developed in *Amolops*, *Huia*, and *Meristogenys* (Gan et al. 2015, Kuramoto et al. 1984). Finally, other body features of *R. sauteri* (relatively narrow oral sucker and extensive dorsal tail fin) underline the morphological differences between this and to other Asian gastromyzophorous tadpoles, implying possible separate origins and different adaptive scenarios.

We are fully aware that phylogenetic and taxonomic problems persist in our studied taxa. These need to be addressed in the future. Broad thorough geographic sampling of adult and larval forms is a prerequisite to solve phylogenetic quandaries with any amphibian taxa, especially in the species rich tropical realm. Moreover, integrating independent sources of evidence (e.g. DNA, morphology, distribution) is an optimal strategy to accurately and convincingly validate the taxonomic position of doubtful amphibian taxa from hyperdiverse hotspots (Dayrat 2005, Padial et al. 2009, Padial et al. 2010). Distantly related frog species that converged onto similar morphotypes (i.e., ecomorphs) are common in tropical biodiversity hotspots (Bossuyt and Milinkovitch 2002) and can confound taxonomic decisions; examples are documented in Stuart (2008).

Our results are also further evidence that the taxonomic diversity of Sumatran frogs is still significantly underestimated (Iskandar and Colijn 2000, Stuart et al. 2006, Inger et al. 2009), despite the recent increase of am-

phibian species described from the island (e.g. Teynie et al. 2010, Matsui et al. 2012, Hamidy and Kurniati 2015, Smart et al. 2017, Wostl et al. 2017). This also holds true for other herpetofauna, such as reptiles (Orlov and Ryabov 2002, David and Das 2003, Das 2005, Harvey et al. 2015, Wostl et al. 2016). Large scale and strategic sampling efforts are of the utmost priority in order to reveal the true faunal diversity and distribution patterns on this incredibly biodiverse island.

Acknowledgements

This study was funded by the Deutsche Forschungsgemeinschaft (DFG Ha2323/12-1) and by a stipend for U. Arifin provided by the Deutscher Academischer Austauschdienst–Indonesian German Scholarship Program (DAAD–IGSP, 91548731). Some parts of the study were funded by the National Science Foundation (NSF) DEB-1146324 to E. N. Smith and M. B. Harvey, Volkswagen Foundation (I/79 405) to A. Haas, and Rufford Small Grants (RSG) 15779-1 to U. Smart. The Synthesis of Systematic Resources Access program (SYNTHESYS; NL-TAF-4882 and GB-TAF-4412) supported U. Arifin during examination of type specimens and other materials. The authors thank the School of Life Sciences-Institute of Technology Bandung, Indonesian Science Institute, RISTEK, Director General KKH–PHKA as well as Balai Besar Taman Nasional Gunung Leuser (BBTNGL), Balai Besar Taman Nasional Kerinci-Seblat (BBTNKS), Balai Taman Nasional Batang Gadis (BTNBG) and all Balai Konservasi Sumber Daya Alam (BKSDA) in Sumatra which made this research possible. Permits for research and collecting (SIP) in Sumatra and Java were kindly provided by RISTEK to E. N. Smith and team during the years 2013 to 2016: 149–150/SIP/FRP/SM/V/2013, 152/SIP/FRP/SM/V/2013, 149-A/SIP/FRP/SM/XII/2013, 151-A/SIP/FRP/SM/XII/2013, 153–154-A/SIP/FRP/SM/XII/2013, 193–197/SIP/FRP/SM/VI/2015, and 209–210/SIP/FRP/SM/VI/2015. For U. Arifin and team, research and collecting permit were kindly provided by Ministry of Forestry, Directorate General of Forest Protection and Nature Conservation: SI.10/Set-3/2014 and SI.298/Set-3/2014, S.49/KKH-2/2014, S.825/KKH-2/2014. We thank Ester Dondorp (Naturalis Biodiversity Center, Leiden) and Jeff Streicher (Natural History Museum, London) for their support during work of U. Arifin at both museums. We are grateful to Jamili Nais, Director of Research Sabah Parks, Economic Planning Unit, Prime Ministers department, Malaysia, for issuing collecting permit and providing essential help to A. Haas and team. We thank the Sarawak Forest Department and Sarawak Forestry Corporation, in particular Nur Afiza Binti Umar, Dayang Nuriza Binti Abang Abdillah, Mohamad bin Kohdi, Engkamat Anak Lading Datu Haji Ali Yusop and Mohd. Shabudin Sabki, for providing advice and issuing permits to S.T. Hertwig and A. Haas: NCCD.907.4.4(Jld.VI)-107, Park Permit 56/2011, export permit 09813. We thank Jimmy McGuire, David Bickford, and Jens Vindum for tissue samples, and Andri Irawan for specimen materials. We are very grateful to Ganjar Cahyadi, Novari Fajria, Amir Hamidy, Agus Yasin, Yoghi Budianto, Zainal, Kamarudin, Carmidi, Hajidin, Zamrin, Agusman, Aidil, Zainudin, Rikha, Sumarto, Darlizon, Muhardi, Samin, Hasbalah, Alfian, Adrinaldi, Abdullah, Mistar Kamsi, Dewi Roesma, Risky Dharma, Ari Arfama, David Gusman, Preddy Syahputra, Mantra Sanjaya, Dr. Nia Kurniawan and his group of herpetology students at Brawijaya University and many other people for all support during field work in Sumatra and Java. Annamarie Vogt, Dimitrij Trovinov, Katharina Gebauer, and Manuel Schweizer provided excellent support in the lab, and Lea Waser provided the illustration for morphological measurement. Ulrich Manthey kindly provided literature. David McLeod and two other anonymous reviewers for reviewing our manuscript.

References

Aguayo R, Lavilla EO, Candioti VMF, Camacho T (2009) Living in fast-flowing water: morphology of the gastromyzophorous tadpole of the bufonid *Rhinella quechua* (*R. veraguensis* Group). Journal of Morphology 270: 1431–1442. https://doi.org/10.1002/jmor.10768

Altig R (2007) A primer for the morphology of anuran tadpoles. Herpetological Conservation and Biology 2(1): 71–74.

Altig R (2006) Discussions of the origin and evolution of the oral apparatus of anuran tadpoles. Acta Herpetologica 1(2): 95–105.

Altig R, Johnston GF (1989) Guilds of anuran larvae: relationships among developmental modes, morphologies, and habitats. Herpetological Monographs 3(1989): 81–109. https://doi.org/10.2307/1466987

Biju SD, Garg S, Mahony S, Wijayathilaka N, Senevirathne G, Meegaskumbura M (2014) DNA barcoding, phylogeny and systematics of Golden-backed frogs (*Hylarana*, Ranidae) of the Western Ghats-Sri Lanka biodiversity hotspot, with the description of seven new species. Contributions to Zoology 83(4): 269–335.

Blyth E (1855) Report of the Curator; Zoological Department, for March meeting. Journal of the Asiatic Society of Bengal 24: 187–188.

Blyth E (1856 "1855") Report for October Meeting, 1855. Journal of the Asiatic Society of Bengal 24: 711–723.

Boistel R, Grosjean S, Lötters S (2005) Tadpole of *Atelopus franciscus* from French Guyana, with comments on other larvae of the genus (Anura: Bufonidae). Journal of Herpetology 39(1): 148–153. https://doi.org/10.1670/0022-1511(2005)039[0147:TOAFFF]2.0.CO;2

Bossuyt F, Milinkovitch M (2002) Convergent adaptive radiations in Madagascan and Asian ranid frogs reveal covariation betweenlarval and adult traits. PNAS 97: 6585–6590. https://doi.org/10.1073/pnas.97.12.6585

Boulenger GA (1882) Catalogue of the Batrachia Salientia s. Ecaudata in the Collection of the British Museum. Second Edition. London: Taylor and Francis.

Boulenger GA (1884) Descriptions of new species of reptiles and batrachians in the British Museum.—Part. II. Annals and Magazine of Natural History, Series 5, 13: 396–398. https://doi.org/10.1080/00222938409459259

Boulenger GA (1891) On new or little-known Indian and Malayan reptiles and batrachians. Annals and Magazine of Natural History, Series 6, 8: 288–292. https://doi.org/10.1080/00222939109460437

Boulenger GA (1893) Descriptions of new reptiles and batrachians obtained in Borneo by Mr. A. Everett and Mr. C. Hose. Proceedings of the Zoological Society of London 1893: 522–528.

Boulenger GA (1909) Descriptions of four new frogs and a new snake discovered by Mr. H. Sauter in Formosa. Annals and Magazine of Natural History Series 8, 4: 492–495. https://doi.org/10.1080/00222930908692704

Boulenger GA (1920) Reptiles and batrachians collected in Korinchi, West Sumatra, by Messrs. H.C. Robinson and C. Boden Kloss. Journal of the Federated Malay States Museums 8: 285–306.

Castresana J (2000). Selection of conserved blocks from multiple alignments for their use in phylogenetic analysis. Molecular Biology and Evolution 17: 540–552. https://doi.org/10.1093/oxfordjournals.molbev.a026334

Chan KO, Brown RM (2017) Did true frogs 'dispersify'?. Biology letters 13(8): 20170299. https://doi.org/10.1098/rsbl.2017.0299

Che J, Pang J, Zhao H, Wu GF, Zhao EM, Zhang YP (2007) Phylogeny of Raninae (Anura: Ranidae) inferred from mitochondrial and nuclear sequences. Molecular Phylogenetics and Evolution 43(1): 1–13. https://doi.org/10.1016/j.ympev.2006.11.032

Cope ED (1865) Sketch of the primary groups of Batrachia s. Salientia. Natural History Review. New Series 5: 97–120.

Cope ED (1868) An examination of the Reptilia and Batrachia obtained by the Orton Expedition to Equador and the Upper Amazon, with notes on other species. Proceedings of the Academy of Natural Sciences of Philadelphia 20: 96–140.

Dayrat B (2005) Towards integrative taxonomy. Biological Journal of the Linnean Society 85(3): 407–415. https://doi.org/10.1111/j.1095-8312.2005.00503.x

David P, Das I (2003) A new species of the snake genus *Amphiesma* (Serpentes: Colubridae: Natricinae) from western Sumatra, Indonesia. Raffles Bulletin of Zoology 51(2): 413–420.

Das I (2005) Revision of the genus *Cnemaspis* Strauch, 1887 (Sauria: Gekkonidae), from the Mentawai and adjacent archipelagos off western Sumatra, Indonesia, with the description of four new species. Journal of Herpetology 39(2): 233–247. https://doi.org/10.1670/61-02A

Dereeper A, Guignon V, Blanc G, Audic S, Buffet S, Chevenet F, Dufayard JF, Guindon S, Lefort V, Lescot M, Claverie JM (2008) Phylogeny.fr: robust phylogenetic analysis for the non-specialist. Nucleic Acids Research 36: 465–469. https://doi.org/10.1093/nar/gkn180

de Queiroz K (2005) A unified concept of species and its consequences for the future of taxonomy. Proceedings-California Academy of Sciences 56: 196–215.

Dever JA, Fuiten AM, Konu Ö, Wilkinson JA (2012) Cryptic Torrent Frogs of Myanmar: An examination of the *Amolops marmoratus* species complex with the resurrection of *Amolops afghanus* and the identification of a new species. Copeia 2012: 57–76. https://doi.org/10.1643/CH-10-180

Duellman WE (2001) Hylid frogs of Middle America. Society for the Study of Amphibians and Reptiles, USA.

Dubois A (1992) Notes sur la classification des Ranidae (Amphibiens anoures). Bulletin Mensuel de la Société Linnéenne de Lyon 61: 305–352.

Fei L, Ye Cy, Jiang Jp (2010) Phylogenetic systematics of Ranidae. Herpetologica Sinica/Liang qi pa xing dong wu xue yan jiu 12: 1–43.

Frost DR, Grant T, Faivovich J, Bain RH, Haas A, Haddad CF, De Sá RO, Channing A, Wilkinson M, Donnellan SC, Raxworthy CJ (2006) The amphibian tree of life. Bulletin of the American Museum of Natural History 297: 1–370. https://doi.org/10.1206/0003-0090(2006)297[0001:TATOL]2.0.CO;2

Frost DR (2017) Amphibian Species of the World: an Online Reference. Version 6.0 (accessed 23. April 2017). Electronic Database accessible at http://research.amnh.org/herpetology/amphibia/index.html. American Museum of Natural History, New York, USA.

Gan L, Hertwig ST, Das I, Haas A (2015) The anatomy and structural connectivity of the abdominal sucker in the tadpoles of *Huia cavitympanum*, with comparisons to *Meristogenys jerboa* (Lissamphibia: Anura: Ranidae). Journal of Zoological Systematics and Evolutionary Research 54(1): 1–14.

Günther ACLG (1858) Neue Batrachier in der Sammlung des britischen Museums. Archiv für Naturgeschichte. Berlin 24: 319–328. https://doi.org/10.5962/bhl.part.5288

Günther ACLG (1872) On the reptiles and amphibians of Borneo. Proceedings of the Zoological Society of London 1872: 586–600.

Goebel AM, Donnelly JM, Atz ME (1999) PCR primers and amplification methods for 12S ribosomal DNA, the control region, cytochrome oxidase I, and cytochromebin bufonids and other frogs, and an overview of PCR primers which have amplified DNA in amphibians successfully. Molecular Phylogenetics and Evolution 11(1): 163–199. https://doi.org/10.1006/mpev.1998.0538

Gosner KL (1960) A simplified table for staging anuran embryos and larvae with notes on identification. Herpetologica 16: 183–190.

Grosjean S, Ohler A, Chuaynkern Y, Cruaud C, Hassanin A (2015) Improving biodiversity assessment of anuran amphibians using DNA barcoding of tadpoles. Case studies from Southeast Asia. Comptes Rendus Biologies 338(5): 351–361. https://doi.org/10.1016/j.crvi.2015.03.015

Grossmann W, Manthey U (1997) Amphibien & Reptilien Südostasiens. Natur und Tier Verlag, Münster.

Guayasamin JM, Bustamante MR, Almeida-Reinoso DIEGO, Funk WC (2006) Glass frogs (Centrolenidae) of Yanayacu Biological Station, Ecuador, with the description of a new species and comments on centrolenid systematics. Zoological Journal of the Linnean Society 147(4): 489–513. https://doi.org/10.1111/j.1096-3642.2006.00223.x

Haas A, Das I (2011) Describing east Malaysian tadpole diversity: status and recommendations for standards and procedures associated with larval amphibian description and documentation. Bonner Zoologische Monographien 57: 29–46.

Hamidy A, Kurniati H (2015) A new species of tree frog genus *Rhacophorus* from Sumatra, Indonesia (Amphibia, Anura). Zootaxa 3947(1): 049–066. https://doi.org/10.11646/zootaxa.3947.1.3

Harvey MB, o'Connell KA, Barraza G, Riyanto A, Kurniawan N, Smith NE (2015) Two new species of *Cyrtodactylus* (Squamata: Gekkonidae) from the Southern Bukit Barisan Range of Sumatra and an estimation of their phylogeny. Zootaxa 4020(3): 495–516. https://doi.org/10.11646/zootaxa.4020.3.5

Hillis DM, Bull JJ (1993) An empirical test of bootstrapping as a method for assessing confidence in phylogenetic analysis. Systematic Biology 42: 182–192. https://doi.org/10.1093/sysbio/42.2.182

Huelsenbeck JP, Ronquist F (2001) MrBayes: Bayesian inference of phylogenetic trees. Bioinformatics Applications Note 17(8): 754–755. https://doi.org/10.1093/bioinformatics/17.8.754

Huelsenbeck JP, Rannala B (2004) Frequentist properties of Bayesian posterior probabilities of phylogenetic trees under simple and complex substitution models. Systematic Biology 53: 904–913. https://doi.org/10.1080/10635150490522629

Inger RF (1985) Tadpoles of the forested regions of Borneo. Fieldiana 26: 1–89.

Inger RF (1966) The systematics and zoogeography of the Amphibia of Borneo. Fieldiana Zoology 52: 1–402.

Inger RF (1986). Diets of tadpoles living in a Bornean rain forest. Alytes 5(4): 153–164.

Inger RF, Gritis PA (1983) Variation in Bornean frogs of the Amolops jerboa species group, with description of two new species. Field Museum of Natural History. https://doi.org/10.5962/bhl.title.5644

Inger RF, Kottelat M (1998) A new species of ranid frog from Laos. Raffles Bulletin of Zoology 46: 29–34.

Inger RF, Voris HK (2001) The biogeographical relations of the frogs and snakes of Sundaland. Journal of Biogeography 28(7): 863–891. https://doi.org/10.1046/j.1365-2699.2001.00580.x

Inger RF, Iskandar DT (2005) A collection of amphibians from West Sumatra, with description of a new species of *Megophrys* (Amphibia: Anura). The Raffles Bulletin of Zoology 53(1): 133–142.

Inger RF, Stuart BL, Iskandar DT (2009) Systematics of a widespread Southeast Asian frog, *Rana chalconota* (Amphibia: Anura: Ranidae). Zoological Journal of Linnaean Society 155(1): 123–147. https://doi.org/10.1111/j.1096-3642.2008.00440.x

Inger RF, Stuebing RB (2009) New species and new records of Bornean frogs (Amphibia: Anura). The Raffles Bulletin of Zoology 57(2): 527–535.

Iskandar DT, Mumpuni (2004) *Chalcorana crassiovis*. (errata version published in 2016) The IUCN Red List of Threatened Species 2004: e.T58580A89367065. Downloaded on 16 April 2017.

Kumar S, Stecher G, Tamura K (2016) MEGA7: Molecular Evolutionary Genetics Analysis Version 7.0 for Bigger Datasets. Molecular Biology and Evolution 33(7): 1870–1874. https://doi.org/10.1093/molbev/msw054.

Katoh K, Standley DM (2013) MAFFT multiple sequence alignment software version 7: improvements in performance and usability. Molecular Biology and Evolution 30(4): 772–780. https://doi.org/10.1093/molbev/mst010

Kearse M, Moir R, Wilson A, Stones-Havas S, Cheung M, Sturrock S, Buxton S, Cooper A, Markowitz S, Duran C, Thierer T, Ashton B, Mentjies P, Drummond A (2012) Geneious basic: an integrated and extendable desktop software platform for the organization and analysis of sequence data. Bioinformatics 28(12): 1647–1649. https://doi.org/10.1093/bioinformatics/bts199

Kluge AG (1989) A concern for evidence and a phylogenetic hypothesis of relationships among *Epicrates* (Boidae, Serpentes). Systematics Zoology 38: 7–25. https://doi.org/10.2307/2992432

Kluge AG (2004) On total evidence: for the record. Cladistics 20: 205–207. https://doi.org/10.1111/j.1096-0031.2004.00020.x

Kok PJ, Kalamandeen M (2008) Introduction to the taxonomy of the Amphibians of Kaieteur National Park, Guyana. Abc Taxa, Belgium.

Kuramoto M, Wang CS, Yü HT (1984) Breeding, larval morphology and experimental hybridization of Taiwanese Brown Frogs, *Rana longicrus* and *R. sauteri*. Journal of Herpetology 18(4): 387–395. https://doi.org/10.2307/1564101

Lanfear R, Calcott B, Ho SY, Guindon S (2012) PartitionFinder: Combined Selection of Partitioning Schemes and Substitution Models for Phylogenetic Analyses. Molecular Biology and Evolution 29(6): 1695–1701. https://doi.org/10.1093/molbev/mss020

Liu W, Yang D, Ferraris C, Matsui M (2000) *Amolops bellulus*: A new species of stream-breeding frog from western Yunnan, China (Anura: Ranidae). Copeia 2000(2): 536–541. https://doi.org/10.1643/0045-8511(2000)000[0536:ABANSO]2.0.CO;2

Miller MA, Pfeiffer W, Schwartz T (2010) Creating the CIPRES Science Gateway for inference of large phylogenetic trees. In Proceedings of the Gateway Computing Environments Workshop (GCE, pp 1–8). New Orleans, LA. https://doi.org/10.1109/GCE.2010.5676129

Manthey U, Denzer W (2014) Südostasiatische Anuren im Fokus Spezies der Gattung *Huia* (sensu lato) Yang, 1991 (amphibia: Anura: Ranidae). Sauria 36(4): 31–48.

Malkmus R, Manthey U, Vogel G, Hoffmann P, Kosuch J (2002) Amphibians and Reptiles of Mount Kinabalu (North Borneo). A. R. G. Gantner K G, Koeltz Scientific Books, Koenigstein.

Matsui M, Nabhitabhata J (2006) A new species of *Amolops* from Thailand (Amphibia, Anura, Ranidae). Zoological Science 23(8): 727–732. https://doi.org/10.2108/zsj.23.727

Matsui M, Shimada T, Liu WZ, Maryati M, Khonsue W, Orlov N (2006) Phylogenetic relationships of Oriental torrent frogs in the genus *Amolops* and its allies (Amphibia, Anura, Ranidae). Molecular Phylogenetic and Evolution 38(3): 659–666. https://doi.org/10.1016/j.ympev.2005.11.019

Matsui M, Yambun P, Sudin A (2007) Taxonomic relationships of *Ansonia anotis* (Inger, Tan and Yambun 2001) and *Pedostibes maculatus* (Mocquard 1890), with a description of a new genus (Amphibia, Bufonidae). Zoological Science 24: 1159–1166. https://doi.org/10.2108/zsj.24.1159

Matsui M, Shimada T, Sudin A (2010) A New Species of *Meristogenys* (Amphibia, Anura, Ranidae) from Sabah, Borneo. Zoological Science 27: 61–66. https://doi.org/10.2108/zsj.27.61

Matsui M, Mumpuni, Hamidy A (2012) Description of a new species of *Hylarana* from Sumatra (Amphibia, Anura). Current Herpetology 31(1): 38–46. https://doi.org/10.5358/hsj.31.38

McDiarmid, Altig A (1999) Tadpole: The Biology of Anuran Larvae (pp. 453). The University of Chicago Press.

Mulcahy DG, Beckstead TH, Sites Jr JW (2011) Molecular systematics of the *Leptodeirini* (Colubroidea: Dipsadidae) revisited: Species-tree analyses and multi-locus data. Copeia 2011: 407–417. https://doi.org/10.1643/CH-10-058

Noble GK (1929) The adaptive modifications of the arboreal tadpoles of *Hoplophryne* and the torrent tadpoles of *Staurois*. Bulletin American Museum of Natural History 58: 291–334.

Nodzenski E, Inger RF (1990) Uncoupling of related structural changes in metamorphosing torrent-dwelling tadpoles. Copeia 1990(4): 1047–1054. https://doi.org/10.2307/1446488

Ngo A, Murphy RW, Liu W, Lathrop A, Orlov NL (2006) The phylogenetic relationships of the Chinese and Vietnamese waterfall frogs of the genus *Amolops*. Amphibian-Reptiles 27: 81–92. https://doi.org/10.1163/156853806776052010

Oberhummer E, Barten C, Schweizer M, Das I, Haas A, Hertwig ST (2014) Description of the tadpoles of three rare species of *Megophryid* frogs (Amphibia: Anura: Megophryidae) from Gunung Mulu, Sarawak, Malaysia. Zootaxa 3835(1): 059–079. https://doi.org/10.11646/zootaxa.3835.1.3

Oliver LA, Prendini E, Kraus F, Raxworthy CJ (2015) Systematics and biogeography of the *Hylarana* frog (Anura: Ranidae) radiation across tropical Australasia, Southeast Asia, and Africa. Molecular Phylogenetic and Evolution 90: 176–192. https://doi.org/10.1016/j.ympev.2015.05.001

Orlov NL, Ryabov SA (2002) A new species of the genus *Boiga* (Serpentes, Colubridae, Colubrinae) from Tanahjampea island and description of (Black Form) of *Boiga cynodon* complex from Sumatra (Indonesia). Russian Journal of Herpetology 9(1): 33–56.

Padial JM, Castroviejo-Fisher S, Köhler J, Vilà C, Chaparro JC, De la Riva I (2009) Deciphering the products of evolution at the species level: the need for an integrative taxonomy. Zoologica Scripta 38(4): 431–447. https://doi.org/10.1111/j.1463-6409.2008.00381.x

Padial JM, Miralles A, De la Riva I, Vences M (2010) The integrative future of taxonomy. Frontiers in Zoology 7(16): 1–14. https://doi.org/10.1186/1742-9994-7-16

Pauly GB, Hillis DM, Cannatella DC (2004) The history of a nearctic colonization: molecular phylogenetics and biogeography of the Neartic toads (*Bufo*). Evolution 58: 2517–2535. https://doi.org/10.1111/j.0014-3820.2004.tb00881.x

Pyron A, Wiens JJ (2011) A large-scale phylogeny of Amphibia including over 2800 species, and a revised classification of extant frogs, salamanders, and caecilians. Molecular Phylogenetics and Evolution 61(2): 543–583. https://doi.org/10.1016/j.ympev.2011.06.012

Rambaut A, Suchard M, Xie W, Drummond A (2014) Tracer v. 1.6. Institute of Evolutionary Biology, University of Edinburgh.

Rao D, Yang D (1994) The study of early development and evolution of *Torrentophryne aspinia*. Zoological Research 15: 142–157.

Ronquist F, Huelsenbeck JP (2003) MrBayes 3: Bayesian phylogenetic inference under mixed models. Bioinformatics 19(12): 1572–1574. https://doi.org/10.1093/bioinformatics/btg180

Ribeiro-Júnior MA, Gardner TA, Ávila-Pires TC (2008) Evaluating the effectiveness of herpetofaunal sampling techniques across a gradient of habitat change in a tropical forest landscape. Journal of Herpetology 42(4): 733–749. https://doi.org/10.1670/07-097R3.1

Ryan WBF, Carbotte SM, Coplan JO, O'Hara S, Melkonian A, Arko R, Weissel RA, Ferrini V, Goodwillie A, Nitsche F, Bonczkowski J, Zemsky R (2009) Global Multi-Resolution Topography synthesis. Geochemistry Geophysics Geosystems 10(3): Q03014. https://doi.org/10.1029/2008GC002332.

Rueda-Solano LA, Vargas-Salinas F, Rivera-Correa M (2015) The highland tadpole of the harlequin frog *Atelopus carrikeri* (Anura: Bufonidae) with an analysis of its microhabitat preferences. Salamandra 51: 25–32.

Schlegel H (1837) Abbildungen neuer oder unvollständig bekannter Amphibien, nach der Natur oder dem Leben entworfen, herausgegeben und mit einem erläuternden Texte begleitet. Part 1. Düsseldorf: Arnz & Co..

Shimada T, Matsui M, Nishikawa K, Eto K (2015) A New Species of *Meristogenys* (Anura: Ranidae) from Sarawak, Borneo. Zoological Science 32(5): 474–484. https://doi.org/10.2108/zs140289

Shimada T, Matsui M, Sudin A, Mohamed M (2007) Identity of larval *Meristogenys* from a single stream in Sabah, Malaysia (Amphibia: Ranidae). Zoological Journal of Linnaean Society 151: 173–189. https://doi.org/10.1111/j.1096-3642.2007.00319.x

Shimada T, Matsui M, Yambun P, Lakim M, Mohamed M (2008) Detection of two cryptic taxa in *Meristogenys amoropalamus* (Amphibia, Ranidae) through nuclear and mitochondrial DNA analyses. Zootaxa 1843: 24–34.

Shimada T, Matsui M, Yambun P, Sudin A (2011) A taxonomic study of Whitehead's torrent frog, *Meristogenys whiteheadi*, with descriptions of two new species (Amphibia: Ranidae). Zoological Journal of Linnaean Society 161: 157–183. https://doi.org/10.1111/j.1096-3642.2010.00641.x

Smart U, Sarker GC, Arifin U, Harvey MB, Sidik I, Hamidy A, Kurniawan N, Smith EN (2017) A new genus and two new species of arboreal toads from the highlands of Sumatra with a phylogeny of Sundaland toad genera. Herpetologica 73: 63–75. https://doi.org/10.1655/Herpetologica-D-16-00041.

Stamatakis A (2014) RAxML Version 8: A tool for phylogenetic analysis and post-analysis of large phylogenies. Bioinformatics 30: 1312–1313. https://doi.org/10.1093/bioinformatics/btu033

Stuart BL (2008) The phylogenetic problem of *Huia* (Amphibia: Ranidae). Molecular Phylogenetic and Evolution 46(1): 49–60. https://doi.org/10.1016/j.ympev.2007.09.016

Stuart BL, Chan-ard T (2005) Two new *Huia* (Amphibia: Ranidae) from Laos and Thailand. Copeia 2005(2): 279–289. https://doi.org/10.1643/CH-04-137R3

Stuart BL, Inger RF, Voris HK (2006) High level of cryptic species diversity revealed by sympatric lineages of Southeast Asian forest frogs. Biology Letters 2: 470–474. https://doi.org/10.1098/rsbl.2006.0505

Talavera G, Castresana J (2007) Improvement of phylogenies after removing divergent and ambiguously aligned blocks from protein sequence alignments. Systematic Biology 56: 564–577. https://doi.org/10.1080/10635150701472164

Teynie A, David P, Ohler A (2010) Note on a collection of Amphibians and Reptiles from Western Sumatra (Indonesia), with the description of a new species of the genus *Bufo*. Zootaxa 2416: 1–43.

Tschudi JJv (1838) Classification der Batrachier mit Berücksichtigung der fossilen Thiere dieser Abtheilung der Reptilien. Neuchâtel: Petitpierre.

Van Kampen PN (1910) Beitrag zur Kenntnis der Amphibienlarven des indischen Archipels. Natuurkundig Tijdschrift voor Nederlandsch-Indië 69: 25–48.

Van Kampen PN (1923) The amphibia of the Indo-Australian archipelago. EJ Brill, ltd.

Van Tuijl L (1995) Revised catalogue of the type specimens of recent amphibians and reptiles in the "Zoölogisch Museum", University of Amsterdam, The Netherlands. Bulletin. Zoölogisch Museum, Universiteit van Amsterdam 14: 125–144.

Waser LE, Schweizer M, Haas A, Das I, Jankowski A, Min PY, Hertwig ST (2016) From a lost world: an integrative phylogenetic analysis of *Ansonia stoliczka*, 1870 (Lissamphibia: Anura: Bufonidae), with the description of a new species. Organisms Diversity & Evolution 1–17. https://doi.org/10.1007/s13127-016-0294-2

Watters JL, Cummings ST, Flanagan RL, Siler CD (2016) Review of morphometric measurements used in anuran species descriptions and recommendations for a standardized approach. Zootaxa 4072(4): 477–495. https://doi.org/10.11646/zootaxa.4072.4.6

Wostl E, Sidik I, Trilaksono W, Shaney KJ, Kurniawan N, Smith EN (2016) Taxonomic status of the Sumatran Pitviper *Trimeresurus* (*Popeia*) *toba* David, Petri, Vogel & Doria, 2009 (Squamata: Viperidae) and other Sunda Shelf species of the subgenus *Popeia*. Journal of Herpetology 50(4): 633–641. https://doi.org/10.1670/15-045

Wostl E, Riyanto A, Hamidy A, Kurniawan N, Smith EN, Harvey MB (2017) A taxonomic revision of the *Philautus* (Anura: Rhacophoridae) of Sumatra with the description of four new species. Herpetological Monographs 31(1): 70–113. https://doi.org/10.1655/HERPMONOGRAPHS-D-16-00007.

Yang DT (1991) Phylogenetic systematics of the *Amolops* group of ranid frogs of southeastern Asia and the Greater Sunda Islands. Fieldiana: Zoology New Series 63: 1–42. https://doi.org/10.5962/bhl.title.2854

Appendix 1

Specimens examined

(* bold = measured, star (*) = sequenced)

Sumaterana crassiovis comb. n. (adults, n = 262)

Provinsi Aceh. – Kabupaten Pidie, Mountain above Geumpang, Transmigrasi community, old road to mining camp, 4.85824°N, 96.21348°E, 1090 m a.s.l., UTA.A64868; Kabupaten Bener Meriah, road between Bireun-Takengon, 4.82623°N, 96.74841°E, 924 m a.s.l., UTA.A64856-60; Kabupaten Bener Meriah, foot of Berni Terlong, near Desa Rambune, pantan Pediangah, Tihmang gagah, 4.76379°N, 96.78131°E, 1184 m a.s.l., UTA.A64853; Kabupaten Aceh Tengah, Taman Buru Linge-Isaq, 4.37958°N, 97.29158°E, 1000 m a.s.l., **MZB.AMPH.29196, MZB.AMPH.29198, ZMH.A14168–69**; Kabupaten Gayo Lues, Kampung Ise-Ise, 4.25511°N, 97.18366°E, 1129 m a.s.l., UTA.A64855; Kabupaten Gayo Lues, Kedah, Blangkajeren, Rain Forest lodge, 3.97806°N, 97.25314°E, 1376 m a.s.l., UTA.A64851, UTA.A64852; Kabupaten Gayo Lues, Marpunge, Taman Nasional Gunung Leuser, 3.79289°N, 97.64417°E, 1190 m a.s.l., **MZB.AMPH.29188, MZB.AMPH.29190, MZB.AMPH.29192, MZB.AMPH.29194, ZMH.A14216–17, ZMH.A14219**; Kabupaten Nagan Raya, Road from Nagan Raya to Terangun, 3.95839°N, 96.85218°E, 795 m a.s.l., UTA.A64864–66; Kabupaten Aceh Selatan, Gunung Putri Tidur near Tapak Tuan, 3.2921°N, 97.19642°E, 481 m a.s.l., UTA.A64867; Kabupaten Gayo Lues, Marpunge, Taman Nasional Gunung Leuser, 3.77103°N, 97.63801°E, 1065 m a.s.l., **MZB.AMPH.29186*, ZMH.A14218.**

Provinsi Sumatera Utara. – Kabupaten Dili Serdang, Sungai DAM Bumi Perkemahan Sibolangit, 3.27347°N, 98.53586°E, 881–965 m a.s.l., **MZB.AMPH.29326***, MZB.AMPH.29327–29, **MZB.AMPH.29330–37**; Kabupaten Dili Serdang, Sungai Batu Belah Bumi Perkemahan Sibolangit, 3.27522°N, 98.53613°E, 880–965 m a.s.l., MZB.AMPH.29338–39, **MZB.AMPH.29340–41**, MZB.AMPH.29342–44; Kabupaten Dili Serdang, Sungai Derek Bumi Perkemahan Sibolangit, 3.27688°N, 98.53472°E, 877–908 m a.s.l., MZB.AMPH.29345–47, Kabupaten Karo, sungai Taman Wisata Alam Deleng Lancuk, 3.19668°N, 98.39298°E, 1416–1427 m a.s.l., MZB.AMPH.29348–49, **MZB.AMPH.29350**, MZB.AMPH.29351, **MZB.AMPH.29352**, MZB.AMPH.29353–54; Kabupaten Karo, Kecamatan Berastagi, Air Terjun Sikulikap, 3.24047°N, 98.53878°E, 1156 m a.s.l., **MZB.AMPH.23492–93**, UTA.A64879–81; Kabupaten Toba Samosir, Gunung Pangulubao, 2.60514°N, 99.04629°E, 1397 m a.s.l., **MZB.AMPH.23496–97**, **MZB.AMPH.23506**, **UTA.A64833***, UTA.A64882–86; Kabupaten Hambung Hasundutan, Gunung Pinapan, 2.18325°N, 98.60513°E, 1309 m a.s.l., MZB.AMPH.23498; Kabupaten Tapanuli Selatan, slope of Gunung T. Anjing, 1.68449°N, 99.34737°E, 1253 m a.s.l., MZB.AMPH.23505; Kabupaten Mandiling Natal, Huta Baringin Julu, Taman Nasional Batang Gadis, 0.66636°N, 99.57191°E, 1271 m a.s.l., UTA.A64894–902, **MZB.AMPH.23507–11**, **UTA.A64835***, **MZB.AMPH.23513–14**; Kabupaten Mandailing Natal, slope of Dolok Malea above Kampung Mompang, 0.97500°N, 99.57959°E, 991 m a.s.l., **MZB.AMPH.23499–501, MZB.AMPH.23503–04**, UTA.A64887–93; Kabupaten Mandailing Natal, road between Panyabungan and Natal, 0.72544°N, 99.54497°E, 804 m a.s.l., MZB.AMPH.23490–91.

Provinsi Sumatera Barat. – Kabupaten Pasaman, Kecamatan Panti, Stream 3 Cagar Alam Rimbo Panti, 0.35220°N, 100.04933°E, 425 m a.s.l., **MZB.AMPH.29200*, MZB.AMPH.29202, MZB.AMPH.29204, ZMH.A14170–73**; Kabupaten Pasaman, Kecamatan Panti, Stream 1 Batu Ampar, Cagar Alam Rimbo Panti, 0.35056°N, 100.04490°E, 450–500 m a.s.l., **MZB.AMPH.29206, MZB.AMPH.29208, MZB.AMPH.29210, ZMH.A14191–92**; Kabupaten Pasaman, Kecamatan Panti, Stream 1 Batu Ampar, Cagar Alam Rimbo Panti, 0.34789°N, 100.03748°E, 1000 m a.s.l., MVZ271526*; Kabupaten Payakumbuh, Kecamatan Pangkalan Koto Baru, Road from Payakumbuh to Pangkalan, 0.01905°N, 100.72205°E, 621 m a.s.l., UTA.A64847; Kabupaten Payakumbuh, small creek next to main road connecting Payakumbuh-Riau, 0.01916°S, 100.72226°E, 606–624 m a.s.l., **MZB.AMPH.29320*, MZB.AMPH.29322, MZB.AMPH.29324, ZMH.A14223–25**; Kabupaten Solok, Kecamatan Gunung Talang, Stream 1 Lubuak Sulasiah, 0.95782°S, 100.57112°E, 1040–1084 m a.s.l., MZB.AMPH.29212, MZB.AMPH.29214, MZB.AMPH.29216, MZB.AMPH.29218, MZB.AMPH.29220, MZB.AMPH.29222, MZB.AMPH.29224, ZMH.A14206–13; Kabupaten Solok, Kecamatan Gunung Talang, Stream 2 Lubuak Sulasiah, 0.94529°S, 100.54630°E, 1104 m a.s.l., MZB.AMPH.29226; Kabupaten Solok, Kecamatan Gunung Talang, Desa Kayu Jao, 0.99717°S, 100.63952°E, 1270 m a.s.l., ZMH.A14195; Kabupaten Solok, Kecamatan Gunung Talang, Stream 1 Desa Kayu Jao, 0.99557°S, 100.64334°E, 1315–1350 m a.s.l., MZB.AMPH.29228, MZB.AMPH.29230, ZMH.A14198; Kabupaten Solok, Kecamatan Gunung Talang, Stream 2 Kayu Jao, 0.99980°S, 100.63550°E, 1195 m a.s.l., MZB.AMPH.29232, MZB.AMPH.29234, ZMH.A14221–22; Kabupaten Solok, Road from Kayu Aro-Padang near Surian, 1.13573°S, 100.80255°E, 1417 m a.s.l., MZB.AMPH.22341, UTA.A62438; Kabupaten Solok Selatan, Muara Labuh, Taman Nasional Kerinci Seblat, 1.45534°S, 101.00020°E, 640–643 m a.s.l., **MZB.AMPH.29253, MZB.AMPH.29255, ZMH.A14136–37** Kabupaten Solok Selatan, Padang Aro, Taman Nasional Kerinci Seblat, 1.559317°S, 101.31072°E, 605 m a.s.l., **ZMH.A14197***; Kabupaten Solok Selatan, Batang Blangir, Padang Aro, Taman Nasional Kerinci Seblat, 1.61750°S, 101.24780°E, 975 m a.s.l., **MZB.AMPH.29237, MZB.AMPH.29241, MZB.AMPH.29243, MZB.AMPH.29245, MZB.AMPH.29247, MZB.AMPH.29239, ZMH.A14179–84**; Kabupaten Solok Selatan, stream at the foot hill of Lake Bontak, Taman Nasional Kerinci Seblat, 1.60325°S, 101.26391°E, 850 m a.s.l., MZB.AMPH.29249, MZB.AMPH.29251, ZMH.A14226–28.

Provinsi Jambi. – Kabupaten Kerinci, trail to Danau Tujuh, 1.71076°S, 101.36986°E, 1506 m a.s.l., MZB.AMPH.22221, MZB.AMPH.22222, MZB.AMPH.22223, MZB.AMPH.22334, UTA.A64904, UTA.A64905, UTA.A64906; Kabupaten Kerinci, road between Sungai Penuh and Tapan, west of crest, 2.04139°S, 101.31462°E 1250 m a.s.l., MZB.AMPH.22345; Kabupaten Kerinci, Gunung Kunyit, Taman Nasional Kerinci-Seblat, 2.26013°S, 101.49512°E, 1355 m a.s.l., **MZB.AMPH.22336**, **MZB.AMPH.22338**, **MZB.AMPH.22339***, **MZB.AMPH.22340**,

UTA.A64907–13; Kabupaten Kerinci, Bukit Tapan, Taman Nasional Kerinci Seblat, 2.06988°S, 101.26235°E, 726 m a.s.l., MZB.AMPH.29257; 2.06543°S, 101.26771°E, 787 m a.s.l., ZMH. A14193; Kabupaten Kerinci, Sungai Kunyit, Bukit Tapan, Taman Nasional Kerinci Seblat, 2.06925°S, 101.28656°E, 909–916 m a.s.l., MZB.AMPH.29259, MZB.AMPH.29261, MZB. AMPH.29263, MZB.AMPH.29265, MZB.AMPH.29267, MZB. AMPH.29269, ZMH.A14201–05.

Provinsi Bengkulu. – Kabupaten Lebong, Stream at Camp 2 Desa Seblat Ulu, Taman Nasional Kerinci Seblat, 2.95330°S, 102.13955°E, 758-774 m a.s.l., **ZMH.A14166–67, MZB. AMPH.29271**; Kabupaten Lebong, Stream at Camp 3 Desa Seblat Ulu, Taman Nasional Kerinci Seblat, 2.95100°S, 102.16345°E, 716–723 m a.s.l., **MZB.AMPH.29273**, **MZB.AMPH.29275***, **MZB.AMPH.29277**; Kabupaten Lebong, Stream at Camp 1 Desa Seblat Ulu, Taman Nasional Kerinci Seblat, 2.95330°S, 102.13955°E, 723 m a.s.l., **MZB.AMPH.29276**, **ZMH.A14165**.

Provinsi Sumatera Selatan. – Kabupaten Pagar Alam Selatan, road from Manna to Pagar Alam, 4.11296°S, 103.10007°E, 772 m a.s.l., UTA.A64870, UTA.A64873–75, UTA.A64877; Kabupaten Muara Enim, Gunung Patah near Desa Segamit, 4.21742°S, 103.46823°E, 1545 m a.s.l., UTA.A64849; Kabupaten Muara Enim, Sungai Lematan Desa Batu Surau, 4.13725°S, 103.58640°E, 1048–1069 m a.s.l., **MZB.AMPH.29312, MZB.AMPH.29314, MZB.AMPH.29316, MZB.AMPH.29318, ZMH.A14149*, ZMH.A14150–53**; Kabupaten Ogan Komering Ulu Selatan, Kecamatan Kisam Tinggi, Gunung Nanti, Desa Gunung Megang, 4.24586°S, 103.83415°E, 1048–1062 m a.s.l., **MZB. AMPH.29302, MZB.AMPH.29304, MZB.AMPH.29306, MZB.AMPH.29308, ZMH.A14140–43, MZB.AMPH.29310**; 4.24543°S, 103.8352°E, 874 m a.s.l., **ZMH.A14139***.

Provinsi Lampung. – Kabupaten Lampung Barat, Curug Berdua, Gunung Abung, Desa Purajaya, 5.03730°S, 104.54828°E, 956–979 m a.s.l., **MZB.AMPH.29282, MZB. AMPH.29284, MZB.AMPH.29286, MZB.AMPH.29288*, MZB.AMPH.29290**, **ZMH.A14144–48**; Kabupaten Lampung Barat, Sumber Jaya, 5.04456°S, 104.44930°E, 1022 m a.s.l., MZB.AMPH.29292, MZB.AMPH.29294, ZMH.A14214–15; Kabupaten Lampung Barat, Road Liwa to Krui, 5.06458°S, 104.05465°E, 673 m a.s.l., MZB.AMPH.22344, MZB. AMPH.22343, UTA.A62440; Kabupaten Lampung Barat, Sungai Pauh, Gedong Surian, 5.06651°S, 104.46261°E, 935–961 m a.s.l., ZMH.A14200, MZB.AMPH.29279, ZMH.A14199; Kabupaten Tanggamus, Air Terjun Talang Ogan, 5.37933°S, 104.66043°E, 754–717 m a.s.l., **MZB.AMPH.29296, MZB. AMPH.29298, MZB.AMPH.29300, ZMH.A14185*–86, ZMH.A14188, ZMH.A14186**.

Sumaterana crassiovis comb. n. (tadpoles, n = 21)

Provinsi Sumatera Barat. – Kabupaten Lima Puluh Koto, Desa Tanjuang Bungo, 0.15188°N, 100.47468°E, 388 m a.s.l., **MZB. AMPH.29363**; Kabupaten Payakumbuh, Stream next to the road between Payakumbuh-Riau 0.01917°S, 100.72226°E, 600–627 m a.s.l., **MZB.AMPH.29355***, **MZB.AMPH.29356, ZMH.A12649** (n = 6); Kabupaten Solok Selatan, Muara Labuh, Taman Nasional Kerinci-Seblat, 1.45534°S, 101.00020°E, 640–643 m a.s.l., **MZB.AMPH.29359, ZMH.A12650***; Kabupaten Solok Selatan, Kecamatan Sangir, Desa Padang Aro, Taman Nasional Kerinci-Seblat, 1.61750°S, 101.24780°E, 975 m a.s.l., **MZB.AMPH.29361, ZMH.A12651, ZMH.A12652** (n = 5).

Provinsi Sumatera Selatan. – Kabupaten Muara Enim, Desa Batu Surau, 4.13725°S, 103.58640°E, 1048-1069 m a.s.l., **MZB. AMPH.29364**, **MZB.AMPH.29365***.

Sumaterana montana sp. n. (adults, n = 28)

Provinsi Aceh. – Kabupaten Bener Meriah, foot of Berni Terlong, near Desa Rambune, pantan Pediangah, Tihmang gagah, 4.77054°N, 96.79341°E, 1377 m a.s.l., UTA.A64930; Kabupaten Gayo Lues, Stream Along Road S. (up) from Ise-Ise, 4.22357°N, 97.18655°E, 1827 m a.s.l., UTA.A64931, UTA.A64932, UTA. A64933, UTA.A64934; Kabupaten Gayo Lues, Stream in Lemon Grass Plantation, 3.97234°N, 97.23405°E, 1638 m a.s.l., UTA. A64935; Kabupaten Gayo Lues, Kedah, Blangkajeren, Rain forest lodge, 3.9771°N, 97.25256°E, 1355 m a.s.l., UTA.A64929; Kabupaten Gayo Lues, Marpunge, Taman Nasional Gunung Leuser, 3.79289°N, 9.764.417°E, 1190 m a.s.l., MZB.AMPH.29375, **ZMH.A14164***.

Provinsi Sumatera Utara. – Kabupaten Karo, Gunung Sibuatan, Above Kampung Naga Linga, 2.91076°N, 98.46313°E, 1625 m a.s.l., **MZB.AMPH.23522–24, UTA.A64834***, UTA. A64929; Kabupaten Toba Samosir, Gunung Pangulubao, 2.60441°N, 99.04599°E, 1392 m a.s.l., UTA.A64927; UTA. A64926; Kabupaten Samosir, vicinity of Tele, 2.55397°N, 98.59806°E, 1774 m a.s.l., **MZB.AMPH.23516*** (paratype), **MZB.AMPH.23517** (paratype), **UTA.A64829** (paratype); 2.54691°N, 98.61414°E, 1780 m a.s.l., **MZB.AMPH.23518–20** (paratype)**, UTA.A64830–32** (paratype); Kabupaten Simalungung, Simpang Tele, 2.52733°N, 98.63364°E, 1800 m a.s.l., Kabupaten Hambung Hasundutan, 2.18325°N, 98.60513°E, 1309 m a.s.l., UTA.A64928.

Provinsi Bengkulu. – Kabupaten Lebong, Desa Seblat Ulu, Taman Nasional Kerinci Seblat, 2.88525°S, 102.12993°E, 2000 m a.s.l., **ZMH.A14194** (paratype); 2.88413°S, 102.13073°E, 2033 m a.s.l., **MZB.AMPH.29377*** (holotype).

Sumaterana dabulescens sp. n. (adults, n = 38)

Provinsi Aceh. – Kabupaten Pidie, Krueng Meriam, Tangse, 4.938417°N, 95.98375°E, 314 m a.s.l., **UTA.A64921** (paratype); 4.93852°N, 95.98294°E, 323 m a.s.l., **UTA.A64922** (paratype)**, UTA.A64923** (paratype); Kabupaten Pidie, Kecamatan Tangse, Stream along Tangse-Geumpang road, 4.93869°N, 95.9825°E, 333 m a.s.l., **UTA.A64924** (paratype); Kabupaten Pidie, Desa Mane, 4.92091°N, 96.12275°E, 761 m a.s.l., **MZB. AMPH.29381** (paratype)**, MZB.AMPH.29383** (paratype), **MZB.AMPH.29385** (paratype)**, MZB.AMPH.29387**(paratype)**, MZB.AMPH.29389** (paratype), **ZMH.A14154-58** (paratype)**, UA.2014.0397** (paratype); 4.91926°N, 96.12300°E, 747 m a.s.l., **MZB.AMPH.29392, MZB.AMPH.29384, ZMH.A14187, ZMH.A14190**; 4.89949°N, 96.13168°E, 700 m a.s.l., **ZMH.A14188**; Kabupaten Aceh Tengah, Road Takengon-Bierut, Enang-Enang Resort, 4.88649°N, 96.72689°E, 604 m a.s.l., **UTA.A64917** (paratype), UTA.A64918; Kabupaten Bener Meriah, 4.82623°N, 96.74841°E, 924 m a.s.l., **UTA.A64919** (paratype); Kabupaten Pidie, Road Tutut

to Geumpang, 4.65267°N, 96.09203°E, 593 m a.s.l., UTA. A64920; Kabupaten Aceh Tengah, Sungai Air Jambu, Taman Buru Linge Isaq, 4.36482°N, 97.24783°E, 440 m a.s.l., **MZB. AMPH.29396*** (holotype)**, MZB.AMPH.29398** (paratype)**, MZB.AMPH.29400** (paratype)**, MZB.AMPH.29402** (paratype)**, ZMH.A14159** (paratype)**, ZMH.A14161–62** (paratype)**, UA.2014.0214** (paratype); Kabupaten Aceh Tengah, red water stream, Taman Buru Linge Isaq, 4.37958°N, 97.29158°E, 1000 m a.s.l., **ZMH.A14163**; Kabupaten Aceh Tengah, Taman Buru Linge-Isaq, 4.338036°N, 97.28096°E, 600 m a.s.l., **MZB. AMPH.29405, MZB.AMPH.29407–09, ZMH.A14174**;.

Sumaterana dabulescens sp. n. (juvenile, n = 1)

Provinsi Aceh. – Kabupaten Pidie, Kecamatan Mane, Desa Mane, 4.92334°N, 96.12215°E, 792 m a.s.l., **MZB.AMPH.29378***.

Sumaterana dabulescens sp. n. (tadpoles, n = 8)

Provinsi Aceh. – Kabupaten Pidie, Kecamatan Mane, Stream 3 Mane, 4.91926°N, 96.12300°E, 747 m a.s.l., **MZB. AMPH.29410** (n = 5)**, MZB.AMPH.29411*, ZMH.A12655, MZB.AMPH.29413**.

Supplementary material 1

List of sequences and GenBank accession number

Authors: Umilaela Arifin, Utpal Smart, Stefan T. Hertwig, Eric N. Smith, Djoko T. Iskandar, Alexander Haas

Data type: molecular data

Copyright notice: This dataset is made available under the Open Database License (http://opendatacommons.org/licenses/odbl/1.0/). The Open Database License (ODbL) is a license agreement intended to allow users to freely share, modify, and use this Dataset while maintaining this same freedom for others, provided that the original source and author(s) are credited.

Link: https://doi.org/10.3897/zse.94.22120.suppl1

Supplementary material 2

Illustration of morphological characters

Authors: Umilaela Arifin, Utpal Smart, Stefan T. Hertwig, Eric N. Smith, Djoko T. Iskandar, Alexander Haas

Data type: species data

Explanation note: Illustration of morphological characters measured in this study: A) for adults, B) for tadpoles. Explanation for each acronym available in Tables 2 and 3. Illustration by L. Waser.

Copyright notice: This dataset is made available under the Open Database License (http://opendatacommons.org/licenses/odbl/1.0/). The Open Database License (ODbL) is a license agreement intended to allow users to freely share, modify, and use this Dataset while maintaining this same freedom for others, provided that the original source and author(s) are credited.

Link: https://doi.org/10.3897/zse.94.22120.suppl2

Supplementary material 3

Pairwise genetic distance

Authors: Umilaela Arifin, Utpal Smart, Stefan T. Hertwig, Eric N. Smith, Djoko T. Iskandar, Alexander Haas

Data type: molecular data

Explanation note: Pairwise genetic distance (uncorrected p) within crassiovis-group and all taxa used in this study based on 16S sequence, calculated using MEGA 7.1.025. Values are in percentage (%).

Copyright notice: This dataset is made available under the Open Database License (http://opendatacommons.org/licenses/odbl/1.0/). The Open Database License (ODbL) is a license agreement intended to allow users to freely share, modify, and use this Dataset while maintaining this same freedom for others, provided that the original source and author(s) are credited.

Link: https://doi.org/10.3897/zse.94.22120.suppl3

Zoosyst. Evol. 94 (1) 2018, 195–209 | DOI 10.3897/zse.94.22289

PENSOFT

museum für naturkunde

Ontogeny of *Hemidactylus* (Gekkota, Squamata) with emphasis on the limbs

Wessel van der Vos[1], Koen Stein[2,3], Nicolas Di-Poï[4], Constanze Bickelmann[1]

1 *Museum für Naturkunde Berlin, Leibniz Institute for Evolution and Biodiversity Science, Invalidenstrasse 43, 10115 Berlin, Germany*
2 *Earth System Science – AMGC, Vrije Universiteit Brussel, Pleinlaan 2, 1050 Brussels, Belgium*
3 *Royal Belgian Institute of Natural Sciences, Earth and History of Life, Rue Vautier 29, 1000 Brussels, Belgium*
4 *Institute of Biotechnology, Research Program in Developmental Biology, University of Helsinki, Finland*

http://zoobank.org/122E692A-9E01-47FB-A386-D4E707620460

Corresponding author: *Constanze Bickelmann* (constanze.bickelmann@mfn.berlin)

Received 15 November 2017
Accepted 12 February 2018
Published 9 March 2018

Academic editor:
Johannes Penner

Key Words

Gecko
in-ovo development
staging table
limb development
bone histology
μCT
immunohistochemistry
ossification
ecomorphological specialization

Abstract

Squamate reptiles constitute a major component of the world's terrestrial vertebrate diversity, encompassing many morphotypes related to ecological specialization. Specifically, Gekkota, the sister clade to most other squamates, have highly specialized autopodia, which have been linked to their ecological plasticity. In this study, a developmental staging table of the gecko *Hemidactylus*, housed at the Museum für Naturkunde, is established. Twelve post-ovipositional stages are erected, monitoring morphological embryological transitions in eye, ear, nose, heart, limbs, pharyngeal arches, and skin structures. Ecomorphological specializations in the limbs include multiple paraphalanges, hypothesized to aid in supporting the strong muscles, that are situated adjacent to metacarpal and phalangeal heads. Furthermore, some phalanges are highly reduced in manual digits III and IV and pedal digits III, IV, and V. Development, composition, and growth of limb elements is characterized in detail via μCT, histochemistry, and bone histological analysis. Using known life history data from two individuals, we found an average lamellar bone accretion rate in the humeral diaphysis comparable to that of varanids. Various adult individuals also showed moderate to extensive remodeling features in their long bone cortices, indicating that these animals experience a highly dynamic bone homeostasis during their growth, similar to some other medium-sized to large squamates. This study of *in-ovo* development of the gecko *Hemidactylus* and its ecomorphological specializations in the adult autopodia, enlarges our knowledge of morphological trait evolution and of limb diversity within the vertebrate phylum.

Introduction

Gekkota (Squamata; lizards, snakes and amphisbaenians *sensu* Wiens et al. 2012) is a speciose and ecologically diverse clade with a cosmopolitan distribution (Carranza and Arnold 2006). Yet, molecular and morphological data for squamate interrelationships disagree substantially (Losos et al. 2012); however, according to the molecular data, Gekkota are, together with Dibamidae, sister to all other squamates (Wiens et al. 2012, Pyron et al. 2013). Although squamate reptiles contribute greatly to vertebrate diversity in modern ecosystems, and exhibit a wide range of morphological variation in their limbs related to ecological specialization, underlying developmental and molecular mechanisms remain yet poorly studied (Sanger 2012, Pyron et al. 2013). However, importantly, the incorporation of taxa from all higher clades in the study of development and molecules is essential for understanding evolutionary patterns of development (Millinkovitch and Tzika 2007, Sanger 2012).

Some gekkotan species have the extraordinary ability of being able to cling to smooth surfaces and of inverted locomotion because of the properties of their specialized autopodia (Autumn et al. 2002, Russell 2002, Pianka and Sweet 2005). Such ability is associated with adhesive toepads which are located ventrally on the distal part of the digits (Ruibal and Ernst 1965, Russell 2002, Gamble et al. 2012). In Gekkota, adhesive toepads have first been reported in fossils from Lower Cretaceous amber deposits of Myanmar (Arnold and Poinar 2008). They evolved and were lost independently several times within this lineage, and allowed them to enter novel ecological habitats (Pianka and Sweet 2005, Gamble et al. 2012). Further eco-specializations in Gekkota include the presence of paraphalanges, unique structures only found in the gekkotan clade and hypothesized to aid both in the attachment of strong muscles in the digits and in the grasping power of the limb by applying pressure to the adhesive toepads (Russell and Bauer 1988). These apomorphic elements are located laterally to the interphalangeal joints and occasionally on the dorsal and ventral sides, and vary in number, shape and size (Wellborn 1933, Russell and Bauer 1988, Gamble et al. 2012). Paraphalanges are either cartilaginous or bony structures (Wellborn 1933, Russell and Bauer 1988, Gamble et al. 2012). Paraphalanges have been correlated with functional demands, such as grasping and/or climbing, rather than phylogeny (Russell and Bauer 1988, Vickaryous and Olson 2007, Gamble et al. 2012). They have evolved and were lost multiple times within Gekkota (Gamble et al. 2012).

Besides these general gekkotan traits, one gekkotan genus shows additional ecomorphological specializations in both fore- and hind limbs: *Hemidactylus* (Fig. 1). It is placed within Gekkonidae, as sister to *Cyrtodactylus* (Pyron et al. 2013). It has highly reduced phalanges (Russell 1975, 1977, Gamble et al. 2012). More specifically, the antepenultimate phalanx is highly reduced in digits III and IV of the manus, with a phalangeal count of 2-3-4-5-3 (Russell 1975, 1977). The pes shows a phalangeal count of 2-3-4-5-4, with an additional reduced phalanx in digit V (Russell 1975, 1977). Although phalangeal elements are also reduced in other geckos, the degree of reduction is never as pronounced as in *Hemidactylus* (Gamble et al. 2012).

Here, we present a morphological staging table for *Hemidactylus* based on external embryonic developmental traits and compare these to other squamate taxa. We make further references to characterize limbs which display ecomorphological specializations, and which we study using different approaches such as bone histology, μCT, and immunohistochemistry. Enlarging the database of well documented developmental character traits of organisms allows for a more detailed and comprehensive knowledge of vertebrate morphological diversity. The described ecomorphological specializations in the autopodia of the adult phenotype make *Hemidactylus* an ideal candidate for eco-evo-devo studies (Gilbert and Epel 2009).

Material and methods

Institutional abbreviations

AC – Comparative Anatomy, Musée d'Histoire Naturelle, Paris, France; CA – Cold Archive, Museum für Naturkunde Berlin, Leibniz Institute for Evolution and Biodiversity Science, Berlin, Germany; MK – Museum Koenig, Bonn, Germany; ZMB – Museum für Naturkunde Berlin, Leibniz Institute for Evolution and Biodiversity Science (former Zoologisches Museum Berlin), Berlin, Germany.

Figure 1. An adult *Hemidactylus* female (three years old).

Animal care

The study organism *Hemidactylus* is a yet unidentified species based on a pregnant female which was collected in Sudan in 2011 (Fig. 1; ZMB 87075 to 87077; Kirchhof et al. work in progress). Live animals are housed in an animal-care facility at the Museum für Naturkunde Berlin; dead animals are preserved in alcohol in the herpetological collection and the Cold Archive at the Museum für Naturkunde Berlin. Temperature in the breeding room is set to 26-28 °C and photoperiod is maintained at 12 hours daylight: 12 hours of darkness. Seasonal cycles are not mimicked. Animals are fed with house crickets (*Acheta domesticus*), fruits, vitamins and calcium powder twice weekly. Females are allowed to oviposit naturally. Eggs are laid in clutches of one to two. Duration of post-ovipositional development is approximately 60 days, comparable to that of the Madagascar Ground Gecko *Paroedura pictus* (Noro et al. 2009). Embryos were sacrificed in accordance with German Law on *Tierschutzgesetz*, and *TierSchVersV*. Embryos were fixed in 4 % pFA in 1X Phosphate buffered saline (PBS) for 24 h to 48 h, depending on size, dehydrated and stored in 100 % methanol at -20 °C in the Cold Archive at the Museum für Naturkunde Berlin (Tab. 1).

μCT analysis

μCT scans were performed using a Phoenix nanotom X-ray|s at the Museum für Naturkunde Berlin (Suppl. material 1: SOM Tab. 1). Scans were reconstructed to a 3D volume using datos|x (Version 2.0, GE Sensing & Inspection Technologies GmbH phoenix|x-ray). Data were analyzed and visualized with VolumeGraphics Studio Max (Version 2.2., Volume Graphics). Scanned hands were from an adult specimen (Fig. 2; ZMB 87075, SVL 42 mm, over one year old), and a juvenile (Fig. 5C; ZMB 87077, SVL 17 mm, two days old). Datasets and models are deposited here https://doi.org/10.7479/qs1j-mnjp.

Bone Histology

We used two histo-technological procedures: (i) azan stained microtome paraffin sections and (ii) ground petrographic sections.

For azan staining, limbs were embedded (Leica EG 1160 and Shandon Hypercenter XP) in paraffin, and sectioned with a microtome (Leica 2000R). Sections were treated following the standard protocol by Heidenhain. In detail, sections were washed or immersed in xylene paraffin (ten minutes), xylene (twice five minutes), aniline alcohol (five minutes), wash in aquadest, azocarmine (25 minutes), wash in aquadest, wash in acetic acid, and 5 % phosphotungstic acid (two times 20 seconds), one to three hours in 5 % phosphotungstic acid. Hereafter, the tissue was placed in the aniline blue orange dye (4.5 minutes), washed with aquadest, 96 % alcohol, absolute alcohol, and finally four times xylene for five minutes each. Azan stains both bone and cartilage: dark blue indicates bone and light blue cartilage. Red indicates muscle fibers, and the nuclei are stained dark red. A forelimb of a hatchling (Fig. 5A; cross section no. A5_F_13a, specimen ZMB 87077) and a juvenile (Fig. 5B; cross section no. A4_F_21a, specimen ZMB 87076, SVL 33 mm, one year old), and an adult (Fig. 6B, D, E; ZMB 87078, SVL 47 mm, over one year old) were embedded in paraffin and sectioned. Cross sections are stored at the Museum für Naturkunde Berlin.

For ground sections (Fig. 6A, C), macerated bones were dehydrated in 70 % alcohol for 48 hours and embedded in epoxy resin (Araldite 2020), cut along the desired surface, mounted on glass slides and ground to a thickness of 75 to 50 μm. To enhance contrast, prevent detachment due to rehydration and generally protect the section, a coverslip was added. Femoral sections of *Iguana iguana* (AC1896 288), *Varanus timorensis* (MK52920) and *Tupinambis teguixin* (MK53531) were studied at the histotheca facilities of the Museum d'Histoire Naturell in Paris.

Morphometry

Photographs of embryos were taken with a Leica M205C camera. Photomicrographs for histomorphometric analysis of lamellar bone apposition rates were taken on a Zeiss Axioskop (HBO 50) with Leica firecam (DFC 420) and processed in a Leica Application Suite. All measurements were taken using ImageJ (Rasband 1997) (Tabs 1, 2).

Table 1. Developmental age range and external length measurements of *Hemidactylus* stages A to L. All embryos were studied to identify key features characteristic for each stage.

Stage	Developmental days post oviposition	Snout vent length (range in mm)	Forelimb measurement (mean in mm)	Hind limb measurement (mean in mm)	Number of studied specimens
A	4–5	9.3–11.5	n/a	n/a	3
B	6	17.4–20.1	0.2	0.3	2
C	9–14	14.1–17.6	0.7	0.6	4
D	11–30	18.9–24.7	1.5	1.4	11
E	8–30	21.0–24.0	1.8	1.8	7
F	42–56	23.8–24.0	2.8	2.8	2
G	15–36	23.8–27.2	2.8	2.8	6
H	38–50	26.4–31.1	3.7	3.5	6
I	35–56	29.0–34.2	4.9	4.8	10
J	40	32.8–34.2	5.3	6.5	2
K	40–58	36.0–39.4	6.2	6.7	3
L	50–60	37.5–41.9	6.8	6.9	2

Table 2. Histomorphometric data obtained from humeri of an adult (ZMB 87078) and a 'stage I' (CA2017_014). These data were used to calculate average apposition and lamellar bone accretion rates.

	Humerus ZMB 87078		Humerus CA2017_014
Life history data	Adult, Born 10.12.15, deceased 22.03.17		Stage I development
Total days lived	468		25 (unborn)
Days since onset ossification	493		0
Humerus shaft width (µm)	587.6		161.0
	posterior cortex	anterior cortex	
Non-remodeled Cortical thickness (µm)	139.4	91.2	0.1
No. of lamellae in cortex	40	29	1

Immunohistochemistry

Immunohistochemistry was performed on sections, with a rabbit polyclonal anti-*Sox9* antibody (Merck Millipore). *SOX9* is an early marker of cartilage, tendons and ligaments (Sugimoto et al. 2013). Samples were deparaffinized in xylene and rehydrated through ethanol steps into 1X PBS. Antigen retrieval was accomplished by citrate buffer treatment (pH = 6.0). Protease XXV treatment (Thermo Scientific) for 15 min was followed by non-specific binding with 5 % goat serum (Sigma). Primary antibody (polyclonal, rabbit, Millipore) was incubated overnight. Staining was achieved by DAPI and Fluoroshield (Sigma).

Results

Morphological staging table

A morphological staging table of *Hemidactylus* establishing twelve post-ovipositional developmental stages is presented here (Figs 2, 3; Tab. 1). For this purpose, differences in pharyngeal arches, otic pit, olfactory pit, optic cup, and other characters are studied in detail. In the following, each stage is presented listing key features which have been established in other squamate staging tables and which have been considered suitable for characterizing the ontogenetic development (Tab. 3; e.g. Noro et al. 2009, Wise et al. 2009, Khannoon 2015).

Stage A

Ear: The otic pit is present and located dorsally to the hyoid arch (Fig. 2A, B). The cartilage capsule lies dorsally to the otic pit (Fig. 2B).

Eye: The eye is composed of an optic cup that has not yet fully enclosed the lens (Fig. 2A).

Heart: The heart shows the distinct s-shape resulting from the curvature of the developing ventricle. It protrudes from the thoracic cavity.

Nose: The snout starts to form at the rostral end of the head. The olfactory pit is visible as a sickle shaped rim with its curvature pointing to the cranial side and the two points of the rim facing ventrally, towards the heart (Fig. 2B). Between the anterior ends of the rim towards the middle of the dorsal end of the rim, there is a small membrane covering the pit.

Pharyngeal arches: The mandibular pharyngeal arch is prominent, with a small bud from the maxillary that has just started to bud out (Fig. 2A). Posterior to the mandibular pharyngeal arch, the hyoid arch is present. It slightly overlaps the mandibular arch ventrally at the proximal part. Ventral to the hyoid arch is a small slit, marking the future distinction between the hyoid arch and the third arch.

Stage B

Ear: The cartilage capsule dorsal to the otic pit is enlarged (Fig. 2C).

Eye: The optic cup has almost enclosed the lens, except for a small gap rostro-ventrally. Note that this is not the characteristic choroid fissure. The optic cup shows faint pigmentation at the caudal-dorsal margin (Fig. 2D).

Head: The mesencephalon protrudes prominently in the cranial direction.

Heart: The heart and its placement in the thoracic cavity have not changed in comparison to the previous stage (Fig. 2D).

Limbs: Both fore- and hind limbs appear as small buds (Fig. 2C).

Nose: The rim of the olfactory pit is still partially covered by a membrane.

Pharyngeal arches: The maxillary process has not proceeded its development compared to the previous stage. The mandibular and hyoid arches, including the gap between them (Fig. 2D; indicated by the plus), have increased in size and show a sharper medial turn at their distal ends, and the segregation of the ventral part of the hyoid arch is more distinct than in the previous stage (Fig. 2D). The fourth arch and the associated pharyngeal slit are present posterior to the hyoid arch (Fig. 2C; indicated by the asterisk).

Stage C

Ear: The otic pit is enlarged and extends antero-posteriorly beyond the mandibular and hyoid arches. There is less overlap with the cartilage capsule.

Eye: The eye is enlarged and pigmented; it is referred to as the retina pigmented epithelium. The choroid fissure is present, and an unpigmented caudal-rostral line divides the optic cup into a distal and a proximal part (Fig. 2E, F; indicated by the cross).

Limbs: Both limb buds are proximo-distally longer than wide. The apical ectodermal ridge (AER) is distinct (Fig. 2G).

Nose: The external nares have developed, replacing the olfactory pit (Fig. 2E, F). This process of the fronto-nasal process replaces the olfactory rim. The dorsal side of the covering membrane is now connected to the maxillary process.

Pharyngeal arches: The maxillary process is linked to the dorsal side of the fronto-nasal process. The mandibu-

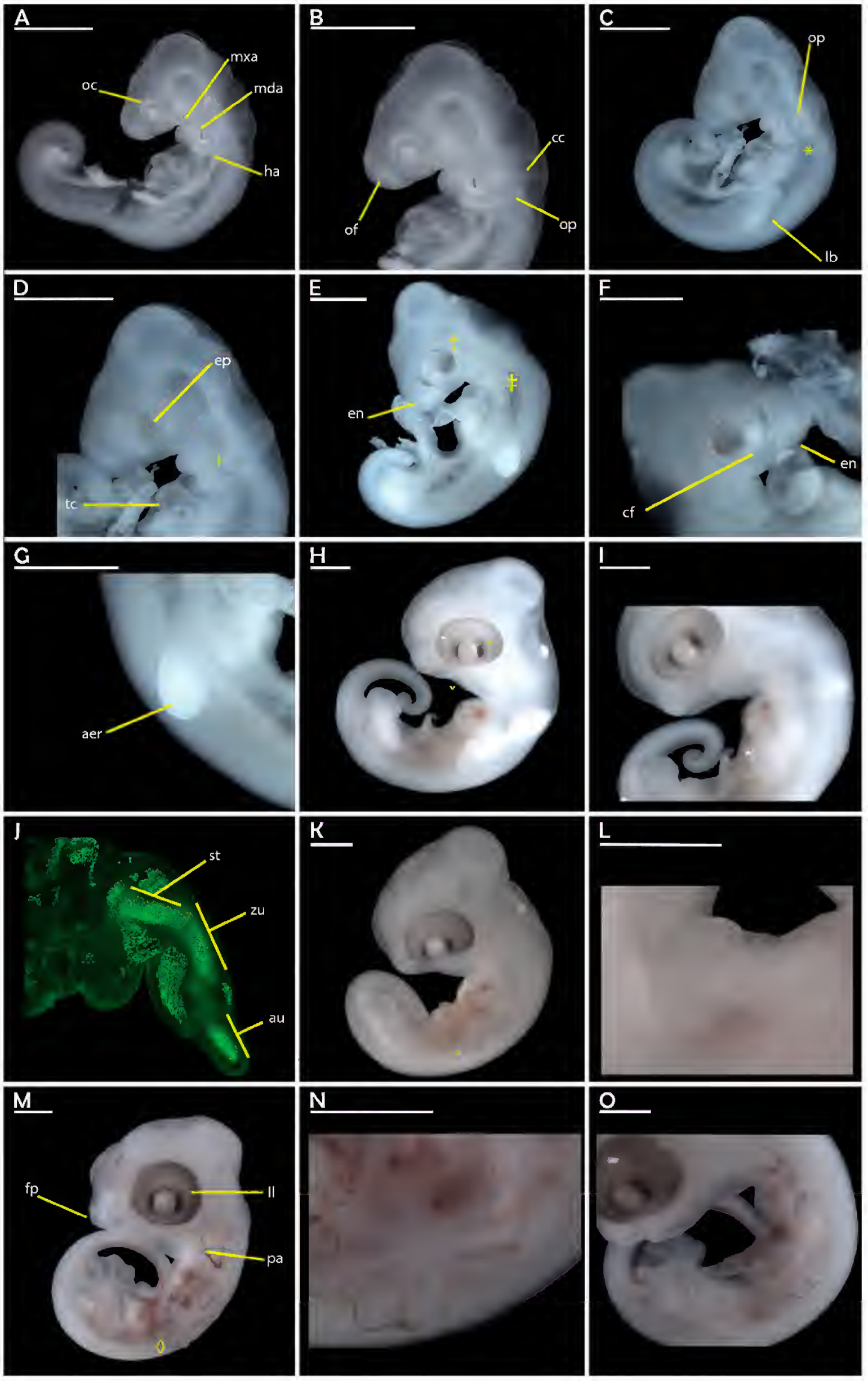

Figure 2. Overview of embryonic developmental stages A to F, erected in this study. Stage A is depicted in **(A, B)** and represented by CA2017_007. **(C, D)** show the representative CA2017_003 for stage B. Stage C **(E–G)** is represented by CA2017_006. CA2017_005 represents stage D in **(H–J)**. Note the immunohistochemistry for *SOX9* expression in a limb cross section in **(J)**. Stage E is shown in **(K–L)**, represented by CA2017_010. CA2017_012 represents stage F in **(M-O)**. Except for **(J)**, all pictures in lateral view. Scale bars equal 1mm. Abbreviations: **aer** – apical ectodermal ridge; **au** – autopod; **cc** – cartilage capsule; **cf** – choroid fissure; **en** – external nares; **ep** – eye pigmentation; **fp** – frontal nasal process; **ha** – hyoid arch; **lb** – limb bud; **ll** – lateral lines; **mda** – mandibular arch; **mxa** – maxillary process; **oc** – optic cup; **of** – olfactory pit; **op** – otic pit; **pa** – pharyngeal arches; **st** – stylopod; **tc** – thorac cavity; **zu** – zeugopod.

lar arch has budded out. The slit between the mandibular and the hyoid arch is reduced. The fourth and the fifth arches are present as small buds (Fig. 2E; indicated by the double-cross).

Stage D

Ear: The otic vesicle is less prominent in comparison to former stages.

Eye: The eye displays darker pigmentation, including its extension rostrally and caudally to the lens (Fig. 2H; indicated by the upside caret), which is here interpreted as the precursor of the iris.

Heart: The heart is fully enclosed inside the thoracic cavity.

Limbs: Fore- and hind limbs show the paddle shape typically seen in other amniote embryos at corresponding stages (Fig. 2H, I). An elbow angle between the stylopod and zeugopod starts developing. *SOX9*, the precursor of cartilage, is expressed in the presumptive stylopod, zeugopod, and autopod regions (Fig. 2J). Expression is also distinct in the presumptive regions of the strong limb muscles (Fig. 2J).

Nose: The rim of the olfactory pit is completely closed. The maxillary and the medial nasal prominence overlay the stomodeum.

Pharyngeal arches: The mandibular arch and the hyoid arch are now indistinguishable from one another (Fig. 2H; indicated by the downside caret), and the fourth arch has begun to grow, becoming larger than the initial bud. The mandibular arch reaches to the midline of the eye, and the maxillary prominence has taken up a position anterior to the eye.

Stage E

Ear: The otic vesicle further extends over the length of the mandibular and hyoid arch.

Eye: Lines that are visible lateral to the eye, or primordial iris, flanking the lens, have differentiated further.

Limbs: The most pronounced differences between stages D and E are identifiable in the limbs. In both fore- and hind limb, the interdigital tissue is retreating (Fig. 2K, L; indicated by the circle). A blood vessel is present at the distal margin of the forming autopod, which is antero-posteriorly wider than it is proximo-distally long (Fig. 2K).

Nose: Deep furrows between the nasal and maxillary prominences are developing further and show invaginations in this region.

Pharyngeal arches: The prominence of the mandibular and hyoid arches is now located anterior to the lens.

Stage F

Ear: The otic capsule has now become a small pit on the lateral side of the head.

Eye: The optic cup is darkly pigmented. The lateral pigmented lines now enclose the lens (Fig. 2M).

Limbs: Recession of the interdigital tissue is extensive (Fig. 3M-O; indicated by the rhomb). The autopodia have increased in size, most notably across the antero-posterior axis (Fig. 2N).

Nose: The olfactory pit has disappeared. The fronto-nasal process is fully fused (Fig. 3M).

Pharyngeal arches: The pharyngeal arches do not show the distinction between the different arches anymore (Fig. 2M).

Stage G

Ear: No further development in comparison to the former stage (Fig. 3A).

Eye: The optic cup has completely encircled the lens. The lateral pigmented lines of the lens start to encircle the lens and intensify in pigmentation.

Head: Cephalic projections, except for the mesencephalon, have disappeared. The head resembles that of a hatchling. Internally, only the calcified endolymphatic sacs and statolithic masses are visible in the μCT scans (Fig. 3B).

Limbs: The autopodia show further recession of the interdigital tissue, prominently segregating digits I to V. The elbow angle is at 90°. First signs of slightly swollen patches on the ventral side of the digits are visible (Fig. 3C).

Nose: The nose has become a pit laterally at the rostral end of the snout (Fig. 3A).

Jaw: Upper and lower jaws are fully formed.

Urogenital bud: The urogenital bud is located medially between the hind limbs (Fig. 3A).

Stage H

Eye: There are four distinct changes that are present in the eye at this stage: (i) The lens has changed from a matte white color to a more shining white color. (ii) The iris starts to cover the margins of the lens. (iii) The black pigmented tissue, starting out as the optic cup, has a glassy appearance. (iv) The hollow pan surrounding the lens is lighter than the rest of the eyeball.

Head: The head surface is smooth with few irregularities. The mesencephalon is still identifiable. Skull bones, such as parietal and surangular, start ossifying (Fig. 3E).

Limbs: The digits are almost free of interdigital tissue, and the distal phalanges start showing claw formation (Fig. 3D, F). Limb elements are still cartilaginous (Fig. 3E). On the ventral side of the digits, swollen pads are distinct, representing the precursors of the adhesive toepads (Fig. 3D, F).

Stage I

Eye: The iris surrounding the lens starts to display a wavy pattern but is still confined along the margin (Fig. 3G).

Head: More or less all skull bones are ossifyed (Fig. 3H).

Limbs: Claws have developed on all digits. Adhesive toepads are more prominent at this stage: one can discriminate the wavy skin and swellings on the toepads (Fig. 3I). All long bones have started ossifying, as well as the metacarpals in the forelimbs (Fig. 3H). In the hind limbs, metatarsals have ossified further compared to the forelimbs, and ossification of the proximal phalanges has just set in (Fig. 3H).

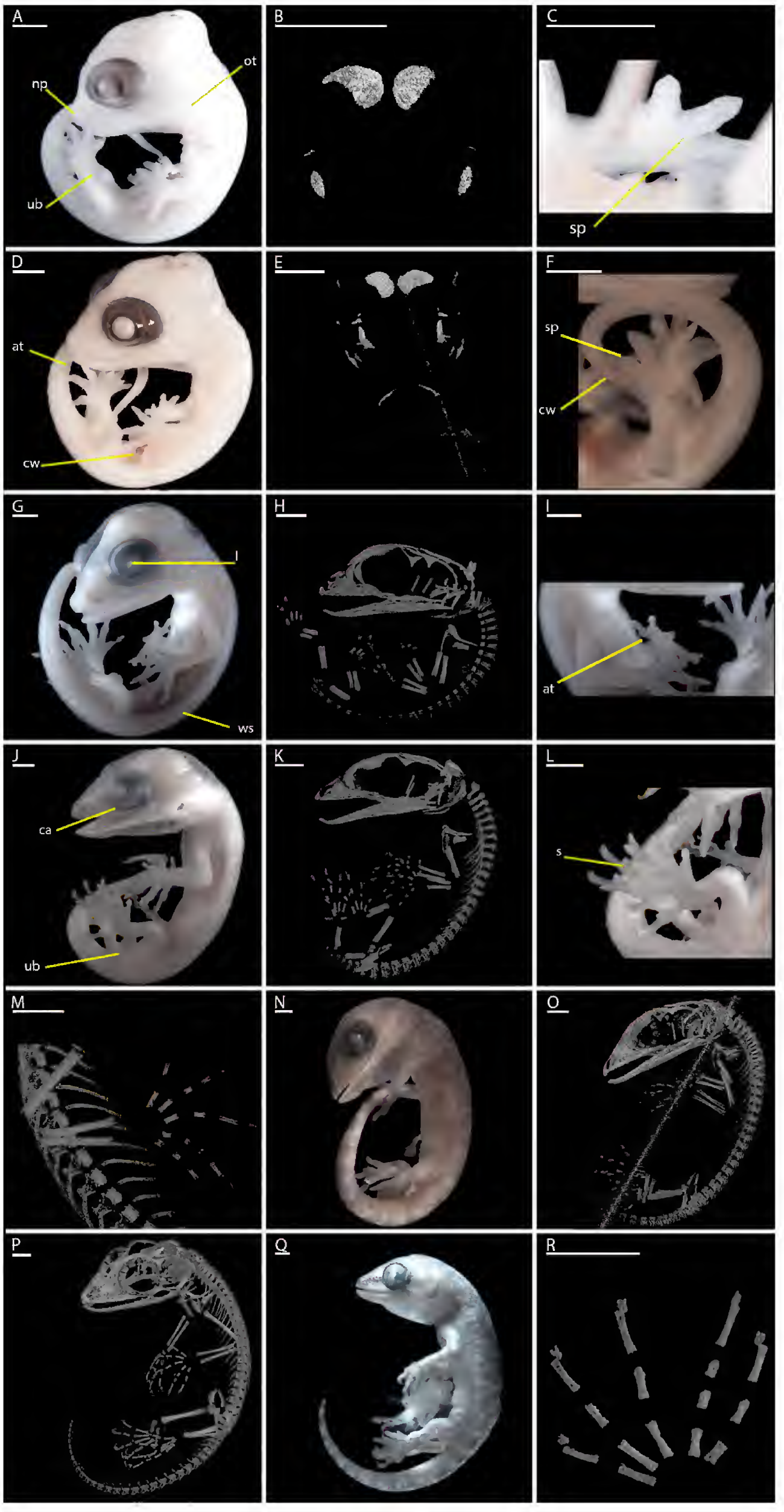

Figure 3. Overview of embryonic developmental stages G to L, erected in this study, including μCT data. Stage G is shown in **(A–C)**, its representative is CA2017_004. CA2017_011 represents stage H in **(D–F)**. **(G–I)** show stage I represented by CA2017_014. Stage J is depicted in **(J–M)**, represented by CA2017_008. Stage K is CA2017_013 and shown in **(N, O)**. **(P–R)** show CA2017_002 for stage L. **(B)** and **(E)** are in cranial view, **(R)** in dorsal view, and all others in lateral view. Scale bars equal 1mm. Abbreviations: **at** – adhesive toepads; **ca** – cornea; **cw** – claw formation; **l** – lens; **np** – nose pit; **ot** – otic capsule; **s** – scansors; **sp** – swollen pads; **ub** – urogenital bud; **ws** – wrinkly skin.

Skin: The skin starts to get wrinkly, a precursor stage prior to scale formation of the skin (Fig. 3G). Scale formation starts on the tail and proceeds cranially.

Stage J

Eye: Within the eye, the cornea is developing, and the eye socket begins to enclose the eye (Fig. 3J). The iris has a distinct shape, with projections pointing to the medial part of the lens.

Head: The mesencephalon has started to retract, exposing a smooth skull.

Limbs: The limbs are fully developed. Even the scales, although not yet fully pigmented, are present on the limbs. The scansors on the ventral adhesive toepads of the digits now show a rough wavy texture (Fig. 3L). The most distal part of the adhesive toepads no longer connects dorsally to the ventral part of each digit. All phalangeal elements have started ossifying (Fig. 3K, M).

Nose: The nose has moved to the most rostral side of the snout; it will not change position hereafter.

Skin: Scales now cover the entire body. The skin is dark.

Urogenital bud: The urogenital bud has started retreating into the body (Fig. 3J).

Stage K

Eye: The eye is located inside the socket, and the scale ridge surrounding it starts to develop (Fig. 3N). The scleral plates of the sclerotic ring start ossifying (Fig. 3O).

Head: Fully scaled.

Limbs: Ossification of the long bones continues (Fig. 3O).

Skin: All scales are pigmented. Scales are present on the upper and lower jaw.

Stage L

Eye: There is a rim on the cranial side of the eye, starting dorsally and wrapping around the upper part of the socket all the way to the midline (Fig. 3Q). The sclerotic ring is fully ossified (Fig. 3P).

Limbs: Phalanges and metacarpals and -tarsals continue ossifying, with the epiphyses not yet being ossified (Fig. 3R). Yet, neither paraphalanges nor carpals or tarsals have started ossifying (Fig. 3R).

Skin: The scales, present on tail, back, limbs, and head show differences in pigmentation and color (Fig. 3Q).

Limb ossification

The phenomenon of limb reduction is of great interest in evolutionary biology (e.g. Shapiro 2002), and especially among squamates, it is frequently found and has been linked to functional demands. Among the many mechanisms and patterns observed that go hand in hand with limb reduction, skeletal heterochrony can be one of them (Shapiro 2002, Hugi et al. 2012). *Hemidactylus* has reduced phalangeal elements, which could represent an evolutionary step along the path of digit loss (Hopson 1995). In that regard, we analysed limb ossification in *Hemidactylus* limbs.

Between fore- and hind limbs, no heterochronic differences in size and shape were monitored at any developmental stage (Figs 2, 3; Tab. 1). Ossification sets in slightly earlier in hind autopodial elements compared to the forelimb ones (Fig. 3H). Reduced phalanges ossify at the same time and in the same order as other phalanges (Fig. 3).

Histochemical staining and μCT scanning show that the paraphalangeal elements of *Hemidactylus* are present in three different shapes (Figs 4, 5): (i) nubbin-like ones laterally and dorsally at the distal end of all metacarpals, as well as at the dorsal side at the distal end of each last phalanx (Fig. 4; labeled in orange); (ii) rhomb-shaped ones distal-lateral to phalanx 1 in digits II, III, IV, and V, as well as phalanx 2 in digit IV (Fig. 4; labeled in red); and (iii) oval paraphalanges located ventrally at metacarpal heads of digits II to V (Fig. 4; labeled in yellow). All paraphalanges are bony in one-year-old adults (ZMB 87075, ZMB 87076) (Fig. 4, 5B). Yet, ossification starts only after hatching; in the two-day-old specimen (ZMB 87077) it has not yet started.

Long bone histology and histomorphometry

The long bones of one-year-old adult individuals show a lamellar bone matrix with no vascular spaces (Fig. 6). Growth lines may sometimes be present in the primary cortex of individuals over one year old, but in some individuals they are absent or have been resorbed by medullary expansion. These individuals also show intense endosteal remodelling features in the diaphyseal cortex, as seen in longitudinal section (Fig. 6A, B). Different generations of resorption and redeposition of endosteal bone can be seen along the margin of the innermost cortex, expressed by the cross-cutting relations of the resorption lines. Such remodeling features in the endosteal region can also be observed in other lizard species, such as varanid, tegu and iguanid lizards (Fig. 7), but only *Tupinambis* shows true secondary osteons in the innermost cortex among sampled squamates.

From an adult individual of known age (ZMB 87078, 468 days old, 493 days since onset of ossification, Fig. 6B, D, E; Tab. 2), we calculated the average daily lamellar bone apposition rate since the onset of ossification until time of death at 0.1 lamellae per day, equivalent to an average periosteal accretion rate of 0.4 μm per day. We used the following formulae to calculate accretion rates:

$$Average[apposition.rate] = \left(\frac{W_{adult.hum} - W_{onset.oss}}{2}\right) \times \left(\frac{1}{N°_{days.onset.oss}}\right)$$

$$Average[lamellar.accretion.rate] \left(\frac{W_{adult.hum} - W_{onset.oss}}{2}\right) \times \left(\frac{1}{N_{days\ onset\ oss}}\right) \times \left(\frac{N°_{lamellae.primcortex}}{W_{primcortex}}\right)$$

Where apposition.rate is the daily accretion rate (in μm/day), lamellar.accretion.rate is the number of lamellae deposited per day, $W_{adult.hum}$ is the width of the adult humerus (in μm), $W_{onset.oss}$ is the humeral width at the onset of ossification (in μm), $N°_{days.onset.oss}$ is the age of the adult individuals, in days, since the onset of ossification, $W_{primcortex}$ is the thickness of the primary cortex in the adult individual, and $N°_{lamellae.primcortex}$ is the number of lamellae counted in the primary cortex of the adult individual (Measurements in Tab. 2).

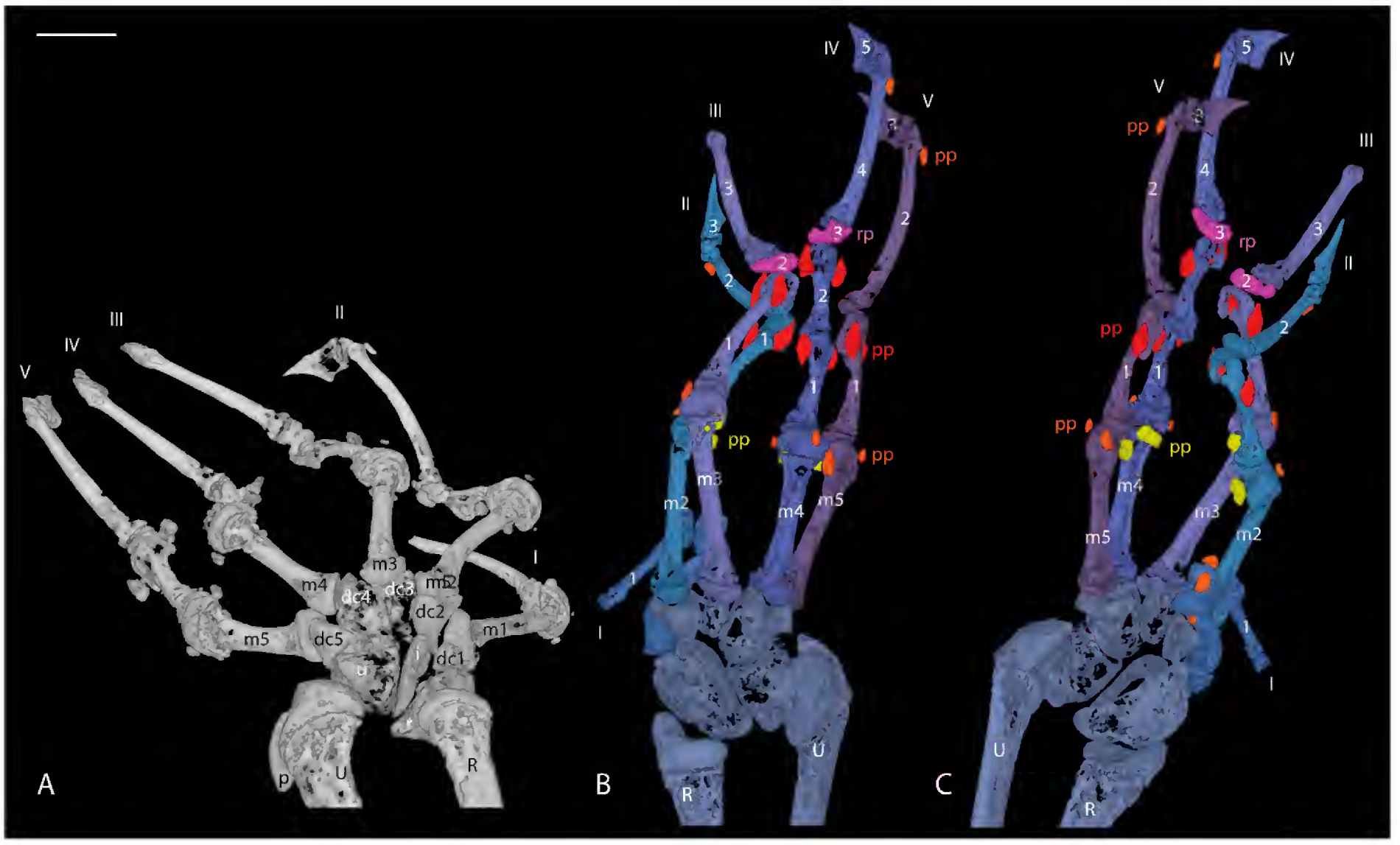

Figure 4. μCT images of the manus of an adult *Hemidactylus* (ZMB 87075). Left **(A)** and right **(B, C)** manus in dorsal **(A, B)** and ventral **(C)** view. Large lateral paraphalanges are shown in red, small nubbin-like ones laterally and dorsally in orange, and ventral ones in yellow. Note the reduced antepenultimate in pink in **(B, C)**. Scale bar is 500 μm. Abbreviations: **dc** – distal carpals; **m** – metacarpals; **p** –pisiform; **pp** – paraphalanges; **R** – radius; **r** – radiale; **rp** – reduced phalanges; **U** – ulna; **u** – ulnare; **1-5** – phalanges 1-5; **I-V** – digits I-V.

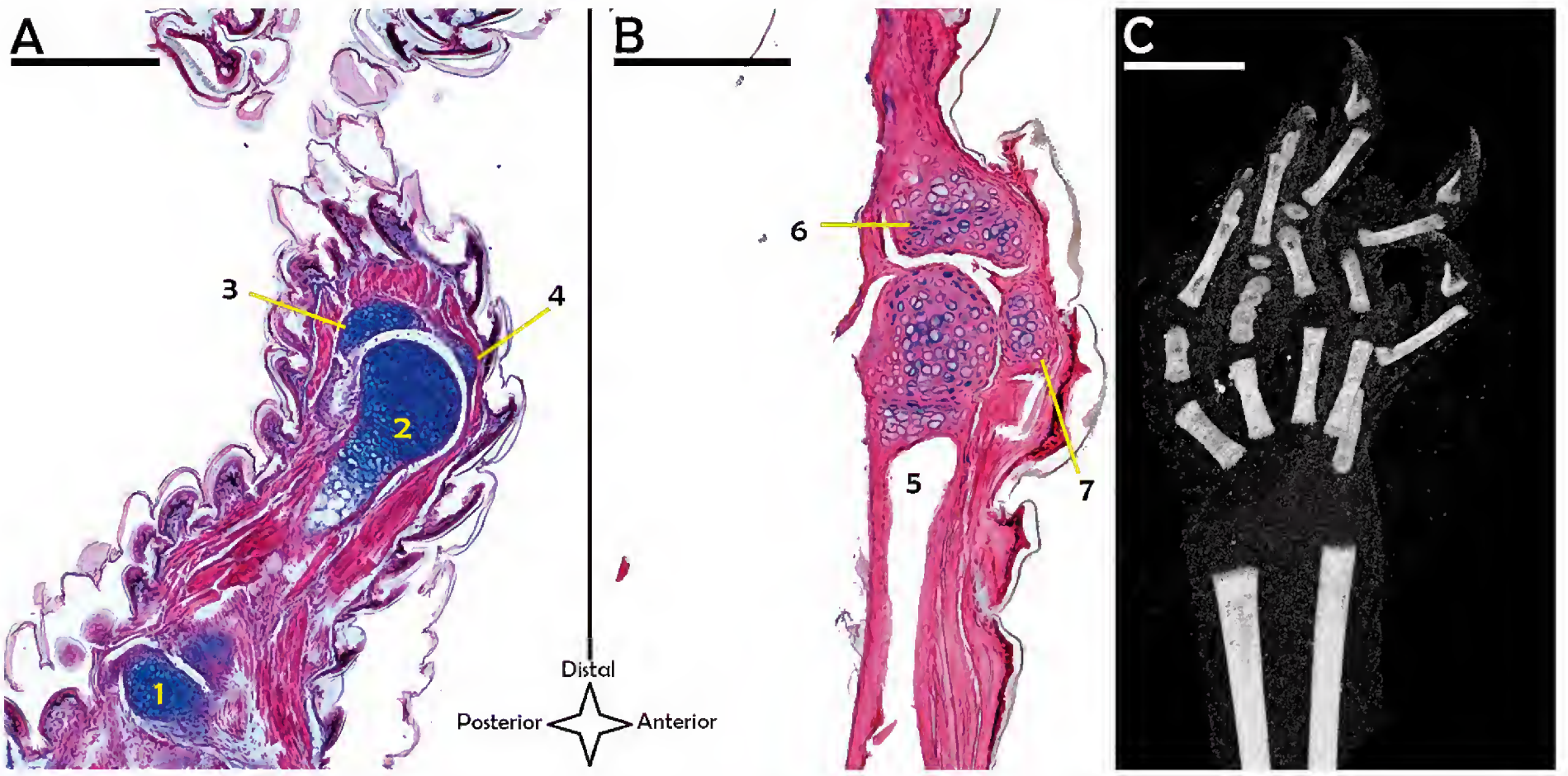

Figure 5. Forelimb of juvenile *Hemidactylus*, stained with azan **(A, B)** and scanned by μCT **(C)**. **(A)** and **(C)** are of the hatchling ZMB 87077 (cross section no. in A is A5_F_13a), and **(B)** of the juvenile ZMB 87076 (cross section no. A4_F_21a). Note the yet unossified paraphalanges in both. In contrast, reduced phalangeal elements have started ossifying. Radius and ulna are not yet fully ossified, and carpal elements are as yet unossified. Numericals indicate: **1** – trapezium; **2** – metacarpal; **3** – phalanx; **4** – paraphalanx; **5** – metacarpal; **6** – phalanx; **7** – paraphalanx. Scale bars in **(A)** and **(B)** equal 200 μm, and scale bar in **(C)** is 550 μm.

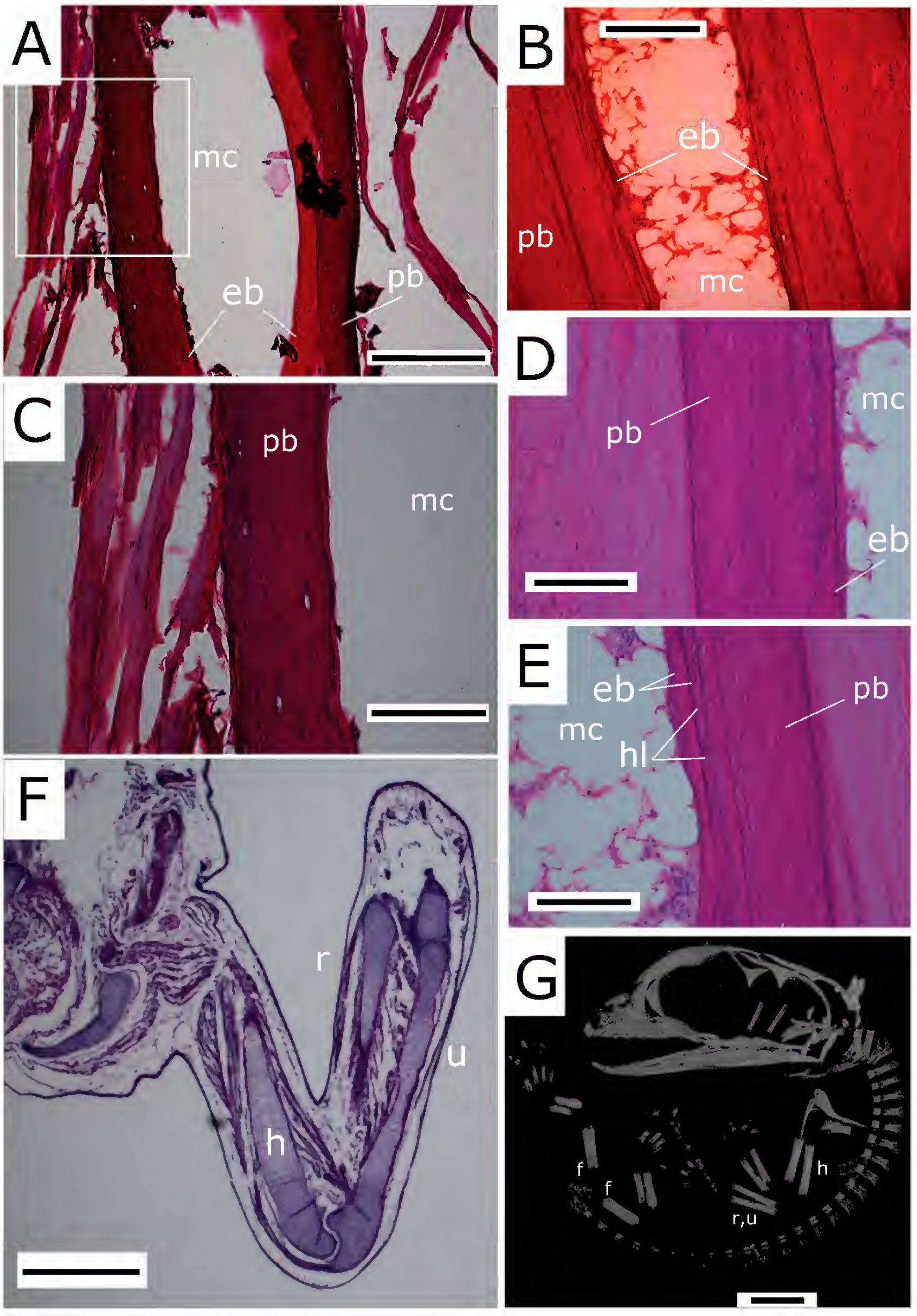

Figure 6. Bone histology of *Hemidactylus* long bones. Adult specimen CA2017_001 (cross section no. H63_FR_B5; **A, C**), ZMB 87078 (cross section no. A12_FL_6b, one year old, SVL 47 mm; **B, D, E**), and developmental stage I specimen CA2017_015 **(F)** and CA2017_014 **(G)**. **(A–E)** Longitudinal sections (HE staining) of the humeral shaft showing a clear pattern of alternating bone lamellae in the periosteal cortex and remodeling in the endosteal region. **(C)** Close-up of boxed area in **(A)**. **(D, E)** Magnification of cortical bone of similar areas in **(B)**. **(F, G)** Onset of ossification in individuals, 25 days before hatching, as seen in histological sections **(F)** and μCT scans **(G)**. Abbreviations: **eb** – endosteal bone; **f** – femur; **h** – humerus; **hl** – Howship lacunae; **mc** – medullary cavity; **pb** – periosteal bone; **r** – radius; **u** – ulna. Scale bars in **(A, B)** equal 200 μm, in **(C–E)** 100 μm, in **(F)** 500 μm, and 1 mm in **(G)**.

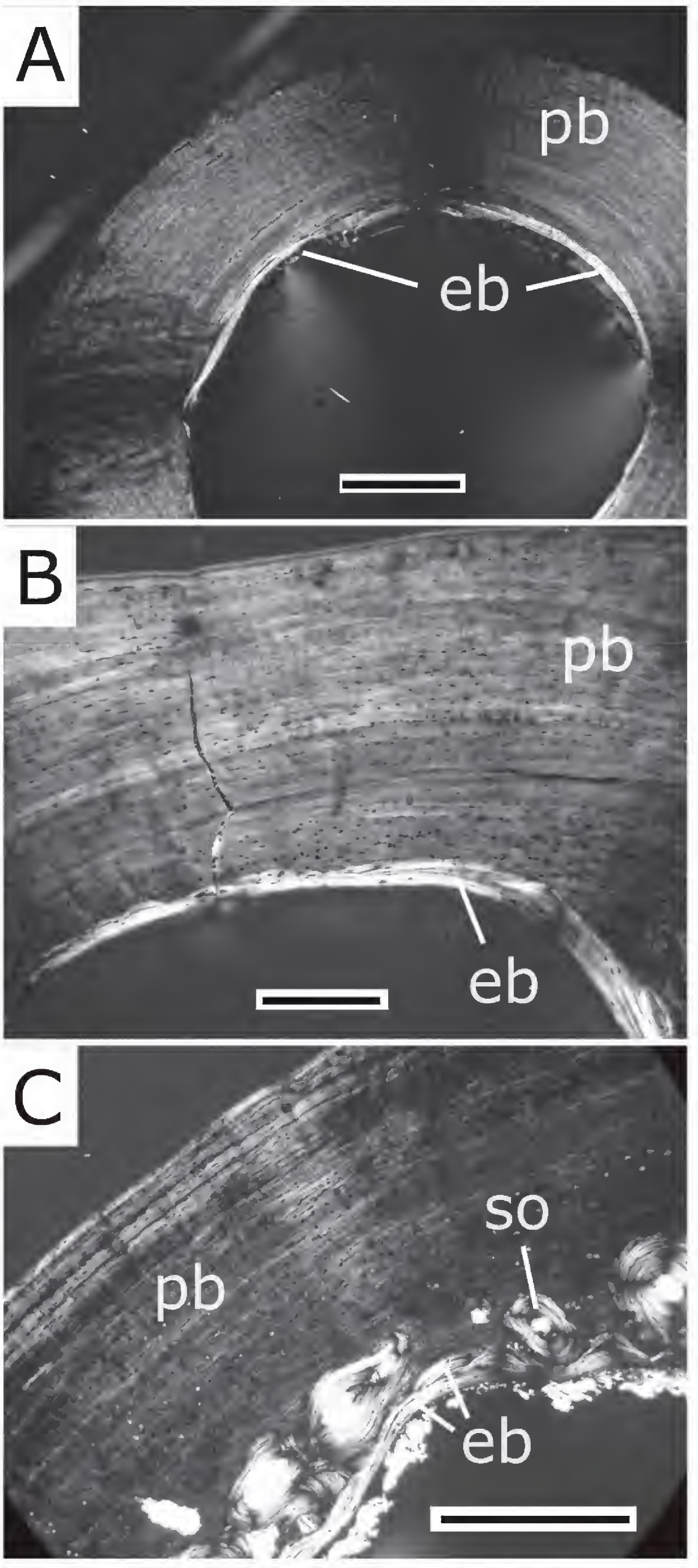

Figure 7. Lamellar bone histology and endosteal remodeling in other squamate lizards. **(A)** Cross section of an *Iguana iguana* femur (AC1896 288). **(B)** Cross section of a *Varanus timorensis* femur (MK52920). **(C)** Cross section of *Tupinambis teguixin* femur (MK53531). All images were taken under cross polarized light. Note the cross cutting relations in the endosteal bone of *V. timorensis* and *Tupinambis*. Also note the more extensive layer of remodeling with secondary osteons in the innermost cortex of *Tupinambis*. Abbreviations: **eb** – endosteal bone; **pb** – periosteal bone; **so** – secondary osteon. Scale bar in **(A)** equals 1 mm, in **(B)** 250 μm, and in **(C)** 500 μm.

Discussion and conlusions

Comparative embryology

The *in-ovo* development of the gecko *Hemidactylus* was defined into twelve stages post-oviposition based on morphological embryonic characters (Figs 2, 3). In contrast to other staging tables, somite formation is not taken into account as they are not clearly identifiable (Hamburger and Hamilton 1951, Muthukkaruppan et al. 1970, Theiler 1989, Sanger et al. 2008). The comparisons of days post-oviposition proved to be a poor indicator of actual development of the embryo (Tab. 1), which we attribute to variations in oviposition timing between females and/or to fluctuation in temperature (26-28°C) in the breeding room. Such discrepancy is not unusual considering the poikilothermic physiology of *Hemidactylus*; shifts in temperature are known to have effects on the developmental age of individuals (Atkinson 1994, Andrews 2004, Goodman 2008, Dayananda et al. 2017). A similar range was also monitored in *Eublepharis macularius* (Wise et al. 2009), *Nothobachia ablephara* and *Calyptommatus sinebrachiatus* (Roscito and Rodrigues 2012). Instead, our study groups erected stages based on morphological events regarding the ear, eye, head, heart, limbs, fronto-nasal process, pharyngeal arches, skin, and thorax development (Figs 2, 3; Tabs 1, 3). Since limb morphogenesis is an often used and a very informative criterion in vertebrate developmental biology, it is also a focus in this study. We not only generated a framework in which to communicate the development of *Hemidactylus*, but we also made direct comparisons with other staging tables available for a diverse range of squamate species (Tab. 3), thus allowing comparative heterochronic studies. In fact, in squamates, the differential timing of fore- and hind limb is rather synchronous (Bininda-Emonds et al. 2007). Interestingly, this is also the case in *Hemidactylus,* which shows no heterochrony in limb development (Tab. 1), in contrast to other gekkotan taxa in which forelimb development is slightly advanced (Noro et al. 2009, Wise et al. 2009). Furthermore, in *Paroedura*, which has a comparable

Table 3. Comparison of squamate staging tables. Differing stages were horizontally aligned based on key characters. Comparing different staging tables allows for the study of heterochrony within squamates, here including geckos, lacertids and iguanians. Focused on limb development, darkening shades of gray indicate (i) both limb buds present after oviposition, (ii) interdigital tissue starts retreating, (iii) develops claws on all 5 digits, (iv) first sign of scales on limbs, and (v) limbs fully developed apart from size. Abbreviations: dpo – days post-oviposition; S, St – embryonic stage.

This study	Noro et al. (2009)	Khannoon (2015)	Wise et al. (2009)	Roscito and Rodrigues (2012)	Roscito and Rodrigues (2012)	Py-Daniel et al. (2017)	Sanger et al. (2008)	Muthukkarruppan et al. (1970)
Hemidactylus sp.	*Paroedura pictus*	*Tarentola annularis*	*Eublepharis macularius*	*Nothobachia ablephara*	*Calyptommatus sinebrachiatus*	*Tropidurus torquatus*	*Anolis sagrei*	*Calotes versicolor*
	0 dpo							Stage 27
	1 dpo							Stage 28
Stage A	2 dpo		St 28		St 1			
Stage B	3-4-5 dpo		St 29	St 1	St 2-3	St 28	3	Stage 29
	6-7 dpo	S29		St 2		St 29	4-5	
Stage C	8-9-10 dpo		St 30		St 4	St 30	6	Stage 30
		S30						
	12 dpo			St 3				Stage 31
Stage D	14 dpo		St 31	St 4	St 5	St 31		
		S31		St 5		St 32		
					St 6			Stage 32
	16 dpo		St 32					
Stage E	18 dpo	S32	St 33	St 6	St 7	St 33-34	7-8	Stage 33
Stage F	20-22 dpo	S33	St 34	St 7	St 8	St 35	9	Stage 34
				St 8	St 9-10			
Stage G	24 dpo	S34		St 9	St 11	St 36	10	Stage 35
	26 dpo		St 35				11	
Stage H	28 dpo	S35	St 36			St 37		Stage 36
Stage I	30 dpo	S36	St 37			St 38	12-13-14	
								Stage 37
								Stage 38
Stage J	35 dpo	S37	St 38			St 39	15-16-17	Stage 39
			St 39					
		S38	St 40					Stage 40
Stage K	40-45-50 dpo	S39	St 41		St 12	St 40	18	Stage 41
Stage L	55-60 dpo		St 42			St 41-42	19	Stage 42

developmental period, limb budding starts at the third day of oviposition (Noro et al. 2009). In contrast, we observe that in *Hemidactylus*, limb budding does not start as early as stage B (Fig. 2, Tab. 1). Later in development, Noro et al. (2009) identify a pattern of heterochrony in the limbs of *Paroedura*, which they attribute to the development of the digits in the gekkotan clade. However, findings of this study do not support this assumption (Figs 2, 3). Instead, we found interspecific variation during limb development within eight squamate species including geckos, lacertids, and iguanians: (i) concerning limb bud formation after oviposition, (ii) retraction of the interdigital tissue, (iii) claw development on the ultimate phalanges, (iv) scale formation on the limbs, and (v) termination of limb development (Tab. 3). Among geckos, for example, scale formation on the limbs starts at stage J and 35 dpo in *Hemidactylus* and *Paroedura*, respectively, whereas in *Tarentola* and *Eublepharis*, it is developed at an earlier stage (S35 and St 37, respectively).

Long bone histomorphometrics

Bone histology shows rapid accretion and endosteal remodeling of lamellar bone in the long bone cortices at later phases in ontogeny. The lamellar bone formation rate is similar to rates seen in the nearly avascular fibulae of wild *Varanus niloticus* (de Buffrénil and Castanet 2000), suggesting that absolute matrix production rate could be similar in different squamates. The intense remodeling in adult *Hemidactylus* indicates a dynamic balance of cortical bone thickness during growth. Interestingly, in contrast to *Hemidactylus*, *Iguana*, and *Varanus timorensis*, the *Tupinambis* (Fig. 7) in our study also produces secondary osteons, and generally experiences more advanced remodeling. This difference may be the result of the combination of the relatively large size and foraging behavioral ecology of *Tupinambis*. The studied *Hemicactylus* and *V. timorensis* also typically forage for food, but they retain relatively small body sizes, and their lacuno-canalicular networks may provide enough flux to maintain a healthy bone homeostasis without the need for additional blood vessels inside the bony cortex.

Eco-specializations of the limbs of Hemidactylus

Our detailed analysis of ecomorphological specializations in the limbs of *Hemidactylus* also reveal that, in contrast to earlier observations (Russell and Bauer 1988), paraphalanges are bony in the adult, as revealed by μCT (Figs 3, 4). However, these ossify only after hatching, as shown by μCT scanning and azan staining (Figs 4, 5). Furthermore, data from the μCT indicate that more paraphalanges in various different shapes are present in *Hemidactylus* (Fig. 4), when compared to other gekkotans (Gamble et al. 2012). These structures have been suggested to aid in the support of the scansors (Russell and Bauer 1988, Gamble et al. 2012). In fact, they evolved also multiple times independently in geckos, alongside adhesive toepads (Gamble et al. 2012). Paraphalanges have been suggested to represent sesamoid bones (Russell and Bauer 1988, Gamble et al. 2012). Sesamoids are neomorphic ossifications present in tendons and/or ligaments, located near joints. They are often mistaken for accessory ossicles because both share various imaging characteristics (Nwawka et al. 2013). However, we agree with their previous identification as paraphalanges, because their existence correlates with the modified tendons and muscles controlling the scansors (Russell and Bauer 1988, Gamble et al. 2012). Among Squamata, a variety of different sesamoid bones are present in the hands and feet (Fontanarrosa and Abdala 2016, Regnault et al. 2016). In fact, phalangeal sesamoids, located dorsally on the penultimate phalanges, are ancestral to all Lepidosauria (squamates and rhynchocephalians), whereas metacarpal sesamoids likely evolved only later within squamates (Regnault et al. 2016). Penultimate phalangeal sesamoids are, in fact, present in most squamates (Regnault et al. 2016). Metacarpal and metatarsal sesamoids are of variable occurrence in Gekkota (Regnault et al. 2016). Although some sesamoids have been linked to lifestyle, functional interpretations are to be inferred with caution (Fontanarrosa and Abdala 2016, Regnault et al. 2016). In humans, e.g., sesamoids likely result from an interplay of intrinsic genetic factors and phylogeny, and extrinsic mechanobiological factors (Sarin et al. 1999).

Reduced phalanges ossify at the same time schedule as the other phalangeal elements in *Hemidactylus* (Figs 3, 4), but their ecological relevance is yet to be determined in this species. This trait is also found in non-related and ecologically different fossil synapsids, such as *Biarmosuchus*, *Titanophoneus*, *Lycaenops*, *Thrinaxodo*n, and even the mammaliaform *Docofossor* (Hopson 1995, Luo et al. 2015). However, phalanx number varies widely in non-mammalian tetrapods (Richardson and Chipman 2003). Hopson (1995) suggested that these reduced disc-like structures were eventually lost. Gamble et al. (2012), on the other hand, linked phalanx reduction with the evolution of adhesive toepads. Furthermore, Russell (1977) suggested that the reduced phalanx is used to raise the penultimate phalanx, thereby altering the angle of the claw relative to the substrate for a more beneficial grip. Phalanx variation has been developmentally associated with either heterochronic shifts (Richardson and Oelschläger 2002), or the involvement of mutations in expression patterns and molecular pathways of BMPs and other transcription factors (Cooper et al. 2014, Luo et al. 2015). Studying the latter in *Hemidactylus* remains an avenue for future research. This study provides the morphological framework essential for the study of such kinds of ecological traits from a molecular perspective, that is, by means of gene expression and transcriptome analyses.

Author contributions

CB designed the study. CB and WvdV collected gecko embryos. WdV carried out experiments in the morphology & histology lab. CB compiled μCT datasets. KS carried

out bone histology experiments. CB, KS, and WvdV analyzed data. NDP provided reagents and lab facilities for immunohistochemical analyses, and commented on an earlier version of the manuscript. CB, KS, and WvdV wrote the manuscript. All authors approved the final version.

Acknowledgements

Johannes Müller (Berlin) provided the parental *Hemidactylus* generation and helped with animal husbandry; we thank him also for discussion. Annett Billepp and Petra Grimm (Berlin) are thanked for animal care-taking. We thank Julia Eymann (Helsinki) for help with immunohistochemical analyses. We thank Jutta Zeller (Berlin) for help with and preparation of histological sections and staining. Kristin Mahlow (Berlin) is thanked for help with μCT scanning. Frank Tillack (Berlin) kindly helped with taking photos of live animals. We furthermore thank Vivian de Buffrénil (Paris) for access to comparative material of *Varanus timorensis*, *Tupinambis teguixin*, and *Iguana iguana* at the histology library of the Musée d'Histoire Naturelle. We also thank Brandon Kilbourne (Berlin) for language editing of an earlier version of the manuscript. We acknowledge critical and helpful comments by Torsten Scheyer (Zurich) and Johannes Penner (Freiburg). CB and WvdV were funded by the German Research Foundation (DFG, BI 1750/3-1 to CB); KS was funded by a postdoctoral mandate of the Research Foundation Flanders (FWO).

References

Andrews RM (2004) Patterns of embryonic development. In: Deeming DC (Ed.) Reptilian Incubation: Environment, Evolution And Behaviour. Nottingham University Press, Nottingham. 75–102.

Arnold EN, Poinar G (2008) A 100 million year old gecko with sophisticated adhesive toe pads preserved in amber from Myanmar. Natural History 1847: 6–68.

Atkinson D (1994) Temperature and organism size - a biological law for ectotherms? Advances in Ecological Research 25: 1–58. https://doi.org/10.1016/S0065-2504(08)60212-3

Autumn K, Sitti M, Liang YA Peattie AM, Hansen WR, Sponberg S, Kenny TW, Fearing R, Israelachvili JN, Full RJ (2002) Evidence for van der Waals adhesion in gecko setae. Proceedings of the National Academy of Sciences of the United States of America 99: 12252–12256. https://doi.org/10.1073/pnas.192252799

Bininda-Emonds O, Cardillo M, Jones KE, MacPhee RDE, Beck RMD, Grenyer R, Price SA, Vos RA, Gittleman JL, Purvis A (2007) The delayed rise of present-day mammals. Nature 446: 507–512. https://doi.org/10.1038/nature05634

de Buffrenil V, Castanet J (2000) Age estimation by skeletochronology in the Nile monitor (*Varanus niloticus*), a highly exploited species. Journal of Herpetology 34: 414–424. https://doi.org/10.2307/1565365

Carranza S, Arnold EN (2006) Systematics, biogeography, and evolution of *Hemidactylus* geckos (Reptilia: Gekkonidae) elucidated using mitochondrial DNA sequences. Molecular Phylogenetics and Evolution 38: 531–545. https://doi.org/10.1016/j.ympev.2005.07.012

Cooper KL, Sears KE, Uygur A, Maier J, Baczkowski KS, Brosnahan M, Antczak D, Skidmore JA, Tabin CJ (2014) Patterning and post-patterning modes of evolutionary digit loss in mammals. Nature 511: 41–45. https://doi.org/10.1038/nature13496

Dayananda B, Penfold S, Webb JK (2017) The effects of incubation temperature on locomotor performance, growth and survival in hatchling velvet geckos. Journal of Zoology. https://doi.org/10.1111/jzo.12460

Fontanarrosa G, Abdala V (2016) Bone indicators of grasping hands in lizards. PeerJ 4: e1978. https://doi.org/10.7717/peerj.1978

Gamble T, Greenbaum E, Jackman TR, Russell AP, Bauer AM (2012) Repeated origin and loss of adhesive toepads in geckos. PLoS ONE 7: e39429. https://doi.org/10.1371/journal.pone.0039429

Gilbert F, Epel D (2009) Ecological developmental biology: integrating epigenetics, medicine and evolution. Sinauer Associates Inc, Sunderland, Massachusetts, 480 pp.

Goodman RM (2008) Latent effects of egg incubation temperature on growth in the lizard *Anolis carolinensis*. Journal of Experimental Zoology Part A: Ecological Genetics and Physiology 309: 525–533. https://doi.org/10.1002/jez.483

Hamburger V, Hamilton H (1951) A series of normal stages in the development of the chick embryo. Journal of Morphology 88: 231–272. https://doi.org/10.1002/jmor.1050880104

Hopson JA (1995) Patterns of evolution in the manus and pes of non-mammalian therapsids. Journal of Vertebrate Paleontology 15: 615–639. https://doi.org/10.1080/02724634.1995.10011252

Hugi J, Hutchinson MN, Koyabu D, Sánchez-Villagra MR (2012) Heterochronic shifts in the ossification sequences of surface-and subsurface-dwelling skinks are correlated with the degree of limb reduction. Zoology 115: 188–198. https://doi.org/10.1016/j.zool.2011.10.003

Khannoon ER (2015) Developmental stages of the climbing gecko *Tarentola annularis* with special reference to the claws, pad lamellae, and subdigital setae. Journal of Experimental Zoology Part B Molecular and Developmental Evolution 324: 450–464. https://doi.org/10.1002/jez.b.22630

Losos JB, Hillis DM, Greene HW (2012) Who speaks with a forked tongue? Science 338: 1428–1429. https://doi.org/10.1126/science.1232455

Luo Z-X, Meng Q, Ji Q, Zhang Y-G, Neander AI (2015) Evolutionary development in basal mammaliaforms as revealed by a docodontan. Science 347: 760–764. https://doi.org/10.1126/science.1260880

Millinkovitch MC, Tzika A (2007) Escaping the mouse trap: The selection of new evo-devo model species. Journal of Experimental Zoology 308B: 337–346. https://doi.org/10.1002/jez.b.21180

Muthukkaruppan V, Kanakambika P, Manickavel V, Veeraraghaven K (1970) Analysis of the development of the lizard, *Calotes versicolor*. Journal of Morphology 130: 479–490. https://doi.org/10.1002/jmor.1051300407

Noro M, Uejima A, Abe G, Manabe M, Tamura K (2009) Normal developmental stages of the Madagascar Ground Gecko *Paroedura pictus* with special reference to limb morphogenesis. Developmental Dynamics 238: 100–109. https://doi.org/10.1002/dvdy.21828

Nwawka OK, Hayashi D, Diaz LE, Goud AR, Arndt III WF, Roemer FW, Malguria N, Guermazi A (2013) Sesamoids and accessory ossicles of the foot: anatomical variability and related pathology. Insights Imaging 4: 581–593. https://doi.org/10.1007/s13244-013-0277-1

Pianka ER, Sweet SS (2005) Integrative biology of sticky feet in geckos. BioEssays 27: 647–652. https://doi.org/10.1002/bies.20237

Py-Daniel R, Kennedy Soares De-Lima A, Campos Lima F, Pic-Taylor A, Rodrigues Pires Junior O, Sebben A (2017) A staging table of

post-ovipositional development for the South American collared lizard *Tropidurus torquatus* (Squamata: Tropiduridae). The Anatomical Record 300: 277–290. https://doi.org/10.1002/ar.23500

Pyron RA, Burbrink FT, Wiens JJ (2013) A phylogeny and revised classification of Squamata, including 4161 species of lizards and snakes. BMC evolutionary biology 13: 93. https://doi.org/10.1186/1471-2148-13-93

Rasband WS (1997) ImageJ. US National Institutes of Health, Bethesda, MD.

Regnault S, Jones MEH, Pitsillides AA, Hutchinson JR (2016) Anatomy, morphology and evolution of the patella in squamate lizards and tuatara (*Sphenodon punctatus*). Journal of Anatomy 228: 864–876. https://doi.org/10.1111/joa.12435

Richardson MK, Oelschläger HHA (2002) Time, pattern, and heterochrony: a study on hyperphalangy in the dolphin embryo flipper. Evolution and Development 4: 435–444. https://doi.org/10.1046/j.1525-142X.2002.02032.x

Richardson MK, Chipman AD (2003) Developmental constraints in a comparative framework: a test case using variations in phalanx number during amniote evolution. Journal of Experimental Zoology Part B Molecular and Developmental Evolution 296: 8–22. https://doi.org/10.1002/jez.b.13

Roscito JG, Rodrigues MT (2012) Embryonic development of the fossorial gymnophthalmid lizards *Nothobachia ablephara* and *Calyptommatus sinebrachiatus*. Zoology 115: 302–318. https://doi.org/10.1016/j.zool.2012.03.003

Ruibal R, Ernst V (1965) The structure of the digital setae of lizards. Journal of Morphology 117: 271–293. https://doi.org/10.1002/jmor.1051170302

Russell AP (1975) A contribution to the functional analysis of the foot of the Tokay gecko, *Gekko gecko*. Journal of Zoology 176: 437–476. https://doi.org/10.1111/j.1469-7998.1975.tb03215.x

Russell AP (1977) The phalangeal formula of *Hemidactylus* Oken: A correction and a functional explanation. Anatomia, Histologia, Embryologia 6: 332–338. https://doi.org/10.1111/j.1439-0264.1977.tb00443.x

Russell AP (2002) Integrative functional morphology of the gekkotan adhesive system (Reptilia: Gekkota). Integrative and Comparative Biology 42: 1154–1163. https://doi.org/10.1093/icb/42.6.1154

Russell AP, Bauer AM (1988) Paraphalangeal elements of gekkonid lizards: a comparative survey. Journal of Morphology 197: 221–240. https://doi.org/10.1002/jmor.1051970208

Sanger TJ, Losos JB, Gibson-Brown JJ (2008) A developmental staging series for the lizard genus *Anolis*: a new system for the integration of evolution development, and ecology. Journal of Morphology 296: 129–137. https://doi.org/10.1002/jmor.10563

Sanger TJ (2012) The emergence of squamates as model systems for integrative biology. Evolution and Development 14: 231–233. https://doi.org/10.1111/j.1525-142X.2012.00541.x

Sarin VK, Erickson GM, Giori NJ, Bergmann AG, Carter DR (1999) Coincident development of sesamoid bones and clues to their evolution. The Anatomical Record 257: 174–180. https://doi.org/10.1002/(SICI)1097-0185(19991015)257:5<174::AID-AR6>3.0.CO;2-O

Shapiro MD (2002) Developmental morphology of limb reduction in *Hemiergis* (Squamata: Scincidae): chondrogenesis, osteogenesis, and heterochrony. Journal of Morphology 254: 211–231. https://doi.org/10.1002/jmor.10027

Theiler K (1989) The House Mouse: Atlas Of Embryonic Development. Springer-Verlag, New York Inc, New York.

Vickaryous MK, Olson MW (2007) Sesamoids and ossicles in the appendicular skeleton. In: Hall BK (Ed.) Fins into Limbs: Evolution, development, and transformation. The University of Chicago Press, Chicago, 323–341.

Wellborn V (1933) Vergleichende osteologische Untersuchungen an Geckoniden, Eublephariden und Uroplatiden. Sitzung der Gesellschaft Naturfreunde, Berlin.

Wiens JJ, Hutter CR., Mulcahy, D. G., Noonan BP, Townsend TM, Sites Jr JW, Reeder TW (2012) Resolving the phylogeny of lizards and snakes (Squamata) with extensive sampling of genes and species. Biology Letters 8: 1043–1046. https://doi.org/10.1098/rsbl.2012.0703

Wise PAD, Vickaryous MK, Russell AP (2009) An embryonic staging table for in ovo development of *Eublepharis macularius*, the leopard gecko. The Anatomical Record: Advances in Integrative Anatomy and Evolutionary Biology 292: 1198–1212. https://doi.org/10.1002/ar.20945

Supplementary material 1

SOM Table

Authors: Wessel van der Vos, Koen Stein, Nicolas Di-Poï, Constanze Bickelmann

Data type: Adobe PDF file

Explanation note: μCT scanning details for specimens used in this study and depicted in Figures 2, 4-6.

Link: https://doi.org/10.3897/zse.94.22289.suppl1

Zoosystematics and Evolution

94 (**1**) 2018

http://zse.pensoft.net

Leibniz Association